

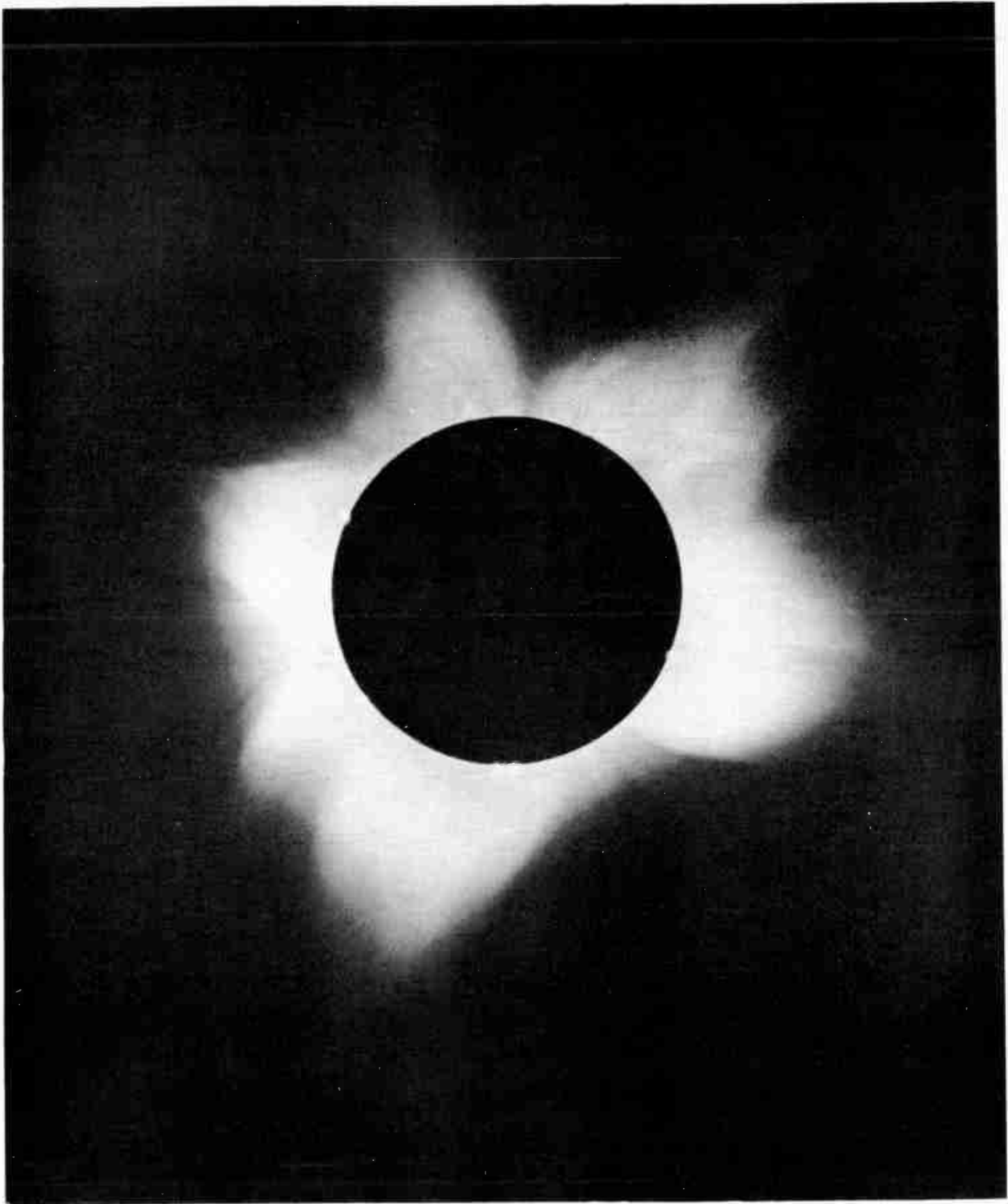
ELEMENTARY MANUAL
— *of* —
RADIO PROPAGATION

by DONALD H. MENZEL

PRENTICE — HALL

ELEMENTARY MANUAL
OF
RADIO PROPAGATION

R.P. BRADY
REPRESENTING
INDMAR, USN, SEATTLE



The Solar Corona, June 19, 1936.

Courtesy National Geographic Society

ELEMENTARY MANUAL

• OF •

RADIO PROPAGATION

BY

DONALD H. MENZEL

*Professor of Astrophysics; Chairman, Department of
Astronomy, Harvard University. Associate Director
for Solar Research, Harvard College Observatory*

New York

PRENTICE-HALL, INC.

1948

COPYRIGHT, 1948, BY
PRENTICE-HALL, INC.
70 Fifth Avenue, New York

ALL RIGHTS RESERVED. NO PART OF THIS BOOK
MAY BE REPRODUCED IN ANY FORM, BY MIMEO-
GRAPH OR ANY OTHER MEANS, WITHOUT PERMIS-
SION IN WRITING FROM THE PUBLISHERS.

PRINTED IN THE UNITED STATES OF AMERICA

TO
DR. J. H. DELLINGER
CHIEF OF THE CENTRAL RADIO PROPAGATION LABORATORY
OF THE NATIONAL BUREAU OF STANDARDS
*Pioneer in the field of radio propagation and
in the effects of variable solar activity
upon radio phenomena*

PREFACE

IT IS SCARCELY NECESSARY TO REMIND A COMMUNICATIONS officer or a radio operator of the importance of maintaining effective radio communication in time of war or peace. We have an efficient, powerful radio transmitter, and we are all set to send a signal, but what makes us think that our signal will ever reach its intended destination? What experiences will the wave undergo in its excursion from our transmitter to wherever we wish it to go?

Many things can happen to the radio wave in the course of its travel through space. The operator must know enough about what may occur, about the transmission characteristics of radio waves, to be able to steer the best course and select the best frequency from those at his disposal for each particular problem that he meets. If he chooses too high a frequency, the "mirror" that exists high in the earth's atmosphere may fail to reflect the beam, in which case the signal will wing its way out into interplanetary space. This might be fine for communication with the moon or the as yet hypothetical inhabitants of Mars, but it is highly impractical for communication on earth. If the operator selects too low a frequency, the waves may be too heavily absorbed in their passage through the atmosphere. Communication would be impossible under that situation, too.

Unfortunately there is no permanent "road map" of the sky along which we can steer our signal, for the passable sky-lanes are not paved, and a road usable now may have a "detour" sign posted on it an hour from now. Fortunately, however, it is not too complicated for us to construct a road map for any required time and from it choose the frequency we must use to send our signal and insure its safe trip.

We shall use certain terms so frequently that some abbreviations are desirable. The lowest useful high frequency and the maximum useful frequency we shall call respectively the LUHF and the MUF. The optimum working frequency condenses to OWF. Most ionospheric experts pronounce the abbreviations instead of saying the letters. Thus we hear "loof," "mewf," and "ouf." The technical jargon sounds like gibberish to the uninitiated, but the procedure saves time and effort.

The range of frequencies useful for communication purposes depends upon a large number of factors, the most important of which are: the location of the points of

transmission and reception, the distance between the stations, the time of day, the time of year, and the state of solar activity. There will be consideration on our map for each of these factors. By following the rules outlined in this elementary manual, we shall be able to analyze and predict the behavior of radio signals over any type of circuit and have further understanding of the whys and wherefores of our complicated but interesting communication system.

During the war the radio lanes were crowded. Delays resulting from failure to use the right frequencies had serious consequences. At an early date the armed services set up Wave Propagation Committees under the Communication Boards of the Joint and Combined Chiefs of Staff. The Joint (U.S. Army-Navy) Committee established the "Interservice Radio Propagation Laboratory" (I.R.P.L.), at the National Bureau of Standards, Washington, D.C. The Combined (U.S.-British) Committee maintained international liaison among the Allied Nations.

The records of ionospheric activity available prior to the war were entirely inadequate for military purposes. The Allied Nations joined in a project of building a network of ionospheric stations. I.R.P.L. analyzed the incoming data and put out forecasts several months in advance of the expected average ionospheric conditions. Studies of the sun and of variations in the earth's magnetism aided in the prediction problem.

The Army and the Navy maintained separate organizations for the practical utilization of the fundamental data supplied by I.R.P.L. This manual is an elaboration of a training pamphlet the author prepared for use of Navy personnel. Speed of analysis was of great importance. The methods presented here were developed in part by the author and in part by I.R.P.L. These methods were carefully tested and checked against tens of thousands of individual transmissions over an enormous variety of circuits. The results of the comparison were entirely satisfactory.

I am particularly indebted to Dr. J. H. Dellinger and Dr. Newbern Smith of I.R.P.L. for many helpful conferences and for permission to use illustrations prepared by them. Major Dana K. Bailey, U.S. Signal Corps, gave helpful advice.

The United States Weather Bureau made available

much valuable material related to meteorological phenomena. I wish to thank Dr. F. W. Reichelderfer, Chief of the Bureau, and Dr. E. Dillon Smith for permission to use basic facts and illustrations contained in their publication on meteorological factors affecting propagation of radio waves on frequencies above 30 megacycles. The Navy Department Aerology section placed additional material of this type at my disposal. Mr. Martin Katzin and Captain John L. Reinartz of the Naval Research Laboratory furnished experimental data. A very complete study of the higher frequencies was carried on by O.S.R.D. (Office of Scientific Research and Development), under the chairmanship of Dr.

Charles R. Burrows. The program was carried out on an international basis.

Finally, I wish to express particular appreciation to the members of my own organization within the Navy for assistance in preparing the original manuscript. I regret that I cannot mention here the names of all who helped, but I wish to acknowledge the aid of Dr. Albert Whiteman and Dr. William Eberlein. Miss Catherine Barber assisted me in preparation of the final manuscript.

The United States Navy Department has given official permission for publication of this book. The material, however, represents the views of the author and does not necessarily carry official Navy endorsement.

DONALD H. MENZEL

CONTENTS

CHAPTER	PAGE
1. WHAT HAPPENS TO A RADIO WAVE?	1
2. THE USE OF MAPS AND CHARTS IN RADIO PROPAGATION PROBLEMS	5
3. STRUCTURE OF THE IONOSPHERE AND WORLD MUF MAPS	14
4. PREPARATION OF GREAT-CIRCLE MAPS	36
5. EVALUATION OF DISTANCE BETWEEN TWO STATIONS	42
6. DETERMINATION OF MAXIMUM USABLE FREQUENCIES.	44
7. THE ABSORPTION PROBLEM AND RADIO NOISE	47
8. CALCULATION OF LOWEST USEFUL HIGH FREQUENCIES.	56
9. VARIABILITY OF THE SUN.	113
10. IONOSPHERIC VARIATIONS	117
11. GROUND WAVE TRANSMISSION	120
12. PROBLEMS OF BROADCAST AND LOWER FREQUENCIES.	131
13. SOME INTRODUCTORY REMARKS ABOUT VHF, UHF, AND SHF	134
14. THE CALCULATION OF COVERAGE DIAGRAMS FOR STANDARD ATMOSPHERIC CONDITIONS FOR RADIO FREQUENCIES GREATER THAN 30 MEGACYCLES.	136
15. THE FIELD IN THE SHADOW ZONE UNDER STANDARD CONDITIONS	172
16. HOW ATMOSPHERIC CONDITIONS CAUSE LARGE VARIATIONS FROM STANDARD-SET PERFORMANCE	176
17. M CURVES, AN INDEX OF EXPECTED COVERAGE	181
18. PROPAGATION EFFECTS DEDUCED FROM WEATHER CONDITIONS	197
19. OPERATIONAL APPLICATIONS IN TROPOSPHERIC PROPAGATION	203
APPENDIX 1. THEORY OF IONOSPHERIC PROPAGATION.	209
APPENDIX 2. THEORY OF TROPOSPHERIC PROPAGATION.	212
APPENDIX 3. DEFINITIONS.	218
INDEX	221

LIST OF ILLUSTRATIONS

THE SOLAR CORONA	FRONTISPIECE		
1. ESCAPE OF HIGH-FREQUENCY WAVES	2	42. ABSORPTION INDEX CHART, JANUARY	62
2. REFLECTION OF WAVES	3	43. ABSORPTION INDEX CHART, FEBRUARY	63
3. SCHEMATIC DRAWING OF THE THREE IONOSPHERIC LAYERS	14	44. ABSORPTION INDEX CHART, MARCH	64
4. MEASUREMENT OF THE IONOSPHERIC MESH	15	45. ABSORPTION INDEX CHART, APRIL	65
5. (a) SCHEMATIC IONOSPHERE RECORD	15	46. ABSORPTION INDEX CHART, MAY	66
(b) OBSERVED VARIATION OF VIRTUAL HEIGHT WITH WAVE-FREQUENCY, MARCH 14, 1939	16	47. ABSORPTION INDEX CHART, JUNE	67
(c) OBSERVED VARIATION OF VIRTUAL HEIGHT WITH WAVE-FREQUENCY, DECEMBER 18, 1939	17	48. ABSORPTION INDEX CHART, JULY	68
6. GEOMETRY OF REFLECTIONS	18	49. ABSORPTION INDEX CHART, AUGUST	69
7. E-LAYER 2000-MUF, IN MC, PREDICTED FOR MARCH, 1945	19	50. ABSORPTION INDEX CHART, SEPTEMBER	70
8. E-LAYER 2000-MUF, IN MC, PREDICTED FOR JUNE, 1945	20	51. ABSORPTION INDEX CHART, OCTOBER	71
9. E-LAYER 2000-MUF, IN MC, PREDICTED FOR SEPTEMBER, 1945	21	52. ABSORPTION INDEX CHART, NOVEMBER	72
10. E-LAYER 2000-MUF, IN MC, PREDICTED FOR DECEMBER, 1945	22	53. ABSORPTION INDEX CHART, DECEMBER	73
11. SIEVELIKE PATTERN OF IONOSPHERE	23	54. NOMOGRAM GIVING VARIATION OF <i>Kd</i>	74
12. F_2 -4000-MUF, IN MEGACYCLES, W ZONE, PREDICTED FOR MARCH, 1945	24	55. NOMOGRAM GIVING VARIATION OF <i>Kd</i>	75
13. F_2 -4000-MUF, IN MEGACYCLES, W ZONE, PREDICTED FOR JUNE, 1945	25	56. WORLD AURORAL-ZONE CHART	76
14. F_2 -4000-MUF, IN MEGACYCLES, W ZONE, PREDICTED FOR SEPTEMBER, 1945	26	57. ABSORPTION OF AURORAL ZONE	77
15. F_2 -4000-MUF, IN MEGACYCLES, W ZONE, PREDICTED FOR DECEMBER, 1944	27	58. LUHF NOMOGRAM FOR LARGE VALUES OF <i>Kd</i> FOR GENERAL USE, NOISE GRADE 1	78
16. F_2 ZERO-MUF, IN MEGACYCLES, E ZONE, PREDICTED FOR MARCH, 1945	28	59. LUHF NOMOGRAM FOR LARGE VALUES OF <i>Kd</i> NOISE GRADE 1½	79
17. F_2 ZERO-MUF, IN MEGACYCLES, E ZONE, PREDICTED FOR JUNE, 1945	29	60. LUHF NOMOGRAM FOR LARGE VALUES OF <i>Kd</i> NOISE GRADE 2	80
18. F_2 ZERO-MUF, IN MEGACYCLES, E ZONE, PREDICTED FOR SEPTEMBER, 1945	30	61. LUHF NOMOGRAM FOR LARGE VALUES OF <i>Kd</i> FOR OPEN OCEAN, NOISE GRADE 2½	81
19. F_2 ZERO-MUF, IN MEGACYCLES, E ZONE, PREDICTED FOR DECEMBER, 1944	31	62. LUHF NOMOGRAM FOR LARGE VALUES OF <i>Kd</i> NOISE GRADE 3	82
20. NOMOGRAM FOR TRANSFORMING E-LAYER 2000-MUF TO EQUIVALENT MAXIMUM USABLE FREQUENCIES AND OPTIMUM WORKING FREQUENCIES DUE TO COMBINED EFFECT OF E LAYER AND F_1 LAYER AT OTHER TRANSMISSION DISTANCES	32	63. LUHF NOMOGRAM FOR LARGE VALUES OF <i>Kd</i> NOISE GRADE 3½	83
21. NOMOGRAM FOR TRANSFORMING F_2 -LAYER ZERO-MUF TO EQUIVALENT MAXIMUM USABLE FREQUENCIES AT OTHER TRANSMISSION DISTANCES	33	64. LUHF NOMOGRAM FOR LARGE VALUES OF <i>Kd</i> NOISE GRADE 4	84
22. NOMOGRAM FOR TRANSFORMING F_2 -LAYER 4000-MUF TO EQUIVALENT MAXIMUM USABLE FREQUENCIES AT OTHER TRANSMISSION DISTANCES	34	65. LUHF NOMOGRAM FOR LARGE VALUES OF <i>Kd</i> NOISE GRADE 4½	85
23. NOMOGRAM FOR TRANSFORMING F_2 -ZERO-MUF AND F_2 -4000-MUF TO EQUIVALENT MAXIMUM USABLE FREQUENCIES AT INTERMEDIATE TRANSMISSION DISTANCES; CONVERSION SCALE FOR OBTAINING OPTIMUM WORKING FREQUENCIES	35	66. LUHF NOMOGRAM FOR LARGE VALUES OF <i>Kd</i> NOISE GRADE 5	86
24. WORLD MAP SHOWING ZONES COVERED BY PREDICTED CHARTS, AND AURORAL ZONES	36	67. LUHF NOMOGRAM FOR LARGE VALUES OF <i>Kd</i> FOR CONTINENTAL LAND AREAS, NOISE GRADE 2½	87
25. OVERLAY, SAN FRANCISCO-MOSCOW PATH	37	68. LUHF NOMOGRAM FOR LARGE VALUES OF <i>Kd</i> NOISE GRADE 3	88
26. GREAT CIRCLE MAP	38	69. LUHF NOMOGRAM FOR LARGE VALUES OF <i>Kd</i> NOISE GRADE 3½	89
27. DISTANCE CIRCLE MAP	39	70. LUHF NOMOGRAM FOR LARGE VALUES OF <i>Kd</i> NOISE GRADE 4	90
28. COMPLETED OVERLAY, SAN FRANCISCO-MOSCOW PATH	40	71. LUHF NOMOGRAM FOR LARGE VALUES OF <i>Kd</i> NOISE GRADE 4½	91
29. DISTANCE NOMOGRAM	41	72. LUHF NOMOGRAM FOR LARGE VALUES OF <i>Kd</i> NOISE GRADE 5	92
30. WORK SHEET FOR DISTANCE BETWEEN STATIONS	42	73. LUHF NOMOGRAM FOR SMALL VALUES OF <i>Kd</i> FOR GENERAL USE, NOISE GRADE 1	93
31. DISTANCE NOMOGRAM	43	74. LUHF NOMOGRAM FOR SMALL VALUES OF <i>Kd</i> NOISE GRADE 1½	94
32. RECORD SHEET FOR DETERMINATION OF MUF FOR A PATH LESS THAN 4000 KM	45	75. LUHF NOMOGRAM FOR SMALL VALUES OF <i>Kd</i> NOISE GRADE 2	95
33. CALCULATION OF MUF FOR PATH GREATER THAN 4000 KM	45	76. LUHF NOMOGRAM FOR SMALL VALUES OF <i>Kd</i> FOR OPEN OCEAN, NOISE GRADE 2½	96
34. REQUIRED FIELD INTENSITIES (PHONE), NOISE GRADE 1	48	77. LUHF NOMOGRAM FOR SMALL VALUES OF <i>Kd</i> NOISE GRADE 3	97
35. REQUIRED FIELD INTENSITIES (PHONE), NOISE GRADE 2	49	78. LUHF NOMOGRAM FOR SMALL VALUES OF <i>Kd</i> NOISE GRADE 3½	98
36. REQUIRED FIELD INTENSITIES (PHONE), NOISE GRADE 3	50	79. LUHF NOMOGRAM FOR SMALL VALUES OF <i>Kd</i> NOISE GRADE 4	99
37. REQUIRED FIELD INTENSITIES (PHONE), NOISE GRADE 4	51	80. LUHF NOMOGRAM FOR SMALL VALUES OF <i>Kd</i> NOISE GRADE 4½	100
38. REQUIRED FIELD INTENSITIES (PHONE), NOISE GRADE 5	52	81. LUHF NOMOGRAM FOR SMALL VALUES OF <i>Kd</i> NOISE GRADE 5	101
39. WORLD MAP INDICATING NOISE ZONES FOR THE PERIOD MAY THROUGH SEPTEMBER	53	82. LUHF NOMOGRAM FOR SMALL VALUES OF <i>Kd</i> FOR CONTINENTAL LAND AREAS, NOISE GRADE 2½	102
40. WORLD MAP INDICATING NOISE ZONES FOR THE PERIOD NOVEMBER THROUGH MARCH	54	83. LUHF NOMOGRAM FOR SMALL VALUES OF <i>Kd</i> NOISE GRADE 3	103
41. WORK SHEET FOR CALCULATION OF LUHF	56	84. LUHF NOMOGRAM FOR SMALL VALUES OF <i>Kd</i> NOISE GRADE 3½	104
		85. LUHF NOMOGRAM FOR SMALL VALUES OF <i>Kd</i> NOISE GRADE 4	105
		86. LUHF NOMOGRAM FOR SMALL VALUES OF <i>Kd</i> NOISE GRADE 4½	106
		87. LUHF NOMOGRAM FOR SMALL VALUES OF <i>Kd</i> NOISE GRADE 5	107
		88. AUXILIARY POWER INDEX	108
		89. GENERAL NOMOGRAM RELATING DISTANCE, POWER, AND FIELD INTENSITY FOR LARGE VALUES OF <i>Kd</i>	109
		90. GENERAL NOMOGRAM RELATING DISTANCE, POWER, AND FIELD INTENSITY FOR SMALL VALUES OF <i>Kd</i>	110
		91. EXAMPLE OF LUHF AND MUF CURVES PLOTTED	111
		92. WORK SHEET FOR CALCULATION OF LUHF FOR SHORT DISTANCES	111
		93. NOMOGRAM FOR COMPUTING (<i>Kd</i>) ₃₀₀₀	112
		94. SOLAR DISK WITH SUNSPOTS	113
		95. SUNSPOTS	113
		96. PROMINENCE	114
		97. SUNSPOT VARIATION WITH TIME	115
		98. CHANGES IN EARTH'S MAGNETISM AND CESSATION OF RADIO REFLECTIONS FROM IONOSPHERE ACCOMPANYING BRIGHT ERUPTION IN SOLAR CHROMOSPHERE	116

99. LIMITING GROUND WAVE FIELD INTENSITY (TWICE FREE SPACE FIELD)	121	136. NOMOGRAM FOR COMPUTING S	165
100. GROUND WAVE INTENSITY FOR SEA WATER	122	137. NOMOGRAM FOR COMPUTING C	166
101. GROUND WAVE INTENSITY FOR AVERAGE SOIL	123	138. NOMOGRAM FOR COMPUTING H	167
102. GROUND WAVE INTENSITY FOR POOR SOIL	124	139. NOMOGRAM FOR COMPUTING H	168
103. HEIGHT-GAIN FOR SEAWATER	125	140. NOMOGRAM FOR COMPUTING h_2	169
104. HEIGHT-GAIN FOR AVERAGE SOIL	126	141. NOMOGRAM FOR COMPUTING S WHEN $B \geq 4$	170
105. HEIGHT-GAIN FOR POOR SOIL	127	142. NOMOGRAM FOR COMPUTING C WHEN $B \geq 4$	171
106. POWER CORRECTION FACTOR	128	143. HEIGHT-GAIN NOMOGRAM	172
107. SHADOW LOSS NOMOGRAM	129	144. NOMOGRAM FOR COMPUTING X AND $17.588 X$	174
108. GEOMETRY OF THE CURVED EARTH	135	145. NOMOGRAM FOR CALCULATING Z	175
109. FIELD INTENSITIES IN FREE SPACE	137	146. OPTICAL REFRACTION	176
110. COVERAGE DIAGRAM	138	147. STANDARD PROPAGATION	177
111. COVERAGE DIAGRAM	139	148. SUPERREFRACTION	178
112. COVERAGE DIAGRAM	140	149. SHOOTING AT A MIRAGE	179
113. COVERAGE DIAGRAM	141	150. NONTRAPPING CONDITIONS	181
114. COVERAGE DIAGRAM	142	151. TRAPPING CONDITIONS	182
115. COVERAGE DIAGRAM	143	152. FLAT EARTH—CURVED RAYS	183
116. WORK SHEET FOR COVERAGE DIAGRAM CALCULATIONS	145	153. CURVED EARTH—STRAIGHT RAYS	183
117. WORK SHEET FOR COVERAGE DIAGRAM CALCULATIONS	146	154. PSEUDO-ADIABATIC DIAGRAM	184
118. WORK SHEET FOR COVERAGE DIAGRAM CALCULATIONS	147	155. EXPLANATION OF PSEUDO-ADIABATIC DIAGRAM	185
119. WORK SHEET FOR COVERAGE DIAGRAM CALCULATIONS	148	156. M NOMOGRAPHIC CHART	187
120. WORK SHEET FOR COVERAGE DIAGRAM CALCULATIONS	149	157. STANDARD ATMOSPHERE, TEMPERATURE ($^{\circ}F$)	188
121. WORK SHEET FOR COVERAGE DIAGRAM CALCULATIONS	150	158. MOISTURE DISTRIBUTION IN THE STANDARD ATMOSPHERE	188
122. COVERAGE DIAGRAM ON LINEAR HEIGHT SCALE	151	159. M CURVES FOR DRY AND MOIST ATMOSPHERES	189
123. COVERAGE DIAGRAM ON LINEAR HEIGHT SCALE	152	160. TRAPPING NOMOGRAM $f_{mc} = 75$	191
124. COVERAGE DIAGRAM ON CURVED-EARTH CHART	152	161. TRAPPING NOMOGRAM $f_{mc} = 100$	192
125. COVERAGE DIAGRAM ON CURVED-EARTH CHART	153	162. TRAPPING NOMOGRAM $f_{mc} = 200$	193
126. WORK SHEET FOR COVERAGE DIAGRAM CALCULATIONS	154	163. TRAPPING NOMOGRAM $f_{mc} = 600$	194
127. NOMOGRAM FOR COMPUTING Y	156	164. TRAPPING NOMOGRAM $f_{mc} = 700$	195
128. NOMOGRAM FOR COMPUTING B	157	165. TRAPPING NOMOGRAM $f_{mc} = 3000$	196
129. NOMOGRAM FOR COMPUTING α	158	166. PROCESS OF SUBSIDENCE	198
130. NOMOGRAM FOR COMPUTING α	159	167. AEROLOGICAL SOUNDINGS BEFORE AND AFTER SUBSIDENCE CROSS-SECTION AA OF FIGURE 166	199
131. NOMOGRAM FOR COMPUTING α	160	168. PPI SCOPES	206
132. NOMOGRAM FOR COMPUTING α	161	169. PPI SCOPES	207
133. NOMOGRAM FOR COMPUTING α	162	170. PPI SCOPES	208
134. NOMOGRAM FOR COMPUTING S	163	171. PPI RECORDS SHOWING EXTENDED RANGES	208
135. NOMOGRAM FOR COMPUTING S	164		

ELEMENTARY MANUAL
OF
RADIO PROPAGATION

• CHAPTER ONE •

WHAT HAPPENS TO A RADIO WAVE?

ALL SIGNALING BY MEANS OF RADIO OCCURS AS THE result of waves that travel from a transmitter to a receiver. These waves, which are electromagnetic in character, arise from the presence of rapidly alternating currents in the antenna of the transmitter. Oscillating vacuum tubes within the transmitter are responsible for this alternating current. From the antenna, the electromagnetic waves spread out in all directions with the velocity of light. The distant receiving antenna intercepts only a small fraction of the wave energy that is radiated by the antenna of the transmitter. The receiving set amplifies these minute electrical impulses and converts them into signals that can be audibly detected or otherwise recorded.

We shall dispose of the radio set itself in these few words, because this manual has little concern for the details of the transmitter and receiver. We shall want to know only the power output of the former and assume that the latter is a communications equipment of high sensitivity. The limit of its receptive power should depend on the external static level or upon the inevitable noise level of a perfect receiver.

Our problem begins when the waves leave the transmitter antenna and ceases when they enter the receiver antenna. In other words, we seek to know what happens to the radio wave in its path through space, where it ordinarily moves with the speed of light, 186,000 miles per second.

A young friend of ours, when asked how radio transmission was possible, answered that the radio waves left a tower way up high and went straight to a receiver. When shown how waves traveling in this fashion would soon leave the curved earth's surface and travel straight on out into space, he remembered "that some waves hit 'the sky' and came back down again." "What part of the sky?" was the next question. "Um, the clouds, I guess." "How about communication on a clear day?" No answer.

Well, our young friend was partly right. The waves do hit clouds high up in the sky, but not the puffy white clouds of summer or the dark snow clouds of winter. These clouds are far higher, invisible ones of electricity,

which we shall discuss in detail later on.

Two types of waves travel from the transmitter to the receiver. First, we shall consider the so-called *sky wave*, which travels through the atmosphere. Second, there is a *ground wave*, which skirts along the curved surface of the earth. The distance of ground-wave travel is limited and, therefore, it is seldom of importance for communication over distances of more than a few hundred miles. We rely on the sky wave for long-range communication.

When the receiving station lies far from the transmitter, well around the curve of the earth, transmission would be impossible were it not for the presence of several layers of electricity high above the surface of the earth, at altitudes of from 60 to 250 miles (the "clouds" of our young friend). These layers act as "mirrors," reflecting back to earth the waves that otherwise would be lost in interplanetary space. This upper region of the atmosphere consists of electrically charged particles originally emitted by the sun, and molecules and atoms whose electrons have been torn from them as the result of ultraviolet radiation. Charged particles are commonly referred to as *ions*; hence, the reflecting layers are usually referred to as the *ionosphere*. Since electrification is controlled by the sun, the state of the upper atmosphere is always changing as the sun rises and sets.

The ground wave is bent to follow the earth's curvature. The conductivity of the earth's surface (land or sea) and the frequency of the signal (as well as the power employed) determine the effective range of the ground wave. The longer waves (lower frequencies) penetrate more readily the shadow cast by the earth's horizon. Thus, higher frequencies display shorter ranges than the lower frequencies. Unlike the extremely variable reflective properties of the ionosphere, which change from hour to hour, day to day, and year to year, properties affecting the ground wave, for a given location, are practically constant with the time.

Although we have very loosely referred to the ionosphere as a sort of mirror, we might more appropriately have compared it to a sieve. Whether a ball will or will not pass through the mesh of a sieve depends upon the

sizes of the ball and of the mesh openings, as well as upon the angle at which the ball strikes the surface. In this analogy, the radio waves behave much like balls. High-frequency radiations, or short waves, correspond to small balls; low-frequency oscillations, or long waves, correspond to large balls.

The ionospheric sieve enclosing the spherical earth is, as has already been indicated, not uniform. Over that portion of the earth where the sun's rays strike nearly vertically, the sieve openings are small. This charac-

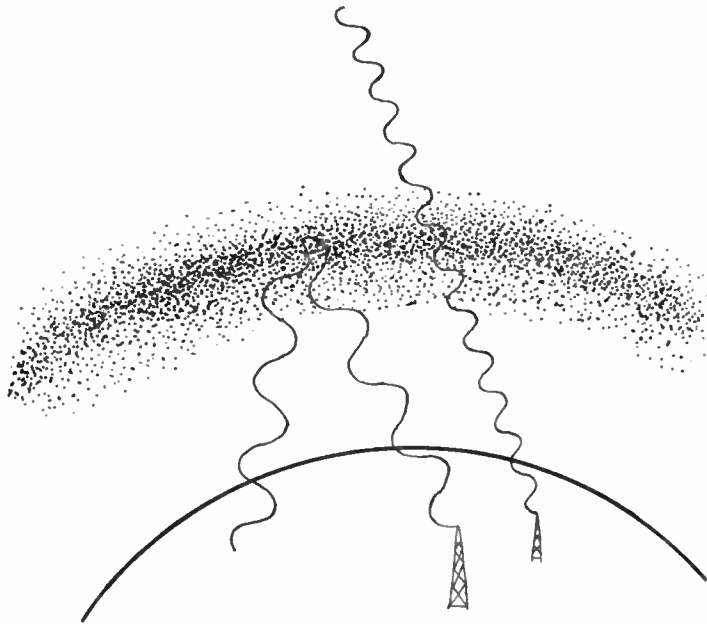


Fig. 1(a). *Escape of High-Frequency Waves.*

teristic arises from the fact that here the solar radiation produces the greatest electrification. In all directions from this point beneath the sun, the size of the mesh openings tends to increase. Some exceptions to this rule will be pointed out later, but this statement is roughly correct. On the night side of the earth, where no sunlight is falling to produce ions and electrons, the mesh is wide indeed.

It should now be obvious, on the basis of the analogy, that if a station operator happens to choose too small a ball (too high a frequency) the ball will penetrate the mesh and will not be sent back toward the earth. (See Fig. 1.) Such a frequency is clearly useless for transmission. For this reason, if we are to be sure that our signal will be received at a distant station, we must make a careful study of the effective "mesh" of the ionosphere all along the path so as to make certain that the energy is always reflected. The balls must be large enough—that is, the frequencies must be low enough—to insure that nowhere will they be able to escape.

It follows from the above discussions that, for a transmitting station in any location, there always exists some

frequency so high that it will pass directly through the ionosphere. A mesh far larger than a ball will, nevertheless, act as a reflector if the ball happens to strike it glancingly. Everything else being equal, then, if we wish to send a radio signal from Washington to San Francisco, we can employ a higher frequency (smaller ball) than we can over the shorter path from Washington to New York. On the longer path, the rays will strike the ionosphere at a much more glancing angle than on the shorter path. Thus, the upper limit of usable fre-

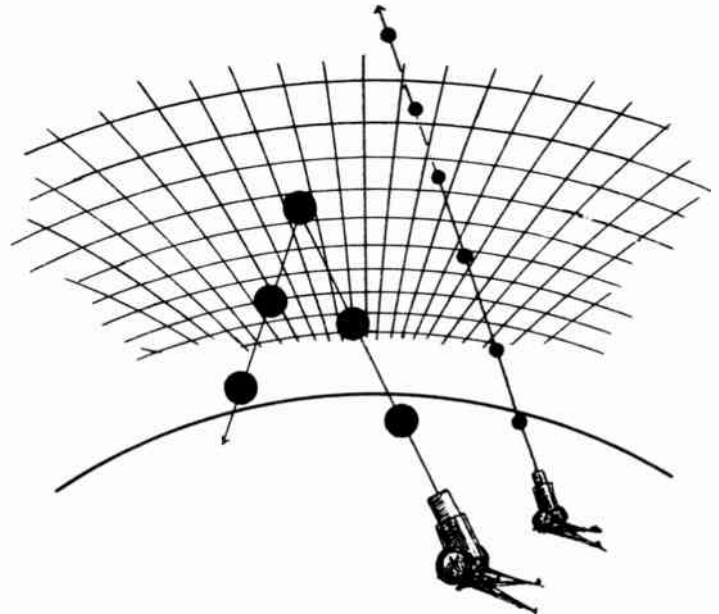


Fig. 1(b). *Analogy.*

quency depends upon the distance between the transmitting and receiving stations, as well as upon the ionospheric mesh. The height of the reflecting layer, which controls the angle at which the wave strikes the mesh, is also a determining factor.

If the frequency adopted is high enough to permit escape of vertical rays, but still low enough to allow reflection at some oblique angle, the situation is such as is illustrated in Fig. 2. Balls of the same size (corresponding to a transmitter radiating constant frequency) are being shot upward in all directions. Those that are nearly vertical pass through the mesh; those that strike the ionospheric sieve at greater angles are reflected.

The boundary between reflection and nonreflection is fairly sharp. Thus, out to some distance from the transmitter, except for areas immediately surrounding the antenna where direct and ground waves give reception, there will be a zone of silence (shaded in our illustration Fig. 2). We may say that the wave *skips* over this intermediate region. The distance from the transmitter to the edge of the skip zone is called the *skip distance*. Most radio operators are familiar with the effect. Thus,

around nightfall, as the ionospheric mesh widens, letting waves through which were previously reflected, we may lose communication with a station and yet be able to hear more distant ones on the same frequency. Radio operators refer to the phenomenon as a "station going into skip."

An additional complication of radio propagation arises from the fact that the wave loses its intensity as it travels over long paths. Part of this loss comes from the simple spreading of the beam. A distant light always appears fainter than a nearby one of the same wattage. In addition

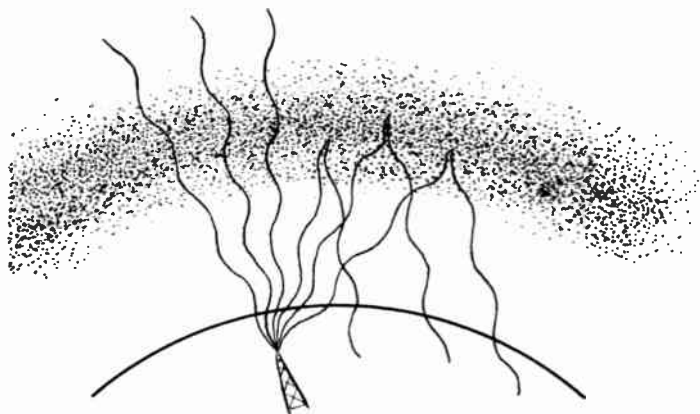


Fig. 2(a). Reflection of Waves.

to this effect, however, there is an actual absorption of the radio beam, a diminution of intensity resulting from the presence of ions and electrons in regions just below the ionosphere. The radio waves are "dimmed" in much the same way that light waves are dimmed in the presence of fog or clouds of dust.

The absorption is greatest when the beam travels over atmospheric areas close to the point where the sun shines vertically, for the sun causes the electrification of the lower absorbing layer in much the same way that it produces the electrification of the higher reflecting ionospheric layer. The absorption at night is practically zero. We can represent this absorption roughly by the presence of additional meshes through which the waves (balls) must pass in order to reach the ionosphere. The network of the absorbing layers, however, is loosely strung and traps the balls that become entangled, whereas the ionospheric mesh, if sufficiently small, lets the waves bounce off, like balls from the face of a tennis racket.

In addition to the maximum at the subsolar point, the absorption also increases in the neighborhood of the

earth's two magnetic poles, which deflect the electrical charges shot earthward from the sun and concentrate them in these regions where they act to absorb the radio signal. The high concentration of electrified particles in these polar regions causes the earth's upper atmosphere to glow, producing the phenomenon of aurorae.

The lower frequencies (the larger balls) find penetration of the absorbing layer more difficult than do the higher frequencies. Thus, of two sets of radio waves, originally equally intense, and traveling similar distances, the one with lower frequency will be weakened

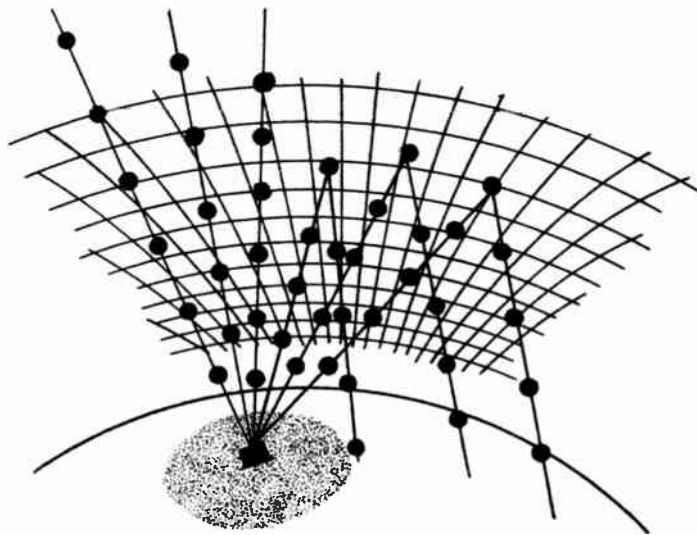


Fig. 2(b). Analogy.

more than the one of higher frequency. It may, in fact, be so completely absorbed that the signal will be far too weak for the receiver to pick up.

At some time or other, most of us have skipped stones on a pond. We select a small flat stone and see how many times we can make it bounce across the surface of the water. A big round rock will sink out of sight, whereas the correctly shaped pebble will dance right along. This absorbing effect in the ionosphere is much the same. The absorbing layer (the water) will catch the low frequency (big rock), whereas the higher frequency (little pebble) will bounce off.

As a consequence of absorption, we are forced to use higher frequencies which will not be completely "blacked out" by radio noise. As a consequence of the sieve and the size of its meshes, we are forced to use lower frequencies. Between the two limits of the lowest useful high frequency (LUHF) governed by the absorption and the maximum usable frequency (MUF) determined by the ionospheric mesh, we find a band of frequencies useful for signaling purposes. If the MUF should happen to be lower than the LUHF, the operator is out of luck.

No transmission is possible under these circumstances unless the absorption in the night hemisphere of the earth is low enough to allow the signal to be transmitted around the world over the longer path.

The electrical noise, either of the receiver or of the atmosphere, also sets a limit to the receivable signal. The stray radio waves arriving from distant lightning flashes produce an electrical noise that may completely overpower any faint trace that remains of the original

signal. Atmospheric conditions are widely variable both with time and over the surface of the earth. Our knowledge of the distribution of the limiting noise level is fragmentary at this time, and further revisions will certainly be necessary.

But with the knowledge we have, we can calculate our LUF and MUF, construct our road map, and, between these two limiting curves, choose the correct route numbers, our optimum or usable frequencies.

• CHAPTER TWO •

THE USE OF MAPS AND CHARTS IN RADIO PROPAGATION PROBLEMS

IN VIEW OF THE FACT THAT THE IONOSPHERE VARIES IN its propagation characteristics from time to time at a given place or from place to place at a given time, the investigator finds it necessary to employ maps and charts in his studies. The only perfect map from the standpoint of absolute accuracy in all details is one made on the surface of a sphere. Spheres, however, are bulky, unwieldy to use, and altogether impractical when a large number of charts have to be published. For these reasons, one must resort to the use of flat maps, with their inevitable distortions.

The number of possible types of maps is infinite, but a certain few have special characteristics for different types of problems. In this book, we use several maps with different "faces," although they are basically the same type. For various reasons, such as finding the location of transmitting or receiving stations, the operator may have occasion to meet many different kinds of map projections. In order that the possible difference in projection between his reference map and those employed here may not confuse him or lead him to question the authenticity of either, we shall explain the special characteristics of a few types that he may encounter.

The reference lines on any map are, of course, the latitude and longitude lines. Latitude is measured in angular units north or south of the equator. For the purpose of the present work, one can ignore the difference between astronomic and geocentric latitude, which arises from the fact that our earth is not a perfect sphere. Longitude is measured east or west from the zero meridian passing through the Observatory at Greenwich, England.

Longitudinal meridians and the equator are two specific examples of *great circles* drawn upon the surface of the earth. The center of all great circles is the center of the globe. A great circle divides the earth exactly in half. Small circles, such as parallels of latitude, do not lie in planes that pass through the center of the earth.

It is important to our study to realize the significance of great-circle paths because the shortest distance between two points on the sphere is that measured along a great

circle, and radio waves tend to follow this path. In some map projections, great circles become curves resembling neither arcs nor straight lines. We shall learn later how to measure distance between two points along such great-circle paths.

A great circle drawn from one station through a second is often called the *bearing*, although, in the strictest sense, the bearing is the angle between that great circle and the meridian running to the north. Bearings range from 0° to 360° and are measured from the north in a clockwise sense—that is, from north toward the east. Thus, a station lying due NE would have a bearing of 45° , and one lying NW would have a bearing of 315° .

The difficulties of presenting a sphere on a flat map are comparable to those encountered in trying to flatten out the skin of a peeled orange. We can readily see how impossible it is to wrap a flat sheet of paper around a globe and then to trace the map upon this sheet of paper. The flat paper will fold, warp, crinkle, or tear as we try to fashion it into a curved surface. Suppose we stretch a sheet of transparent rubber to fit the globe smoothly and trace the map upon its surface. When we remove the sheet of rubber from the sphere and allow it to relax into its natural shape, the distortions that would appear show to a certain extent what happens when we try to represent a sphere on a plane surface.

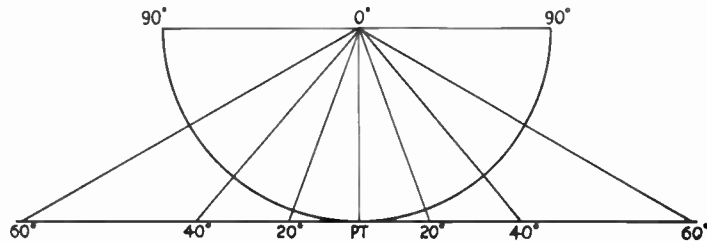
An ideal map would have these main properties:

- (1) It should represent the countries, continents, oceans, and so forth in their true shape and true relative size.
- (2) Great circles (the shortest distance between two points on the sphere) should go into straight lines (the shortest distance between two points on a plane).
- (3) It should be easy to read the latitude and longitude coordinates of any place on the map, or, conversely, given the latitude and longitude, to plot the position.
- (4) The distance of every place to every other place on the map should bear a constant ratio to the corresponding distance on the earth.
- (5) The map should represent as much of the earth as

possible without being of too awkward a size.

Unfortunately, no single flat map can possess all these characteristics. Various projections have been devised, however, which have some of these traits to the exclusion of others.

Two primary classifications of map projections exist—those involving polar coordinates and those involving cylindrical coordinates. There are, of course, a large number of specialized projections that do not fall into these classifications, but these do not have the properties of symmetry possessed by the primary groups and are

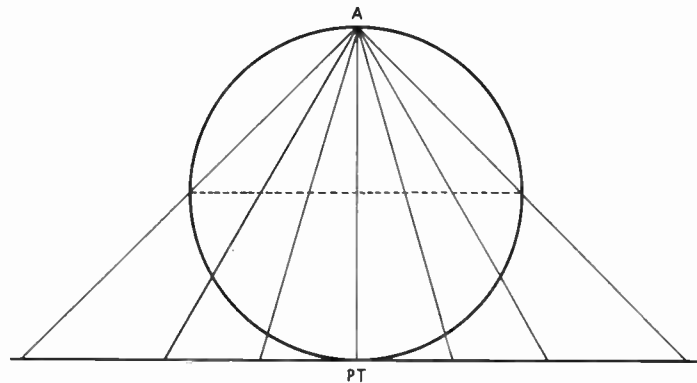


GNOMONIC PROJECTION

usually developed for very special problems.

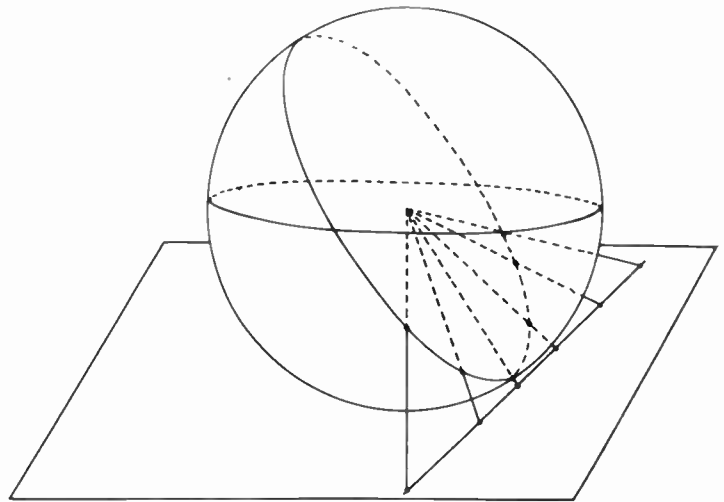
Polar or azimuthal projections are usually made upon a plane tangent to the sphere at some one point. Bearings from this point are laid off uniformly around the map. If the North or South Pole is the center, then the angle is simply equal to the longitude. Several types of projections fall into this group:

The *gnomonic projection* has the advantage that great circles go into straight lines. This projection is made upon a plane tangent to the sphere at some point, with the projecting lines drawn from the center of the sphere. Around the point of tangency, the map is a fairly true representation, but as the distance from this point increases, the map becomes more and more stretched out. It is impossible to represent even a whole hemisphere on this projection, because the 90° line would never cross the plane. To project angles close to 90° would require a map of tremendous size. We may choose different points



STEREOGRAPHIC PROJECTION

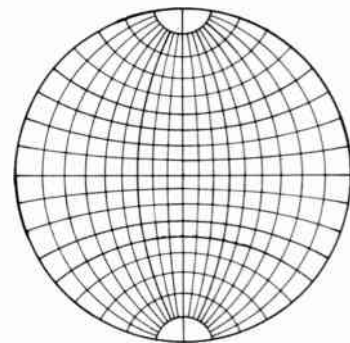
of tangency, and thereby represent the whole sphere by several maps. The gnomonic projection is particularly useful for plotting bearings because of its property that great circles go into straight lines. But the angles of the

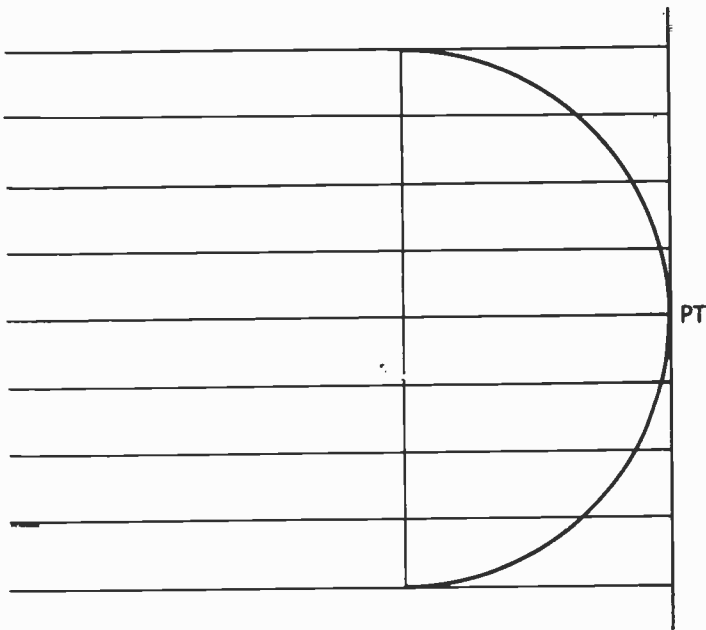


bearings are distorted except for those from the point of tangency.

The *stereographic projection* has less distortion than the gnomonic projection. Here, the point of projection is a point on the sphere diametrically opposite the point of tangency. *A* represents the antipodal point from *PT*, the point of tangency. All circles, great or small, go into circles or straight lines. This projection can be used to represent considerably more than one hemisphere, but the entire earth cannot be pictured simultaneously. The distortions increase the nearer one approaches point *A*.

The *orthographic projection* may be compared to a photograph of the moon. The point of projection is at infinity. Its distortions are of the opposite type from projections discussed previously. Whereas the space between equal degrees of latitude on the foregoing maps increases with distance from the point of tangency, in this projection, the space between, say, 80° and 90° , is less than that





ORTHOGRAPHIC PROJECTION

between 70° and 80° , and so forth. Because of the "squashed-in" effect along the outer edges, this type of projection is rarely used for maps. Circles go into ellipses or circles.

The *azimuthal equidistant projection*, like all polar projections, conserves bearings from the point of tangency, and gives correctly the distances from that point to any other point on the surface. Thus, if the North Pole is the tangent point, the various parallels of latitude form equally spaced circles. The representation of a single hemisphere is particularly good on this form of map, and the projection is favored by many cartographers. One can fit the entire world into such a projection. The South Pole, however, is not a point, but a circle bordering the picture.

The *azimuthal equal-area projection* is often used when the relative areas, but not necessarily the shapes of the areas, are important. The map resembles the one previously described, except that successive parallels of latitude are spaced closer together.

Maps involving *cylindrical projections* have been designed for certain desirable features. An easy way to visualize this projection is to imagine a sheet of paper wrapped around the sphere at the equator.

A *cylindrical equal-area projection* unrolls with equally spaced longitude lines, but the latitude lines appear closer together as they approach the poles, to allow for the greater stretching that has taken place as the distance from the equator increases.

To avoid this violent distortion in the polar regions we may modify this projection—make the latitude parallels equally spaced—but in so doing we lose the equal-area

property of the preceding projection. This new projection thus obtained is called the *cylindrical equal-distance projection*.

The *Mercator projection* is the most familiar type of cylindrical projection. As can be seen, this representation undergoes a noticeably great enlargement from 40° to 80° . The distortion near the equator is less. It is not extended beyond 80° because of this exaggeration, and the poles lie at infinity. It is from maps of this sort in geography books that some people get the misconception that Greenland is larger than South America. Actually, Greenland is smaller than Ecuador.

Maps are not limited to the location of cities or coast lines, but may be employed for many purposes. For example, we shall find that one of the most important uses of maps is the determination of great circles between two points. It should be noted that only on the gnomonic projection are great circles represented as straight lines; on all other projections, the great circles go into curves. The student will be familiar with the use of maps to report altitudes, with the aid of contour lines. Such contour lines are often drawn on weather charts to indicate barometric pressure, or lines of equal temperature. Similarly, the ionospherist employs contour lines on maps of the world to show conditions of the ionosphere.

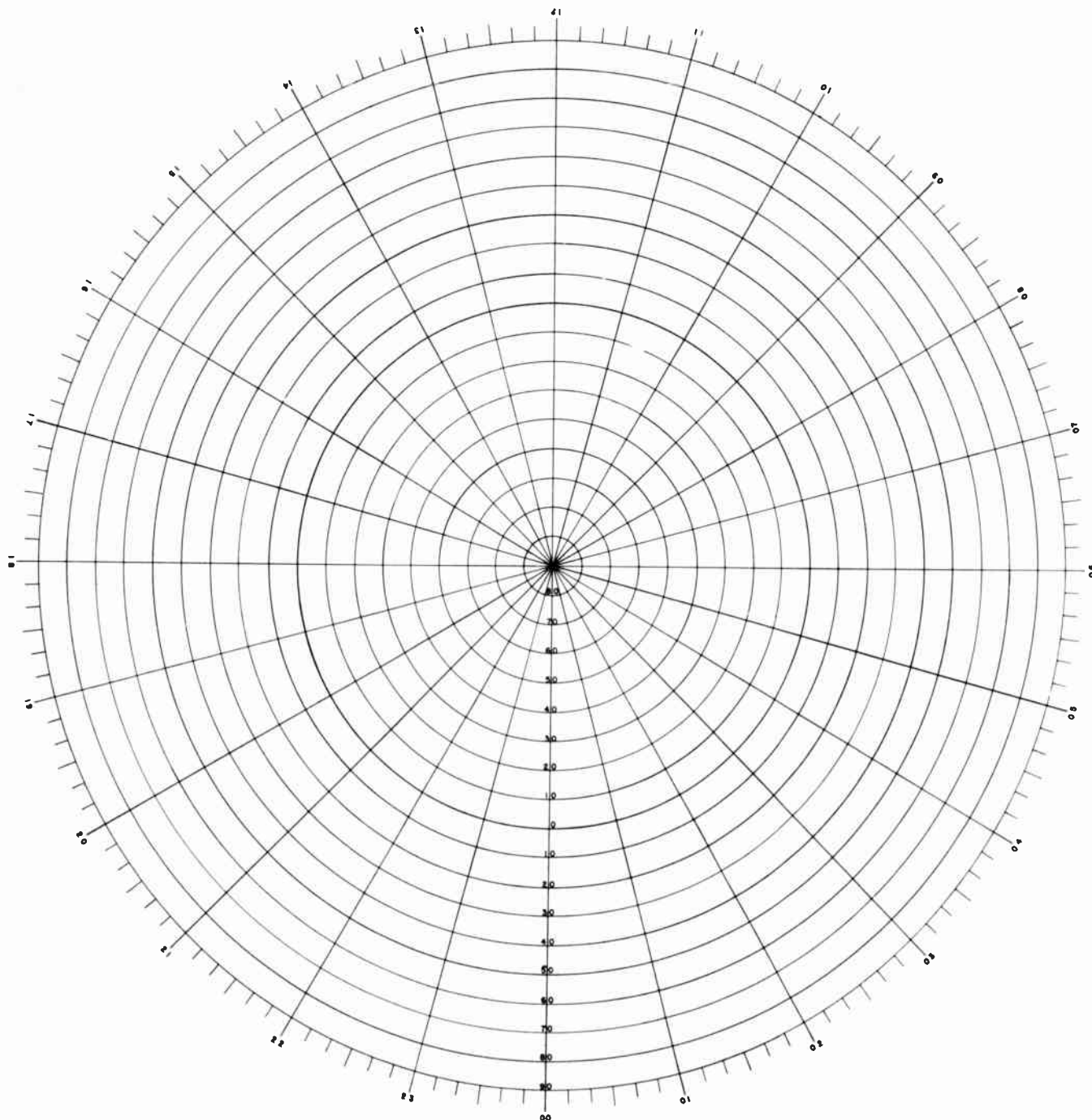
The most convenient type of map for ionospheric studies, and the type we have adopted in this book, is a modified simple cylindrical projection (Fig. 24). Note that the longitude divisions are equal and the latitude divisions are equal, but they are not equal to each other. The longitude divisions are smaller in order to make the map a convenient page size. Great circles will be curves on this projection. A method for drawing these curves is explained later.

Closely associated with consideration of map-making is the calculation of *time*. The calculations appearing in this book are carried out with respect to Greenwich Civil Time, (abbreviated hereafter as GCT). GCT is, of course, the local time at the 0° longitude meridian at Greenwich, England, to which we have referred previously.

GCT runs from 0 to 24 hours, from midnight to midnight. Roughly, we may say that GCT represents the number of hours that has elapsed since the sun was directly *below* the meridian of Greenwich. Since the earth turns 360° in 24 hours, we have these relationships.

$$\begin{aligned} 360^\circ &= 24 \text{ hours} \\ 15^\circ &= 1 \text{ hour} \\ 1^\circ &= 4 \text{ minutes of time} \\ 1' &= 4 \text{ seconds of time} \end{aligned}$$

Standard meridians are marked off at 15° (or one-

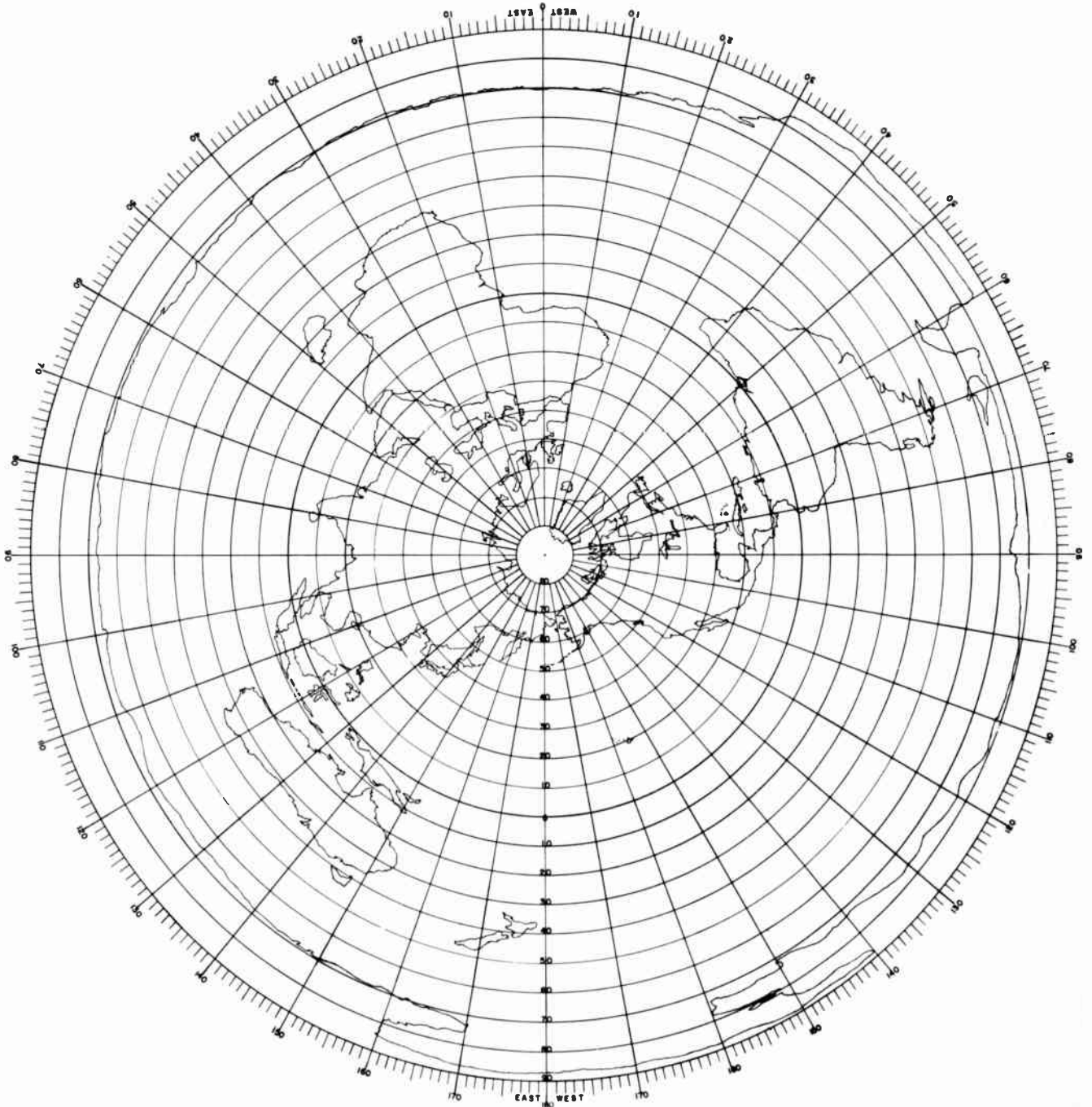


AZIMUTHAL EQUIDISTANT PROJECTION

hour) intervals from the meridian at Greenwich, east or west. The United States has four time divisions. The time in each division is the local civil time of the Standard Meridian nearly central. Thus, the area included in the division for Eastern Standard Time is determined by the 75° meridian line and is 75°/15°, or 5 hours, different from Greenwich. When the sun is directly overhead at Greenwich and England is eating lunch, it is just before sunrise in California—4:00 a.m., eight hours before Greenwich. In the Union of Soviet Socialist Republics, on the other hand, the sun has already passed overhead.

Hence, for Greenwich noon, their clocks register some time in late afternoon or early evening.

The system of standard-time zones is merely a useful fiction. In the strictest sense, each meridian has its own local civil time. A person sitting in a chair 10 feet to the east of you would have a time $\frac{1}{100}$ second later. This amount may seem small, but it adds up to almost five seconds per mile. Think of the confusion that would result if trains and airlines had to operate on local rather than standard time. On a train moving east, one would have to set his watch continuously ahead in order to have



MAP OF THE EARTH ON THE AZIMUTHAL PROJECTION

the correct time. How much simpler it is to save up the seconds and minutes, and then move the watch ahead or back in jumps of a full hour!

But the ionosphere does not operate on standard time. The electrification of the reflecting layers moves with the sun, and one should use local civil time (LCT) for exactness in determination of ionospheric records. GCT is the local civil time for all stations on the meridian of Greenwich.

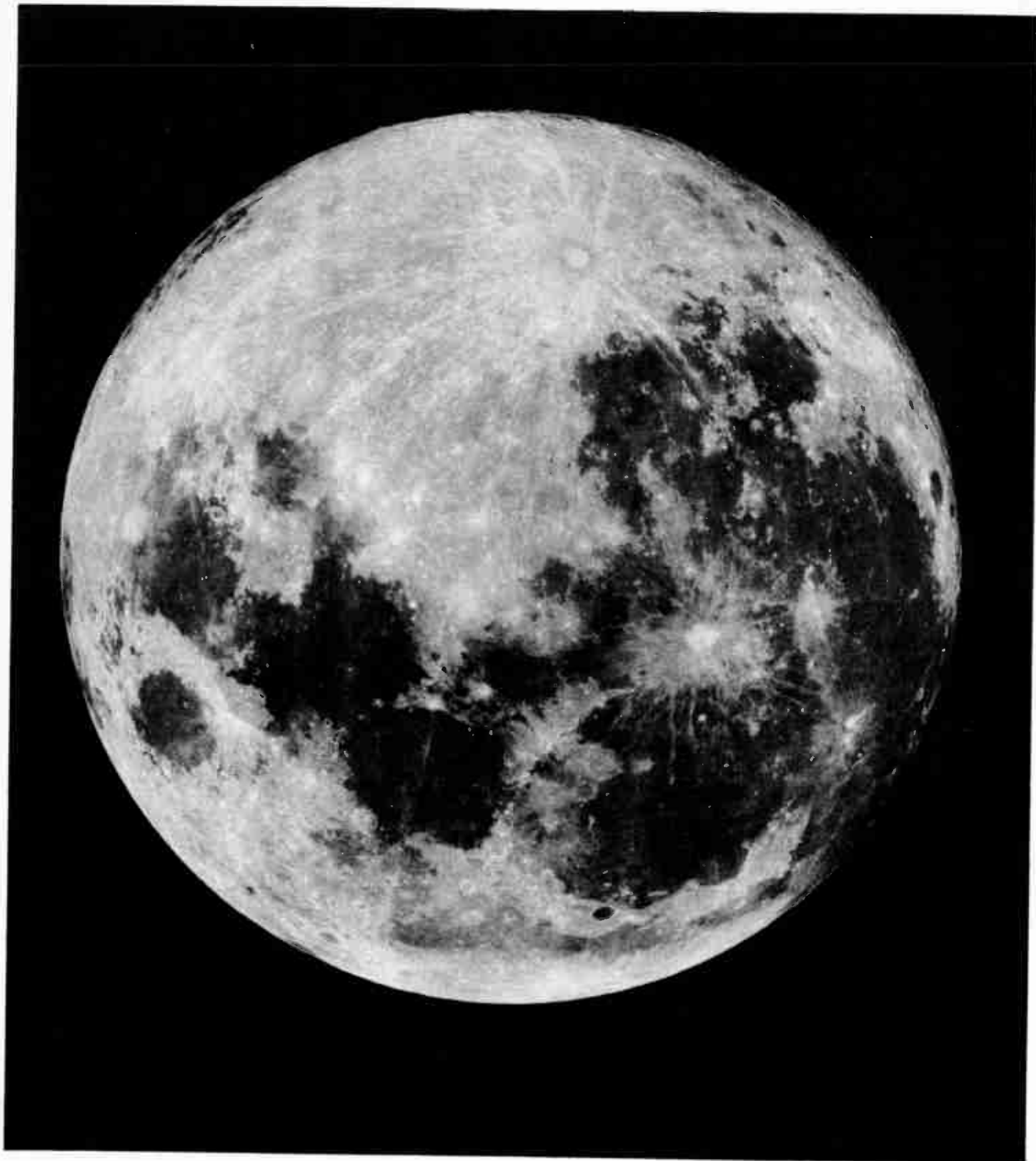
$$LCT = GCT \pm \text{longitude}/15.$$

Use the + sign for East longitude and the - sign for West longitude. Or inversely,

$$GCT = LCT \pm \text{longitude}/15.$$

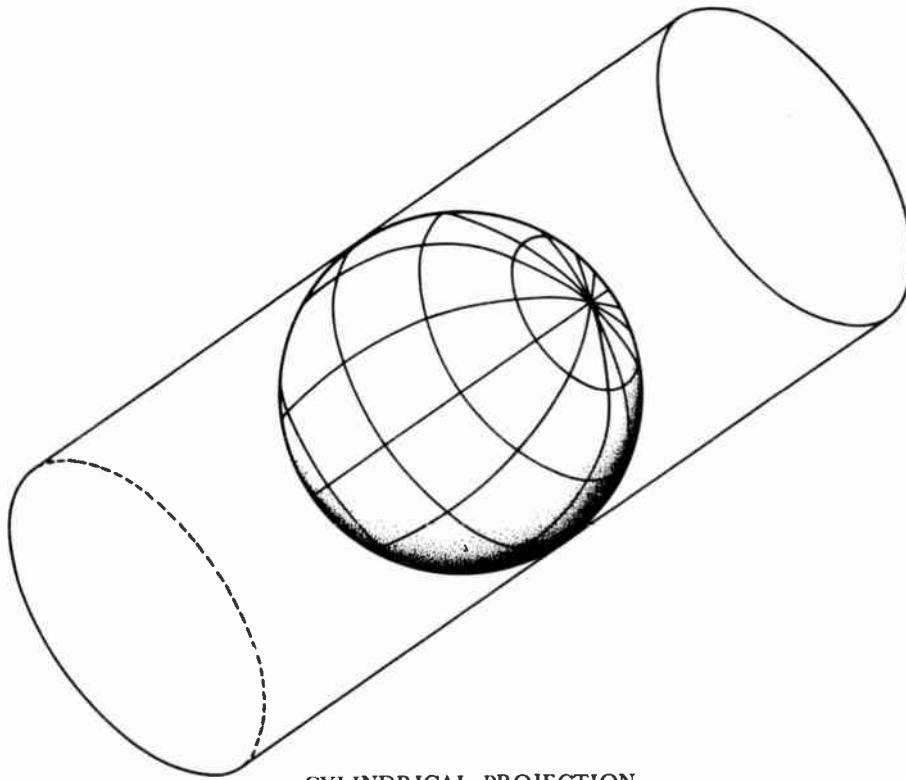
Use the + sign for West longitude and the - sign for East longitude.

The above equations will enable the operator to convert his calculations made in GCT to his own civil time, if he so desires. He might add an extra column to the left of the GCT column in the worksheets and record his own time. Or, if he is making the calculations for a cer-



Courtesy Lick Observatory, University of California

ORTHOGRAPHIC PROJECTION. PHOTOGRAPH OF THE FULL MOON



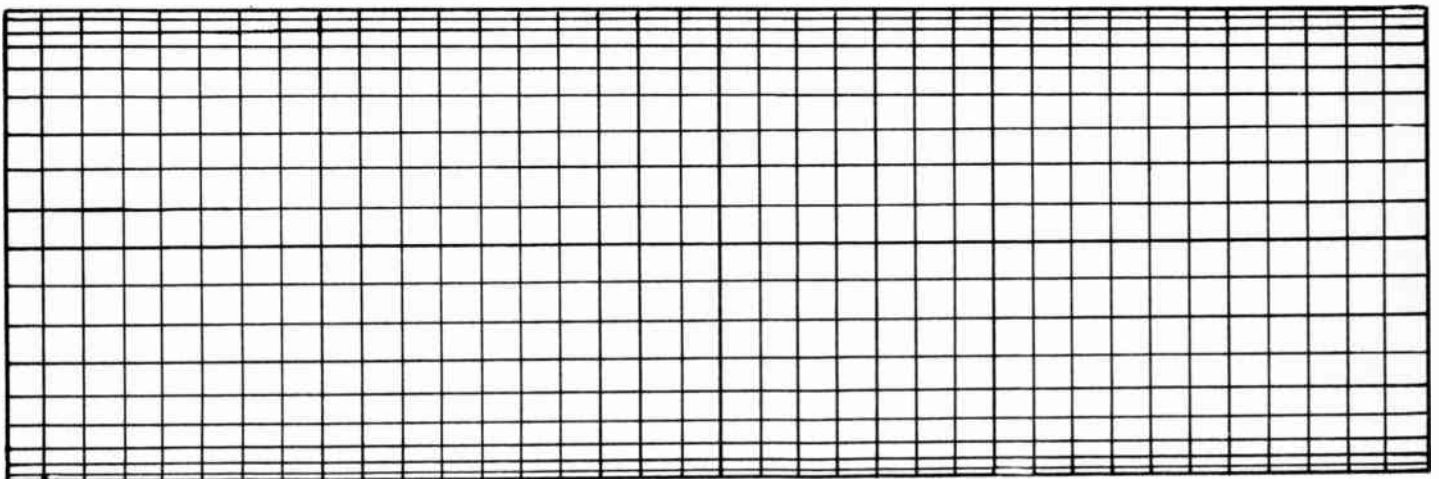
CYLINDRICAL PROJECTION

tain hour of his civil time, he may use the second equation to find out what GCT he should use in following through the method of calculation outlined in this handbook.

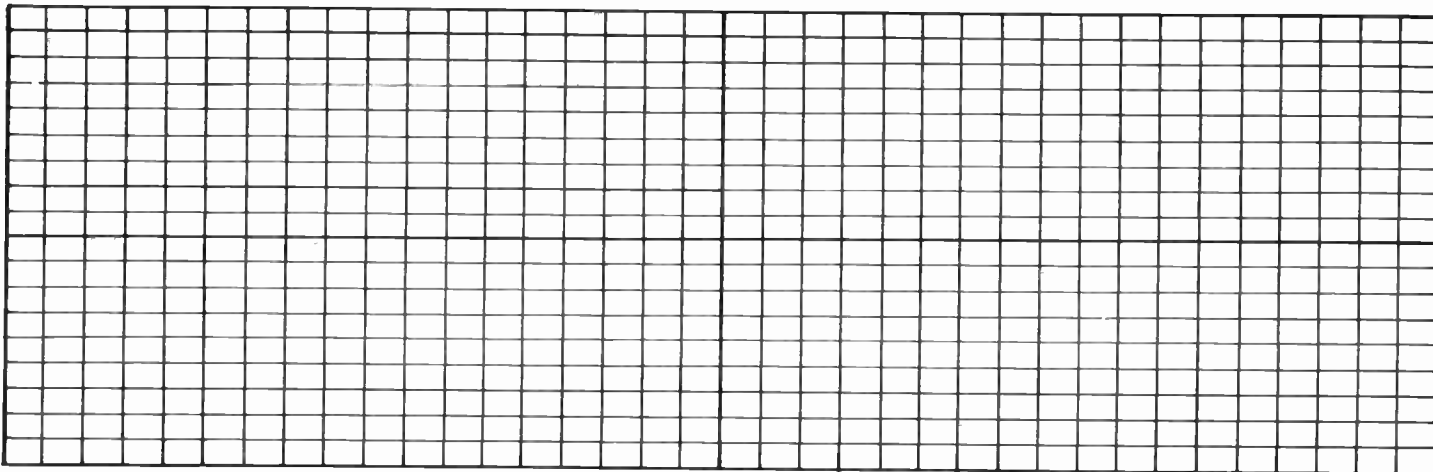
The reader may have gained the impression that local civil time is the same as sun time—that is, the time indicated by the apparent position of the sun or read from a sun dial. Actually, the two are not quite equivalent, although the discrepancy does not exceed 16 minutes. The source of the difference between the two kinds of time is as follows. Civil time, whether local or standard,

must progress at a uniform rate throughout the year. The sun, however, does not move uniformly across the sky. Its path takes it south of the equator in the winter and north in the summer. In addition, the earth swings about the sun in an ellipse rather than in a circle. Its rate of motion, not a constant, also affects the apparent motion of the sun. The difference between local civil time and apparent solar time is called the *equation of time*, ET. Thus,

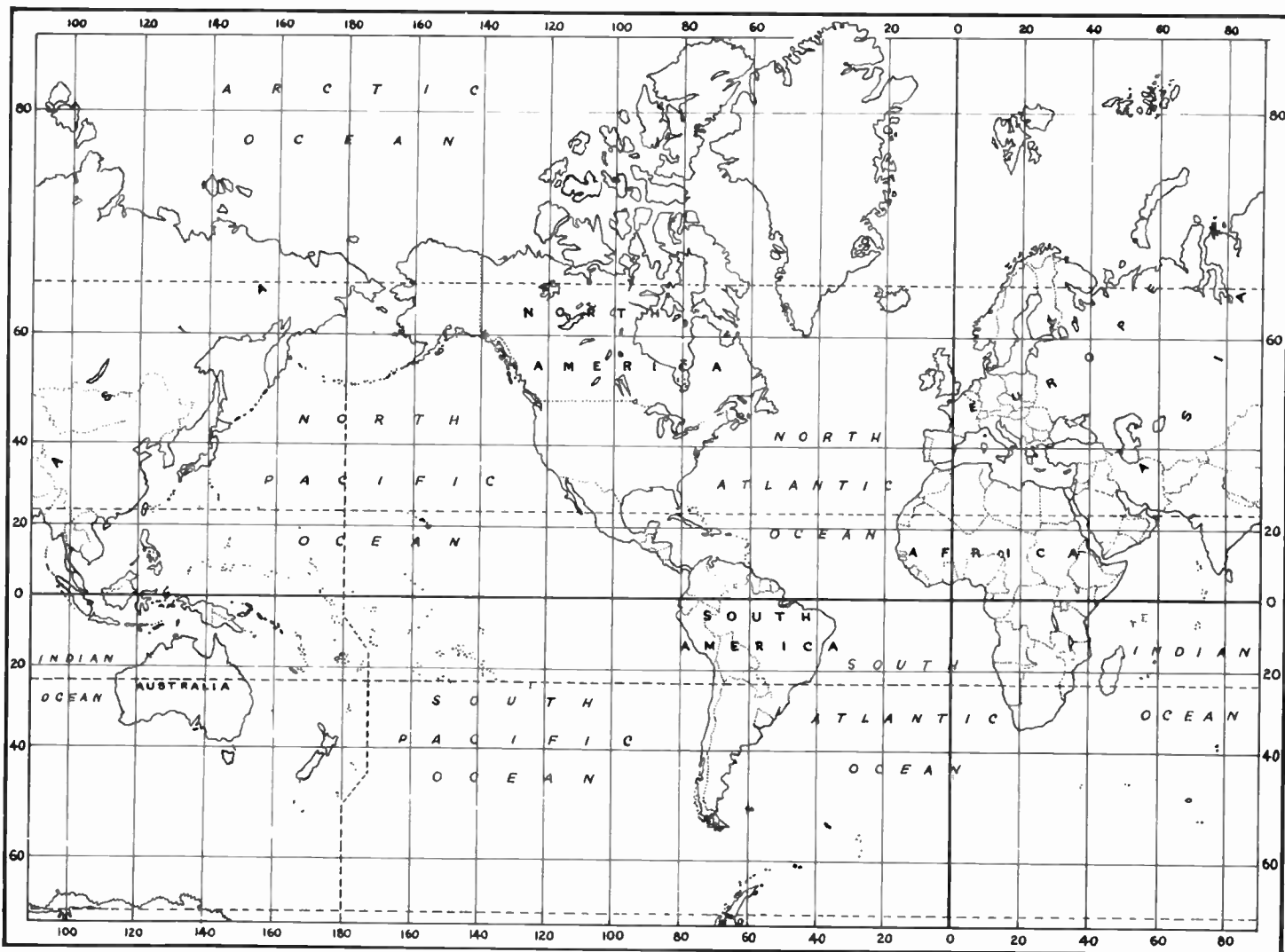
$$\begin{aligned} \text{LCT} &= \text{AST} + \text{ET} \\ \text{AST} &= \text{LCT} - \text{ET} \end{aligned}$$



CYLINDRICAL EQUAL-AREA PROJECTION



CYLINDRICAL EQUIDISTANT PROJECTION



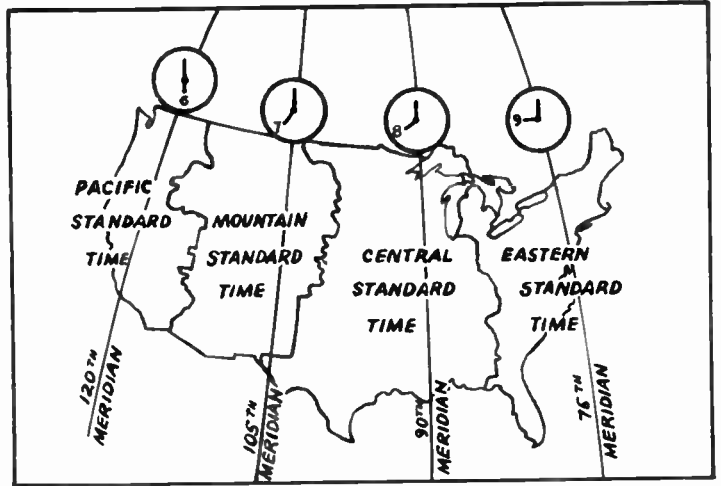
MERCATOR PROJECTION

The values of ET are tabulated for the 1st and 15th of various months.

Date	ET	Date	ET
Jan. 1	- 3 min	Jan. 15	- 9 min
Feb. 1	-14 min	Feb. 15	-14 min
Mar. 1	-13 min	Mar. 15	- 9 min
Apr. 1	- 4 min	Apr. 15	0 min
May 1	+ 3 min	May 15	+ 4 min
June 1	+ 2 min	June 15	0 min
July 1	- 3 min	July 15	- 6 min
Aug. 1	- 6 min	Aug. 15	- 5 min
Sept. 1	0 min	Sept. 15	+ 4 min
Oct. 1	+10 min	Oct. 15	+14 min
Nov. 1	+16 min	Nov. 15	+16 min
Dec. 1	+11 min	Dec. 15	+ 5 min

We employ *nomograms* as well as maps in our calculations. Nomograms are extremely useful for solving many types of problems. We could write a mathematical formula for solving problems, such as the relationship between the latitude of two places, and the difference of longitude and the required distance. The equation is involved, however, and its use requires some mathematical ability. With the nomogram, anyone can get the result quickly and simply. A nomogram is usually a chart with three (or more) scales. Locate two points on different lines and connect them with a straight line. The required answer appears at the intersection of this connecting line with some other line on the chart. This explanation may sound somewhat involved, but the procedure is simple in actual practice.

In this book, we shall employ the kilometer, rather than the mile or nautical mile, as the standard of distance for parts of the analysis. The calculations are often simpler and more direct in the metric system. To reduce kilometers to nautical miles, multiply by 0.540. To reduce kilometers to statute miles, multiply by 0.621. The circumference of the earth is almost exactly 40,000 kilometers, or 10,000 kilometers to a quadrant.



TIME ZONES OF THE UNITED STATES

• CHAPTER THREE •

STRUCTURE OF THE IONOSPHERE AND WORLD MUF MAPS

WHEN WE PLAN A TRIP, WE NATURALLY TAKE INTO account the geography of the route, whether we have oceans to sail over, mountains to climb, deserts to cross. In sending our radio wave on its travels, we should know something about the geography or, more accurately, the *aerology*, of the route it will follow.

at heights of from 60 to 250 miles above the surface of the earth, considered the possibility that still other lower layers might be discovered at a later date. Therefore, they reserved some letters ahead of *E* in the alphabet—just in case. Indeed, the lower fringes of the *E* layer are often referred to as the *D* layer.

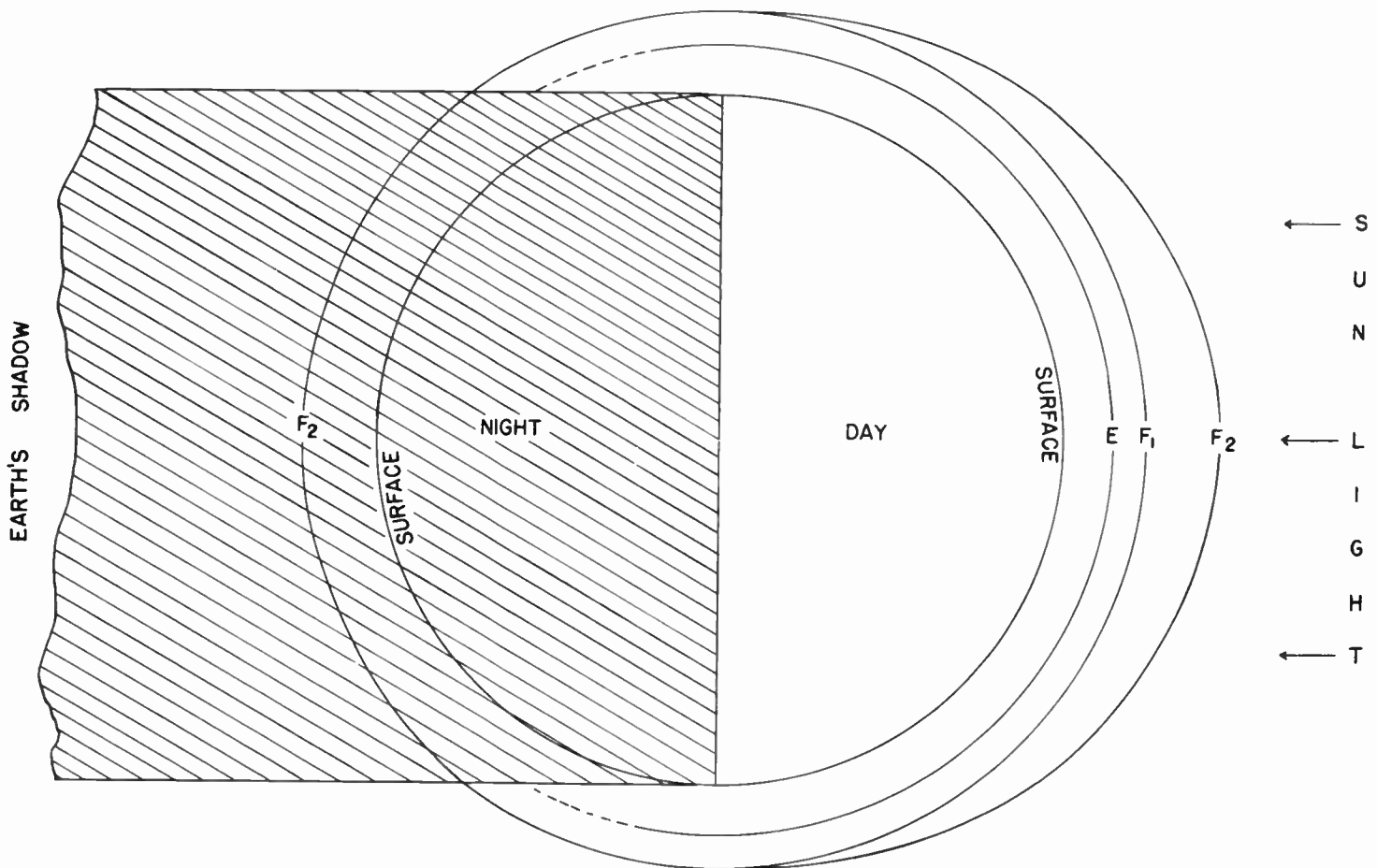


Fig. 3. Schematic Drawing of the Three Ionospheric Layers.

The ionosphere consists, as we have pointed out in Chapter 1, of several electrified layers. These are drawn schematically in Fig. 3. The three layers are designated by the letters *E*, *F*₁, and *F*₂—*E* being the lowest. You may wonder why this labeling starts with *E* instead of *A*, *B*, *C*, and so forth. Scientists, discovering these layers

The *E* layer has a well-defined maximum at a height of about 70 miles (110 km) above the earth's surface. The so-called *F* region is higher and lies above the earth from 90 to 250 miles (145 to 400 km). This region may have a fairly complicated structure. At night, there is usually a single maximum, known as the *F* (or *F*₂) layer. Dur-

ing the day, however, this layer separates into two parts, the F_2 rising and the F_1 sinking somewhat below the night height.

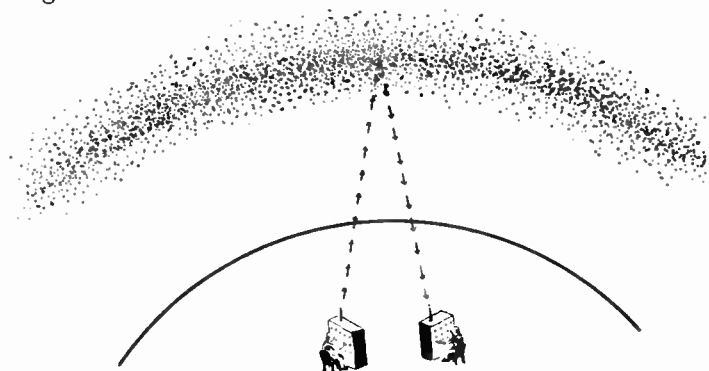


Fig. 4. Measurement of the Ionospheric Mesh.

Before undertaking our detailed calculations, we must have a certain amount of information about ionospheric conditions of the various layers over the surface of the earth. We need to know how high, how dense, and how variable these layers are. The experiments that have been set up to secure these data for us are strikingly demonstrated by the ball-and-mesh analogy of Chapter 1. The transmitter sends up short pulses at regular intervals, between which the frequency is slowly varied. A receiver stands by to pick up the returned echoes. The situation is similar to that depicted in Fig. 4. Low frequencies (long waves or large balls) are returned, and high frequencies (short waves or small balls) escape. A ball of critical size will exist—that is, a *critical frequency*,

which just will be reflected in the vertical path. Measurements of this critical frequency indicate the size of the ionospheric mesh.

From the time it takes for the signal to traverse the path from transmitter to the ionosphere and back to the receiver, we may estimate the effective or *virtual* height of the ionosphere. The waves travel at 186,000 miles a second in free space. Hence, a delay of 0.001 second (1 millisecond) indicates that the total path length up and down, or round trip, is 186 miles. The one-way path—that is, the ionospheric height, is half that distance, or 93 miles. The value of the vertical height is usually somewhat greater than the true height, because the waves are slowed down a little during their passage through the ionosphere. A record, corrected for this lag, is shown in Figs. 5a and 5b.

The actual records contain additional complications. A record of this type appears in Fig. 5b. Note, first of all, that the lines are tilted; the higher frequencies are reflected at greater heights. Also, the critical frequencies are not sharply defined, as in the idealized record of Fig. 5a. Instead, there is a pronounced curvature as if the ionospheric height rose sharply at the critical frequency. This upward curving arises from the afore-mentioned fact that waves near the critical frequency are markedly slowed down. The virtual height increases though the true height must remain the same. At times, the lag produced by the slowing down of a pulse may introduce a serious error in any device where the determination of

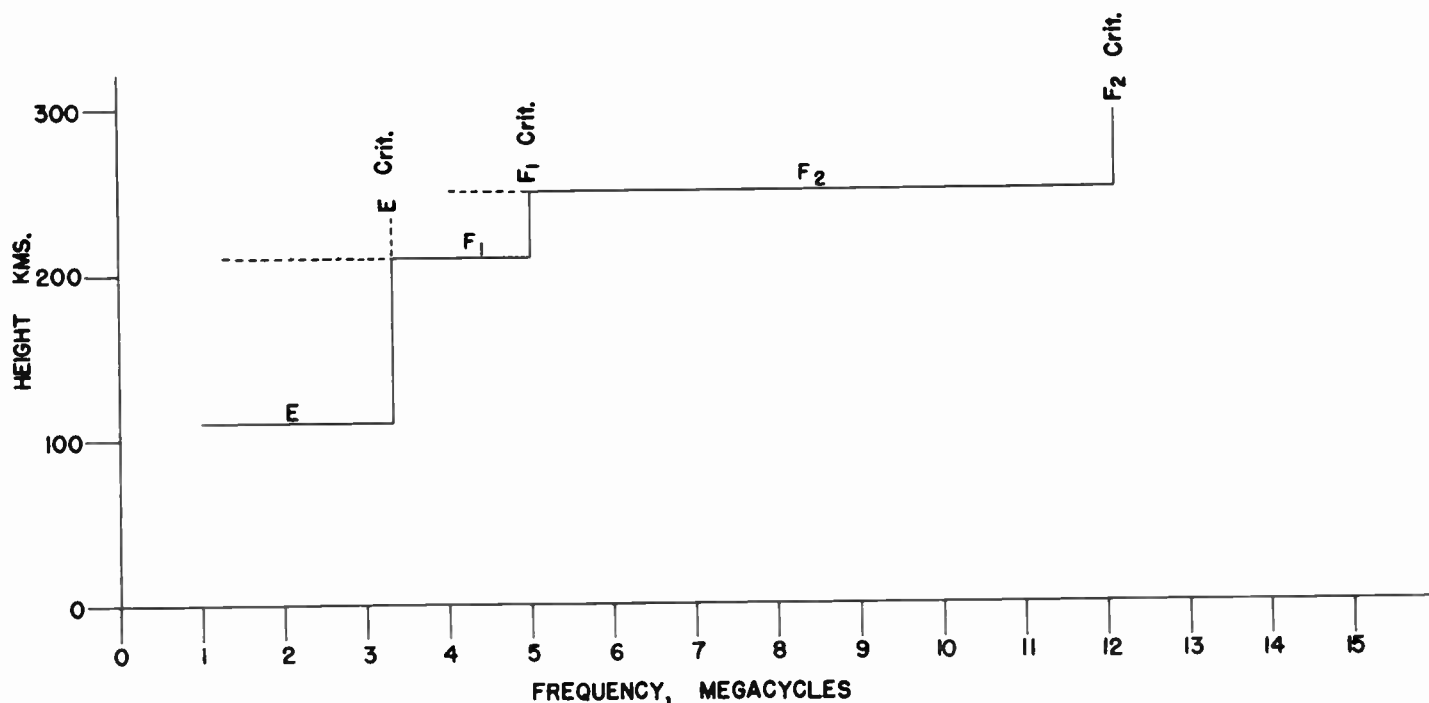


Fig. 5.(a). Schematic Ionosphere Record.

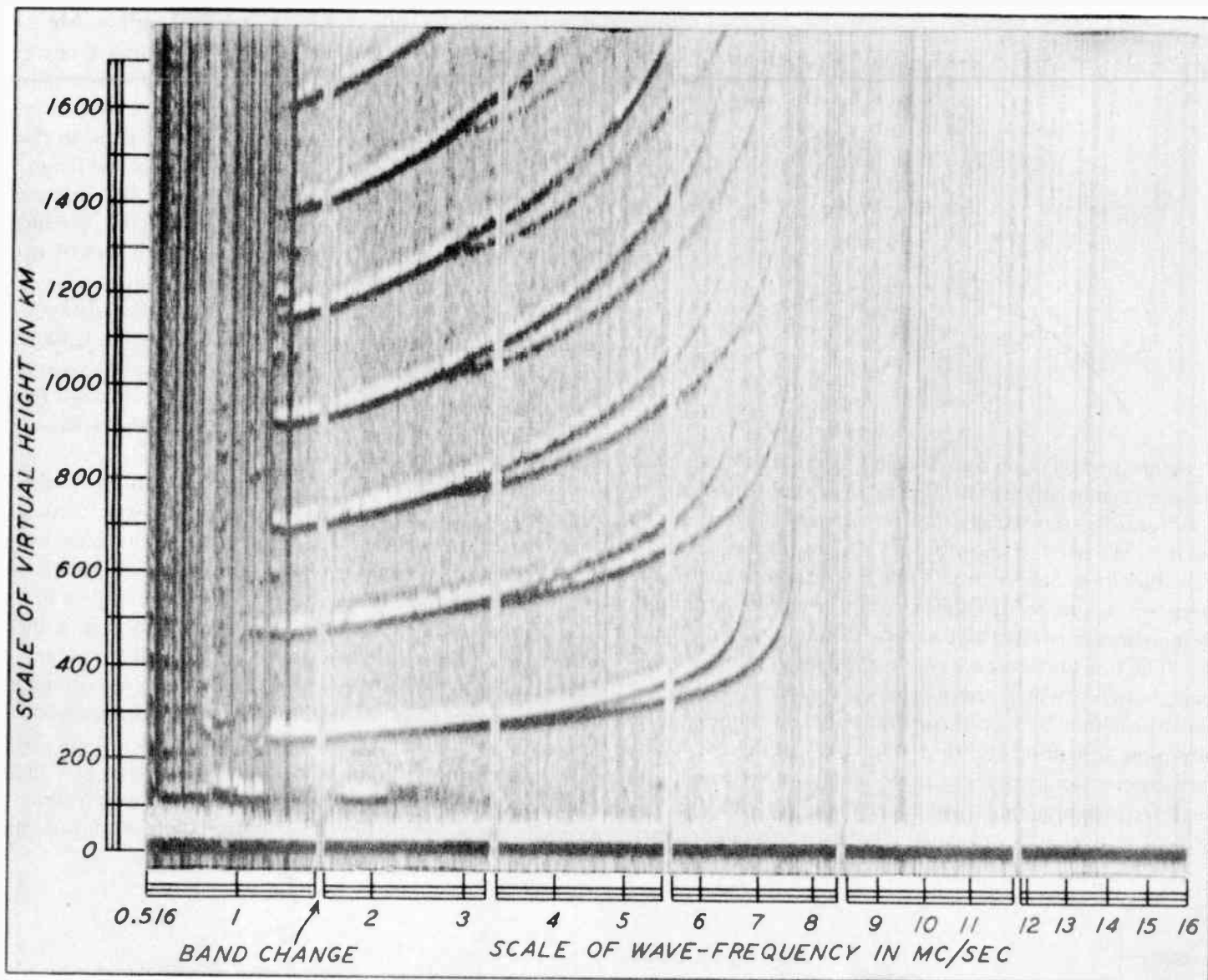


Fig. 5(b). Observed variation of virtual height with wave-frequency. Watheroo Magnetic Observatory, March 14, 1939, 20^h 15^m to 20^h 30^m local time (120° east meridian).

exact time intervals is important. SS Loran, for example, may be subject to such uncertainties at various times of day. Fig. 5c presents another sample record.

Returning again to Fig. 5b, we note the fact that the F layer, especially the F_2 , appears to consist of two parts. One part extends to somewhat higher frequencies. This apparent doubling is an effect of the earth's magnetic field. A plane-polarized radio wave—that is, one whose vibrations are in a definite plane, splits into two components during its passage through the ionosphere. These two waves are elliptically polarized—that is, their planes of polarization rotate, and the amplitudes of the vibration change according to the instantaneous orientation of the planes.

In the optics of certain crystals, a somewhat analogous

splitting occurs with respect to polarized light waves, which are, in effect, miniature radio waves. Here, we call the phenomenon *birefringence*, which means that the medium has two indices of refraction according to the types of polarization of the incident light.

In the radio application, we borrow from optics the terms *ordinary wave* and *extraordinary wave*. The former rotates to the left and the latter to the right. The effect arises from the fact that both the passing radio wave and the earth's magnetic field simultaneously exert forces on the free electrons in the ionosphere.

The principal difference between the two types of waves, from the viewpoint of radio propagation, is that the effective ionospheric mesh is slightly smaller for the extraordinary than for the ordinary wave. In other

words, the critical frequency of the former exceeds the latter usually by a sizeable fraction of a megacycle. At first sight, it would appear that the extraordinary wave would be the factor controlling the maximum usable frequency. For distances up to about 1500 km, the extraordinary wave may play a significant role for communication purposes, but it is more readily absorbed than the ordinary wave. In consequence, we shall employ the ordinary wave as a standard. Remember, however, that the ionosphere may reflect the extraordinary wave at somewhat higher frequencies for communications over the shorter ranges.

One other feature of the actual ionospheric records deserves special mention—namely, the repetition of the record at double the height. This duplication comes from signals that have made two round trips, including a reflection at the earth's surface. Often several such

multiples show on the records.

A recent and very important development in the taking of ionospheric records is the adaptation of motion-picture photography to the instruments. The records, taken at the rate of one or more per minute, are projected at the normal speed of 16 to 24 frames per second. The motions of the ionosphere, as the layers develop normally or as they are disturbed by incoming blasts of solar radiation or charged corpuscles, are spectacular. One clearly sees that the ionosphere is far from being constant or uniform.

The relationship between the extraordinary and ordinary criticals, f_x and f_o , depends upon a quantity f_h , known as the *gyro frequency*. This quantity corresponds to the natural period of a free electron circling in the earth's magnetic field. The value of f_h is about 0.7 to 0.8 megacycle near the geomagnetic equator, and it

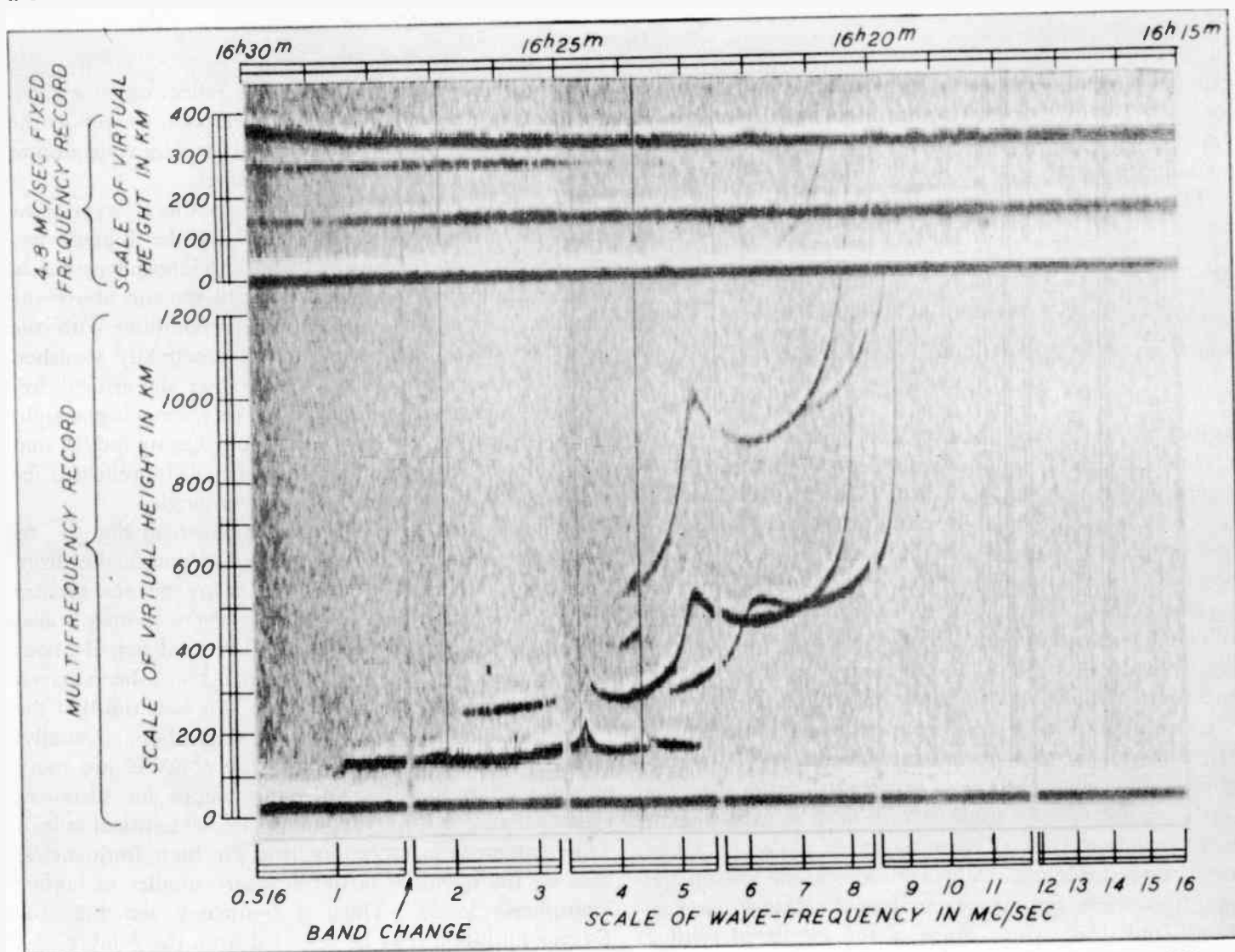


Fig. 5(c). Observed variation of virtual height with wave-frequency, Watheroo Magnetic Observatory, December 18, 1939, 16^h 15^m to 16^h 30^m local time (120° east meridian).

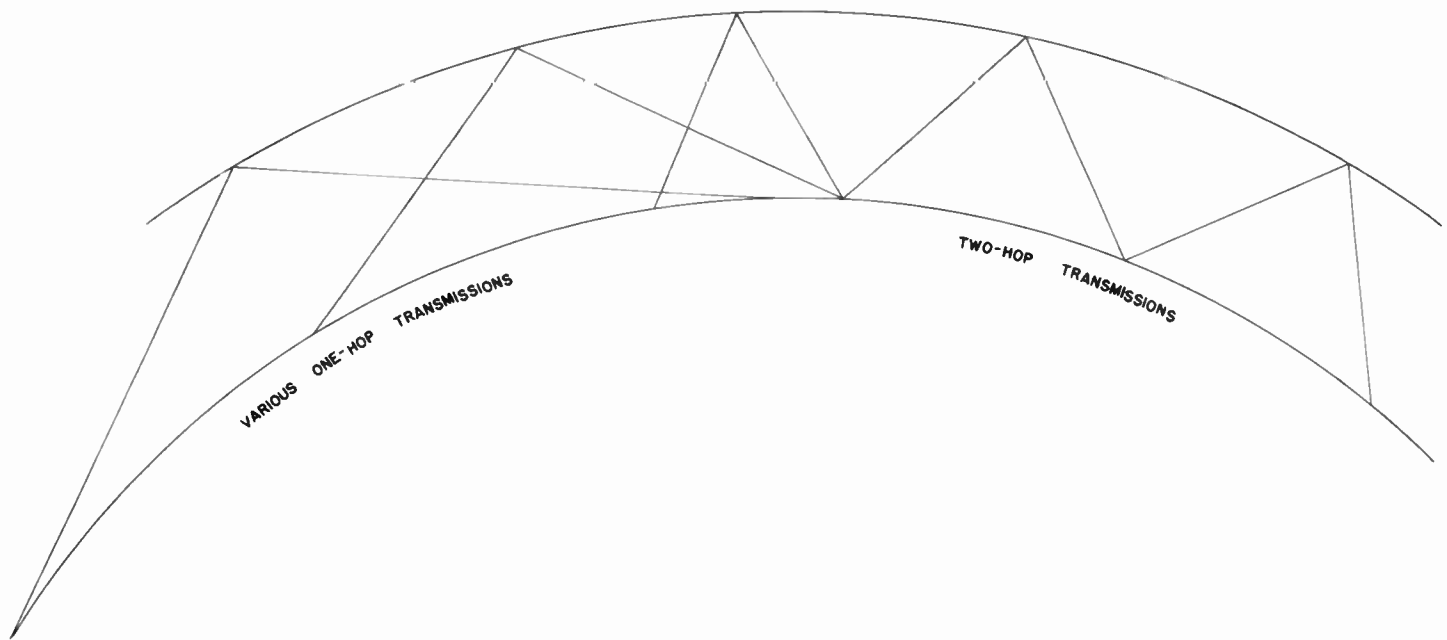


Fig. 6.

gradually increases at the rate of about 0.09 megacycle for each 10° of geomagnetic latitude until it attains a value of 1.5 to 1.6 megacycles in the auroral zones surrounding the magnetic poles.

The equation relating the three quantities is

$$f_0^2 = f_z(f_z \pm f_h), \quad (1)$$

or

$$f_z = \sqrt{f_0^2 + (f_h/2)^2} \pm f_h/2, \quad (2)$$

which gives the approximate condition that

$$f_z \sim f_0 \pm f_h/2, \quad (3)$$

as long as f_0 is greater than about 4 megacycles.

Note that these equations predict two extraordinary waves, one at a higher and one at a lower frequency than f_0 . The latter, however, is unimportant for communication purposes because it is highly absorbed. It is rarely observed, except on ionospheric records taken near the magnetic poles.

The extraordinary wave occasionally shows for the E layer, but only for F_2 and, occasionally, for F_1 does it ever appreciably control the frequency limit for radio signals.

In order to obtain continuous records of the critical frequencies, scientists have established numerous ionospheric observing stations at strategic locations on the earth. Some of these stations have been in existence for years, such as the one at Washington, D. C.; others are of more recent building. A central laboratory collects the data from them and experts analyse the data to forecast trends and draw world maps of the predicted critical frequencies (ordinary waves) several months in advance.

Analyses of the ionospheric records tell us how long a trip to the ionosphere our wave will take. We are particularly interested in knowing at what angle the wave

will strike the layer, so that it will reflect on to a given point of reception. The angle of impact, as well as the mesh, is important to fix the critical limit for reflection or transmission of the various frequencies.

Observations of radio echoes from the E layer show that the critical frequency—namely, the highest frequency that will be returned from the ionospheric mesh, depends primarily on the altitude of the sun above the horizon. At night, the electrons recombine with the ions, and the E layer of electricity practically vanishes. From observations, we may map either the critical frequencies themselves, which refer to waves moving straight up and down, or we may apply appropriate factors and map the maximum frequencies that will be reflected for rays striking the E layer at any given angle.

The geometry of the problem is shown in Fig. 6. As the angle of transmission moves farther and farther from the vertical, the rays are reflected to greater and greater distances. At the very maximum, where the ray leaves the earth tangent to the ground, the total hop is about 2400 km for an E layer at 110 km. For E -layer transmission beyond 2400 km, therefore, it is essential that the radio path include more than a single hop. Usually, because of their greater height, the F layers are more effective than multihop E transmissions for distances greater than 2400 km (1500 miles or 1300 nautical miles). This statement is especially true for high frequencies, because the openings of the sieve are smaller in higher ionospheric levels. Thus, a frequency too high for E -layer multihop may be reflected from the F layer.

For our map of maximum reflected frequencies, we shall adopt 2000 km as the distance for greatest effectiveness of E -layer transmissions. As in our analogy, the slanting angle at which the beam strikes the ionosphere

for a 2000-km hop permits reflections of higher frequencies (smaller balls) than would be possible for waves traveling perpendicular to and striking the ionosphere; actually frequencies 4.78 times as large can be reflected. Consequently, if we multiply the observed critical frequency by 4.78, we obtain the maximum usable frequency (MUF) that will just be returned to earth for a hop of 2000 km from the *E* layer.

Figs. 7 to 10 are essentially maps of the *E*-region maximum usable frequencies for 2000-km hops at different seasons. The vertical coordinate is the latitude and the horizontal, the time of day. We cannot specify the longitude because the ionosphere is not fixed relative to the earth, but rotates as the sun rises and sets. More accurately, we may say that the sun and the ionosphere, or rather the *characteristics* of the ionosphere, remain fixed while the earth rotates freely beneath them.

Examine these maps of the ionosphere. The point directly beneath the sun is marked by *x*. The curves representing the MUF's (maximum usable frequencies)

are not quite symmetrical about the sun—there seems to be a tendency for them to be slightly shifted in latitude. The curves are very nearly true circles on the surface of the earth, and the distortions into ovals arise from the previously mentioned deformations that occur when we attempt to map a sphere on a flat surface.

The numbers on the circles represent the MUF's for 2000 km, the values being given in megacycles. Thus, for June at 0615 (6:15 a.m. local time) at latitude 50°N, the 2000 MUF is 12.0 megacycles. To find the critical frequency, we divide by the factor 4.78 (or multiply by 0.21) and get the value of 2.5 megacycles. Frequencies higher than 2.5 megacycles will penetrate if they are sent up vertically. Frequencies greater than 12.0 megacycles will penetrate if used for 2000-km hops.

To obtain the MUF for distances between 0 and 2000 km, or greater distances, Table 1 supplies the necessary multiplying factors. Simply multiply the 2000-km *E* MUF by the factor for the given distance in this table.

We may regard the charts of Figs. 7 to 10 as maps of

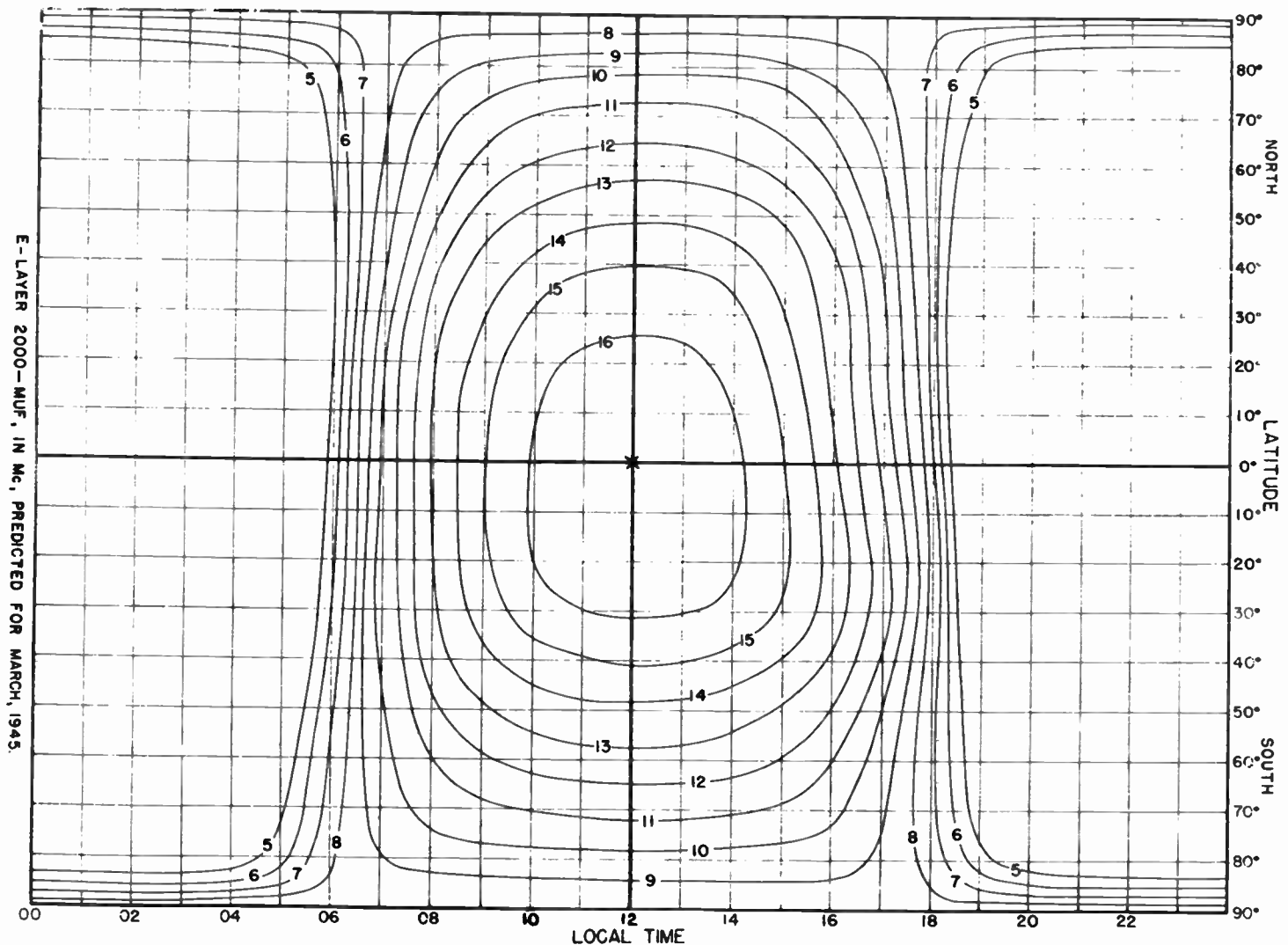


Fig. 7.

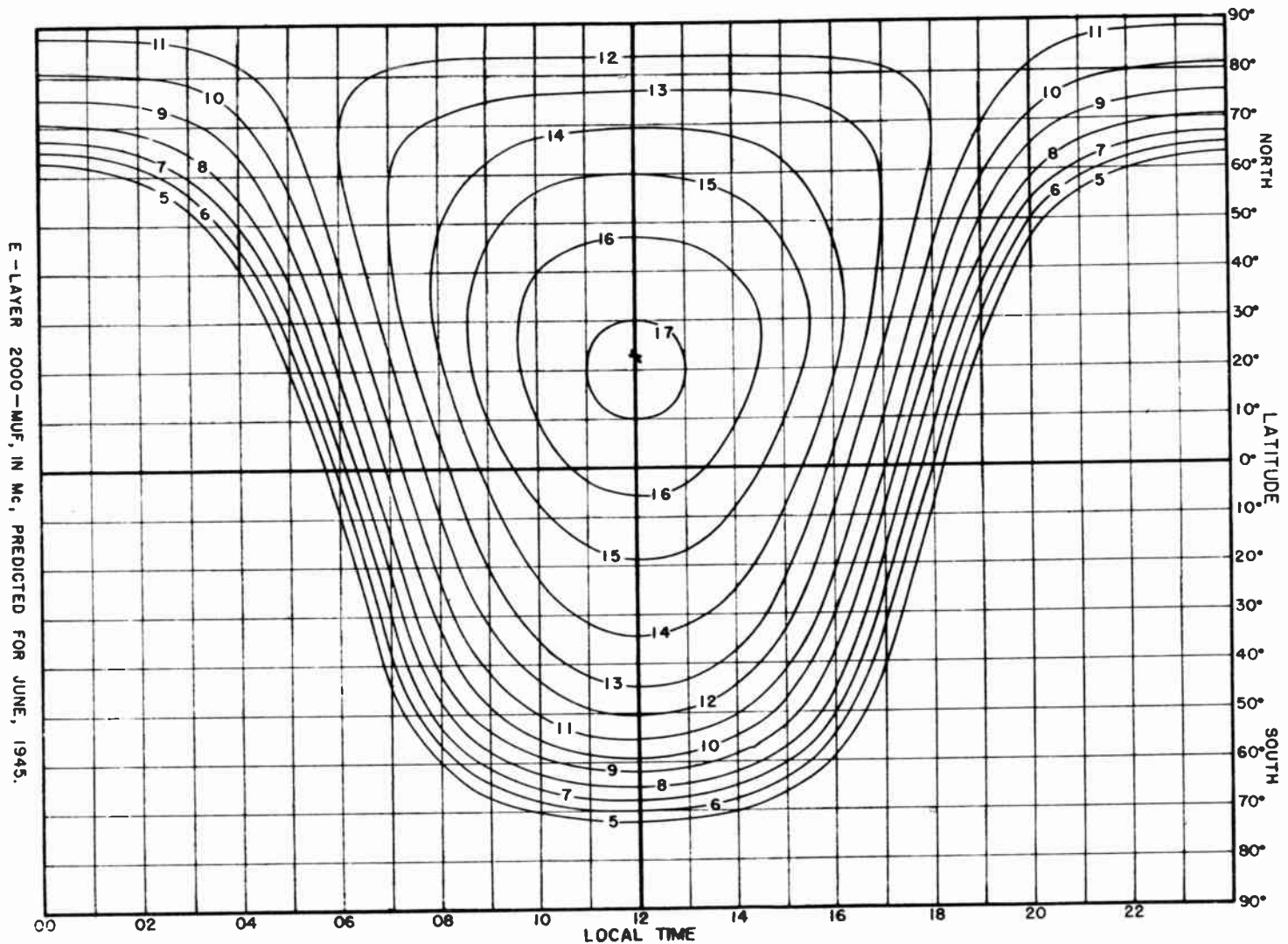


Fig. 8.

the ionospheric mesh referred to in the analogy. The higher frequencies near the subsolar point indicate a smaller mesh, illustrative of the statement previously made that the ionospheric network (especially for the E layer) is smallest when the sun is directly overhead. The map, depicted as a sieve with variable mesh, appears in Fig. 11. This diagram is illustrative and is not to be used for calculations.

The F_1 map shows a mesh very similar to that of the E layer. Both layers are essentially daytime phenomena. The F_1 layer is lowest at noon, with an effective height of about 200 km (125 miles). The altitude generally is greater toward sunrise and sunset.

For predictions of radio propagation, we may combine the effects of the E and F_1 layers, and use the fundamental E maps to forecast the combined effects of both. As far as the maps are concerned, the F_1 layer is the main agent for distances between 2000 and 4000 km. The multiplying factors of Table 1 for converting the 2000-km MUF to the MUF at another distance are simple only because the E and F_1 layers are fairly constant in height.

A nomogram, Fig. 20, furnishes another means of obtaining the MUF for different distance hops. To use it, find the 2000-km MUF on the left-hand scale and the distance, in kilometers, on the right-hand scale. Connect these two points by a straight line. The actual MUF appears at the intersection of the left-center scale with the straight line so drawn. The right-center scale indicates the OWF, the optimum working frequency. Because of unpredictable fluctuations in the E -layer MUF's, one generally finds it safer to employ a frequency 0.97 of the MUF, which defines the OWF.

Above the E and F_1 layers lies a third, the F_2 layer, which is the most important of all for long-range transmissions, especially for those in excess of 4000 km. During the night, the F_1 and F_2 layers coalesce into a single F layer at a height of about 250 km. The splitting occurs about sunrise, the F_1 layer falling to about 200 km and the F_2 rising to 300 to 400 km, or even to 500 km for high latitudes in the summer.

The critical frequency or ion-layer mesh is directly connected with the density of electrons within the layer.

For the E and F_1 layers, the controlling factor is the angle at which the sun's rays strike the upper atmosphere. The sun when directly overhead, produces greater ionization (electrification) than it does when shining at oblique angles. The additional fact that the E and F_1 layers do not vary greatly in height helps to keep the phenomenon relatively simple, with the critical frequencies decreasing fairly uniformly from the subsolar point.

For the F_2 layer, however, which bulges out so tremendously on the daylight side of the earth, the problem becomes more complex. Two opposing factors appear to be affecting this layer. The layer expands as the solar altitude increases, probably as the result of solar heating, and this effect tends to reduce the density of the electrons and lower the critical frequencies. But the additional solar ionizing radiation tends to increase the frequencies. The two processes, expansion and absorption, thus work in opposite directions, and the resultant effect is more difficult to predict.

Apparently, the expansion is somewhat more effective than the solar ionization. Hence, in March and September, when the sun is on the equator and, therefore, symmetrically situated with respect to the northern and southern hemispheres, there is less electron density at the equator than at latitudes 20° north or south. This behavior is exactly opposite to the behavior of the E and F_1 layers, where the density is greatest at or near the subsolar point.

In December, for latitudes in the northern hemisphere where the expansion by heating is less, the F_2 ion density and, consequently, the MUF's are considerably greater than in the summer when the greater expansion more than counteracts the effect of the more direct beam of sunlight. In fact, the $F_1 F_2$ splitting is small in winter. Similar effects occur at the appropriate seasons in the southern hemisphere.

An additional tendency should be noted—namely, that the maximum F_2 MUF's generally occur two or three hours after local noon, a result clearly suggesting that the

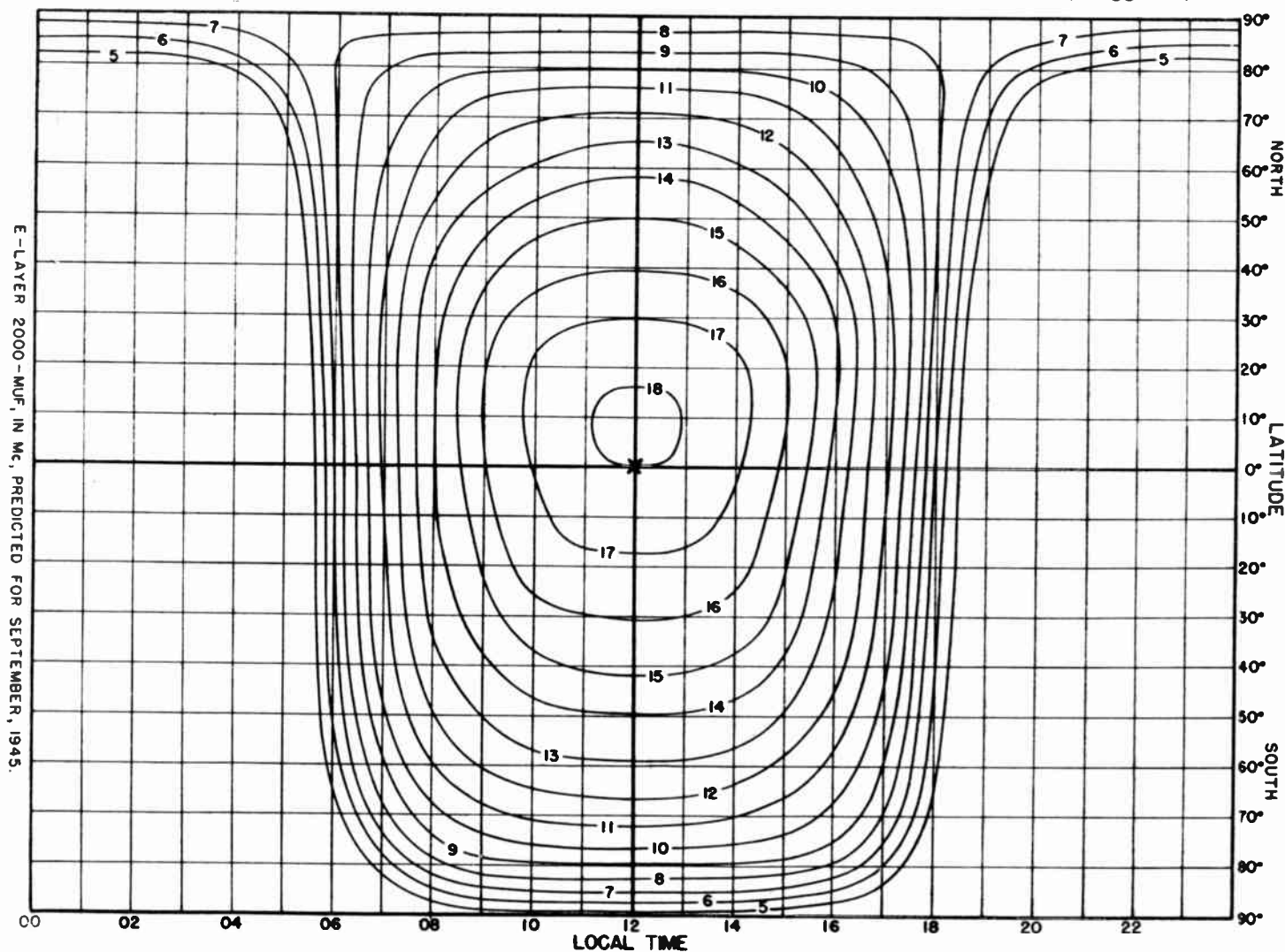


Fig. 9.

TABLE 1
 DISTANCE FACTORS FOR MAXIMUM USABLE FREQUENCY
 To obtain the maximum frequency reflected by the E or F_1 layer, multiply the 2000-km E MUF by the factor for the given distance in this table.

Distance (Km)	Factor for E 2000 MUF	Distance (Km)	Factor for E 2000 MUF
0	.21	2100	1.00
100	.22	2200	1.01
200	.25	2300	1.01
300	.30	2400	1.02
400	.35	2500	1.02
500	.42	2600	1.02
600	.48	2700	1.02
700	.54	2800	1.02
800	.61	2900	1.02
900	.67	3000	1.02
1000	.72	3100	1.01
1100	.77	3200	1.01
1200	.81	3300	1.01
1400	.85	3400	1.00
1300	.88	3500	1.00
1500	.92	3600	.99
1600	.95	3700	.98
1700	.97	3800	.96
1800	.98	3900	.94
1900	.99	4000	.91
2000	1.00		

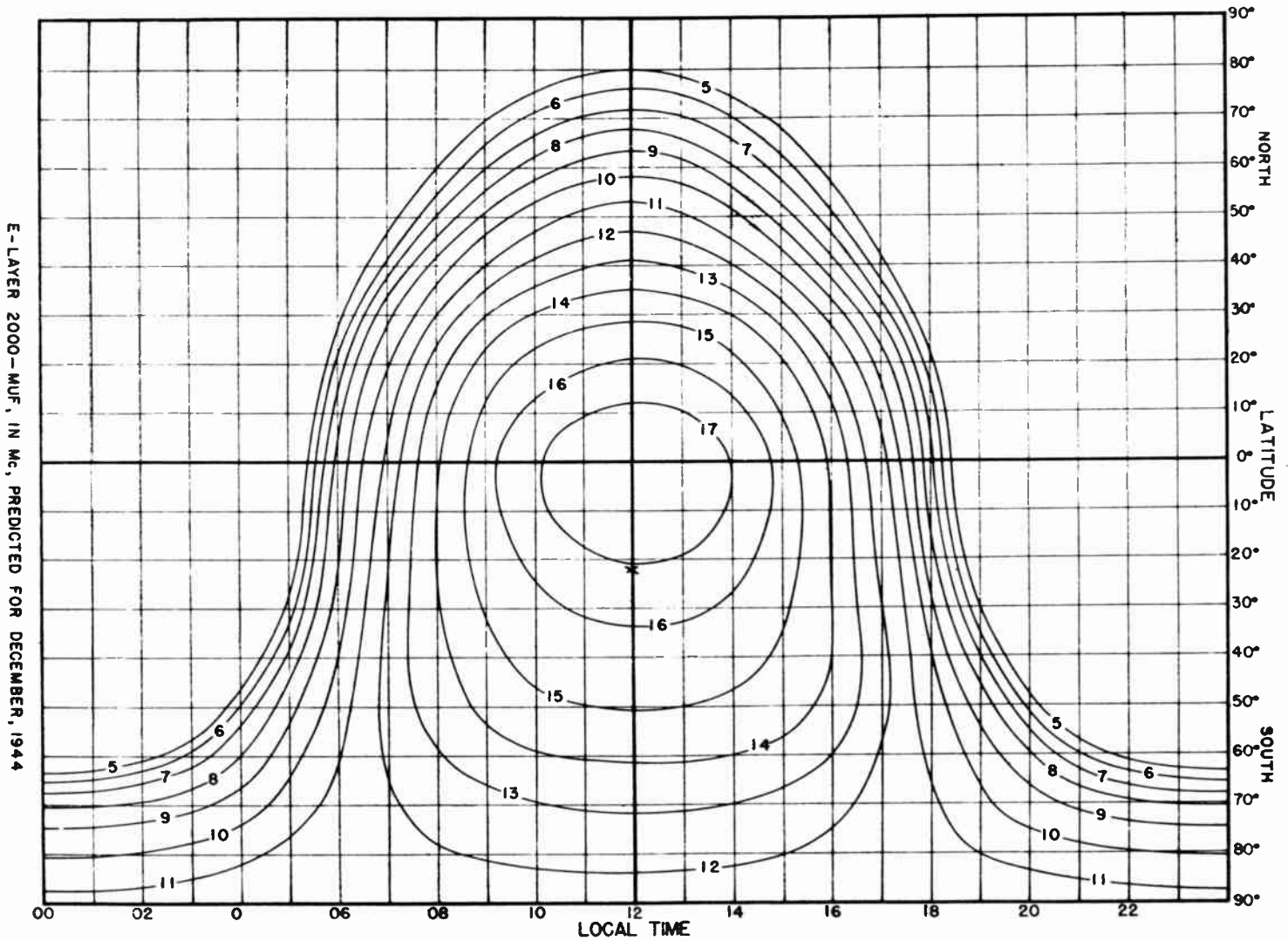


Fig. 10.

ions and electrons do not recombine instantaneously.

A further complication enters as the result of the discovery that the eastern and western hemispheres do not give identical results. This last effect appears to depend upon the magnetic latitude of the place, because the observed distribution of electrons appears to be centered approximately about the magnetic rather than the geographic poles. These magnetic poles do not coincide with the geographic—that is, with the poles of rotation.

One might expect that Tokyo and Los Angeles, say, cities having approximately the same geographic latitude, would show similar ionospheric characteristics at a given time of year. If the sun were the only factor, the ionospheric behavior should be almost identical, because the daily variation of solar altitude is the same at both places, in terms of their respective local times. Actually, we have found that the ionospheric mesh for Tokyo, especially in the uppermost (F_2) layer, is smaller than for Los Angeles. The effect appears to be generally present in

the eastern vs the western hemispheres. The phenomenon is not completely understood, but we attempt to allow for it, in part, by using three maps of the F_2 layer, one each for the Western, Eastern, and Intermediate Zones.

During the night, ionization in the F_2 layer, unlike that in the E and F_1 , does not subside to nearly the vanishing point—a fairly substantial amount remains. Indeed, near the equator, the indications are that there may be a second maximum of ionization, produced perhaps by condensation of the cooling F_2 layer, with resulting concentration of electrons in the layer thus compressed. Nighttime transmissions are controlled almost entirely by the F_2 layer.

The maps of Figs. 12 to 15 show the MUF's for 4000-km F_2 hops. To convert these figures to values for paths of other lengths, multiply by the factors of Table 2. These factors are only average values and are more accurate for distances of from 2000 to 4000 km than for

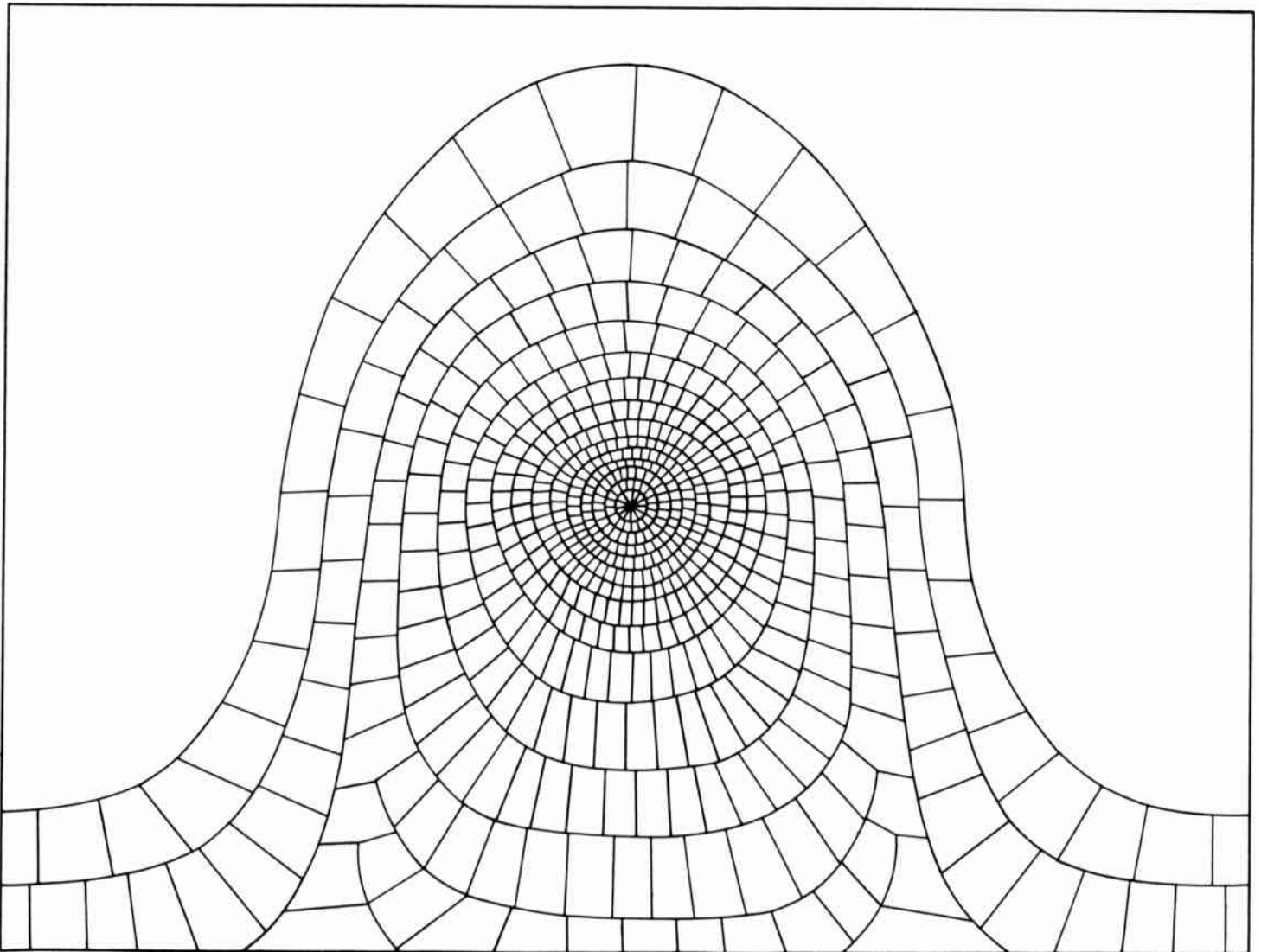


Fig. 11. Sievelike Pattern of Ionosphere.

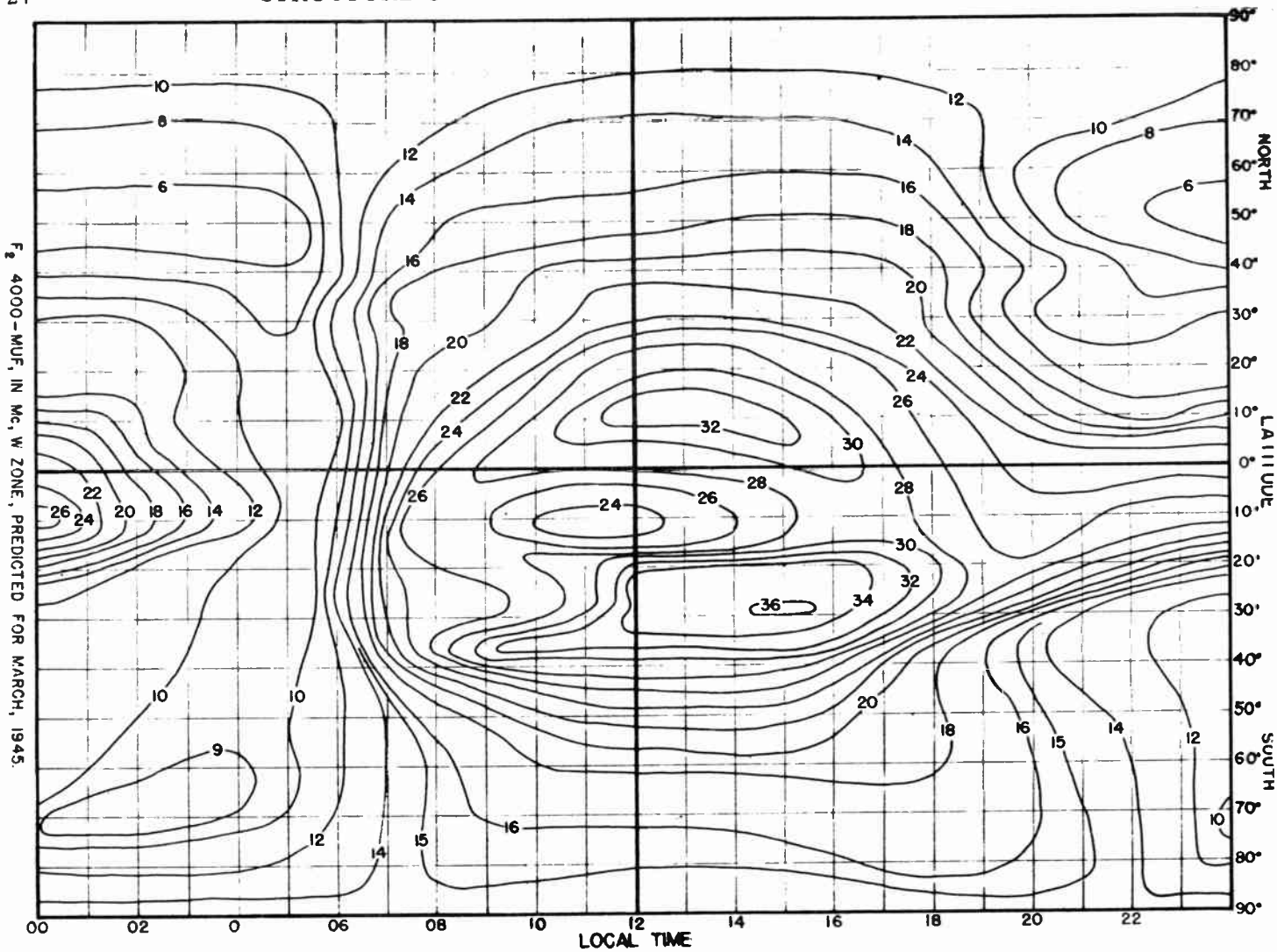


Fig. 12.

TABLE 2
 DISTANCE FACTORS FOR MAXIMUM USABLE FREQUENCY
 To obtain the maximum frequency reflected by the F_2 layer, multiply the F_2 4000 MUF (critical frequency) by the factor for the given distance in the table.

Distance (Km)	Factor for F_2 4000 MUF	Distance (Km)	Factor for F_2 4000 MUF
0	.35	2100	.76
100	.35	2200	.78
200	.35	2300	.81
300	.36	2400	.83
400	.36	2500	.85
500	.37	2600	.86
600	.38	2700	.88
700	.40	2800	.90
800	.42	2900	.91
900	.44	3000	.92
1000	.46	3100	.93
1100	.48	3200	.95
1200	.51	3300	.96
1300	.54	3400	.97
1400	.57	3500	.98
1500	.60	3600	.98
1600	.63	3700	.99
1700	.65	3800	.99
1800	.68	3900	1.00
1900	.71	4000	1.00
2000	.73		

shorter distances. For the E and F_1 layers, the method of simple conversion factors was amply accurate only because the heights of the layers were reasonably constant. The height of the F_2 layer, however, fluctuates greatly from hour to hour and month to month. Hence, as we apply the tabulated factors for hops less than 2000 km, the resultant MUF may not be correct. In consequence, zero-distance MUF's, so calculated, may differ considerably from the true critical frequencies. It must be emphasized that these MUF maps are for the year 1945.

To increase the accuracy for short-distance MUF's, it is preferable to use a world map of the critical frequencies rather than the 4000 MUF's. To the zero-distance MUF, as read from the map, apply the approximate factor from Table 3 to convert to MUF's for the given distance. It is to be noted that this procedure, also, is approximate and that the MUF's calculated independently from the 4000- and zero-MUF charts may not be in complete agreement.

World maps of the zero-MUF's or critical frequencies are given in Figs. 16 to 19, corresponding to the 4000-MUF maps previously given. The nomograms of Figs. 20 to 22 may be used as an alternative method for converting the standard MUF's to approximate MUF's at other distances or to the OWF (optimum working frequency). These nomograms give results equivalent to those of the tables. The OWF for the F_2 layer is 85 percent of the MUF. The OWF is considered best—that is, optimum, because it is sufficiently below the MUF to allow for the very considerable fluctuations that may occur in the F_2 layer. If the OWF is higher than the LUHF, it is the most satisfactory for transmissions.

For the F_2 layer, satisfactory agreement for all distances may be obtained by the following procedure. For a given point on the surface of the earth, read off both the zero- and 4000-MUF values. Lay a straightedge between the points on the 4000- and zero-MUF scales of the nomogram of Fig. 23. Find the vertical line representative of the distance of the hop (that is, the distance

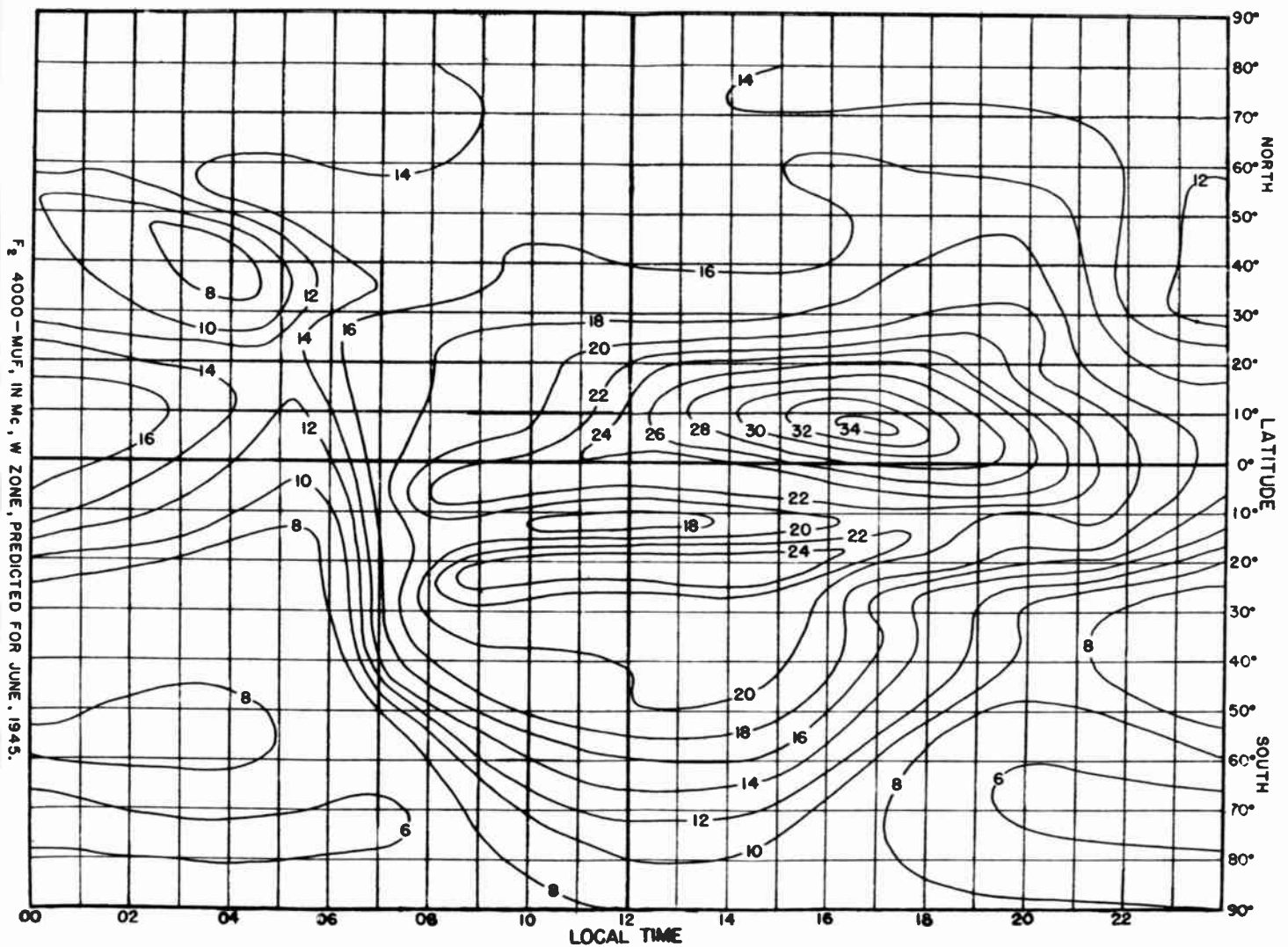


Fig. 13.

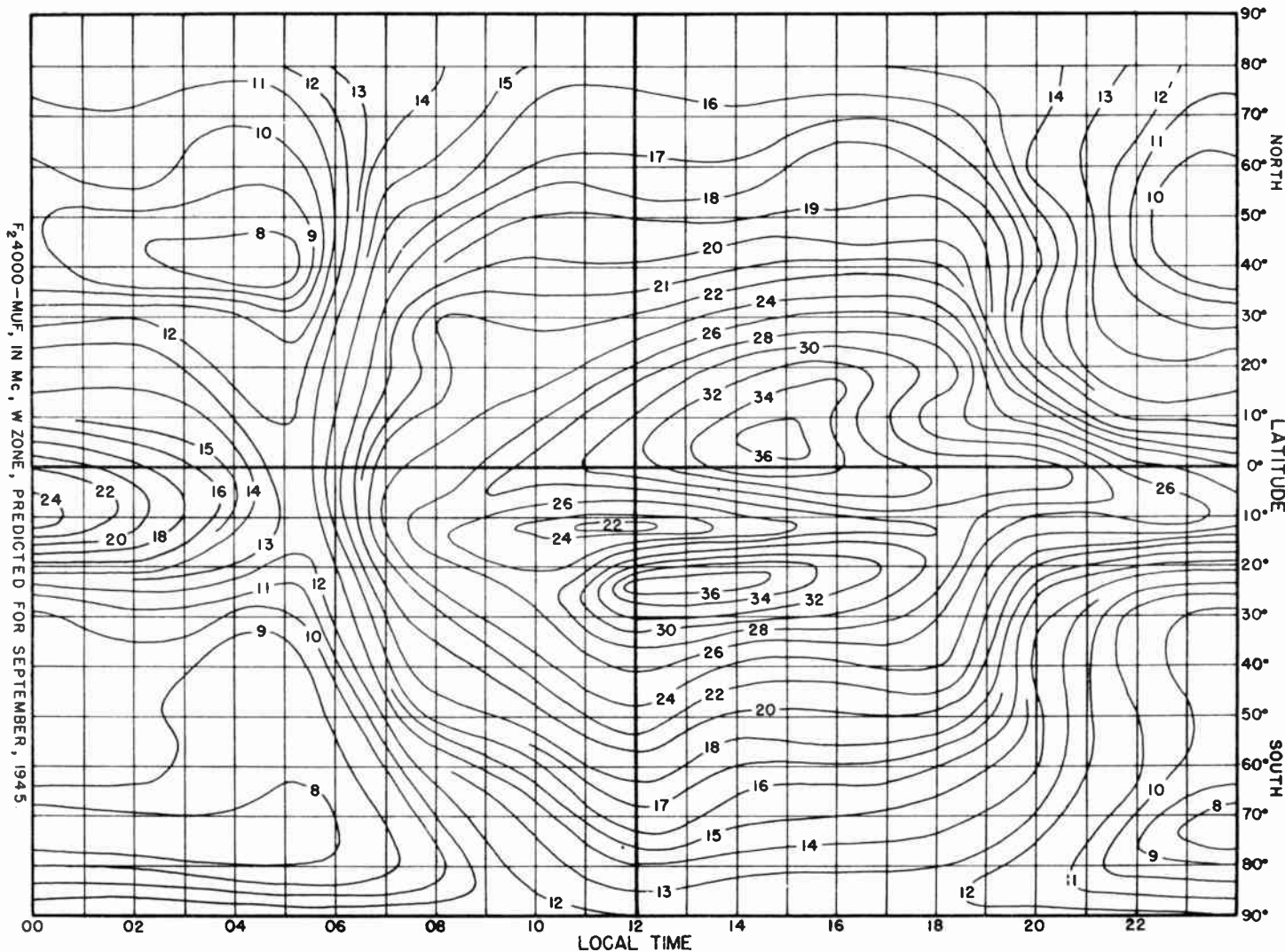


Fig. 14.

TABLE 3
DISTANCE FACTORS FOR MAXIMUM USABLE FREQUENCY
 To obtain the maximum frequency reflected by the F_2 layer, multiply the zero kilometer F_2 MUF by the factor for the given distance in the table.

Distance (Km)	Factor for F_2 zero MUF	Distance (Km)	Factor for F_2 zero MUF
0	1.00	2100	2.16
100	1.00	2200	2.22
200	1.01	2300	2.29
300	1.02	2400	2.35
400	1.03	2500	2.40
500	1.05	2600	2.45
600	1.09	2700	2.50
700	1.14	2800	2.55
800	1.19	2900	2.59
900	1.25	3000	2.62
1000	1.31	3100	2.65
1100	1.38	3200	2.69
1200	1.45	3300	2.72
1300	1.54	3400	2.75
1400	1.62	3500	2.77
1500	1.71	3600	2.79
1600	1.79	3700	2.81
1700	1.86	3800	2.83
1800	1.94	3900	2.84
1900	2.02	4000	2.85
2000	2.09		

between sending and receiving stations) and read off the MUF by following the point of intersection along a line parallel to the diagonals to one of the external scales. The scale at the right is to convert MUF directly to OWF.

We recall from the earlier discussion that all these charts refer to the ordinary wave. Since the F_2 transmissions up to 1500 km, and occasionally for greater distances, may be controlled by the extraordinary wave, the student may prefer to correct his zero-MUF's for the approximate gyrofrequency, to give the extraordinary rather than the ordinary critical frequency. The writer prefers to work entirely with the ordinary wave, whose values tend to lie on the conservative side. But it is worth while remembering the general effect of the extraordinary wave—at certain times of day, particularly when the absorp-

tion is high, the extraordinary wave may be more effective than the somewhat lower frequency designated by the ordinary-wave MUF.

New E , F_1 - and F_2 -MUF charts are issued each month by the Central Radio Propagation Laboratory, located at the National Bureau of Standards, Washington, D. C. These current maps should be used in place of the illustrative figures reproduced in the text.

Copies of the publication series D, may be obtained as follows:

- | | |
|-----------------------------|---|
| Army . . . TB 11-499 series | Adjutant General |
| Navy . . . CNC-13-1 series | Registered Publications Section,
Division of Naval Communica-
tions |
| Others . . CRPL-D series | Central Radio Propagation Lab-
oratory |

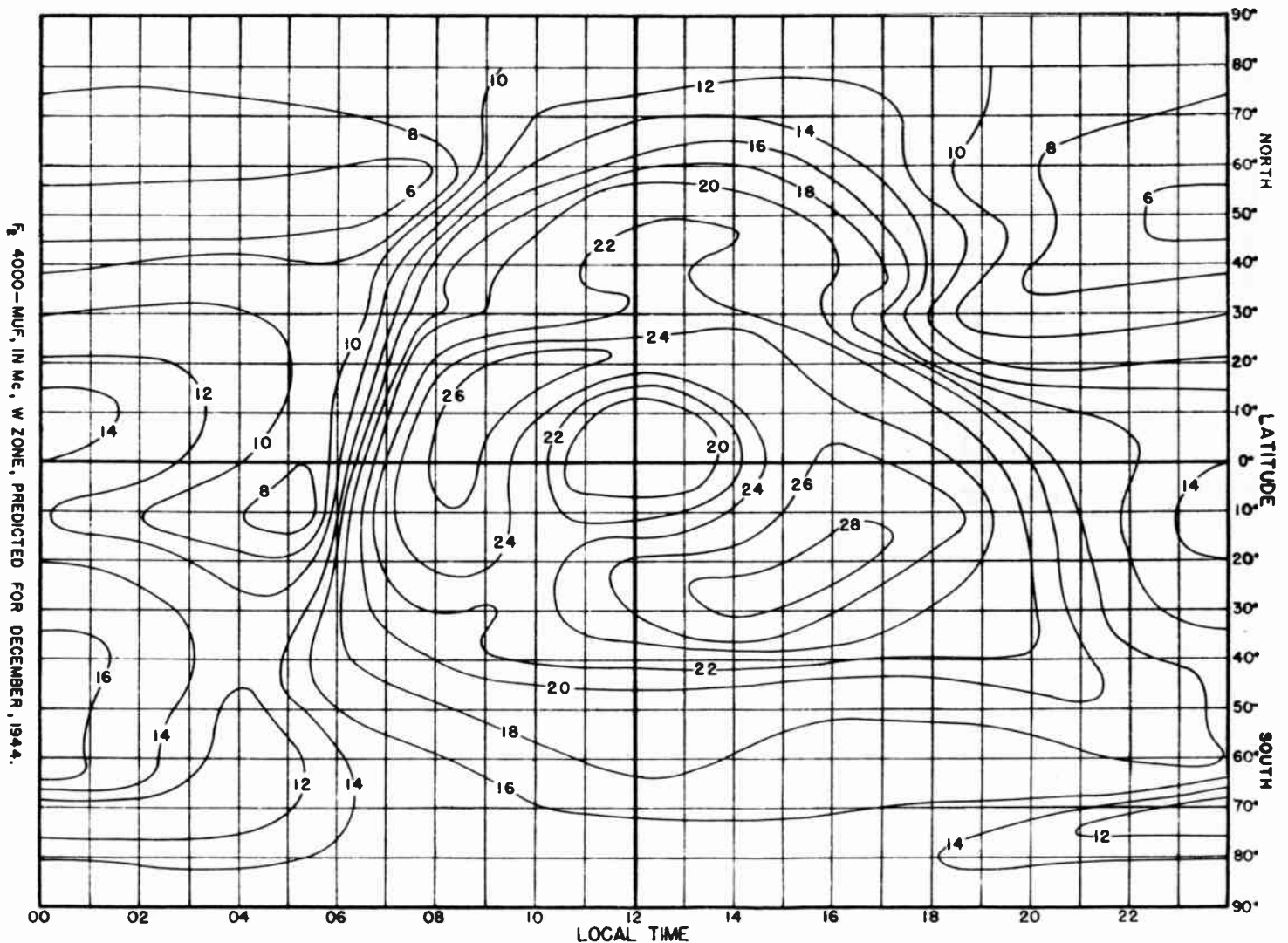


Fig. 15.

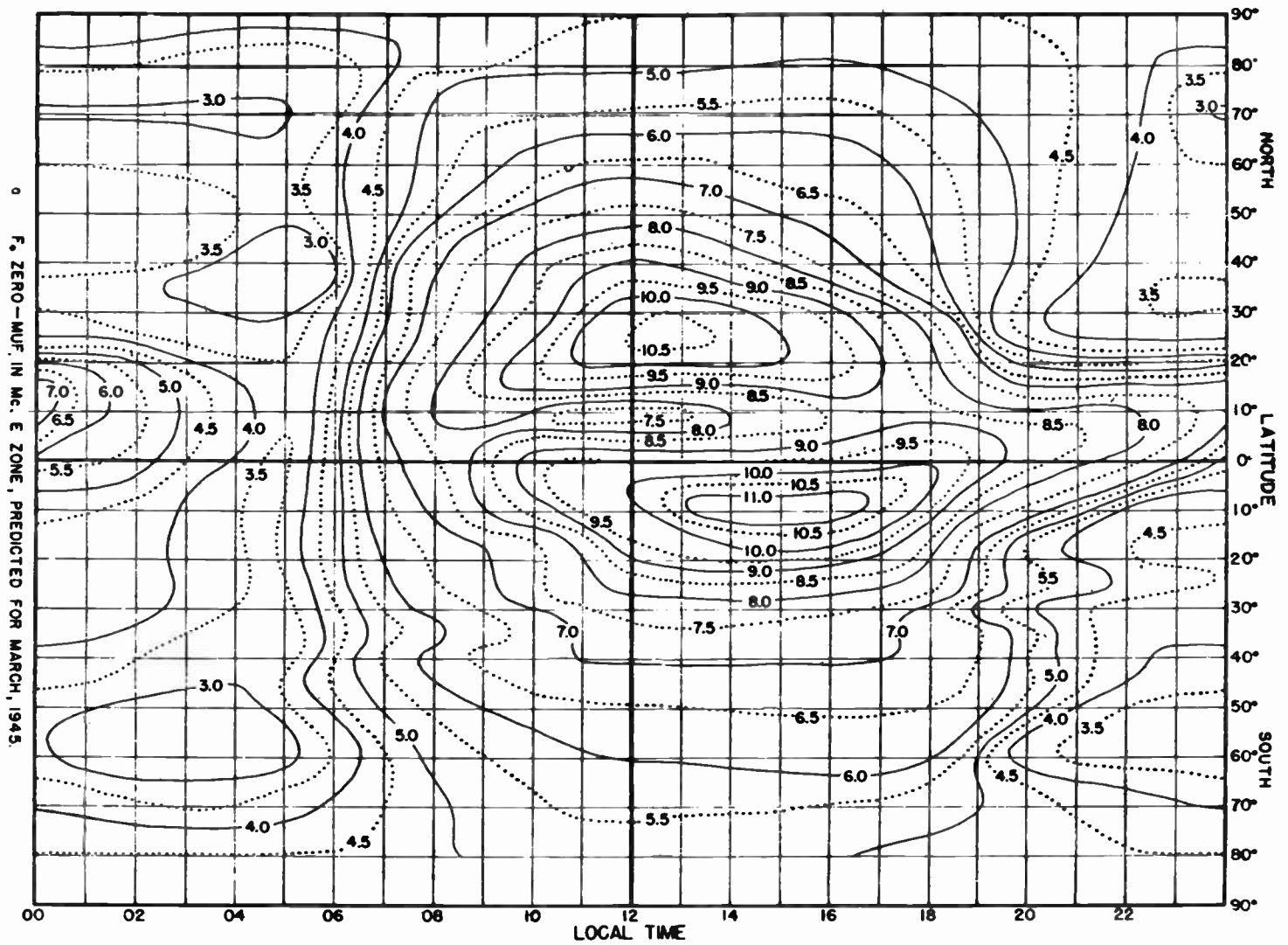


Fig. 16.

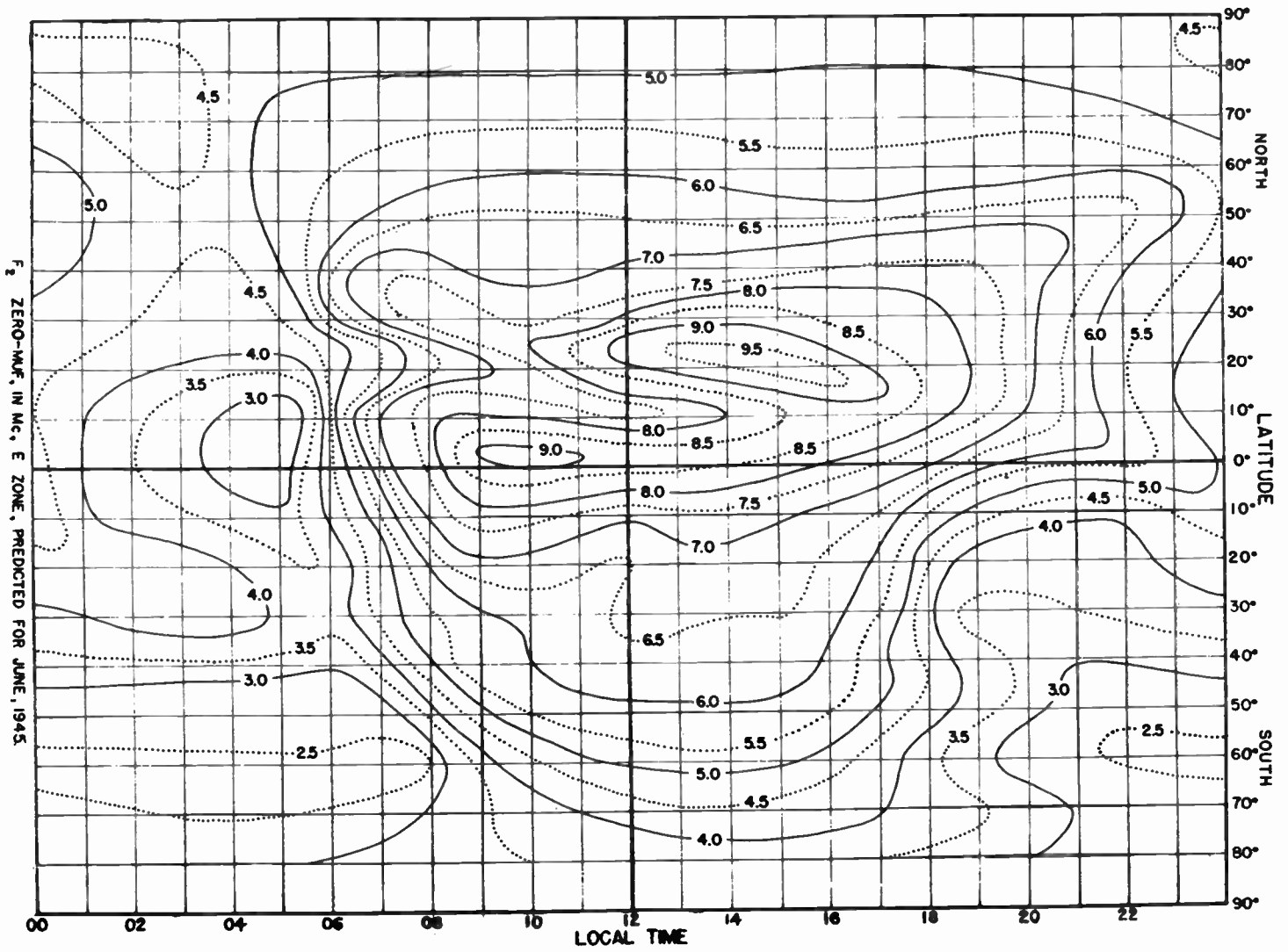


Fig. 17.

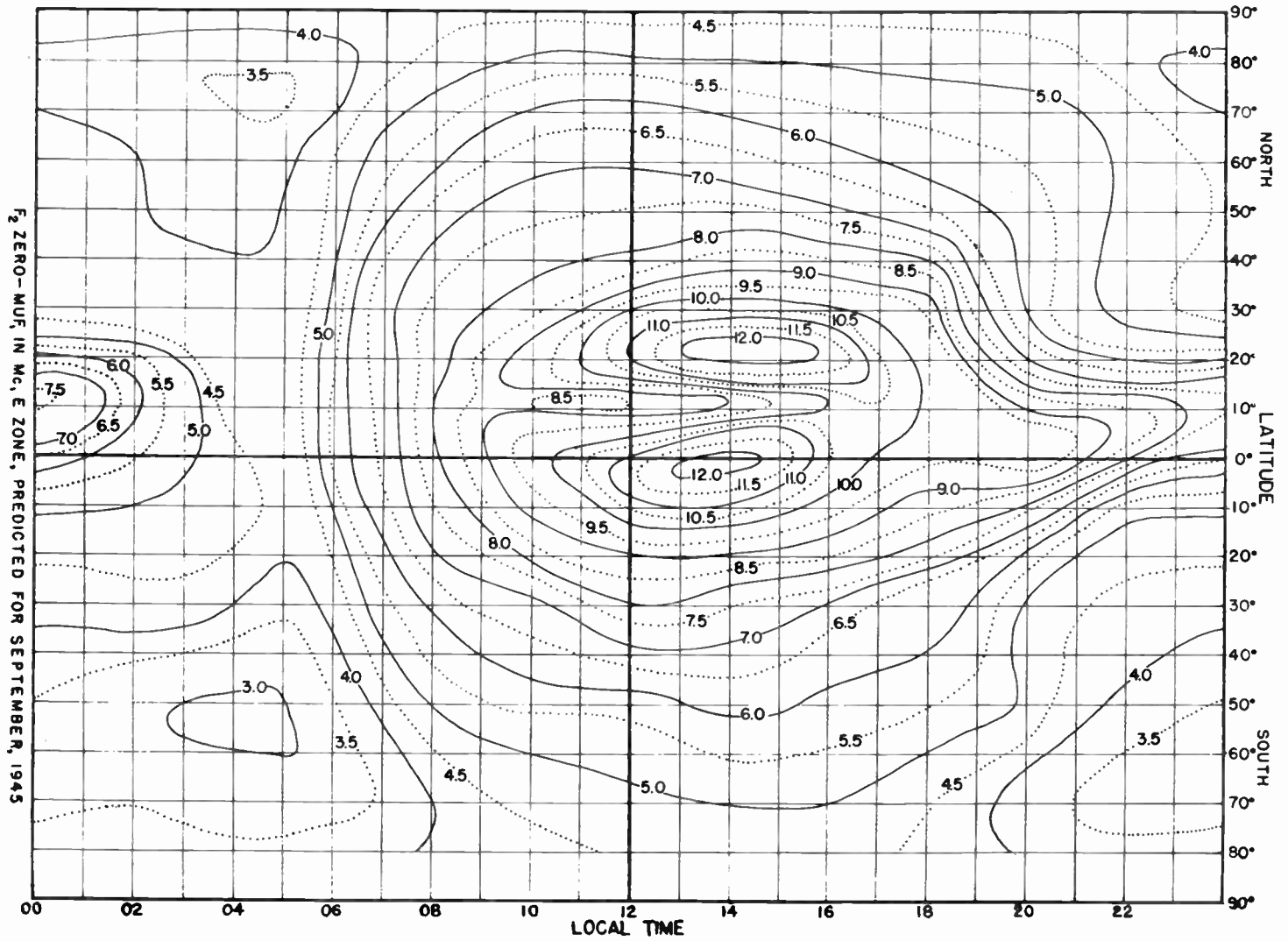


Fig. 18.

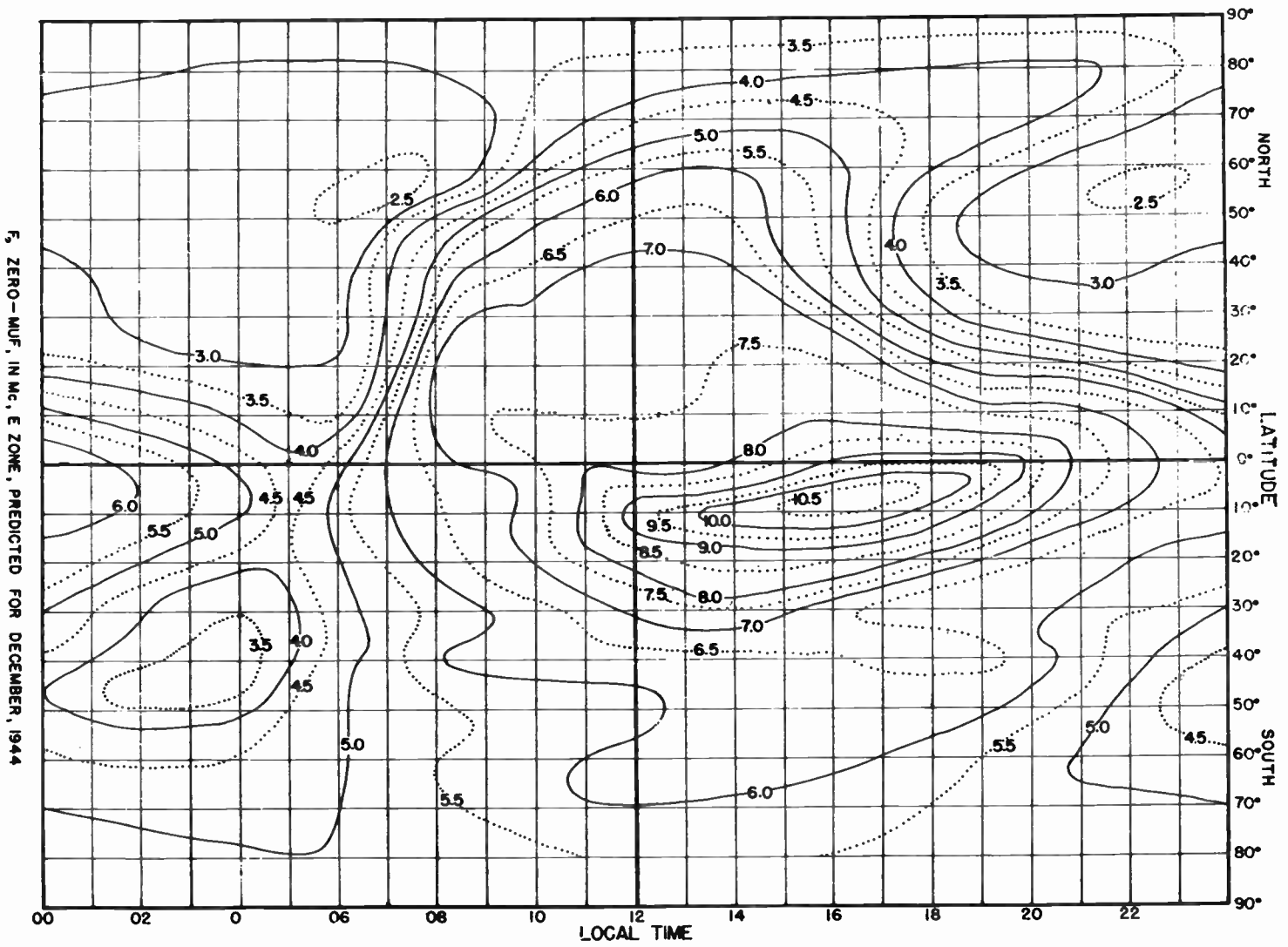
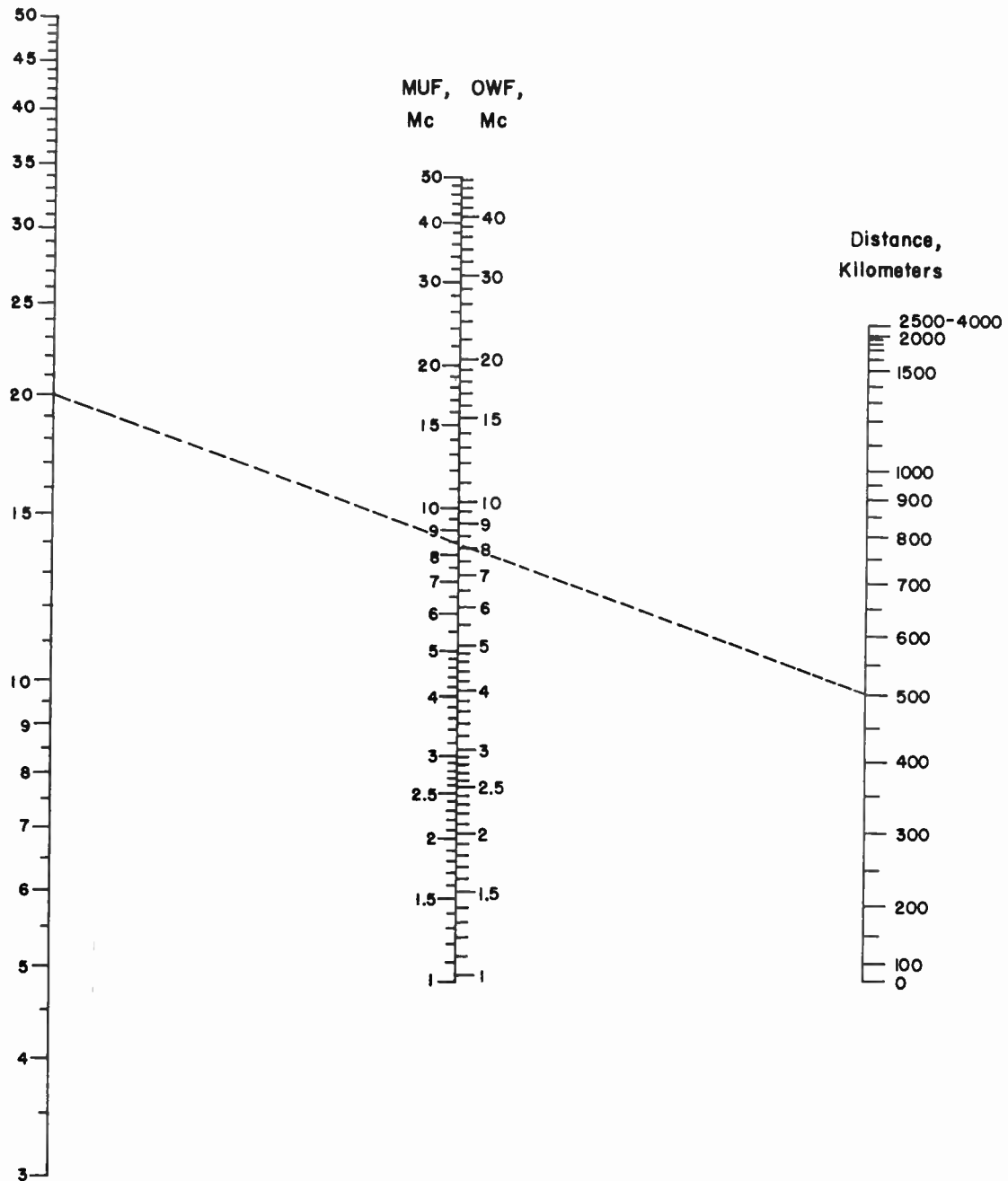


Fig. 19.

2000-Km E muf,
Mc

1 km = 0.62137 mile = 0.53961 naut. mi.
1 mile = 1.60935 km = 0.86836 naut. mi.
1 naut. mi. = 1.85325 km = 1.1516 mi.



Example shown by
dashed lines:

Distance = 500 Kilometers

2000-km E muf = 20 Mc

Combined E-and F₁-Layer muf = 8.4 Mc

Combined E-and F₁-Layer owt = 8.1 Mc

Fig. 20. Nomogram for Transforming E-Layer 2000-MUF to Equivalent Maximum Usable Frequencies and Optimum Working Frequencies Due to Combined Effect of E Layer and F₁ Layer at Other Transmission Distances.

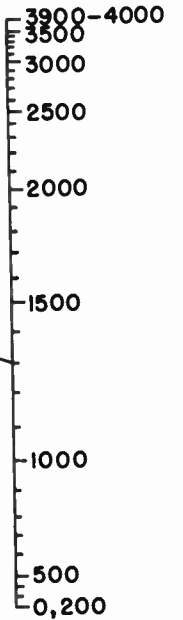
F_2 ZERO-MUF
MEGACYCLES



F_2 - LAYER MUF,
MEGACYCLES



DISTANCE,
KILOMETERS



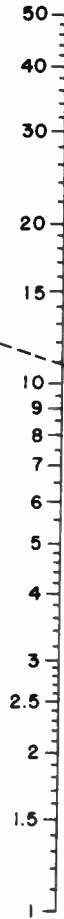
EXAMPLE SHOWN BY
DASHED LINES:
DISTANCE = 1300 KILOMETERS
 F_2 ZERO - MUF = 7.1 MC
 F_2 - LAYER MUF = 10.9 MC

Fig. 21. Nomogram for Transforming F_2 -Layer Zero-MUF to Equivalent Maximum Usable Frequencies at Other Transmission Distances.

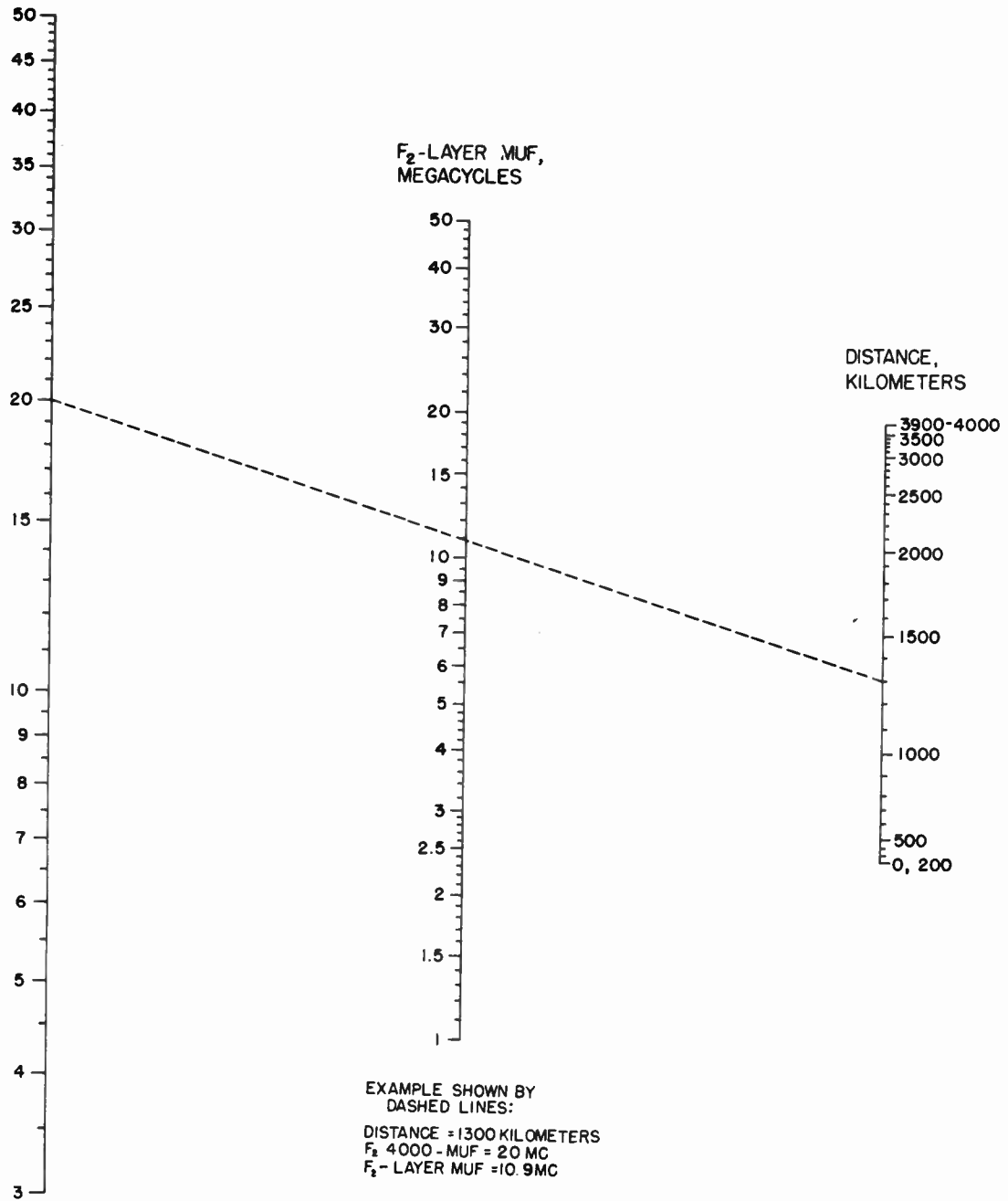
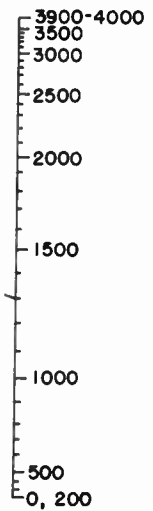
F_2 4000-MUF,
MEGACYCLES



F_2 -LAYER MUF,
MEGACYCLES



DISTANCE,
KILOMETERS



EXAMPLE SHOWN BY
DASHED LINES:
DISTANCE = 1300 KILOMETERS
 F_2 4000 - MUF = 20 MC
 F_2 - LAYER MUF = 10.9 MC

Fig. 22. Nomogram for Transforming F_2 -Layer 4000-MUF to Equivalent Maximum Usable Frequencies at Other Transmission Distances.

1 km = 0.62137 mile = 0.53961 naut. mi.
 1 mile = 1.60935 km = 0.86836 naut. mi.
 1 naut. mi. = 1.85325 km = 1.1516 mi

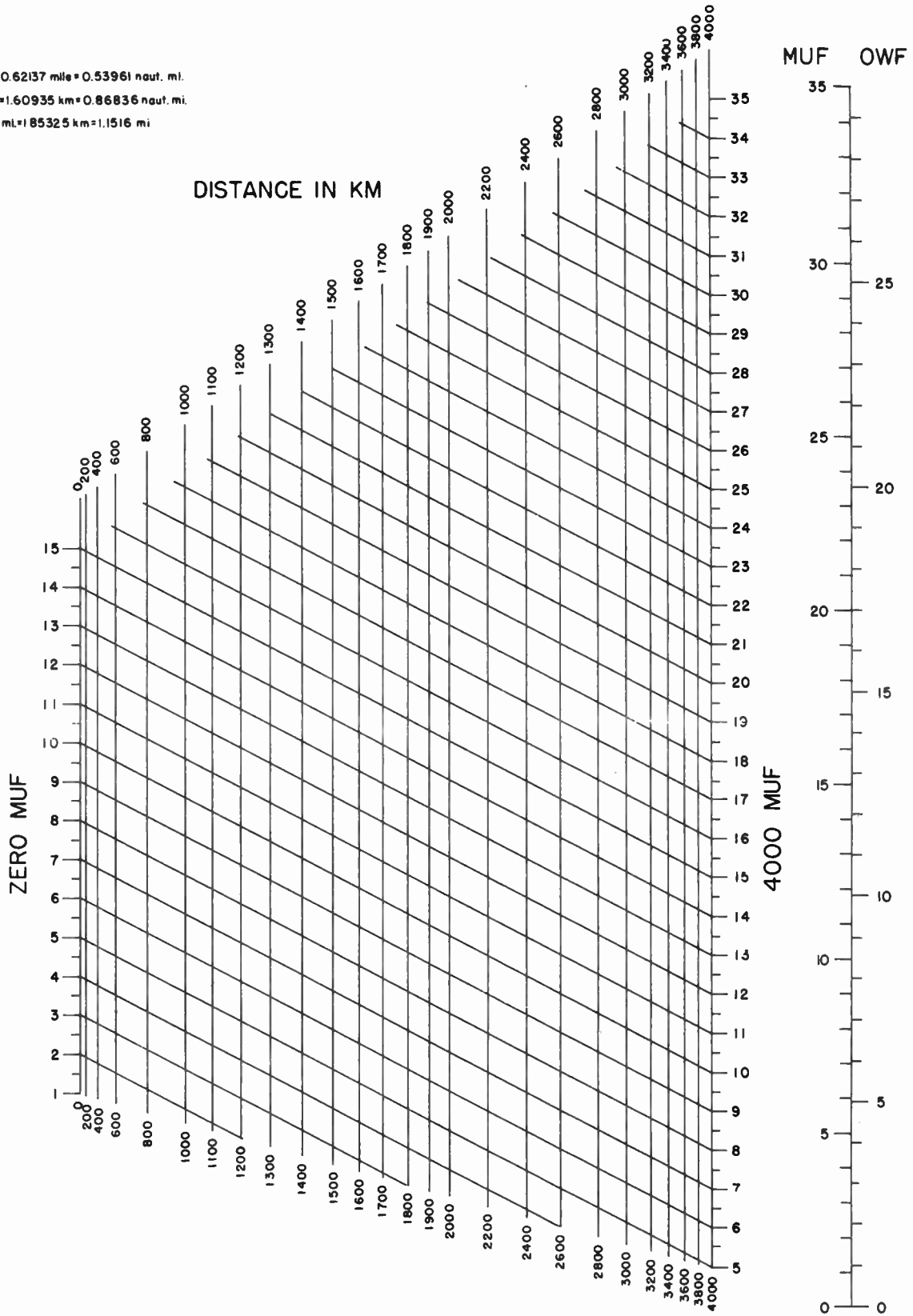


Fig. 23. Nomogram for Transforming F_x -Zero-MUF and F_x -4000-MUF to Equivalent Maximum Usable Frequencies at Intermediate Transmission Distances; Conversion Scale for Obtaining Optimum Working Frequencies.

• CHAPTER FOUR •

PREPARATION OF GREAT-CIRCLE MAPS

PROVIDED WITH THE BACKGROUND INFORMATION OF THE earlier chapters, we are ready, at last, to start our paper and pencil work. With some transparent paper, some work sheets, and a pencil, let's begin.

represent the shortest distance between two points. Radio waves tend to follow paths of this variety.

In Chapter 2, we stated that an accurate representation of the complete map of the earth cannot be made on

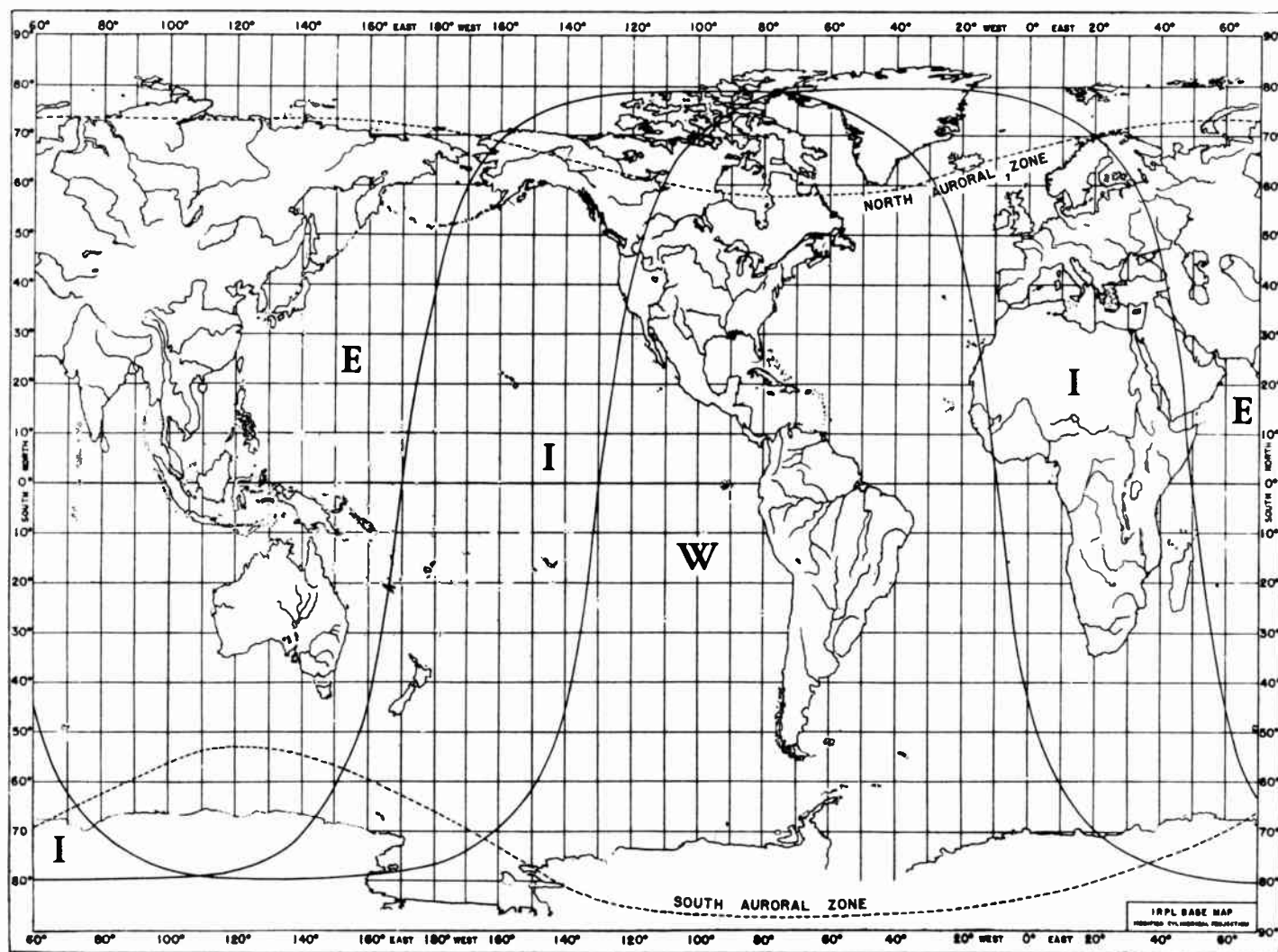


Fig. 24. World Map Showing Zones Covered by Predicted Charts, and Auroral Zones.

First of all, we must plot on a map the positions of our transmitting and receiving stations and connect them by an arc of a circle whose center is also the center of the earth—a so-called “great circle.” Great circles on the surface of the globe, like straight lines on a flat surface,

a flat sheet of paper. Because of the distortions, great-circle paths on a chart will usually be greatly deformed and may not even have any resemblance to the circular form.

We can best illustrate the successive steps to be

employed by calculation of an actual case. Let us take, for example, a path from San Francisco to Moscow, cities whose positions are as follows:

	<i>Latitude</i>	<i>Longitude</i>
San Francisco	37.8° N	122° W
Moscow	55.8° N	37.5° E

Fig. 24 shows a map of the earth (plotted on the cylindrical projection). The scale of this map is identical with those of the ionospheric charts, which were presented in the previous chapter. Let us place our sheet of transparent paper upon this map and put dots at the positions of the two stations. Also, for reference, draw the Greenwich (zero) meridian, the equator, and the two meridians through the stations. The transparent chart will then appear as in Fig. 25.

Now, let us pick up our sheet of transparent paper and superpose it on Fig. 26. The latter depicts great circles, which are the lines tending to radiate from the center of the chart. Keeping the equators coincident on both charts, slide the transparency horizontally (that is, parallel to the equator) until you find a great circle that will

connect or nearly connect the two stations. If no circle given on the map passes exactly through the two stations, you will have to guess approximately where the circle lies that does so. Draw in this great circle on the transparency. Mark the positions of the terminals of the vertical line *Q-Q*.

Now, transfer your sheet to Fig. 27, placing it so that the lines *Q-Q* coincide on both. Ordinarily, it is preferable to make the map of double length, repeating the path after an interval of 360°. The circles (which look like ellipses on the chart) are spaced at intervals of 1000 km. These small circles thus mark out equal distances along the great circles. Note that the equator is almost precisely 40,000 km in length, or 10,000 km to a quadrant. This property makes the kilometer more useful to the student of the ionosphere than either the mile or nautical mile. Along the great circle connecting the two stations, mark off with short lines the intersections of the great-circle path and the 1000-km small circles. The completed map is shown in Fig. 28.

The map you have thus prepared depicts the locations

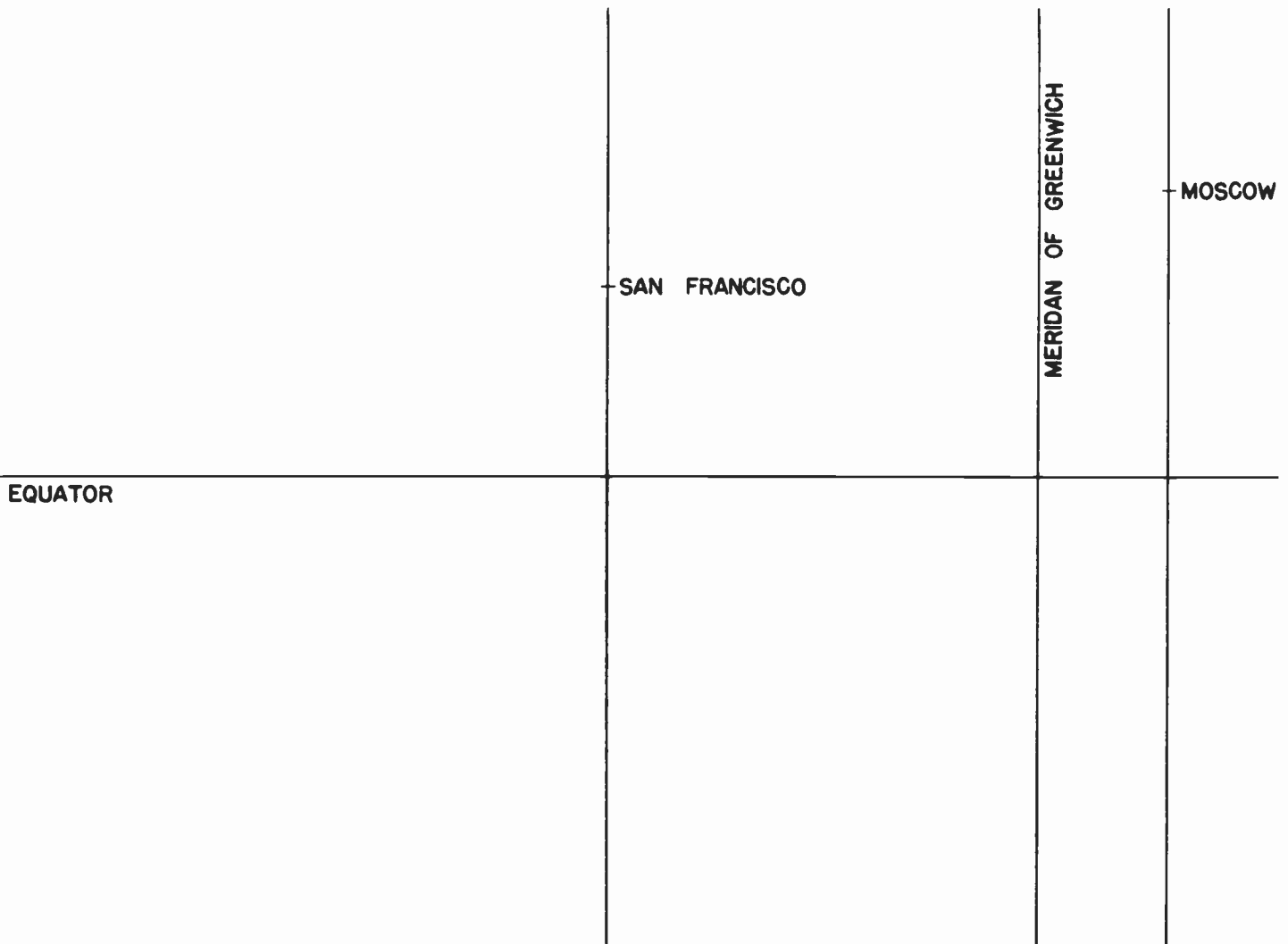


Fig. 25. Overlay, San Francisco-Moscow Path.

of the two stations upon the surface of the earth and the great-circle radio path between them. You have also marked the equator and three meridians, which constitute sufficient identification for the exact location of the path. Note that one may, if he wishes, continue the

great-circle path to run the long way around. In some problems, we may have to distinguish between the long path and the short path. Occasionally, the longer path is an easier mode of travel for the radio wave, especially when a large portion of the long path is in darkness.

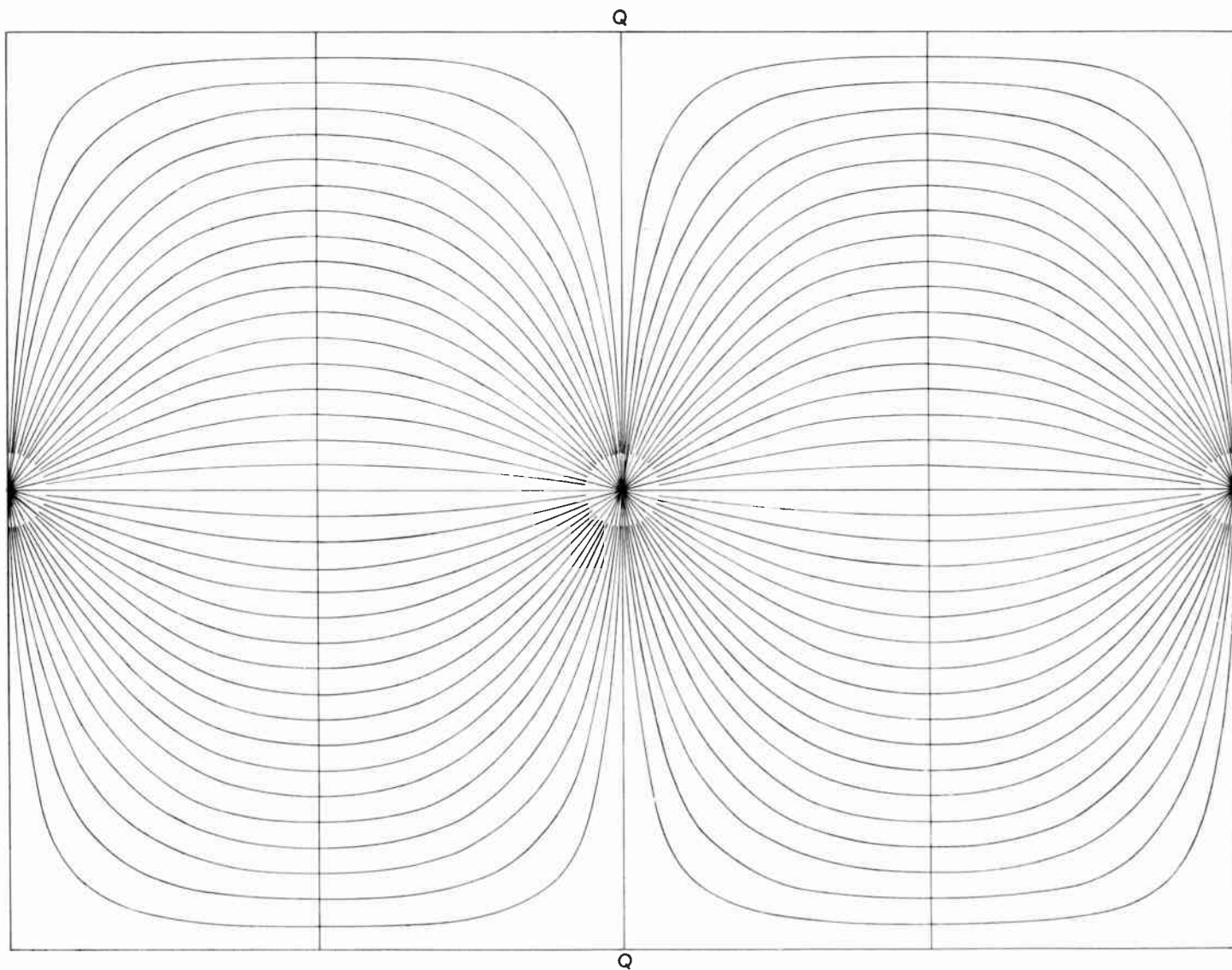


Fig. 26. Great Circle Map.

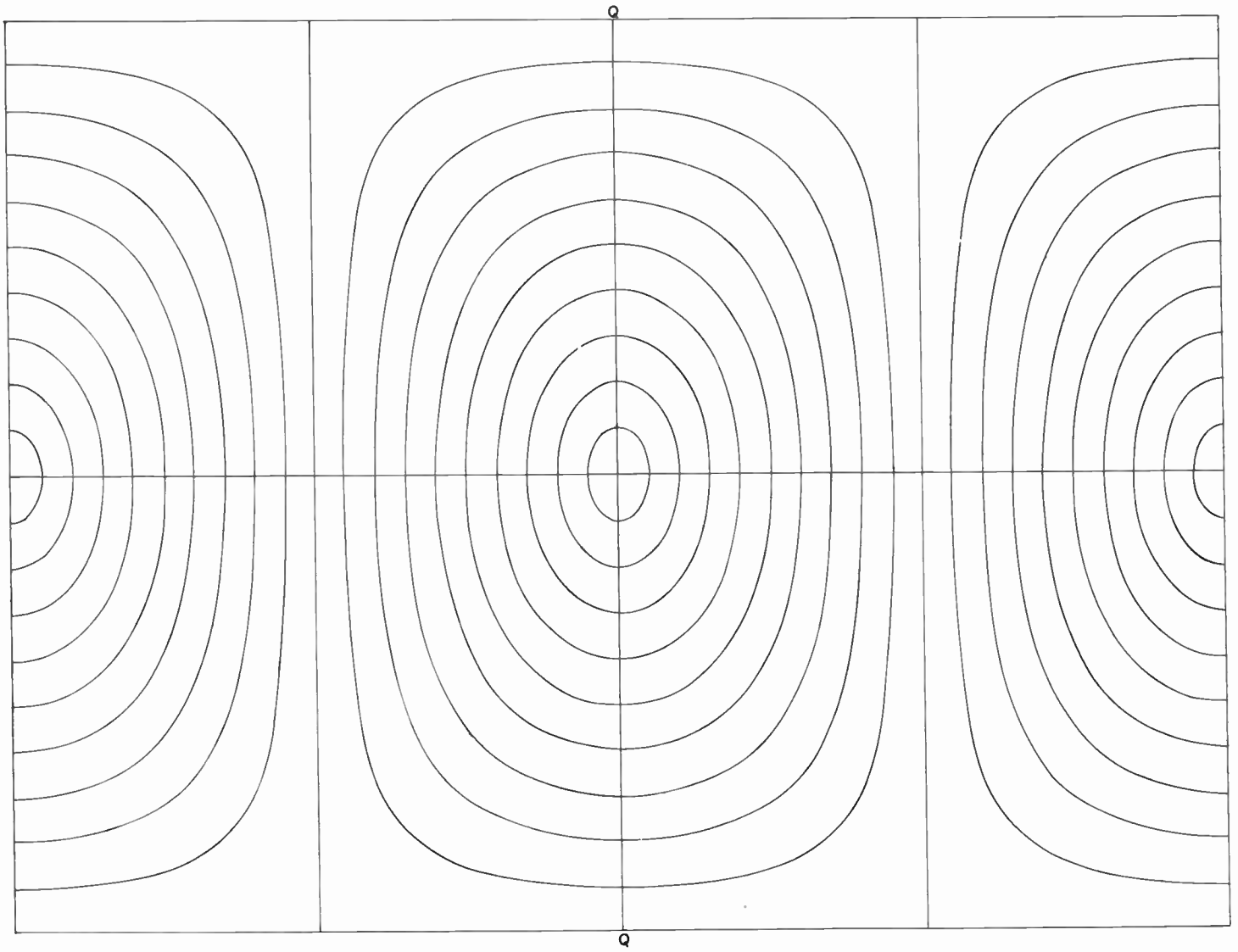


Fig. 27. Distance Circle Map.

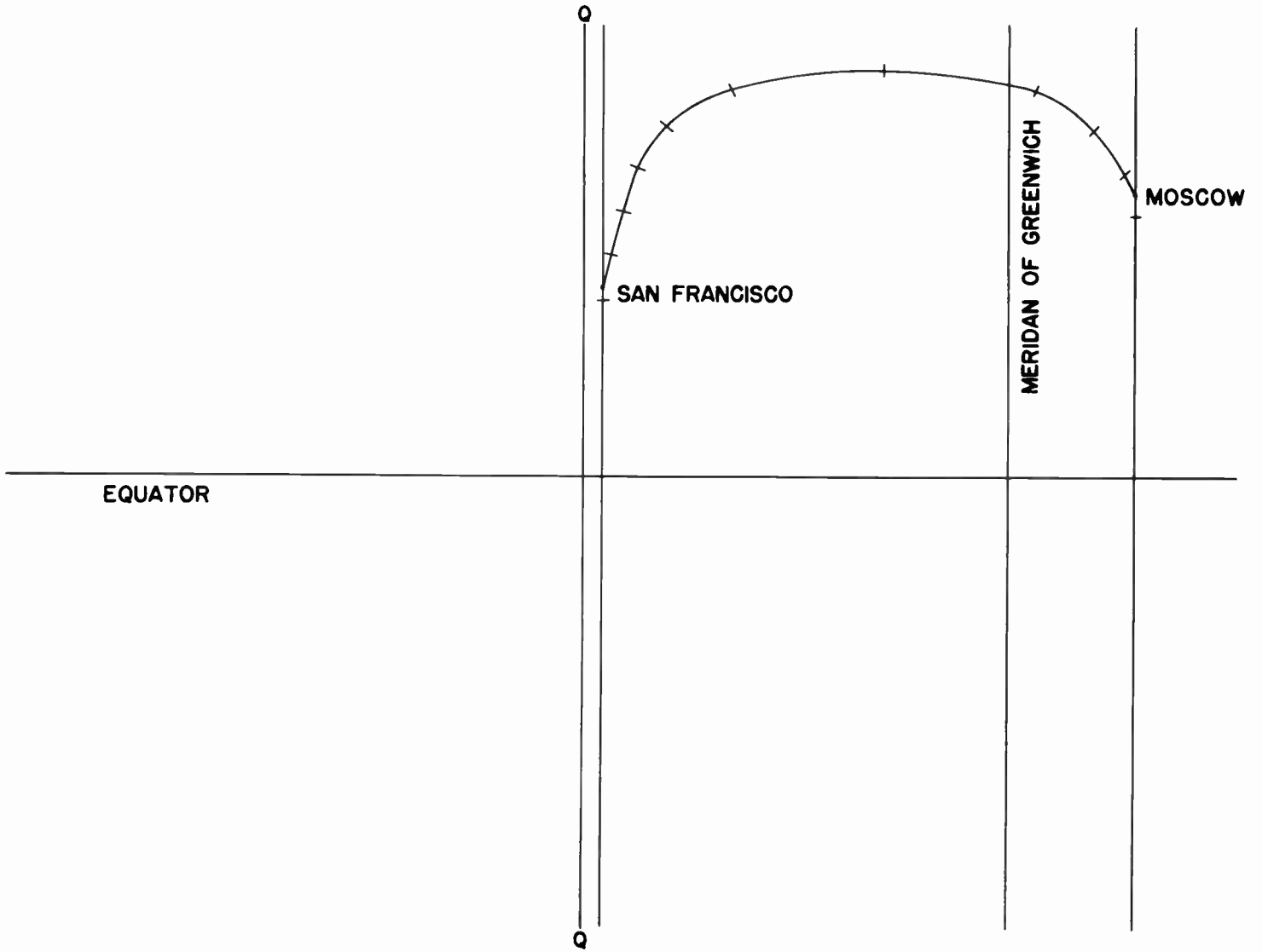


Fig. 28. Completed Overlay, San Francisco-Moscow Path.

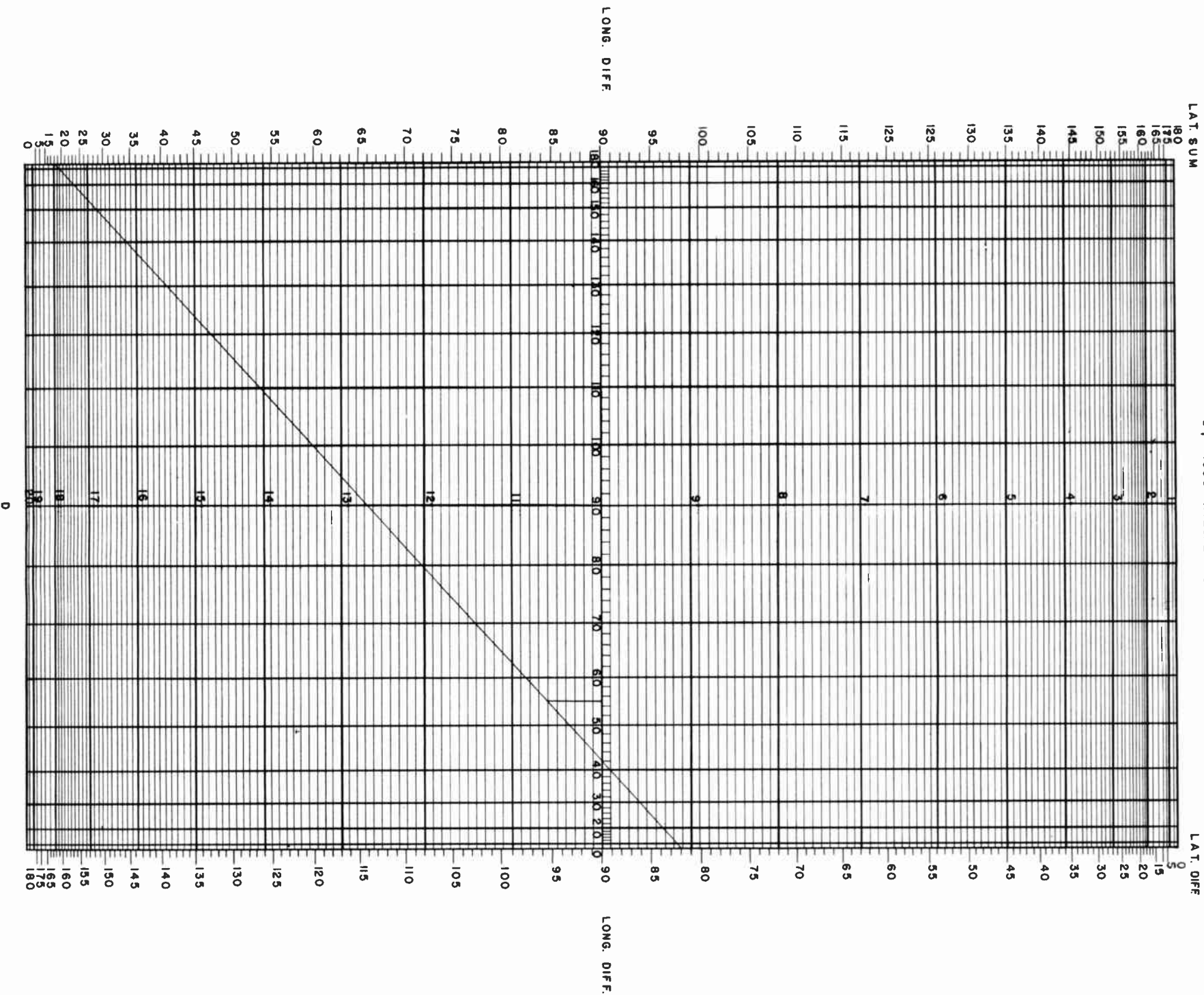


Fig. 29. Distance Nomogram.

• CHAPTER FIVE •

EVALUATION OF DISTANCE BETWEEN TWO STATIONS

WE NOW WISH TO DETERMINE THE GREAT-CIRCLE DISTANCE between the stations. We may add up the 1000-km segments on our previously prepared map, and evaluate the fractions left over at the ends. Or, if we desire greater accuracy, we may employ the nomogram of Fig. 29, and evaluate the distance directly.

To use the nomogram for the present case, we must know the sum of the latitudes and the difference of the latitudes of the two stations, as well as the difference in longitude. Thus, for the San Francisco-Moscow path we have

$$\begin{aligned} \text{Latitude sum} &= 93.6^\circ \\ \text{Latitude difference} &= 18.0^\circ \\ \text{Longitude difference} &= 159.5^\circ \end{aligned}$$

Referring to Fig. 29, connect 93.6° on the latitude-sum line with 18.0° on the latitude-difference line. The line, so drawn, crosses the chart at a diagonal angle. Find the value 159.5° on the longitude-difference scale running horizontally across the top or bottom of the chart and note the intersection of the line previously drawn with the vertical line at 159.5° . This point of intersection falls near one of the remaining horizontal lines on the chart. The figure on this line, read from the vertical central scale, is the distance in thousands of kilometers. The value of the present example is 9400 km.

When both stations are south of the equator, the sum

and difference will be negative since south latitudes are considered minus. Employ the nomogram, however, precisely as if the station lay in the northern hemisphere. When one station is north and the other south of the equator—for example, at latitudes 43° and -21° , we subtract and add algebraically, minus a minus becoming plus. Thus,

$$\begin{aligned} \text{Latitude sum} &= 43 + (-21) = 43 - 21 = 22 \\ \text{Latitude difference} &= 43 - (-21) = 43 + 21 = 64 \end{aligned}$$

If either figure comes out negative, as for example, Latitude sum = $17 + (-21) = 17 - 21 = -4$,

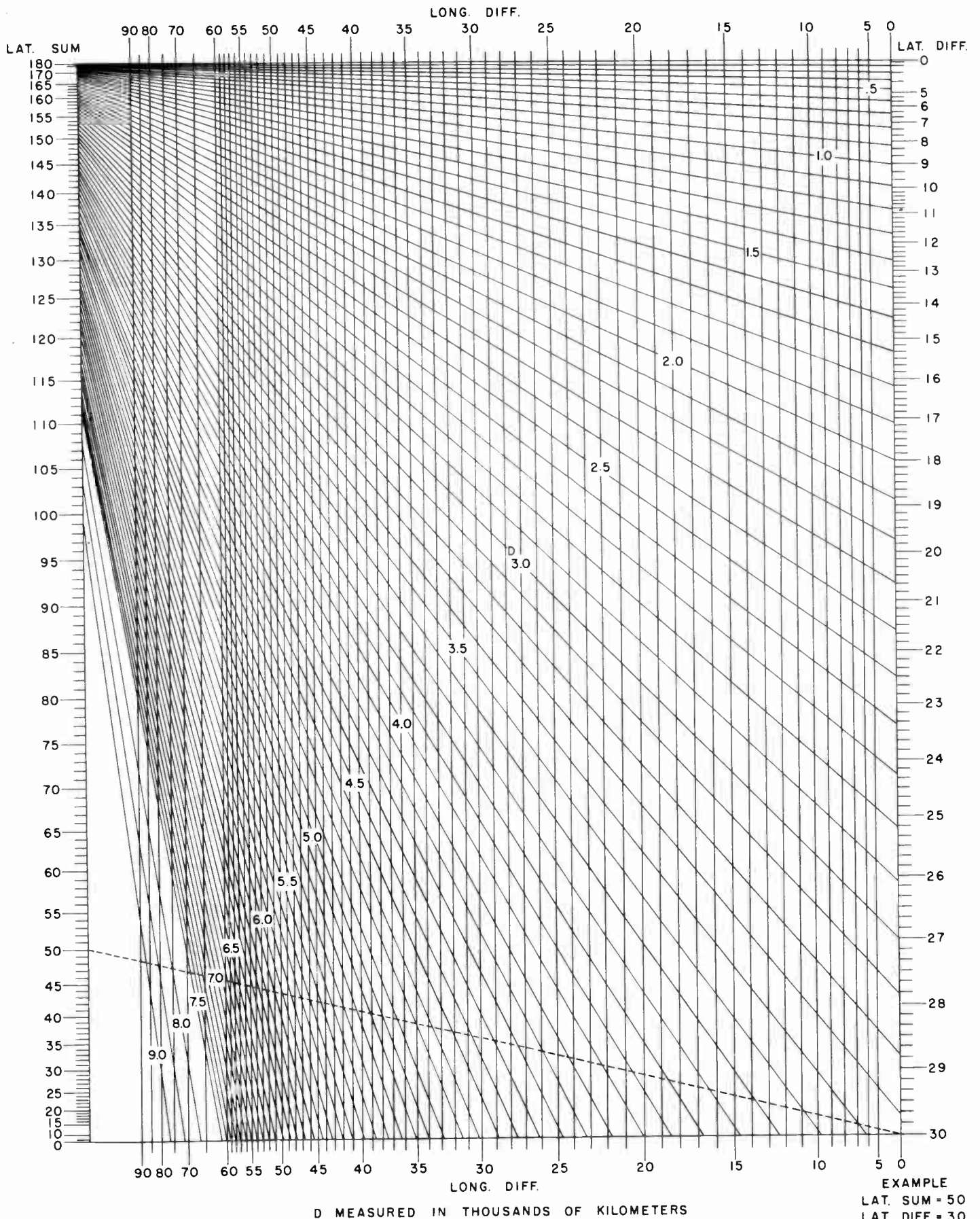
treat the value as positive—that is, use: latitude sum = +4. A sample work sheet for the distance calculations appears in Fig. 30.

For nearby stations, for which latitude difference may be small, the nomogram of Fig. 31 is preferable to that of Fig. 29. The procedure for using it is identical with the foregoing, except that certain of the lines are now inclined so that the scale for small distances is considerably magnified.

These calculations give the short path—that is, the minimum distance between the stations. Since the total length of a great circle is 40,000 km, the long-path distance is merely 40,000 minus the derived short-path value.

STATION A _____ LATITUDE STATION A _____ LATITUDE STATION B _____ LATITUDE SUM (A+B) _____ LATITUDE DIFFERENCE _____	STATION B _____ LONGITUDE STATION A _____ LONGITUDE STATION B _____ LONGITUDE DIFFERENCE _____ DISTANCE IN KILOMETERS _____
STATION A _____ LATITUDE STATION A _____ LATITUDE STATION B _____ LATITUDE SUM (A+B) _____ LATITUDE DIFFERENCE _____	STATION B _____ LONGITUDE STATION A _____ LONGITUDE STATION B _____ LONGITUDE DIFFERENCE _____ DISTANCE IN KILOMETERS _____

Fig. 30. Work Sheet for Distance between Stations.



EXAMPLE
 LAT. SUM = 50
 LAT. DIFF = 30
 LONG. DIFF = 30
 D = 4.46

Fig. 31. Distance Nomogram.

• CHAPTER SIX •

DETERMINATION OF MAXIMUM USABLE FREQUENCIES

THE ANALOGY OF THE SIEVE, GIVEN IN CHAPTER 1, clearly illustrates the various processes that we must employ in predicting the maximum usable frequency (MUF)—that is, the highest frequency that will not escape through the network of the ionosphere.

Chapter 3 presented several illustrative maps of the ionospheric mesh for various months and discussed the procedure for determining the MUF for a hop of a given length. In Chapter 4, we prepared a map of the great-circle path of the radio wave. In Chapter 5 we calculated the distance between the stations.

If the distance is less than 4000 km (2500 miles or 2200 nautical miles), the E and F_1 layers may be the determining factors for daytime transmission. Ordinarily, however, they will dominate only for distances between 600 and 2700 km. The F_2 layer will usually control for distances up to about 600 and beyond 2700 km during the day, and will always control during the night, except when “sporadic E ” is present.

If the distance between the stations is less than 4000 km, put a cross on your drawing at the mid-point of the great-circle path. This cross represents the control point or point where the wave is reflected from the ionosphere. For tracks longer than 4000 km, put crosses at the points 2000 km from each station. The region between the two crosses represents the portion of the path controlling the MUF. Next, place the transparent chart in its original position upon the cylindrical projection of the earth (Fig. 24). If the transmission distance is less than 4000 km, record on your work sheet the zone, I , E , or W , in which the control point falls. If the distance is greater than 4000 km, record all the zones through which the path between the two control points passes. In addition, mark the boundaries between these same zones on the great-circle path between the two stations.

Now superpose the great-circle transparency upon the F_2 -zero or 4000-MUF map for the zone in which the control point falls. (For distances above 4000 km, where two or more zones are involved, use the map of the zone in which the first control point falls.) Make sure that the equators on the two charts are coincident. Slide the transparency horizontally along the equator

until the 0° meridian on the transparency is coincident with the vertical line on the lower chart that represents the local time at Greenwich. (For conversion to local time at the transmitter or receiver, see Chapter 2.) A given position of the map corresponds to a certain time of day, and the horizontal sliding represents the rotation of the earth with respect to a stationary ionosphere. The reason for a double-length map, with repeated path as recommended in Chapter 4, is now apparent. When a portion of the track slides out of the picture, a corresponding portion reappears on the opposite side. The value of the local time for any given station may be read at the base of the meridian which passes through it.

With the transparency superposed on the 4000-MUF map, note the *lowest* value of the MUF at the cross for paths of 4000 km and less. If the path is greater than 4000 km, note the lowest MUF located along the transmission path between the two control points, if this portion of the path is entirely included by a single zone. If more than one zone is involved, note the lowest MUF between the first control point and the first zone boundary. Repeat the process for the other zones, using the MUF map appropriate for the zone, and note the lowest MUF value along the remainder of the path up to the second control point. Choose the lowest of these values as the 4000-km MUF. Multiply this figure by the distance factors in Table 2. The result is the approximate MUF for the given distance.

If the distance is between 0 and about 2000 km, one may get a more accurate MUF from use of the zero- rather than the 4000-MUF map of the ionosphere. The procedure is essentially the same as that of the foregoing paragraph. Note the zero MUF at the mid-point of the path, and then apply the factors of Table 3 or the nomogram of Fig. 21 to obtain the MUF for the actual path distance.

If higher accuracy is desired, some extra work is necessary. Use both the 4000- and the zero-MUF charts as explained in the previous paragraphs to determine the lowest F_2 MUF's between the two control points on the path. Then employ the nomogram of Fig. 23 to get the actual MUF for the given distance. This procedure

RECORD SHEET FOR DETERMINATION OF MUF FOR A PATH LESS THAN 4000 KM.

FROM (A) _____ LAT. _____ LONG. _____ TO (B) _____ LAT. _____ LONG. _____
 PREDICTED FOR _____ DISTANCE _____ KM. ZONE OF CONTROL POINT _____
 DISTANCE FACTOR F_2 4000 _____ DISTANCE FACTOR $E-F_2$ 2000 _____

1	2	3	4	5	6
GREENWICH CIVIL TIME	F_2 4000 MUF MOS.	CORRECTED MUF COL. 2 x F_2 4000 DISTANCE FACTOR	$E-F_1$ 2000 ⁹ MUF MCG.	CORRECTED MUF COL. 4 x $E-F_1$ 2000 DISTANCE FACTOR	PREDICTED MUF (OR OWF) (SEE TEXT)

Fig. 32.

CALCULATION OF MUF FOR PATH GREATER THAN 4000 Kms.

STATION A (TRANSMITTER) _____ STATION B (RECEIVER) _____
 DISTANCE IN KM. _____ ZONE OF CONTROL PATH _____

GCT	ZONE I		ZONE II		ZONE III		DISTANCE FACTOR	MUF XDF (CORRECTED) MUF	OWF (85% OF CORRECTED MUF)
	F_1	F_2 MUF	F_1	F_2 MUF	F_1	F_2 MUF			

Fig. 33.

makes a partial allowance, at least, for the fact that the F_2 height varies with time of day. The Tables 2 and 3 and associated nomograms rely on an average F_2 height.

For shorter paths, one should ordinarily compute values for both the E , F_1 , and F_2 layers. The procedures for the former are essentially the same as for the F_2 layer, except that one need not distinguish between the different zones. The distance factors appear in Table 1 and the nomogram of Fig. 20. Adopt for the actual MUF the *greater* of the two figures obtained. If the E , F_1 MUF exceeds the F_2 , the signal will not penetrate to the latter layer at all. If the E , F_1 MUF is lower, the F_2 will act to reflect frequencies transmitted through the lower-lying E , F_1 . Sample record sheets for longer and shorter paths appear in Figs. 32 and 33. The columns labeled *corrected MUF* are the 2000- and 4000-km MUF's read from the charts, multiplied by the appropriate distance factors. The final column gives the predicted MUF's, the higher of the values E , F_1 or F_2 . Because of daily unpredictable fluctuations in the ionosphere, one may preferably enter in this last column 97 per cent of the correct MUF for the E , F_1 layer or 85 per cent of the F_2 values, whichever is higher. These are safety factors, adjusted to make the optimum working frequency (OWF) as reliable as possible for days on which the ionospheric mesh may be abnormally large. The scale of Fig. 23 may be used for the F_2 conversion of MUF to OWF. Note that the uncertainties are less for the E , F_1 layer than for the F_2 layer.

If an operator uses the F_2 MUF as his transmission frequency on a path of less than 4000 km, the receiving station will lie just on the outside edge of the skip zone. Points any nearer to the transmitter will receive signals

erratically, if at all.

The basic E , F_1 and F_2 charts change not only from month to month, as previously indicated, but also from year to year. The values of the frequencies are closely associated with the state of solar activity, as evidenced by the sun spots and other solar phenomena. Their effects will be discussed in more detail in a later chapter.

For paths in excess of 4000 km, only the F_2 calculation is ordinarily required. Rarely would the E , F_1 dominate over a very long path.

There is one additional point that may have occurred to the reader. Suppose that the transmission is required over a path of 5000 km. This distance is too great for one-hop F_2 . Should we then not consider the transmission as resulting from two hops, each of 2500 km, and determine the MUF separately for each, applying the 2500-km distance factor? The argument appears to be logical. We have definite evidence, especially from the Loran records, of multihop transmissions. In the early stages of our ionospheric applications during World War II, we actually attempted to apply this apparent improvement. Many test cases indicated, however, that the effective MUF was considerably higher than the figures derived from such calculations. The simpler method previously explained proved to give better agreement with the observations.

These studies and applications of ionospheric measurements to the solution of transmission problems represent a new science. During the next few years our basic knowledge should be rapidly increasing. Eventually, many refinements should be possible in the prediction methods.

• CHAPTER SEVEN •

THE ABSORPTION PROBLEM AND RADIO NOISE

THE CALCULATIONS OF MAXIMUM USABLE FREQUENCY make no use of the stated power of the transmitter. For a signal to be received at all, the frequency must lie below the MUF. There is, however, a second condition that must be fulfilled. Radiation spreads out from the transmitting antenna, and thus dwindles in intensity with distance. In addition, the beam is absorbed, lower frequencies being more affected than higher ones.

For a signal to be receivable, the electric field produced at the distant point must exceed the noise level of the receiver or the noise level of the atmosphere (static), whichever is greater. For the frequencies between 1.5 and 30 megacycles, the latter will usually be the determining factor. Radio noise is by no means constant. It changes with time of day and is different for various locations on the face of the earth. Local thunderstorms, especially in the tropics, may raise the noise level to a very high value. In nontropical regions, the noise levels depend on atmospherics transmitted from the tropical storm centers, as well as on local thunderstorms. All noise-zone boundaries are farther north during the northern summer, when the tropical storm centers are farther north.

Figs. 34 to 38 depict the field intensities required for reliable reception of a phone signal. To apply these curves to other types of transmissions—for example, CW, printing, and so forth—we introduce the corrections given in Table 7 of the following chapter. The variations with time and frequency are caused by noise conditions, which have been classified into five different grades according to the areas of the world shown in Figs. 39 and 40, on a scale of 1 to 5 of increasing static interference.

Note that the shapes of the noise curves in the range from 20 to 40 hours—that is, during the night—are quite similar, although the magnitude of the noise increases at the rate of 8 to 10 db* for each grade. These curves for night conditions, when ionospheric absorption is small, represent the approximate distribution of static interference with frequency as actually produced by

* "The difference in loudness level between two sounds is defined as the common logarithm of the ratio of the two intensities, the unit difference being called a *bel*." A decibel, abbreviated db, is a unit one tenth this size.

thunderstorms. There has been some modification of these curves by propagation effects, but the statement applies most accurately for noise grade 5, because the receivers are then close to the actual sources of interference.

The remaining curves, for other hours, represent the modification of the noise curves by radio propagation. For grade 5 (Fig. 38) the chief modification is a slight decrease in noise level because of ionospheric absorption. Frequencies in the range of 1 to 5 megacycles are weakened more than the others because the absorption is greatest near 1.5 to 2 megacycles.

Receivers located in noise grade 4 are somewhat more distant from the tropical noise centers. The over-all weakening is caused by this distance and by the fact that storms in these areas are less violent than those of grade 5. The big daytime dip from 0700 to 1100 comes from the increased ionospheric absorption. This dip would apply to noon and afternoon hours also, if areas 5 were the only noise centers. But local thunderstorms within the areas are common around noon and continue through the afternoon. These disturbances tend to raise the general noise level.

In noise grade 3, the local showers are much less effective, and they tend to occur later. Thus the noon value shows the heavy minimum at 1.8 megacycles, caused by the absorption. The magnitude of the minimum increases for grades 1 and 2. The tendency for 1600 to lie above that for 0800 is a residual effect of the afternoon showers.

The nighttime noise usually exceeds that of the daytime. The main exception to this rule occurs for grades 1 to 3, for frequencies greater than about 12 megacycles. This effect is mainly one of skip. During the night, the ionospheric MUF's are not high enough to transmit noise from the distant storm centers. Thus, for frequencies in excess of about 12 megacycles, the receiving conditions are generally better at night.

From the above discussion, the reader may have gained the impression that our approach to the noise problem is somewhat naive and artificial. That impression is correct. Actually, the problems of radio noise

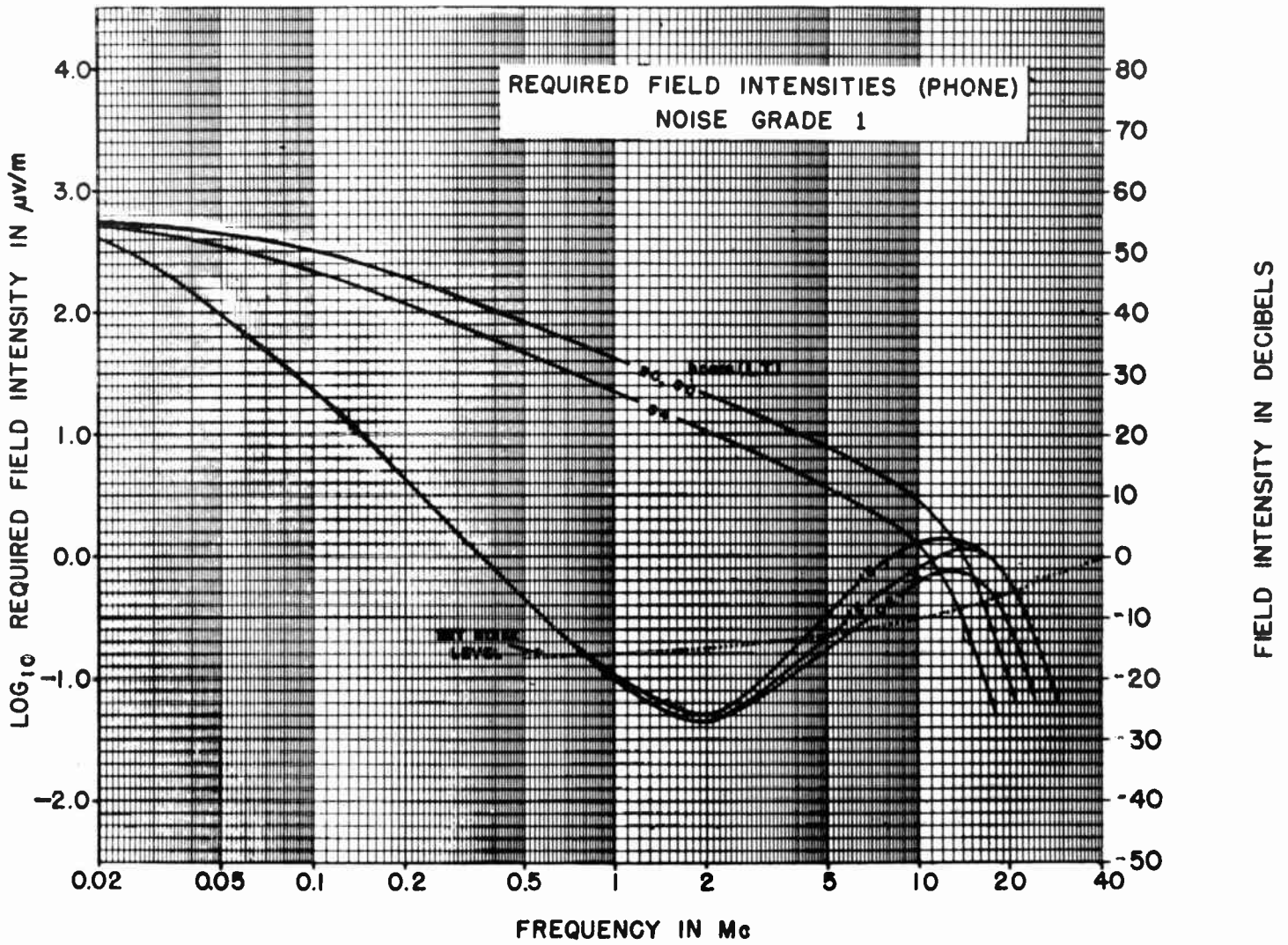


Fig. 34.

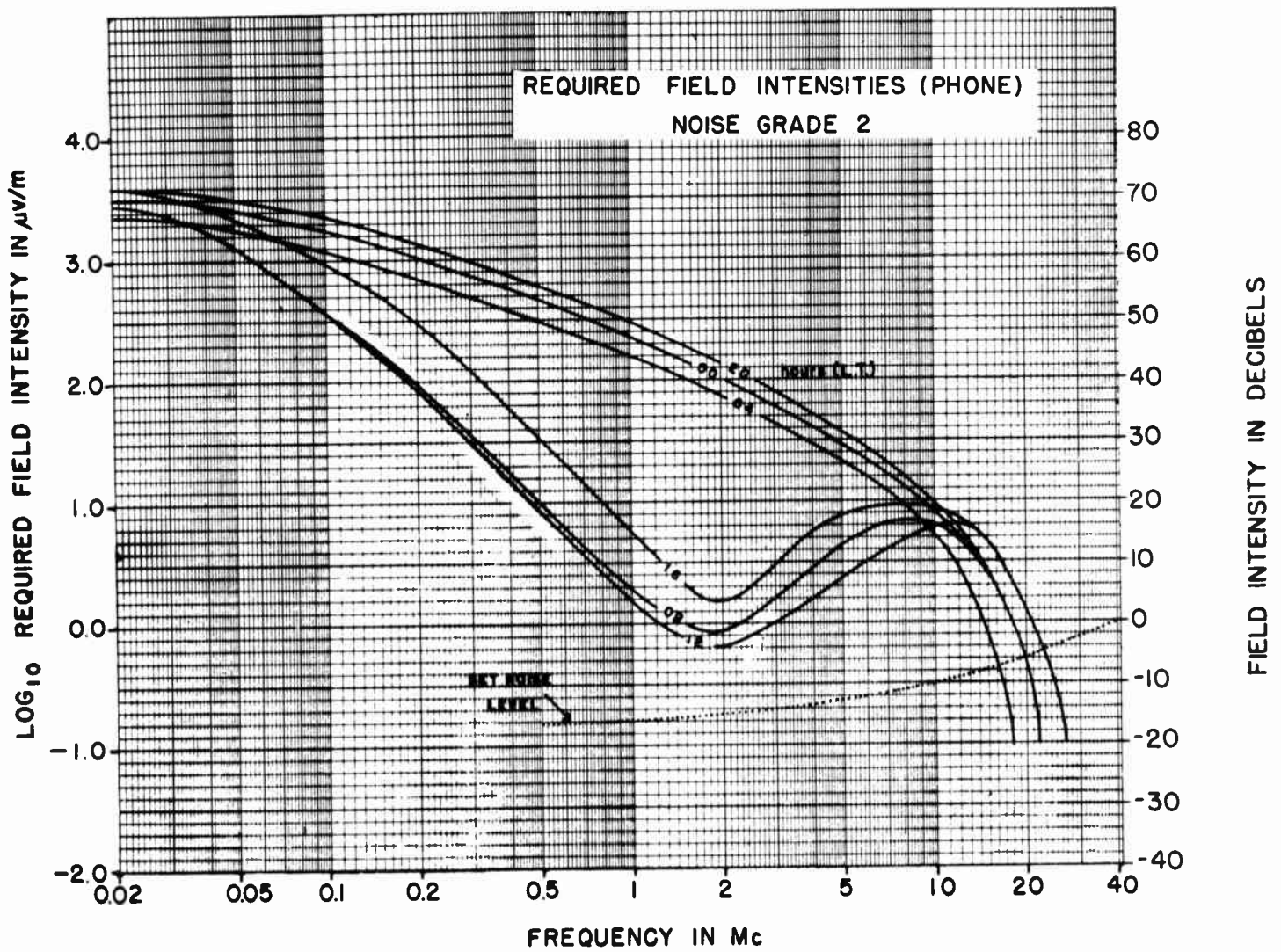


Fig. 35.

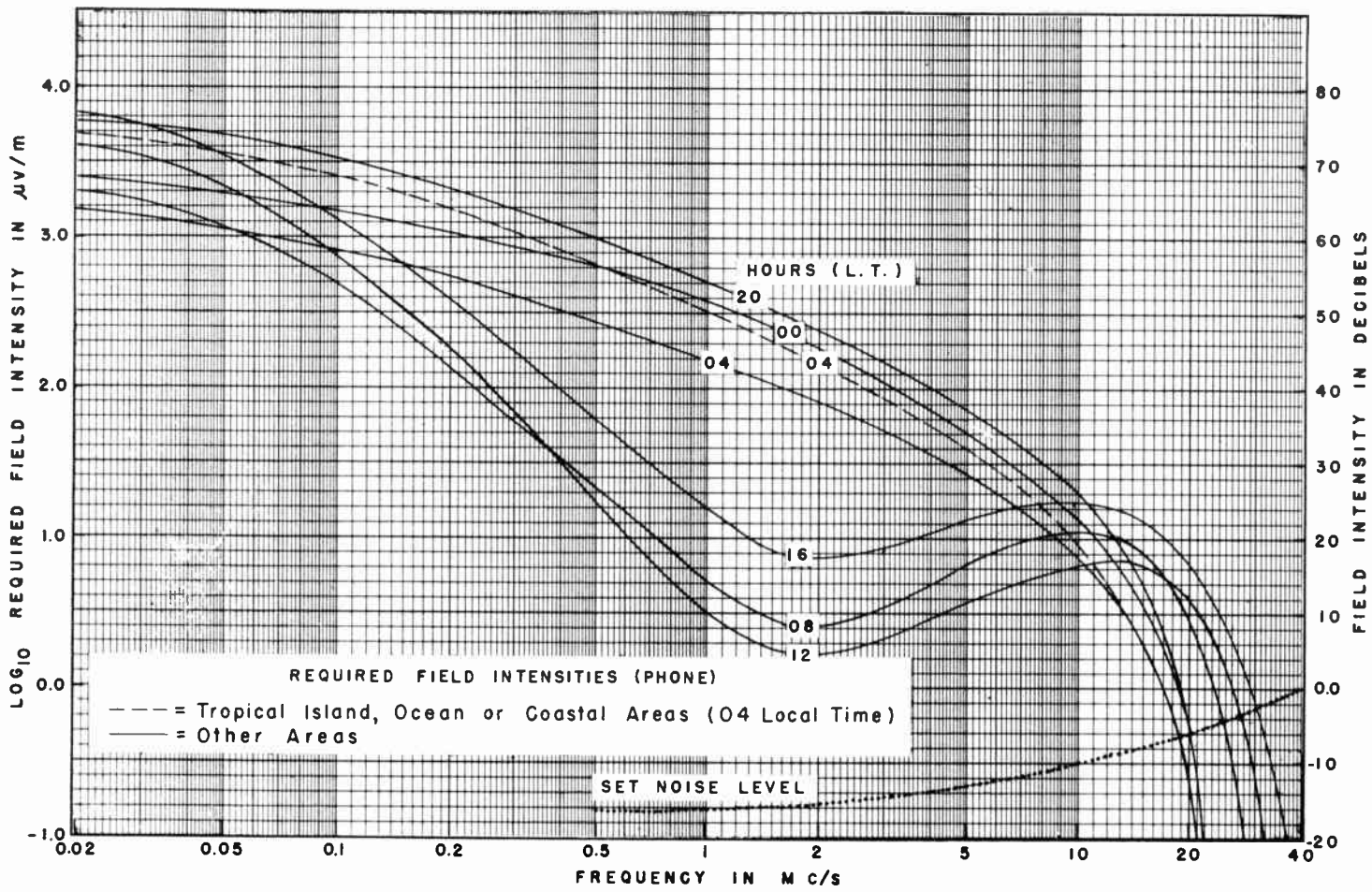


Fig. 36.

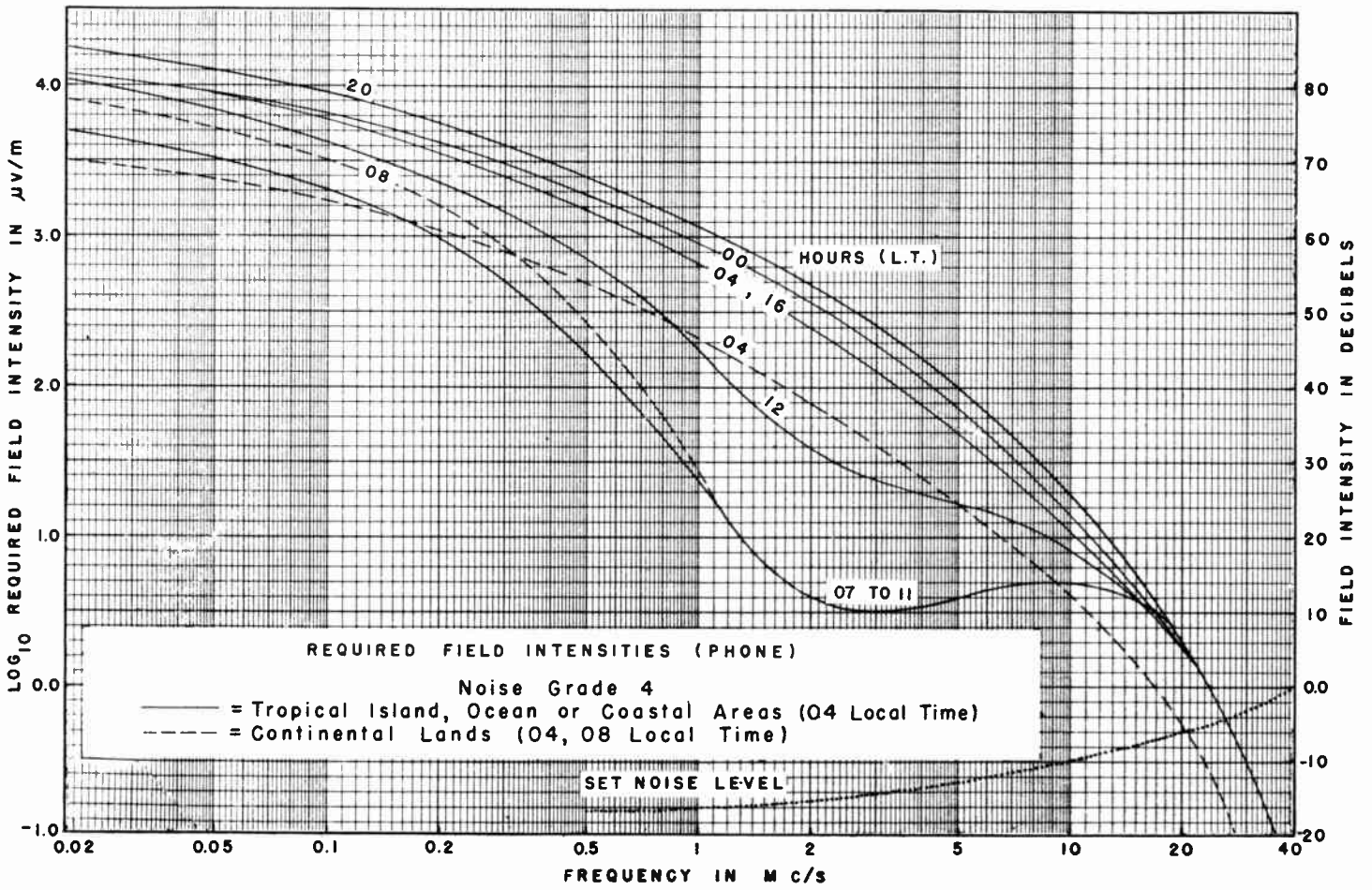


Fig. 37.

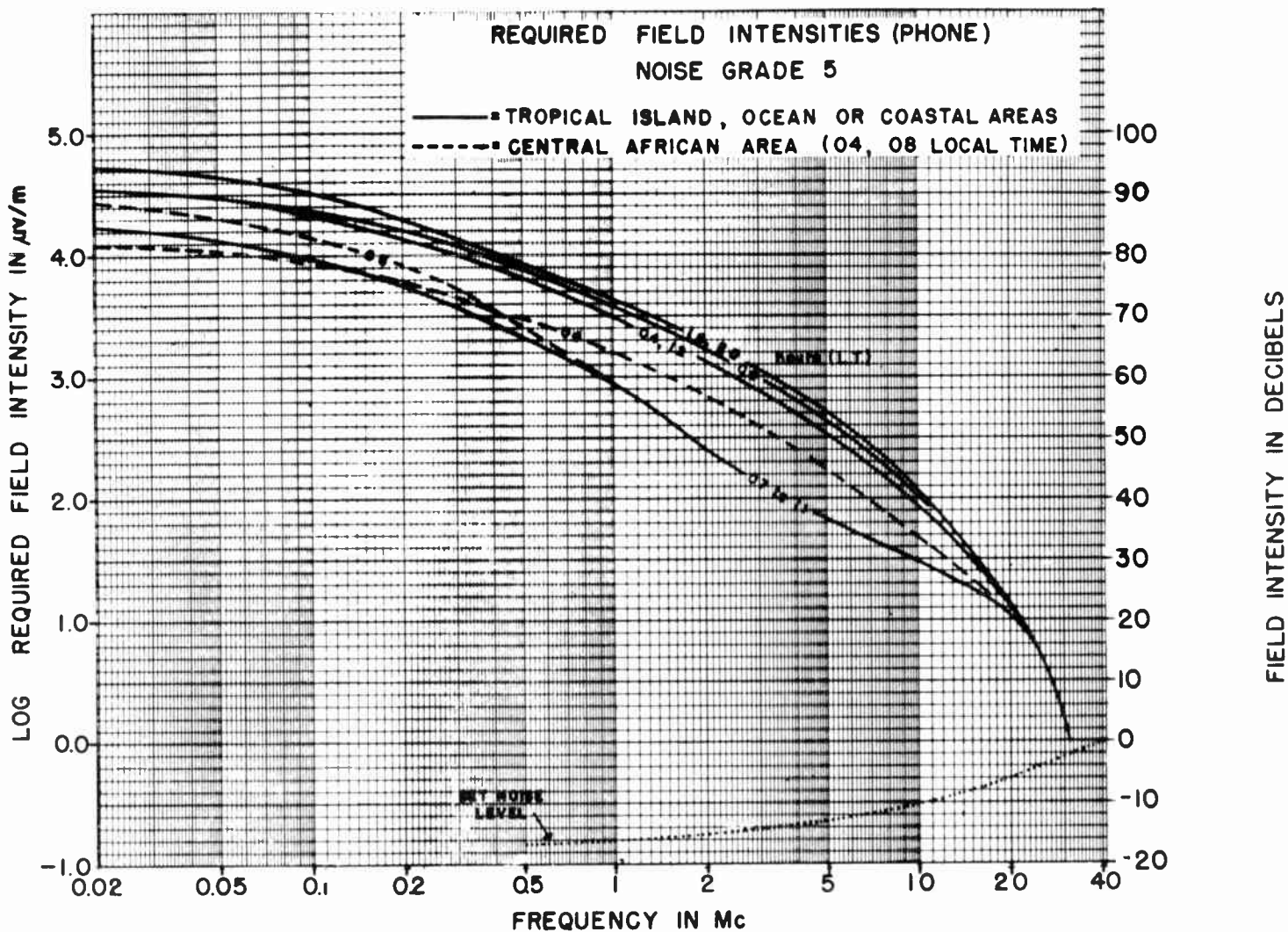


Fig. 38.

are extremely involved—almost as complicated as the weather. The noise levels here outlined have been derived from a rather arbitrary analysis. The data require checking—extensive checking—by actual measures, which are still unavailable. During World War II, the Allies planned an extensive program of noise measurement, but the war ended shortly after the studies were begun.

Despite the preliminary character of the above analysis, the hopeful fact remains that studies and checks of the theory on thousands of circuits and hundreds of thousands of transmissions have shown excellent agreement of the LUHF's with their theoretical values. This analysis was made by the military. It is true that individual circuits occasionally gave trouble. There were some transmissions that came through in spite of noise, absorption, and interference; and vice versa.

A detailed analysis of noise must take into account the variations with bearing. Unavoidable inaccuracies exist that arise from weather uncertainties. A scheduled

storm may fail to occur or an unexpected storm will appear in an unlikely area. For this reason, the calculated LUHF's have uncertainties amounting to one and occasionally two megacycles, according to the nature of the path and time of day. The forecasts for long circuits are likely to be more accurate than for short circuits. Those for daytime conditions are more accurate than the forecasts for night.

The world maps purposely omit the transition months of April and October. The noise variability seems to be greatest for those times of year. If one wishes to forecast for these months, he will find it safer to make the calculation for the noise grades from both maps. The result will indicate the probable range of uncertainty. The other alternative is to average the noise grades for both maps.

The original five noise grades were found to represent too large an interval. In preparation of the LUHF nomograms, which will be discussed in detail in the next chapter, we find it desirable to add grades $1\frac{1}{2}$, $2\frac{1}{2}$, $3\frac{1}{2}$,

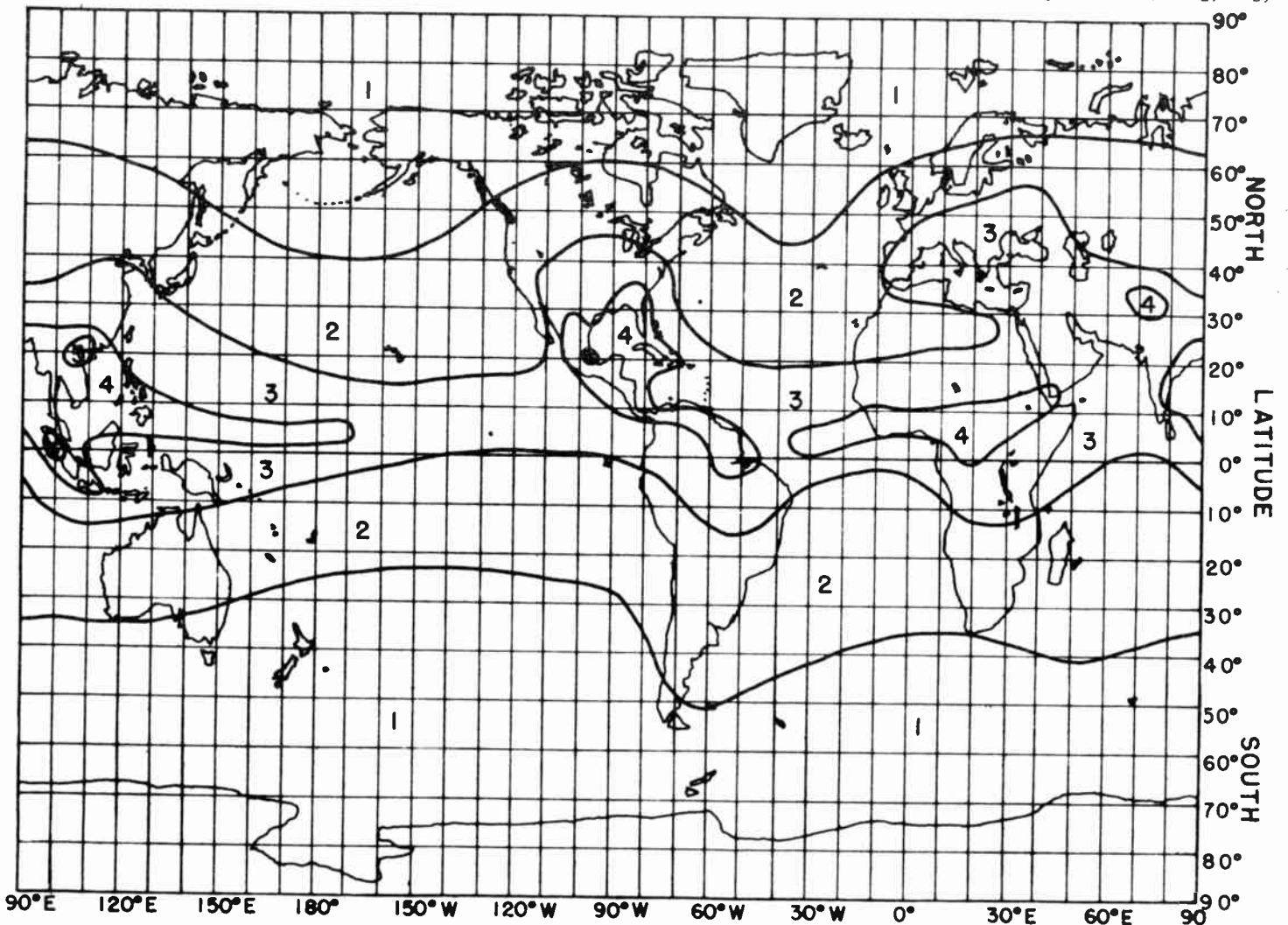


Fig. 39. World Map indicating noise zones for the period May through September. Figures in zones give noise grades corresponding to those used in Figs. 34 through 38.

and $4\frac{1}{2}$ to those already considered. When a receiving station lies on the boundary, or less than one fourth of the way into the neighboring region, one may usefully employ the half noise grades in the LUHF calculations.

The MUF sets a *maximum value* for the transmitted frequency. Absorption calculations, considered along with the radio noise level, set a *lower limit* for the frequency. The value is known as the LUHF, lowest useful high frequency. The LUHF depends upon the transmitter power, whereas this quantity did not enter into the calculations of the MUF.

Important to note is the manner in which the calculations predict the overpowering value of the absorption and the rapidity with which the radio signal appears or disappears at the point of reception at a given time of day. The phenomenon is especially striking for long paths. To improve the reception, it is usually much more effective to raise the frequency than to increase the power. The frequency must, however, remain below the MUF. Best transmission occurs, when the

LUHF is appreciably less than the MUF, at the OWF (optimum working frequency).

If the LUHF *exceeds* the MUF for a given circuit at a given time, transmission will be impossible unless by chance the absorption over the inverse great-circle path, the opposite way around the earth, will permit a significant signal. Occasionally, erratic transmissions, scattered reflection radiation by the auroral zone or ionospheric clouds, will be observed when the theory indicates that no signal is possible. The reception, however, is usually unreliable and will usually be subject to severe fading. The variation of noise levels from the average is so large that reception or the absence of reception cannot be guaranteed for a particular day, even though the calculations represent average conditions fairly well. The required signal strength will be higher if the operator is inexperienced or if the receiving set is poor. It will be lower if the receiving antenna is directional, with the transmitter and noise centers on different bearings from the receiver. We cannot, however, make quanti-

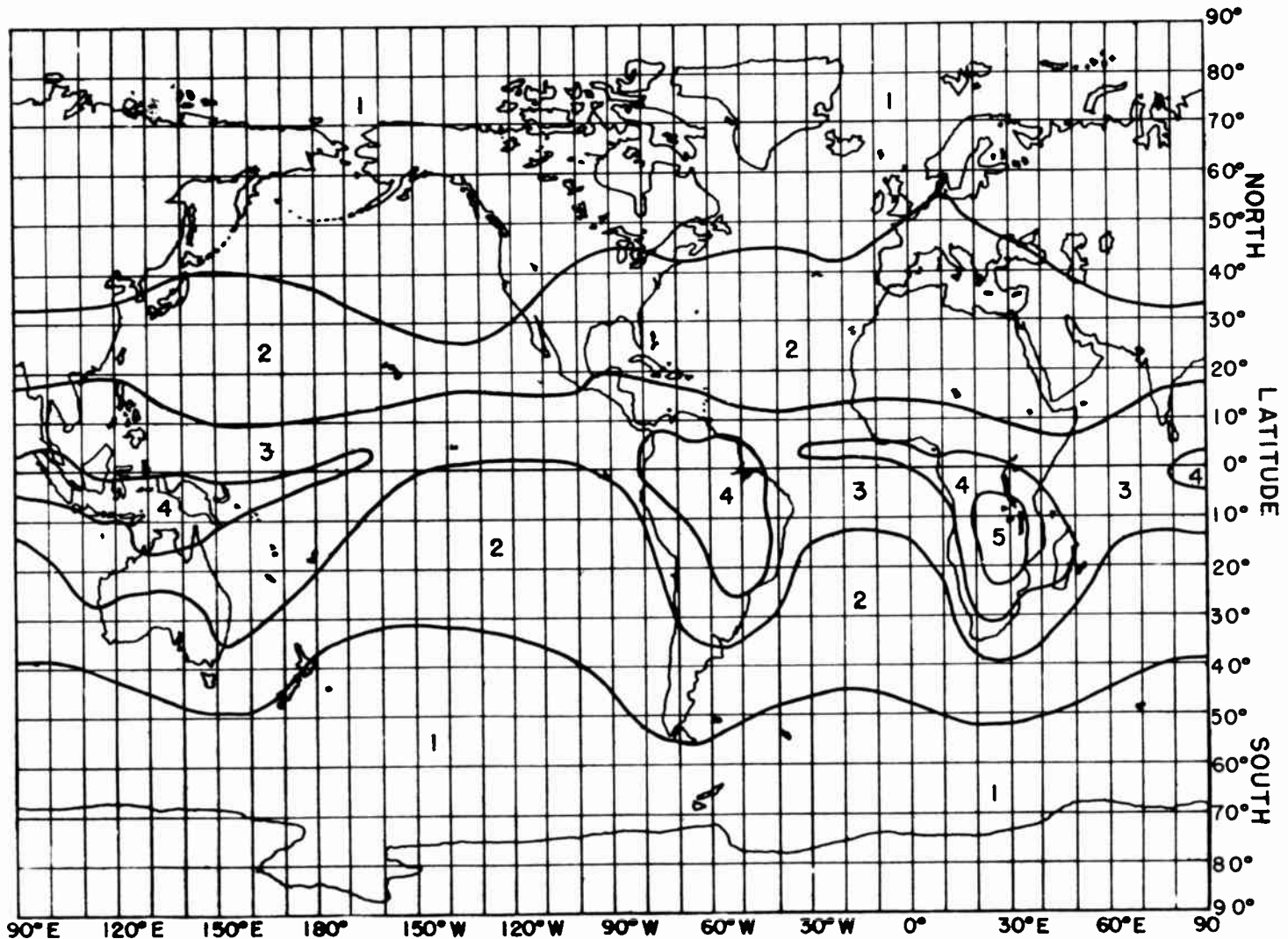


Fig. 40. World Map indicating noise zones for the period November through March. Figures in zones give noise grades corresponding to those used in Figs. 34

tative refinements of this latter sort at the present time. These considerations should, nevertheless, enter into the selection of transmitter sites and the laying out of circuits for commercial purposes.

The calculation of the absorption loss along a radio transmission path is a cumbersome process at best. The following procedure is the simplest available, at present, for the determination of this important propagation factor.

We consider the absorption to be produced by two distinct distributions of electricity in the earth's atmosphere. The first is supposed to be symmetrical with respect to the sun, the absorption being greatest at the subsolar point and dwindling to zero shortly after sunset. For a given transmission path, this contribution to the absorption varies with time of day and must be computed at one- or two-hour intervals, if the behavior of the circuit is desired for the entire day.

This absorption appears to occur in the lowest portions of the *E* layer, which are sometimes called the *D* regions. Electrons are responsible for the absorption, but the densities rarely reach proportions sufficient to give reflections of frequencies above 1.5 megacycles. Since sunlight is responsible for the production of electrons,

we take the total absorption to be proportional to the total amount of sunlight falling along the path. The amount includes the fraction lying beyond the sunrise-sunset line at the earth's surface, where the absorbing layer may still be illuminated by twilight rays.

The second cluster of electricity that contributes to the absorption is distributed in rings in the north and south auroral zones. The poles or centers of these zones lie fairly close to the so-called magnetic poles of the earth, which do not coincide with the poles of rotation. If the transmission path does not cut either of the auroral zones, the absorption caused by this region may be neglected.

The auroral zone is assumed to be constant with time of day; hence, it is calculated only once. The figure derived, however, is only approximately correct because auroral-zone absorption is often subject to large and unpredictable variations. These are associated with magnetic storms which, in turn, are caused by solar activity. When solar disturbances of the ionosphere occur, the auroral zone tends to expand and may cause transmission difficulties in intermediate latitudes. These effects will be discussed further in Chapters 9 and 10.

tion index K . Read the value of K at the transmitting station K_1 and at the receiver K_2 . Record these values on the work sheet. The K 's on the chart represent the amount of absorption contributed by each point of the path.

Step 3. The portion of the path that lies outside the zero curve represents the part of the great circle in darkness. Using the 1000-km divisions, previously marked on the transmission path, estimate the length in kilometers of that fraction of the path passing through the daylight regions. If the entire path is in daylight, the distance is equal to that between the stations, as previously calculated. Record this distance in the column labeled D' on your work sheet.

Step 4. Fill in the column labeled $K_1 + K_2$ simply by adding the two columns together.

Step 5. From the nomogram (Fig. 54 or 55) determine $(Kd)_{sol}$ —that is, the solar contribution to the absorption constant, as follows: Connect the value of D' on the diagonal scale with $K_1 + K_2$ on the right-hand scale and read off $(Kd)_{sol}$ at the point where the extended line intersects the left-hand scale. This nomogram represents the following equation

$$(Kd)_{sol} = 0.142D' + (K_1 + K_2 - 0.284) \tan \frac{1}{2}D'. \quad (1)$$

This quantity $(Kd)_{sol}$ is proportional to the amount of sunlight falling on the entire path. Actually, the absorption takes place in certain limited regions where the beam traverses the absorbing D layer. We have distributed it over the entire path. The result is satisfactory when the distance separating the stations is greater than about 1700 km. When the stations are nearer than this figure, the $(Kd)_{sol}$ calculated by this procedure is too small. We then employ a method described later.

Step 6. We are now required to determine the auroral absorption. For the measurement of MUF's from the basic monthly chart, you have already prepared a transparent overlay map for the circuit. Superpose this map upon the world auroral zone chart of Fig. 56 making certain that both the latitude and longitude scales coincide.

The curves on Fig. 56 are concentric circles drawn at two-degree intervals about the north and south auroral (geomagnetic) poles. Note the point of closest approach of the great-circle radio path to the auroral pole (N or S), and estimate the distance in degrees from this point to the pole. Since the numbers on the circles are given in degrees, estimate the distance to the nearest one-half degree by interpolating between the curves. Call this result P_d . Since the pole is fixed relative to the earth and stations, only a single reading for a given circuit is

required. The value remains unchanged from month to month.

Now, from the curves of Fig. 57 or from Table 4, read off the value of $(Kd)_{aur}$. $(Kd)_{aur}$ represents the auroral contribution to the absorption factor. If P_d exceeds 37° , set $(Kd)_{aur} = 0$. This calculation is based on the assumption that neither of the stations lies within the auroral zone. If one point is so situated, we should divide the tabulated $(Kd)_{aur}$ by 2 to get the approximate value of the absorption.

TABLE 4

ABSORPTION OF AURORAL ZONE					
P_d (Deg)	$(Kd)_{aur}$	P_d (Deg)	$(Kd)_{aur}$	P_d (Deg)	$(Kd)_{aur}$
0	.84	17	1.13	26½	2.42
1	.84	17½	1.16	27	1.98
2	.84	18	1.19	27½	1.36
3	.84	18½	1.23	28	1.12
4	.84	19	1.27	28½	.92
5	.85	19½	1.32	29	.76
6	.86	20	1.36	29½	.60
7	.87	20½	1.41	30	.48
8	.87	21	1.48	30½	.36
9	.89	21½	1.57	31	.29
10	.91	22	1.65	32	.15
11	.92	22½	1.80	33	.06
12	.94	23	1.96	34	.03
13	.97	23½	2.23	35	.02
14	1.00	24	2.37	36	.02
15	1.04	24½	2.44	37	.01
15½	1.06	25	2.46	38	.00
16	1.08	25½	2.47		
16½	1.11	26	2.47		

Step 7. Perform the addition $(Kd)_{tot} = (Kd)_{sol} + (Kd)_{aur}$. $(Kd)_{tot}$, the total value of Kd , is the fundamental quantity determining the propagation characteristics of radio waves of frequencies in the range 2 to 30 megacycles. The value here determined must be regarded as an average, however. The absorption is subject to rapid and often unexpected fluctuations which, under severe solar disturbances, may lead to radio black-out conditions. The variations are most critical for long circuits, for which the values of Kd are high.

Step 8. To calculate the LUHF, note from Fig. 39 or 40 the location of the receiving station b , with respect to radio noise level and position on land or sea. Choose the appropriate nomogram, Figs. 58 to 72, according to the grade of noise intensity 1 to 5. There are two sets of nomograms for grades 2½ to 5, one set for a land-based receiver, the other for one based on the sea or near the coast. For small values of $(Kd)_{tot}$, use the nomograms Figs. 73 to 87.

The known quantities, already filled in on the work sheet, are T_b , the local receiving time, $(Kd)_{tot}$, and D , the distance. The times, of course, are the local apparent times and not standard times. To get the latter, one must use the procedure described in Chapter 2.

Note the intersection of the straight line connecting Kd and D , with the appropriate time curve. The value of the LUHF for a transmitter operating on power of 1 kw is thus read off directly. For transmitters of other powers, attach the auxiliary index, Fig. 88, setting it to the appropriate power, and proceed as before. Since Fig. 88 forms a part of this book, you should copy it accurately on a strip of semitransparent, stiff white paper. Note that there are two sets of auxiliary scales, one for small and the other for large values of Kd . These correspond to the two sets of nomograms, similarly indicated. One may, for safety, wish to adopt a transmitter power of 6 db or so less than the actual value.

The sliding strip thus prepared is to replace the left-hand index of the nomograms, which refer to a 1-kw transmitter. To use the strip, make the vertical line of the paper coincide with the left-hand vertical line of the nomogram. Then shift the index until the decibel index on the paper corresponds to the effective power of the transmitter. The upper distance scale, reading as before in thousands of kilometers, replaces the old one printed on the nomogram. It is advisable to prepare a number of such scales and to attach them to the individual nomograms with paper clips.

The sliding scale may also be employed with the field-intensity nomograms, Figs. 89 and 90. Comparison of these two nomograms with the LUHF nomograms will show that the latter are based on the former. The triangular gridwork of Figs. 89 and 90 is, in effect, an oblique coordinate system, relating field intensity to frequency, on which we may replot the required field intensity curves of Figs. 34 to 38. If we make such a plot and then remove the basic grid, the resulting diagrams are identical with the LUHF nomograms.

The fundamental field-intensity nomograms represent a solution of the equation

$$F_{db} = F_{db}^0 - S_0(Kd)_{tot}. \quad (2)$$

In this equation, F_{db} is the actual field intensity of a 1-kw transmitter, expressed in decibels above 1 microvolt per meter. The term labeled F_{db}^0 is the field intensity produced by such a transmitter at distance D when there is no absorption. This term, which is nearly independent of the frequency, allows for the loss of energy by simple spreading.

Table 5 gives the relationship between F_{db}^0 and D . The latter quantity is given in thousands of kilometers.

Other values may be interpolated graphically, or read from the intersections of the distance scale and the decibel scale on the left of Figs. 58 to 87.

The term, $S_0(Kd)_{tot}$ represents the decibel absorption loss. S_0 depends upon the frequency. There may be

some minor seasonal variation also, but we neglect it here.

TABLE 5
UNABSORBED FIELD INTENSITY FOR 1-KW RADIATED POWER

D	F_{db}^0
0.1	53
0.2	52
0.4	50
0.6	49
1.0	46
2.0	40
4.0	32
6.0	27
10.0	21
20.0	12
40.0	3

Table 6 clearly demonstrates the greater absorption experienced on the lower frequencies. Values below 3 megacycles are extremely uncertain. But the absorption curve has a maximum in the neighborhood of 1 to 1.5 megacycles, so that lower frequencies, such as the broadcast band, are not as strongly absorbed as the 1 to 2 megacycle range. The absorption factor S_0 varies appreciably with both latitude and time of year in the lower frequency range. No analyses are available at the moment to determine S_0 exactly for the lower frequencies.

TABLE 6
VARIATION OF S_0 WITH FREQUENCY

$f_{\text{megacycles}}$	S_0
3	94
4	50
5	32
6	23
8	13
10	8.3
12	6.2
15	4.0
20	2.3
25	1.5
30	1.08
40	0.62
50	0.40
60	0.28

Actually, two types of absorption exist, although the treatment considered above allows for only one—namely, the energy loss by waves passing through the D region of the ionosphere. Since such waves move very nearly in a straight-line path through the region of active absorption, we speak of the effect as *nondeviative* absorption.

A ray near the MUF, which may pass through the D region with or without appreciable energy loss, will be strongly deviated as it passes through the upper ionospheric layers that are responsible for the MUF. Such a ray, as we saw in Chapter 3, is strongly retarded. The collision processes that tend to remove energy from the radio wave, and which are ordinarily ineffective on a rapidly moving wave in the low-density regions of the upper atmosphere, now have time to act. The signal thus suffers a depletion, which we term *deviative absorp-*

tion. The gyrofrequency also enters to complicate the problem. The absorption varies with latitude and the direction of propagation (N-S or E-W). Because of the great variability of the critical frequencies with latitude and time of day, it becomes difficult to allow for the effects of deviative absorption. Theoretical calculations, moreover, are very sensitive to the small fluctuations that are always present in the ionosphere.

We prefer to base our calculations on the nondeviative assumption. There will be times, however, when a certain small range of frequencies will not be audible even though the simplified theory indicates that there is no absorption. These effects will be most marked for relatively short paths, say from a few hundred to one thousand kilometers. The result may be confused with fading, which is discussed in more detail in Chapter 11.

Note that the calculated LUHF may well differ at the two stations, even though the $(Kd)_{tot}$ is the same. The discrepancy arises from the fact that the local times are different, so that the noise level is not identical at the two locations. The familiar adage of the radio operator, "If you can hear him, you can work him," is thus not necessarily true.

Step 9. In many studies, the LUHF and MUF are all that one requires. It is possible, however, to determine the decibel loss caused by absorption and the spreading of the radio beam with distance. When the frequency is given, one can determine the actual field at the receiver in decibels above one microvolt per meter. We use the nomogram of Fig. 89 for long ranges, or that of Fig. 90 for short ranges. The intensities of the received field must exceed the values given in the noise curves of Figs. 34 to 38. This fact limits the LUHF given by the procedure of step 8. For a given $(Kd)_{tot}$, note that greater field intensities occur on the higher frequencies.

Step 10. When the MUF (or OWF) and LUHF have been computed for a given circuit, it is instructive to draw them as curves. The shaded area between the curves (shown in Fig. 91) indicates the usable range of frequencies. Should the LUHF cross above the MUF, reception will be impossible, unless the long-path absorption allows it.

Analysis of the long path follows the same general procedure as for the short path. The length of the inverse path must exceed 20,000 km. The track may start in the daylight zone, move into darkness, and then cross back again into daylight. When this condition occurs, we calculate $(Kd)_{sol}$ in two parts, one for each fraction of the path in the daylight region. We get K_1 and D_1 , the absorption index at the transmitting station and the distance from the transmitter to the sunset or

zero line. $K_2 = 0$. From the nomogram of Fig. 54 or 55, find $(Kd)_{sol}$. Similarly, get K' and D_1' for the receiving station and compute $(Kd)_{sol}'$. Then $(Kd)_{tot} = (Kd)_{sol} + (Kd)_{sol}' + (Kd)_{aur}$. The last quantity is derived as before, from the P_d for the inverse path.

At first sight, the scale on the nomogram of Fig. 55, which runs up to 40,000 km, seems anomalous. How could a long path ever have 40,000 km in daylight? The answer is that there is an appreciable twilight zone. At certain times of day, for transmissions running roughly north and south or, more accurately, approximately parallel to the sunset line, the entire path may lie in the twilight region, and thus experience some absorption. The case is rarely important, because the direct path, under such circumstances, will usually predominate over the inverse. But the data are given for the sake of completeness.

In using Figs. 54 or 55, you will shortly discover that it is almost impossible to estimate $(Kd)_{sol}$ when D' is close to 20,000 km. When $D' = D = 20,000$ km, the two stations will be at opposite extremities of the earth's surface. We have not one but an infinite number of great-circle paths. There results a sort of "whispering-gallery" effect. The energy diverging from the transmitter tends to collect again at the antipodes. The signal intensity is greatly increased, though certain paths are favored more than others. This augmented signal strength has been observed, but exact calculations are impossible at present.

When $D' = 20,000$ km, with D appreciably greater, we may resolve the difficulty as follows. This condition may occur when one of the stations lies in daylight just 20,000 km away from the opposite sunset line, with the other station located well out in the area of darkness. The situation is for inverse, or long-path, transmission. When the stations themselves lie exactly 20,000 km apart, the great-circle path is not defined; as we pointed out in the previous paragraph, there are an infinite number of great circles possible.

But in the present instance, the path is well-marked. We can calculate $(Kd)_{sol}$ in two steps by arbitrarily marking a point on the track approximately half way to the sunset line. Compute the $(Kd)_{sol}$ for each half of the path separately, and sum to get the total. Note that the long, inverse path may contain two $(Kd)_{aur}$ contributions.

The general method which has just been described is not sufficiently accurate for short distances, from 0 to about 2000 km. In computing short-distance LUHF's, the following steps 2 and 3 replace steps 2 to 5 of the general method.

Step 2. Using Figs. 42 to 53 in the same way as in the

general method, read the value of K at the mid-point of the path (K_m). Record these values on the work sheet (Fig. 92).

• *Step 3.* From the nomogram (Fig. 93) determine $(Kd)_{\text{sol}}$ for E -layer reflection and $(Kd)_{\text{sol}}$ for F_2 -layer reflection, as follows: Connect the value of D for the desired layer with the value of K_m by a straight line and read off $(Kd)_{\text{sol}}$ for the proper layer at the point where the extended line meets the $(Kd)_{\text{sol}}$ scale. Record these values.

Following step 3, proceed with steps 6 to 8 of the general method. These steps must be carried out for both the E and F_2 layers, and will yield two sets of values for the LUHF. The LUHF for the circuit may be determined by the following rule:

If the E -layer LUHF is less than or equal to the E -layer MUF, the E -layer LUHF can be used as the circuit LUHF. If, however, the E -layer LUHF is higher than the E -layer MUF, transmission by reflection from the E layer is not useful. The wave is too completely absorbed.

In such a case, we must investigate the F_2 -layer values to determine whether we can send our signal by reflection from this higher layer. We must compare the F_2 -layer LUHF with the E -layer MUF and choose the greater value as the circuit LUHF. If the F_2 -layer LUHF values happen to be lower than the E -layer MUF, we nevertheless must use the E -layer MUF values as the lower limits of our circuit frequency.

Clearly, we must use frequencies high enough to pass through the E layer if they are to penetrate and be reflected by the F_2 layer. Any frequency lower than the E -layer MUF must be reflected by the E layer; although the frequency may exceed the F_2 -layer LUHF, it never gets through to its intended destination. Therefore, in a situation like this, the F_2 -layer LUHF or E -layer MUF, whichever is the *greater*, sets the lower limit to the circuit frequencies.

The curves of Fig. 91 constitute our road map. From the shaded area between the MUF at the top and the LUHF at the bottom, we may select frequencies at will and be reasonably sure of getting satisfactory transmission for average ionospheric conditions.

The MUF and the LUHF curves exhibit a tendency to rise and fall approximately together. The reason for this characteristic is obvious. During the middle of the day, the ionospheric mesh is smaller than at night, permitting the reflection of higher frequencies. Also, during the day, the absorption resulting from the electrons in the D region is high. Since the absorption is greater for the lower frequencies, the LUHF shows a daytime maximum.

For short paths, both the MUF and LUHF curves are

lower than for long ones. But, as we increase the length beyond 4000 km, the MUF tends to approach a limit while the LUHF continues to rise. Thus, the shaded area for long paths is generally much smaller than for short paths, especially during the daytime.

An increase of power tends to lower the LUHF, but the effect of such increase on the LUHF's for long-distance transmissions is small. There are circuits where a billion billion kilowatts would not produce an appreciable signal on certain frequencies. But raise the frequency by three or 4 megacycles and the transmission may become effective with entirely reasonable powers.

Charts such as Fig. 91 are of great value to the person whose primary duty is the selection of frequencies or the laying out of schedules for communications purposes. Regulations will not permit the use of the OMF at all times. In fact, the operator may consider himself fortunate if, at certain times of day he has one frequency that falls into the shaded area of the chart. But it is important that he know what frequency to choose for the most effective result.

Occasions will arise when frequencies slightly above or below the boundaries of the chart will still give communication. Also under certain circumstances, no frequency at all will get through, even though the road map indicates otherwise. The uncertainty arises from fluctuations within the ionospheric regions. The upper levels of the earth's atmosphere, like the lower regions, experience a type of weather variation. One of these, known as *sporadic E*, will be discussed in Chapter 10.

The use of such charts will remove most of the guesswork in communications problems, where choice of frequencies is involved. A tendency exists for operators to remember occasions when a certain frequency worked like magic on a given difficult circuit. He is likely to give preference to that frequency on all future occasions irrespective of time of day, month, or year. Long-range planning of frequency schedules is almost a necessity because of the cyclic variations of the sun, which will be discussed in the following chapter. It should be mentioned that the (Kd) 's calculated in this section are derived for sunspot minimum. They may well exhibit some increase as the current cycle advances. But further data mostly of observational character, are required to establish the nature of the variations. The CRPL will probably issue revised absorption maps from time to time. If one wishes to be conservative, he will assume a transmitter power 3 or 4 db less than the theoretical value.

On a few circuits, one other effect may enter occasionally to increase the effectiveness of transmission. For

fairly long paths, say from 8000 to 16000 km, where the F_2 layer is dominant in the transmission, we expect to get from 2 to 4 or 5 hops. Each time the waves go through the E layer to suffer reflection from the ground, they are weakened by absorption. It is this absorption we have here assumed to be spread over the path to give an average $(Kd)_{\text{tot}}$.

But, if the downcoming waves strike the E layer at a sufficiently glancing angle, they may suffer reflection and go back up to the F_2 layer without reaching the ground. Since the major absorption occurs in the D region, which lies in the lower portions of the E layer, the weakening is considerably reduced.

We call a transmission from ground to F_2 to E to F_2 to ground an *M-type transmission* because of the M form of the path. Very little is known of the properties of such waves, but they are clearly responsible for occasional transmission anomalies. They are most likely to occur when the mid-point of the path is near local noon, for there the E -layer mesh is smallest and quite as able to reflect downcoming radiation back to the F_2 as to act in the more familiar fashion.

Not enough data are yet available to test completely the phenomenon. Clearly, both MUF's and LUHF's are involved. Roughly, we may expect as a primary condition that the frequency used be less than the 2000-km E MUF near the mid-point of the path. If an M -type reflection occurs, the $(Kd)_{\text{tot}}$ computed by the foregoing procedures will be roughly halved. Thus, the LUHF's will be correspondingly lowered.

The effects of MUF and LUHF are often shown in bearings measured by direction-finding equipment. When the transmission frequency is in the shaded zone, the bearings will generally be reliable. But if any signal at all is received on a frequency outside the range of predicted frequencies, the bearing will generally be poor, the maximum flat or wandering. Also, as a

station moves into skip, the bearing will generally shift toward the direction of higher ionospheric density—that is, toward the sun. The ionosphere is not a perfect reflecting surface: the layers are rough, the electrons often occur in patches and clouds, and the regions are often tilted, especially in the auroral zones.

The values of the LUHF calculated above refer specifically to phone reception for 1 kw of power *actually radiated from the antenna*. Other types of emission, such as CW or machine recording, require, for efficient operation, different ratios of signal to noise than the values here assumed. We may employ the same procedures however, by adopting a fictitious power for the transmitter. For the various services listed below, calculate with a transmitter power greater than the actual value by the number of decibels listed in the following table. A negative sign signifies, of course, a transmitter power less than standard. Use the auxiliary scale of Fig. 88 to make the adjustment.

For example, you are using a transmitter radiating 250 watts on CW aural operation. The actual power is 6 db less than 1 kw, or -6 db. But the sensitivity of CW emission is 17 db greater than for phone. Hence, the effective transmitter power is $-6 + 17 = 11$ db greater than 1-kw phone. If the antenna is directive, include the decibel gain in the given direction. Set the auxiliary index, therefore, to 11 and proceed as explained earlier in the text to evaluate field intensities or LUHF's.

TABLE 7
VALUES TO BE SUBTRACTED FROM REQUIRED FIELD INTENSITIES
FOR COMMERCIAL TELEPHONY

	<i>Satisfactory</i>	<i>Barely Acceptable</i>
Telegraphy (aural)	17 db	25 db
Telegraphy (automatic)	6	14
Telegraphy (printing)	2	10
Commercial telephony	0	8
Commercial broadcasting	-8	0
Facsimile	6	14
Direction finding	0	8

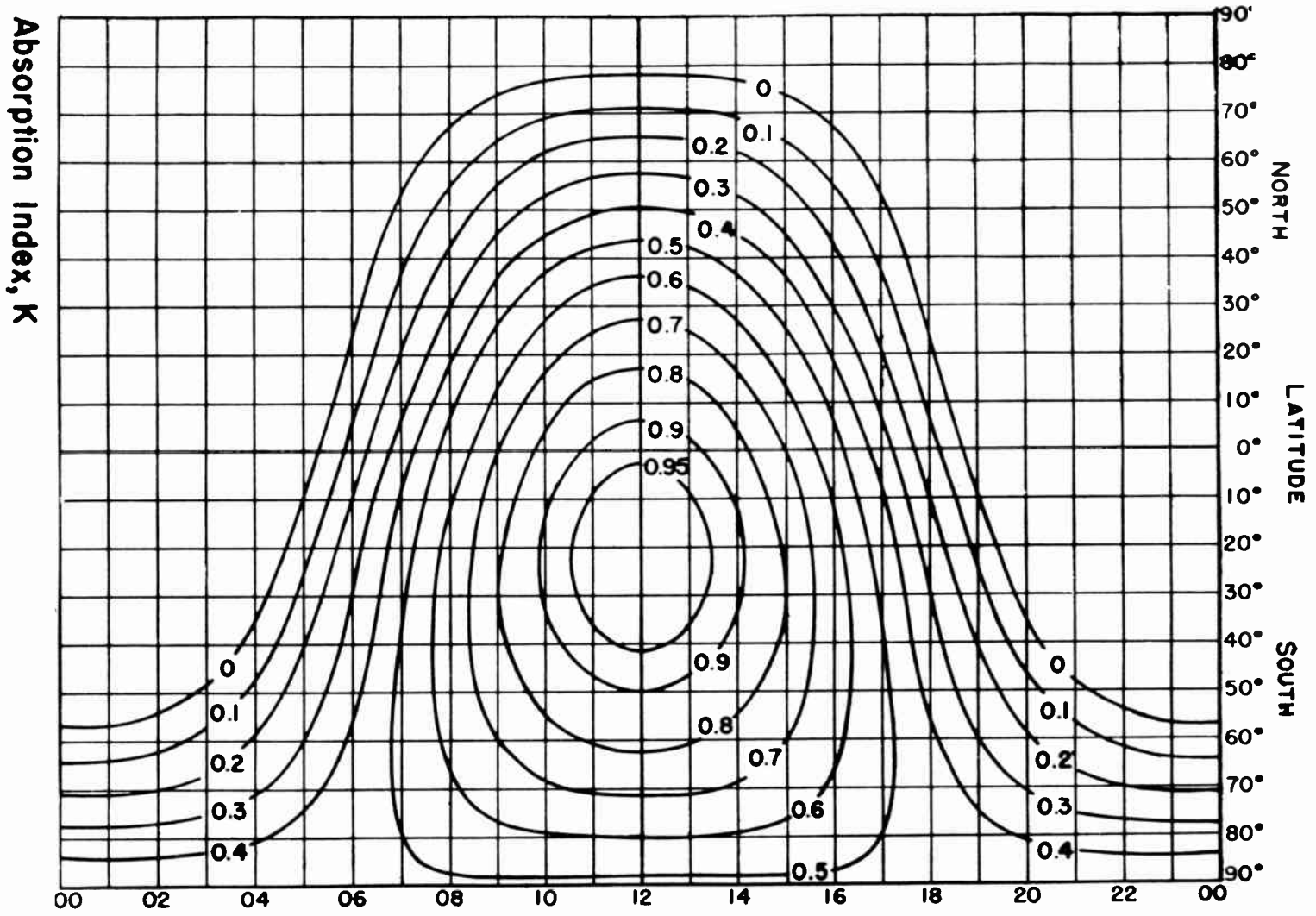


Fig. 42. Absorption Index Chart, January.

Absorption Index, K

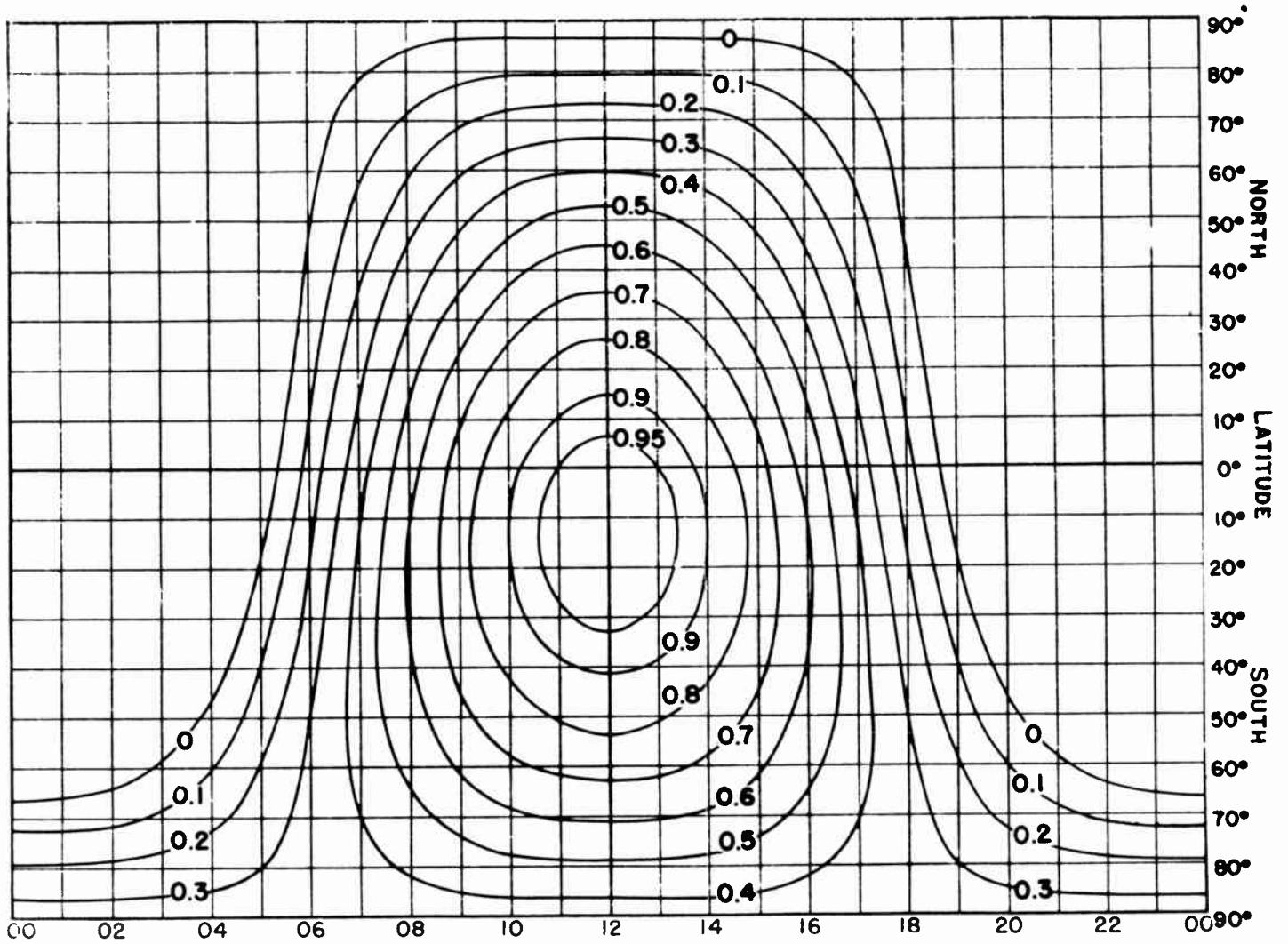


Fig. 43. Absorption Index Chart, February.

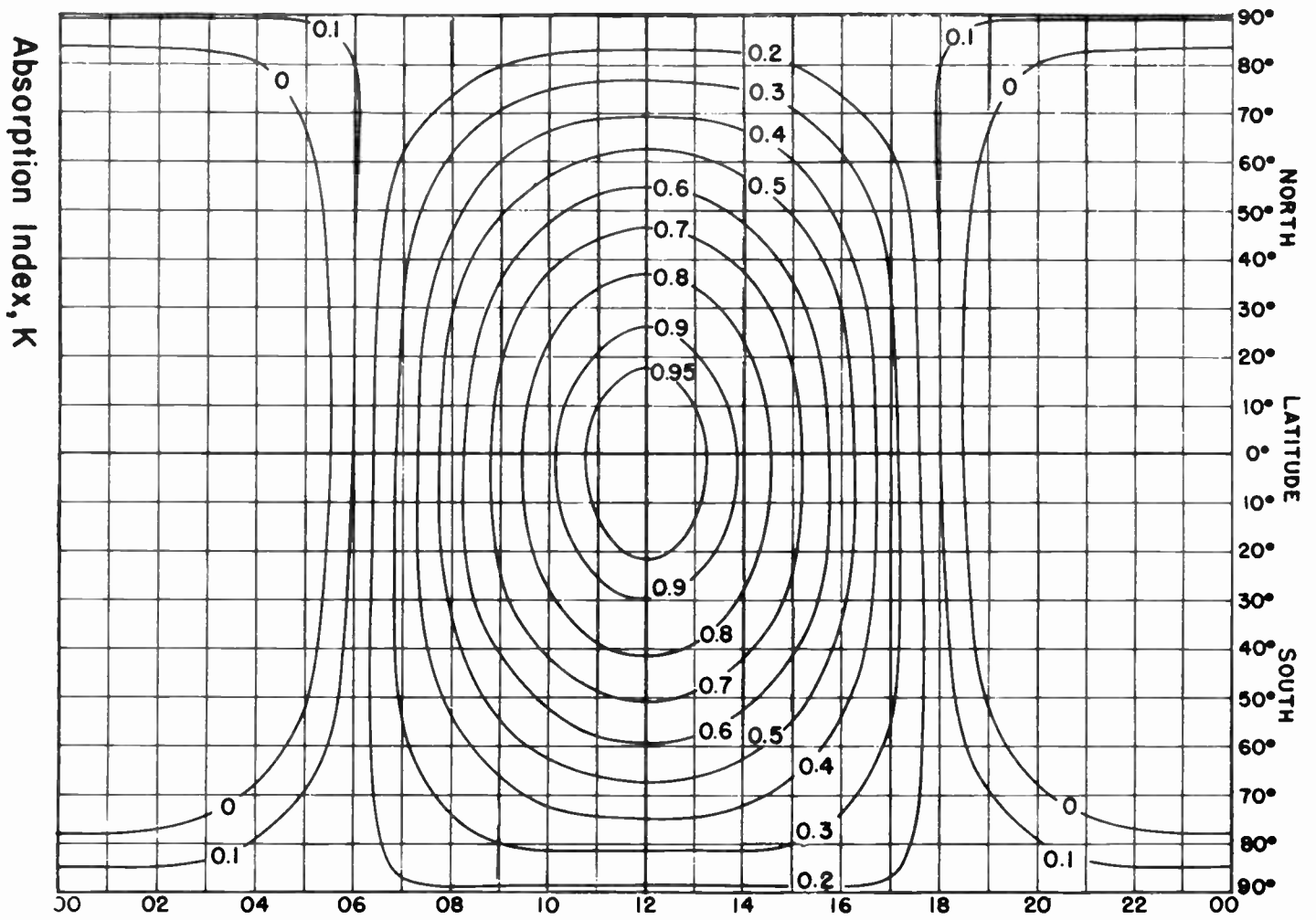


Fig. 44. Absorption Index Chart, March.

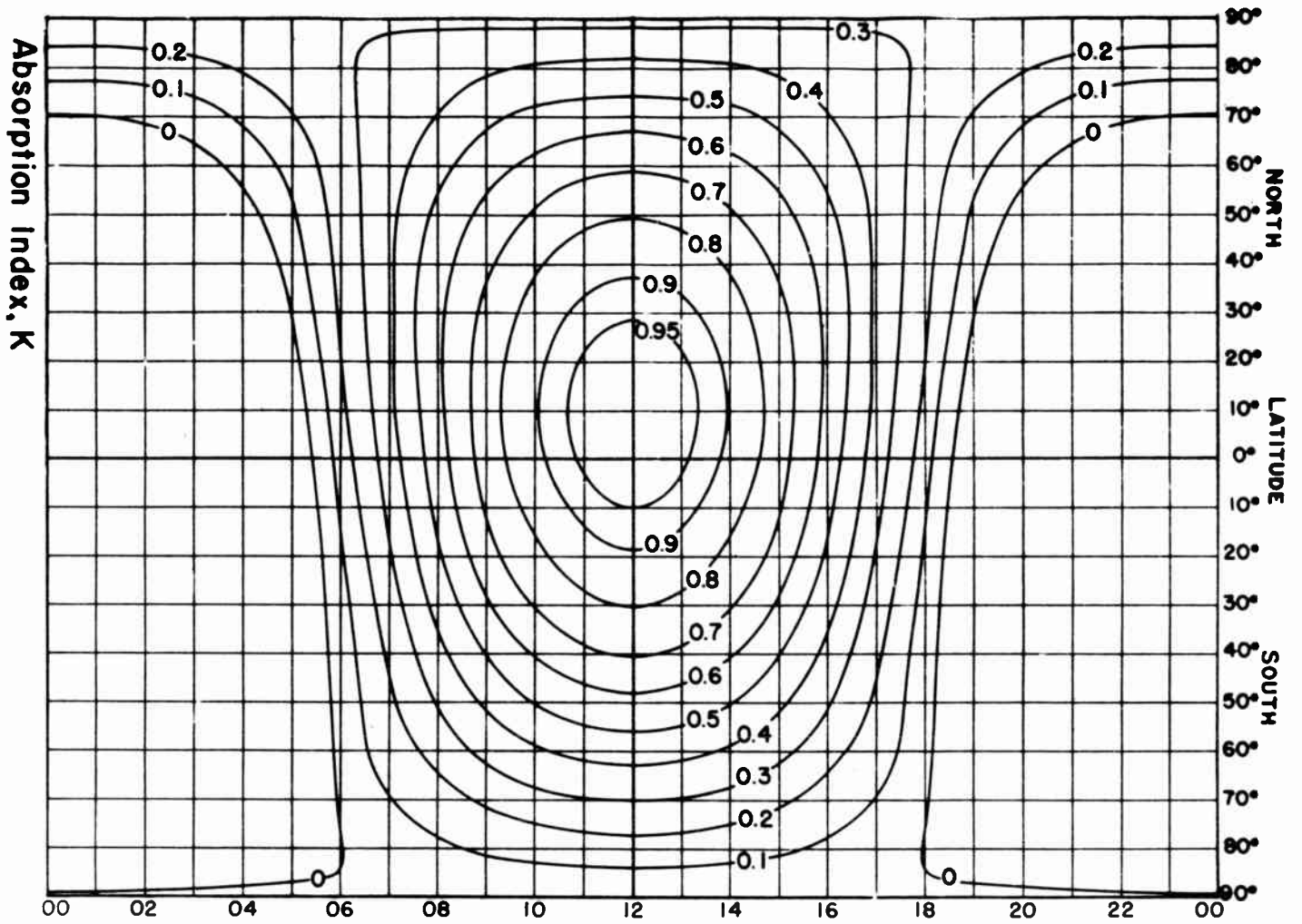


Fig. 45. Absorption Index Chart, April.

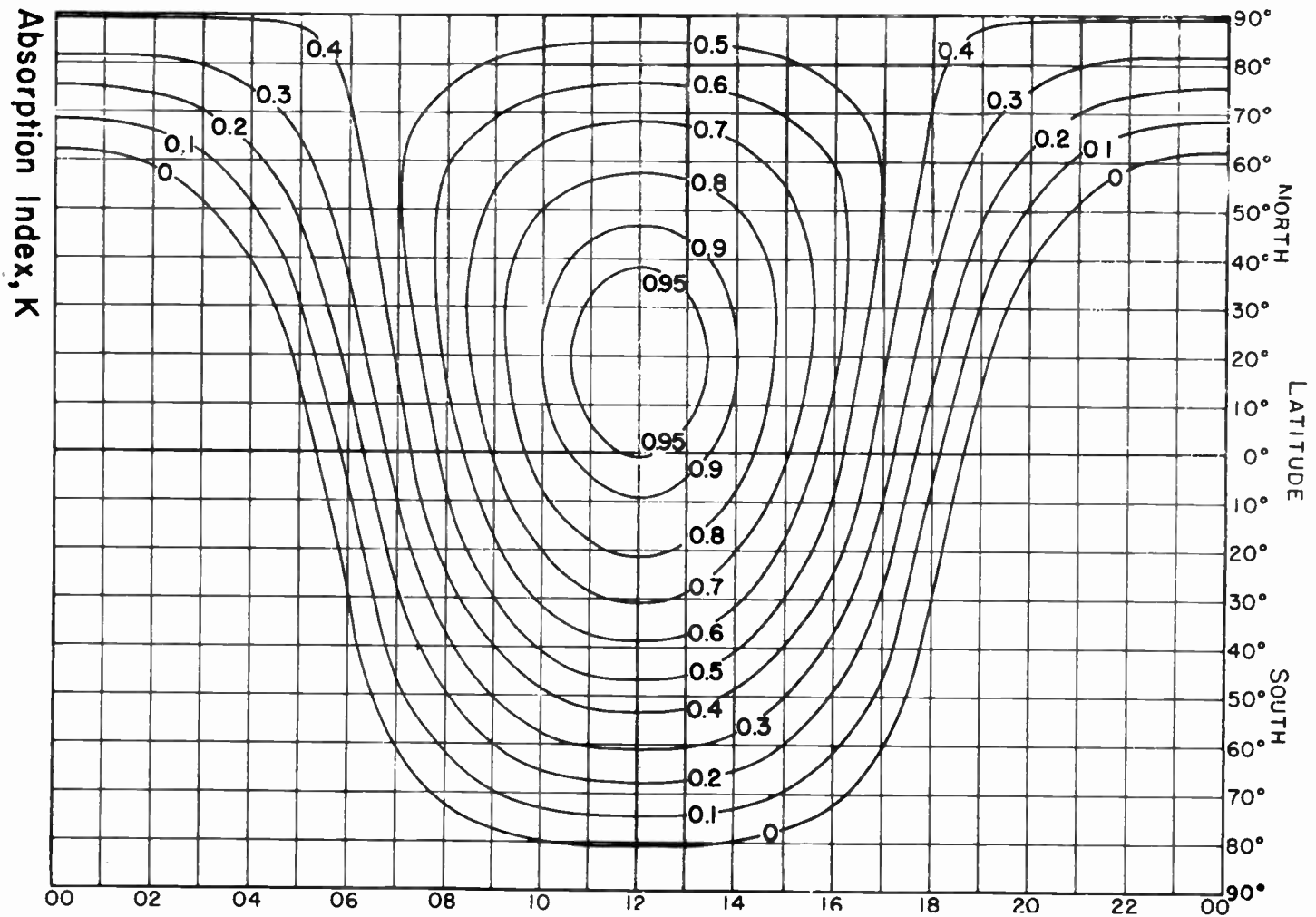


Fig. 46. Absorption Index Chart, May.

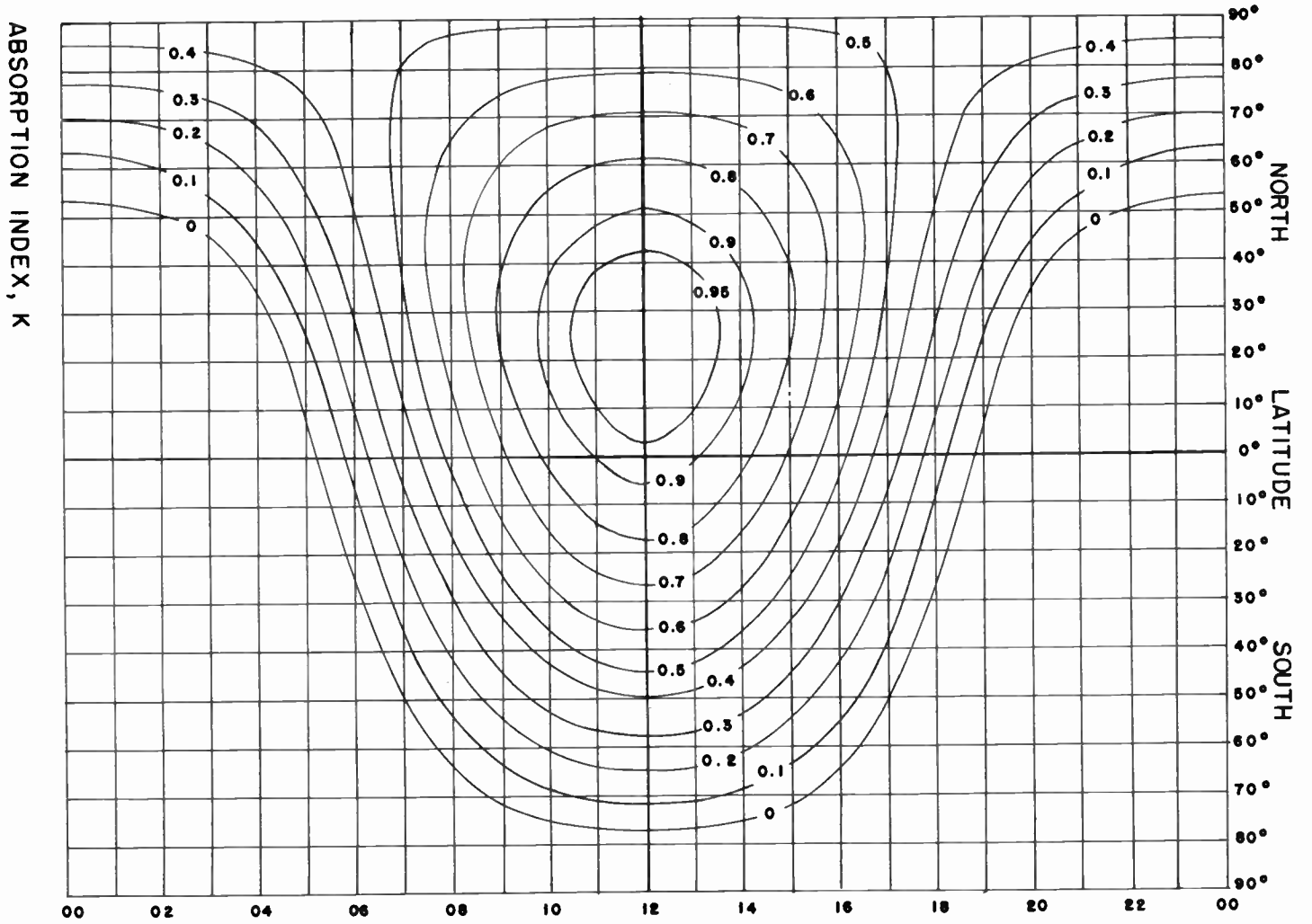


Fig. 47. Absorption Index Chart, June.

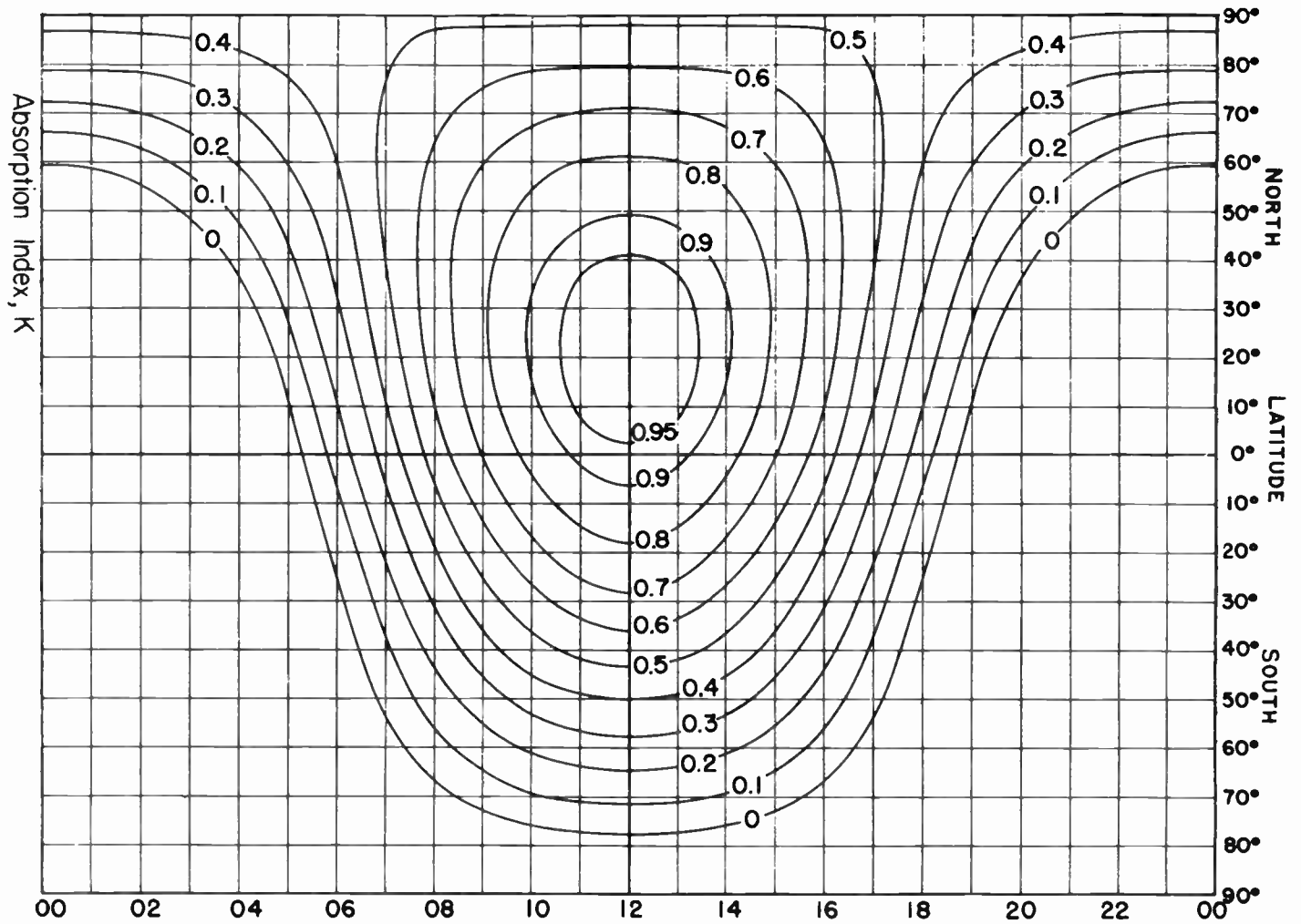


Fig. 48. Absorption Index Chart, July.

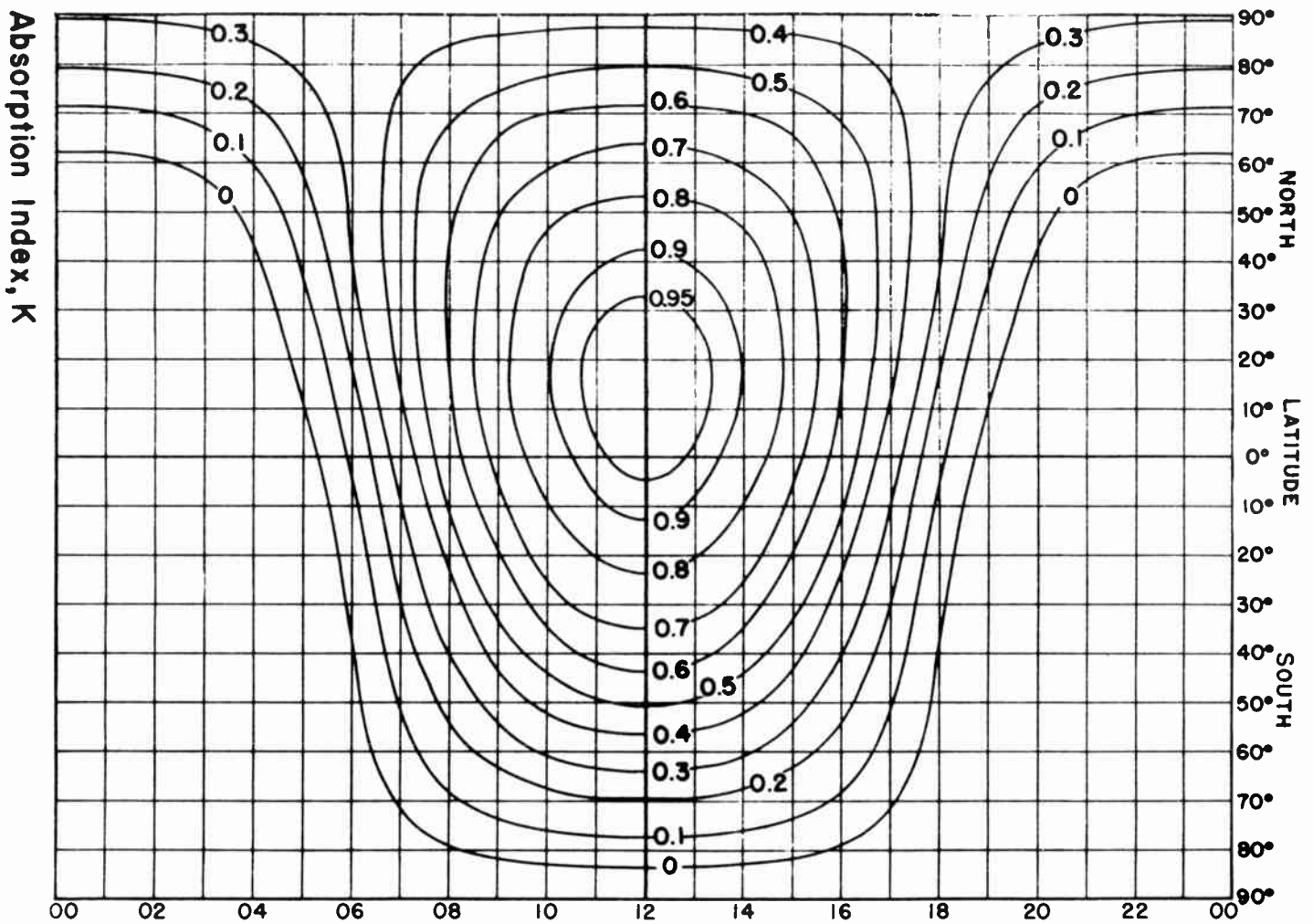


Fig. 49. Absorption Index Chart, August.

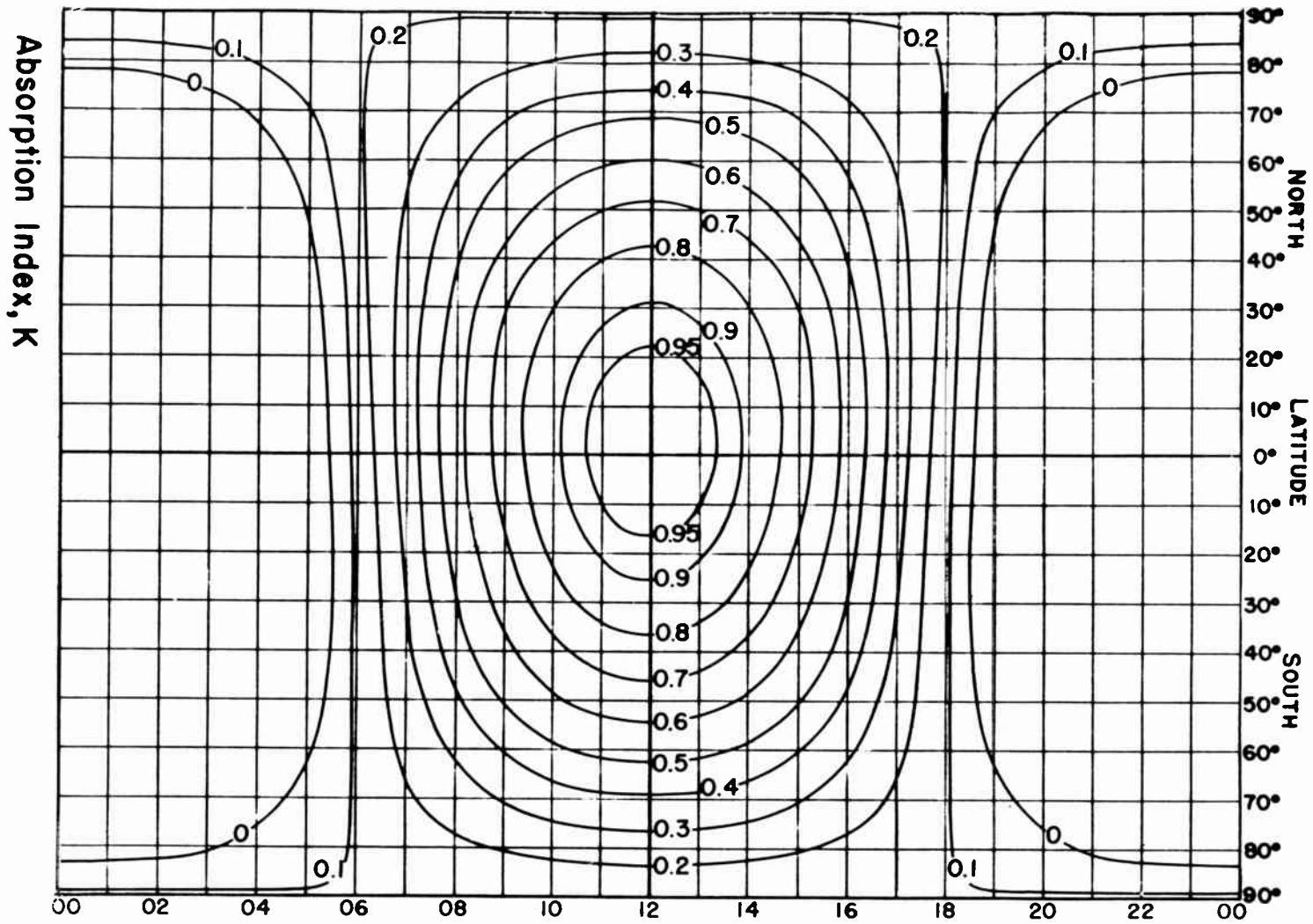


Fig. 50. Absorption Index Chart, September.

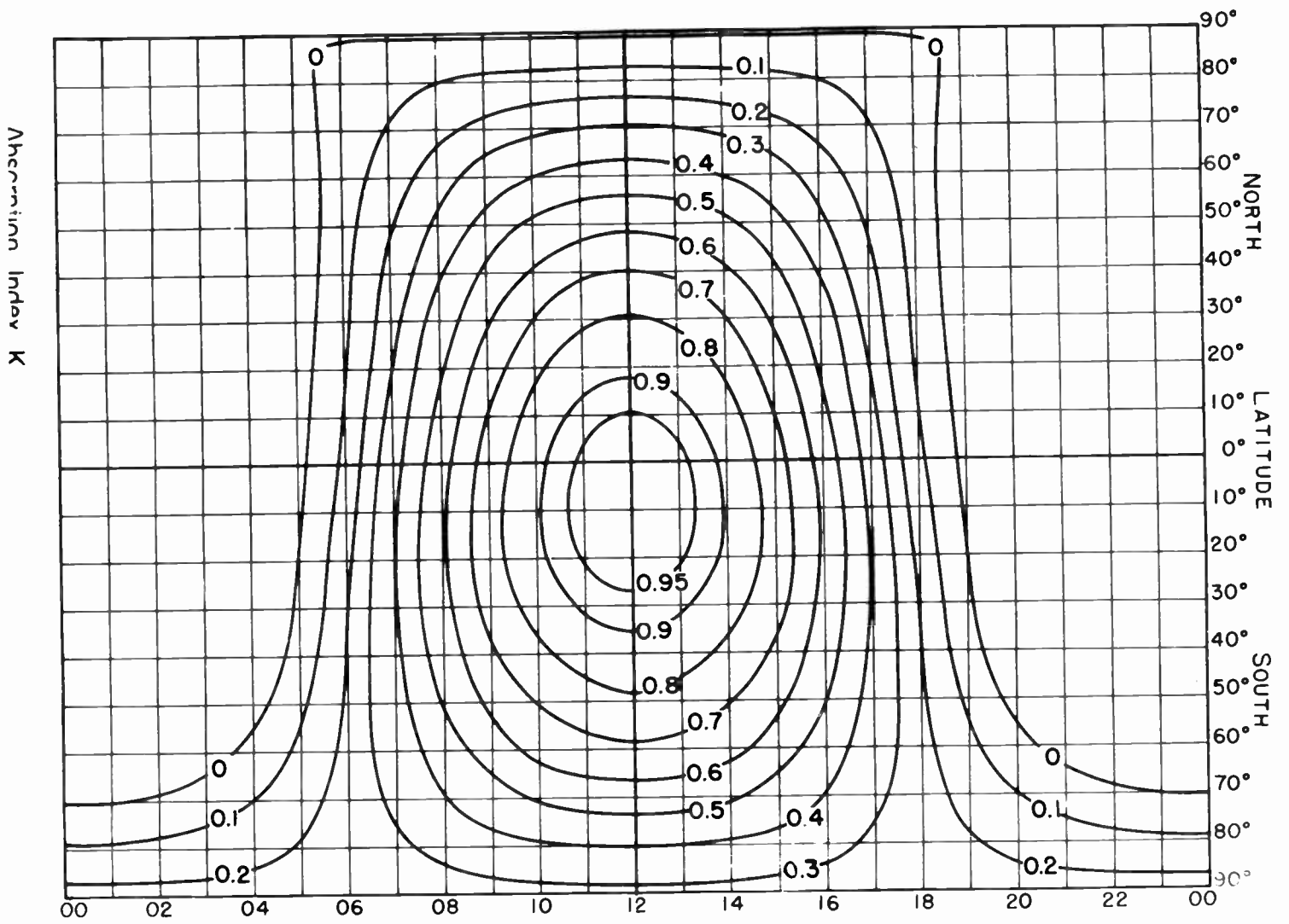


Fig. 51. Absorption Index Chart, October.

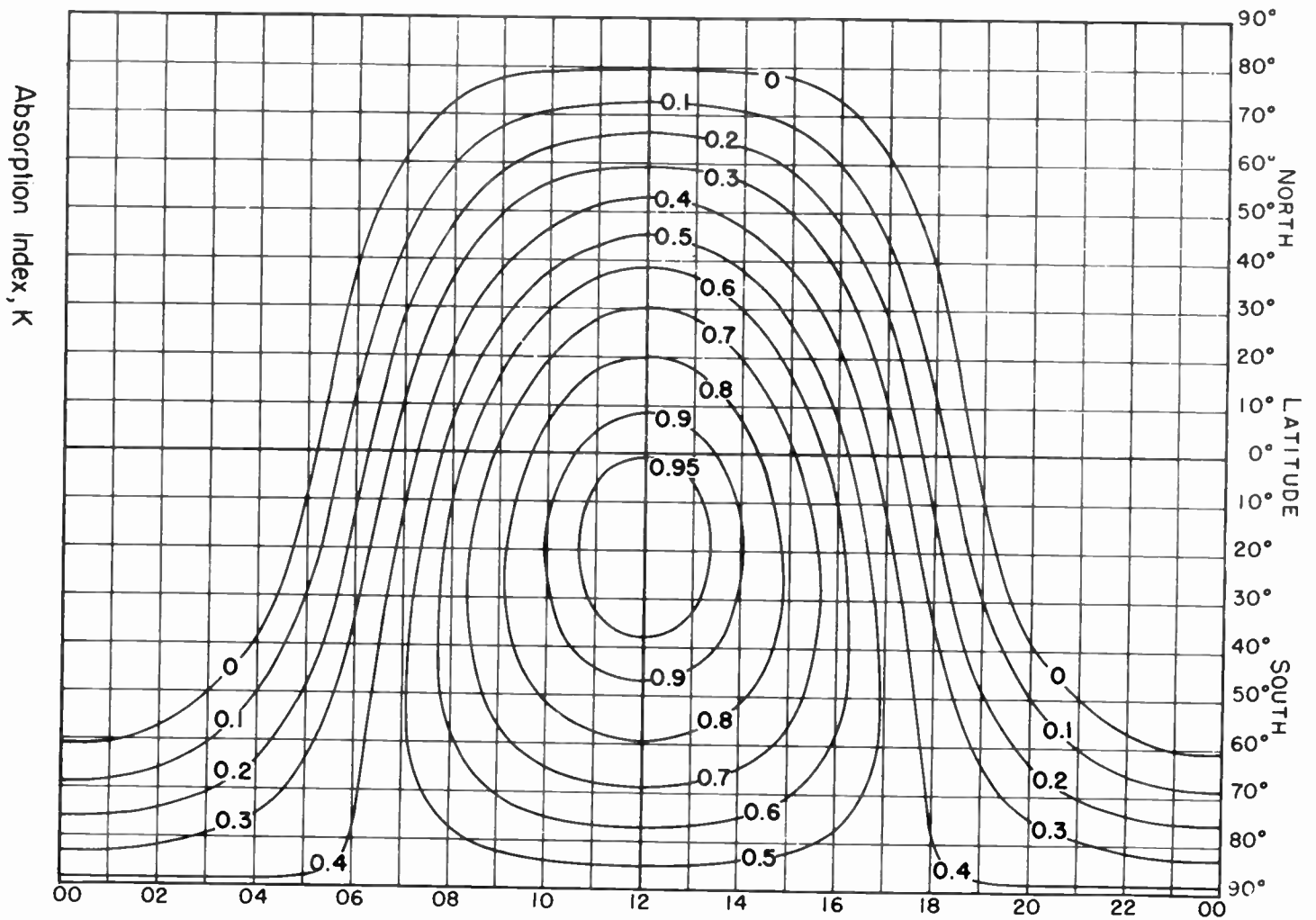


Fig. 52. Absorption Index Chart, November.

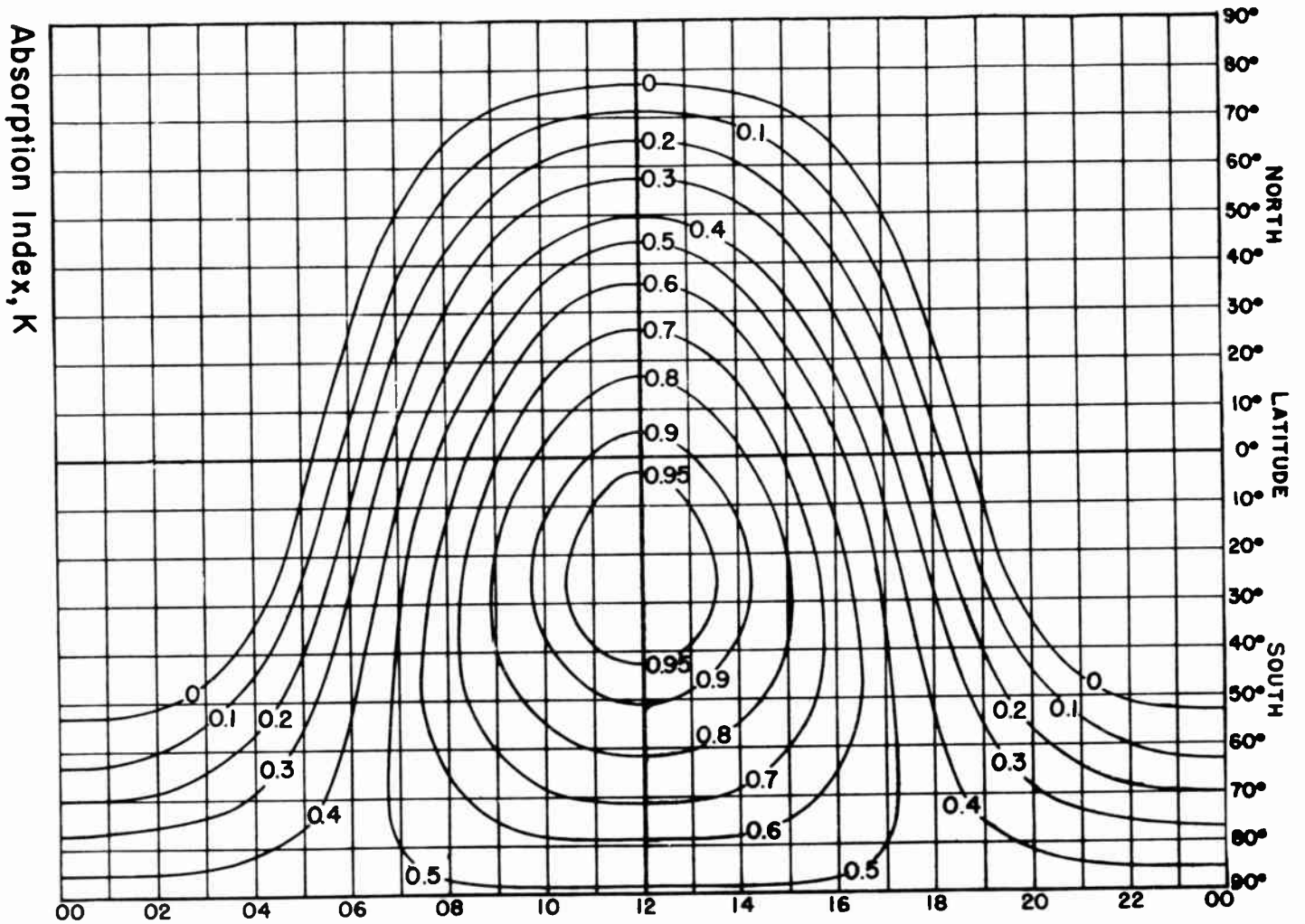


Fig. 53. Absorption Index Chart, December.

CALCULATION OF LOWEST USEFUL HIGH FREQUENCIES

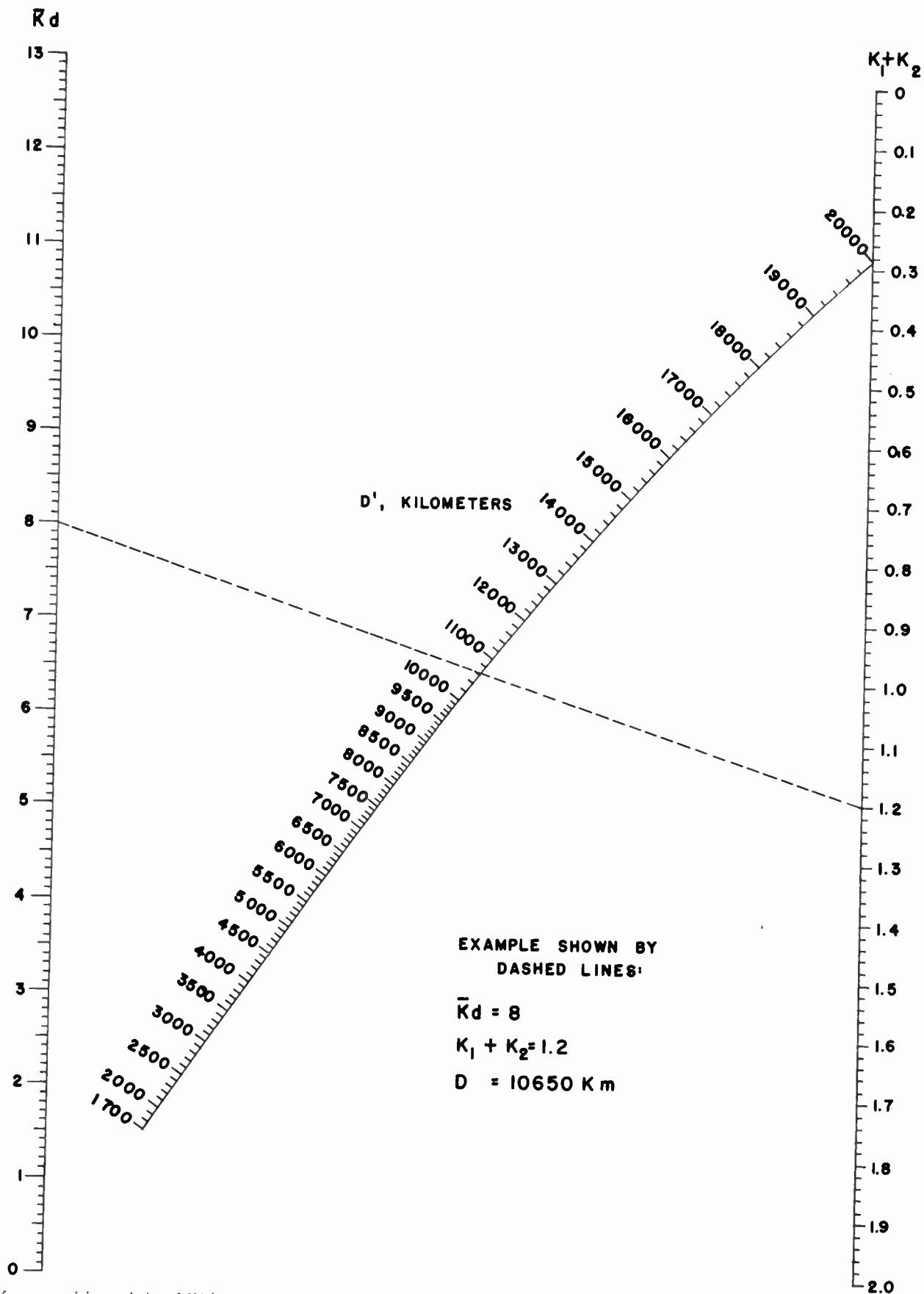


Fig. 54. Nomogram giving variation of $\bar{K}d$ (product of the average absorption index for total transmission path and the transmission distance) with transmission distance, d , and $K_1 + K_2$ (sum of the absorption indexes at terminal points of the transmission path). (Distance in nautical miles, up to 10,794 nautical miles.)

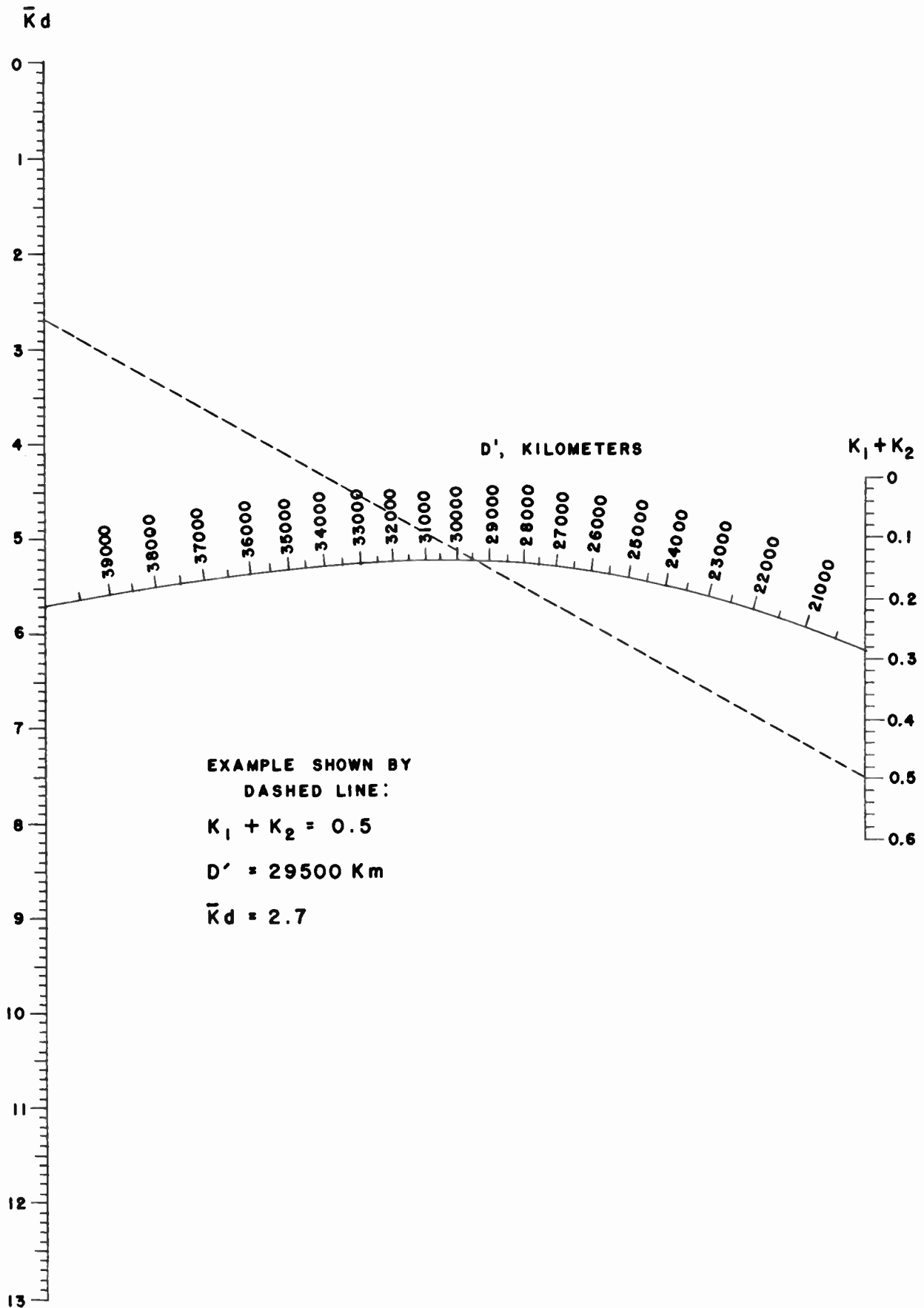


Fig. 55. Nomogram giving variation of Kd with transmission distance, d , and $K_1 + K_2$. (Distance in kilometers, between 20,000 and 40,000 kilometers.)

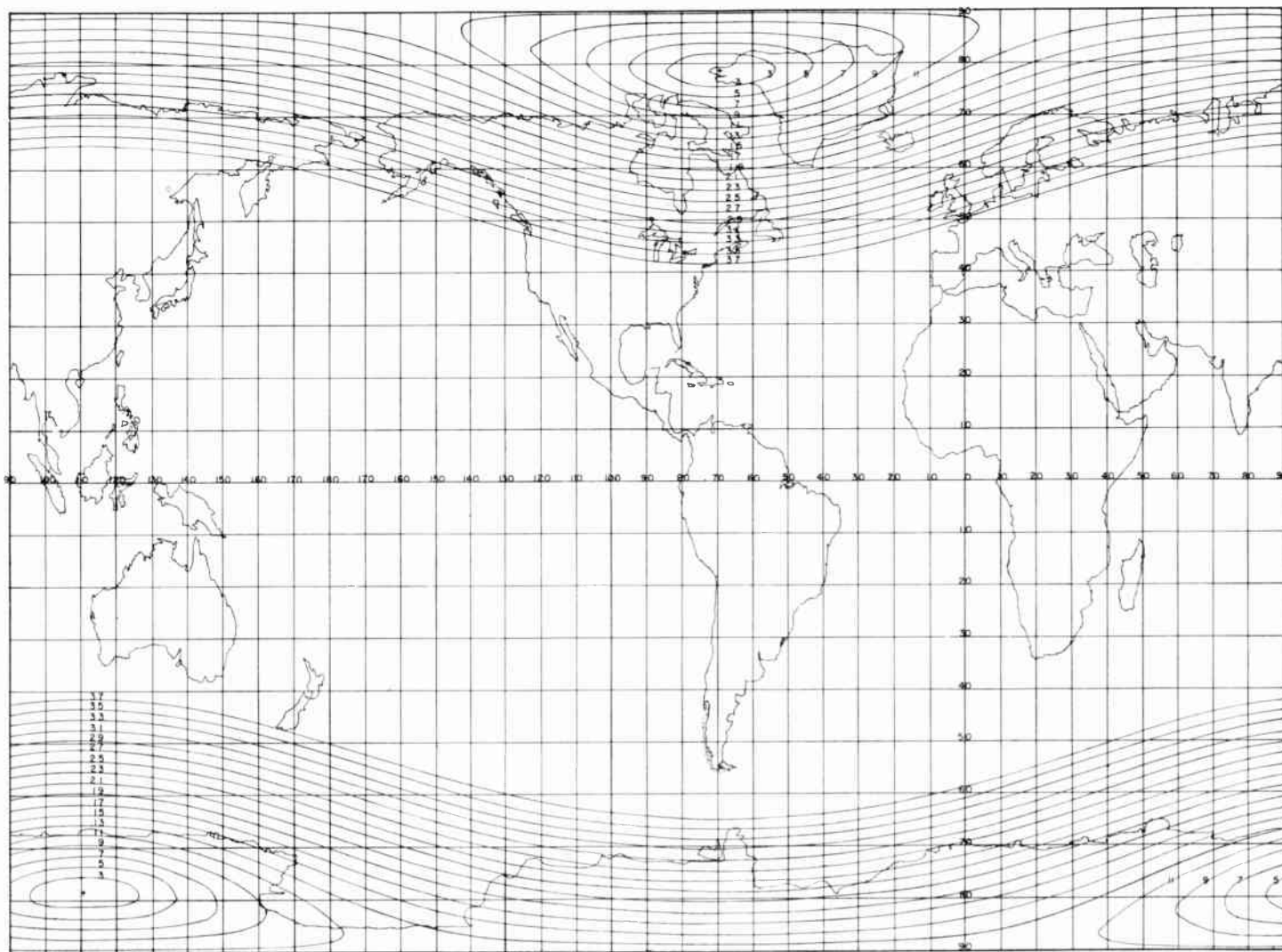


Fig. 56. World Auroral-zone Chart.

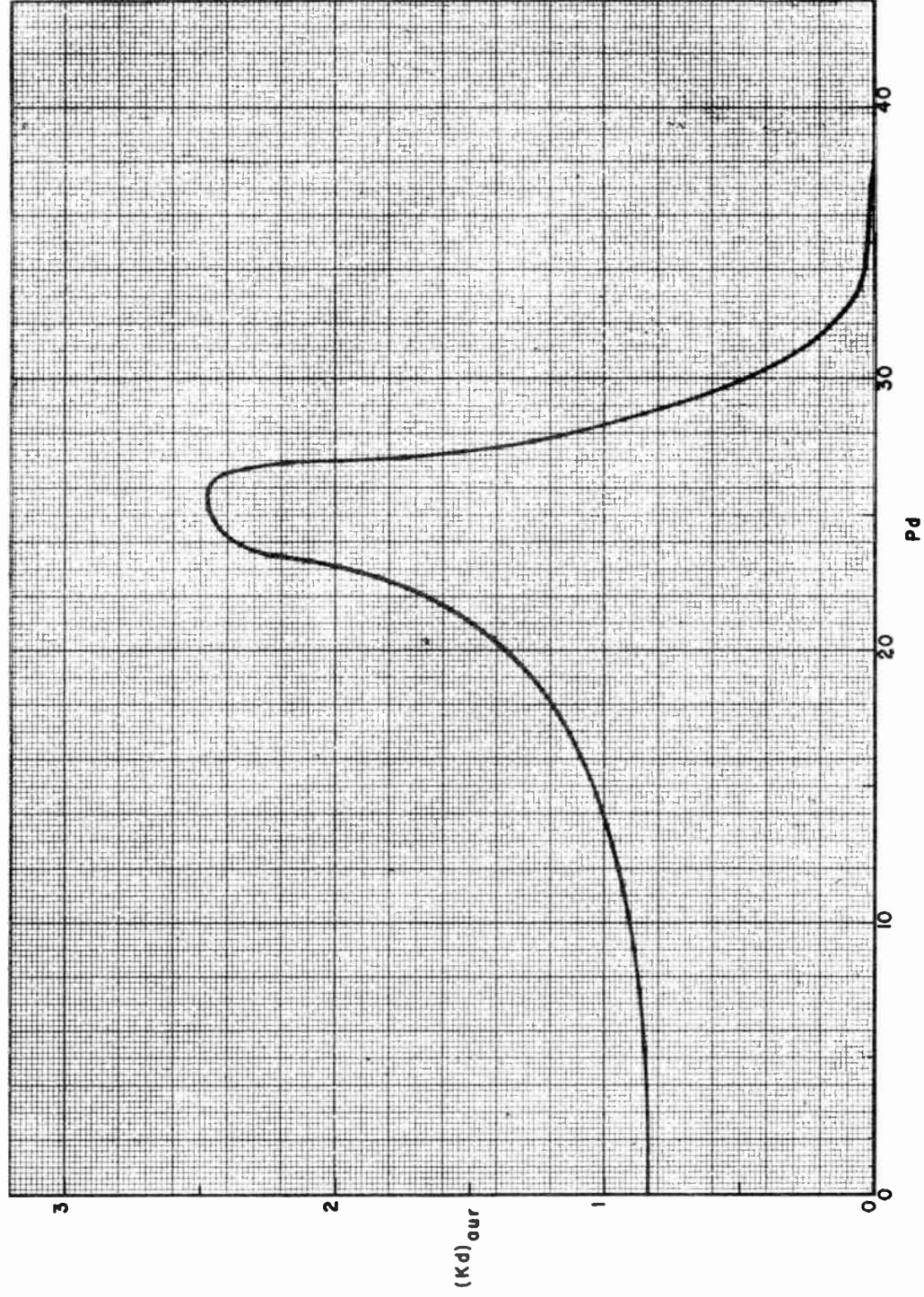


Fig. 57. Absorption of Auroral Zone.

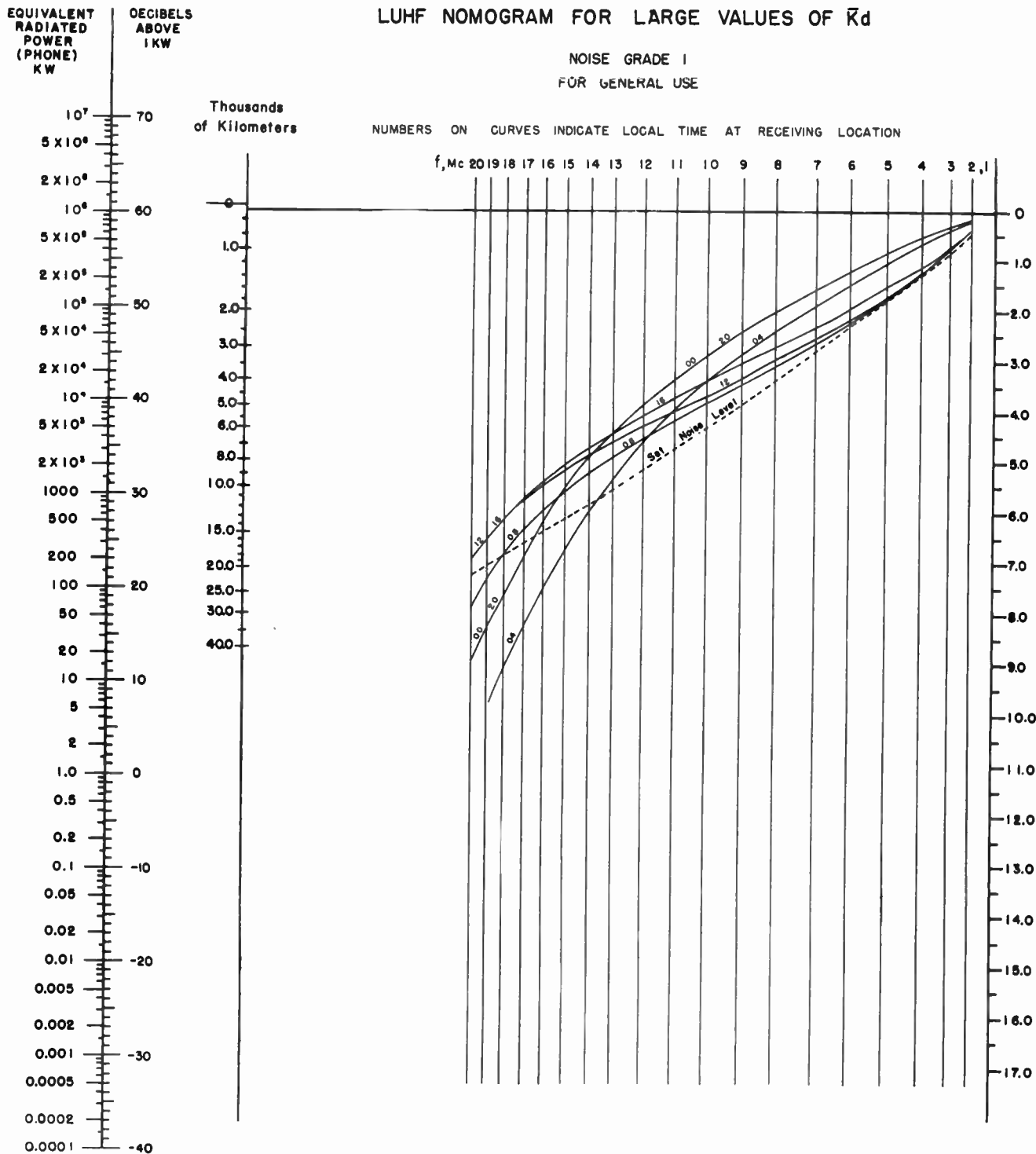


Fig. 58.

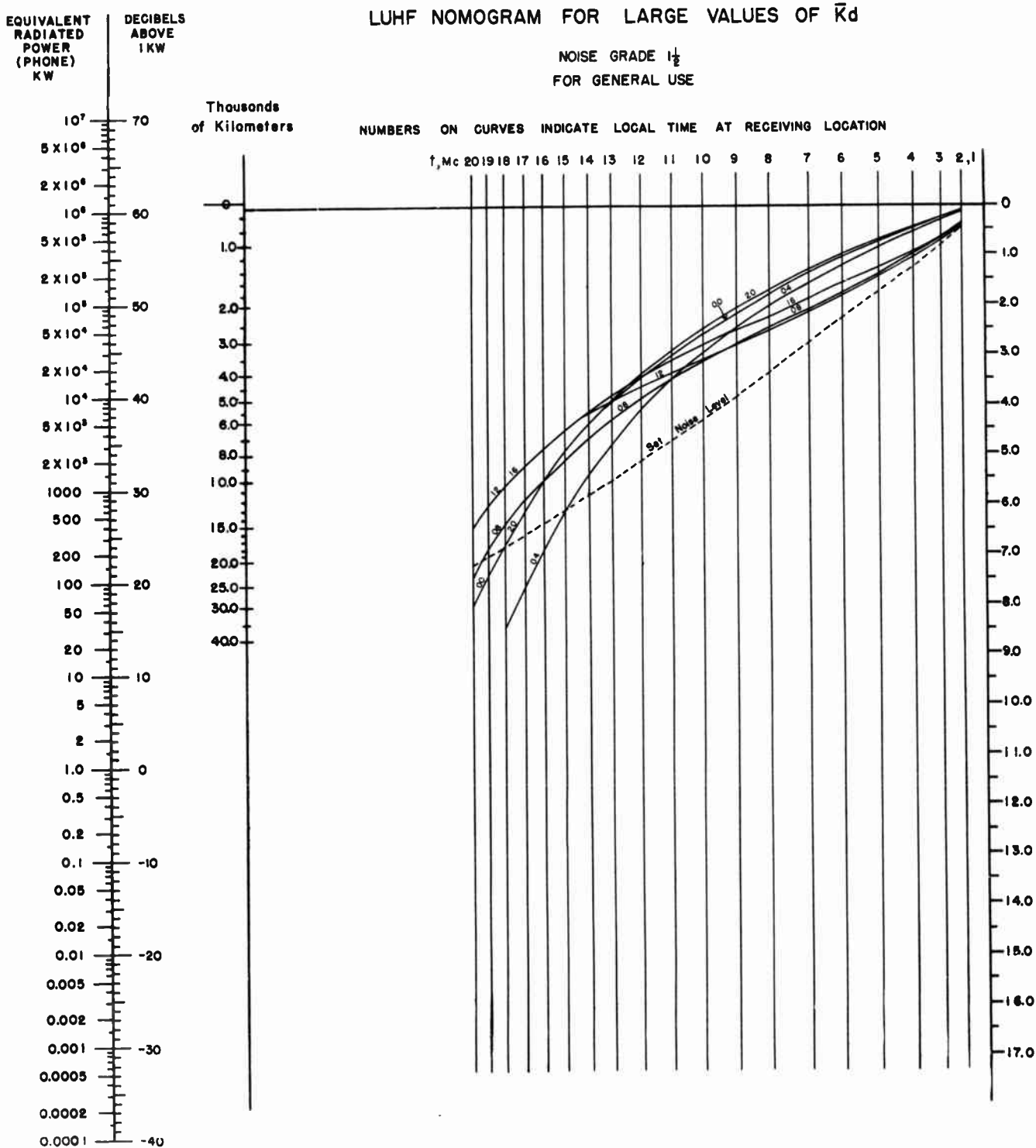


Fig. 59.

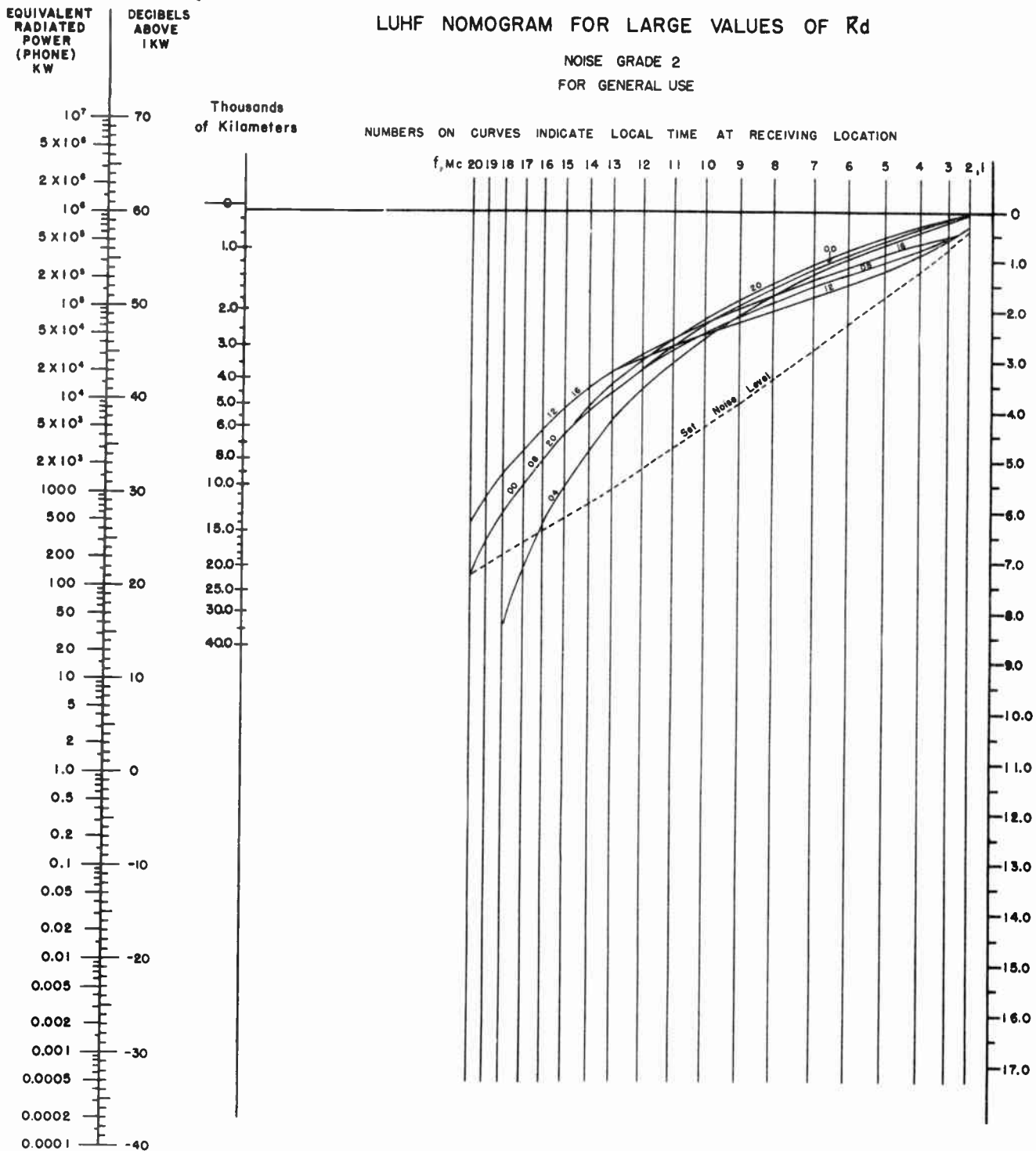


Fig. 60.

LUHF NOMOGRAM FOR LARGE VALUES OF R_d

NOISE GRADE $2\frac{1}{2}$
FOR OPEN OCEAN

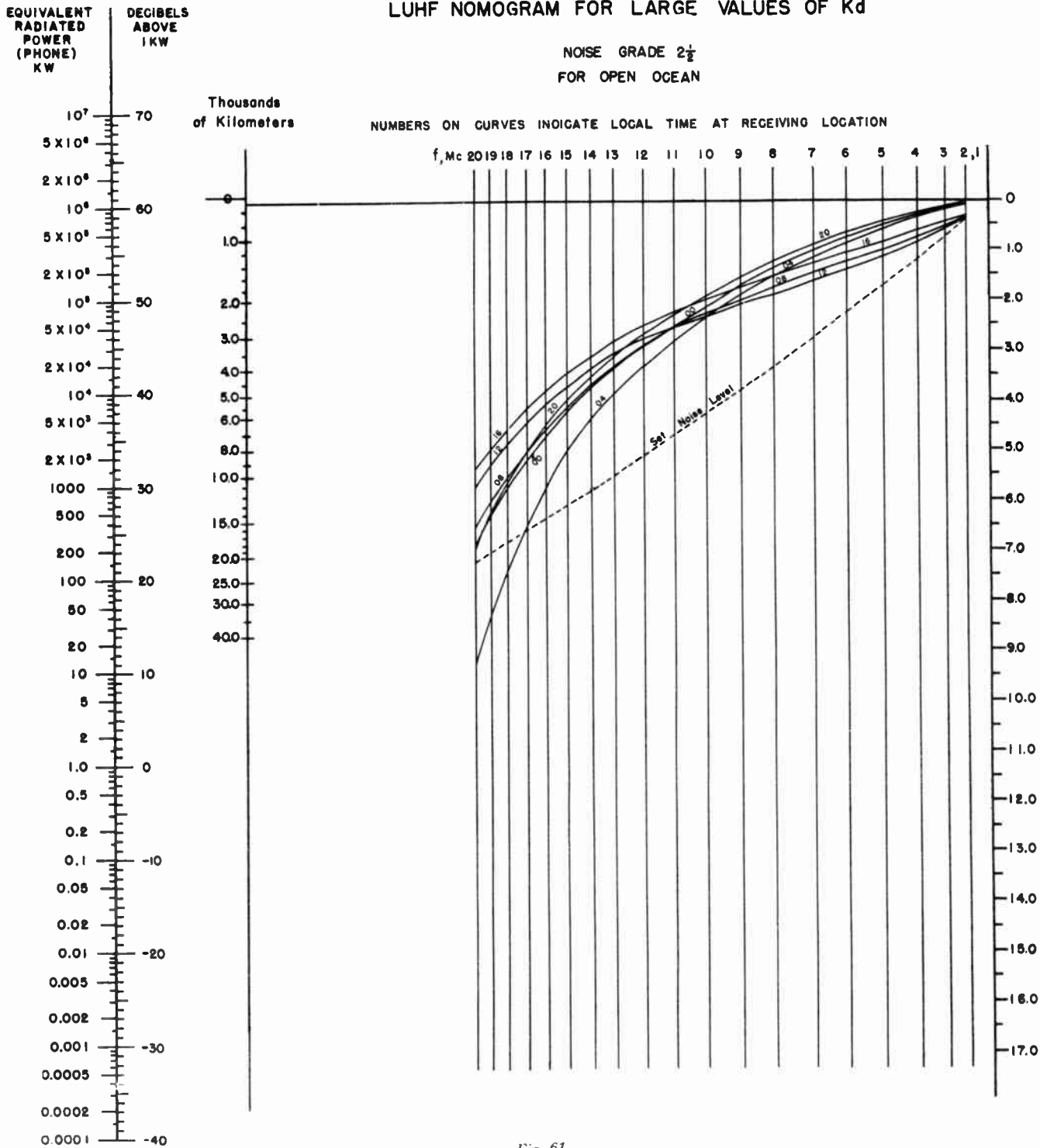


Fig. 61.

LUHF NOMOGRAM FOR LARGE VALUES OF R_d

NOISE GRADE 3
FOR OPEN OCEAN

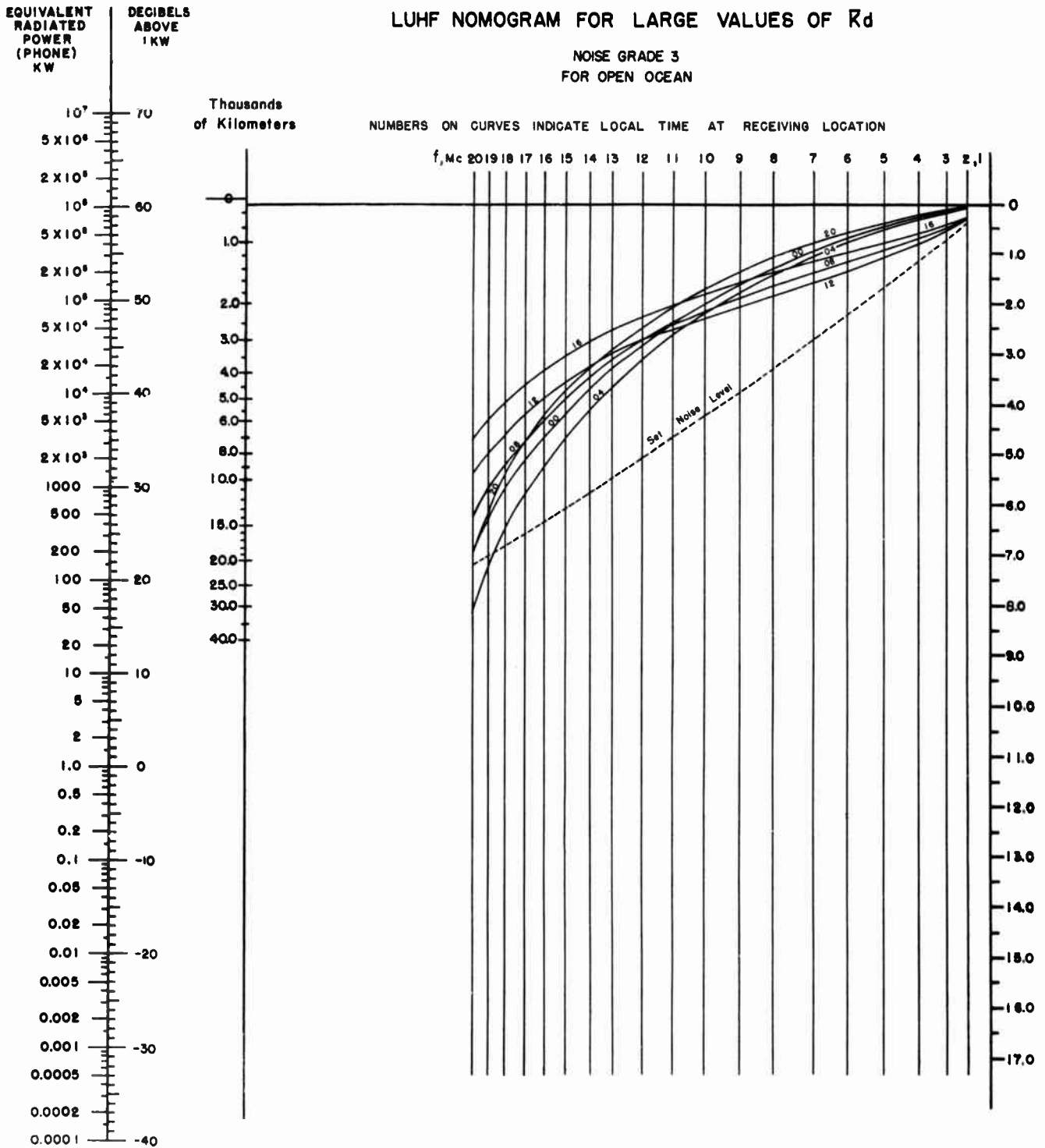


Fig. 62.

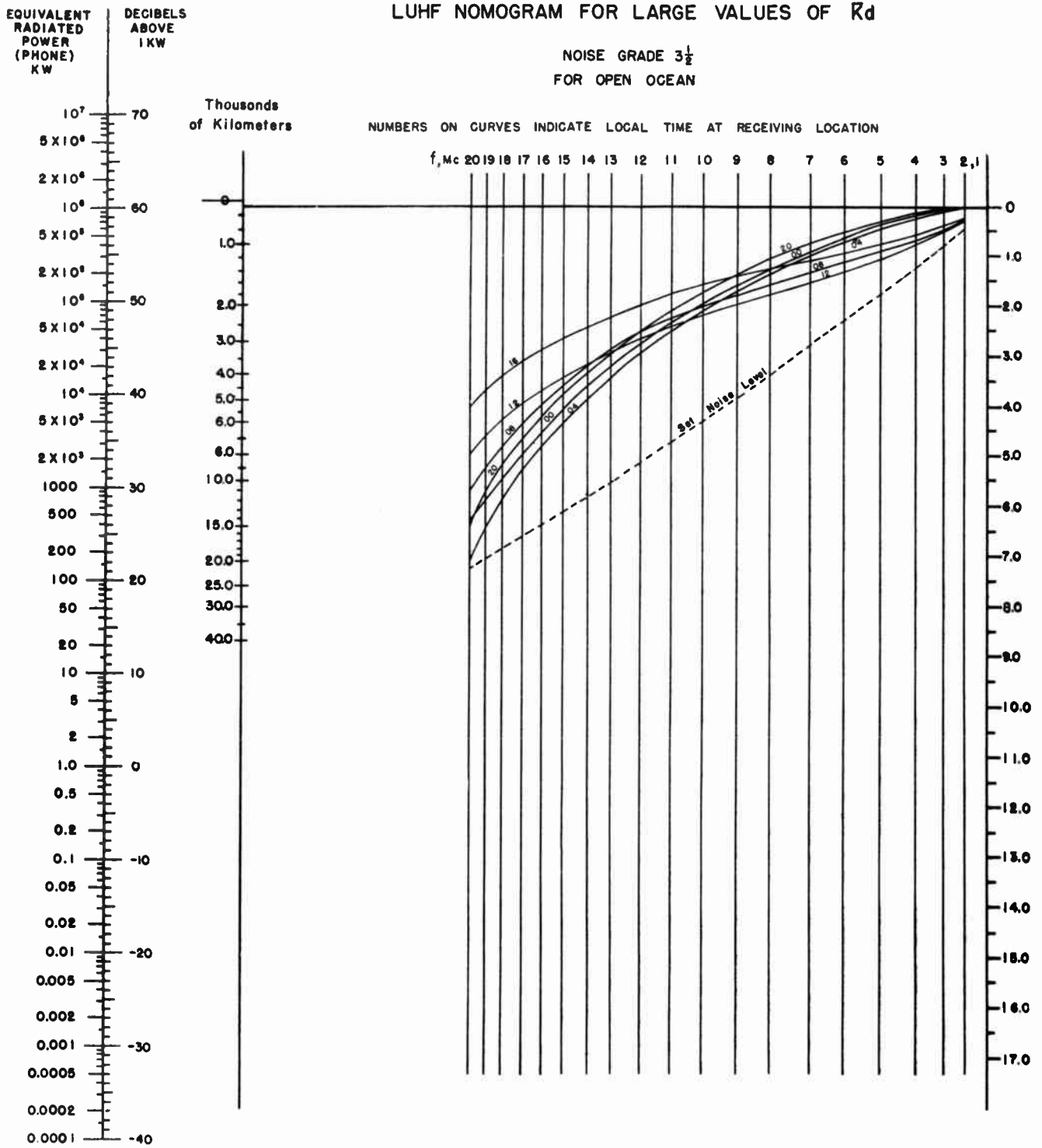


Fig. 63.

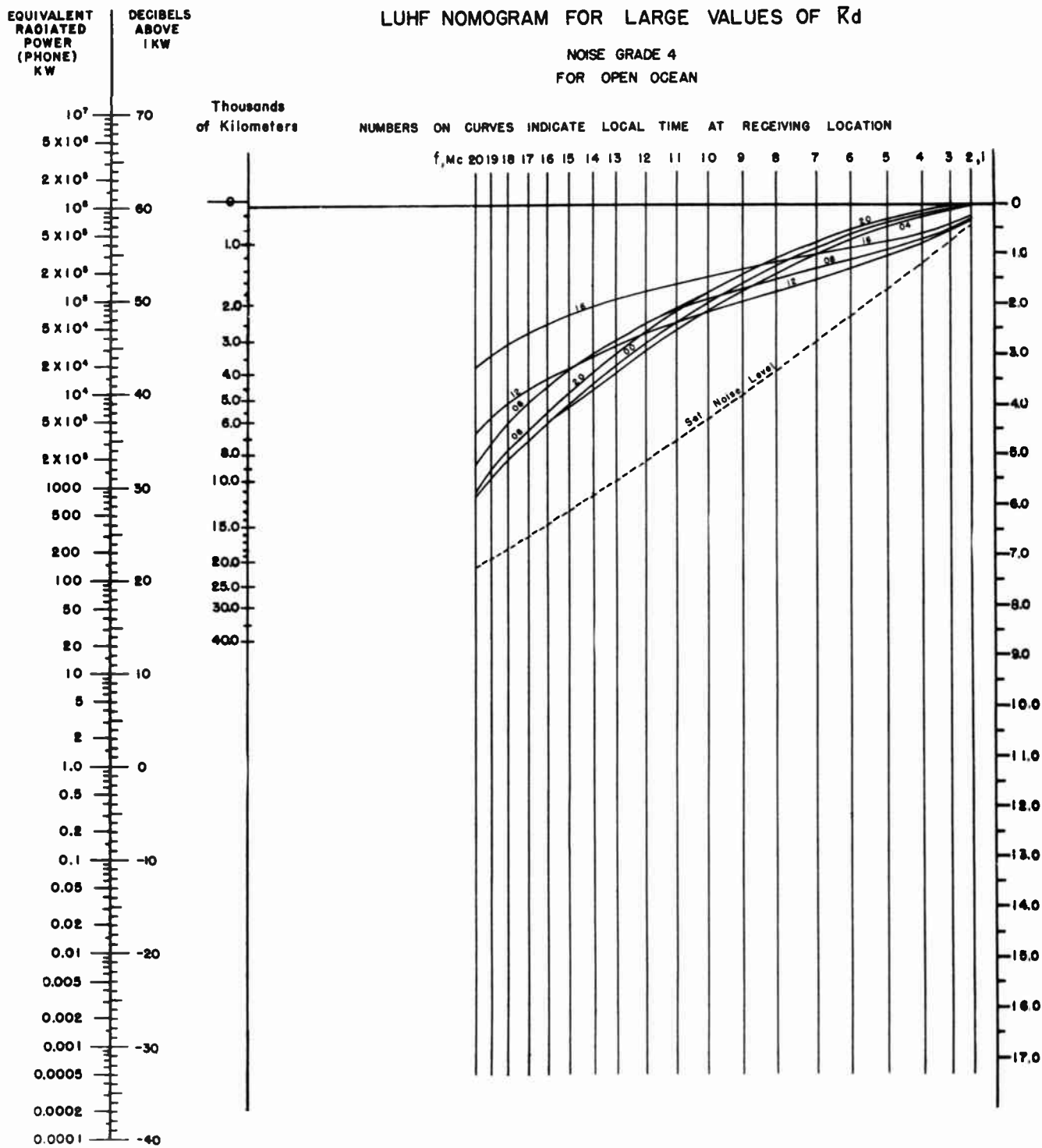


Fig. 64.

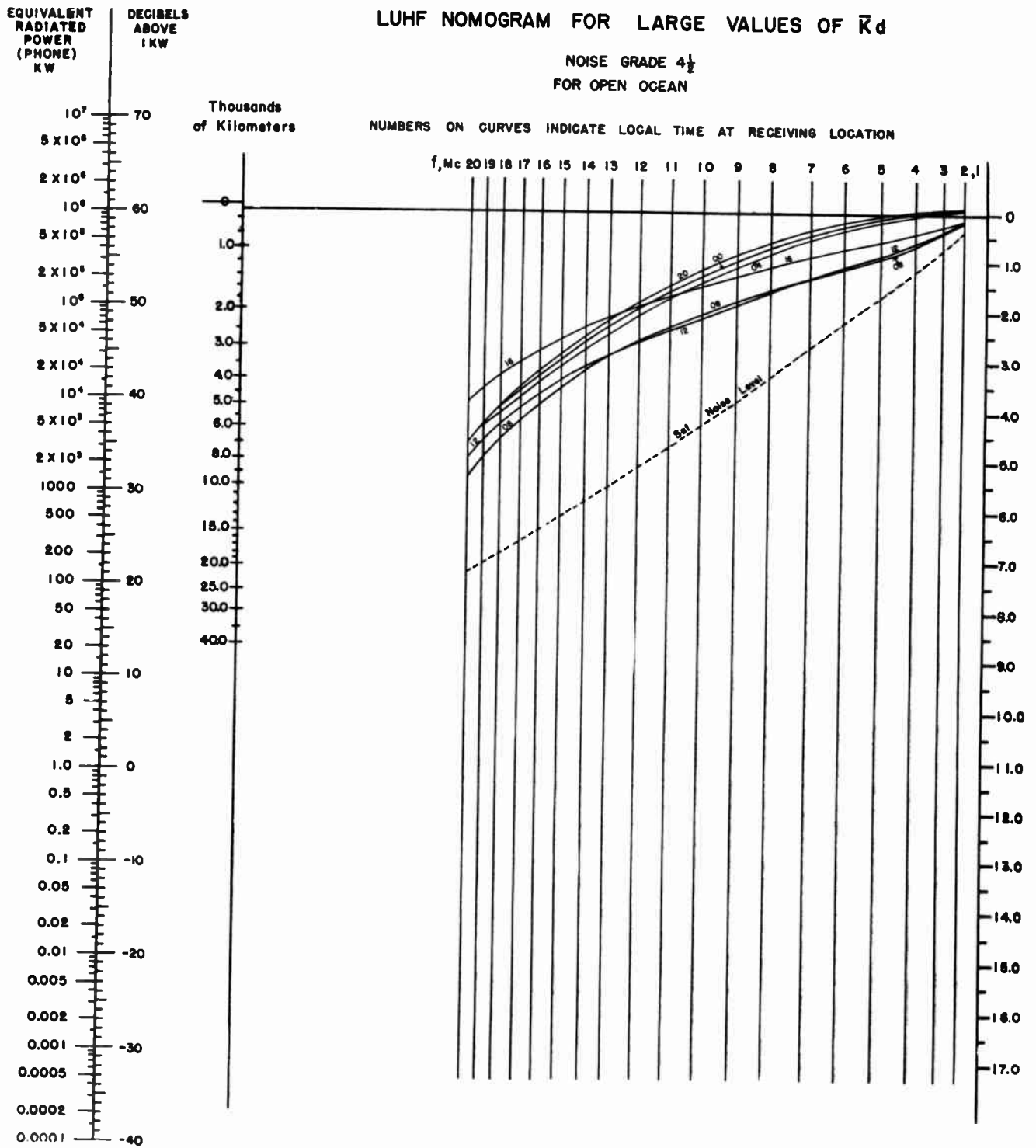


Fig. 65.

LUHF NOMOGRAM FOR LARGE VALUES OF R_d

NOISE GRADE 5
FOR OPEN OCEAN

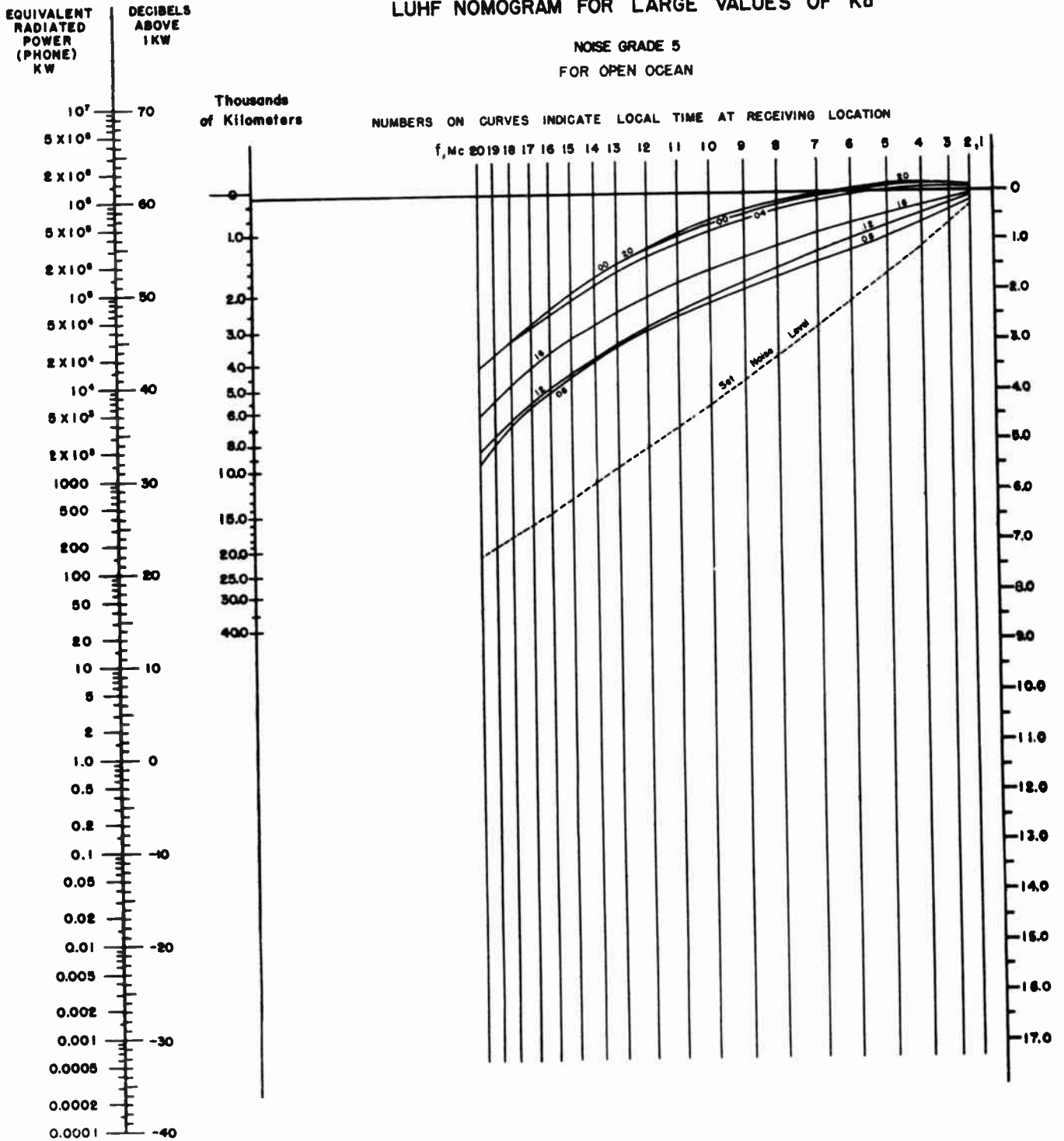


Fig. 66.

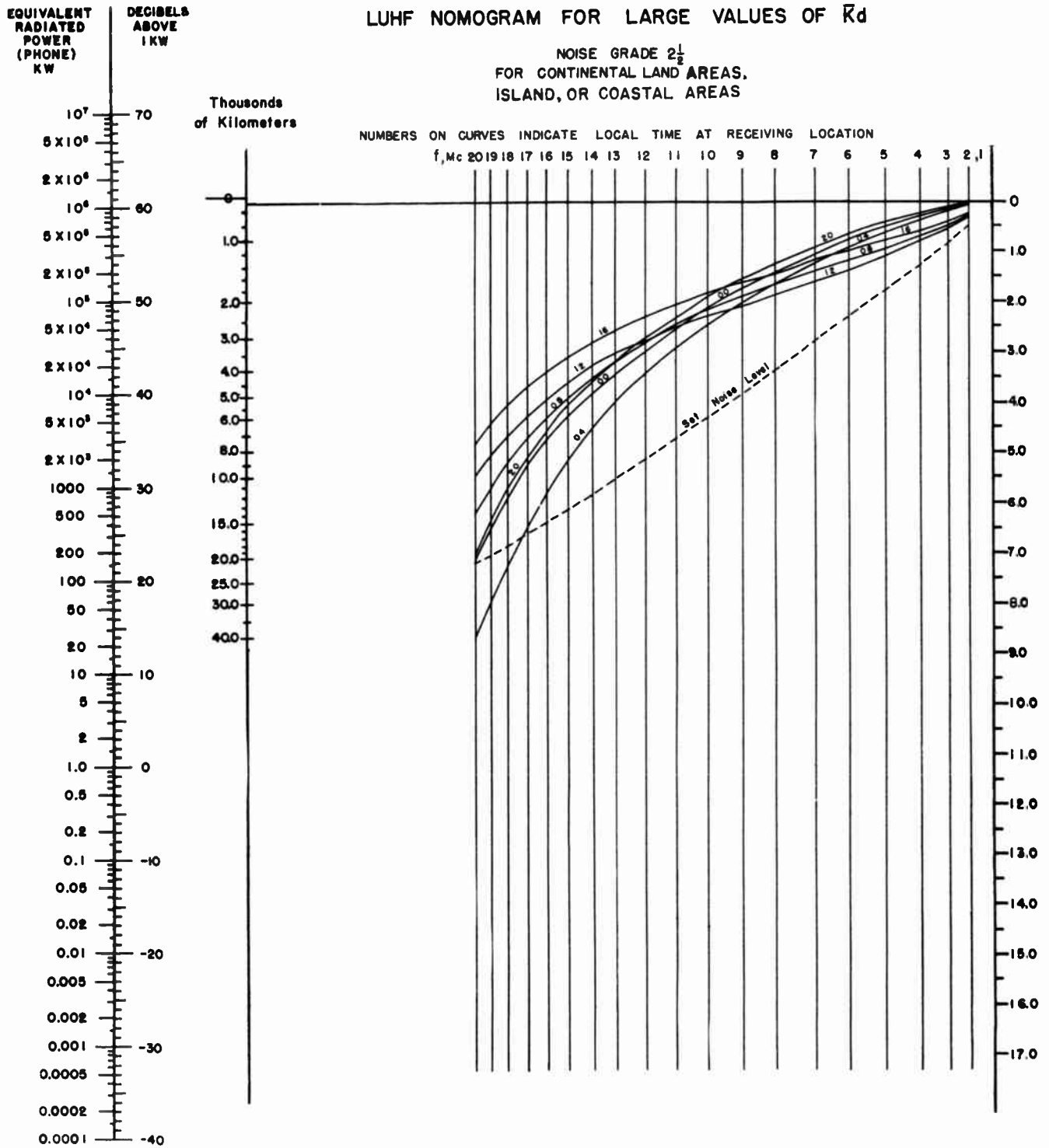


Fig. 67.

LUHF NOMOGRAM FOR LARGE VALUES OF \bar{R}_d

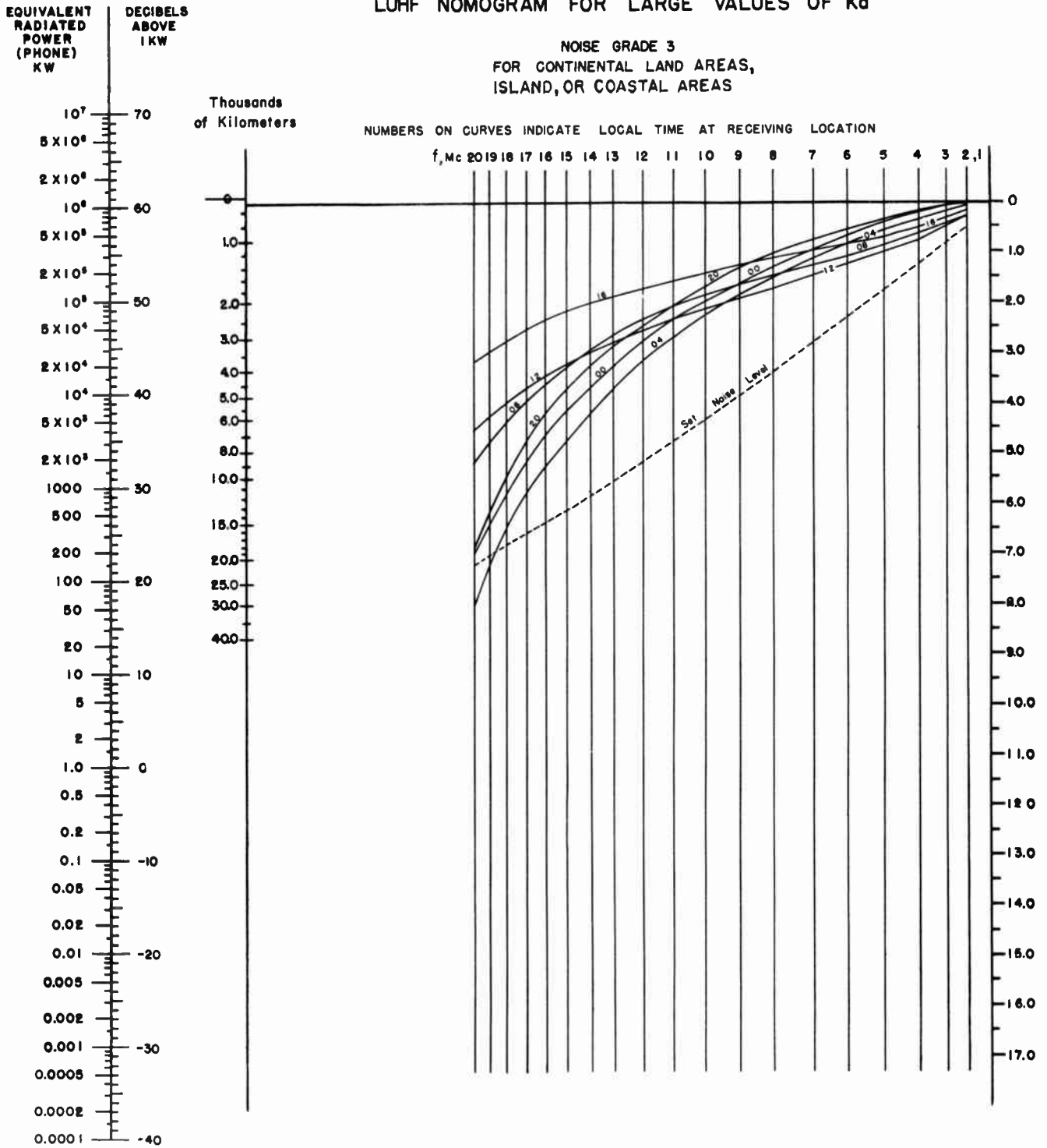


Fig. 68.

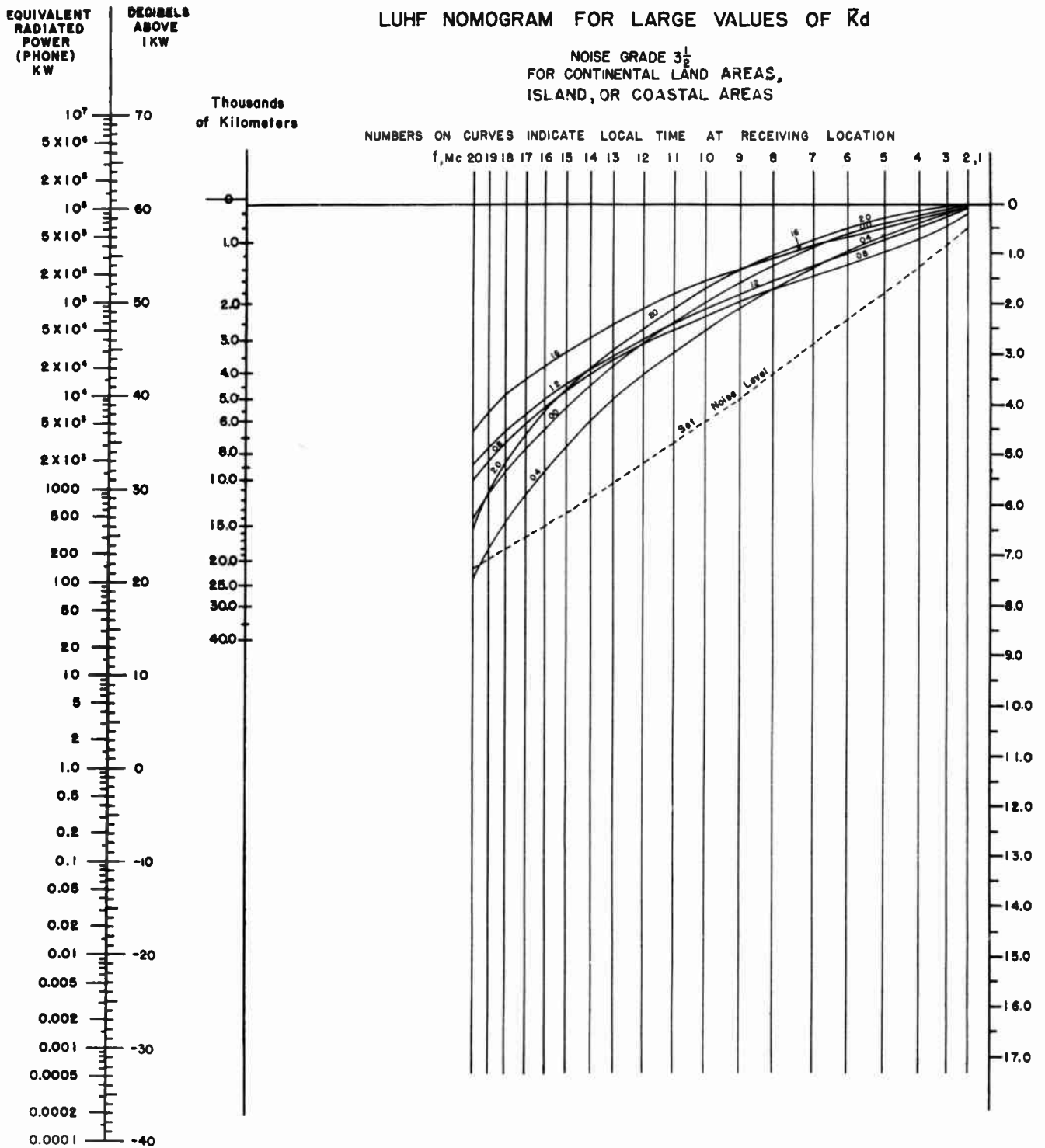


Fig. 69.

CALCULATION OF LOWEST USEFUL HIGH FREQUENCIES

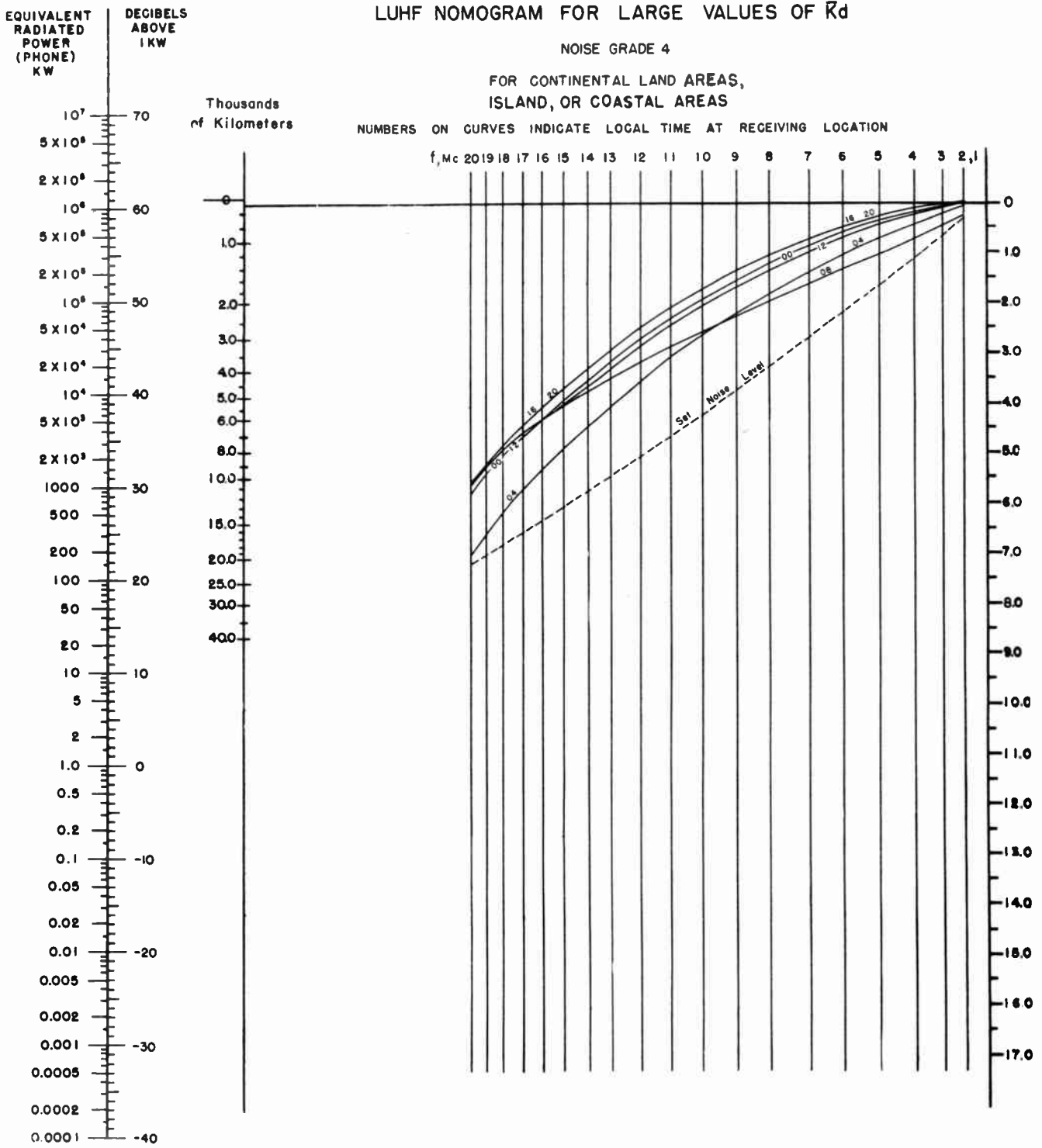


Fig. 70.

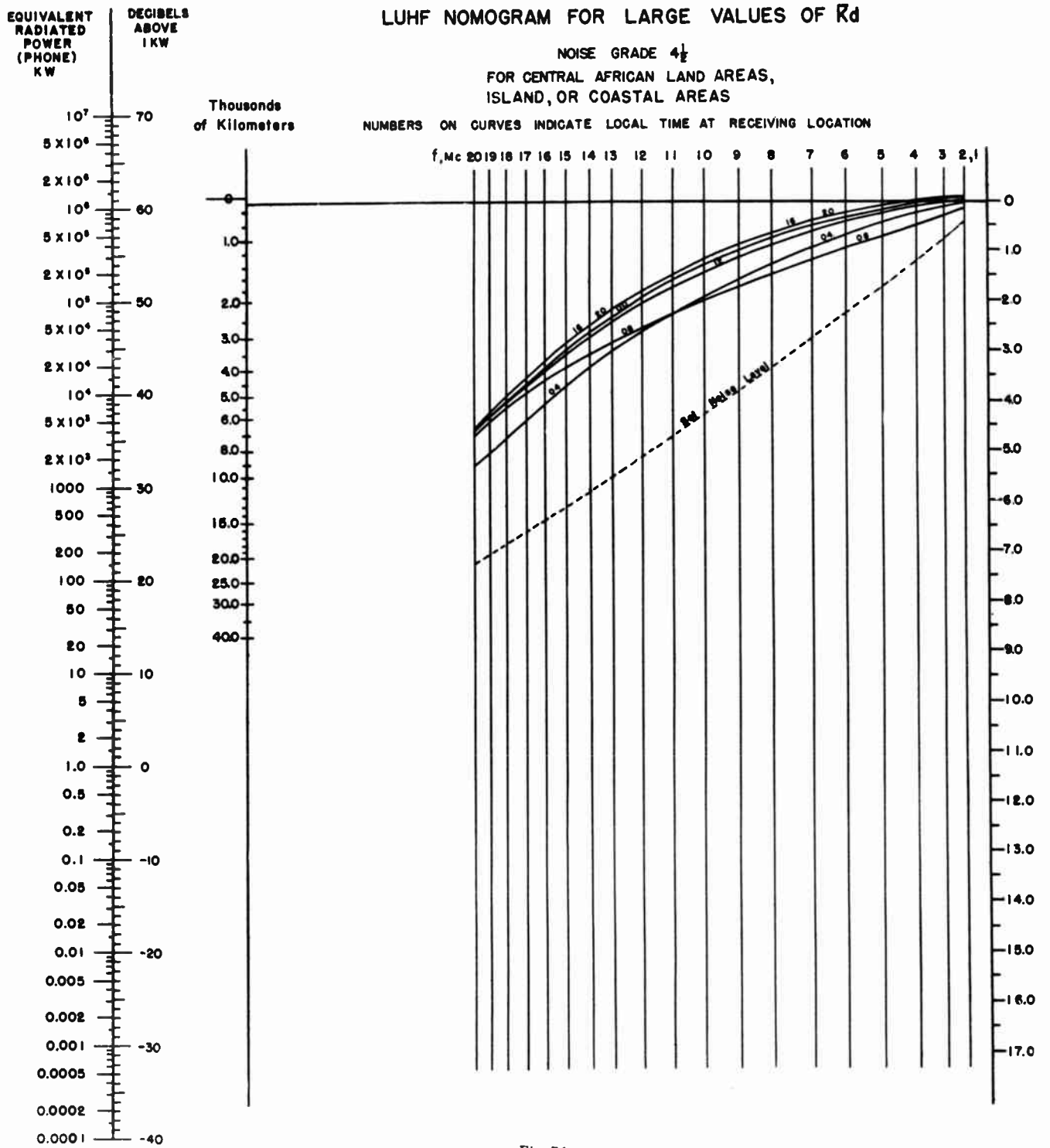


Fig. 71.

LUHF NOMOGRAM FOR LARGE VALUES OF K_d

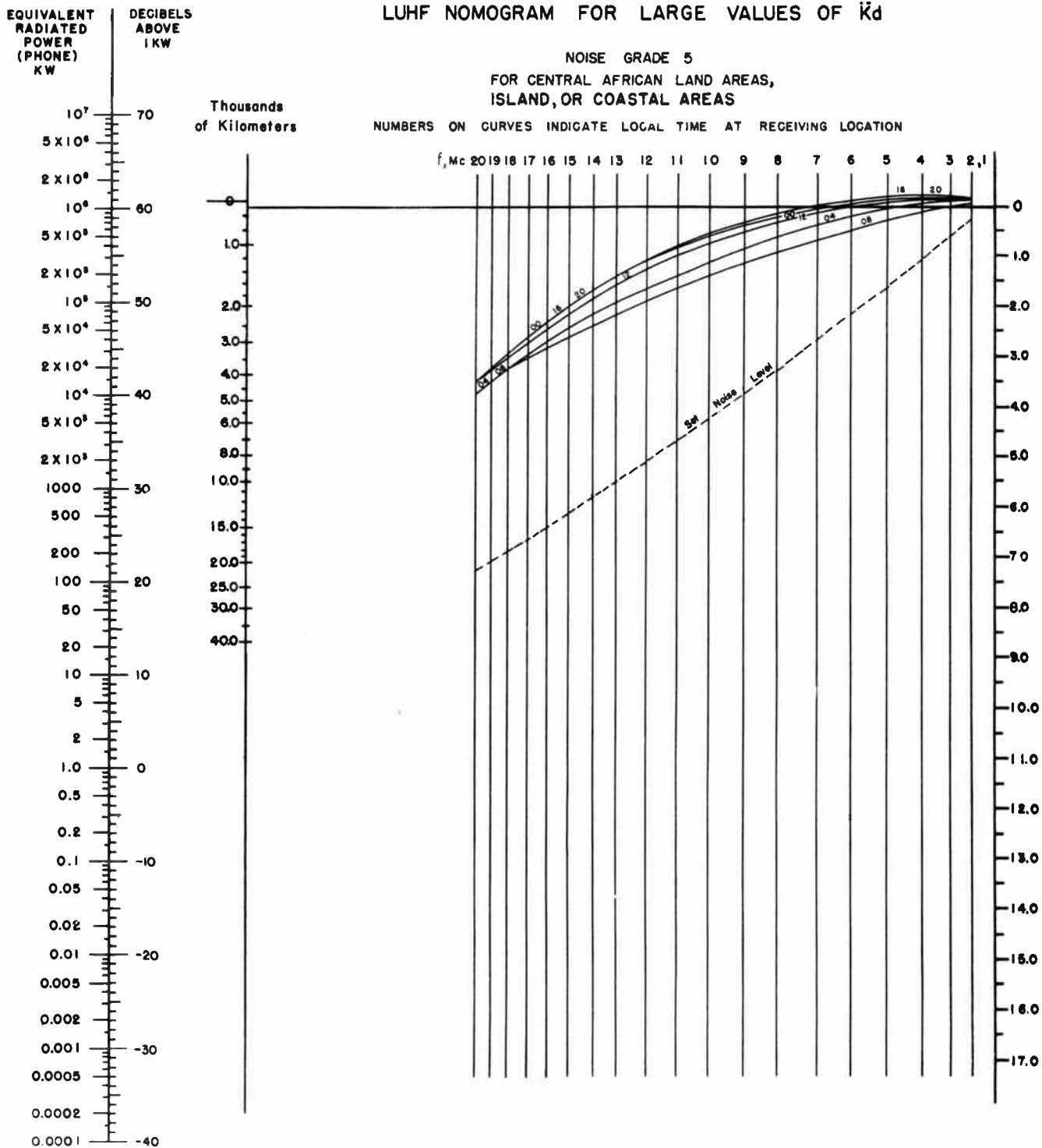


Fig. 72.

LUHF NOMOGRAM FOR SMALL VALUES OF \bar{R}_d

NOISE GRADE $1\frac{1}{2}$
FOR GENERAL USE

NUMBERS ON CURVES INDICATE
LOGAL TIME AT RECEIVING LOCATION

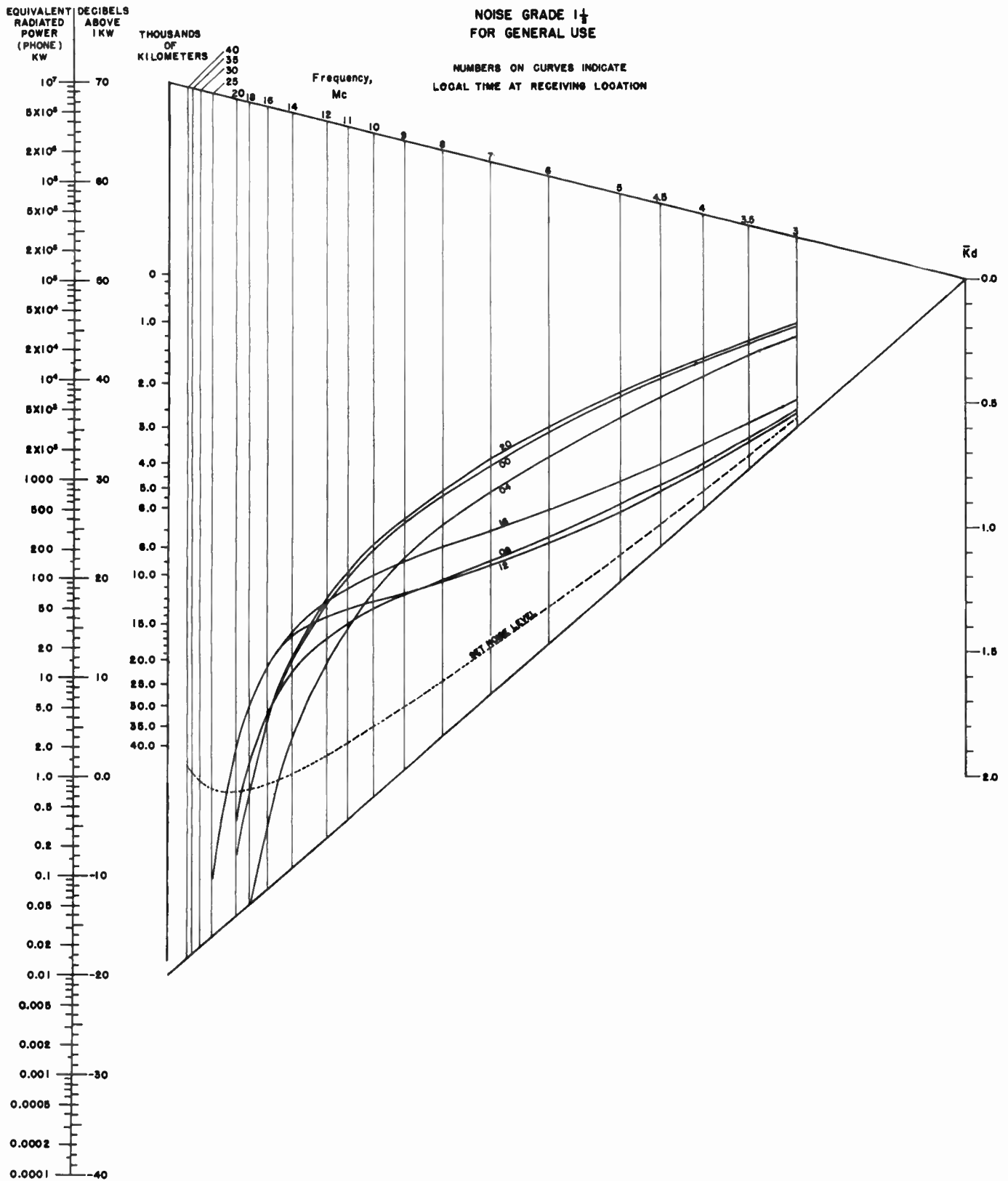


Fig. 74.

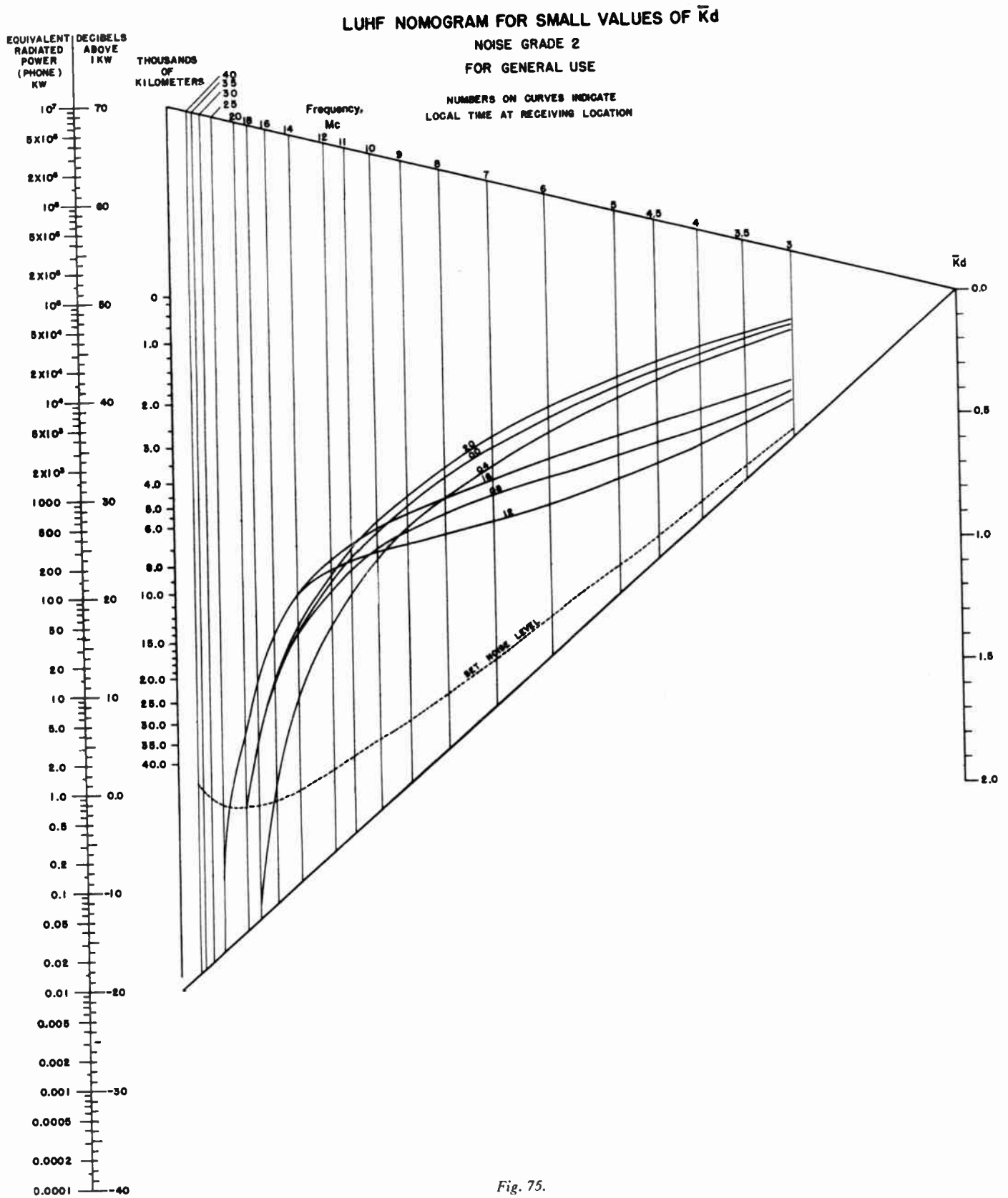


Fig. 75.

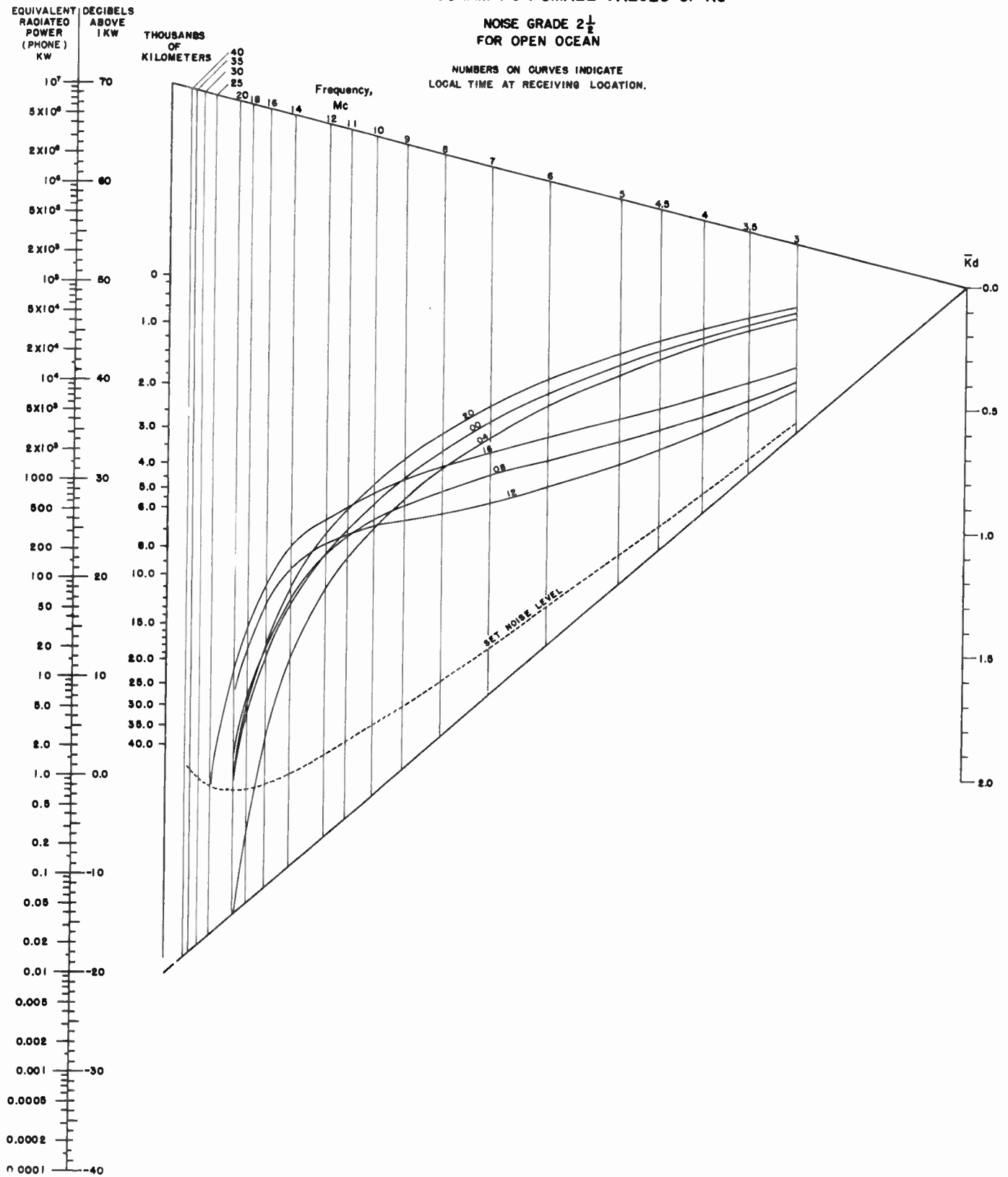
LUHF NOMOGRAM FOR SMALL VALUES OF \bar{K}_d 

Fig. 76.

LUHF NOMOGRAM FOR SMALL VALUES OF \bar{K}_d

NOISE GRADE 3
FOR OPEN OCEAN

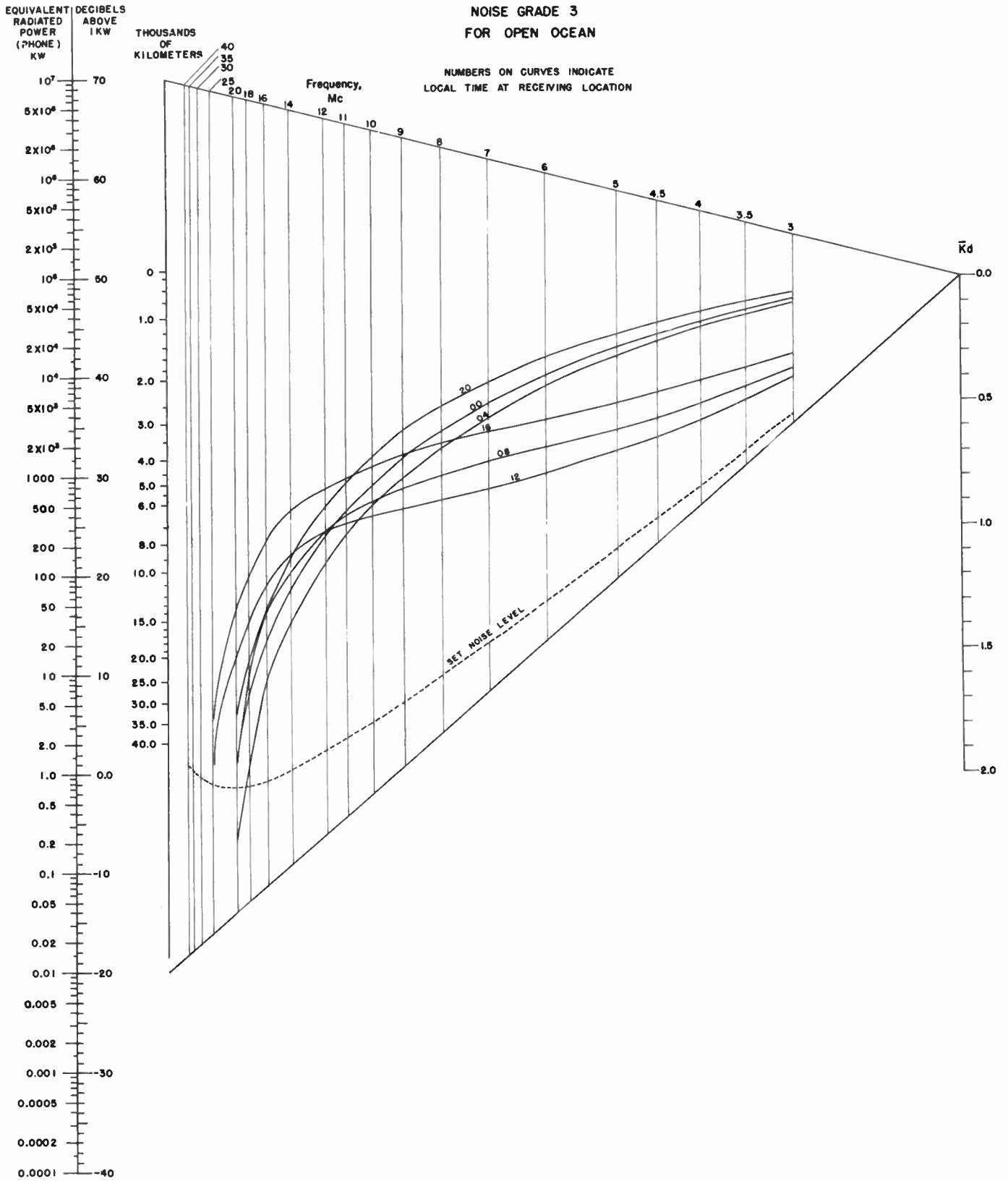


Fig. 77.

LUHF NOMOGRAM FOR SMALL VALUES OF \bar{K}_d

NOISE GRADE $3\frac{1}{2}$
FOR OPEN OCEAN

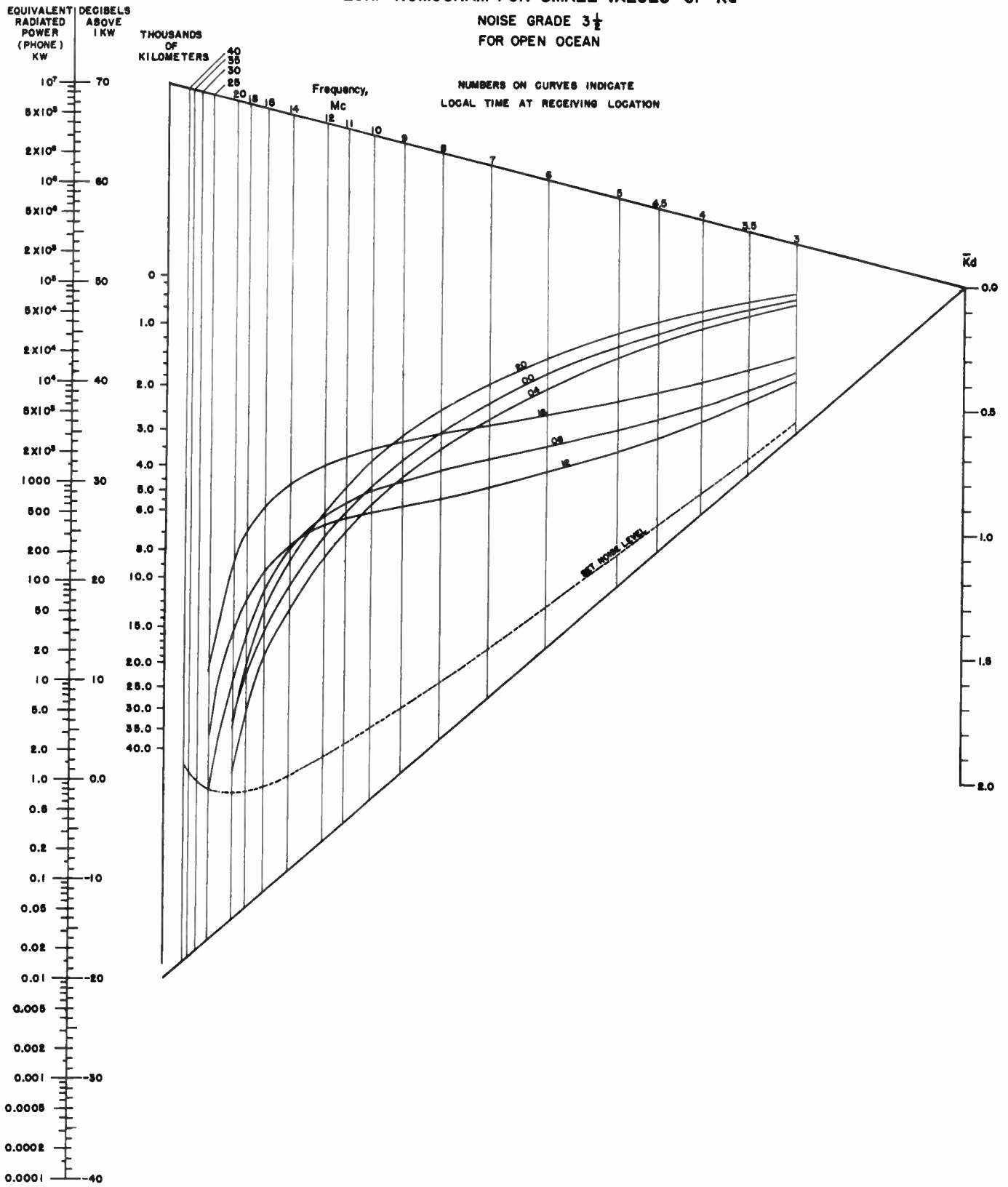


Fig. 78.

LUHF NOMOGRAM FOR SMALL VALUES OF R_d

NOISE GRADE 4
FOR OPEN OCEAN

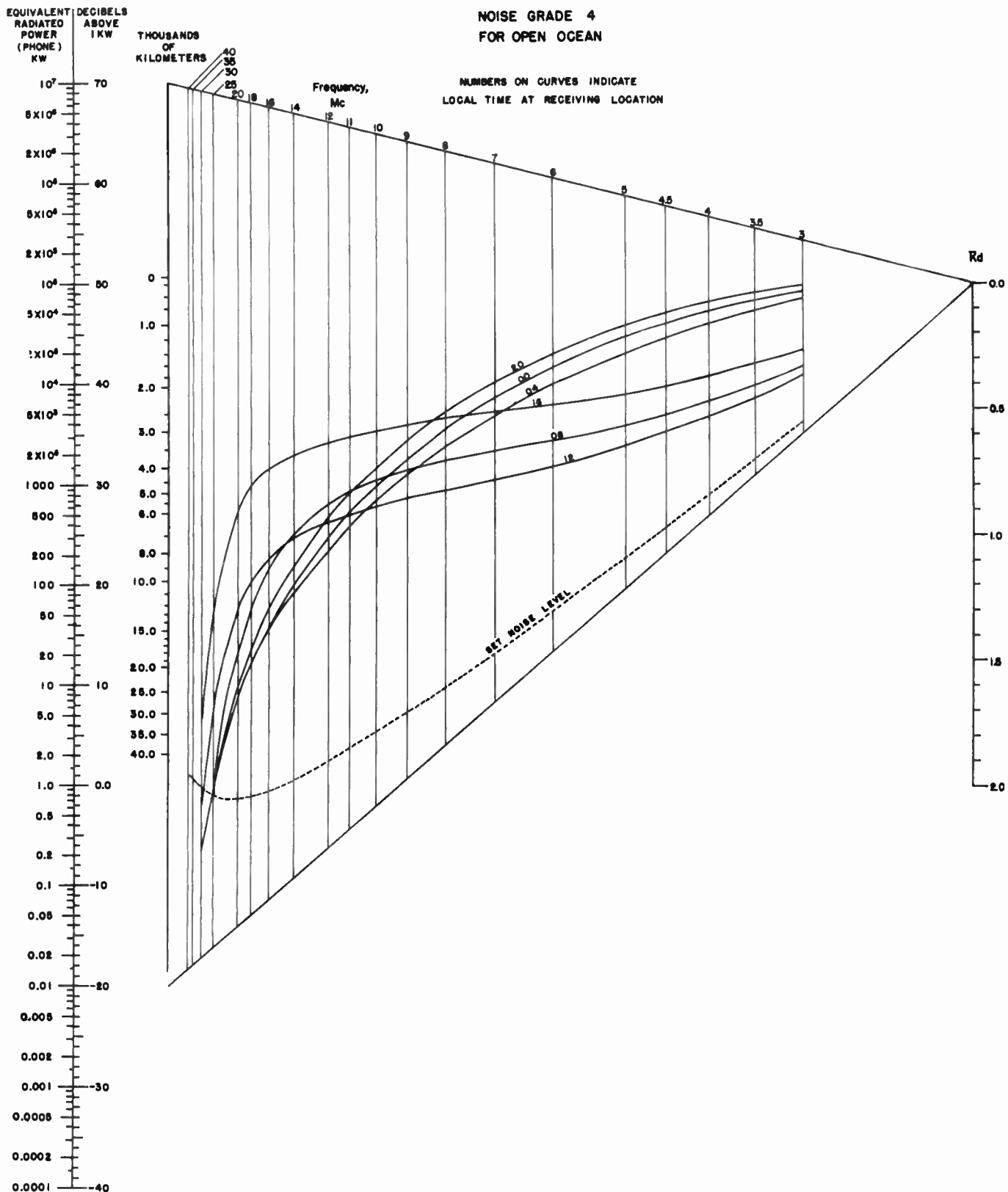


Fig. 79.

LUHF NOMOGRAM FOR SMALL VALUES OF \bar{K}_d

NOISE GRADE $4\frac{1}{2}$
FOR OPEN OCEAN

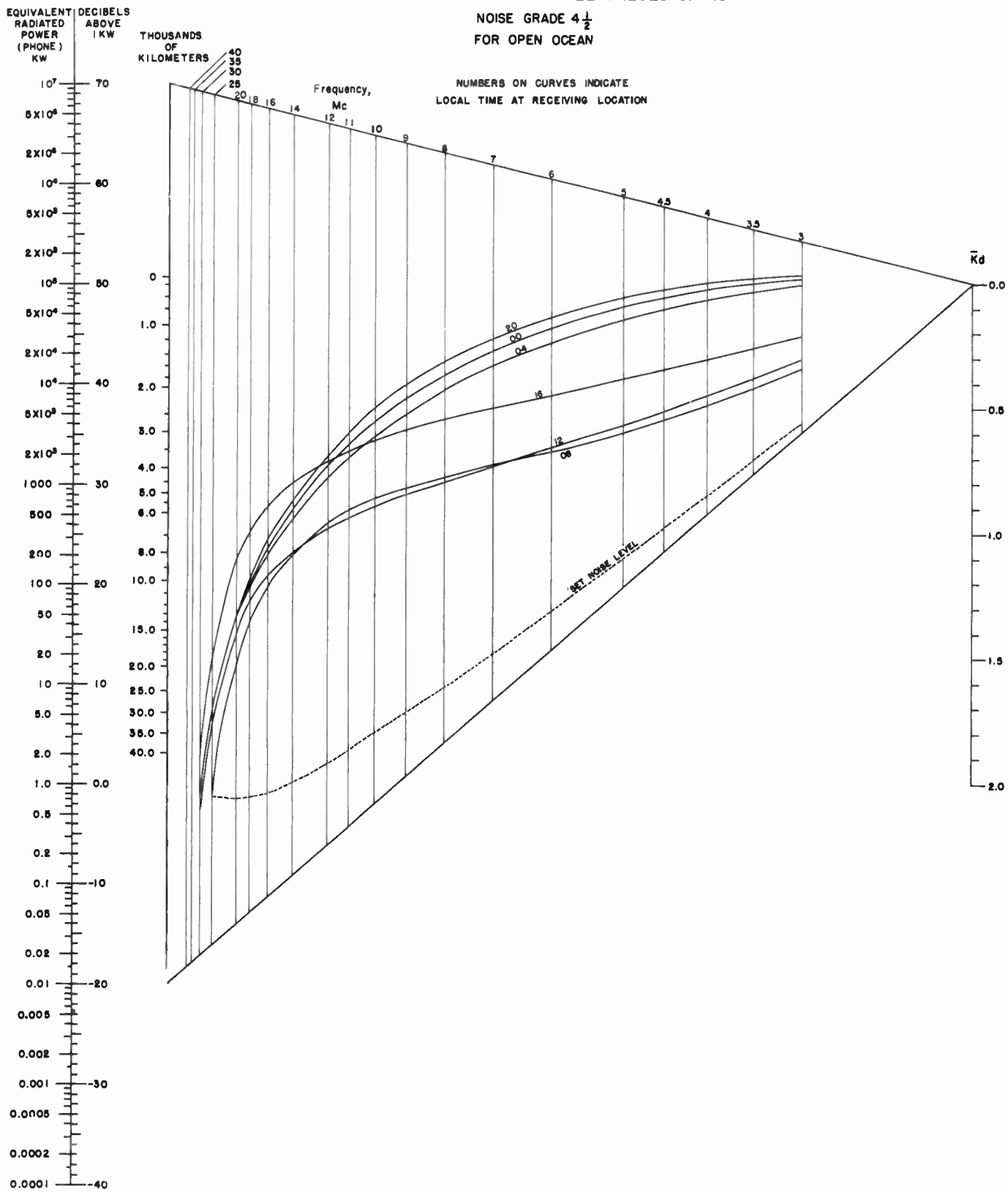


Fig. 80.

LUHF NOMOGRAM FOR SMALL VALUES OF \bar{K}_d

NOISE GRADE 5
FOR OPEN OCEAN

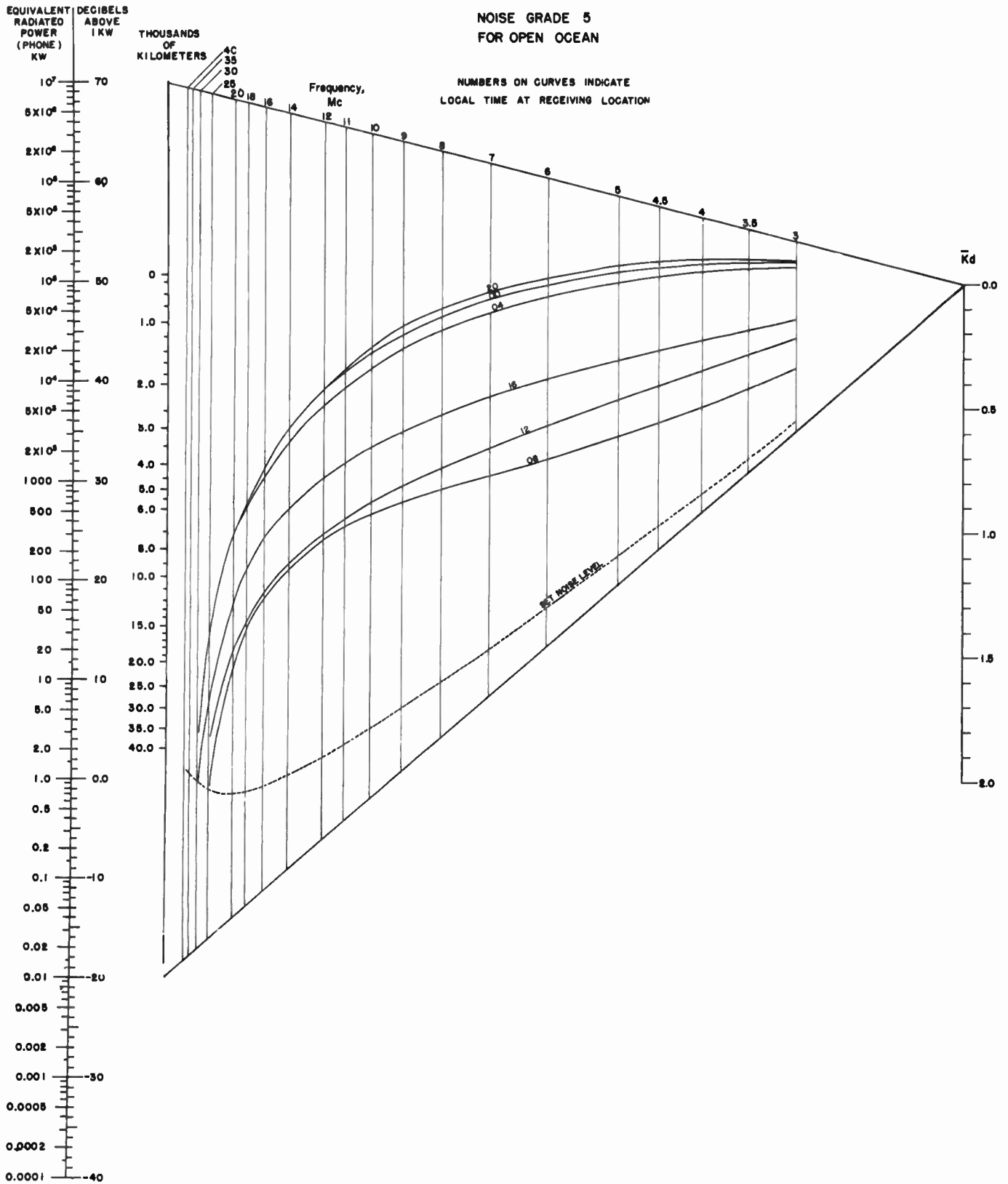


Fig. 81.

LUHF NOMOGRAM FOR SMALL VALUES OF \bar{K}_d

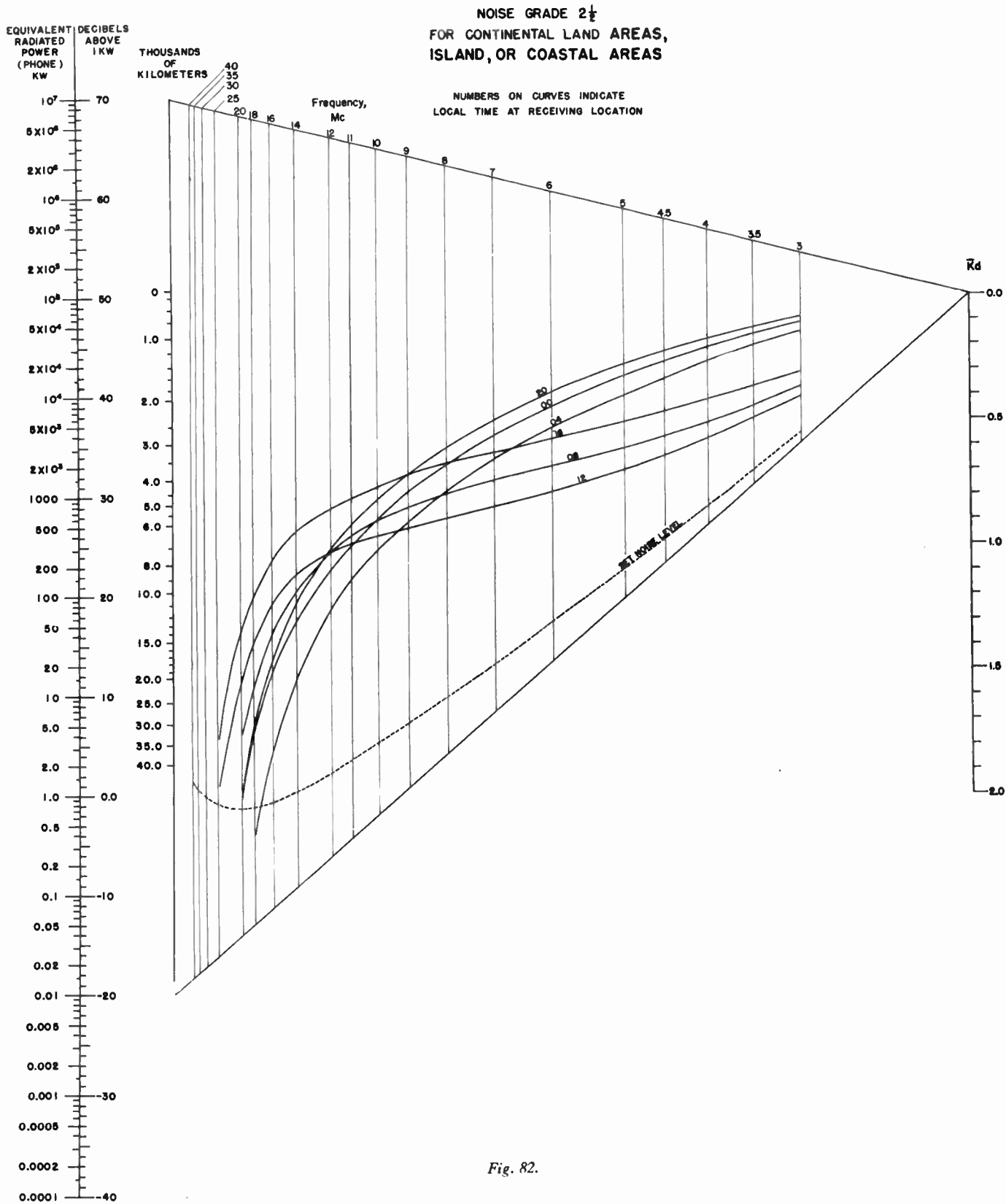


Fig. 82.

LUHF NOMOGRAM FOR SMALL VALUES OF Kd

NOISE GRADE 3
FOR CONTINENTAL LAND AREAS,
ISLAND, OR COASTAL AREAS

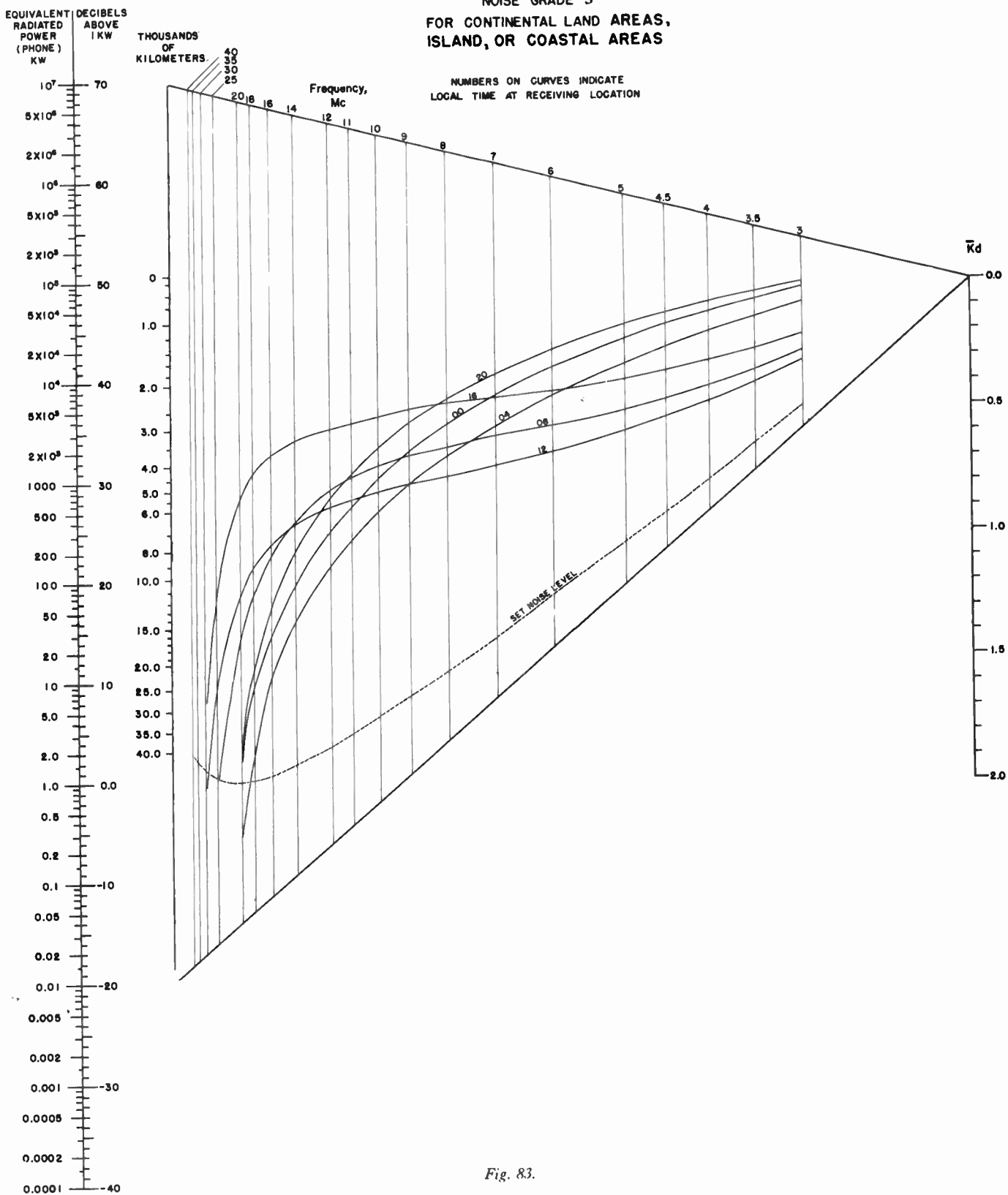


Fig. 83.

CALCULATION OF LOWEST USEFUL HIGH FREQUENCIES

LUHF NOMOGRAM FOR SMALL VALUES OF \bar{K}_d

NOISE GRADE $3\frac{1}{2}$
FOR CONTINENTAL LAND AREAS,
ISLAND, OR COASTAL AREAS

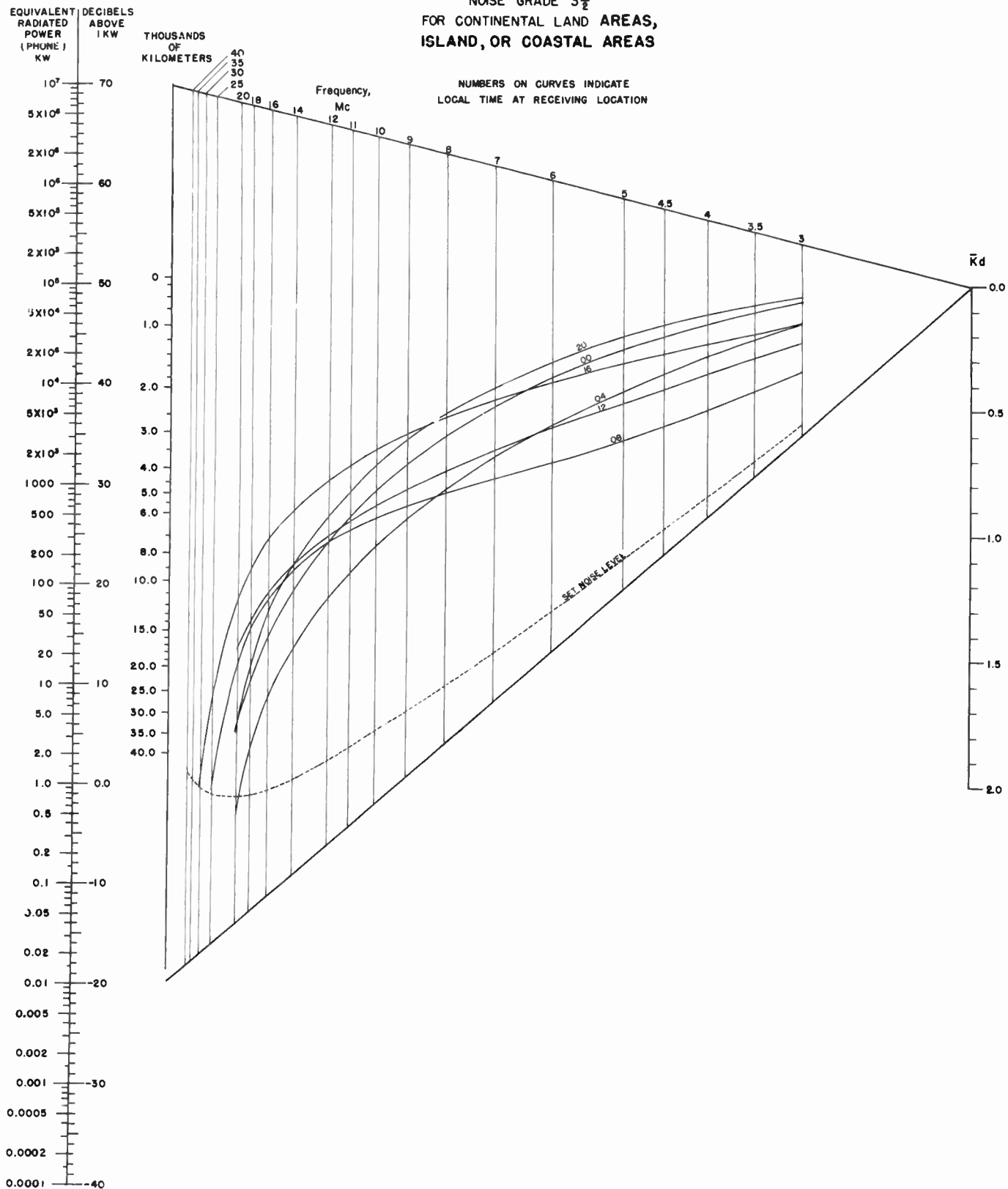


Fig. 84.

LUHF NOMOGRAM FOR SMALL VALUES OF R_d

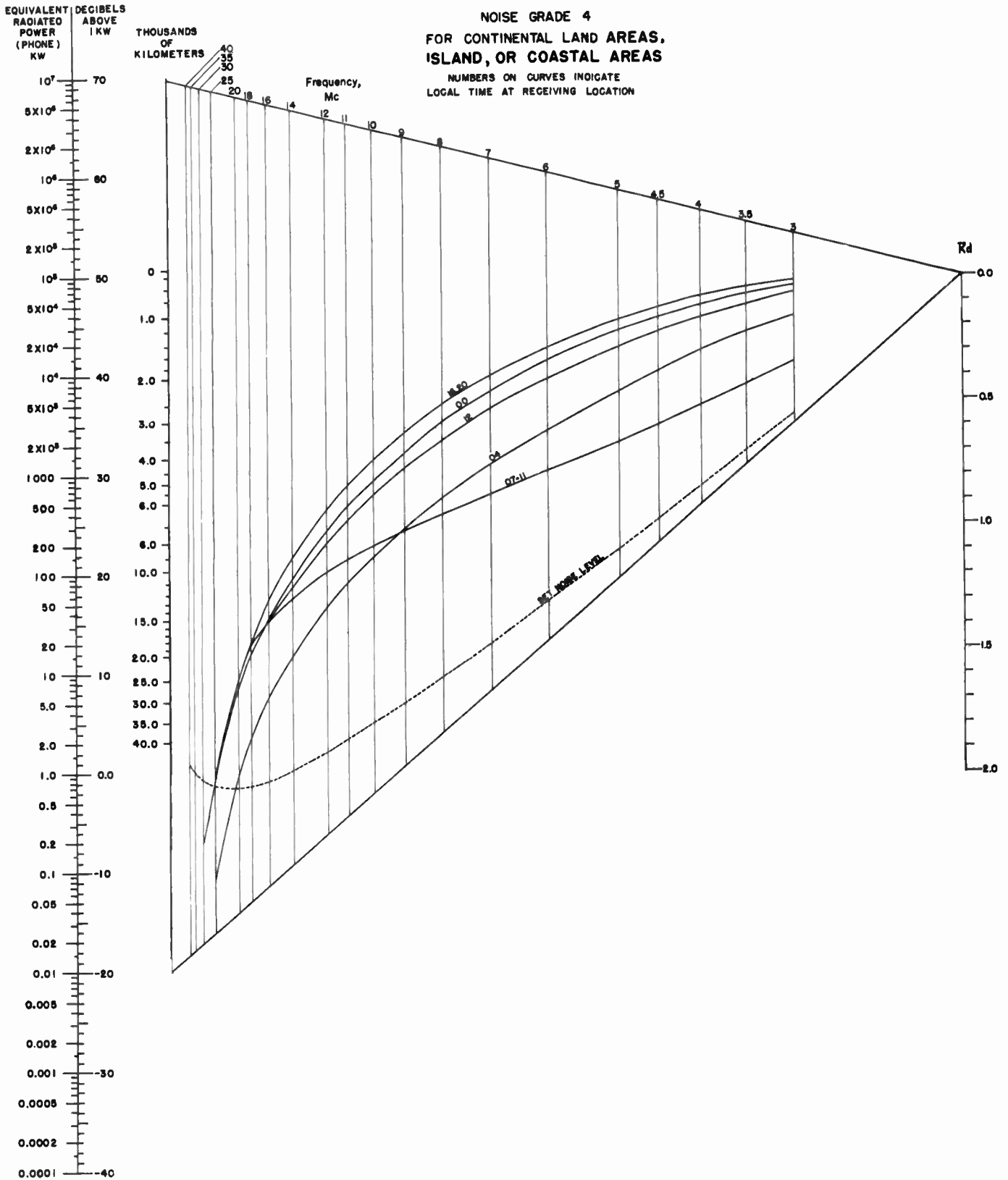


Fig. 85.

LUHF NOMOGRAM FOR SMALL VALUES OF \bar{R}_d

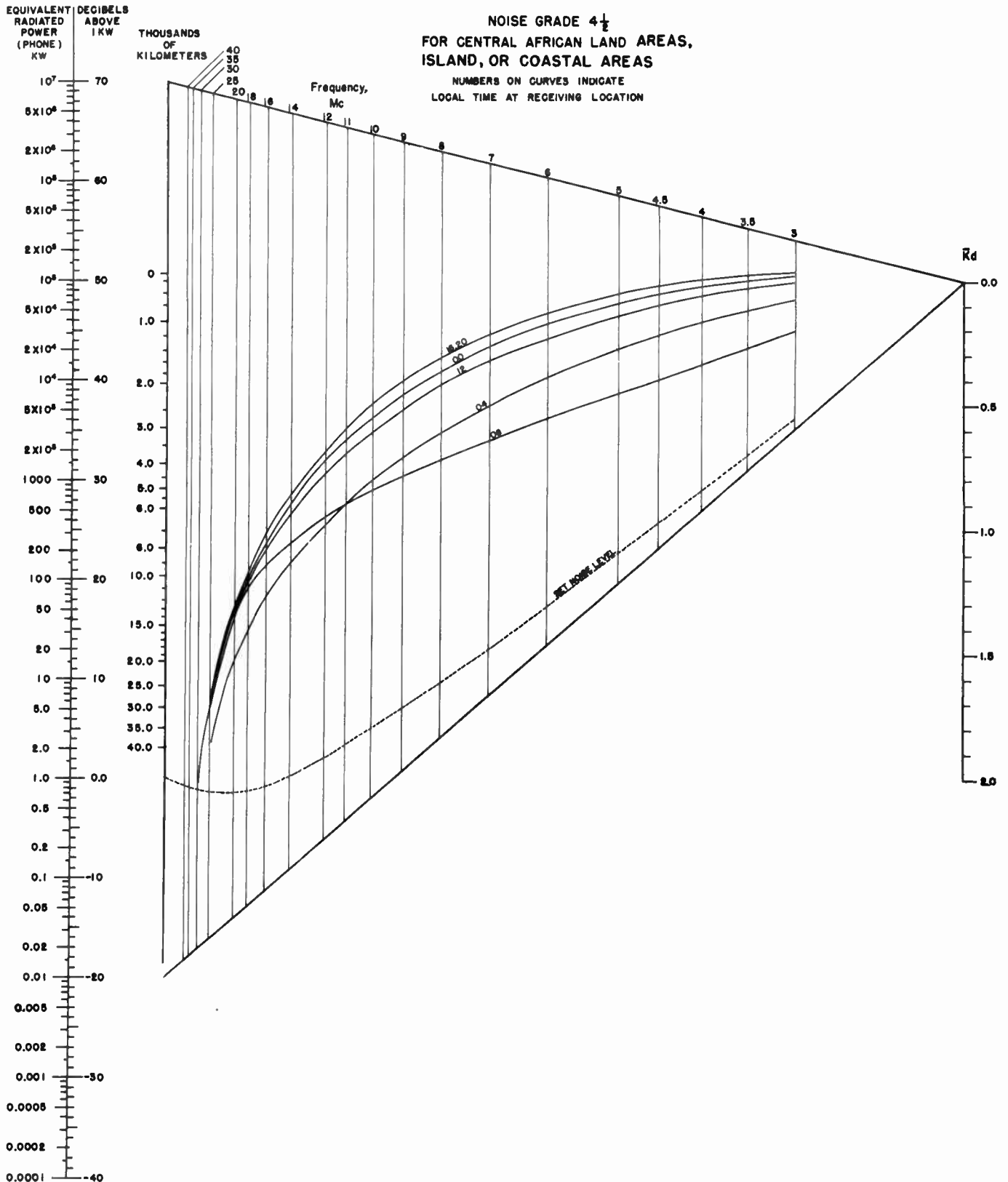


Fig. 86.

LUHF NOMOGRAM FOR SMALL VALUES OF R_d

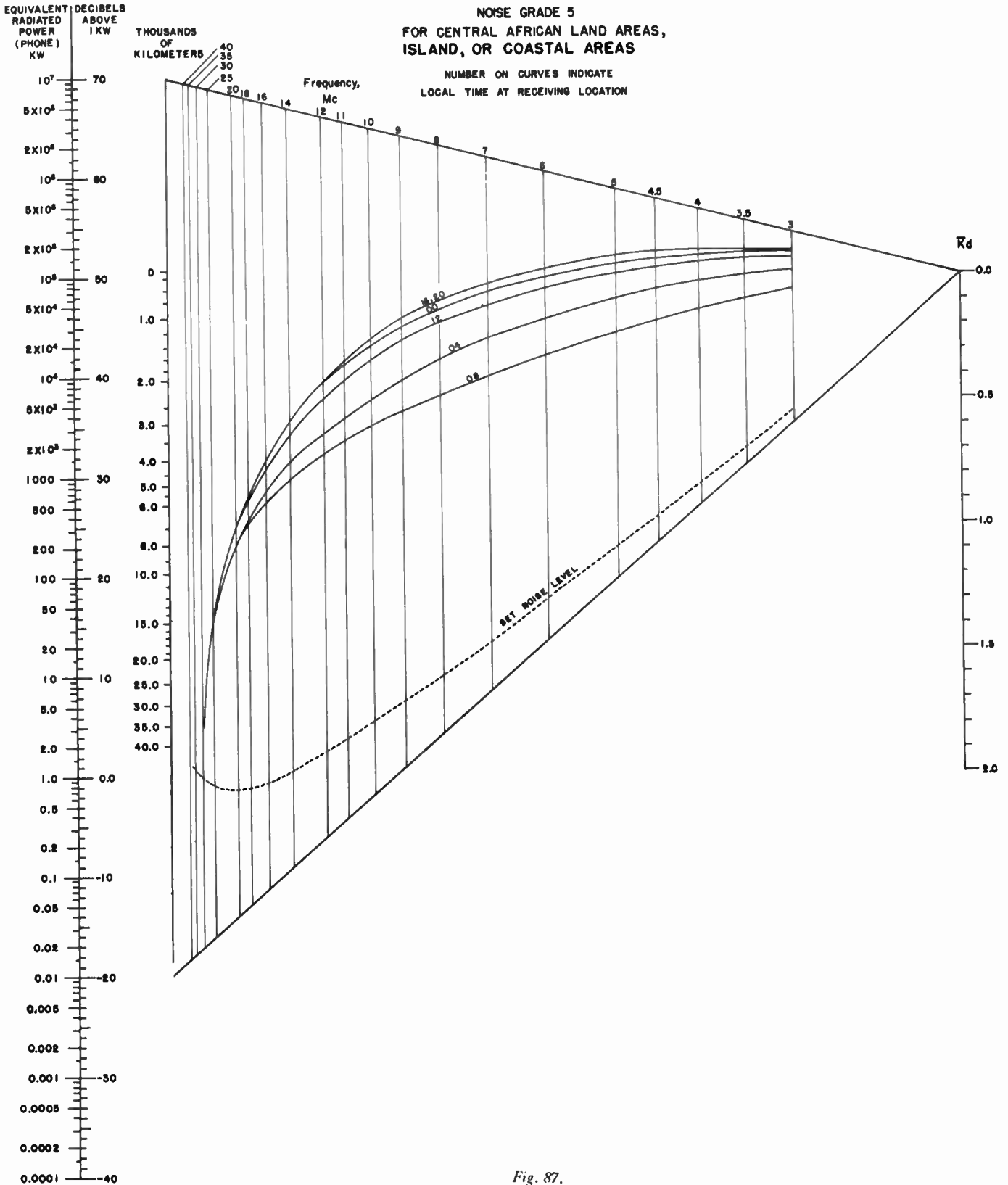


Fig. 87.

AUXILIARY POWER INDEX

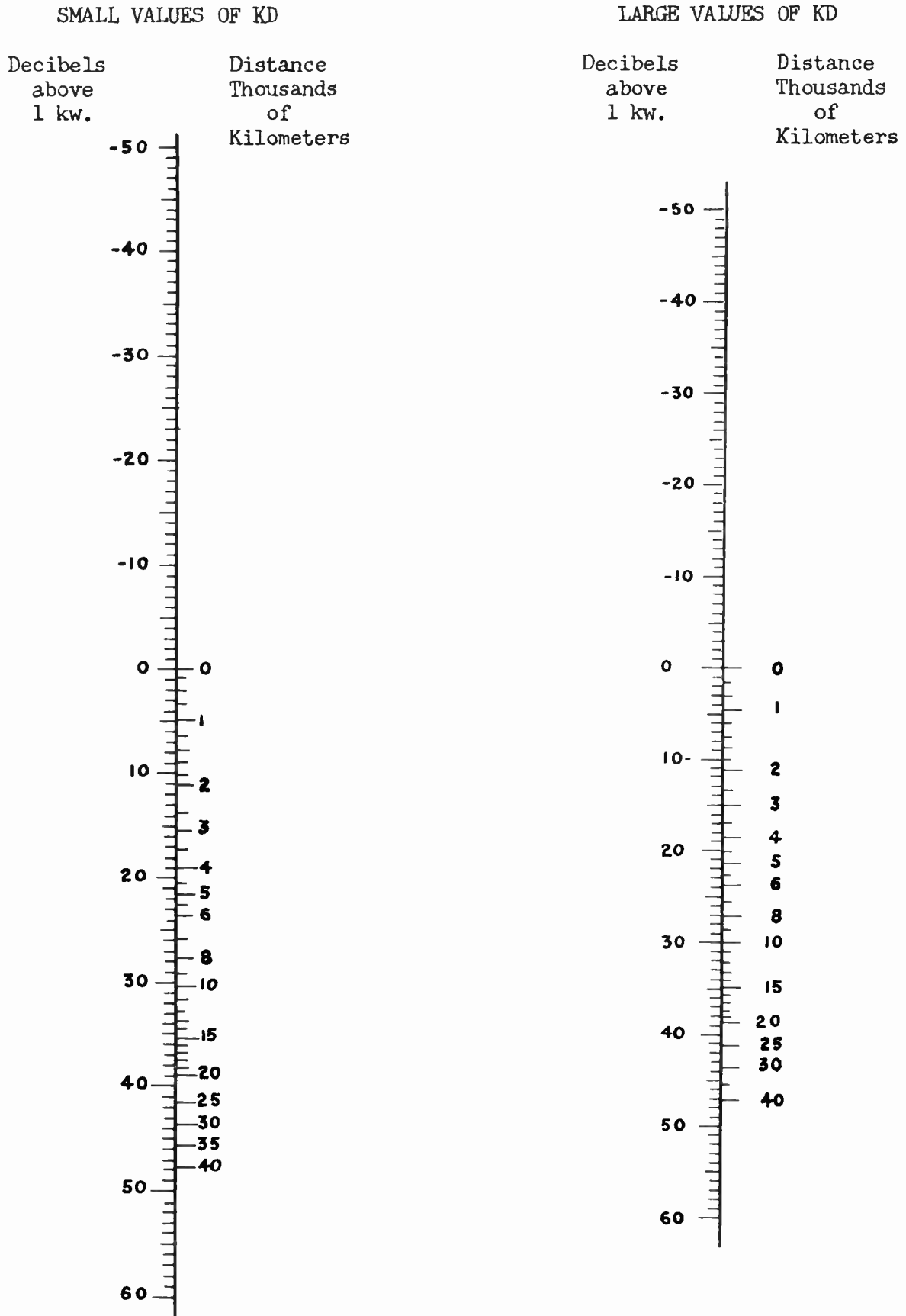


Fig. 88.

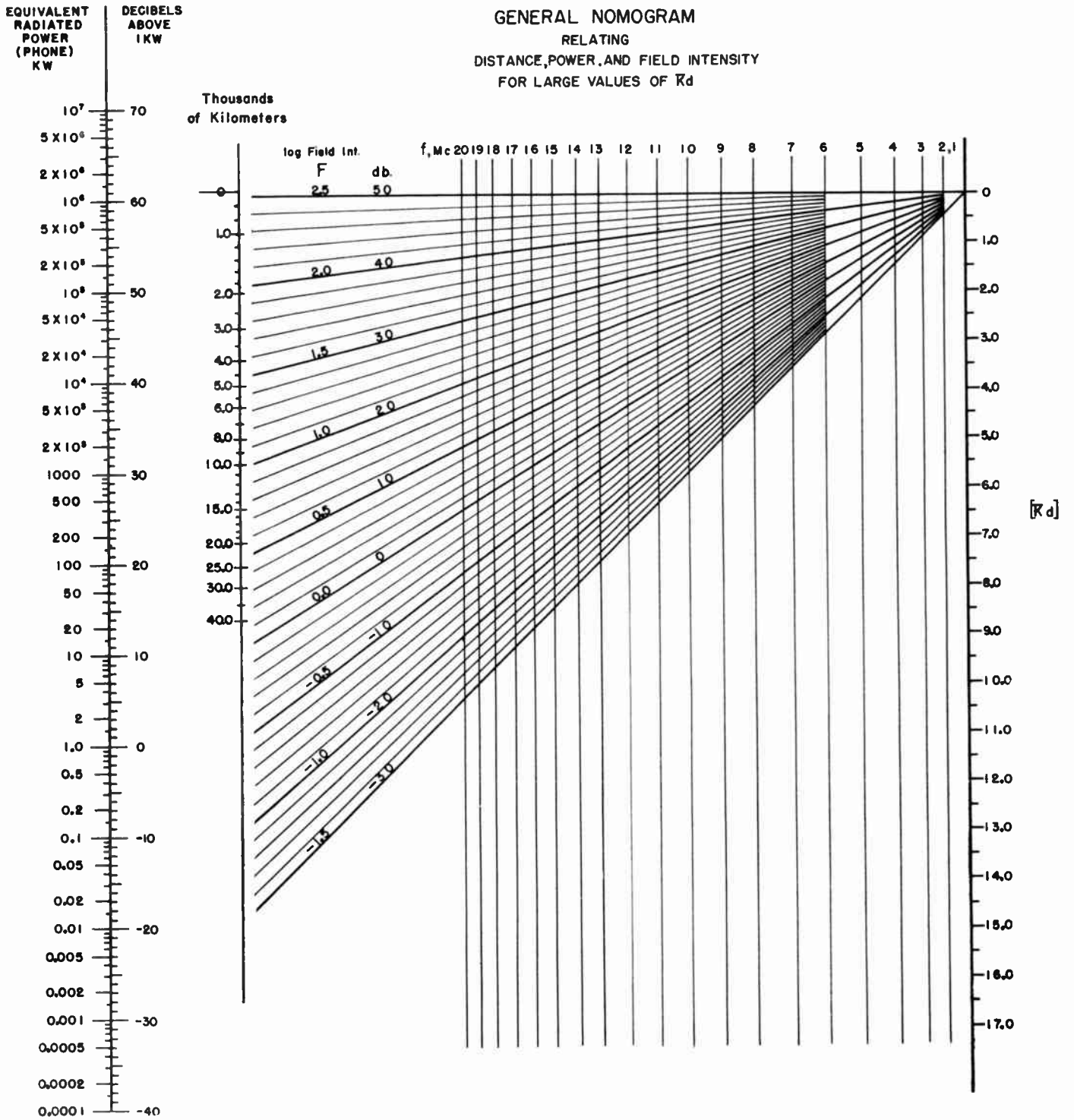


Fig. 89.

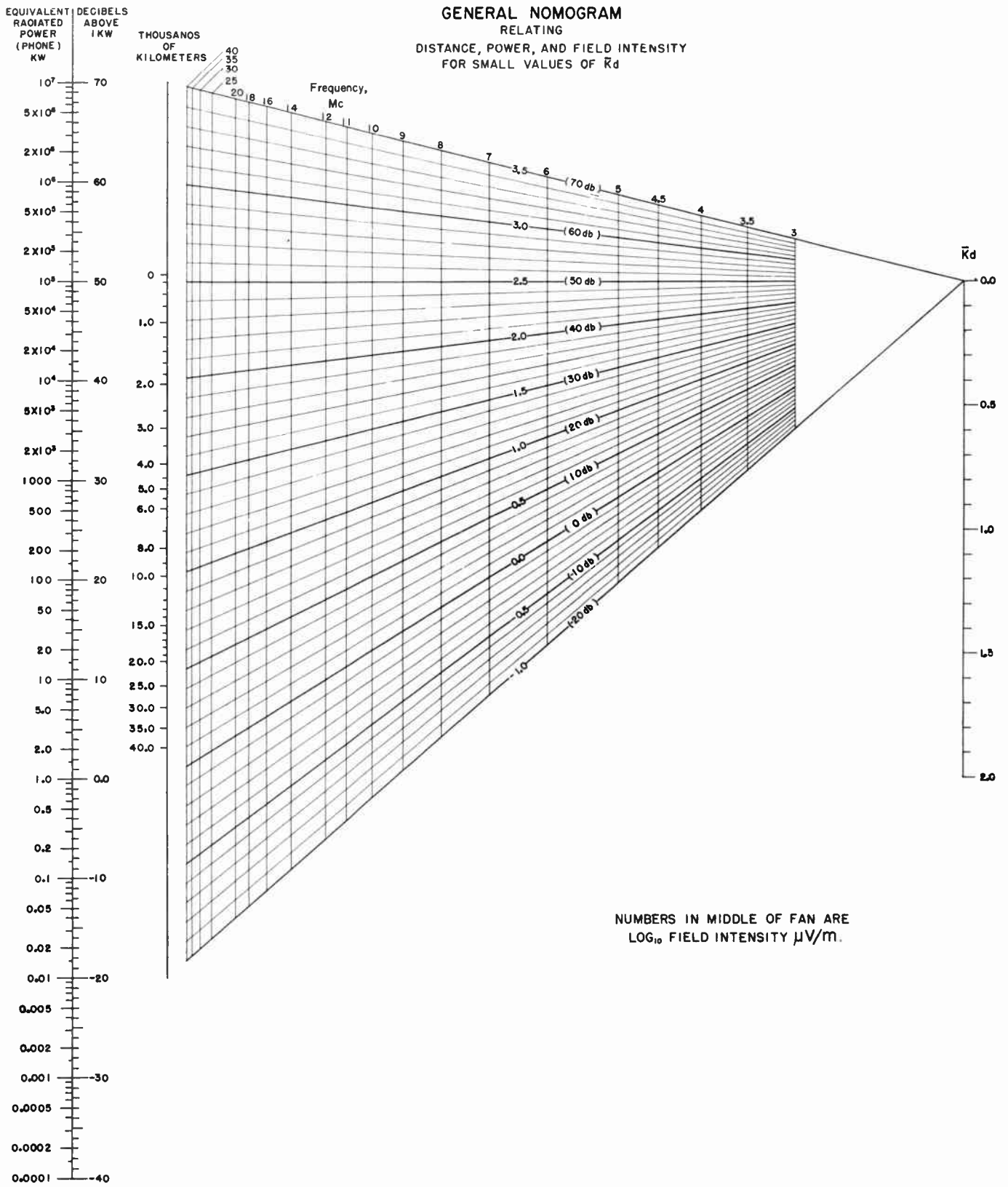


Fig. 90.

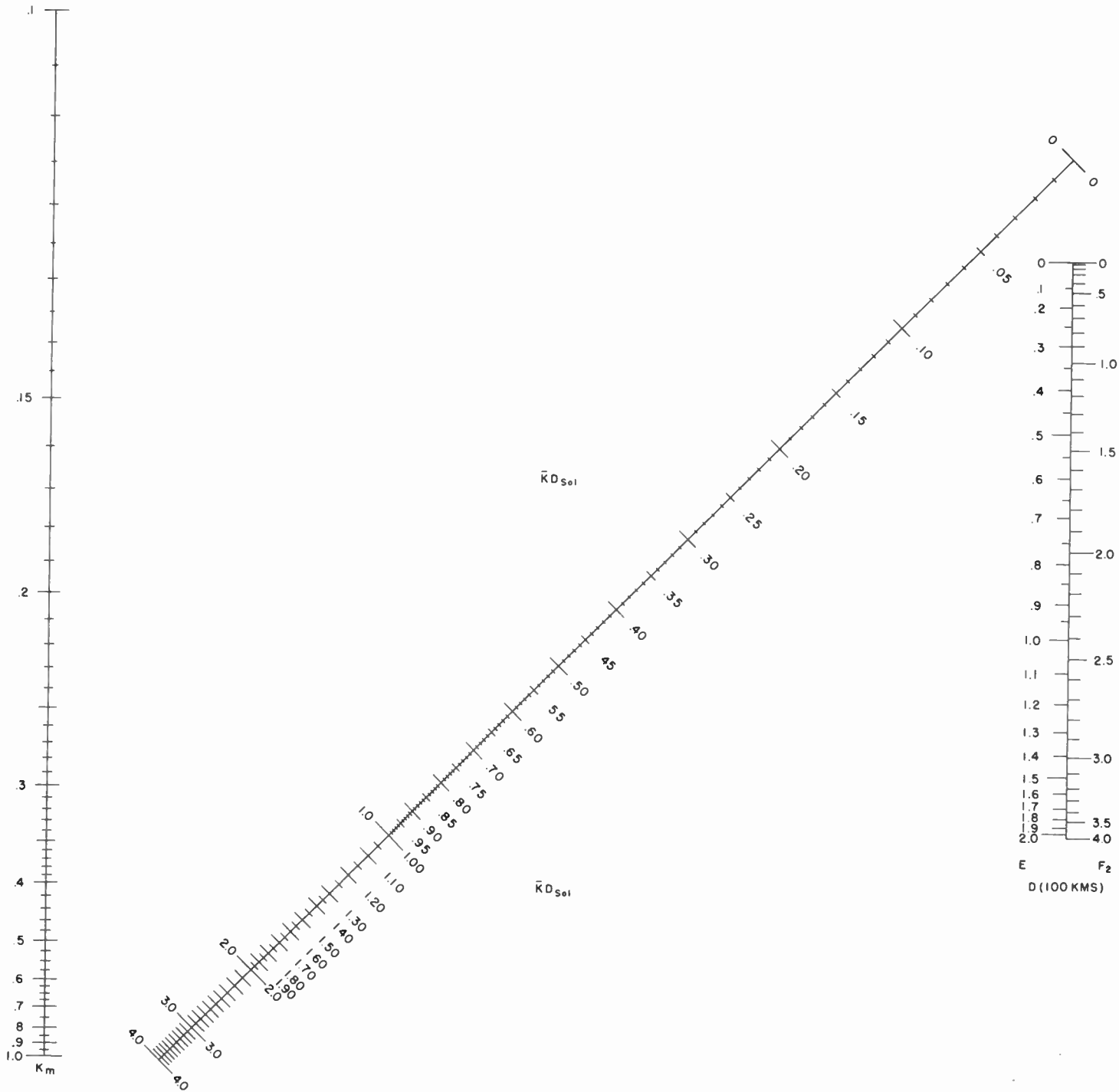


Fig. 93. Nomogram for Computing $(Kd)_{not}$.

• CHAPTER NINE •

VARIABILITY OF THE SUN

OBSERVATIONS SHOW THAT THE IONOSPHERE IS CONTINUOUSLY in a state of rapid fluctuation. Marked variations may occur from hour to hour and even from minute to minute. Solar radiations are responsible for the presence of the electrons in the reflecting *E*, *F*₁, and *F*₂ layers and in the absorbing *D* regions on the lower fringe of the *E* layer. Variations in solar radiation disturb the normal characteristics of the ionospheric layers and may cause disturbances that interfere seri-

Astronomical observations show that the surface of the sun is not uniform in brightness. The whole area is mottled, covered with granulations of tiny bright spots and darker edges. Near the edge of the sun are larger groupings of bright areas, called *faculae*. In addition, there are the most conspicuous of all solar markings, the famed sunspots, which appear as black patches surrounded by a hazy grey edging (Figs. 94 and 95).

The sun appears to be in a constant state of eruption.

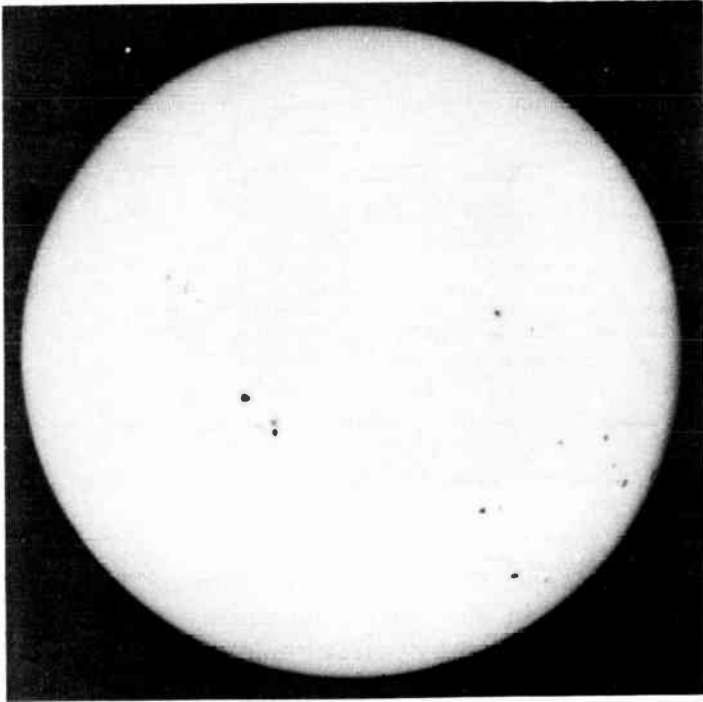


Fig. 94. Solar Disk with Sunspots.



Fig. 95. Sunspots.

ously with communications.

Just how the sun affects the ionosphere is still something of a mystery. Photographs show, however, that the shining solar surface is far from quiescent. The sun is gaseous throughout, so that the visible layers represent the outer solar atmosphere. On the earth, we have occasional winds of high velocity. One-hundred-mile-an-hour gales are called *tornadoes* or *hurricanes*. But on the sun, winds of such magnitude are common. Indeed we sometimes observe large clouds of gas moving with speeds in excess of 100 miles per second.

Enormous geysers of luminous gas shoot from the interior, like fire from a flame thrower. The smallest of these are perhaps several hundred miles across and several thousand miles in length. Occasionally, the shining gas clouds may be 50,000 miles or more across and extend half a million miles into space. These flame-like formations are called *solar prominences*. Figure 96 shows the largest prominence on record, that of June 4, 1946. The sun is hidden behind the occulting black disk. At the time of this picture the arch was rising rapidly. The overall lapse of time for the entire eruption was only one hour

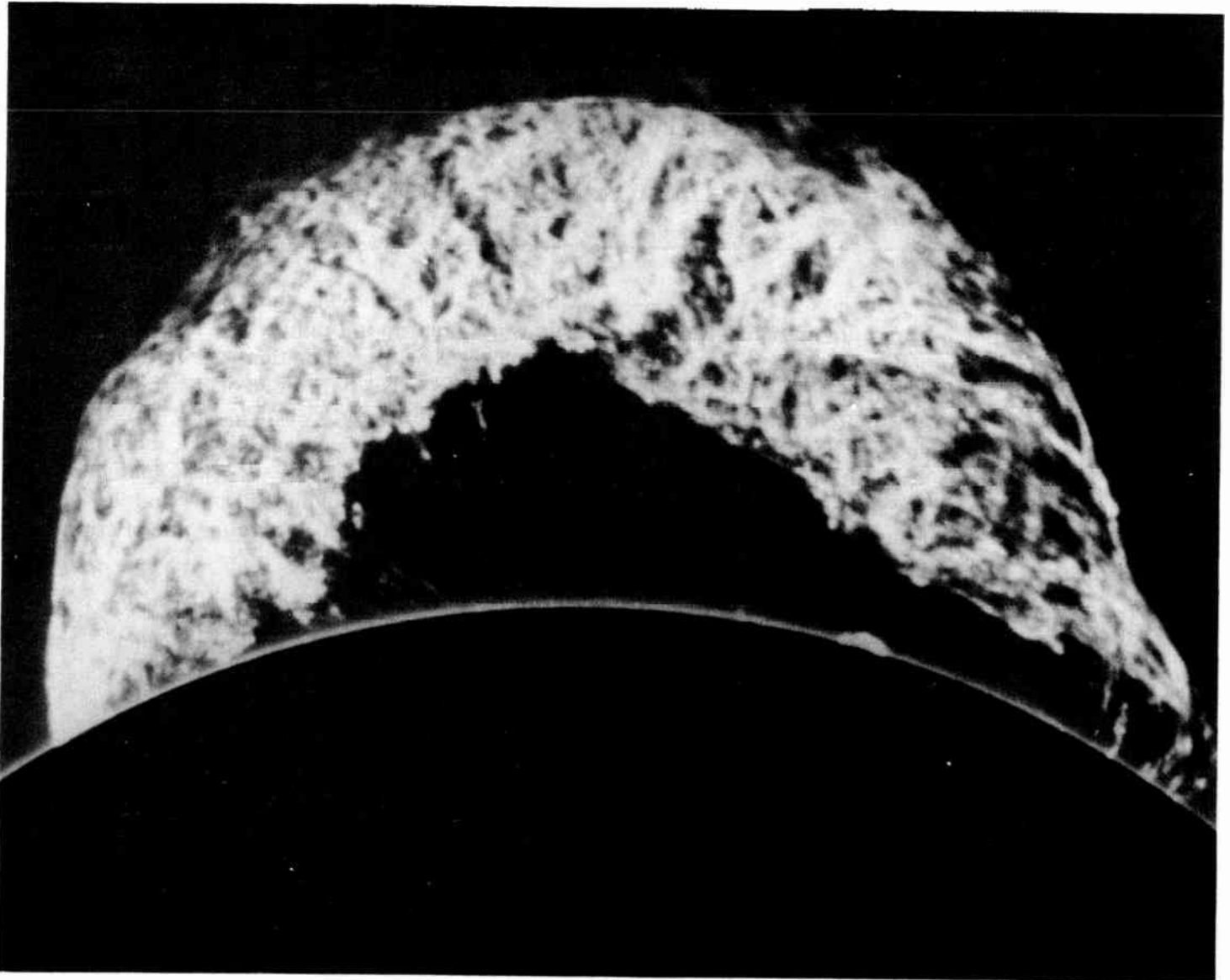


Fig. 96. Prominence.

and twenty minutes. Motion pictures of this and similar eruptions are spectacular. Most of the ejected material appears to fall back on the solar surface. In many cases, prominences seem to form high in the atmosphere and "rain" the luminous gases down toward the surface in graceful curves and arches. The activity is extremely complex.

Many years may pass before we determine the true cause of solar variability. We suspect that a circulation of gases deep in the sun's interior is responsible, and that all of the features mentioned in the previous paragraphs are secondary effects. They are the skin eruptions of the periodic fever that infects the solar body. Since any radiation emitted by the sun must pass through the surface, however, we may examine each of these secondary disturbances to see if it is directly associated with ionospheric effects.

First, consider the sunspots. Sunspots are, in reality, storm areas in the solar atmosphere. Like similar cyclonic, low-pressure disturbances in the earth's atmosphere, they are cooler than their surroundings. The sun's shining surface appears to have a temperature of about 6000 C; that of spots is about 2000° lower, which is, of course, why they appear relatively dark by contrast. We have found no obvious reason why a small region of low temperature would have any profound effect upon the ionosphere. Spots also are known to possess powerful magnetic fields. It is difficult to see how this field can have any direct effect at the distance of the earth. One possible connection we can conceive is that the magnetic lines of force may provide tracks for ions or electrons to escape from the sun. Then, too, the disturbed areas surrounding the spots often emit more ultraviolet radiation than a spotless region.

Finally there is the solar *corona* (Frontispiece), a faint cloud of gas surrounding the sun. Its delicate structure can best be seen at a total solar eclipse when the moon covers the shining disk and hides it from our view. The corona is a sort of "super ionosphere." It consists of highly *electrified atoms*—that is, atoms from which large numbers of electrons are torn. Great as prominence

High-speed corpuscles or radiation! One or the other, or a combination of both, is required to affect the ionosphere. There is little doubt of that! A definite correlation exists between bright flares (a type of prominence) and short-wave fade-outs. These prominences, we have found, possess extremely high temperatures, ranging from 15,000 to 25,000 C. Their relative brilliance, compared with that of the sun, would be far greater in the ultraviolet than in the visual range.

Astronomers, keeping daily records of the numbers of sunspots visible, discovered that the average degree of spottedness changes slowly from minimum to maximum and back to minimum again. The period between successive minima is about eleven years, on the average. The cycle is not exact, and variations of from one to two years are common. Figure 97 shows a plot of the variation of spottedness with time.

We have, thus, come to speak of the *sunspot period*. Numerous terrestrial phenomena, such as the aurora borealis (northern lights), magnetic storms (wandering of the compass needle), and ionospheric characteristics vary so markedly with a similar period that the existence of a physical connection between the sun and the earth is undoubted. There is no question, however, but that the effect of *sunspots* has been greatly overemphasized.

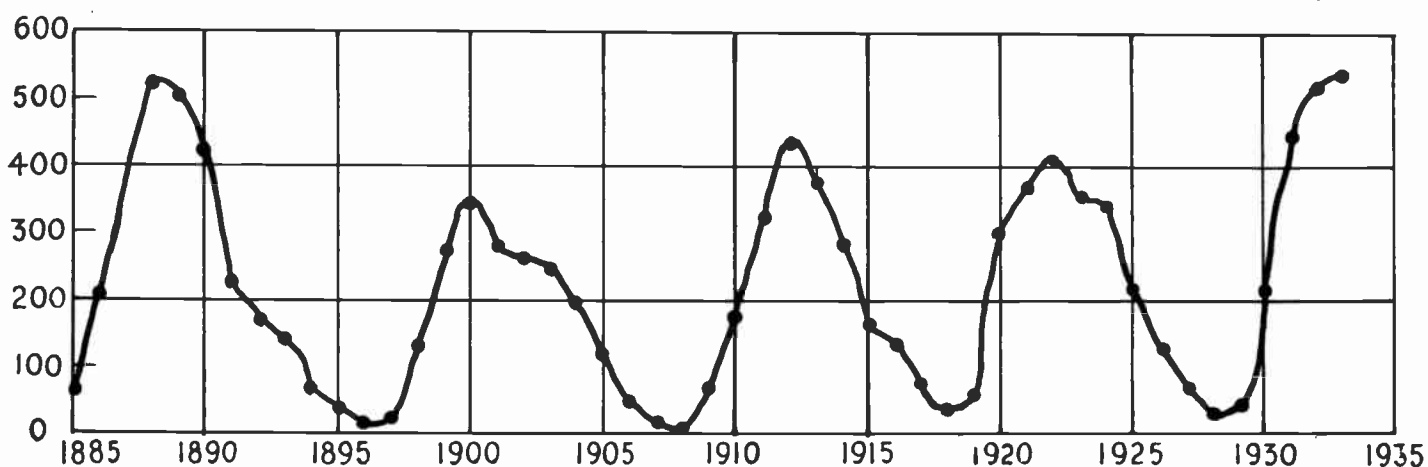


Fig. 97. Number of Sunspot Groups Observed Yearly.

temperatures are, they are negligible compared with the 1,000,000 C values associated with the sun's corona. No completely satisfactory explanation exists. We are inclined to believe that hot gases leaking from the sun's interior may be responsible.

What we do know, however, is this: the corona must emit great quantities of soft X rays and far ultra violet energy. In these regions of the solar spectrum, the corona is probably far brighter than the solar disk. All this short-wave energy is absorbed, however, by the ionospheric layers, and none penetrates to the surface of the earth. To us, the corona is a faint haze, half a million times less brilliant than the sun itself.

The state of the solar atmosphere is continuously variable. Sunspots, faculae, and prominences often change markedly in the course of hours or even minutes. But, superposed on these rapid fluctuations, is a long-scale variability that seems to affect all visible features of the sun. This variation is usually called the *sunspot cycle*, because spots are the most conspicuous of all solar phenomena.

True, they are the most conspicuous feature of the "disease" with which the sun is afflicted. Also, large terrestrial effects occur in the presence of a big, active spot. But spots are almost certainly not the fundamental cause of the observed disturbances here on the earth.

As we have pointed out, the cause of solar variability is still unknown. Observations disclose the fact that the output of solar radiation, especially in the far ultra-violet, may vary considerably. This variability is associated more with the external corona or with the prominences than with the spots. There is evidence that the sun occasionally sends out blasts of ions in addition to radiation. These electrified atoms, bent toward the north and south magnetic poles by the field of the earth, enter the upper atmosphere and cause it to glow, thus producing auroral displays and ionospheric disturbances. Perhaps the aurora results when the earth happens to "brush" the tail of an extended coronal streamer.

Salisbury and Menzel have recently suggested that

intense emission of very long radio waves, from disturbed sunspot areas, may cause the terrestrial disturbances. These waves are supposed to possess wavelengths of the order of 10^4 — 10^5 kms. They may also account, in part, for the high energy excitation of prominences and corona.

The years 1943-44 marked the lowest point in the current sunspot cycle. Beginning with 1945 and for

four or five years thereafter, solar activity should be on the increase. The radio operator cannot rely entirely on experience gained during sunspot minimum to predict the behavior of various radio circuits at other phases of the cycle. He must learn how the ionosphere changes with solar activity.

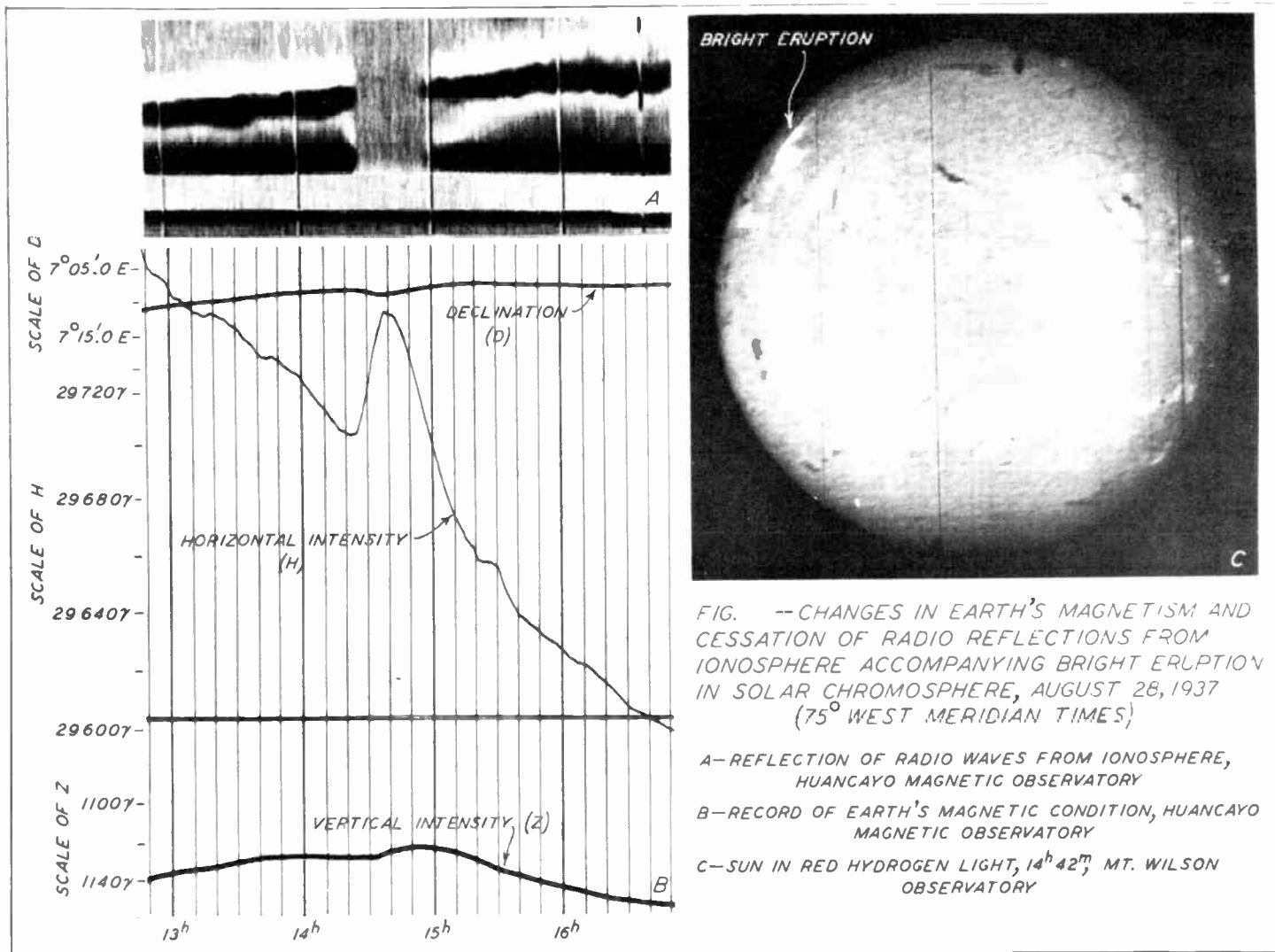


Fig. 98.

• CHAPTER TEN •

IONOSPHERIC VARIATIONS

SOLAR VARIABILITY PRODUCES A NUMBER OF EFFECTS IN the ionosphere. Some appear as rapid fluctuations; others are slow changes over the sunspot cycle.

The values of the MUF's evaluated from procedures given in earlier chapters refer to average undisturbed ionospheric conditions for a given month and year. The 4000-km MUF maps for December 1948 (sun spot maximum) will show a similarity to those of December 1944 (sunspot minimum), except that the frequencies will be considerably greater in 1948. Solar activity results in greater emission of solar ultraviolet radiation which, in turn, causes increased ionization in the upper atmosphere. Thus, MUF's are greater at sunspot maximum than at minimum.

The values of the calculated MUF's may be modified by rapid solar variations. One of the most significant and, in general, unpredictable deviations from normal characteristics lies in the presence of *sporadic E*. As the name indicates, there occur, from time to time, extraneous patches or clouds of ions at heights near the normal *E* layer. Often, the density of electrons is great enough to permit reflection of radio waves whose frequencies are much higher than those returned earthward by the normal *E* layers. As a consequence, the *E*-layer MUF's may be enhanced considerably.

Since normal *E* effectively fades away during the night, and since sporadic *E* may occur at any time, the latter usually affects radio transmission more significantly during the hours of darkness. In temperate latitudes, sporadic *E* is more prevalent in summer than in winter. Curiously, it seems to be stronger near sunspot minimum than near maximum, and thus tends to offset, in part, the generally lower MUF's occurring normally at the minimum phase of the cycle.

The exact nature of sporadic *E* is not known. It appears to increase in intensity near the magnetic poles, a fact suggesting that it may be caused by electric charges (ions) expelled from the sun. In some cases, it appears to be associated with the aurora, but the tendency for the effect to decrease while aurorae and sunspots are increasing is somewhat puzzling. We know that the layers are patchy and transient, and that transmissions

via sporadic *E* reflections may not be reliable, especially at higher frequencies. On occasion, sporadic *E* may reflect waves of frequencies as great as 80 to 100 megacycles and thus cause long-distance transmission on frequencies normally expected to be applicable only to line-of-sight communication.

There appear to be two varieties of sporadic *E*; the reflecting type just described and the *blanketing*, or absorbing type. The latter seems to be directly related to the aurora and ionospheric storms. It may produce very heavy absorption, which is most pronounced during the night hours.

One of the most annoying and altogether unpredictable effects of solar variations upon communication is the so-called *radio fade-out* (or Dellinger effect). Within the course of a minute (usually less) and entirely without warning, a high-frequency radio signal that previously may have been "pounding in" will completely vanish or be materially reduced in strength. The effect occurs simultaneously for all radio circuits lying wholly or in part on the sunward side of the globe. Circuits lying entirely in darkness are unaffected. The operator may well gain the impression that his receiver has suddenly gone "dead." It is best not to start tearing the radio set apart, however, to find the difficulty, because chances are that the sun, *not* the set, is causing the trouble.

Evidence indicates that radio fade-outs occur when the sun has suddenly erupted a brilliant prominence. The increased ultraviolet light from this prominence greatly enhances the density of electrons in the absorbing regions on the lower fringe of the *E* layer. Thus, the absorption is enormously increased so that radio waves can only travel short distances. Fig. 98 shows such an eruption of the sun's surface and the various radio and magnetic disturbances that accompanied the blast.

The solar outbursts increase the value of the absorption index $(Kd)_{\text{min}}$, discussed in Chapter 8. The effects, as for normal absorption, are greatest for long paths and for the lower frequencies. If a fade-out interrupts communication, the operator who wishes to regain contact should turn to a higher frequency, if one is available. Increase of power will generally have little effect. Otherwise, he

will have to wait until the solar outburst subsides, which may be from ten minutes to nearly an hour, according to the magnitude of the eruption. Fade-outs are more frequent at sunspot maximum than at minimum.

Another type of disturbance, not to be confused with the radio fade-out, is the *ionospheric storm*. The name is apt, for the indications are that a violent disturbance of the normal electrified conditions takes place during such an outburst. Again, the cause is undoubtedly solar, although the mechanics of the phenomenon are extremely obscure.

Ionospheric storms are usually accompanied by magnetic storms (erratic variations in the position of the compass needle) and, frequently, by aurorae (northern lights). A disturbance extends generally over both night and day hemispheres and tends to increase in severity toward the auroral zones. Ionospheric storms are somewhat more prevalent in spring and fall than during summer or winter, although they may occur at any season of the year.

The effects of a storm on communications are rarely so sudden as those of the radio fade-out, although marked changes may be observed in the course of a few minutes. The disturbances begin in the F_2 layer and gradually move downward into the other layers, which in general are much less affected. The indications appear first for stations or circuits near the magnetic poles, and the storms tend to be more severe in latitudes far from the equator.

The onset of a storm is marked by severe turbulence in the ionosphere. The well-marked normal stratification of the upper atmosphere is disturbed. The F_2 layer expands rapidly, and electron densities decrease. In consequence, the critical frequencies and MUF's are lowered. Thus, a frequency that would ordinarily lie well below the safe limit may suddenly penetrate the ionospheric mesh and escape into space.

As the storm progresses, a greater-than-normal concentration of electrons tends to form in the lower absorbing fringes of the E , especially for latitudes of the auroral zone. One might roughly describe the phenomenon as an expansion of the auroral zone of absorption shown in Fig. 54. Or one may say that $(Kd)_{min}$ is greatly increased. The lower frequencies, as previously discussed, experience the greatest weakening. Thus, the lowest useful high frequency (LUHF) is increased.

The combination of the lowering of the MUF's and the raising of the LUHF's results in a situation very unfavorable for communication. In many instances, especially for long circuits whose great-circle paths lie close to the auroral zone, the LUHF's may exceed the MUF's, and transmission will be impossible. Relaying

of messages to circuits in lower latitudes is the only solution for such a situation.

An additional unfortunate circumstance is the relatively long duration of the storms. Return to normal conditions usually requires several days. Even after the reflecting layers have recovered their normal characteristics, the absorption may still persist, and thus give an abnormally high LUHF. Ionospheric storms are usually more severe and more frequent during sunspot maximum than during minimum.

Methods of forecasting at least the more pronounced disturbances are in process of development. The tendency of ionospheric storms to recur at 27-day intervals, corresponding to the rotation period of the sun, is of some assistance in the prediction. Unfortunately, the major storms appear not to follow this rule. Also, the 27-day recurrence is less marked near the maximum than at the minimum of the sunspot cycle. Forecasting, at present, is a complicated procedure, based on a combination of ionospheric, magnetic, and solar observations.

The accuracy attained in the ionospheric forecasts is satisfactory, although not perfect. After all, the weatherman makes some mistakes, and the ionosphere is a sort of weather phenomenon. Those who have been closely associated with the work are now concerned with the improvements that will be possible with new and more advanced equipment. A device known as the *coronagraph*, which can record the corona without an eclipse of the sun, is one such instrument.

The coronagraph, invented by Dr. B. Lyot in France, depends for its success on the extremely clear skies of a high-altitude station, optical perfection, and elimination of all scattered or reflected light inside the telescope. During World War II, Dr. Walter O. Roberts, superintendent of the Harvard Station at Climax, Colorado, took daily records of the solar corona. Study of the data revealed relationships between coronal brightness and the magnetic storms. These results, combined with other astronomical records from Mt. Wilson and McMath-Hulbert Observatories, along with magnetic and ionospheric evidence, enabled scientists in Washington, D. C. to forecast radio disturbances about two weeks in advance of their occurrence.

The importance of the coronagraph for ionospheric research is borne out by the fact that the Germans built several such instruments during World War II and had developed plans for an even more elaborate program. Only one coronagraph, that at Climax, was available for Allied use.

Radio-propagation information had a variety of uses during World War II, such as the planning of radio channels and the selection of correct frequency, when

more than one was available. On one particularly difficult circuit, transmissions were impossible for the major part of the day. The study showed that the frequencies, which may have been altogether satisfactory several years earlier when sunspots were more numerous, were far too high. When a new set of frequencies was allocated, contact became possible during almost the entire day.

The beginnings we have made during World War II have opened up an entirely new field for scientific study. Radio-propagation information has many important applications to peacetime industries, as well as to the mechanics of war. There is the long-range planning of frequencies to use for general communication. In the development of new circuits, companies may find certain locations more strategic than others for effective signal transmission. Problems of radio interference are primarily dependent on propagation information for their solution. Prior knowledge of an ionospheric storm will enable more efficient planning of broadcast relays from abroad.

The various companies engaged in commercial aviation will also require propagation data for the maintenance of reliable communications over land and sea. Ship-to-shore service will also benefit from application of this knowledge, which was not available prior to World

War II. All services dependent on Loran or other navigational systems will want to know when, where, and how the procedure will fail because of potential solar disturbances of the ionosphere. Indeed, the utility and further development of such devices depend, to a very large extent, upon our ability to forecast ionospheric conditions in different parts of the world.

Work still needs to be done to improve our knowledge of radio propagation. The present international network of ionospheric stations requires extension. Mobile equipment for exploration, especially of the complicated auroral zone, must be further developed. We need special data to increase the accuracy of absorption, reflection, and radio-noise prediction. Continued analysis of magnetic variations should give a valuable clue. Extensive solar studies, including those of eclipses, will contribute important information that can be gained in no other way. We must have theoretical studies and laboratory measures of the ionization properties of the common gases. Without these additional phases, we should be forced to follow the blind alley of empiricism. With the broad view, there is a reasonable hope that some day we may fully understand the physical, chemical, and astronomical processes that cause the ionosphere and are responsible for its variations.

GROUND WAVE TRANSMISSION

PREVIOUS CHAPTERS HAVE DEALT PRIMARILY WITH THE sky wave, reflected by the ionosphere. Several additional ways exist for transmission of the signal from one antenna to the other. When two stations are fairly close—that is, within two hundred miles or so—a wave may travel directly to the receiving antenna, it may strike the ground and reach the antenna after reflection, and it may follow along the curved surface of the earth. The first two of these, the direct and ground-reflected waves, comprise the so-called *atmospheric wave*. The wave following the curved surface of the earth is termed *surface wave*. Together they form the *ground wave*.

The distance that ground waves travel is limited because they can pass beyond the horizon only by diffraction or bending around the edge of the earth. This process causes marked depletion of signal strength, particularly for waves of high frequency (short wave length). The shadow cast, even by a light wave, is not perfectly sharp. The rate of change from light to deep shadow depends on the wave length. Longer waves show a much more gradual change than short ones; hence, they penetrate much further into the shadow zone. The ground wave is seldom of importance for communication over distances of more than a few hundred miles.

Waves of frequencies higher than about 40 megacycles, about which we shall learn in later chapters, may be strongly reflected downward by lower levels of the air (troposphere). The resulting signal may, therefore, be much stronger than expected. At lower frequencies, however, the signal strength of the ground wave depends on the interaction of the three waves already mentioned.

This interaction depends on both amplitude and phase. A simple analogy will explain these terms. Radio waves are not too unlike the waves produced by a pebble thrown into a quiet pool of water. They consist of alternate ridges and hollows. The height of the ridges or depth of the hollows denotes the amplitude. When two waves join they may be in phase, in which case the crests of one coincide with the crests of the other; or they may join directly out of phase, so that the crests of one coincide with the hollows of the other, thereby canceling the wave motion entirely. In other words, if the crest of

one wave reaches a point simultaneously with the trough of another equally large wave, the waves are said to be 180° out of phase, and the resulting amplitude is seen to be zero. In free space, there would be no surface wave or ground-reflected wave, and the strength of a radio signal would equal the strength of the direct wave, no matter what the frequency.

At the surface of a perfect reflector, the ray changes its phase by 180° . Since it leaves the transmitter with the same phase and amplitude as the direct wave, the two waves will interact to give zero amplitude (signal strength) when the transmitting and receiving antennas are both at ground level. Actually, the ground is not a perfect reflector, especially for the lower frequencies, and there is some residual intensity at the surface. The conducting properties of the ground traversed determine the strength of the surface wave. Some types of ground encountered are better conductors than others.

The signal strength of a wave produced by a standard transmitter varies with frequency and distance, as shown in Figs. 100 to 102, for three different types of conductors. The standard transmitter for which these charts are drawn has a power of 1-kw and a vertical-wire antenna. To calculate signal strength, it is necessary to consider transmitter power, since a 10-kw transmitter produces a stronger signal than one of 1 kw. The power correction in decibels is found from Fig. 106. The type and directivity of antennas is also important. Waves from horizontal antennas are poorly conducted by the ground, so that the surface wave extends only a short distance from the transmitter, and the ground-wave signal strength is low. For this reason, a vertical antenna is usually used in ground-wave transmission. Vertical antennas of any kind can usually be regarded as vertical-wire antennas of increased power.

If either of the antennas is raised, the surface wave becomes weaker, and the angle the reflected wave makes with the ground is increased. As this angle increases, the ground reflects less energy, and the ground-reflected wave becomes weaker than the direct wave. The phase of the reflected wave depends on the electrical properties of the ground, but it is always such that the strength of the

combination of the direct and reflected waves (the atmospheric wave) is less than twice the strength of the direct wave alone. As the height of either antenna is increased, less and less energy is reflected from the ground, so that the strength of the atmospheric wave becomes more nearly equal to the free-space strength. (When both antennas are high, the relative phase of the direct and reflected waves changes because of the difference in path length. However, for moderate heights, this change is less important than the change caused by the increase in the angle of reflection.)

The strength of the ground wave, when the antennas are raised, depends on the strengths and relative phases of the surface and atmospheric waves. As we have said, these waves combine in such a way that the ground-wave strength is approximately equal to the surface-wave strength for low antennas. As the antenna becomes higher, the ground-wave strength increases in a manner that depends upon the frequency and the type of ground. This increase (in decibels) is called the *height gain*. At

distances that are not too short and at moderate antenna heights, the strength of the ground wave, in decibels above one microvolt per meter, may be represented as the sum of the strength of the surface wave and the height gains of the two antennas. Figures 103 to 105 show the height gain for various antenna heights and frequencies over three types of ground.

The strength of the atmospheric wave cannot exceed the sum of the amplitudes of the direct wave and ground-reflected wave, or twice the free-space signal strength, a situation that would arise if the two joined exactly in phase. This limit, given in Fig. 99, provides a useful check on the applicability of the method just described. If a computed signal strength happens to exceed the limiting strength, adopt the limiting strength.

As we have stated, Figs. 100 to 102 show the signal strength produced by a 1-kw, vertical-wire transmitter at various distances over three types of terrain, when both transmitting and receiving antennas are at ground level. To compute the signal strength for a particular circuit,

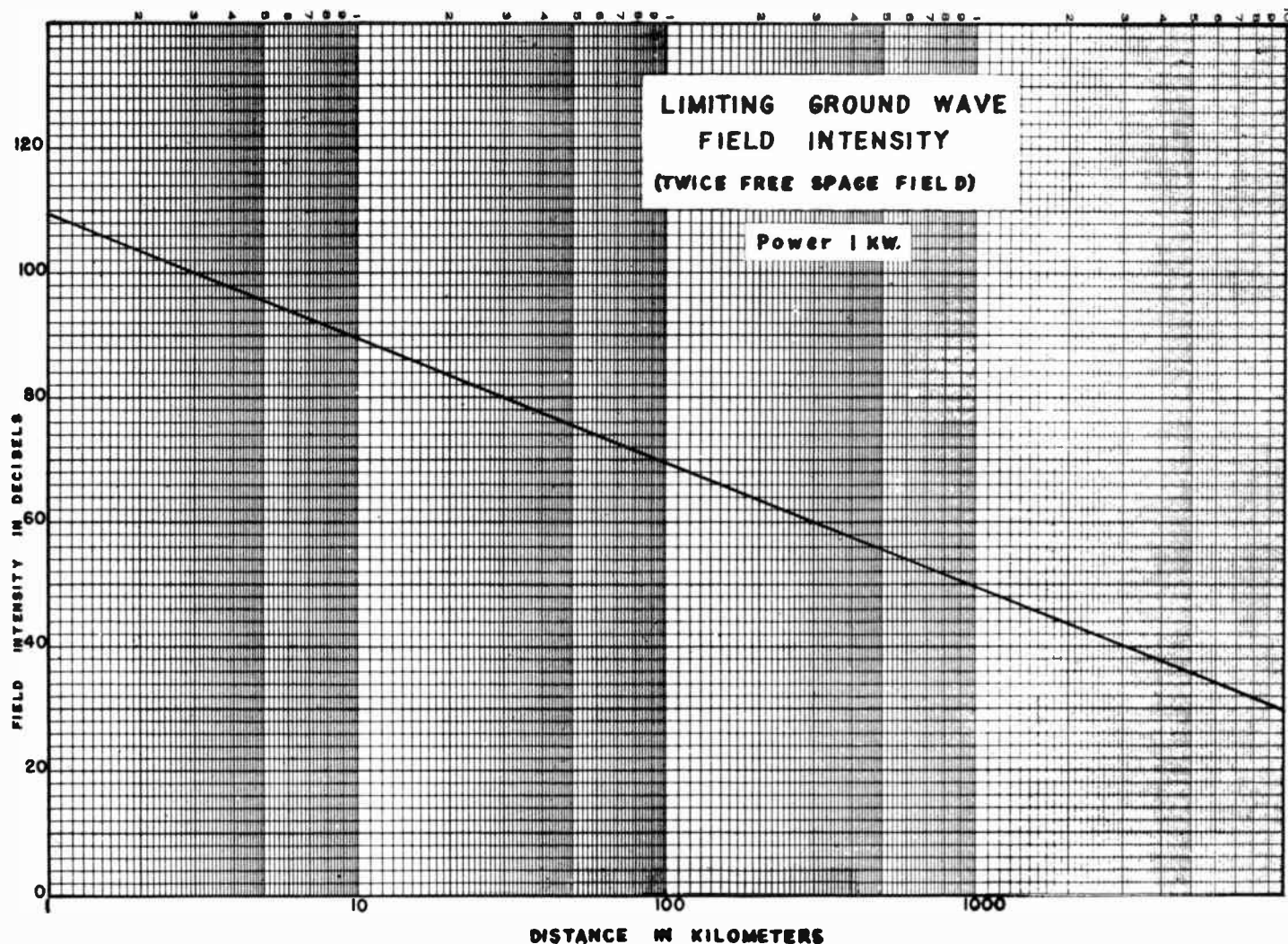


Fig. 99.

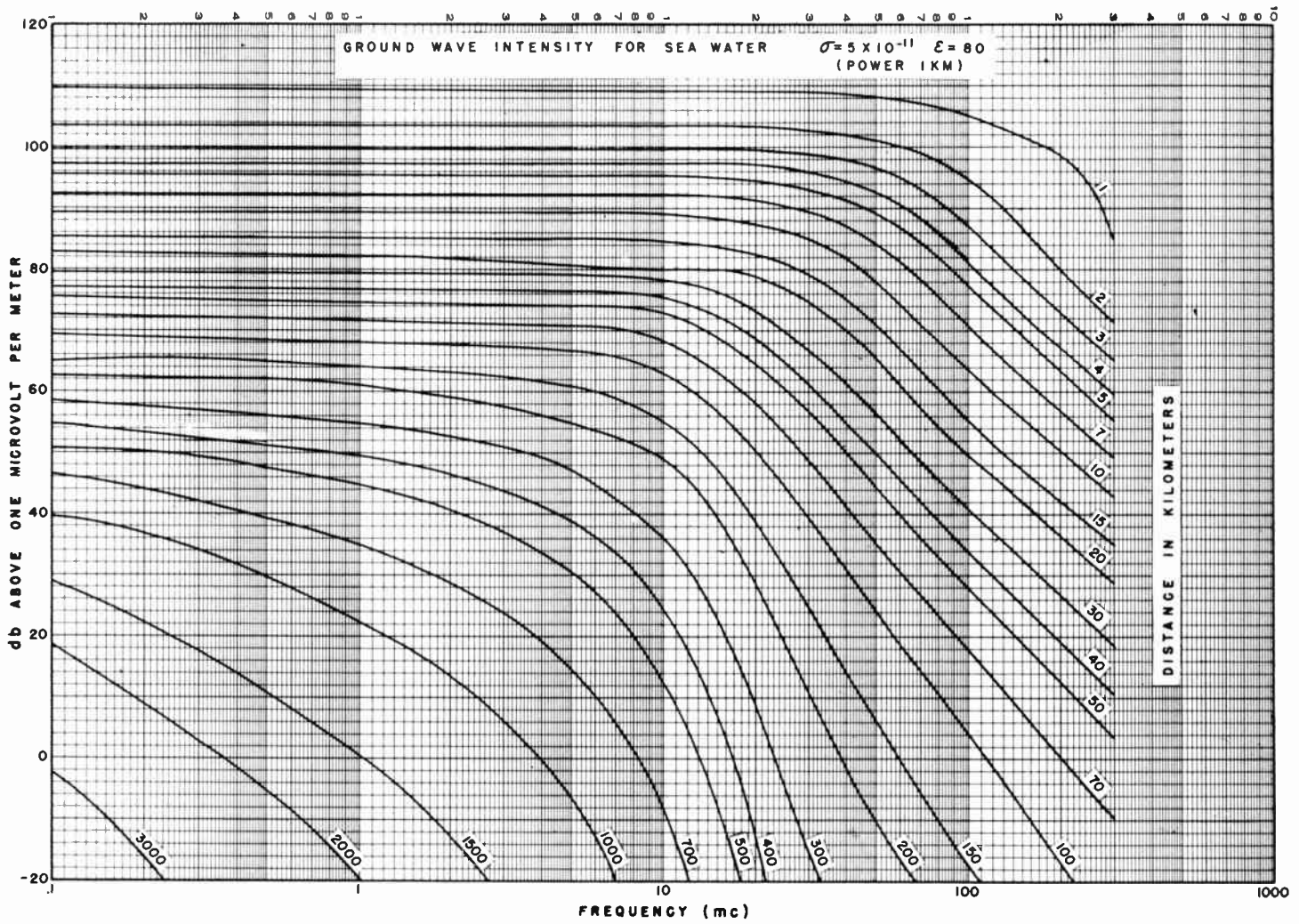


Fig. 100.

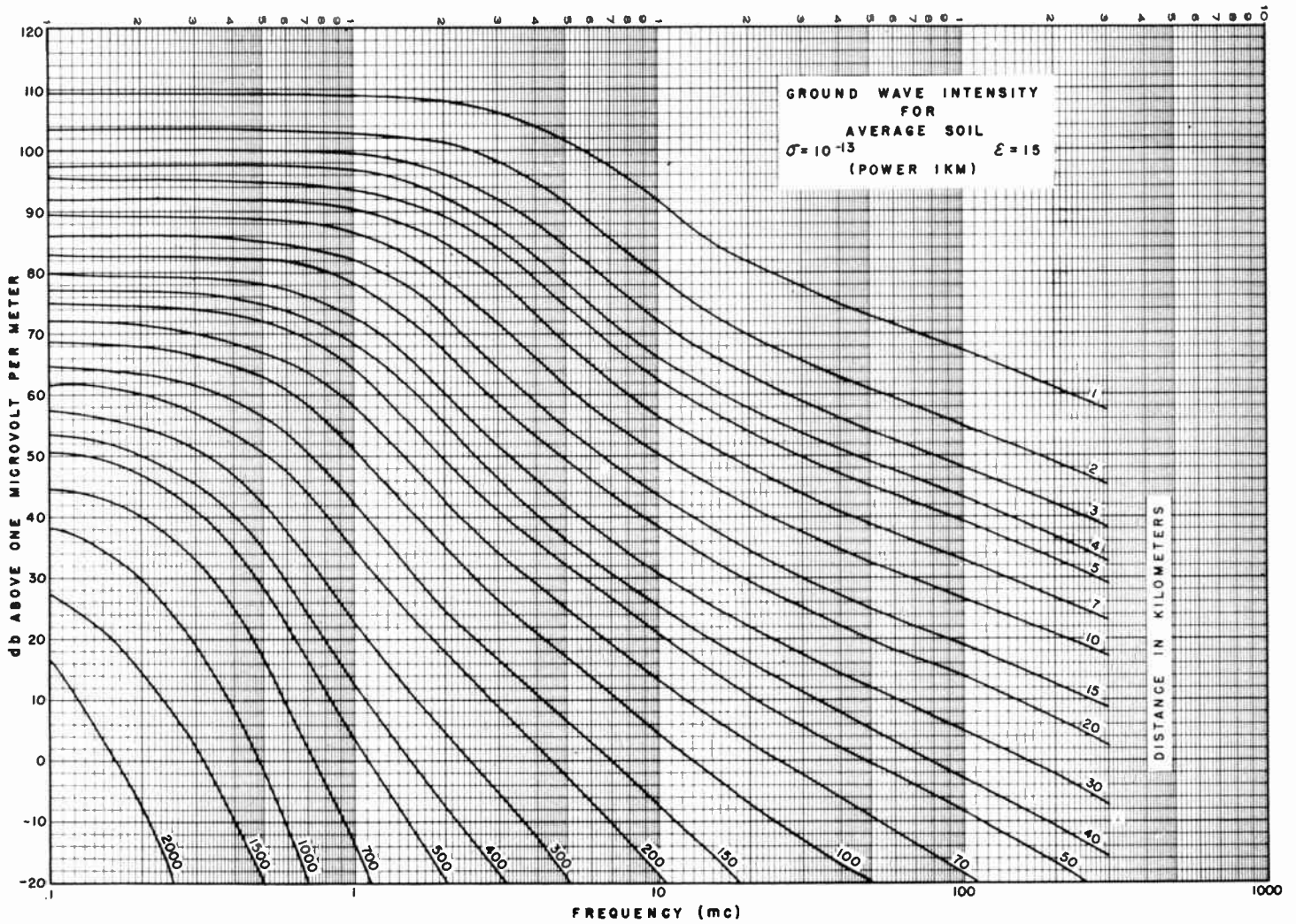


Fig. 101.

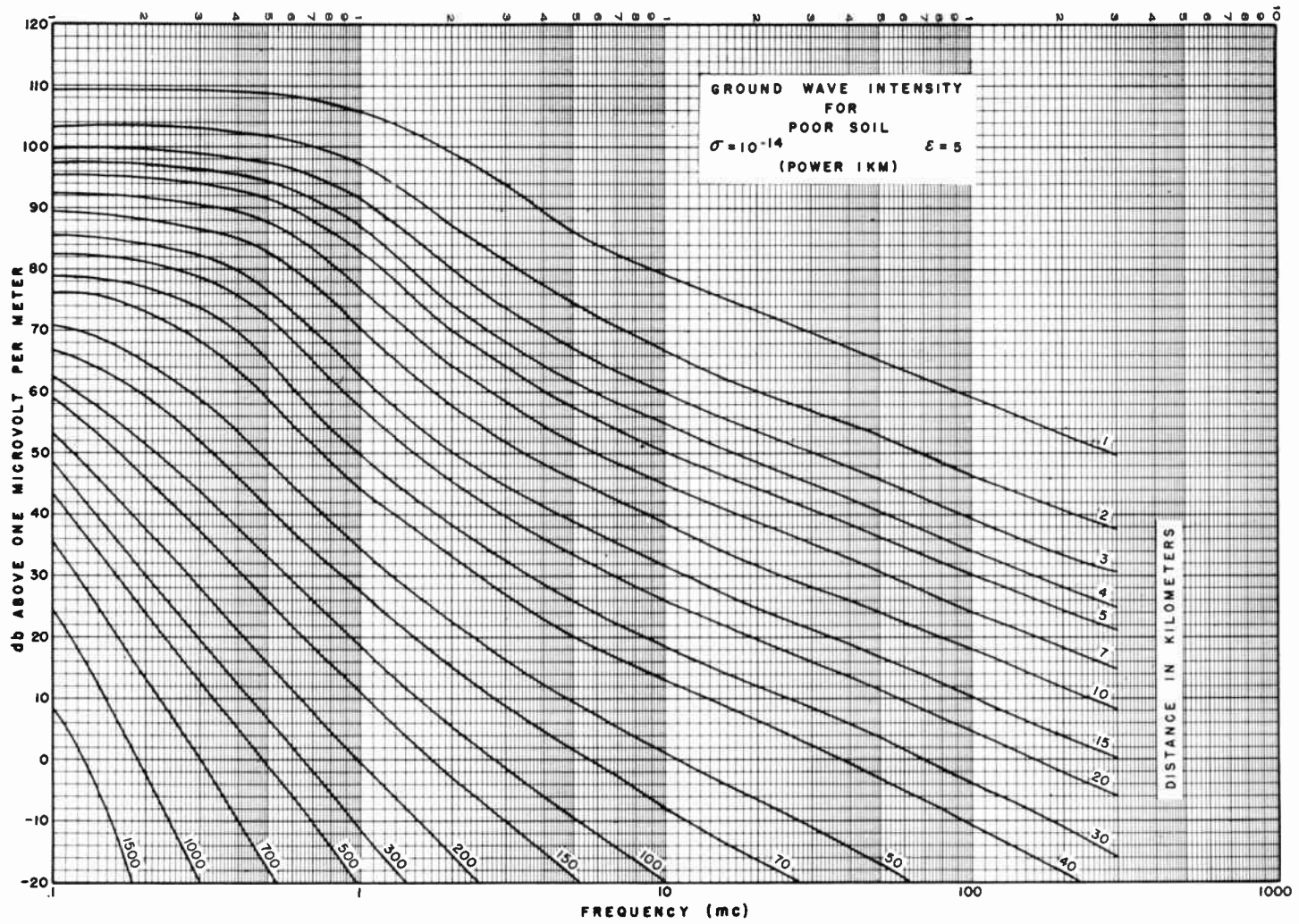


Fig. 102.

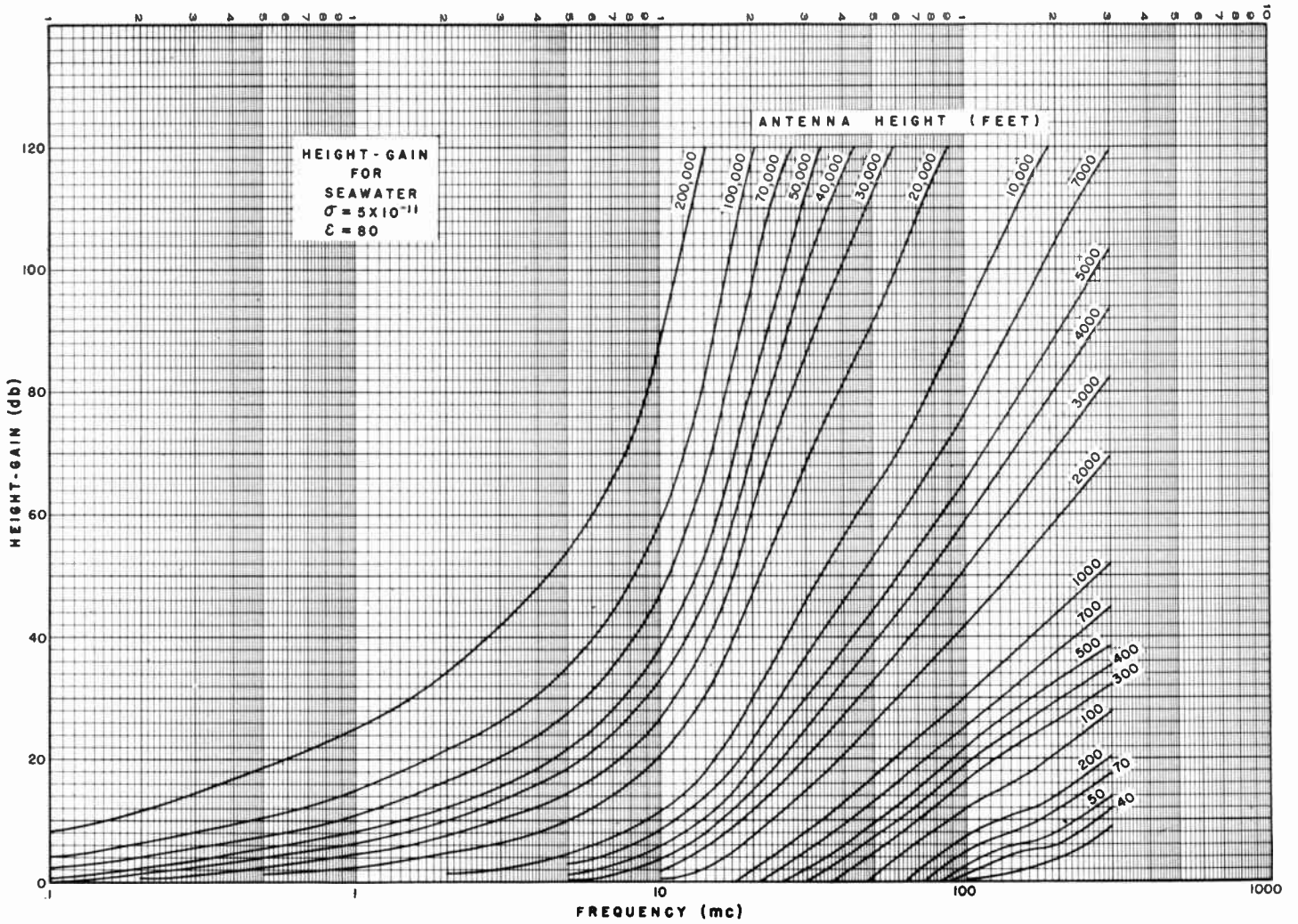


Fig. 103.

take the signal strength from one of the Figs. 100 to 102, and add the height gains of the antennas (Figs. 103 to 105), the power correction of the transmitter (Fig. 106), and any gain that the antennas may have with respect to a vertical wire.

Let us compute, as an example, the strength of a 20-megacycle signal produced by a 100-watt, vertical-wire transmitter at a distance of 100 km over sea water. Let the effective heights of both transmitting and receiving antennas be 2000 feet.

Reference signal strength (Fig. 100).....	50 db
Transmitter height gain (Fig. 103).....	8
Receiver height gain (Fig. 103).....	8
Transmitter power correction (Fig. 106).....	-10
Correction for type of antenna.....	0
Circuit signal strength.....	56

strength for the circuit discussed is

Limiting signal strength (1 kw) (Fig. 99).....	69 db
Transmitter power correction (Fig. 106).....	-10
Free-space signal strength (100 watts).....	59

The correct circuit signal strength is, therefore, 56 db.

In practical cases, the operator is interested in whether the signal is strong enough to exceed the radio noise level rather than in the signal strength in decibels above one microvolt per meter. He must, therefore, compare the computed signal strength with the signal strength that is necessary to exceed the noise (Chapter 7). The signal is barely heard above the noise at such a distance that the computed signal strength is equal to the noise level. To compute this distance, which is called the *ground-wave*

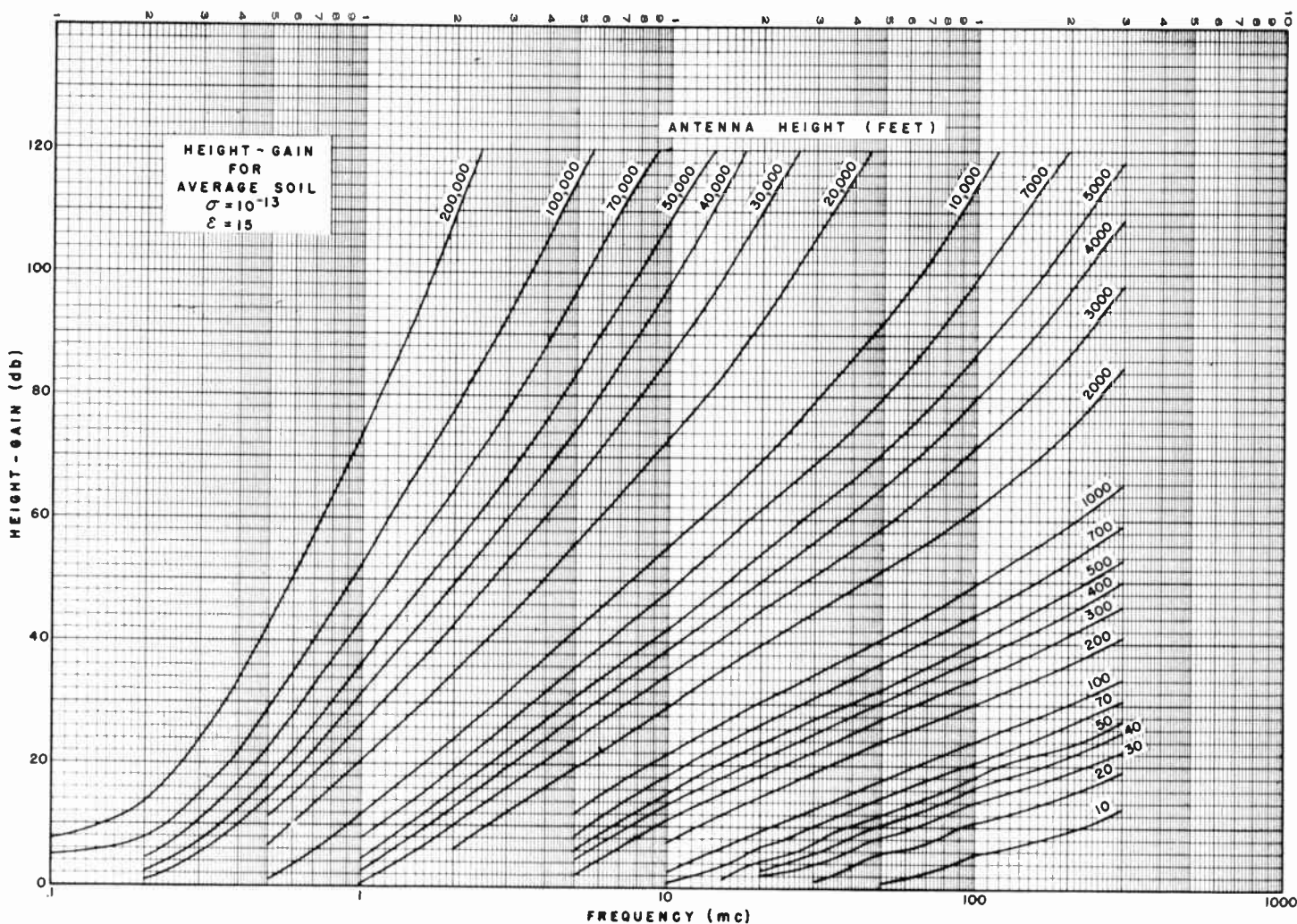


Fig. 104.

As has been stated, the above method of computation may yield too large a value of the circuit signal strength. The limiting signal strength, corrected for power, should also be found. If it is smaller than the computed value, adopt it as the correct signal strength. The limiting

distance range, reverse the procedure of the preceding paragraph. Let us compute the sea-water distance range at 0800 in noise zone 3 for a 20-megacycle signal from the transmitter described above. Let the receiving antenna have an effective height of 2000 feet. Then

	<i>Above 1 Micro-volt Per Meter</i>
Noise level (Fig. 36)	10 db
Correction for antenna type	0
- Transmitter power correction (Fig. 106)	10
- Transmitter height gain (Fig. 103)	- 8
- Receiver height gain (Fig. 103)	- 8
Reference signal strength	4

Fig. 100 discloses that a reference signal strength of 4 db is reached at 320 km. The distance range is then 320 km. A LUHF is usually not computed for ground waves, since the distance range changes quite slowly as the frequency increases.

Caution must be exercised in ground-wave computations. The graphs are based on average conditions, which may be considerably different from the true con-

The height-gain and signal-strength curves are given for a spherical earth (ocean or level ground). If either antenna is on a hill, experience has shown that its effective height for height-gain computations is more than its own effective height by an amount depending on the steepness of the hill, but less than the sum of the heights of the antenna and the hill. The signal strength in hilly country is complicated by the "shadow-loss" from hills in the direct line of propagation. Such obscurations may weaken the signal, whereas reflections from other hills nearby strengthen the signal. These effects are important only at distances of less than a 100 km. Compute the approximate shadow loss from the nomogram of Fig. 107, for which the hill is replaced by a triangle as shown

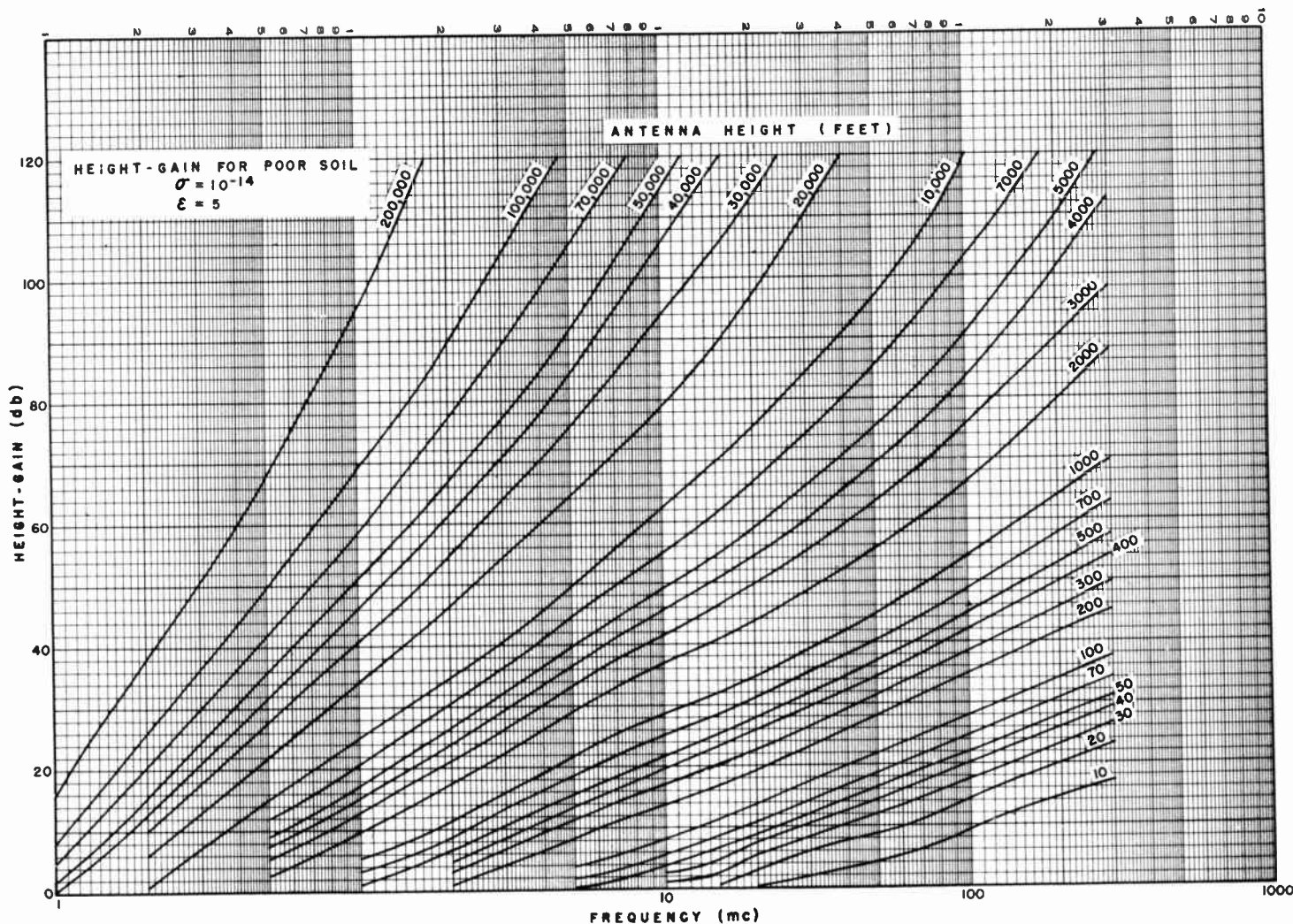


Fig. 105.

ditions in a particular case. The determination of the type of terrain may be particularly difficult. For example, a receiver a mile inland may receive a ground wave from an overseas station as much as 10 db weaker than an equally distant receiver on the coast.

in the sketch at the top of the figure. In the nomogram, D' is the distance between the foot of the perpendicular H and the nearer antenna, whether transmitting or receiving.

Ground-wave is ordinarily more reliable than the sky-

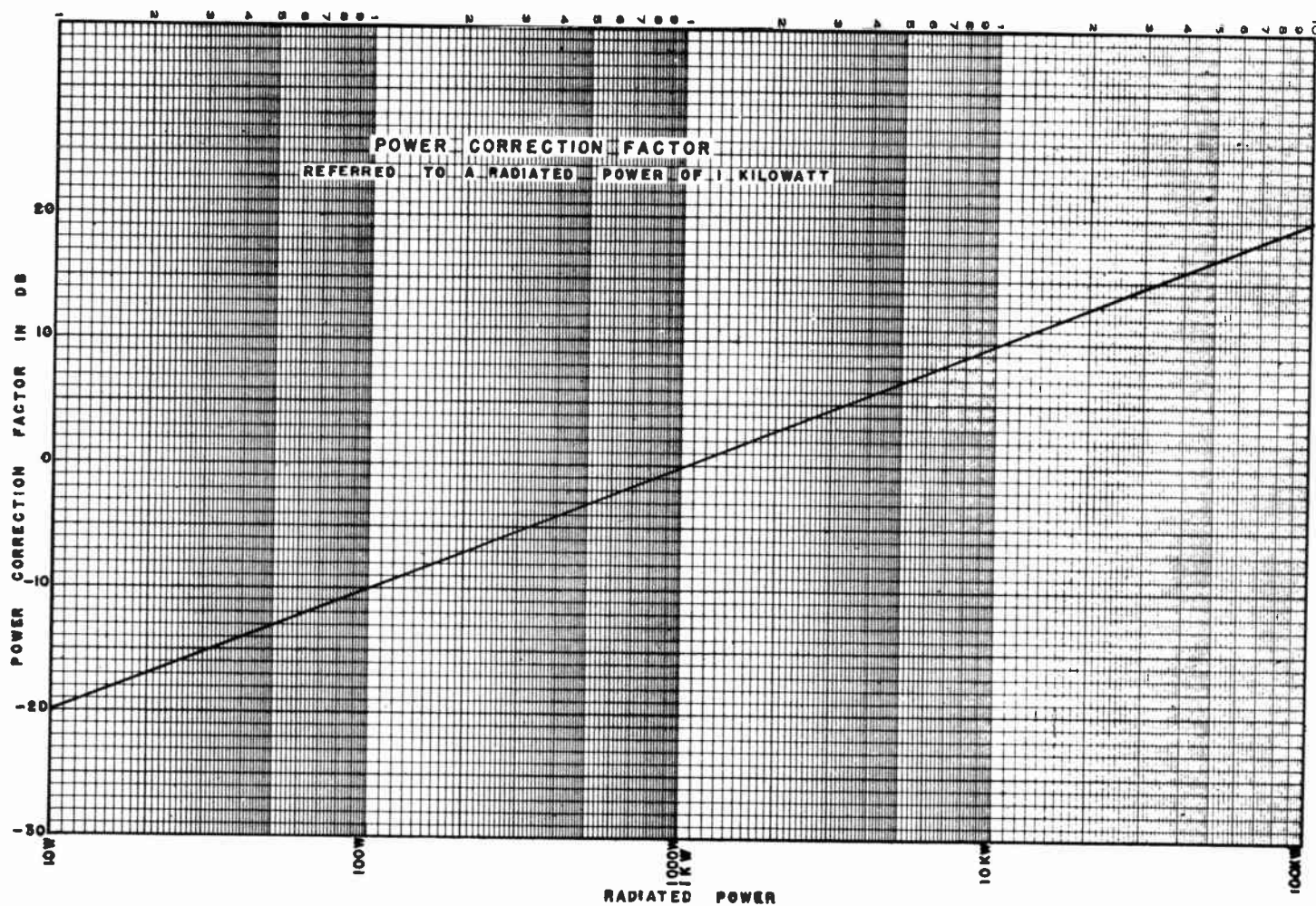


Fig. 106.

wave transmission, because it is less subject to variations. Bearings on the ground wave are usually sharp and steady. Ground-wave Loran is, thus, considerably more reliable than SS (sky-synchronized) Loran. Unfortunately, the ground range is usually very limited, as the calculations of this chapter clearly show.

One further problem that we must discuss is the question of *fading*. This familiar phenomenon of the waxing and waning of a radio signal may arise from a variety of causes, the most common of which is interference of the ground and sky waves. Since the ionospheric height is always fluctuating to some extent, the relative phases of the two waves are continually changing. Sometimes they reinforce each other, and we get a loud signal. At other times, if their intensities are nearly equal, they cancel each other, and the resultant signal strength is very low.

In precisely the same way, we can have fading over longer ranges, produced by the interference of two sky waves. For example a one-hop may interfere with a two-hop transmission. Or we may even have two waves, both of which have suffered single-hop transmission,

arriving and interfering. The phase difference arises from the irregularities of the ionosphere, or from the ordinary and extraordinary waves.

We occasionally find zones known as dead spots, where the signal strength is permanently low. These spots may result from interference of the direct ground wave with a wave reflected from some structure. Dead spots may also exist under culverts, bridges, transmission lines, or within steel structures. The low signal intensity arises from absorption of the direct or sky wave. The existence of such effects should be considered by anyone who plans to install a radio receiving antenna.

Ionospheric variability, particularly that associated with sporadic *E* and the aurora, may produce a type of signal known as *flutter fading*. The patchiness of the ionic clouds and their rapid motions are responsible. When the control point of reflection lies near the dawn or sunset line, we may also expect similar fading. A signal may disappear and return many times before a steady state is reached. Some fading may arise from deviative absorption, but the effect has not been clearly identified.

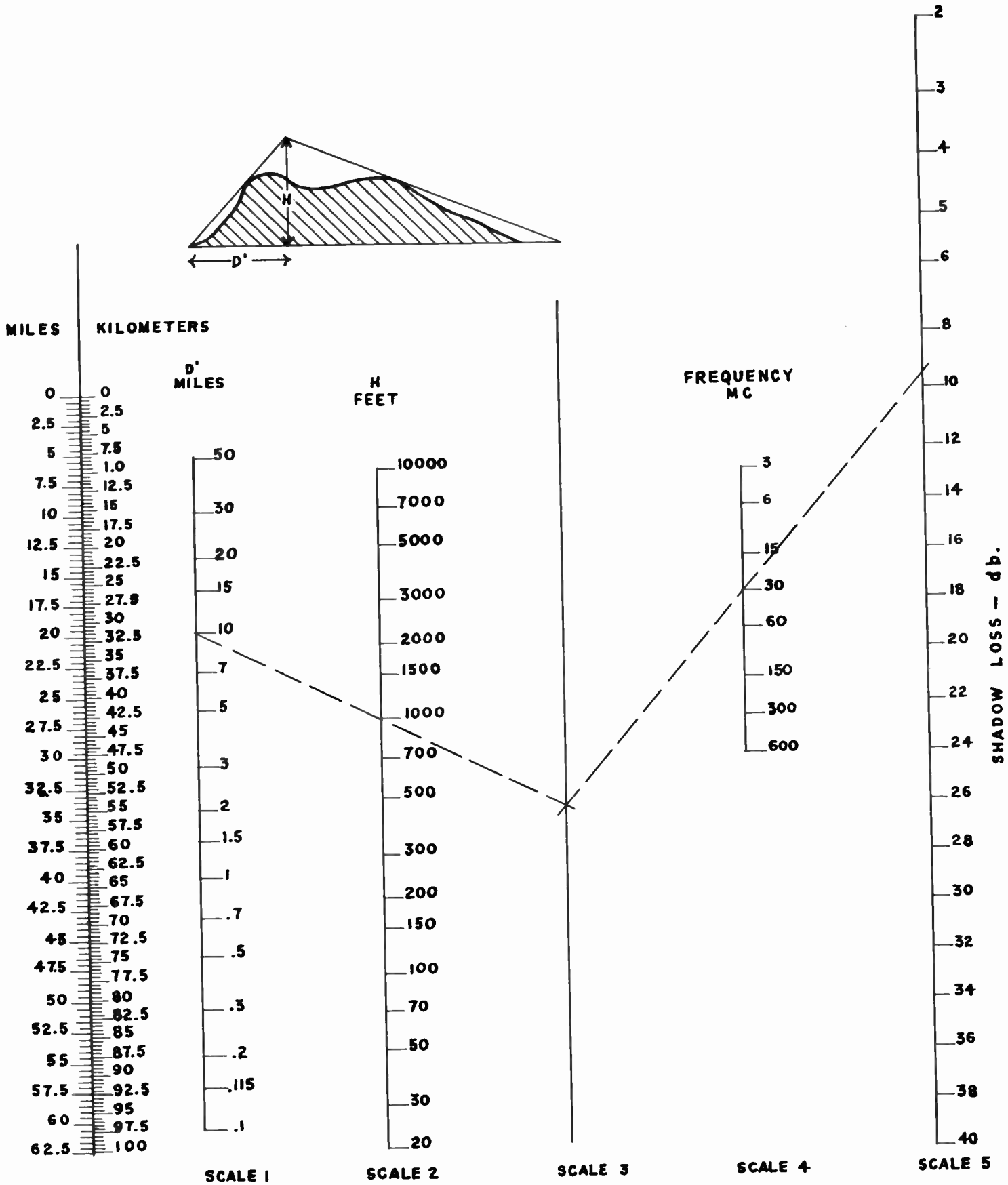


Fig. 107. Shadow Loss Nomogram.

In phone reception, the variable fading with frequency often causes difficulties. Ripples of interference, known as *selective fading*, eliminate various portions of the side bands, and the speech may be severely distorted. Variable polarization of radio waves is another reason for fading. Variable absorption, especially for paths crossing the auroral zone, may also be troublesome.

Although fading is a propagation problem and there is no simple solution, automatic volume control is, perhaps, the simplest method of eliminating all but the most serious interference. Diversity reception—that is, the use of two or more antennas with electronically operated circuits,—is the most effective means yet found for the elimination of fading troubles. The interference rarely will be com-

plete simultaneously at both antennas. The third method for reducing fading trouble is frequency modulation.

Thus far we have said very little about the directional characteristics of antennas. We do not propose to discuss this problem in any detail, because it is primarily one of design rather than of radio propagation. It is clear, however, that certain antenna properties may have a direct effect on radio ranges. The angle of fire will influence the ratio of ionospheric to ground wave, and thus have a marked effect on fading. Also, the decibel gain of an antenna has the same effect as increasing the radiated power in a certain direction. All of these points must be considered in detailed circuit analysis.

PROBLEMS OF BROADCAST AND LOWER FREQUENCIES

IT WILL BE OBSERVED THAT THE GROUND-WAVE CURVES have been extended to frequencies much lower than those considered in the LUHF calculations. For the broadcast frequencies, we could evaluate the equivalent of LUHF's by extending our Table 6 of S_0 to still lower frequencies. The absorption is still high, but has passed through its maximum near 1.8 megacycles. In consequence, lower frequencies suffer less loss than the higher ones in this important band. The LUHF is, therefore, not the lowest, but the highest useful broadcast frequency.

The higher powers and longer wave lengths employed in this frequency range make for considerable extensions of the ground wave. Most often, therefore, the ground wave predominates over the sky wave during daylight hours. The long broadcast ranges for sky-wave transmission occur during the night, when $(Kd)_{\text{min}}$ approaches zero. The field-intensity nomograms of Figs. 89 or 90 will then apply. The auroral absorption on broadcast frequencies occasionally makes itself felt in latitudes as far south as New York City, when solar disturbances of the ionosphere are specially intense.

For satisfactory reception, the requirements of the broadcast frequencies are much more severe than for ordinary commercial work (Table 7). The field intensities required depend markedly upon the density of population, the types of buildings, and so forth. The values specified in the field-intensity curves of Figs. 89 to 90 are based on the best receiving conditions to be found within an area of given noise grade.

In or near large centers of population, man-made electrical noise, from trolley-cars, subways, electrical machinery, and so forth, may rise as much as 40 db above ordinary atmospherics. The large buildings of steel and concrete tend to reduce the ground conductivity, causing great depletion of signal strength. Hence, for factory areas or city business regions, the maximum noise curves of 5, without the diurnal variation, represent the conditions more effectively. Noise curves 4 will apply roughly to residential areas; noise grade 3 to suburban regions or small towns; and noise grade 2 will fit rural conditions. If the location happens to lie within a natural noise area of higher grade, clearly one should use the higher value.

Since districts differ so widely in the character of interference, no general rules can be given. Each area requires special studies. The problem, from the point of view of broadcasting, is not so much one of receiver as of transmitter location. The receivers will obviously be concentrated in the population centers, and the problem for the broadcasting station is how to serve the area best. For the concentrated business districts, the only answer is high power. The actual station location will be dictated by the layout of the residential and suburban service areas. Reception will generally be poor in the area directly beyond the business district of large cities. The shadow effect of the large buildings will be quite pronounced. This consideration applies even more to the higher frequencies used for FM and television.

It is particularly important to note that the daytime and nighttime service areas for broadcast purposes will generally be different. During the day, the ground wave will predominate at all distances, and the range will depend upon the pattern of the field intensity.

At night, however, the sky wave comes into action. The ground wave tends always to diminish with distance from the transmitter and is essentially constant with time. Near the transmitter, however, the sky wave is weak because antenna emission is low directly upward. Thus, the field intensity of the sky wave first increases outward, reaches a maximum, and then decreases at a rate much slower than that of the ground wave.

At some distance from the transmitter, the two curves will cross, and the field intensity is the resultant of the ground and sky waves. Because of ionospheric variability, the phases of the two waves fluctuate, and we find a region (a ring roughly centered about the transmitter) where fading and consequent signal distortion are severe. Beyond that point, when the sky wave dominates over the ground wave, the reception is again satisfactory.

Thus, at night, we find a primary service area of ground-wave reception and a secondary area of sky-wave reception separated by a ring of poor service and high distortion. In the daytime, the primary and secondary service areas are contiguous. The location of the distortion ring will vary, of course, with local conditions

and with the character and height of the antenna, but it will generally fall in the region from about 50 to 150 miles from the broadcast station. Also, the higher the frequency, the smaller will be the radius of the ring because the ground-wave field dies away more rapidly with distance. By using directive antenna with an angle of fire as near as possible to the horizontal, one can increase the range of primary service and reduce the width of the distortion zone.

For the radio waves in the range 1.5 megacycles and above, we found that we could neglect reflections by the E layer at night, except when sporadic E was present. Study of transmissions on broadcast frequencies indicate that the residual nighttime E ionization is sufficient to reflect these lower frequencies, so that the effective ionospheric altitude lies in the zone from 90 to 110 km. Absorption, possibly deviative in character, reduces the sky wave by about 12 db from the intensity for perfect reflection.

The amount of the absorption seems to vary with solar activity, being greatest near sunspot maximum. The periods of minimum, therefore, give greatest signal strength. A tendency also exists for broadcast sky waves to propagate more readily on circuits running north and south than along paths running east and west. This phenomenon is probably associated with the earth's magnetic field and the induced polarizations of the waves. This phenomenon also persists to some extent into the higher-frequency ranges.

Radio waves of frequencies below 100 kc exhibit characteristics that differ markedly from those of the higher frequencies. The properties, however, are consistent with the expected characteristics, deduced by extrapolation from the higher ranges. The ground-wave ranges increase. The ionospheric absorption is less, though still sufficiently intense to produce some weakening of signal strength during the daytime.

At night, however, the signals are less strongly transmitted than during the day. The propagation of the standing waves is actually facilitated by high ionization in the upper atmospheric layers. The difference between night and day signal strengths may amount to as much as 20 db. The actual difference will depend on the season of the year and the location of the path on the surface of the earth. For similar reasons, these long waves, unlike the high frequencies, give greater signal strength at times of greatest solar activity. Thus, when all communication may be impossible on the ordinary frequencies, the very low frequencies offer an effective means of maintaining operating schedules.

For daytime transmissions over sea water, the following formula, devised by Austin and Cohen and improved

by Fuller and others, represents the observed data satisfactorily.

$$E = \frac{3.77 \times 10^6 h I e^{-(\alpha r / \lambda^{1/2})}}{\lambda (r R \sin \theta)^{1/2}} \quad (1)$$

where E is in microvolts per meter, I is the antenna current in amperes, h is the "effective" antenna height, λ is the wave length, R is the earth's radius, and r is the length of the transmission height—all these distances are to be expressed in kilometers. e is the Napierian base, 2.718. θ is the angle subtended by the path at the center of the earth, so that $\theta = r/R$, in radians. The quantity α is a constant, supposedly, although its value seems to vary with the path. For example, European stations received in the Atlantic $\alpha = 0.0018$
American stations received in the Atlantic $\alpha = 0.00142$
European stations received in the Pacific $\alpha = 0.00095$
The reasons for this variation are unknown. The power of λ in the exponent of e , first determined empirically, has been given some theoretical justification. Fuller, however, has shown that a very careful set of observations taken over the 4000-km path from Honolulu to San Francisco are better represented by a factor $\lambda^{1.4}$ instead of $\lambda^{1/2}$.

Out to distances of 700 km, and possibly as far as 2000 km, especially for very long waves (frequencies of about 20 kc), the ground waves will predominate. Beyond this distance, the sky wave begins to take effect, and the signal strength falls off less slowly with distance than the ground-wave calculations indicate. The sky wave on these low frequencies appears to act like a standing wave bounded by two reflecting planes, the ionosphere and the ground. There are interference effects between the ground and sky wave that complicate the problem within a few hundred miles of the transmitter.

Frequencies in the range 100 to 500 kc are intermediate in character between the very low and the broadcast frequencies. Ground-wave ranges and ionospheric absorption are intermediate. Equation (1) expresses the field intensities to a fair degree of accuracy for daytime transmissions, but for nighttime values, the exponential factor should be eliminated.

The segregation of the data into two groups only, of day and night values, appears to be rather arbitrary. Moreover, there is a very large scatter. A reanalysis of the data, employing the parameter (Kd) of the LUHF calculations, would seem to be in order. The following equation, which is similar to, but not quite identical with, that used for the field-intensity nomograms for high frequencies, would appear to be applicable.

$$F_{db} = 26.3 + 10 \log P - 10 \log d \sin (0.1571d) - 10(Kd)S_0, \quad (2)$$

where F_{db} is the field intensity in decibels above one

microvolt per meter; P is the power, in kilowatts; and d is the distance in units of 1000 km. This equation, for $(Kd) = 0$, is an alternative form for Equation (1) with the exponential term omitted. The problem is to find the proper expression for S_0 . From rather meager observational data, it appears that an expression of the following form will apply:

$$S_0 = 2 \times 10^{-3} f_{kc}^{1.4}, \quad (3)$$

where f_{kc} is the frequency in kilocycles. The equation seems to work fairly well for all frequencies in the range of 100 to perhaps 700 kc.

Employing this expression, together with the noise curves, we could work out charts similar to the LUHF nomograms of Figs. 58 to 87. In this sense, however, the derived frequencies would be the highest useful low frequency, HULF, rather than the LUHF. Or one could make up field-intensity nomograms similar to those of Figs. 89 and 90. Because of the semiprovisional character of this equation, however, further studies aimed at increasing the accuracy of the coefficient of $f_{kc}^{1.4}$ in Equa-

tion (3) are desirable. Indeed, the exponent of f_{kc} is not well determined, but the value of 1.4 seems definitely preferable to that of 0.5, used in the Austin-Cohen formula and seems to be confirmed in part by the work of Fuller.

It will be noted that the field intensity equations give infinite intensity at the antipodes. Although this condition is not fulfilled, because the ionosphere does not bring the beam to a precise focus, the high intensities, nevertheless, have been confirmed. The phenomenon already has been referred to in an earlier chapter.

During the past twenty years or more, the trend has been toward the higher and higher frequencies. The greater space available in the upper brackets for wide bands, as well as the low cost of the equipment, has caused this move. New developments, however, will allow the use of greatly improved techniques for low and very low frequencies. It is the author's opinion that these advances will cause a renewal of interest in the lower-frequency ranges during the coming few years.

• CHAPTER THIRTEEN •

SOME INTRODUCTORY REMARKS ABOUT VHF, UHF, AND SHF

RADIO EQUIPMENT OPERATING ON FREQUENCIES ABOVE 30 megacycles has played an increasingly important role in military operations. We rely upon high-bracket radio frequencies for communication in crucial battles; radar warns us of impending attack and trains our guns on enemy targets invisible to the eye; beacons guide our planes through storm and darkness. These frequencies are so high (the balls of our analogy are so small) that they penetrate the ionospheric mesh and are, therefore, not usable for long-distance communication on earth. This escape through the ionospheric mesh is strikingly illustrated by army scientists' recent contact with the moon by means of radar. The primary utility of these frequencies is for short distances, within the line of sight. Sometimes, freakish atmospheric conditions allow high-frequency waves to travel unexpectedly long distances, but these conditions are nonstandard and require special forecasting. Also, as mentioned in Chapter 10, sporadic E , and occasionally F_2 , will sometimes reflect frequencies as high as 80 to 100 megacycles.

Most of us are familiar by now with the general principles of radar. Radar is a radio-wave phenomenon. The pulse methods for determination of ionospheric height by means of a time delay were the first important application of the radar principle. Another forerunner of radar is the radio altimeter used by pilots to find their height above the ground. A transmitter sends out pulses and the objects they strike reflect back an "echo," which the receiver amplifies and reshapes to give a visual picture of the territory scanned.

Radar was a tremendously important factor in the victory of World War II. Its value will continually increase during time of peace. Radar will guide aircraft through fog, clouds, or rain that would ordinarily make flight impossible. Vessels approaching a fog-bound harbor can dock without fear. Icebergs and other navigational hazards can be detected and avoided. Radar's recent excursion to the moon is just the beginning of an extremely important series of scientific studies in interstellar space.

Radar not only "sees" but also tells how far away the object is, by the same technique we employ in measuring

the height of the ionosphere. The time required for the pulse sent out by the transmitter to reach the target and return is a measure of the object's distance. The orientation of the antenna, when it receives the strongest echo, indicates the direction of the target.

Radar depends on the use of very short wave lengths at high levels of power. Longer wave lengths often fail to cover the area just above or on the surface of the sea with enough energy to pick up ships or low-flying airplanes, although such wave lengths were adequate to locate planes at high altitudes. Shorter wave lengths could extend the area of search right down to the sea with vitally important advantages.

Again we shall not concern ourselves with the mechanics of radio or radar equipment, but focus our study on the waves' behavior after they leave the transmitting antenna. One of our first problems is to find the maximum range the waves will travel at a given strength. That is, will radar pick up a plane at 100 or 10 miles? Or, inversely, will the pilot "sight" his airport at 10 or 1 miles? This range will vary according to the required signal strength, the frequency used, the antenna heights, weather and atmospheric conditions, height and topography of area to be surveyed, and so forth. Because formulas including all these factors are extremely involved, we have developed a nomographic method that leads to a graphical representation of the coverage area. This method is outlined in the following chapter for standard atmospheric conditions.

The troposphere, or earth's lower atmosphere, is the medium ordinarily controlling the VHF and higher frequencies. Consequently, we shall talk about tropospheric propagation, as distinguished from the ionospheric propagation of earlier chapters. When the troposphere is turbulent and has no tendency toward stratification, propagation is relatively simple. We thus speak of standard conditions.

Conditions often exist, however, that differ tremendously from the results predicted for the standard atmosphere. On one occasion, a target 1800 miles away was detected by a set whose normal range was less than 100 miles. At the other extreme, enemy planes were some-

times able to slip in undetected almost to the ship. Something strange was happening in the atmosphere that was conducting these waves to greatly extended distances at one time, and producing extremely low ranges at another. Chapter 16 and following chapters explain something of the influence of variable atmospheric conditions upon coverage of VHF, UHF, and SHF communication and radar equipment.

Because this material was first prepared for the U.S. Navy and for use of communications officers at sea, some of the references may have a slightly nautical twist. The principles, however, have a general application to all

types of problems in the frequency ranges under consideration. An effort has been made to include operation over land as well as sea areas. If the coverage appears to be greater for the latter case, it is because sea conditions are simpler. We have no mountain ranges or valleys or vegetated areas in open ocean.

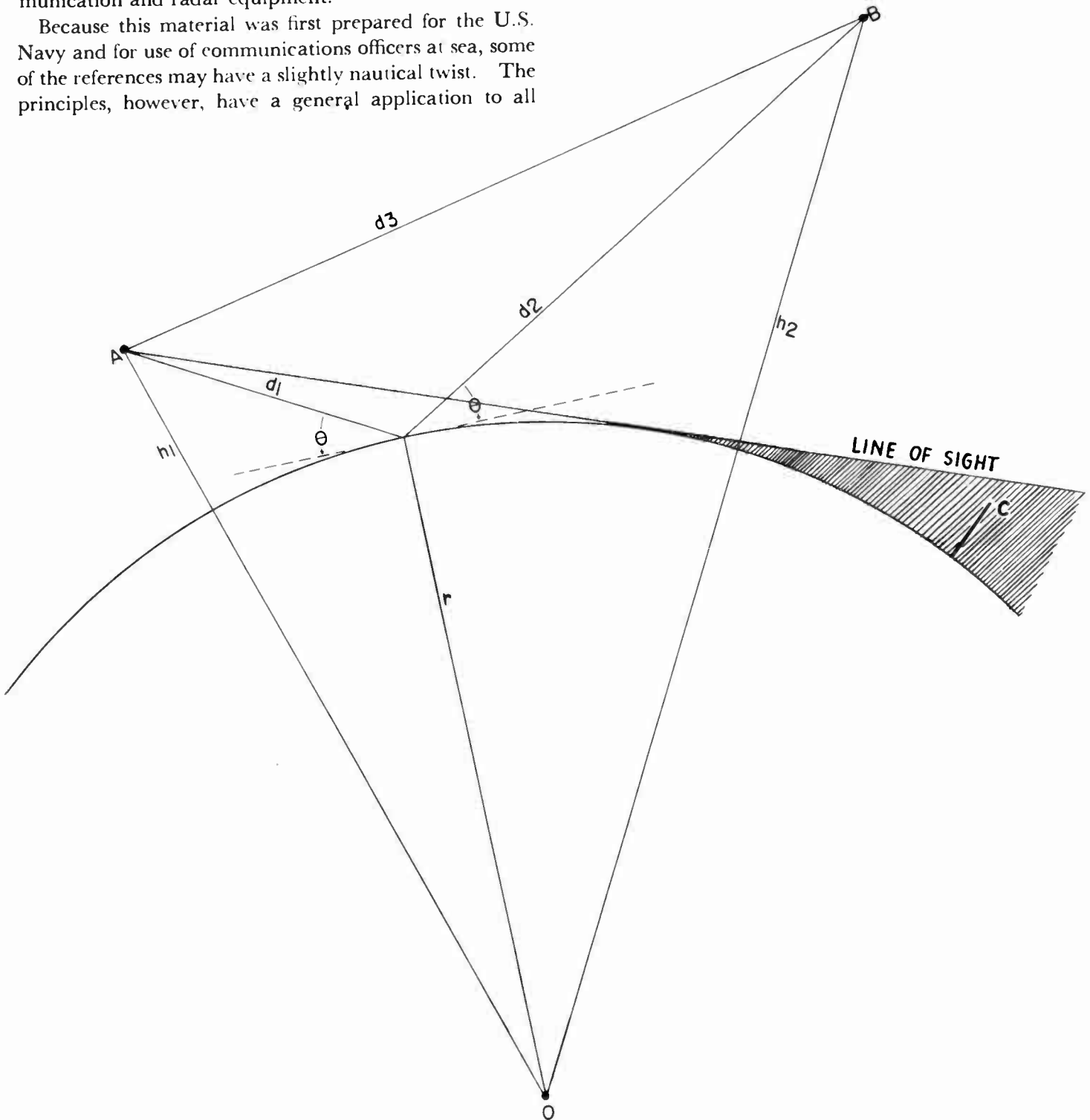


Fig. 108. Geometry of the Curved Earth.

THE CALCULATION OF COVERAGE DIAGRAMS FOR STANDARD ATMOSPHERIC CONDITIONS FOR RADIO FREQUENCIES GREATER THAN 30 MEGACYCLES

A NUMBER OF INDEPENDENT INVESTIGATORS HAVE EXAMINED the problem of determining the field produced by a radio transmitter. The formulas and methods devised have been more complicated than necessary. The purpose of this chapter is to simplify the problems of calculation for two antennas that lie within the line of sight.

Allowance is made for the earth's curvature. The geometrical relationship involved appears in Fig. 108. The arc represents the curved surface of the earth, with center at O . A and B represent two antennas at respective heights h_1 and h_2 above the surface of the earth. AB is the direct path of the radio wave, and ACB is the ground-reflected path of the wave. Antenna C lies in the shadow zone, hidden from the transmitter by the earth's curvature. Some energy penetrates into this region by diffraction.

We also assume that the transmission occurs under standard atmospheric conditions. These conditions prescribe a normal decrease in temperature and moisture content with height. Nonstandard conditions will be considered in later chapters.

For the moment, we shall consider A as the transmitting antenna and B the receiving, although it is clear that the problem is symmetrical and that we may interchange transmitter and receiver without altering the results. The formulas and mathematical calculation involved in deriving them will be omitted from this discussion except where the formulas are simple and where the operator might occasionally find them preferable to the nomograms.

A transmitter with a nondirectional (isotropic) antenna in free space will emit energy equally in all directions. The energy will vary inversely as the square of the distance, and the field intensity, inversely as the distance. The zones of equal energy or field intensity will be spherical surfaces, centered around the transmitter, as in Fig. 109. If the antenna is directional, these free-space surfaces of equal intensity will conform to the antenna

pattern.

But, put one of these antenna near the surface of the earth, so that a reflected wave appears, and the entire pattern changes. The direct and reflected waves interfere with one another. The surfaces of constant field intensity flare out from a region near the base of the antenna to form a sort of cone. At some distance away, the edge of the cone curves sharply around, and the surface returns transmitterward on another cone-like face. If we take a vertical cut through the cones with a plane surface that includes both transmitter and receiver, we obtain a map of the distribution of equal field intensity. The petal-like pattern is shown in Figs. 110 to 115. We call the individual petals *lobes*. The complete lobe picture is known as a *coverage diagram*, because it pictures the potential ranges of a given transmitter-receiver combination.

We shall draw our coverage diagram with reference to a transmitter possessing an isotropic antenna and a power of 1 watt. Other powers or other antenna gains will be discussed later.

The power density produced by this transmitter, at distance S (measured in thousands of yards) and at height h_2 (in feet) above the ground, is measured in decibels (db) *above* the standard of 1 microwatt per square meter. Ordinarily, the power density will be less than this standard figure. Hence, $db = -45$ indicates that the power density is 45 db *below* 1 microwatt per square meter. If the power of the transmitter is, say 500 watts or 27 db above 1 watt, the actual field (DB) would be $27 - 45 = -18$, or 18 decibels below 1 microwatt per square meter.

The simplest case occurs when the transmitter is in free space, as previously discussed. Then, for the 1-watt transmitter,

$$db = -10.2 - 20 \log S \quad (1)$$

The coverage diagram is extremely simple: it is a series of concentric spheres around the transmitter shown in Fig. 109. The circles represent the intersection of the

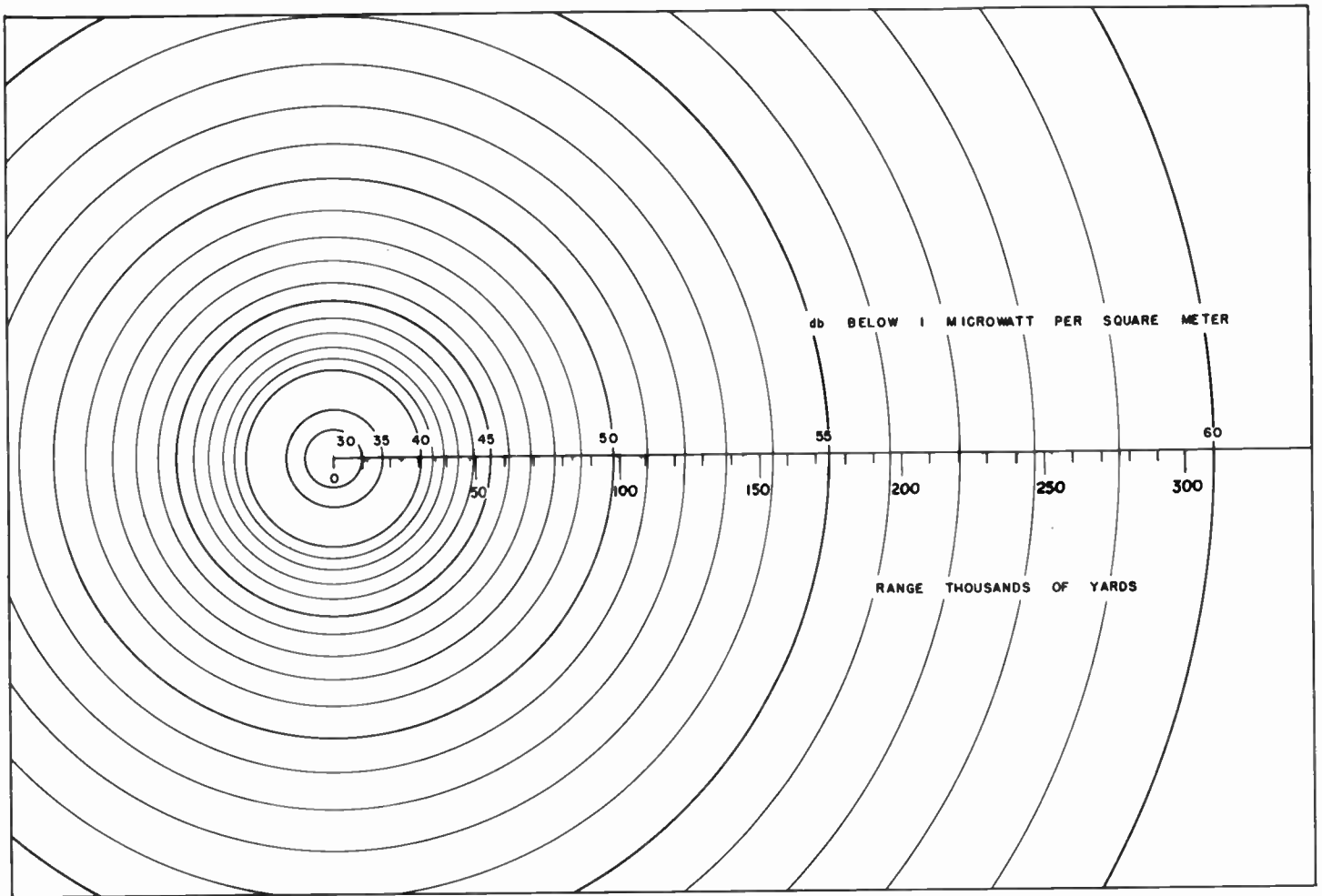


Fig. 109. Field Intensities in Free Space.

sphere with the vertical plane of the transmitter.

Let us work out a problem with this coverage diagram. What range can we expect to obtain with a 20-watt transmitter, used with a receiving antenna, whose gain is 3 db, and a receiver system sensitive to, let us say, 40 db below,—that is, -40 db above, 1 microwatt per square meter? The power of 20 watts is $10 \log 20$, or 13 db above the standard power of 1 watt. Thus, the total effective transmitter power is 16 db greater than that for 1 watt. A receiver 16 db more sensitive would respond to 1-watt power in the same way as the actual receiver would to a 16-db transmission. Add the power and antenna gains and subtract the receiver sensitivity,

$$13 + 3 - (-40) = 56.$$

Now, on the coverage diagram find the distance at which the power density is 56 db below standard. This point lies at $S = 196$. Therefore, the range is 196,000 yards.

In this simple example, it is easier to compute S from the formula, which connects db and S , than to get it from the diagram. But in the actual case of an antenna

near the ground, the quantity, db , depends upon height as well as distance, and the formula is very complicated. Hence, nomograms make the calculations much easier.

The limit of noise level for frequencies above 30 megacycles is generally set by the receiver rather than by atmospherics. Outside interfering signals will occasionally rise above the set noise level. The receiver noise arises from random motions of the electrons in the set itself. Since these motions increase with temperature, the noise similarly increases. The receiver noise, in decibels above 1 microvolt per meter, is

$$(db)_{noise} = -102.6 + 10 \log TRW, \quad (2)$$

where T is the absolute temperature on the Kelvin (Centigrade) scale; R is the resistance component, in ohms, of the impedance across the circuit considered; and W is the effective band width of the receiver.

Such radio noise as actually occurs on these upper-bracket frequencies is subject to the propagation characteristics of such frequencies. Distant storm areas, therefore, do not contribute appreciably to the radio

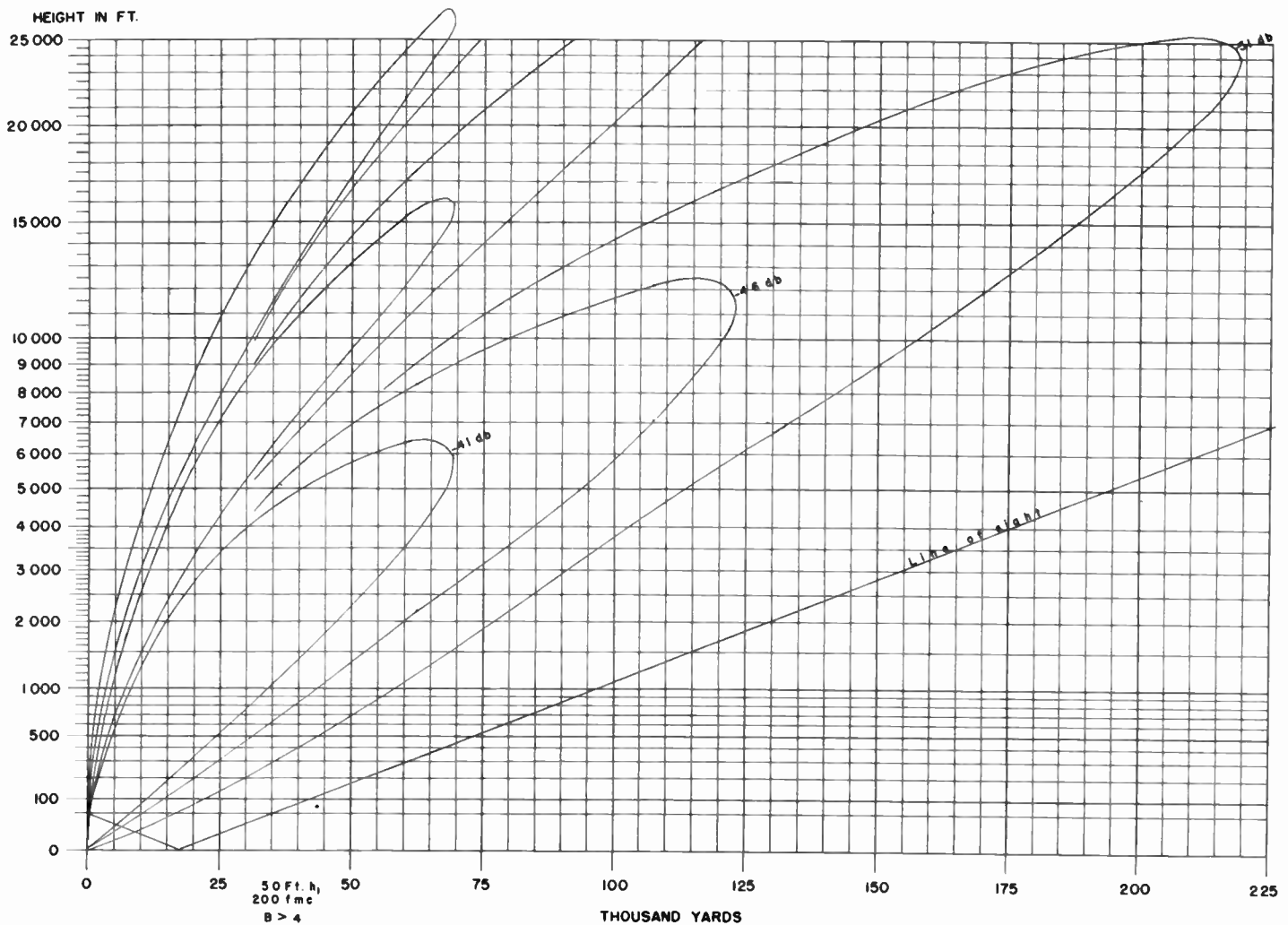


Fig. 110. Coverage Diagram.

noise.

Recent studies have revealed an unexpected source of radio interference: the sun itself. We have already discussed the effect of solar activity on the ordinary radio waves through the medium of ionospheric variation. But for frequencies in the range of from 50 to 200 megacycles, the sun itself acts as a radio transmitter, emitting radio signals that can interfere with reception on these frequencies.

As early as 1937, radio amateurs had reported occasional hissing sounds on 5-meter (60-megacycle) receivers, and had suggested a solar origin for them. But the first definite evidence of such wave lengths came during World War II. Late one afternoon, a number of British radars operating within this frequency band detected a peculiar signal that was first regarded as an enemy countermeasure. Later plotting showed that these bearings all pointed toward the sun. The signals were intense enough to interfere seriously with ordinary radar operation.

The war was fought, it must be remembered, during a period of minimum solar activity. During 1945 and 1946, with the marked rise of solar activity, the frequency and intensity of such solar outbursts had greatly increased. The emission comes from small areas of the sun, probably coincident with the bright solar flares responsible for short-wave radio fade-outs. The precise mechanism is not fully understood, but the observed polarization of the waves suggests that they originate in or near the magnetic fields of active sunspots. The frequencies correspond very nearly to the gyrofrequencies of free electrons in the outer regions of a spot.

The existence of such sources of radio noise is a potential source of trouble for services operating on these frequencies. One-way services, like television, can minimize the interference if the transmitter is set to the north of the service area (in the northern hemisphere). In this way, the directional or semidirectional receiving antennas will be turned away from the sun.

On frequencies ranging from 15 or 20 megacycles

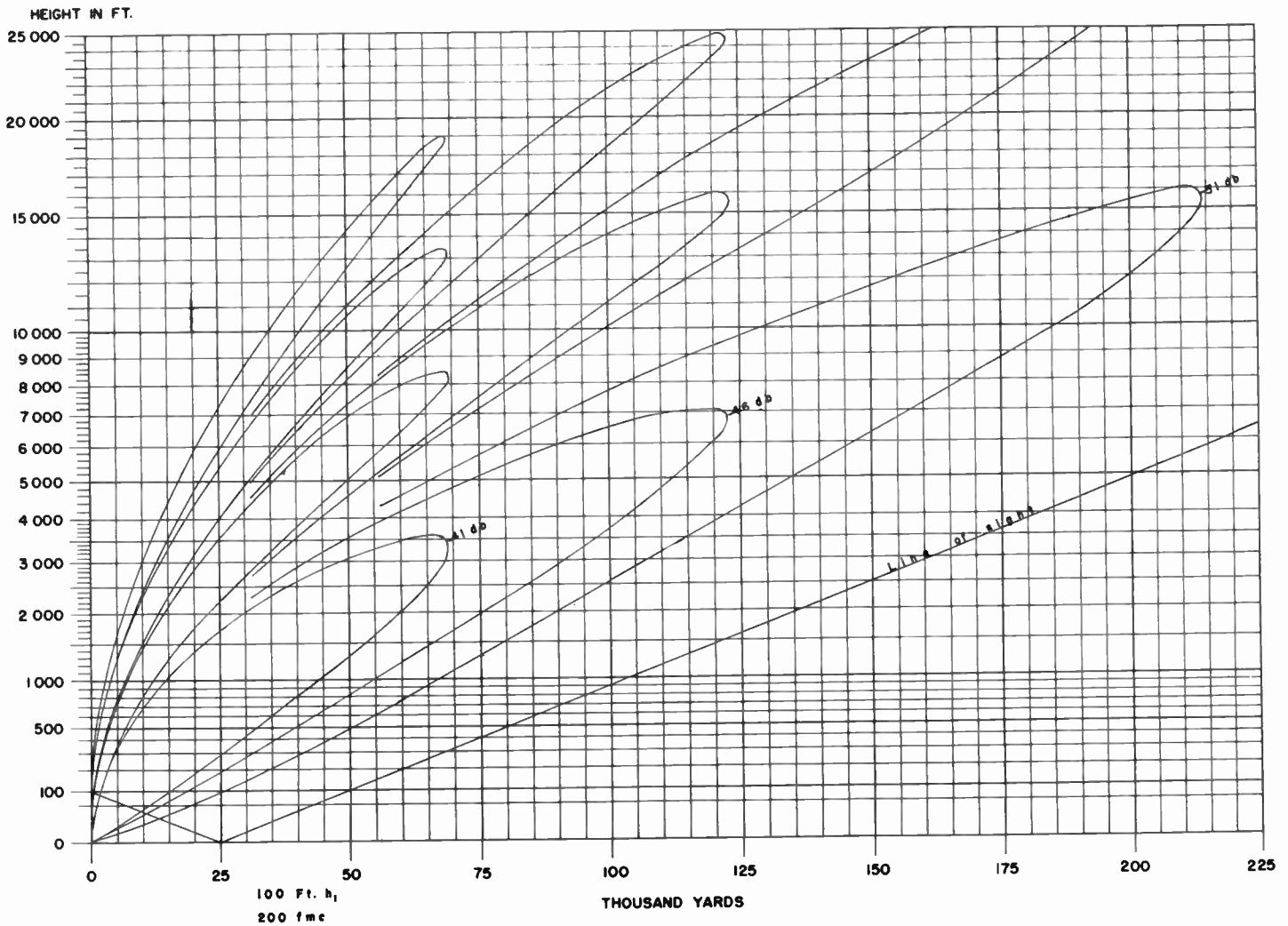


Fig. 111. Coverage Diagram.

upward, additional radio noise has been observed to come from outside our solar system. The maximum appears to coincide fairly well with the center of our own galactic (Milky Way) system, in the constellation of Sagittarius. The source is unknown. Astronomers have suggested that it arises in the depths of interstellar space. It is the author's opinion, however, that the source may be in the atmospheres of the stars.

One other source of interference comes from so-called *precipitation static*. A plane, flying through rain, snow, hail, ice crystals, fog, or even dust storms, may pick up an electrical charge so great that actual discharge will result. This occurs in the form of a corona discharge from the wing tips or other sharp points or surfaces of the plane. The static from the flash is powerful and will generally interfere seriously with the operation of radio equipment. Various methods are employed for eliminating the trouble by mechanical means. For example, a fine trailing wire attached to the plane through a resistance

will disperse the charge gradually and uniformly, so that a minimum of disturbance results.

The concept of power density—that is, the power passing through a unit area, is often more useful in short-wave calculations than field intensity. In all radar applications, for example, the area of a target is involved. If one desires to convert power density, P , in decibels above 1 microwatt per square meter, to field intensity, F , in decibels above 1 microvolt per meter, the formula is

$$F_{db} = P_{db} + 85.77 \quad (3)$$

All the complications arise when the ground-reflected wave interferes with the direct wave, producing, within the line of sight, the aforementioned lobe pattern. The formulas from which we compute coverage are based on the assumption that the ground is a perfect, or nearly perfect, reflector. In certain regions of space, the field intensity of the reflected wave adds on to the direct wave. The resultant field intensity is twice the free-space value,

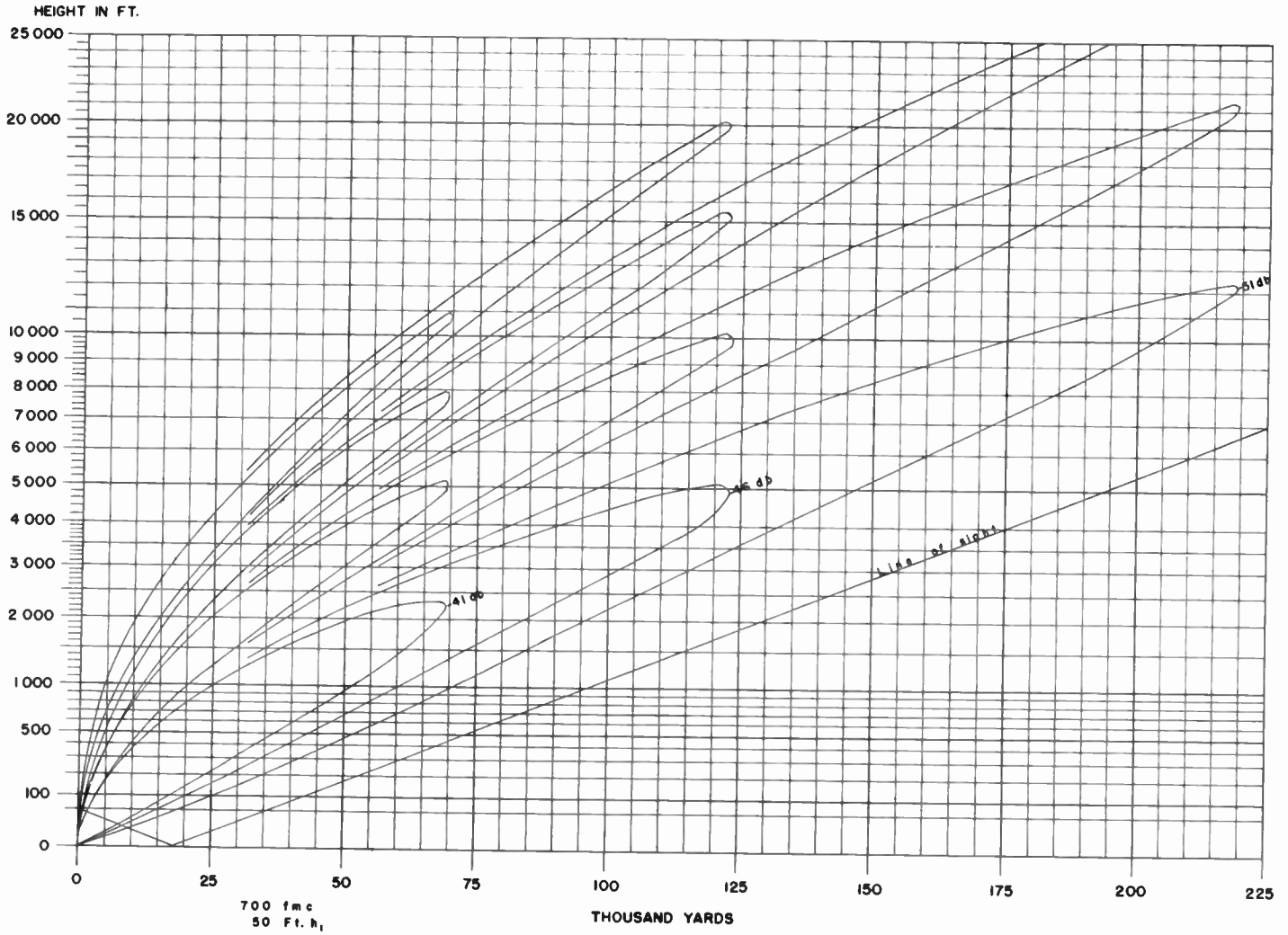


Fig. 112. Coverage Diagram.

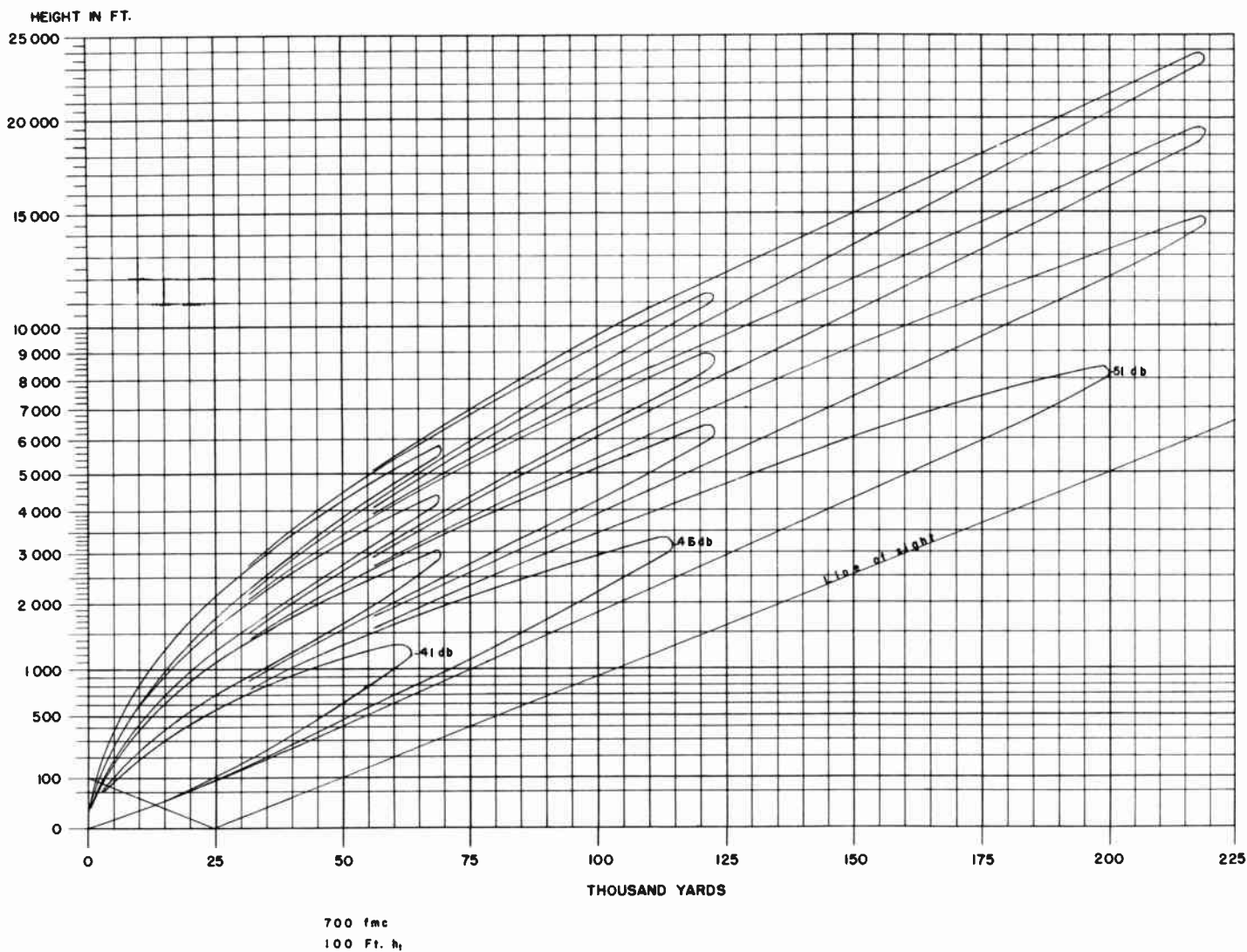


Fig. 113. Coverage Diagram.

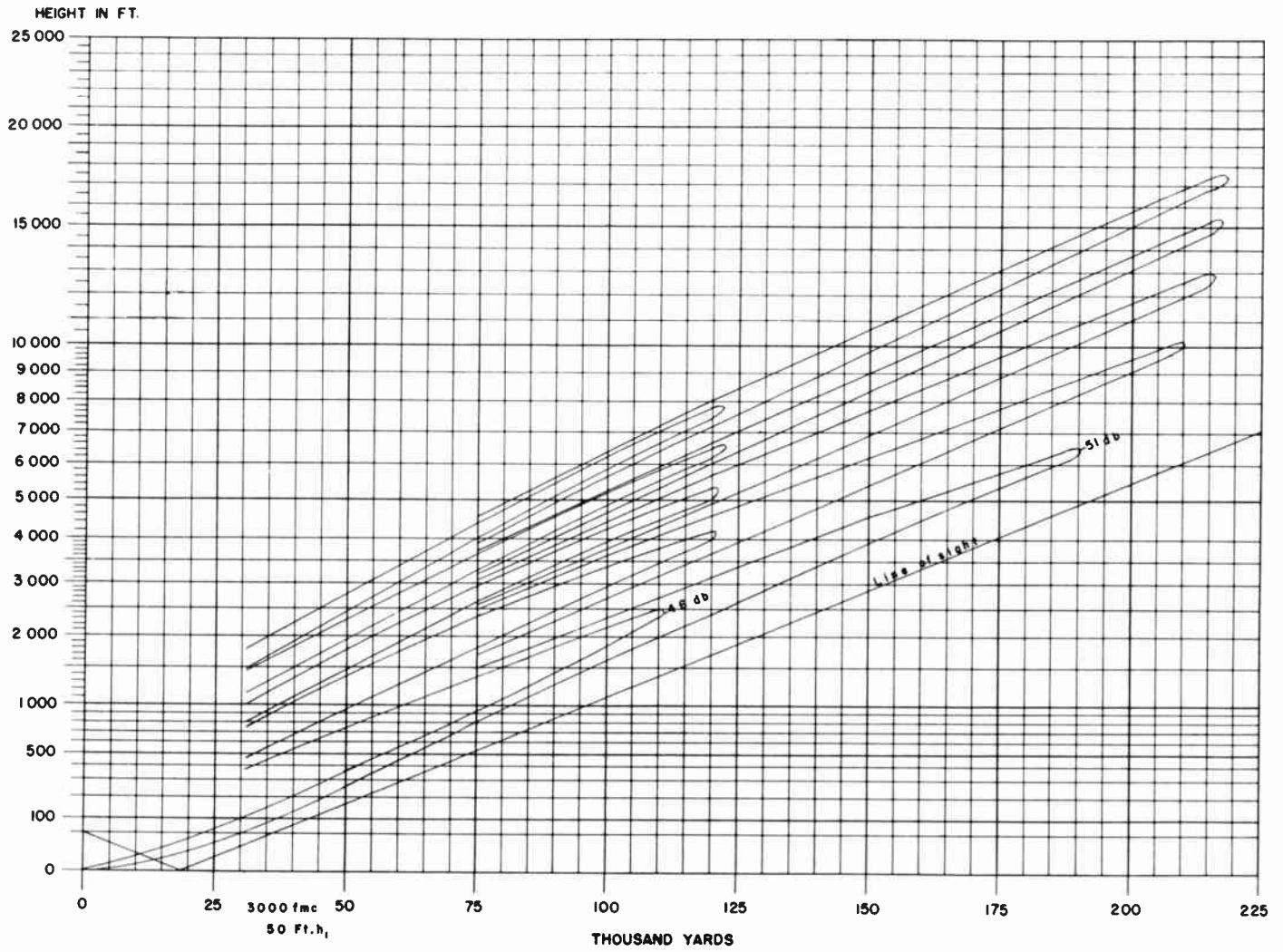


Fig. 114. Coverage Diagram.

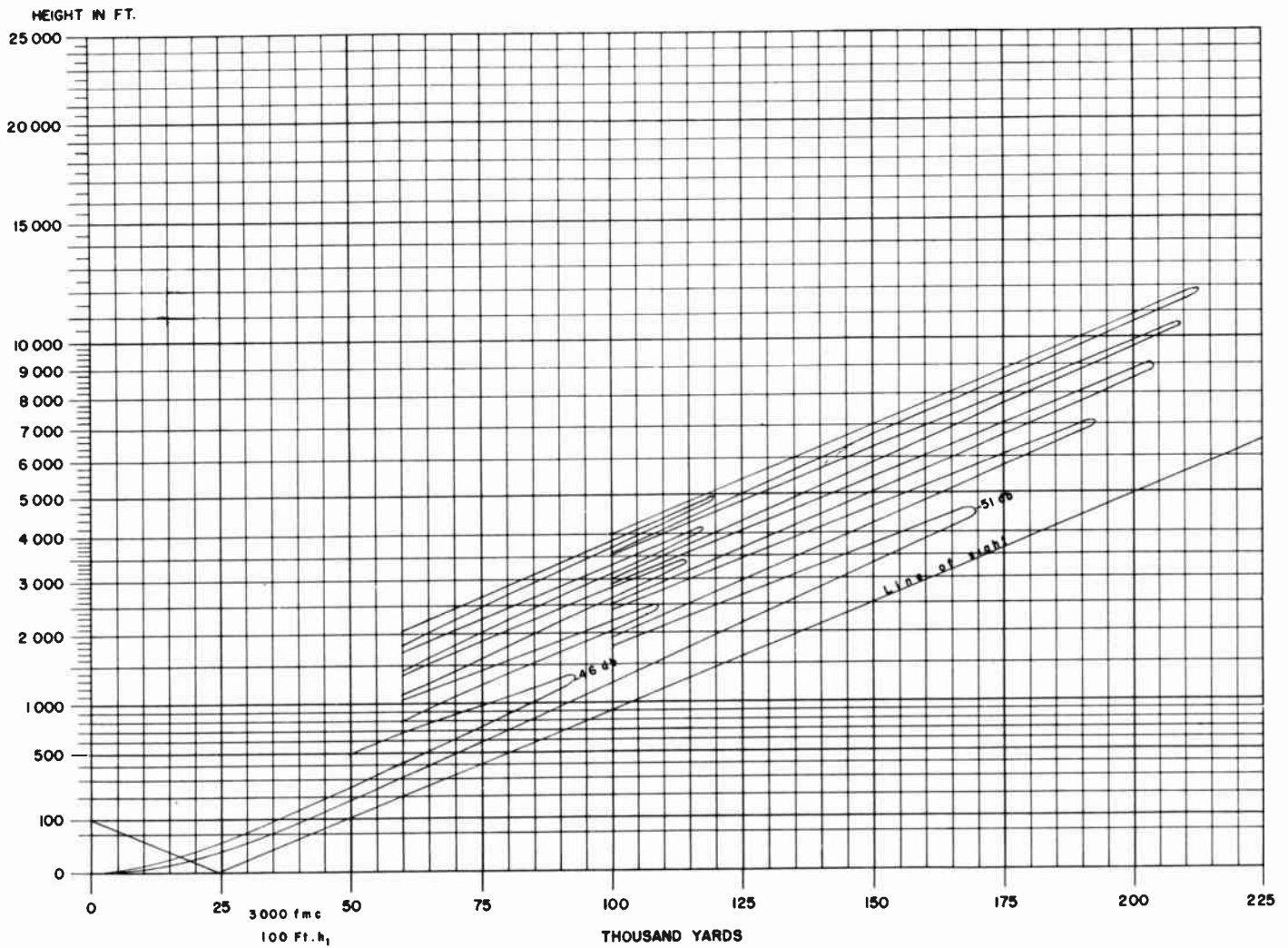


Fig. 115. Coverage Diagram.

and the power density (which goes as the square of the field intensity) is four times, or 6 db, greater than in free space. A comparison of the values at the lobe tips with the power densities from the free-space figure, will generally show this 6-db excess.

In the directions of the lobe maxima, therefore, the ground reflection actually increases the effective range of the set. This increase is accomplished, however, only at the expense of a marked decrease of coverage in the regions between the lobes. Our problem, therefore, is to map out the lobes for a given power density. Actually, we determine at least seven points on each lobe, which are usually sufficient for delineating the coverage pattern. The theory behind the nomogram procedure takes into account the earth's curvature and the refraction or bending effect of a standard atmosphere. We aim to construct a picture similar to those of Figs. 110 to 115. The total number of lobes N is approximately

$$N = 2.03 \times 10^{-3} h_1 f_{\text{megacycles}} \quad (4)$$

for h_1 in feet. These will be distributed over an angle of 90° . Work sheets for six typical operational cases are given in Figs. 116 through 121. The corresponding coverage diagrams appear in Figs. 110 through 115, respectively. Note that the vertical scale on these charts varies as the square root of the height. Tests have shown that the square root of the height scale is the most convenient for depicting coverage. It enlarges the picture near the ground where greater accuracy is needed. It compresses the scale at high altitudes where small variations in atmospheric conditions cause some inaccuracies in the calculated field.

Two of the examples are shown plotted on coverage charts in which the height scale is linear (Figs. 122 and 123). Note how the lobes seem to curl up at the ends and squash together near the transmitter. Finally, in Figs. 124 and 125 are shown two examples of coverage diagrams drawn on curved-earth charts developed at the MIT Radiation Laboratory. These maps greatly exaggerate the earth's curvature.

Let us now proceed to the nomograms and the calculations, which will prove to be simpler than they appear to be at first sight. Look at the work sheets (Figs. 116 through 121). Known values are the frequency $f_{\text{megacycles}}$, the height of the transmitting antenna h_1 , and the decibel level assumed for the power density. The height is in feet; the frequency, in megacycles; and the decibels are the number the power density is above standard. In all practical cases, the decibel level will turn out negative, and we shall occasionally omit the minus sign on charts or nomograms. This procedure should cause no confusion.

We desire to calculate the values of S and h appropri-

ate to define the various lobes. Fill in the top of the work sheet (Fig. 126) with the various quantities db, $f_{\text{megacycles}}$, h_1 , $h_1 f_{\text{megacycles}}$, and Y . The last is obtained directly from the nomogram of Fig. 127.

The first, third, and fourth columns of the work sheet have been filled in in advance; k is a running number, indicating successive points along the lobes; n is the number of the lobe; and b indicates the position of the point on the lobe. For example, $b = \frac{1}{2}$ corresponds to maximum and $b = 0$ to minimum. The other values of b correspond to intermediate points on the lobe. Note that

$$(n - b) = k/6 \quad (5)$$

The quantity B is now filled in, either by slide-rule calculation from the equation

$$B = \frac{6.127 \times 10^{5k}}{h_1^{3/2} f_{\text{megacycles}}} \quad (6)$$

or from the nomogram of Fig. 128. To prepare this nomogram for use, connect $f_{\text{megacycles}}$, the set frequency, to h_1 , the antenna height in feet and note the point where this line intersects the central vertical line. Mark this point with a small dot. It will remain fundamental as long as $f_{\text{megacycles}}$ and h_1 are unchanged. Now, pass a straight line from successive values of k through the point until it strikes the B scale on the left. Read off the values of B and enter in the third column. Continue this process until you obtain a value of B greater than 4, or reach a value of k greater than 27.

The fifth column is headed α (alpha).* It is necessary to compute α only for values of B less than 4. Further, omit this calculation when $b = 0$. Refer to the nomograms of Figs. 129 and 130. Connect the value of Y (previously computed and listed at the top of the work sheet) with successive values of B , and read off the corresponding values of α from one of the three curves, according to the value of b . Note that $b = \frac{1}{6}$ and $b = \frac{5}{6}$ employ the same curves. Similarly, $b = \frac{1}{3}$, $b = \frac{2}{3}$, and $b = \frac{1}{12}$, $b = \frac{11}{12}$, are equivalent. Figs. 131, 132, and 133 can be used alternatively for greater accuracy when B lies in the limited range of their scales. Having filled in the values of α for all cases except $b = 0$, average the two adjacent figures for $b = \frac{1}{12}$ and $b = \frac{11}{12}$ and enter this value in the vacant space for $b = 0$.

We are now ready to calculate S , the distance out to the given lobe point, measured in thousands of yards.

* α is an intermediate parameter used merely to simplify the calculations. Although one does not need to know its precise significance to carry out the computation, the definition may be of some interest. If d_1 is the distance from the antenna to the point of reflection on the surface of the earth, and if r is the earth's effective radius ($\frac{3}{4}$ the earth's true radius), modified for the refraction of a standard atmosphere, the equation: $d_1^2 = 2h_1 r (1 - \alpha)$ defines the quantity α .

WORK SHEET FOR COVERAGE DIAGRAM CALCULATIONS

db = -41
(M.I.T. -90)

$f_{mc} = 200$
 $h_1 = 50$ ft.

$Y = \dots\dots\dots$
 $h_1 f_{mc} = 10000$

K	B	n	b	α	S	C	H	h_2
1	>4	1	$\frac{1}{6}$	—	35	25	1075	Same as H
2		1	$\frac{1}{3}$		60	49	3520	
3		1	$\frac{1}{2}$		69	75	5943	
4		1	$\frac{2}{3}$		60	97	6400	
5		1	$\frac{5}{6}$		35	123	4500	
5.5		1	$1\frac{1}{2}$		17.5	135	2447	
6		2	0			140		
6.5		2	$\frac{1}{2}$		17.5	162	2926	
7		2	$\frac{1}{6}$		35	171	6182	
8		2	$\frac{1}{3}$		60	192	12100	
9		2	$\frac{1}{2}$		69	220	15948	
10		2	$\frac{2}{3}$		60	245	15280	
11		2	$\frac{5}{6}$		35	275	9823	
11.5		2	$1\frac{1}{2}$		17.5	280	5021	
12		3	0			285		
12.5		3	$\frac{1}{2}$		17.5	310	5553	
13		3	$\frac{1}{6}$		35	325	11573	
14		3	$\frac{1}{3}$		60	350	21580	
15		3	$\frac{1}{2}$		69	375	26643	
16		3	$\frac{2}{3}$		60	395	24280	
17		3	$\frac{5}{6}$		35	425	15073	
17.5		3	$1\frac{1}{2}$		17.5	430	7595	
18		3	0			450		
18.5		4	$\frac{1}{2}$		17.5	455	8039	
19		4	$\frac{1}{6}$		35			
20		4	$\frac{1}{3}$		60			
21		4	$\frac{1}{2}$		69		off map	
22		4	$\frac{2}{3}$					
23		4	$\frac{5}{6}$					
23.5		4	$1\frac{1}{2}$					
24		5	0					
24.5		5	$\frac{1}{2}$					
25		5	$\frac{1}{6}$					
26		5	$\frac{1}{3}$					
27		5	$\frac{1}{2}$					

Fig. 116. Work Sheet for Fig. 110.

WORK SHEET FOR COVERAGE DIAGRAM CALCULATIONS

db = -51
(M.I.T. - 100)

$f_{mc} = 200$
 $h_1 = 100$ ft.

$Y = \dots\dots\dots$
 $h_1 f_{mc} = 20000$

K'	B	n	b	α	S	C	H	h_2
1	74	1	$\frac{1}{6}$	—	110	12	3211	Same as H
2		1	$\frac{1}{3}$		188	24	10211	
3		1	$\frac{1}{2}$		219	36.5	15727	
4		1	$\frac{2}{3}$		188	47.5	14629	
5		1	$\frac{5}{6}$		110	60	8551	
5.5		1	$1\frac{1}{2}$		56	68	4314	
6		2	0			73		
6.5		2	$\frac{1}{2}$		56	82	5098	
7		2	$\frac{1}{6}$		110	86	11411	
8		2	$\frac{1}{3}$		188	97	23935	
9		2	$\frac{1}{2}$		219	109	31604	
10		2	$\frac{2}{3}$		188	123	28823	
11		2	$\frac{5}{6}$		110	136	16911	
11.5		2	$1\frac{1}{2}$		56	140	8346	
12		3	0			143		
12.5		3	$\frac{1}{2}$		56	153	9074	
13		3	$\frac{1}{6}$		110	159	19441	
14		3	$\frac{1}{3}$		188	169	37471	
15		3	$\frac{1}{2}$		219	180	off map	
16		3	$\frac{2}{3}$		188	197	off map	
17		3	$\frac{5}{6}$		110	210	25051	
17.5		3	$1\frac{1}{2}$		56	220	12826	
18		3	0			223		
18.5		4	$\frac{1}{2}$		56	227	13218	
19		4	$\frac{1}{6}$		110	235	off map	
20		4	$\frac{1}{3}$		188	250	off map	
21		4	$\frac{1}{2}$		219	260	off map	
22		4	$\frac{2}{3}$					
23		4	$\frac{5}{6}$					
23.5		4	$1\frac{1}{2}$					
24		5	0					
24.5		5	$\frac{1}{2}$					
25		5	$\frac{1}{6}$					
26		5	$\frac{1}{3}$					
27		5	$\frac{1}{2}$					

Fig. 117. Work Sheet for Fig. 111.

WORK SHEET FOR COVERAGE DIAGRAM CALCULATIONS

db = -41
(M.I.T. -90)

$f_{mc} = 700$
 $h_1 = 50$ ft.

$Y = 12.1$
 $h_1 f_{mc} = 35000$

K	B	n	b	α	S	C	H	h_2
1	2.476	1	$\frac{1}{6}$	916	33	6.1	400	395.8
2	74	1	$\frac{1}{3}$		60	13.9	1414	Same as H
3		1	$\frac{1}{2}$		69	20.5	2225	
4		1	$\frac{2}{3}$		60	27.5	2230	
5		1	$\frac{5}{6}$		35	34	1388	
5.5		1	$1\frac{1}{2}$		17.5	38.5	734	
6		2	0			41.5		
6.5		2	$\frac{1}{2}$		17.5	45.5	858	
7		2	$\frac{1}{6}$		35	48	1878	
8		2	$\frac{1}{3}$		60	55	3880	
9		2	$\frac{1}{2}$		69	62	5130	
10		2	$\frac{2}{3}$		60	68	4660	
11		2	$\frac{5}{6}$		35	75	2823	
11.5		2	$1\frac{1}{2}$		17.5	79	1453	
12		3	0			84		
12.5		3	$\frac{1}{2}$		17.5	86	1577	
13		3	$\frac{1}{6}$		35	90	3348	
14		3	$\frac{1}{3}$		60	97	6400	
15		3	$\frac{1}{2}$		69	105	7940	
16		3	$\frac{2}{3}$		60	110	7180	
17		3	$\frac{5}{6}$		35	117	4293	
17.5		3	$1\frac{1}{2}$		17.5	121	2199	
18		3	0			125		
18.5		4	$\frac{1}{2}$		17.5	130	2359	
19		4	$\frac{1}{6}$		35	131	4783	
20		4	$\frac{1}{3}$		60	140	8980	
21		4	$\frac{1}{2}$		69	144	10870	
22		4	$\frac{2}{3}$		60	150	9580	
23		4	$\frac{5}{6}$		35	159	5763	
23.5		4	$1\frac{1}{2}$		17.5	167	3015	
24		5	0			167		
24.5		5	$\frac{1}{2}$		17.5	171	3104	
25		5	$\frac{1}{6}$		35	171	6183	
26		5	$\frac{1}{3}$		60	181	11440	
27		5	$\frac{1}{2}$		69	190	14090	

Fig. 118. Work Sheet for Fig. 112.

WORK SHEET FOR COVERAGE DIAGRAM CALCULATIONS

 $db = -41$
 (M.I.T. -90)

 $f_{mc} = 700$
 $h_1 = 100$ ft.

 $Y = 9.0$
 $h f_{mc} = 70000$

K	B	n	b	α	S	C	H	h_2
1	.875	1	$\frac{1}{6}$	79	33	20.5	220	199
2	1751	1	$\frac{1}{3}$	87	54	54.5	800	787
3	2626	1	$\frac{1}{2}$	92	64	9.40	1200	1198
4	3601	1	$\frac{2}{3}$	94	57	12	1250	1244
5	74	1	$\frac{5}{6}$		35	17.5	820	Same as H
5.5		1	$1\frac{1}{2}$		17.5	19.1	390	
6		2	0		26.5	21	56	
6.5		2	$\frac{1}{2}$		17.5	23	459	
7		2	$\frac{1}{6}$		35	24	1038	
8		2	$\frac{1}{3}$		60	27.5	2230	
9		2	$\frac{1}{2}$		69	32	3030	
10		2	$\frac{2}{3}$		60	35	2680	
11		2	$\frac{5}{6}$		35	38	1528	
11.5		2	$1\frac{1}{2}$		17.5	40	761	
12		3	0		.6	42	25	
12.5		3	$\frac{1}{2}$		17.5	43	814	
13		3	$\frac{1}{6}$		35	45	1773	
14		3	$\frac{1}{3}$		60	48	3460	
15		3	$\frac{1}{2}$		69	52.5	4465	
16		3	$\frac{2}{3}$		60	55	3880	
17		3	$\frac{5}{6}$		35	59	2263	
17.5		3	$1\frac{1}{2}$		17.5	61	1133	
18		3	0		.28	63	18	
18.5		4	$\frac{1}{2}$		17.5	64	1186	
19		4	$\frac{1}{6}$		35	65	2473	
20		4	$\frac{1}{3}$		60	69	4720	
21		4	$\frac{1}{2}$		69	72	5830	
22		4	$\frac{2}{3}$		60	75	5080	
23		4	$\frac{5}{6}$		35	80	2998	
23.5		4	$1\frac{1}{2}$		17.5	81.5	1497	
24		5	0		16	84	13	
24.5		5	$\frac{1}{2}$		27.5	84	1541	
25		5	$\frac{1}{6}$		35	85	3173	
26		5	$\frac{1}{3}$		60	90	5980	
27		5	$\frac{1}{2}$		69	95	7340	

Fig. 119. Work Sheet for Fig. 113.

WORK SHEET FOR COVERAGE DIAGRAM CALCULATIONS

db = -46
(M.I.T. -95)

$f_{mc} = 3000$
 $h_1 = 50$ ft.

$Y = 16.75$
 $h f_{mc} = 150000$

k	B	n	b	a	S	C	H	h_2
1	.575	1	$\frac{1}{6}$.650	53	.200	400	382
2	1.22	1	$\frac{1}{3}$.787	93	1.88	1600	1589
3	1.77	1	$\frac{1}{2}$.853	111	3.95	2400	2393
4	2.4	1	$\frac{2}{3}$.899	100	5.75	2200	2195
5	2.8	1	$\frac{5}{6}$.923	58	7.60	1000	996
5.5		1	$1\frac{1}{12}$					
6	3.4	2	0		10.6			
6.5		2	$\frac{1}{12}$					
7	4.0	2	$\frac{1}{6}$.955	60	10.4	1250	1248
8	74	2	$\frac{1}{3}$		106	14.0	3300	3300
9		2	$\frac{1}{2}$		121	14.7	4200	4200
10		2	$\frac{2}{3}$		106	16.4	3600	3600
11		2	$\frac{5}{6}$		61	18.8	1800	1800
11.5		2	$1\frac{1}{12}$					
12		3	0		2.8	21.0	50	50
12.5		3	$\frac{1}{12}$					
13		3	$\frac{1}{6}$					
14		3	$\frac{1}{3}$					
15		3	$\frac{1}{2}$					
16		3	$\frac{2}{3}$		121	25.0	5450	5450
17		3	$\frac{5}{6}$					
17.5		3	$1\frac{1}{12}$					
18		3	0					
18.5		4	$\frac{1}{12}$					
19		4	$\frac{1}{6}$					
20		4	$\frac{1}{3}$					
21		4	$\frac{1}{2}$		121	34.0	6550	6550
22		4	$\frac{2}{3}$					
23		4	$\frac{5}{6}$					
23.5		4	11.12					
24		5	0					
24.5		5	$\frac{1}{12}$					
25		5	$\frac{1}{6}$					
26		5	$\frac{1}{3}$					
27		5	$\frac{1}{2}$		121	45.0	7850	7850

Fig. 120. Work Sheet for Fig. 114.

WORK SHEET FOR COVERAGE DIAGRAM CALCULATIONS

db = -46
(M.I.T. -95)

$f_{mc} = 3000$
 $h_1 = 100$ ft.

$Y = 13.9$
 $h_1 f_{mc} = 300000$

K	B	n	b	α	S	C	H	h_2
1	.21	1	$\frac{1}{6}$.478	53.5	-2.15	350	300
2	.42	1	$\frac{1}{3}$.581	82.5	-1.29	950	908
3	.63	1	$\frac{1}{2}$.655	93.0	.20	1350	1316
4	.84	1	$\frac{2}{3}$.720	85.0	1.07	1250	1222
5	102	1	$\frac{5}{6}$.778	52.5	2.45	600	568
5.5		1	$1\frac{1}{2}$					
6	1.22	2	0					
6.5		2	$\frac{1}{2}$					
7	1.35	2	$\frac{1}{6}$.828	56.0	4.10	750	733
8	1.55	2	$\frac{1}{3}$.835	94.0	4.70	1850	1834
9	1.85	2	$\frac{1}{2}$.863	109.0	5.70	2550	2536
10	1.95	2	$\frac{2}{3}$.873	98.0	6.60	2200	2187
11	2.1	2	$\frac{5}{6}$.893	57.0	7.80	950	939
11.5		2	$1\frac{1}{2}$					
12	2.3	3	0					
12.5		3	$\frac{1}{2}$					
13		3	$\frac{1}{6}$					
14		3	$\frac{1}{3}$					
15	2.9	3	$\frac{1}{2}$	923	114.0	10.80	3300	3292
16		3	$\frac{2}{3}$					
17		3	$\frac{5}{6}$					
17.5		3	$1\frac{1}{2}$					
18		3	0					
18.5		4	$\frac{1}{2}$					
19		4	$\frac{1}{6}$					
20		4	$\frac{1}{3}$					
21	3.9	4	$\frac{1}{2}$	951	118.0	15.40	4100	4095
22		4	$\frac{2}{3}$					
23		4	$\frac{5}{6}$					
23.5		4	$1\frac{1}{2}$					
24		5	0					
24.5		5	$\frac{1}{2}$					
25		5	$\frac{1}{6}$					
26		5	$\frac{1}{3}$					
27	5.3	5	$\frac{1}{2}$	---	119.0	23.5	4900	4900

Fig. 121. Work Sheet for Fig. 115.

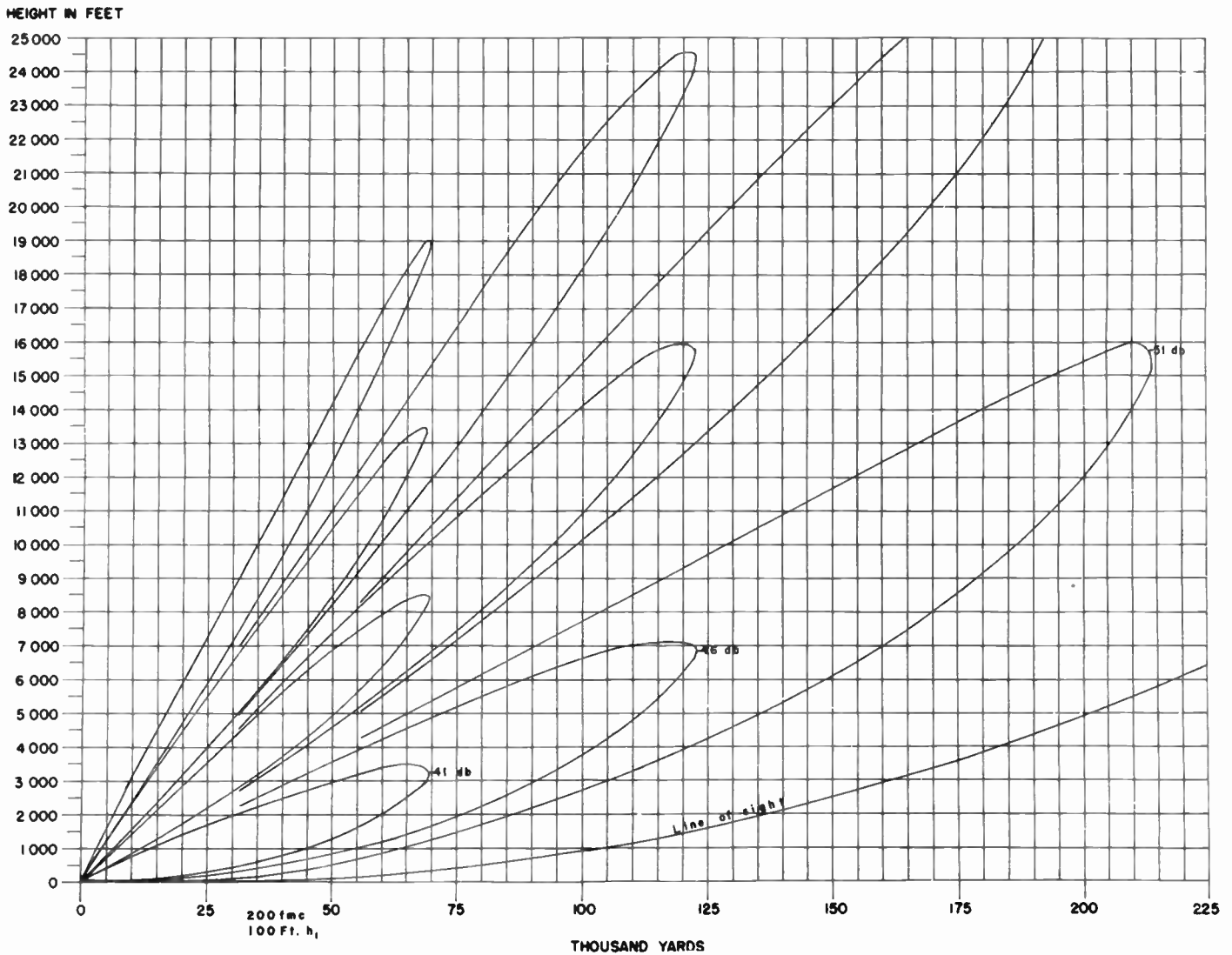


Fig. 122. Coverage Diagram on Linear Height Scale.

This point is determined from the nomograms of Figs. 134 and 135, or 136. Connect the value of α , found on the right-hand scale according to the given value of b , with the decibel scale on the left. The intersection with the center scale serves to fix S .

We next calculate the quantity C , in column 7, from the nomogram of Fig. 137. Connect the product $h_1 f_{\text{megacycles}}$, previously determined, with each value of k , in turn. This process will give a series of points along the center axis. Label these points with the numbers k . Now connect the value of α with the appropriate k point on the center axis. The final result is C , read from the intersection at the left. Note the simple rule for the sign of C , which is minus when α is less than $\frac{2}{3}$ and plus when α is greater than $\frac{2}{3}$.

Turn now to Figs. 138 or 139. Connect C with S and read off the quantity H . Alternatively, we may compute H from the equation

$$H = 0.1612S^2 + CS. \tag{7}$$

Finally, from the nomogram of Fig. 140, determine h_2 as follows. Connect h_1 with α and prolong the line to intersect at the left-hand scale. Then connect this point of intersection with H and extend it to meet the right-hand line. Alternatively, one may determine h_2 by slide-rule calculation from the equation

$$h_2 = H - (1 - \alpha)h_1. \tag{8}$$

The quantity h_2 is the height of the lobe point, in feet, above ground level. We have previously calculated the distance S of this point from the transmitter. A plot, therefore, of the positions of the points for $k = 1, 2, 3, 4, 5, 6$ outlines the lowest lobe. The points 6, 7, 8, 9, 10, 11, 12 outline the second lobe, and so forth, for the given decibel value. The points usually suffice to determine the lobes with all the accuracy desired. By connecting the successive points one can, therefore,

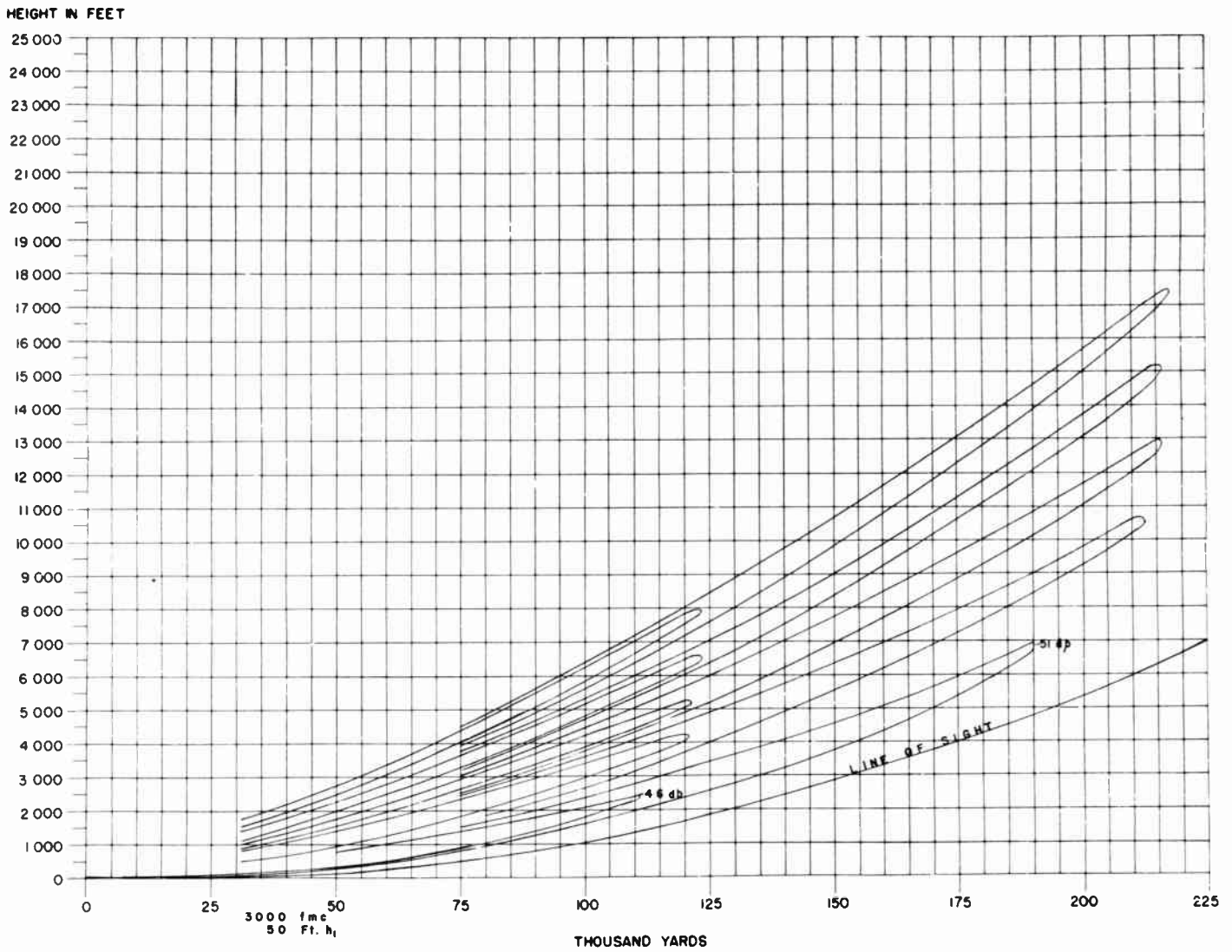


Fig. 123. Coverage Diagram on Linear Height Scale.

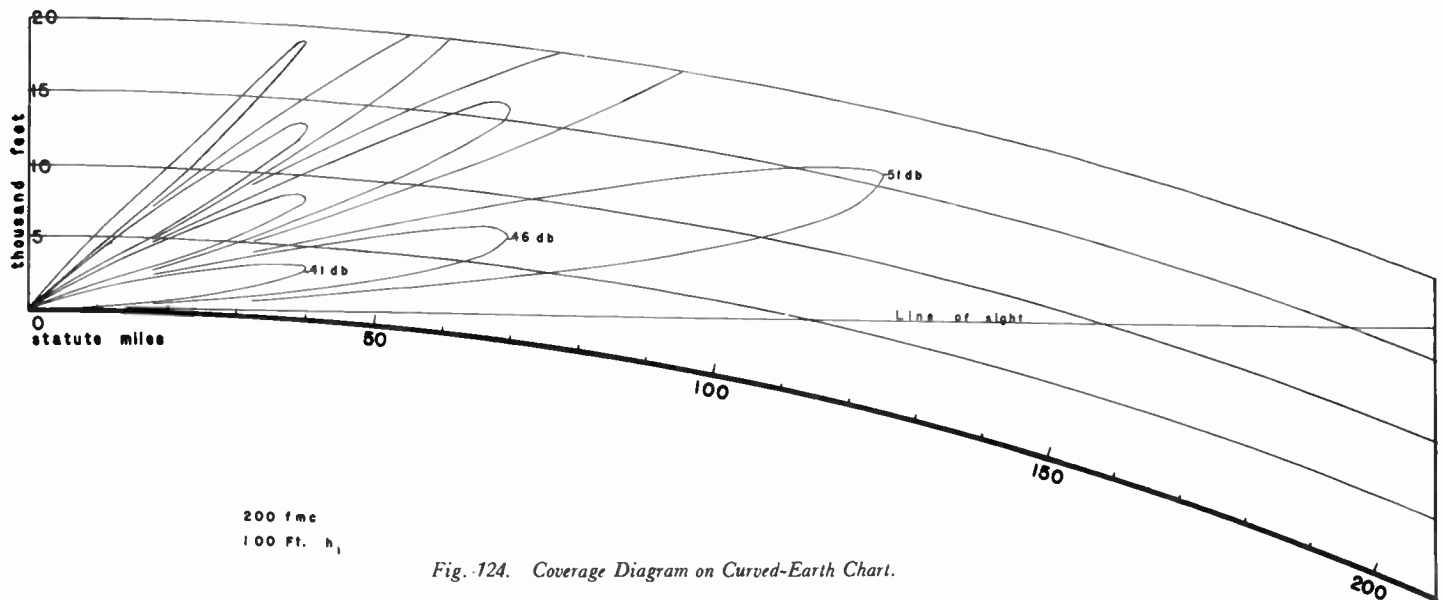


Fig. 124. Coverage Diagram on Curved-Earth Chart.

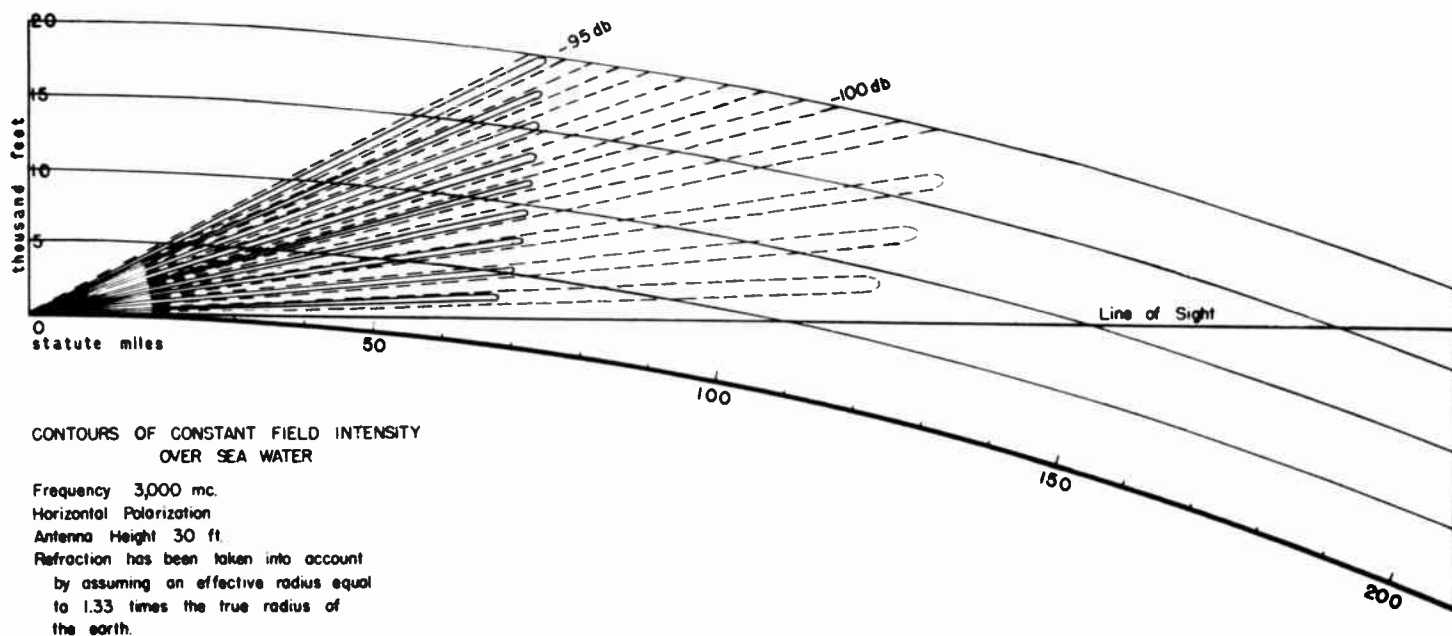


Fig. 125. Coverage Diagram on Curved-Earth Chart.

Courtesy M.I.T. Radiation Laboratory

sketch in the lobe pattern on any coverage diagram.

When B is 4 or greater, the column marked α is no longer necessary. One can then compute S directly from the nomogram of Fig. 141. For $b = \frac{1}{2}, \frac{1}{6}, \frac{1}{3}, \frac{1}{2}, \frac{2}{3}, \frac{5}{6}$, or $1\frac{1}{2}$ —that is, for any value of b other than zero, it is not necessary to know the value of B as long as it exceeds 4, and the calculation may be omitted. For $b = 0$, large values of B cause the lobe minima to fall very close to the transmitter. It is of no great importance to define the points here with any accuracy, since the theoretical values in this region will seldom conform to those actually measured. Small variations in antenna pattern or ground reflectivity cause marked shifts in the positions of lobe minima.

Having found S , proceed as before to evaluate C , H , and h_2 , this time from the nomograms of Figs. 142, 138, 139, and 140. As B increases, it will generally appear that H approaches h_2 , unless the antenna height h_1 is very great. Alternatively, when B is greater than 4, we may calculate C , H , and h_2 from the equations:

$$C = \frac{2.463 \times 10^{3k}}{h_1 f_{\text{megacycles}}} \left(1 - \frac{1}{B^2}\right), \quad (9)$$

$$H = h_2 + h_1/B^2. \quad (10)$$

The foregoing method does not include a nomogram for the determination of α when $b = 0$. Studies have shown that the most practical procedure for evaluating α in this case is by averaging the values previously derived for $b = \frac{1}{2}, 1\frac{1}{2}$. Once α is derived by this method, proceed as before to obtain S from the nomogram of Fig. 141, and continue to derive C , H , and h_2

in turn.

The results are amply accurate—indeed, far more accurate than they will be fulfilled in nature, where minor variations will cause appreciable differences from the theoretical curve, especially at the minima, as previously mentioned.

There will be some cases, usually involving large values of the product $h_1 f_{\text{megacycles}}$, where B will still be small even for $k = 27$. When this condition exists, the lobes tend to be so closely spaced that the individual maxima are difficult to define and even more difficult to draw on a coverage chart. For such conditions, an alternative procedure is recommended. One then records only the B 's for the b values of $\frac{1}{2}$. Thus, for a given decibel value, one determines merely the positions of maxima, plus the lower edge of the lowest lobe. Small variations in reflection coefficients may cause the power density to approach its free-space value. Ground irregularities have a similar effect.

Work sheets for six typical operational cases are given in Figs. 116 to 121. The corresponding coverage diagrams are shown in Figs. 110 to 115, respectively.

It should be emphasized that the lobes here drawn depend on the assumption that there is just as much energy directed downward as there is upward. This condition is fulfilled for longer wave lengths, for which the antennas cannot be made too directive in the vertical plane. But, when SHF is used with a reflector or dish that is tilted upward, the ground-reflected ray may be very much weakened or completely disappear. When this condition obtains, the tips of the lobes move inward

WORK SHEET FOR COVERAGE DIAGRAM CALCULATIONS

db =
(M.I.T.)

f_{mc} =
 h_1 = ft.

Y =
 h_1/f_{mc} =

K	B	n	b	α	S	C	H	h_2
1	>4	1	$\frac{1}{6}$					
2		1	$\frac{1}{8}$					
3		1	$\frac{1}{2}$					
4		1	$\frac{2}{3}$					
5		1	$\frac{5}{6}$					
5.5		1	$1\frac{1}{2}$					
6		2	0					
6.5		2	$\frac{1}{2}$					
7		2	$\frac{1}{6}$					
8		2	$\frac{1}{3}$					
9		2	$\frac{1}{2}$					
10		2	$\frac{2}{3}$					
11		2	$\frac{5}{6}$					
11.5		2	$1\frac{1}{2}$					
12		3	0					
12.5		3	$\frac{1}{2}$					
13		3	$\frac{1}{6}$					
14		3	$\frac{1}{3}$					
15		3	$\frac{1}{2}$					
16		3	$\frac{2}{3}$					
17		3	$\frac{5}{6}$					
17.5		3	$1\frac{1}{2}$					
18		3	0					
18.5		4	$\frac{1}{2}$					
19		4	$\frac{1}{6}$					
20		4	$\frac{1}{3}$					
21		4	$\frac{1}{2}$					
22		4	$\frac{2}{3}$					
23		4	$\frac{5}{6}$					
23.5		4	$1\frac{1}{2}$					
24		5	0					
24.5		5	$\frac{1}{2}$					
25		5	$\frac{1}{6}$					
26		5	$\frac{1}{3}$					
27		5	$\frac{1}{2}$					

Fig. 126.

and the nulls or pockets move out toward the limit of the free-space field.

Rough terrain or land covered with heavy vegetation may act as a very poor reflector. Over such regions, the pattern tends to revert to free-space conditions, but with occasional, almost unpredictable, vagaries. Indeed, VHF-SHF installations near the ground in thickly wooded territory will suffer from 10 to 20 or even more decibel loss. The attenuation will depend markedly upon the direction of polarization of the waves.

VHF-SHF equipment, used in large centers of population, suffer from additional complications of dead spots or multiple reflections. The latter, for television equipment, results in ghost patterns, doubled images, and so forth. This type of interference, however troublesome it may be, is at least relatively constant. The most effective method for overcoming it is by effective design and location of receiver antennas.

In radar operation, the propagation factor pictured in the coverage diagrams comes in twice—once for the direct transmission and once for the returning echo. If P_{db} is the effective power of the transmitter in decibels above 1 watt, if G is the antenna gain in decibels, if A is the effective reflecting area of the target in square meters, and if R_{db} is the limit of sensitivity of the combination of the receiver and receiving antenna area, computed without gain, we have

$$P(db) + 2G + 10 \log A + 2(db) = R_{db} \quad (11)$$

for the limiting signal for the given target. (db) is the

propagation factor from the coverage diagrams, according to the location of the target. Its value must always be negative!

Now, if we know the limiting power R_{db} of our set (which depends upon a number of factors, such as receiver noise, frequency, pulsing rate, and band width) and the additional quantities P_{db} , G , and A , we can calculate (db) , the limiting decibel contour on the coverage diagram. This quantity determines the ranges of the target for different heights. If the free-space value is used, the range in thousands of yards is immediately calculable.

The use of Equation (11) presupposes that we know something about the target areas. These must be determined observationally for the type of target considered. In practice, A will depend upon the aspect as well as upon the nature of the target. A plane observed head-on will possess an effective cross section different from one flying broadside to the set. Also, it should be mentioned that A is the electrical, not the visual, area. A will generally depend on the frequency.

For surface targets, the fact that the field intensity practically vanishes at the ground introduces additional complexities. Since the rate of increase depends markedly upon the frequency, we may integrate the field intensity from the surface to some height h_2 , and introduce a fictitious cross section to represent the phenomenon. The details, however, are too specialized to be given here.

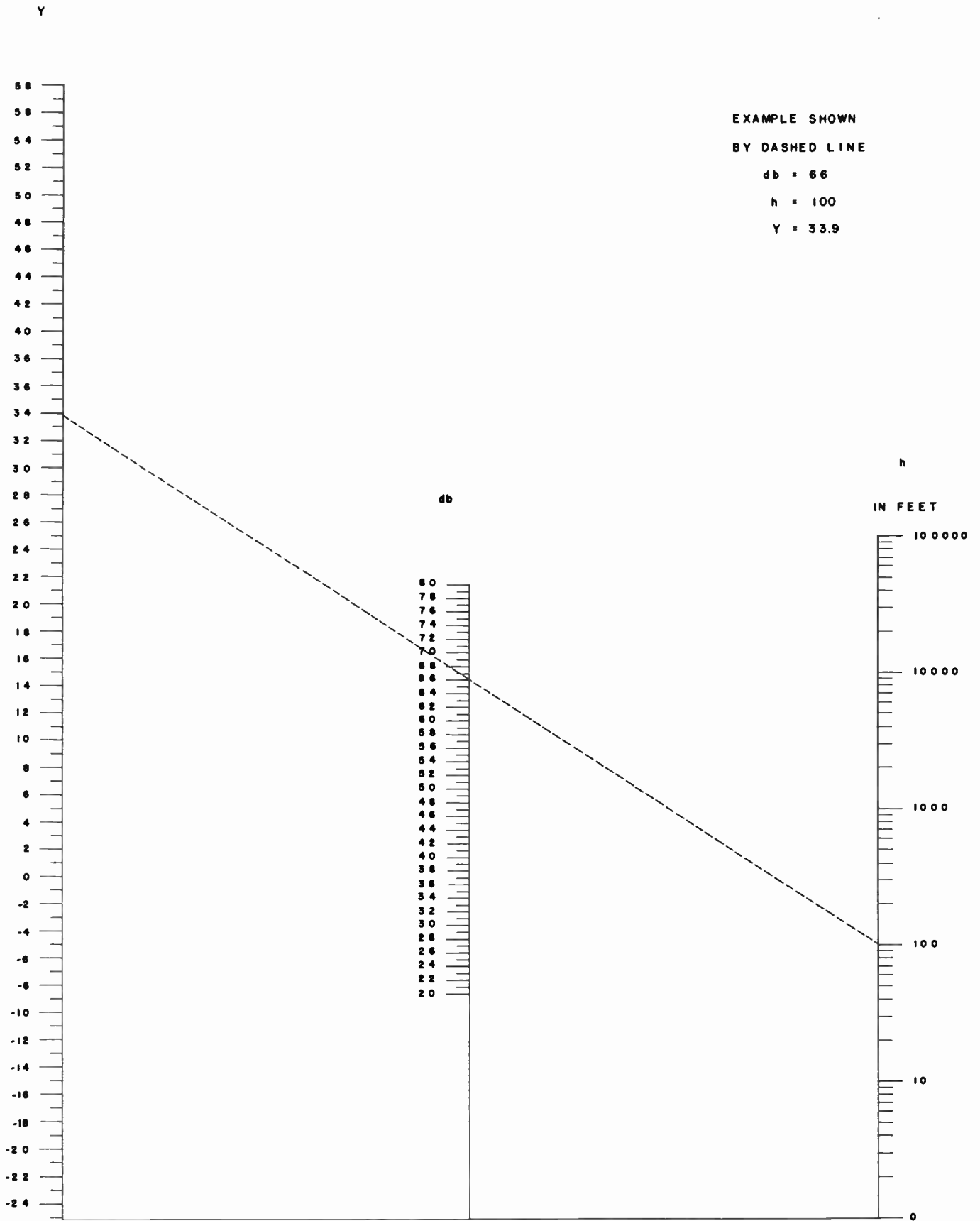


Fig. 127. Nomogram for Computing Y.

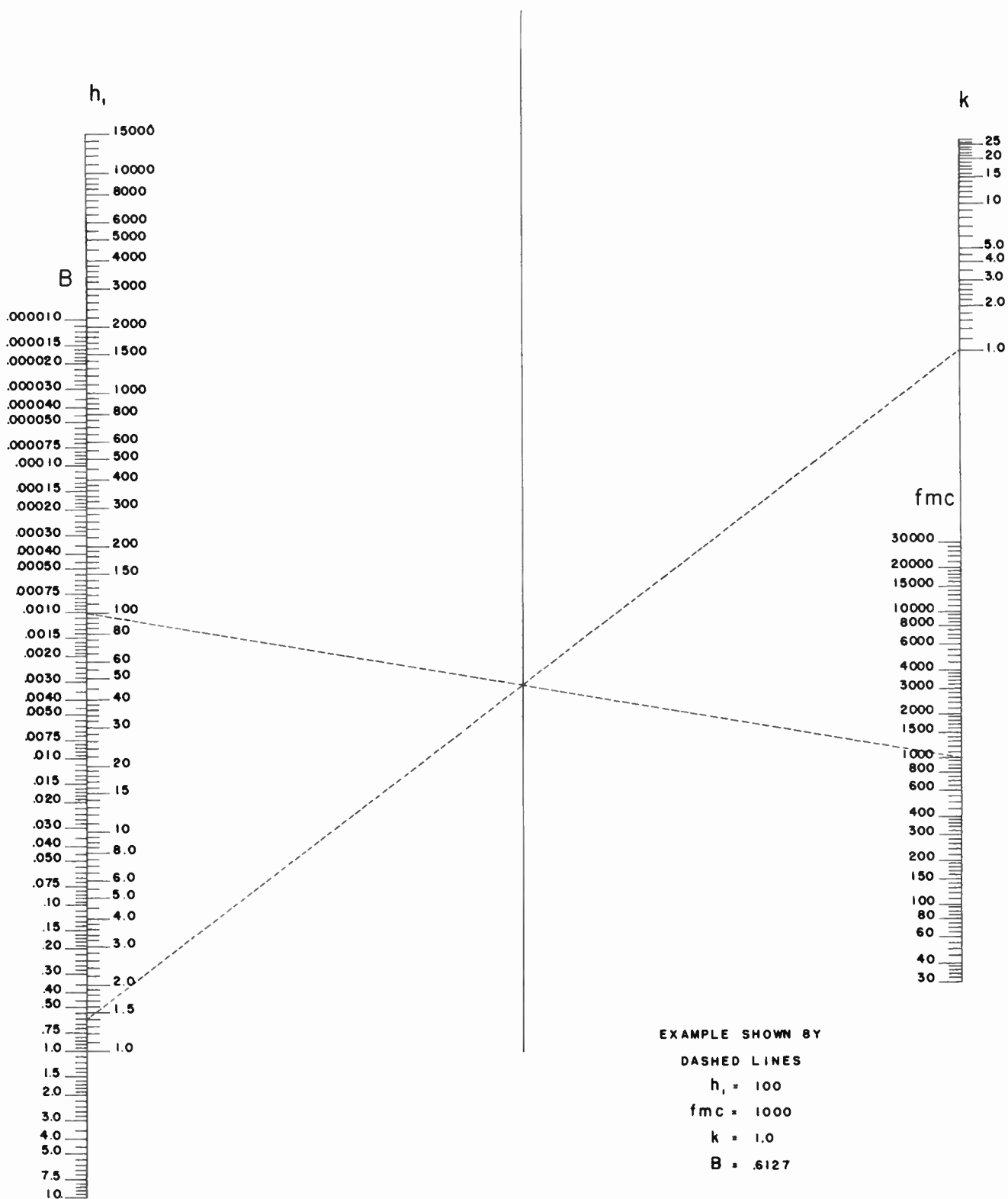


Fig. 128. Nomogram for Computing B.

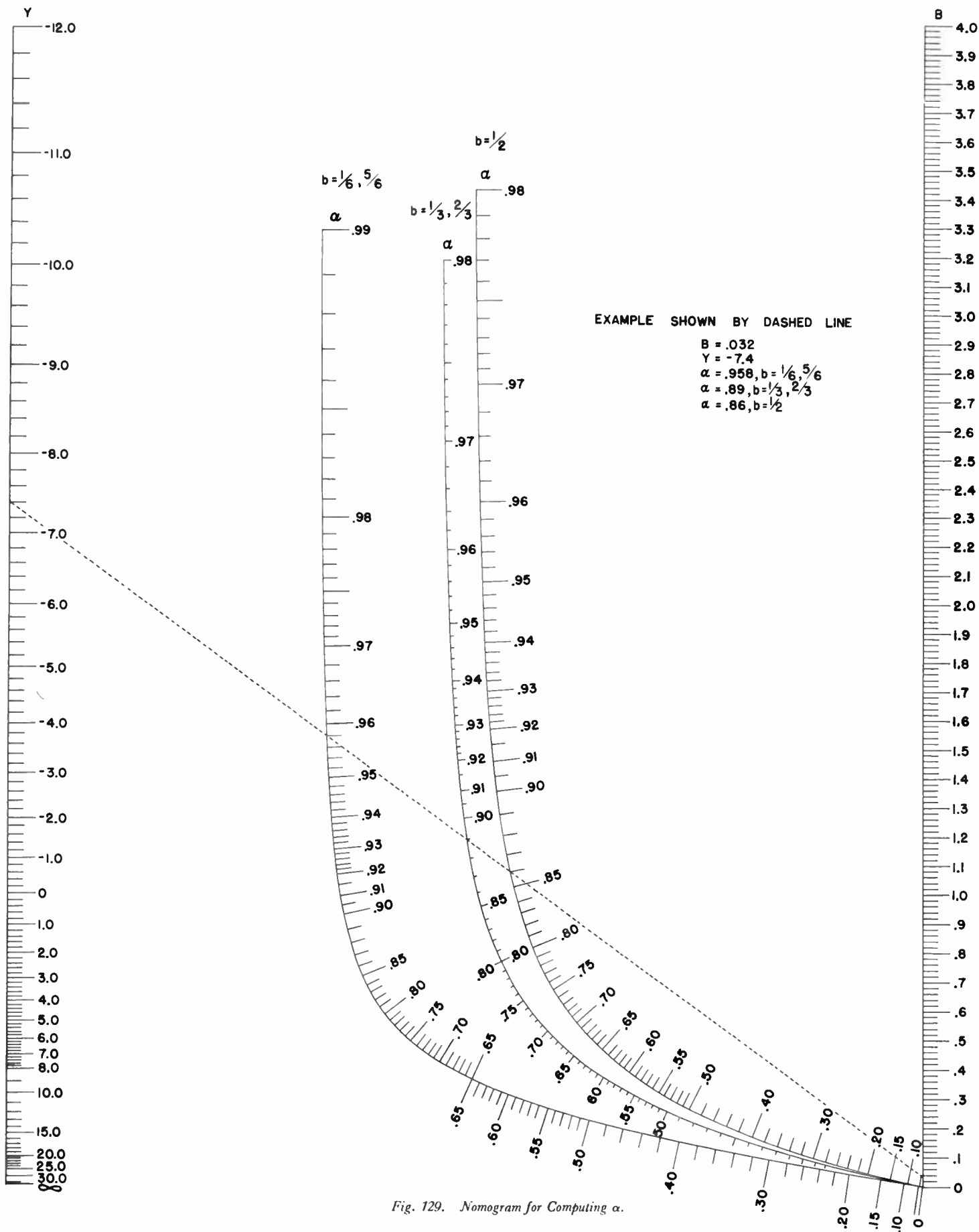


Fig. 129. Nomogram for Computing α .

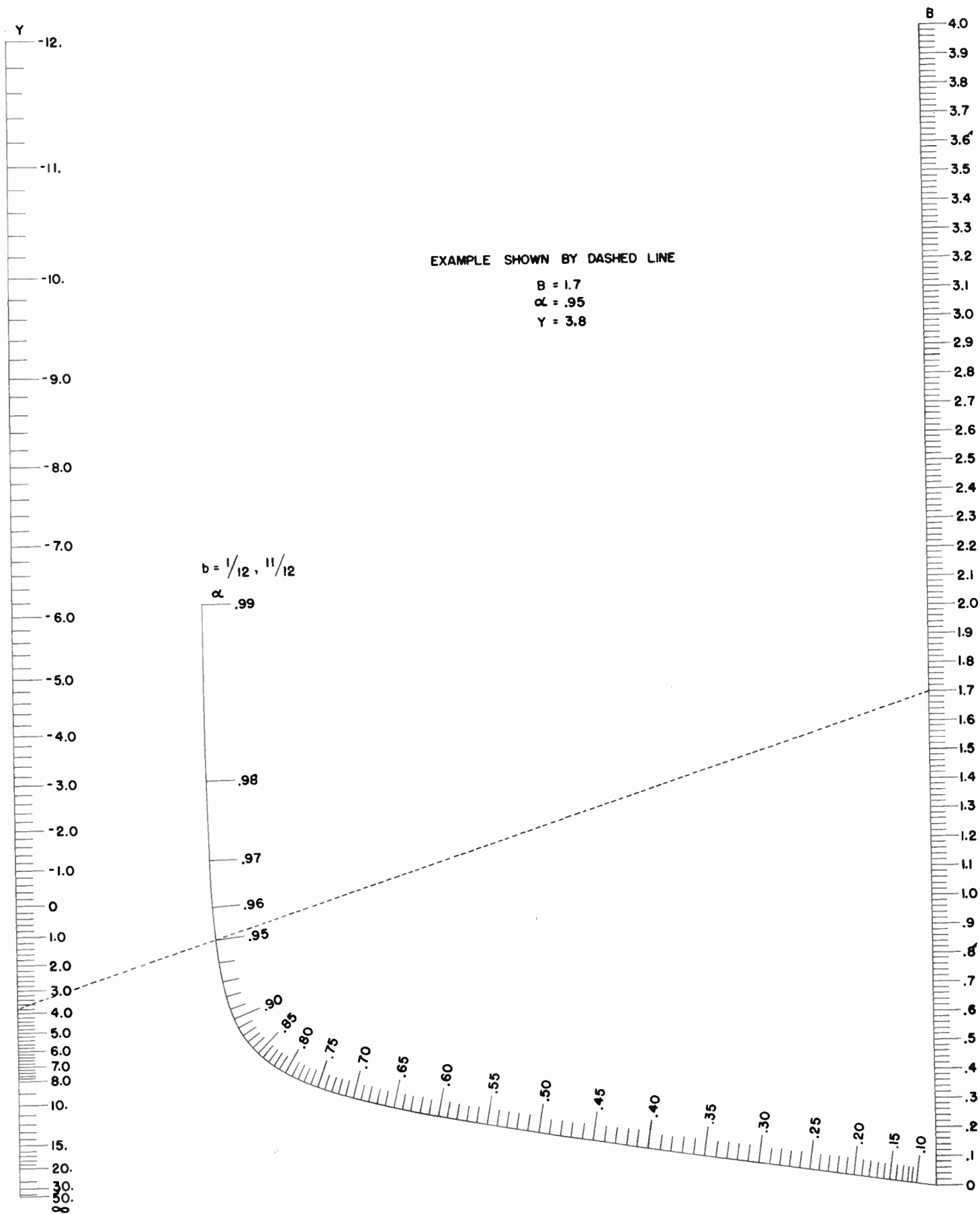


Fig. 130. Nomogram for Computing α .

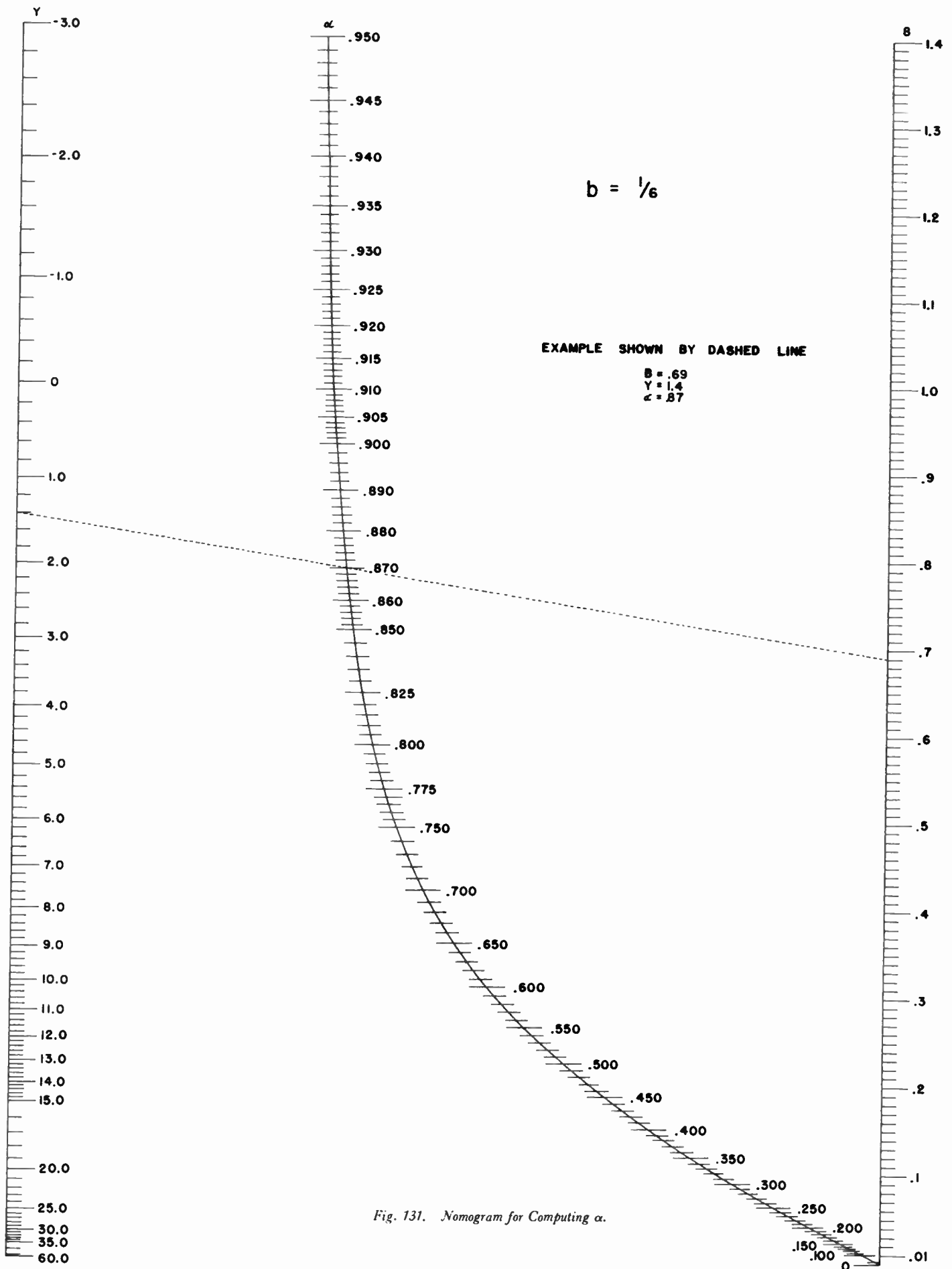


Fig. 131. Nomogram for Computing α .

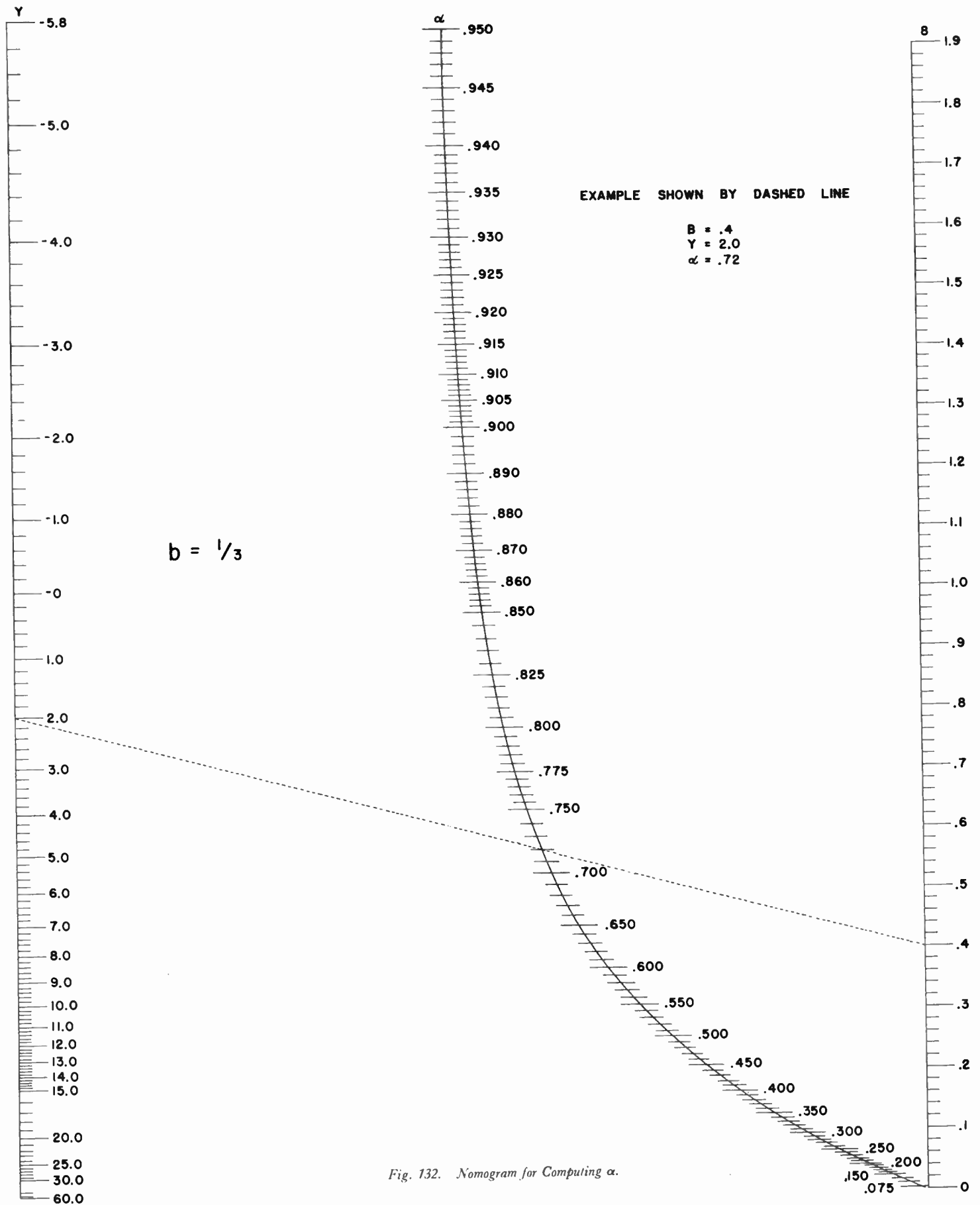


Fig. 132. Nomogram for Computing α .

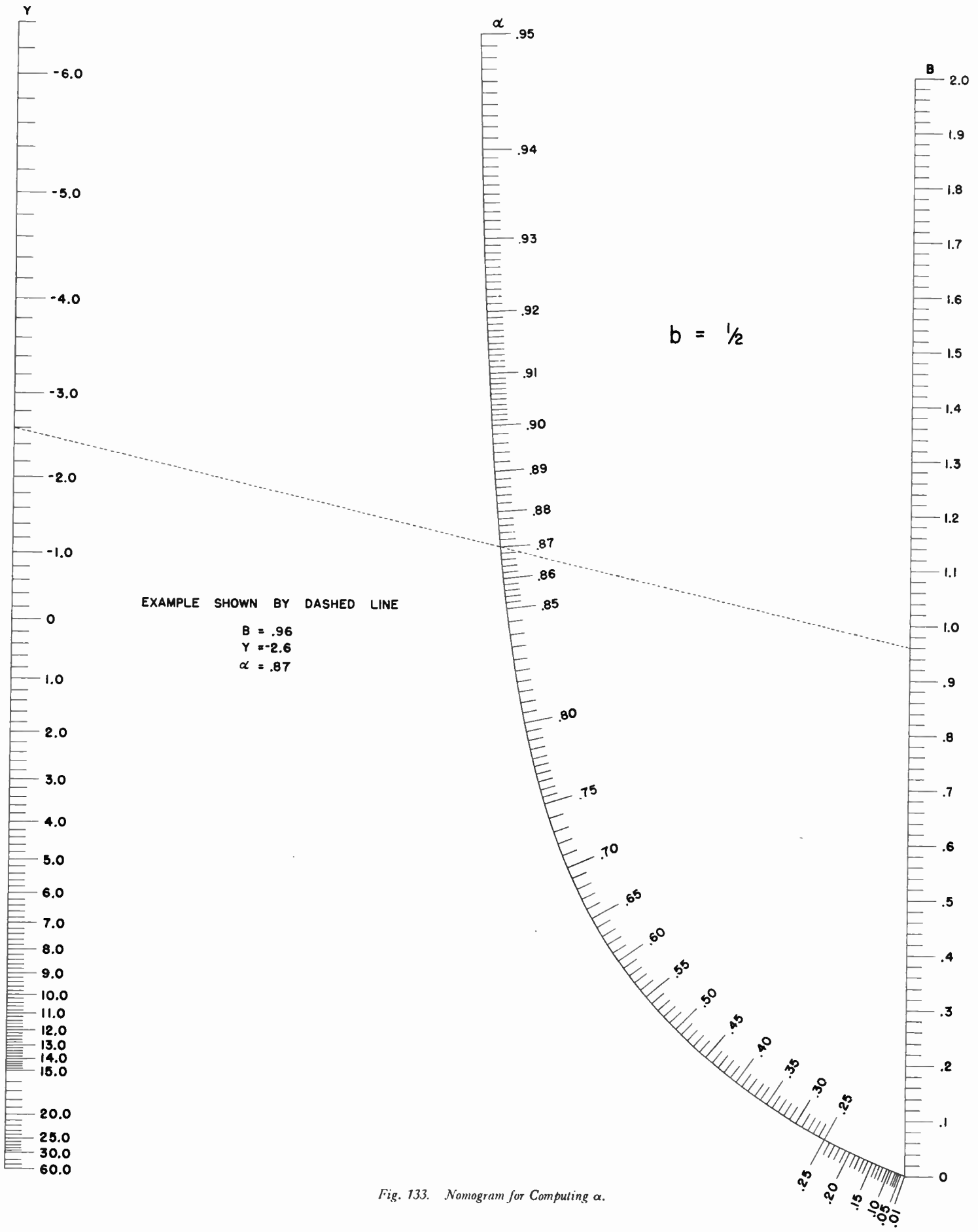


Fig. 133. Nomogram for Computing α .

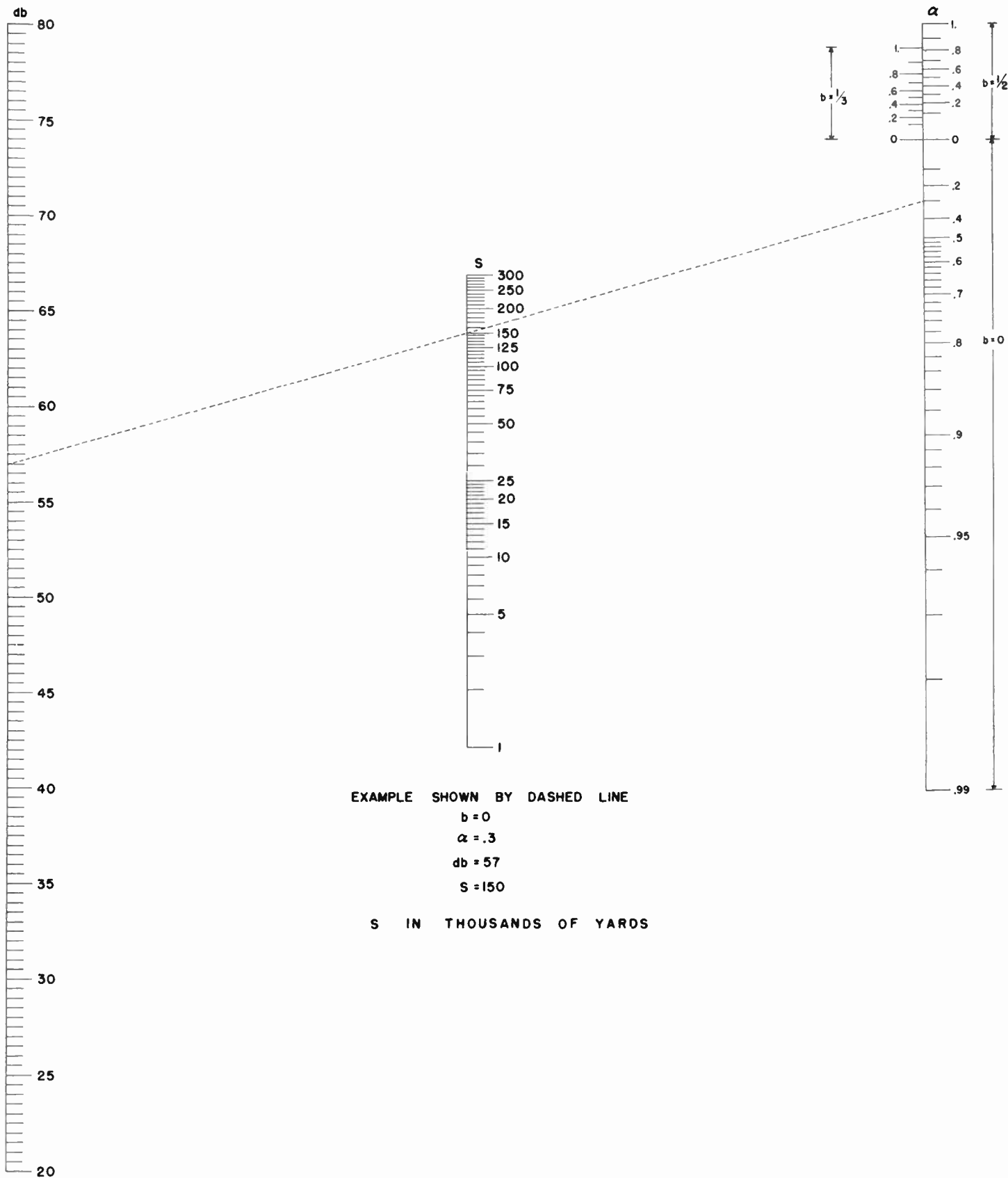


Fig. 134. Nomogram for Computing S.

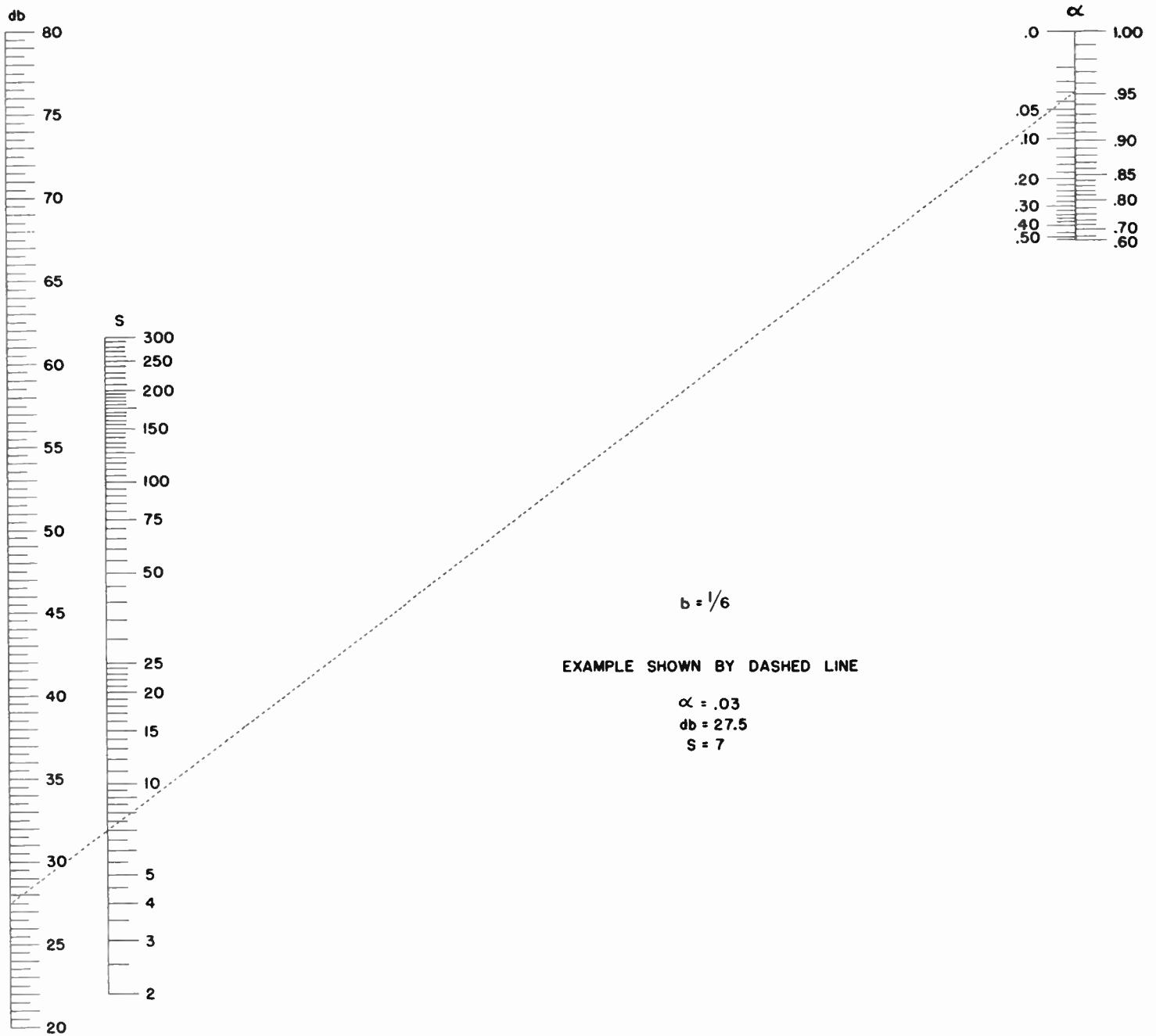


Fig. 135. Nomogram for Computing S.

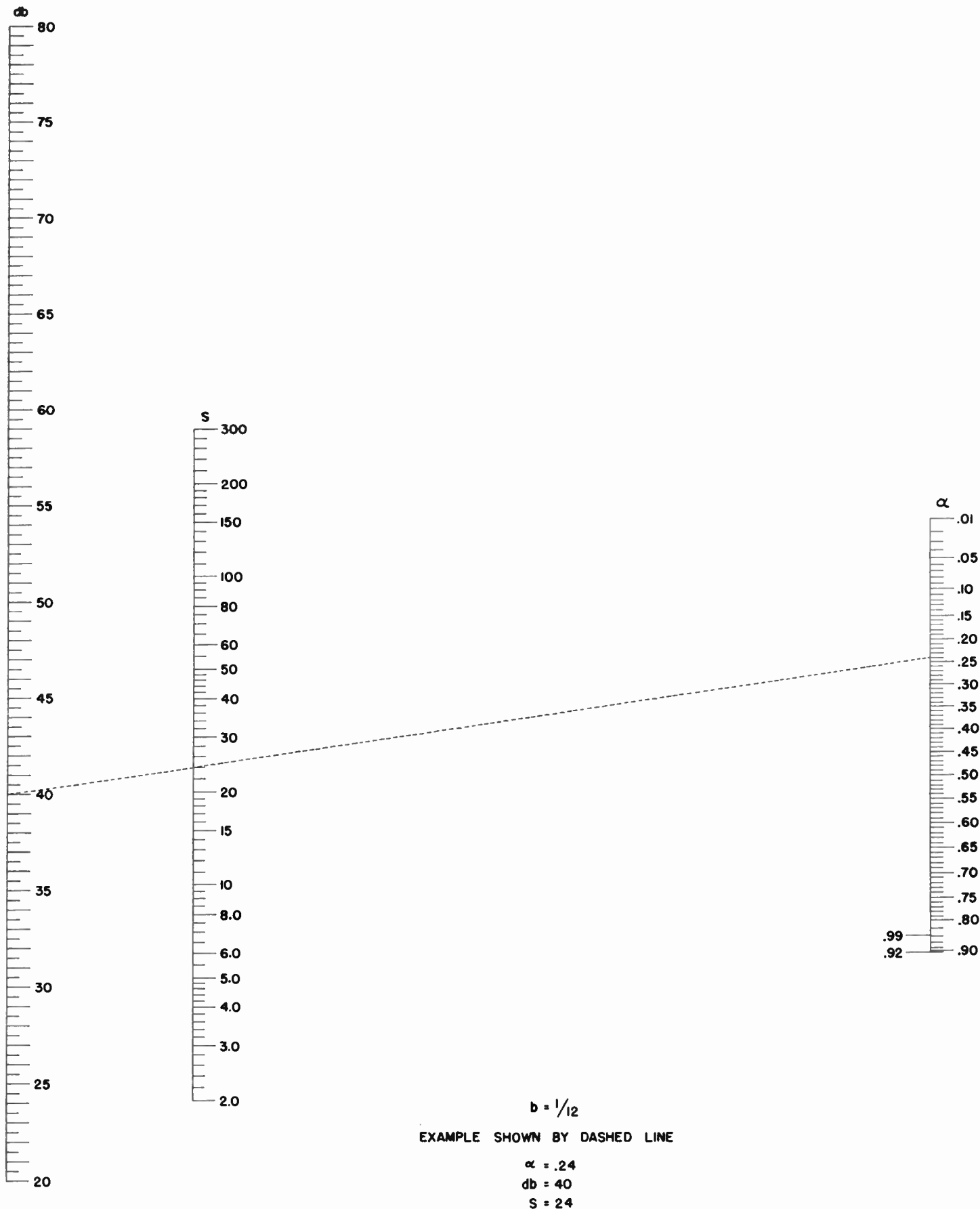


Fig. 136. Nomogram for Computing S.

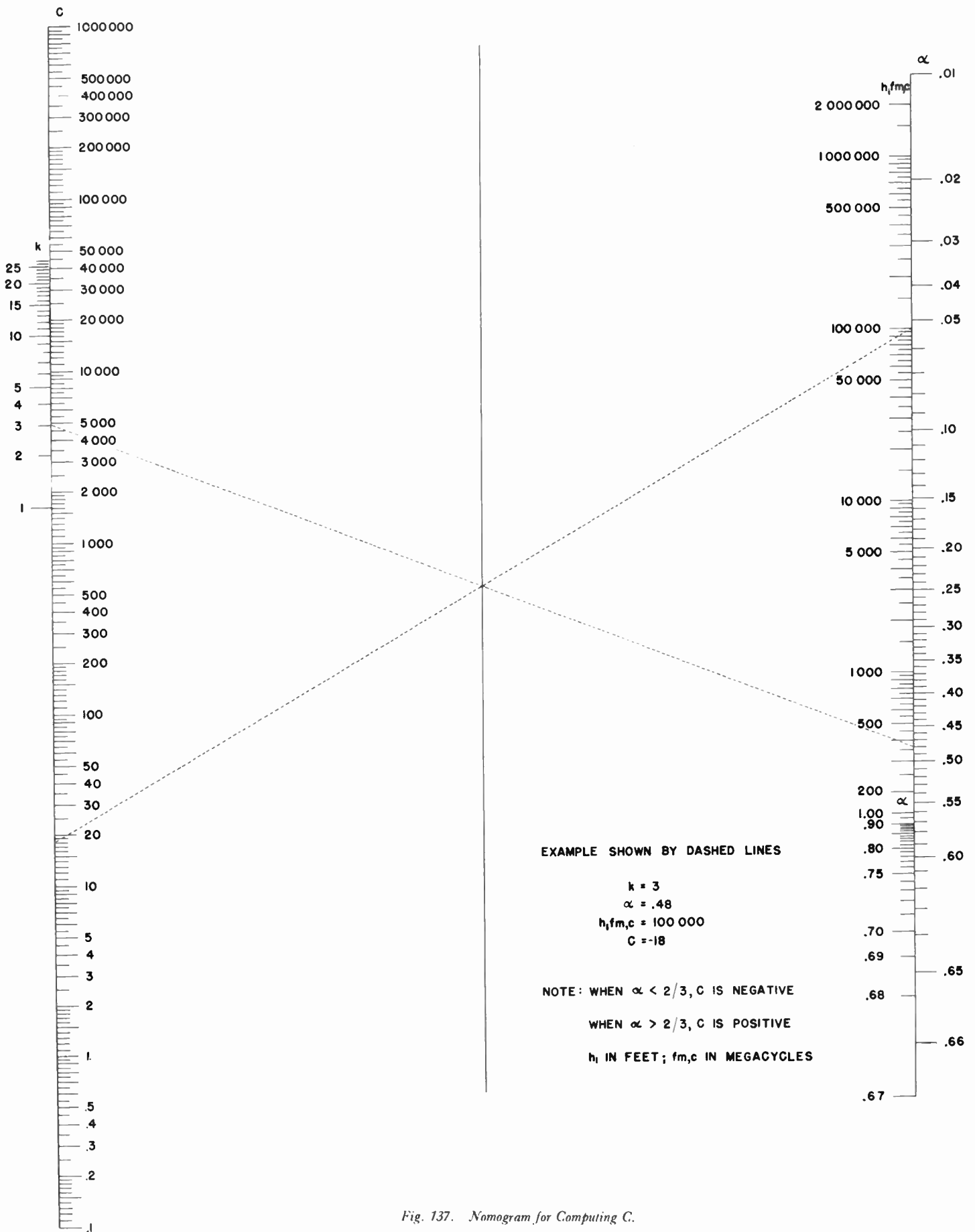


Fig. 137. Nomogram for Computing C.

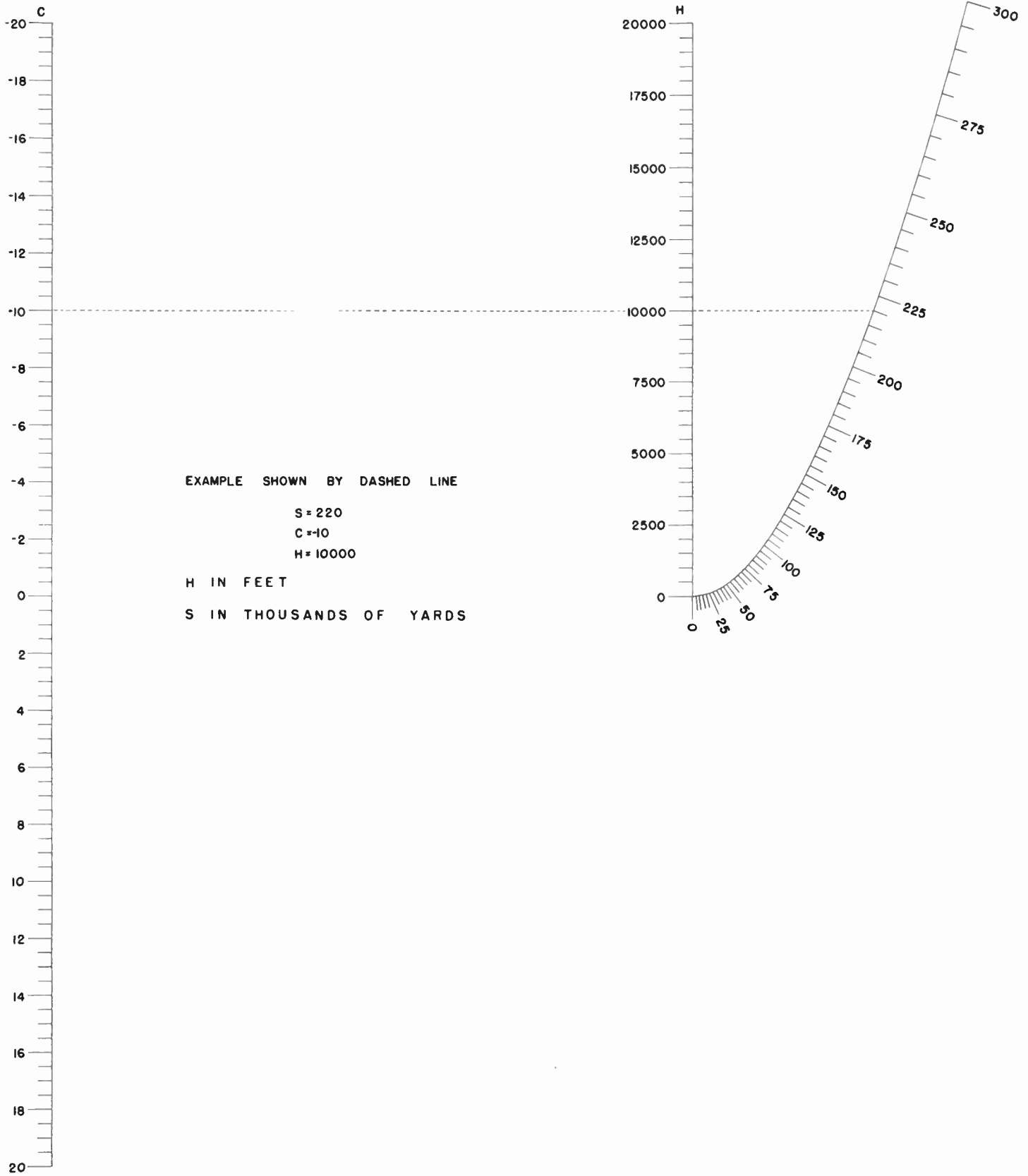


Fig. 138. Nomogram for Computing H.

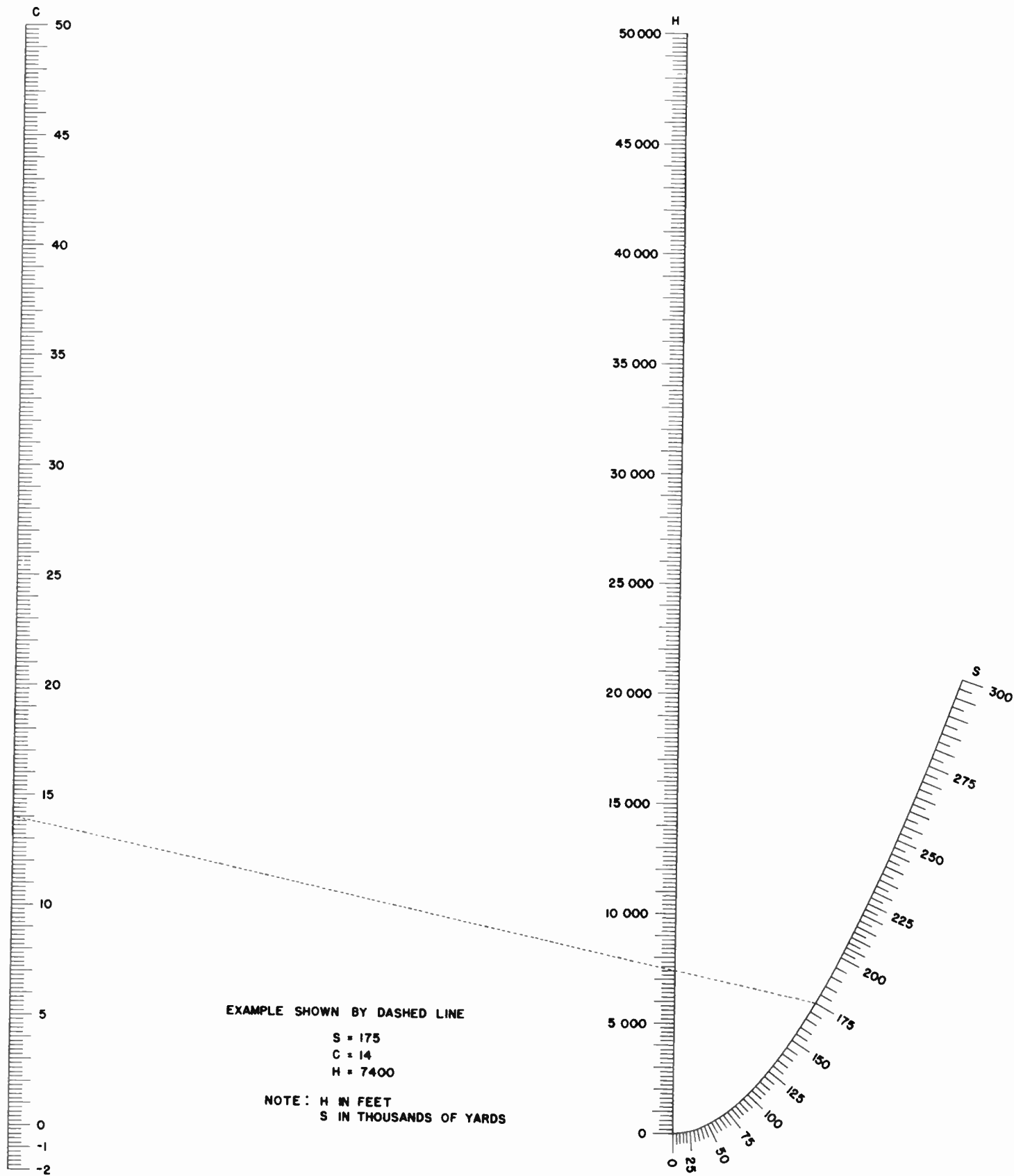


Fig. 139. Nomogram for Computing H.

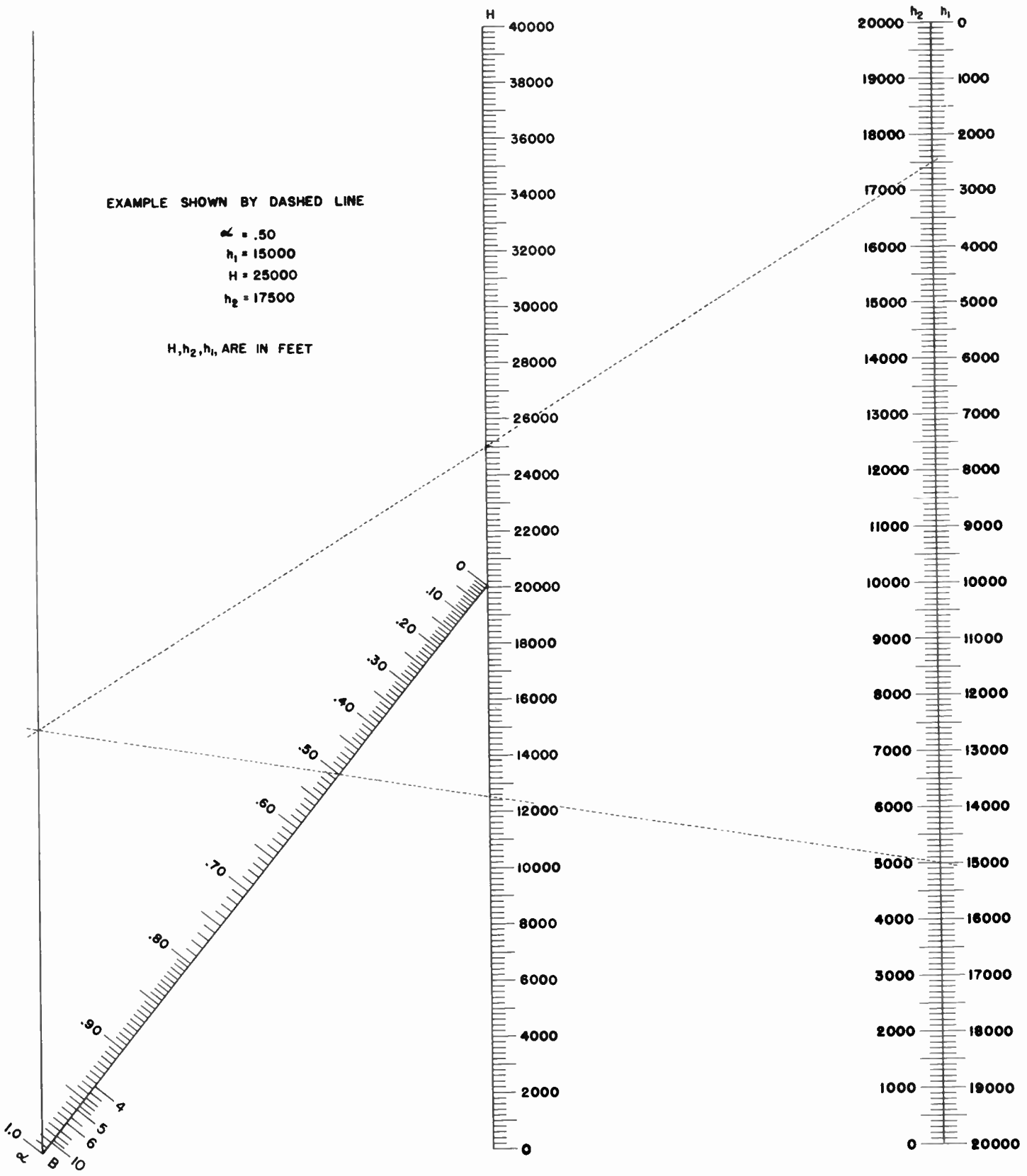


Fig. 140. Nomogram for Computing h_2 .

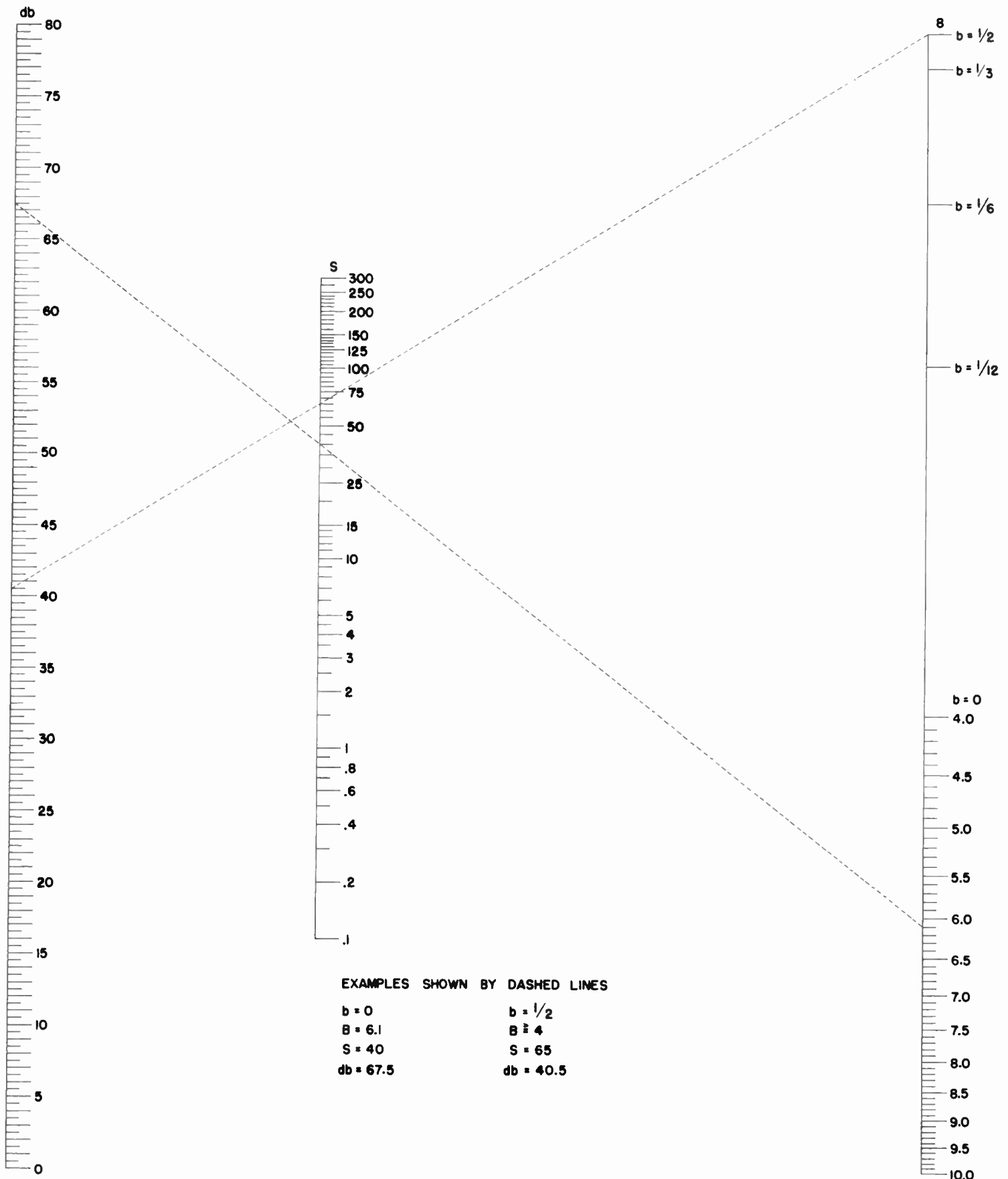


Fig. 141. Nomogram for Computing S when $B \geq 4$.

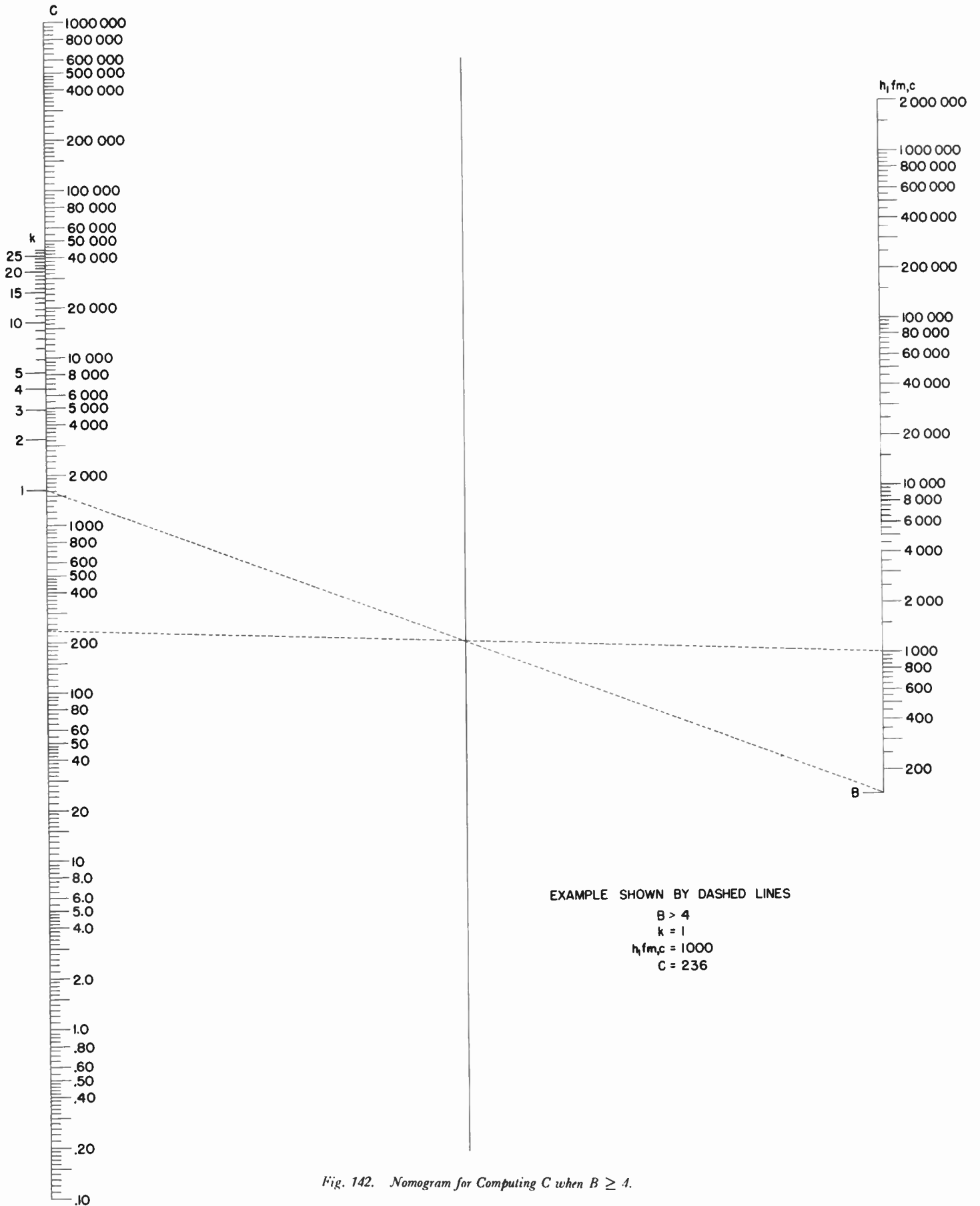


Fig. 142. Nomogram for Computing C when $B \geq 1$.

• CHAPTER FIFTEEN •

THE FIELD IN THE SHADOW ZONE UNDER STANDARD CONDITIONS

WITHIN THE LINE OF SIGHT, THE METHOD JUST DESCRIBED is a quick and satisfactory means of calculating the field of a radio transmitter. When the receiver lies in the shadow zone below the horizon (right-hand shaded area of Fig. 108), this simple theory breaks down, and

one must employ diffraction theory. The radio shadow cast by the edge of the earth is not perfectly sharp. Longer waves penetrate more deeply into the shadow zone than do the shorter ones. The effect is identical with that discussed for ground waves in Chapter 11.

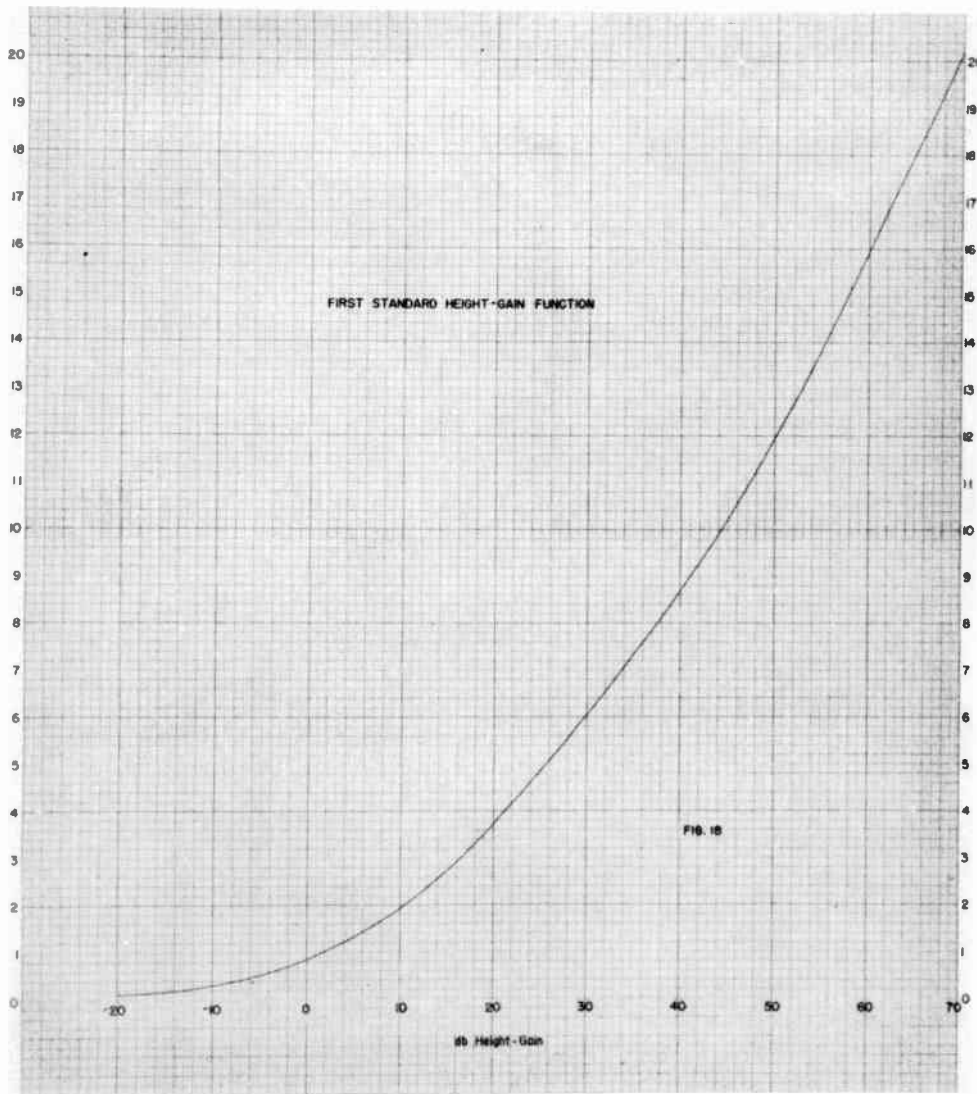


Fig. 143. Height-Gain Nomogram.

We assume, as before, a 1-watt isotropic source that produces a power density db at the receiver in decibels above 1 microwatt per square meter. Then,

$$db = (-22.41 + 1\frac{1}{3} \log_{10} f_{\text{megacycles}}) - (10 \log_{10} S) \\ - (8.448 \times 10^{-2} f_{\text{megacycles}}^{1/3} S) + (\text{transmitter height gain}) \\ + (\text{receiver height gain}), \quad (1)$$

where $(-22.41 + 1\frac{1}{3} \log_{10} f_{\text{megacycles}}) =$ frequency factor;
 $(10 \log_{10} S) =$ cylindrical spreading;
 $(8.448 \times 10^{-2} f_{\text{megacycles}}^{1/3} S) =$ horizontal attenuation;
 $f_{\text{megacycles}} =$ the frequency, in megacycles; and
 $S =$ the horizontal distance between the transmitter and receiver, in thousands of yards.

The height-gain factor is plotted in Fig. 143 as a function of the dimensionless height parameter ζ , where

$$\zeta = 1.433 \times 10^{-4} f_{\text{megacycles}}^{1/3} h. \quad (2)$$

The equation may be employed directly to compute the field at a given point—that is, given $f_{\text{megacycles}}$, S , h_1 , and h_2 , to find the decibel value. It may be employed inversely to locate points on a given decibel contour—that is, given $f_{\text{megacycles}}$, S , h_1 , and decibel value, to find h_2 . In either case, compute the first two terms on the right directly. Compute the attenuation term directly or read it from the nomogram of Fig. 144. Compute ζ_1 directly or from Fig. 145. Enter Fig. 143 with this value of ζ to obtain the transmitter height gain. If h_2 is given, compute ζ_2 and the receiver height gain

similarly, and thus calculate the decibel value. If the decibel value is given, solve for the receiver height gain. Then use Fig. 143 to determine ζ_2 , whence h_2 can be computed directly or from the nomogram of Fig. 145.

EXAMPLE:

GIVEN: $f_{\text{megacycles}} = 3000$, $S = 32$ miles = 56.32 thousand yards, $h_1 = 10$ feet, and $h_2 = 60$ feet.

SOLUTION:

$$1\frac{1}{3} \log_{10} f_{\text{megacycles}} = 11.59, \quad 10 \log S = 15.47, \quad \text{horizontal} \\ \text{attenuation} = 42.9,$$

$$\zeta_1 = 0.30, \quad \text{transmitter height gain} = -10$$

$$\zeta_2 = 1.79, \quad \text{receiver height gain} = 9$$

Then decibel value = -70.2

None of the formulas given is satisfactory for determining the field at points near the tangent ray that marks the shadow boundary. To estimate the field at such a point, first compute its value at several points well above it in the line-of-sight region by the methods described in the preceding chapter. Then compute the field at several points well below it in the *shadow zone* by the above diffraction formula. Obtain, finally, the field at the desired point by graphical interpolation. The ground-wave calculations, as given in Chapter 11, go over into the formulas of the present chapter in the realm of high frequencies.

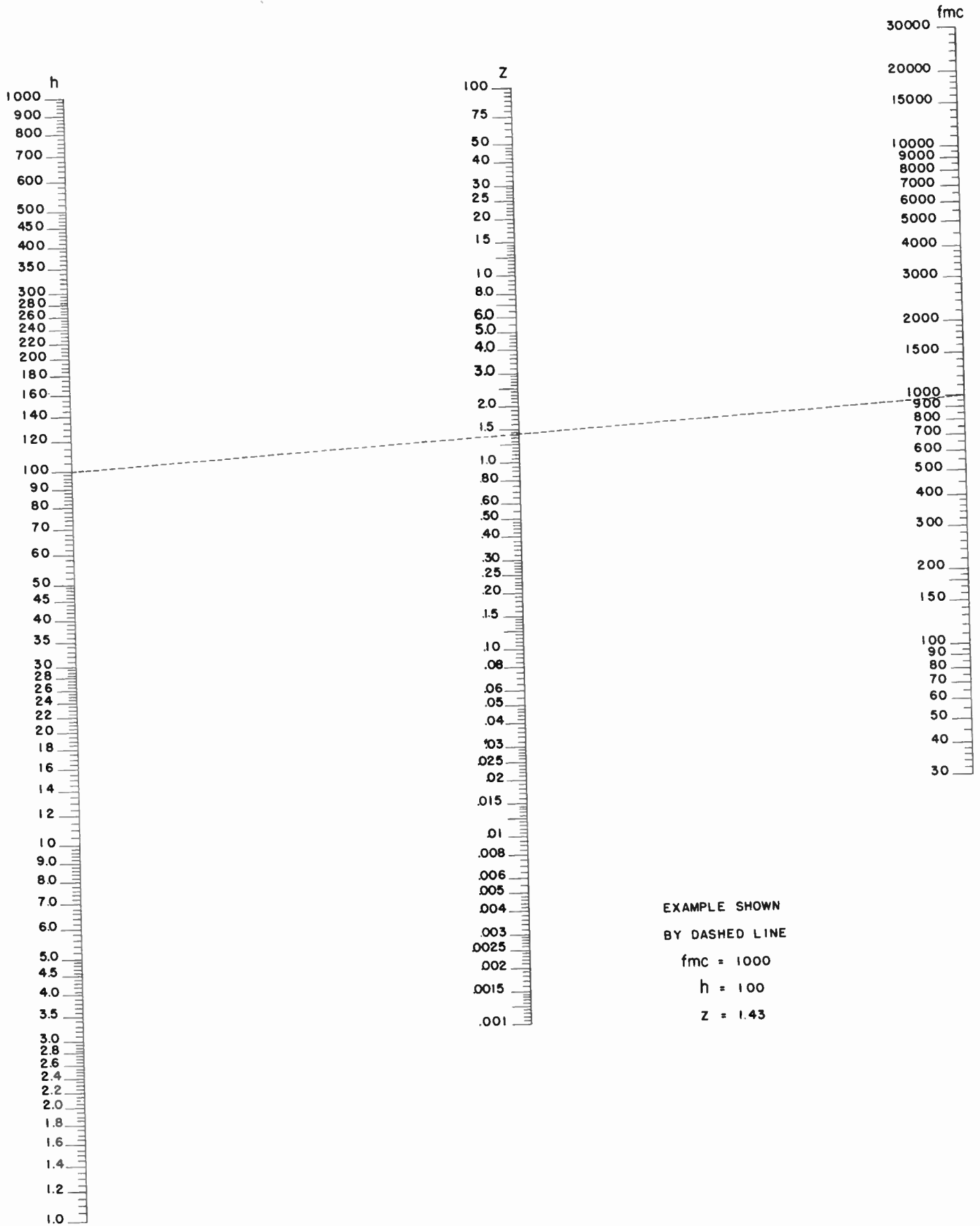


Fig. 145. Nomogram for Calculating Z.

• CHAPTER SIXTEEN •

HOW ATMOSPHERIC CONDITIONS CAUSE LARGE VARIATIONS FROM STANDARD-SET PERFORMANCE

IN THE LAST THREE CHAPTERS, WE HAVE DISCUSSED, primarily, communication under standard atmospheric conditions. Now we must study nonstandard situations, since they occur very often. The full benefits of various communication and radar equipments have not been consistently realized because we have failed to understand completely certain limitations or, rather, peculiarities of high-frequency radio communication, imposed by the atmosphere through which the waves must travel from transmitter to receiver.

eyes. The shore should be well out of sight around the curvature of the earth. And yet, there it is, looming clearly above the horizon. Hastily he checks his charts and finds the position correct. What can the effect be? Oh, yes! Nothing but a mirage! Light rays from the distant coast have been bent around the earth's curvature. Peculiar atmospheric conditions are responsible.

Light waves are bent when they pass from a medium of one density into another. Fig. 146 pictures an example of this familiar effect. Note how the girl's leg

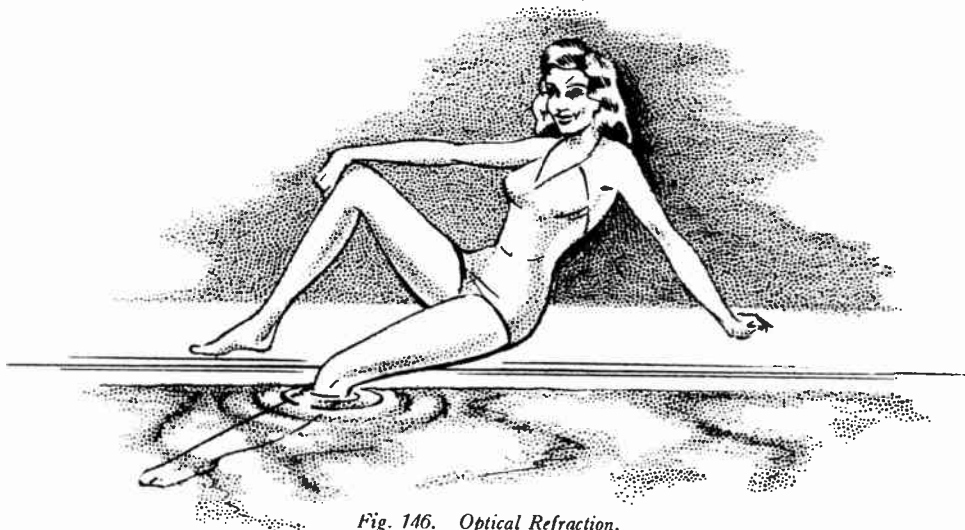


Fig. 146. Optical Refraction.

The ranges and heights to which the signals are effective often exhibit variations over which the operator has no control. Thus, even though he may be confident that his set is functioning perfectly, he may find, to his amazement, that the ranges are abnormally decreased or increased. If the operator fails to understand the causes for these variations and persists in placing blind faith in his equipment, a perilous situation may arise. A pilot, for example, may not be able to find the near-by airfield, or, in the other extreme he may believe he is almost there when actually he is many miles away.

The variability of radio range is an atmospheric phenomenon similar in some respects to an optical mirage. The ship's captain who clearly sees a coast that he knows to be 100 miles away can scarcely believe his

appears to be bent at the water surface. Similarly, the atmosphere is not uniform and may vary so much in density and composition that light waves will travel in curved rather than in straight lines.

Radio waves, like light waves, are also subject to mirage. As we have shown in preceding chapters, waves corresponding to the higher radio frequencies usually penetrate the electric layers of the ionosphere. Hence, an operator of radio sets employing frequencies greater than 30 megacycles often assumes that the energy sent out from the antenna never returns earthward and that his transmission range is confined to the limit of his horizon.

These assumptions, however, may be utterly wrong. The atmosphere may, in effect, provide the operator

with a kind of periscope through which he can see far beyond the horizon. The lower levels of the earth's atmosphere, extending not higher than a few thousand feet above the surface, may, on occasion, bend the high-frequency waves far around the earth's curvature. Many radar operators have observed variations in range and fluctuations in the extent of "ground or sea return" that result from the changes in the lower levels of the atmosphere. At times, they have blamed this inconsistent behavior on the performance of the set itself. Like the ship's captain, they make various checks, but they fail to recognize the presence of a radar mirage because they have never heard of the phenomenon before.

Reports from the field indicate that radio mirages often accompany optical mirages. Both result from the bending of rays in the atmospheric medium away from the regions of low density into the regions of greater density, the amount of this bending being expressed by variations of the refractive index, as will be discussed later. Both types of mirages are not always observed in conjunction, however, because the refractive index for radar wave lengths differs from that for optical wave lengths, and also because external factors, such as haze, materially reduce the possibility of observing optical mirages.

The general problem of radio propagation in the lower atmosphere is quite complex. In order to deal with variation in atmospheric conditions, a radio or radar operator must become "weather conscious." The methods described below will help him to understand

how he can use his knowledge of the weather to evaluate his radio coverage more effectively.

Radars display the variations in coverage that arise from atmospheric conditions more graphically than communication equipment because of visual presentation (PPI scope). For this reason, we shall give special attention to radar problems. But the effects of propagation here discussed apply equally to communication systems, racons, and other services operating on high-bracket frequencies. Indeed the effects may be exaggerated for communication problems, because of the extra sensitivity resulting from one-way transmissions.

Radars send out pulses at regular intervals. These radio waves travel at the velocity of light, the enormous speed of 186,000 statute miles per second. Hence, if the pulsing rate is 1000 per second, for example, the successive pulses are spaced 186 miles or 327,000 yards apart, as shown in Fig. 147. Each pulse dwindles in intensity as it recedes into the distance. Little, if any, energy penetrates into the shadow zone, and a plane in this region will normally not be detected.

Ordinarily, the observer will receive echoes only from the pulse nearest him. The others, more distant, will not send back echoes sufficiently strong to influence the receiver. Among conditions that cause echoes to be received from more distant pulses, the state of the weather is of considerable importance. Under some atmospheric conditions, the waves may be bent downward and follow along or close to the ground. The radio energy may be so highly concentrated in a limited region of space that it appears to be following a duct.

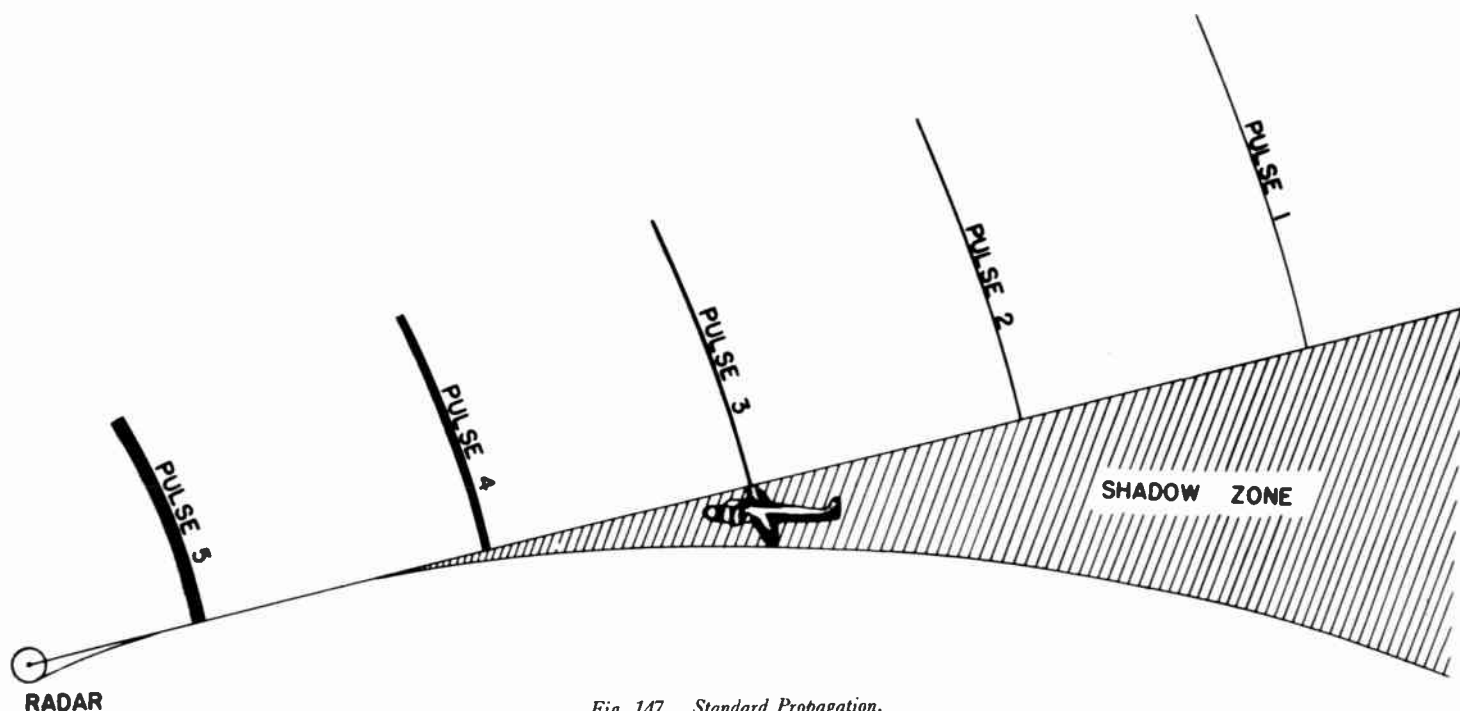


Fig. 147. Standard Propagation.

The phenomenon has been referred to as superrefraction, anomalous propagation, or trapping.

When this condition occurs, the situation is similar to that illustrated in Fig. 148. In this case, suppose that a target plane intercepts pulse number 3. The previous pulse, number 2, will have moved forward except for the small portion forming the echo. The latter will have returned toward the transmitter, and thus will coincide with the position of the outgoing pulse 4. Similarly, the echo from pulse 1 will coincide with the position of pulse 5. Without additional information, the radar operator who measures a returning echo will not be able to tell whether this echo has been reflected from a target at the position actually shown on the diagram or whether the target lies at the nearer position indicated by the pulse with which the actual echo coincides.* Indeed, the possible position may be halfway between the pulses, as shown, because the echo from the plane will reach this point at the same moment that pulse number 4 arrives at the spot. Therefore, the actual uncertainty is half the pulse spacing, or 93 miles in the present example.

It would seem that the operator should be able to distinguish between the pulses by the intensity of the echo. However, when atmospheric conditions lead to the formation of a duct, the concentration of energy is so intense that there is less than normal distinction between the intensity of the echoes from the near and

* It should be noted that, in reality, the radar pulses cannot be so accurately counted. Thus, the numbers 1, 2, 3, and so forth, are chosen merely arbitrarily for illustrative purposes. We must imagine the pulse train as extending on far to the right.

more distant pulses. Thus, in the present example, if his measured range is 70 miles, the actual range may be $70 + 93 = 163$, $70 + 186 = 256$ miles, and so forth. The higher values *may* be more improbable, but the radar evidence alone is insufficient to solve the problem. There are records of radar reception over distances as great as 1,800 miles! In such cases, the presentation on the PPI scope is the superposition of many circular mappings. If an echo shows, the problem is to pick out the particular mapping or sweep that represents the true position of the reflecting object.

The misinterpretation of a signal received under these circumstances, either through ignorance of the presence of a duct or through inability to distinguish between the successive pulses in a duct, may lead to a result such as that shown in Fig. 149, where a ship shells the mirage or "ghost" of a target many times more distant. Such errors have actually happened in operations. A ship has poured numerous broadsides into the empty ocean when the real target was an island several hundred miles away. At last report the island was still "afloat."

Many radar sets are provided with more than one pulse rate. The pulse nearest the transmitter is said to give an echo "on the first sweep." The next nearest pulse is said to give an echo "on the second sweep," and so forth. When the pulse rate is changed, the spacing between the pulses alters accordingly, and one can ascertain more accurately the range of the target. However, the radar officer who uses a single pulsing rate, either from habit or necessity, should always keep clearly in mind the possibility that atmospheric condi-

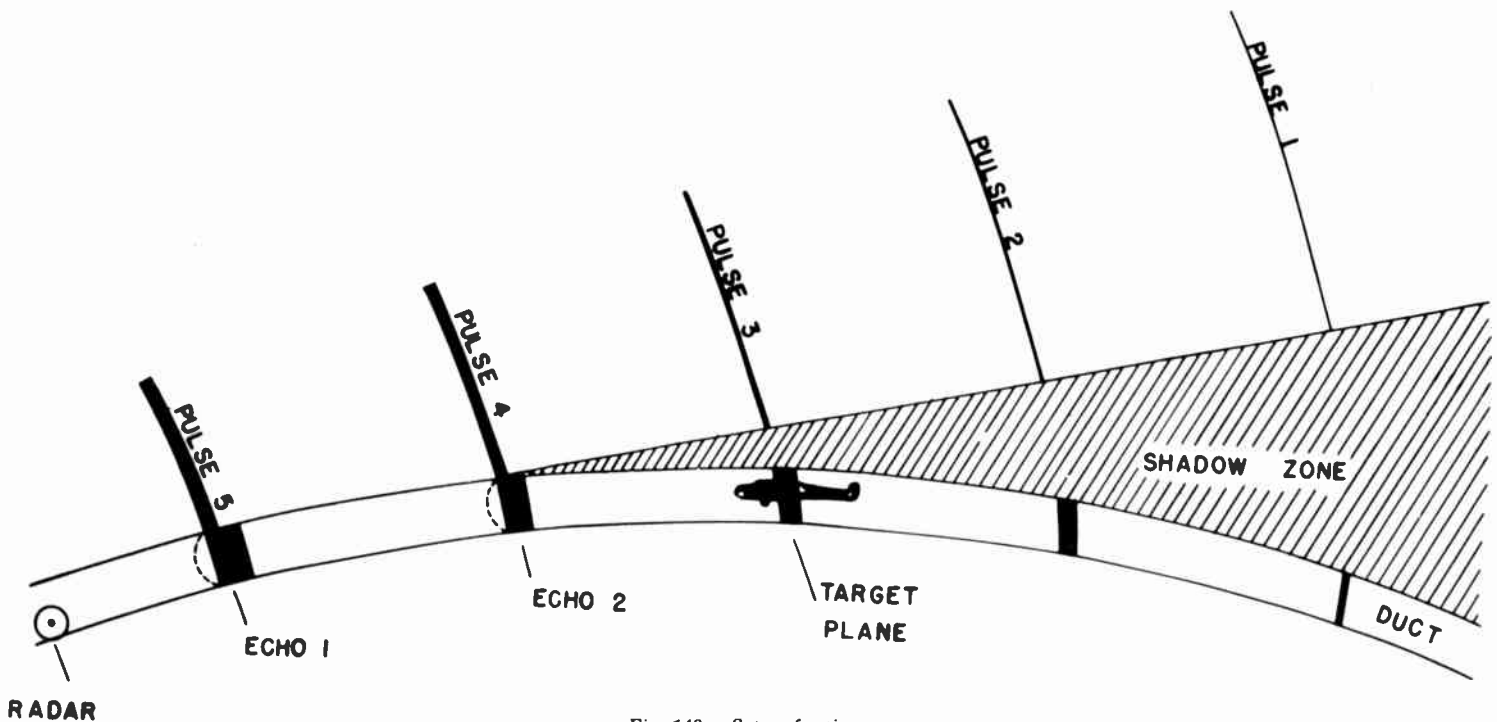


Fig. 148. Superrefraction.

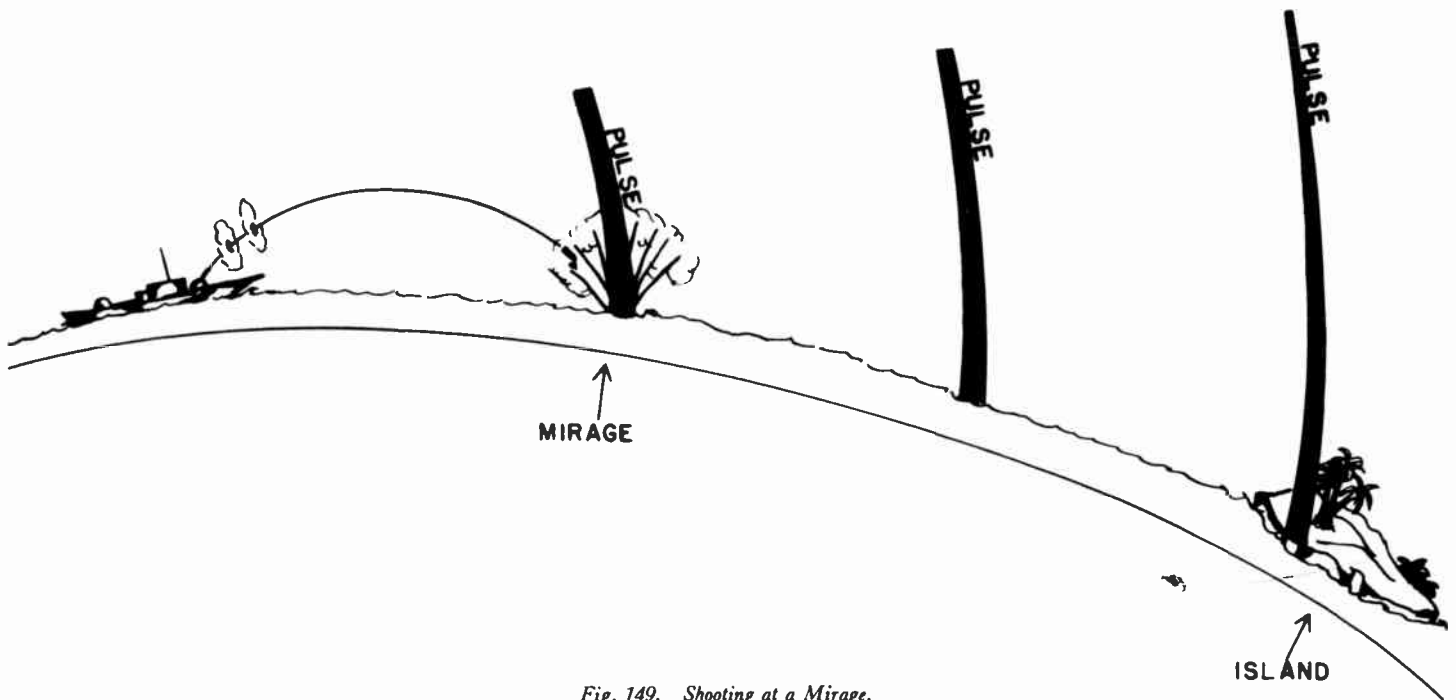


Fig. 149. Shooting at a Mirage.

tions may have caused the formation of a duct and that the true range may be much greater than the observed range. The formula for this greater range (in yards) is as follows:

$$\text{True range} = \text{observed range} + \frac{327,000,000(N - 1)}{2P}, \quad (1)$$

where P is the number of pulses per second and N is an integer 1, 2, 3, and so forth, representing the number of the sweep.

When two pulse rates are possible, the operator should always check to ascertain which sweep is effective. If only one pulse rate is available, he should try to check with another type of set. If a second set with another pulse rate is not available, prior knowledge of atmospheric conditions may give information concerning the probability of occurrence of an exceptional range.

It should be emphasized that the use of two pulse rates is not in itself a guarantee against error in range. If the ratios of the pulse rates can be expressed as the ratios of two integers, there will still be some uncertainty. For example, if the rates are 1200 and 800, say, whose ratios are in the proportion of 3 to 2, the former will give echoes on the fourth sweep coinciding with those of the latter on the third sweep, since

$$\frac{N - 1}{P} = \frac{3}{1200} = \frac{2}{800} = \frac{1}{400}. \quad (2)$$

Costly errors of this sort have been made. Observers actually saw the evacuation of Kiska, but were unable to interpret the radar results because of the seeming agreement between two radars with different pulse rates.

It was not until our forces moved in and found the island deserted that the correct answer was worked out. The newer-type sets, which provide for a variable rate of 10 percent or so, are much more reliable.

A ghost image may often be recognized by severe fading and by the marked fluctuations and scintillations that it undergoes on the scopes. These fluctuations arise from the unusual interference between the radio waves trapped within the duct. Communications signals may show a marked and rapid fading when atmospheric trapping results in extended ranges.

As we described in Chapters 11, under standard conditions, radio waves travel by two paths. The first of these, the *direct wave*, follows a more or less straight route, whereas the second, the *reflected wave*, moves down to the earth's surface and is reflected upward again. These two components of the radio impulse meet again at a distance from the transmitter. Interference results in a great reduction of signal strength in regions where the waves are out of phase.

When radio waves are trapped in a duct, the possibilities of interference are greatly multiplied. At great distances from the transmitter and within the duct, no direct waves exist. All waves will have bounced at least once, and some may have been reflected many times. Small fluctuations of the atmosphere within the duct may, therefore, cause marked changes in the relative phases of the waves. The result is severe fading of the signal strength. The use of a diversity (multiple) antenna system will usually be of great assistance.

Variable atmospheric conditions may affect the ranges

of all equipment operating on frequencies greater than 30 megacycles. The higher the frequency, in general, the greater will be the chances of the formation of a duct. Failure of plane-to-ground communication has been responsible for the loss of many aircraft. Doubtless, most of these communication failures have arisen from difficulties with the sets—drift of operating frequency, and so forth, including failure of the operator to turn the ON switch. Other failures, however, may well be attributable to atmospheric peculiarities which, if their presence had been recognized, would not have disrupted communications. A duct may act as a sort of barrier through which transmission becomes difficult, especially when it takes place at a grazing angle. Communicators both on the ground and in the air should be prepared for sudden changes in signal readability attributable to these effects. To regain or maintain contact under such conditions, one must choose a proper altitude for the plane. Knowledge of the atmospheric conditions enables the communications operator to predict a suitable level for flight. Maintenance of communication is an important factor in air-travel safety.

Before proceeding further, we should emphasize a grave danger inherent in the information that this manual conveys. A careless operator will be inclined to ascribe all abnormal ranges to weather conditions, but this is obviously untrue. Nonstandard refraction almost never occurs at angles of elevation greater than 1° above the horizontal, and is considered exceptional even above

0.5° . Accordingly, any irregularities at higher angles must be attributed to causes other than abnormal propagation. It should be emphasized, therefore, that the analysis of weather conditions and their effects upon radar performance is not a substitute for adequate set testing.

In this connection, use of the echo box is much to be preferred over measurement by means of a so-called standard target, such as a cliff or ship. The standard target, whether it be a corner reflector or some distant mountain, is not a dependable reference for the checking of set performance. The vagaries of trapping may produce uncertainties as great as 40 or 50 db in signal strength.

Even when atmospheric conditions are standard, the rise and fall of the tide may alter the relative path lengths of the direct and ground-reflected waves. The resulting phase shifts produce variations of signal strength amounting to 20 or 30 db. Similarly, the path lengths of only the direct rays arriving from various parts of a comparatively large target may be altered by slight movement of either the target or the radar, causing large fluctuations in signal strength. The pitch and roll of a target ship are often plainly visible on the radar record. It is evident that reference targets are a poor means of maintaining equipment at peak performance and of distinguishing between set failure and abnormal effects arising from peculiar conditions of the propagation path.

M CURVES, AN INDEX OF EXPECTED COVERAGE

WHAT WEATHER CONDITIONS CAUSE THESE UNUSUAL transmission effects? Can one predict in advance when extremely long or very reduced ranges are likely to occur? How does the atmosphere affect radio propagation on frequencies greater than 30 megacycles? In what ways can this information be put to practical use? These are questions to which only partial answers are available at present, but the indications are that knowledge of this entirely new subject has many important applications. The problem is one for combined effort of the aerological, communications, and radar units.

The atmosphere is subject to many changes. Under standard conditions, both the temperature and water-vapor content decrease gradually and almost uniformly with the height above the surface. When this condition

occurs, there will be no duct, and radio propagation will be of the standard type. Figure 150, section A-4, pictures the paths of radio waves propagated under standard conditions. Figure 150, section A-3, also gives a sample standard coverage diagram. The shaded portions represent the areas where there is no coverage; the unshaded areas are the regions in which targets will be detected. For the sake of simplicity, we have omitted the lobes of earlier sections. In Figs. 150 and 151, it was more convenient to represent the earth as flattened out and the rays as curving away from the earth. In reality, the rays are almost straight and the earth curves away from the rays. The two points of view are presented schematically in Figs. 152 and 153.

Occasionally, there may be breaks in the temperature

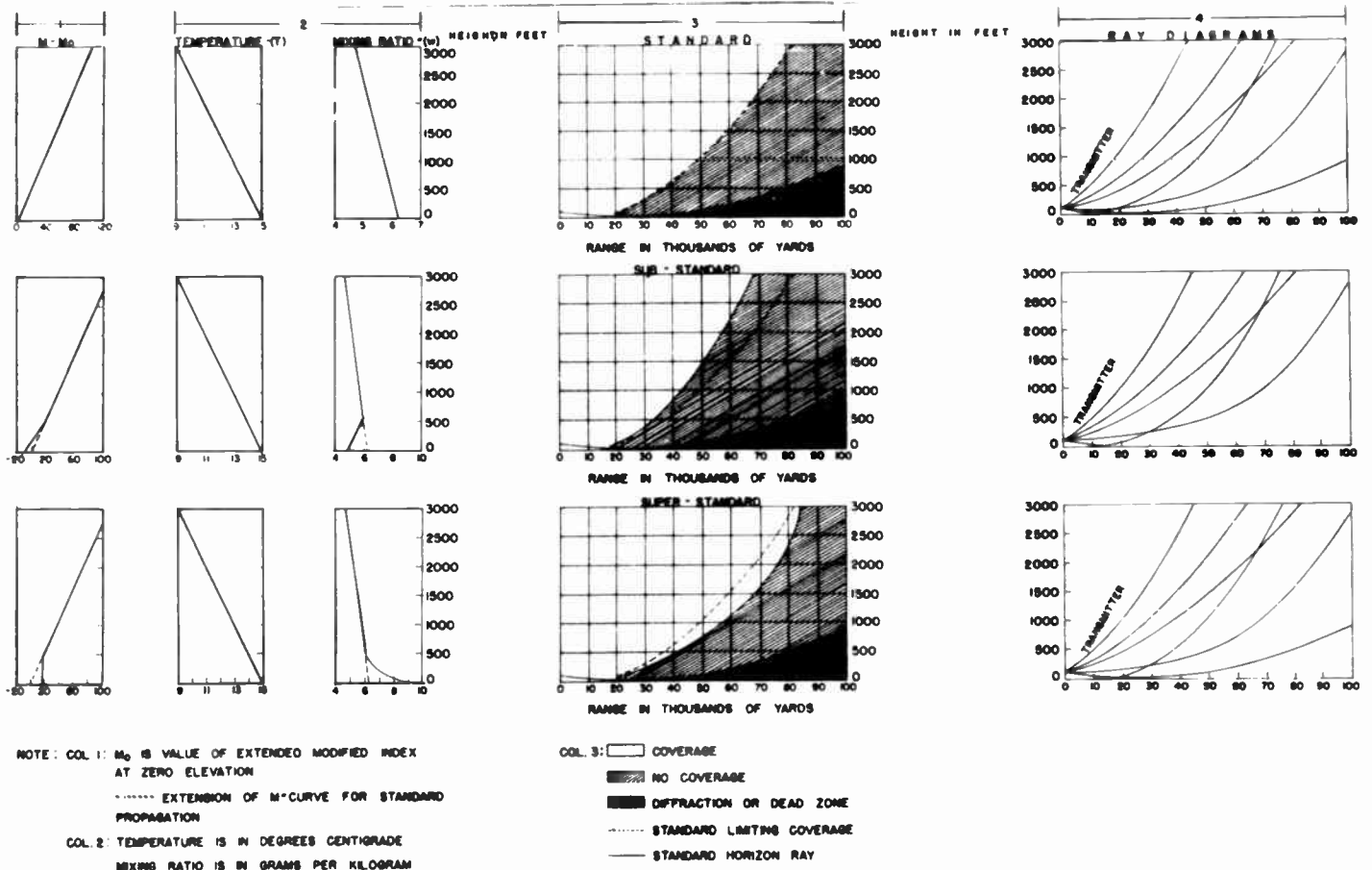


Fig. 150. Nontrapping Conditions.

and moisture curves. The temperature may, for example, first increase with height, then begin to decrease. Such a situation is called a *temperature inversion*. More important, the moisture content of the air may decrease steeply just above the ground. When one or both of these conditions are present, it is possible to obtain downward bending of the radio waves and the extraordinary ranges that indicate the presence of a duct. Temperature inversions, however, unaccompanied by any pronounced moisture difference, usually do not cause serious trapping.

Aerologists, in attempting to analyze the conditions that lead to such range variations, employ the *M curve* (Figs. 150 and 151, col. 1) to picture the expected degree of bending (or refraction). This curve is drawn up from records or forecasts of temperature and moisture change with height above the earth. *M* is the so-called modified index of refraction, modified for the curvature of the earth. As we pointed out in an earlier paragraph of this chapter, a straight ray, plotted with respect to the curved earth's surface, becomes a curved ray when we arbitrarily treat the earth as flat. *M* is a fictitious refractive index, which gives the proper bending to the ray on the flat-earth presentation.

Variations in *M* determine the bending of the rays along their path through the atmosphere. For standard

propagation, the *M* curve becomes a straight line sloping up and to the right at a prescribed rate (Fig. 150, section A-1). A break in the *M* curve is a clear indication of atmospheric conditions associated with nonstandard propagation.

Trapping conditions occur when part of the *M* curve slopes up and to the left—when *M* decreases with height. The top of the duct coincides with the level at which *M* again begins to increase with height. In other words, it is frequently associated with the top of the temperature inversion, although it may not coincide exactly with this level because variations in the distribution of moisture may not precisely follow the temperature curve. If a difference exists, the *M* inversion will generally lie below the temperature inversion.

It should be noted that moisture variations play a more important role in tropical than in polar regions. This is true largely because the atmosphere is capable of holding a great deal more moisture in warm than in cold areas. Nevertheless, there are frequent reports of long radar ranges and very evident trapping from the arctic and antarctic zones.

The bottom of the duct lies either at the ground (Fig. 151, sections A-1 and B-1) or at a level where the value of *M* equals that at the top (Fig. 151, section C-1). Thus the duct may be "surface" or "elevated," according

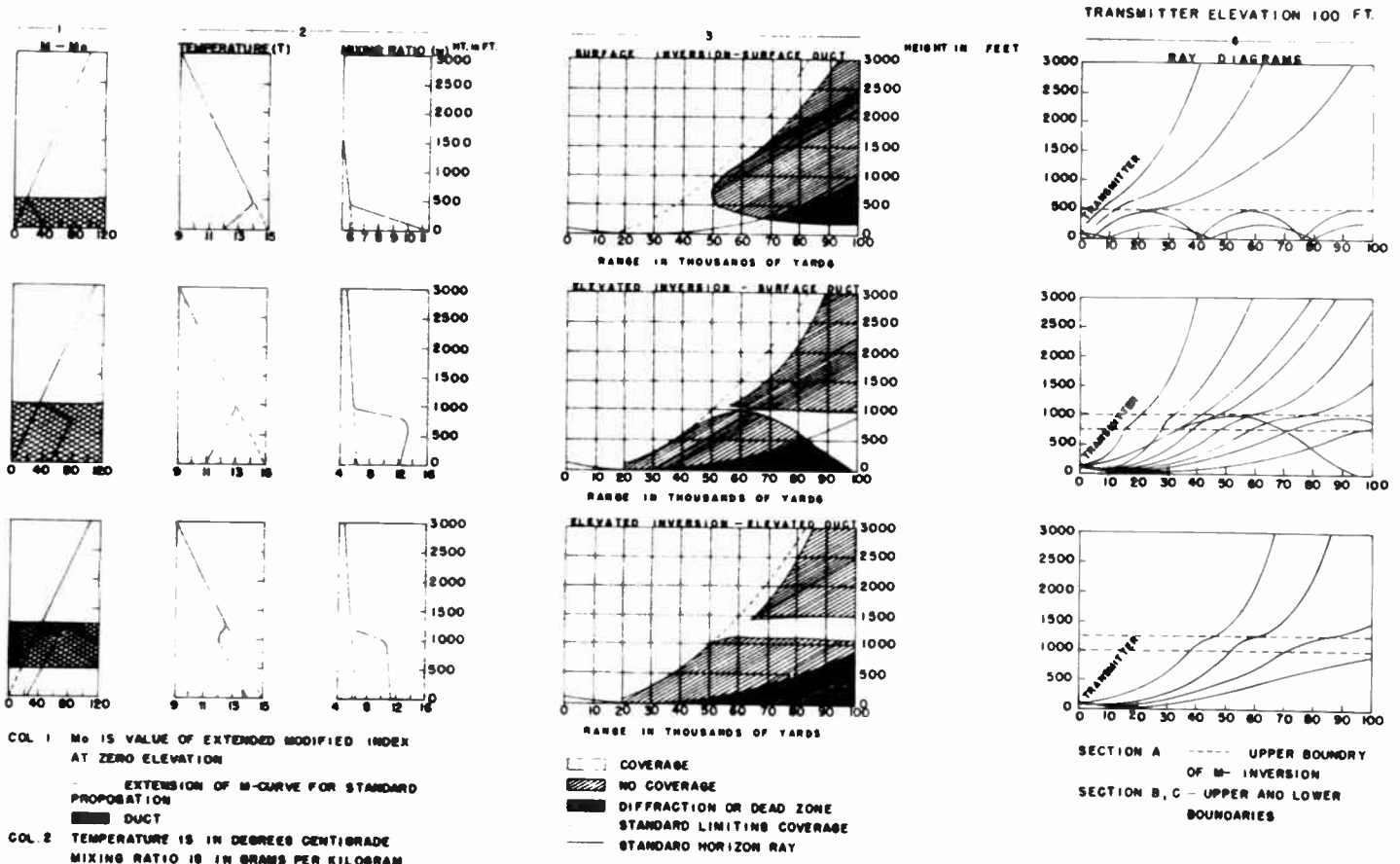


Fig. 151. Trapping Conditions.

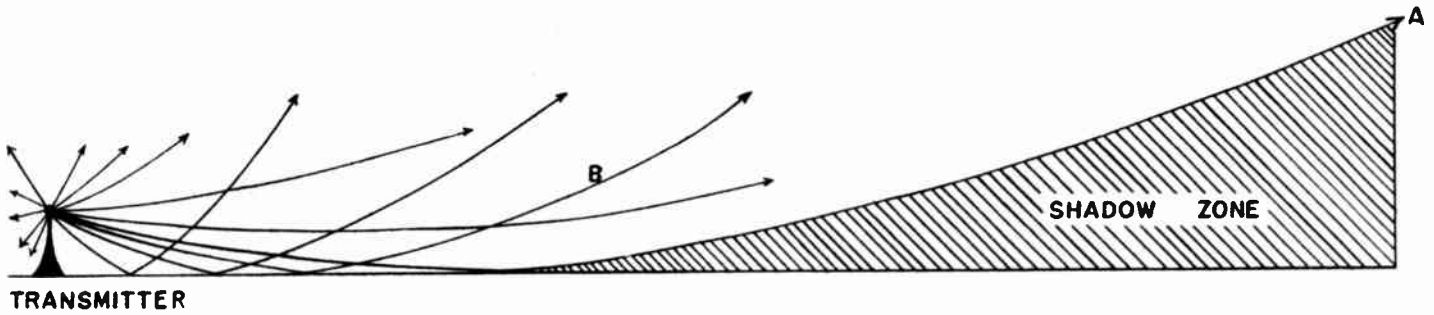


Fig. 152.—Flat Earth—Curved Rays.

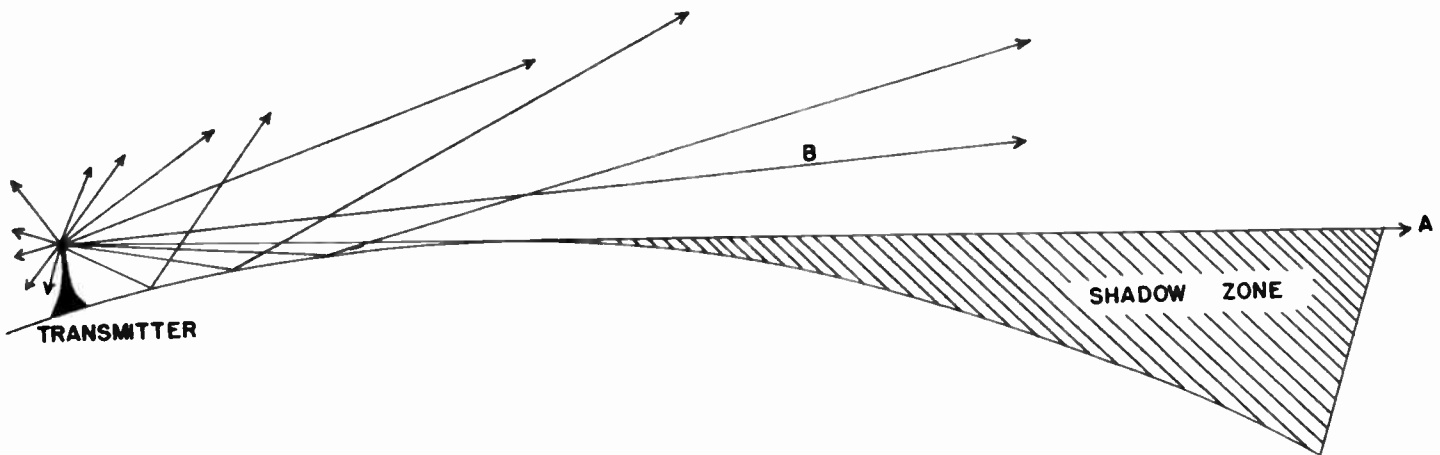


Fig. 153.—Curved Earth—Straight Rays.

to the shape of the *M* curve.

We usually describe an inversion as *surface* if *M* begins to decrease at the surface of the earth. Similarly, we describe an inversion as *elevated* if *M* does not begin to decrease until some point above the surface of the earth. An elevated inversion may give rise to a surface duct.

We have said that the index of refraction, which determines the paths of radio waves through the atmosphere, depends upon the moisture content and the temperature of the various levels above the earth's surface. The quantity *M* is given by the equation

$$M = \frac{79}{T_A} (p - e) + \frac{3.8e(10^6)}{T_A^2} + 0.048h, \quad (1)$$

where *h* is the altitude, in feet, of the given point; *p* is the barometric pressure, in millibars; and *e* is the vapor pressure of the water, also expressed in millibars. *T_A* is the absolute temperature on the Kelvin scale, related to *T_c* or *T_F*, the ordinary Centigrade or Fahrenheit scales, by the equations:

$$\begin{aligned} T_A &= 273 + T_c \\ &= 273 + \frac{T_F - 32}{1.8}. \end{aligned} \quad (2)$$

The quantity *e* may be expressed as

$$e = \frac{p}{623/w + 1}, \quad (3)$$

where *w* is the *mixing ratio*, which defines the actual moisture content of the atmosphere.

Squeeze out all the water from a given sample of air and weigh both the moisture and the dry-air residue. Multiply the weight of the moisture by 1000 and divide by the weight of the dry-air residue. The result is *w*, which may be more simply defined as the *number of grams of moisture per kilogram of dry air*.

In practice, one usually determines *w* indirectly by measures of dry-bulb and wet-bulb temperature. The cooling effect of evaporation from the wet-bulb thermometer depends upon the amount of moisture already present in the atmosphere. Wet- and dry-bulb readings are most frequently converted to relative humidity (RH).

This quantity is the ratio of the number of grams of water contained in a kilogram (or any other fixed amount) of air, to the number of grams that would be contained in completely saturated equal amount of air

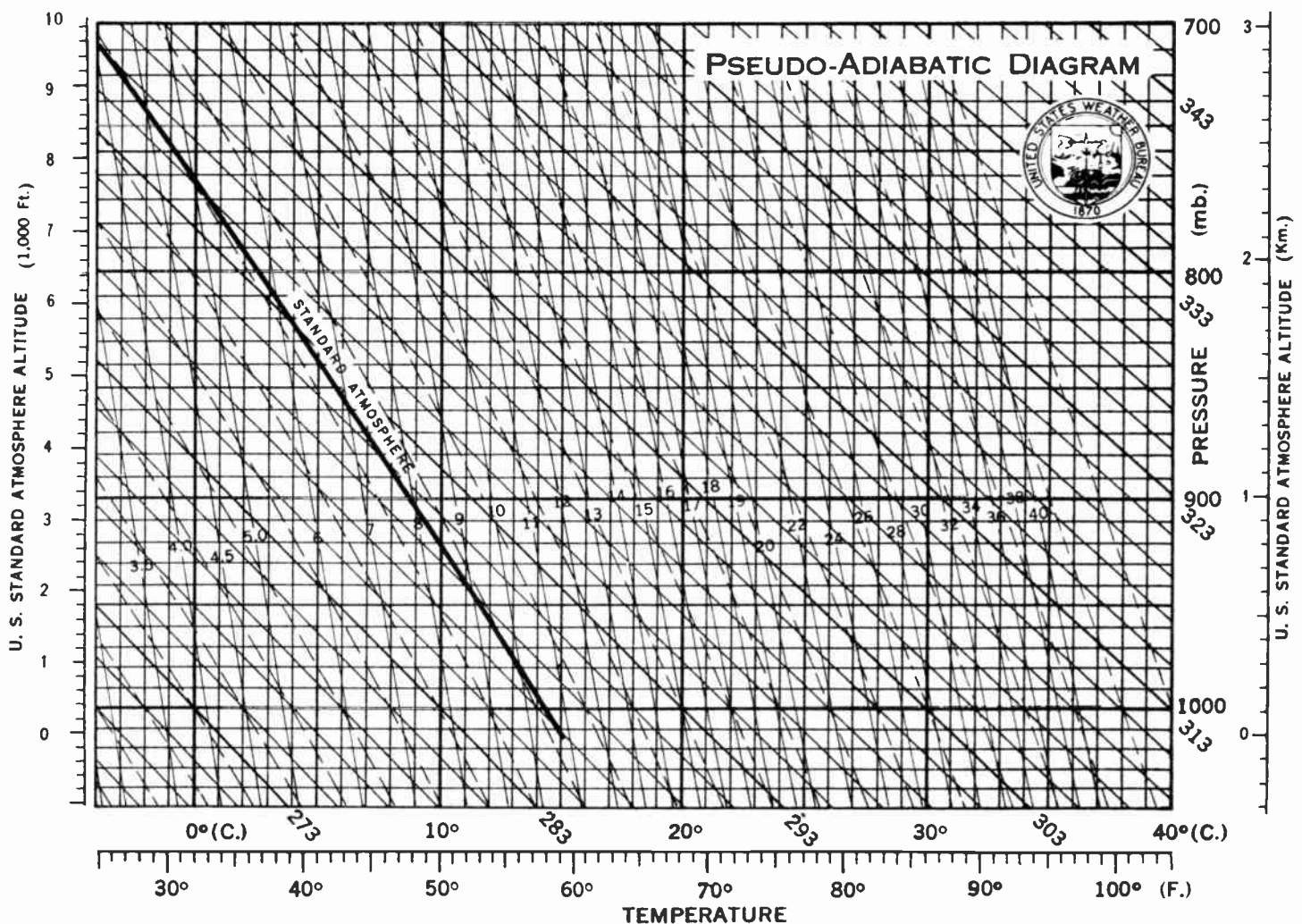


Fig. 154.

at the same temperature. At RH = 100 per cent, the air is completely saturated, and no evaporation occurs. Thus, when dry- and wet-bulb thermometers read alike, we infer that RH = 100.

The maximum amount of moisture that air can hold depends markedly upon its temperature. For example, a sea-level atmosphere with $T_p = 95^\circ$ contains about 37 grams of water per kilogram—that is, $w = 37$. But at 40° , the same air will have a mixing ratio $w = 5.2$. The warmer air thus holds about seven times more water than the cold. In similar fashion, if we vary the pressure the relative humidity fluctuates, even if w remains constant. Evaporation occurs more readily at the lower atmospheric pressures.

From the standpoint of human comfort, relative humidity may be more important than the actual mixing ratio. RH determines the rate of evaporation from the skin, and it is well known that such evaporation tends to cool the body. The radio waves, however, are not governed by such elusive factors as physical comfort. Thus, for radio propagation, w is the fundamental quantity.

The various quantities such as dry- and wet-bulb temperatures, height, RH, barometric pressure, and w are all intimately connected. The relationships are best displayed on what the meteorologists call a *pseudo-adiabatic diagram*, shown in Fig. 154, with an enlarged section for convenience of detailed examination shown in Fig. 155.

The plot is primarily one of height (above sea level) as the vertical coordinate vs. temperature expressed on the centigrade scale. The absolute temperature (273, 283, 293, and so forth) and the Fahrenheit scale are also noted. In addition to the horizontal and vertical lines, there are three sets of inclined lines.

Those lines most nearly horizontal are called *dry adiabats*. Those slightly less inclined and broken into dashes are called *moist* or *pseudoadiabats*. The full lines nearest the vertical represent the mixing ratio w . The numbers crossing the page horizontally refer to this last quantity and are to be considered representative, not of a point, but of the entire inclined line.

We are now ready to interpret the various lines. In physics, an adiabatic process is one in which no heat is

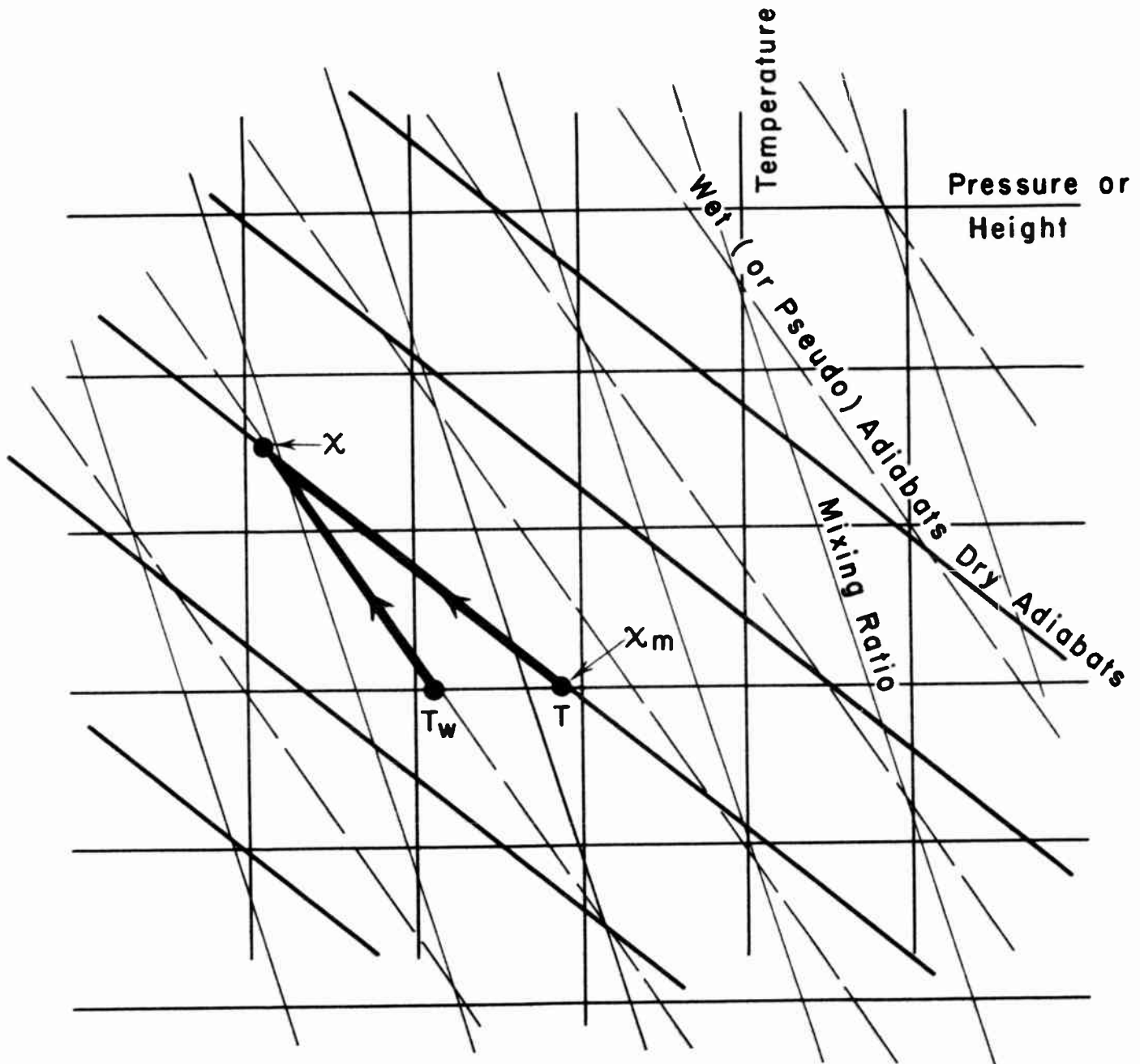


Fig. 155. Explanation of Pseudo-Adiabatic Diagram.

allowed to escape from, or enter into, the medium. Suppose, for example, that we have a quantity of dry air in an insulated cylinder with a piston at one end, so that the gas is free to expand or contract. Let us carry this equipment from nearly sea level to a height of 10,000 feet. As the piston moves out, the gas will expand, always keeping its pressure equal to that of the outside air. The expansion causes the gas to cool and if, as we have supposed, there is no loss or gain of energy to or from the exterior, the process is truly adiabatic.

From the laws of physics and the known properties of air, we can easily determine the final temperature. The diagram of Fig. 154 simplifies the calculation. Suppose that our starting point was at a pressure of

1000 millibars (right-hand vertical scale) or height 180 feet. Also suppose that the initial temperature was 30° C. Find this point of intersection on the chart and follow the dry adiabat curve that slants upward and to the left, until you reach the top of the diagram, pressure 700 millibars and altitude 10,000 feet. From this point, drop vertically down and read the temperature. The value is 0.5° C. The expansion has caused the gas to cool through a range of 29.5° C.

Now, let us perform the same experiment with saturated moist air at the same initial temperature and pressure. As before, the gas starts to cool because of the expansion at higher elevations. But now a new phenomenon occurs. The cooling air, originally saturated

for the starting temperature, cannot hold as much moisture. Fog, dew, or rain begins to form. Just as the process of evaporation cools the air, the inverse process of condensation warms it. Thus, the moist air in the ascending cylinder does not cool off as rapidly as the dry air did in the previous case.

To find out the result, follow up the pseudoadiabat (dashed line), from the same starting point as before to the 10,000-foot level. The temperature of the moist air is 19 C. Thus, the total cooling is only 11° as compared with the value of 29° obtained for dry air.

We call this process pseudoadiabatic because the moist air does not behave like a perfect gas. We further suppose that the rain or mist is removed from the cylinder as fast as it is being formed; otherwise, some of the liberated energy would be used to heat the accumulated moisture. But we are removing, at the same time, some of the original energy, so that the process is not strictly adiabatic.

Points along a pseudoadiabat represent completely saturated air at the different pressures and altitudes. To find out the mixing ratio of saturated air at a given temperature and pressure, find the w curve that runs through this point and run up or down it to the index figure running across the page near the heights of 2500 to 3000 feet. Thus, we find that, for the moist air of our example, with $T_c = 30^\circ$, $p = 1000$, and $w = 28$. For the final situation, $T_c = 19^\circ$, $p = 700$, $w = 19.5$. During the ascent, $28 - 19.5 = 8.5$ grams of water per kilogram of dry air were precipitated.

The observational data for the calculation of M curves usually consist of wet- and dry-bulb readings or their equivalent. The wet-bulb reading T_w , which will be normally less than or, at the extreme, equal to the dry-bulb value, represents the temperature at which the air under examination will just be saturated. Find the two points T_w and T (the dry-bulb value) on the diagram for the height or barometric pressure of the observation. Follow the moist adiabat for the former and the dry adiabat for the latter upward until the two curves intersect. The crossing marks the point where the dry and wet bulbs would give the same temperatures. Hence, if we now move over to the mixing-ratio curve, as previously described, we determine w for the original air sample.

To find the relative humidity, read the w_s for the point T . This figure represents the mixing ratio for a completely saturated atmosphere at the given temperature. Then,

$$\text{RH} = 100w/w_s, \text{ in percent,} \quad (4)$$

—that is, the ratio of the amount of water actually

present to the saturation value.

If one is given T and RH, and lacks the original wet-bulb reading, he can still determine w_s from the diagram and calculate w from the equation above.

The observational procedures for determination of a detailed M curve are rather complicated. They usually involve special meteorological equipment, to be sent up in a free or captive balloon, or a kite. The readings are taken at the ground, relayed by wires from the equipment aloft or by radio telemetering devices from radiosonde.

It is necessary, or at least desirable, to have frequent observations at several points along the radio path, because of the variability of the atmosphere in time and space. Near the ground, the measures should be spaced at intervals of about 10 feet. From altitudes of from 50 to 200 feet, the interval may be increased to 25 feet and expanded proportionally for still greater heights. In view of the fact that the instruments will rarely ascend vertically, some device must be available for triangulation of the altitude.

During World War II, both the Army and Navy trained aerological units in sounding techniques. These groups made numerous surveys of meteorological conditions in many areas, over land and sea. Although the methods are too involved for widespread use, some of the results led to conclusions of rather general applicability. These will be made the basis for discussion of the next chapter. Even though one may not be able to determine a complete M curve, a few observations made with the simplest equipment will often be very useful in indicating the presence of potential trapping.

Let us now turn to the calculation of M values from the known w and T . The fundamental relation has already been given, Equation (1). The nomogram of Fig. 156 (prepared by the U.S. Weather Bureau) provides a simple mechanical solution. Connect the observed dry-bulb temperature on the upper line (1) with the appropriate value of w (2) and note the intersection on the bottom line of the drawing, labeled *turning line* (3). Now connect this point (3) with the height (in feet) of the observation (4). The intersection (5) gives the modified index, M , in so-called M units. The key printed on the left of the nomogram indicates the proper procedure.

The value of h in the nomogram or Equation (1) is the height above any convenient reference level, sea level or not. If the antenna is located on a hill-top, the surrounding level country should be the reference level. It is particularly important to note that, when simultaneous M curves from two or more different locations are to be compared, the zero level should be the same for both.

The quantity M , thus calculated, when multiplied by 10^{-6} , differs from the refractive index by a constant. This constant is unimportant. One may subtract any value he chooses from all the M 's of a given set and the radio propagation will not be affected. We plot M against the height, to give an M curve. The propagation characteristics depend only on the shape of the curve.

It is often convenient to subtract M_0 , the value of the modified index at zero elevation, from all the M values at other heights. If one follows this practice, however, with several M curves at different points along the path, it is not permissible to reduce each curve with its own M_0 . Choose any one of the curves as standard and use the same value of M_0 for all. The other procedure may suppress significant horizontal changes of refractive index. Also, it is possible for very different meteorological conditions to produce identical M curves.

Analysis of many low-level tropospheric weather soundings and their associated M curves indicates the possibility of classifying M curves into several general types. The over-all classification can be made under the major headings of *nontrapping* and *trapping*.

The three principal nontrapping types of M curves, *substandard*, *standard*, and *superstandard*, are shown in column 1 of Fig. 150. They are called *nontrapping* because no duct is present, since M always increases with height. Column 4 of the illustration depicts the effect that the various combinations of aerological conditions will have upon VHF radio waves. Column 2 gives typical aerological soundings that produce the various M curves.

The substandard type of M curve appears in section B of Fig. 150. The characteristic feature of this variety is a break in the M curve at some altitude. The slope of the higher portion is the same as that of the standard atmosphere, but the lower portion meets the horizontal axis at an angle somewhat more acute than that of the standard curve. The substandard case arises from an increase in the moisture content with height, as shown by the associated aerological soundings.

High-frequency radio waves propagated under these conditions tend to be bent upward, and a consequent decrease in the effective range of the equipment may be expected. Should the angle at which the curve meets the horizontal axis become very acute, the danger from

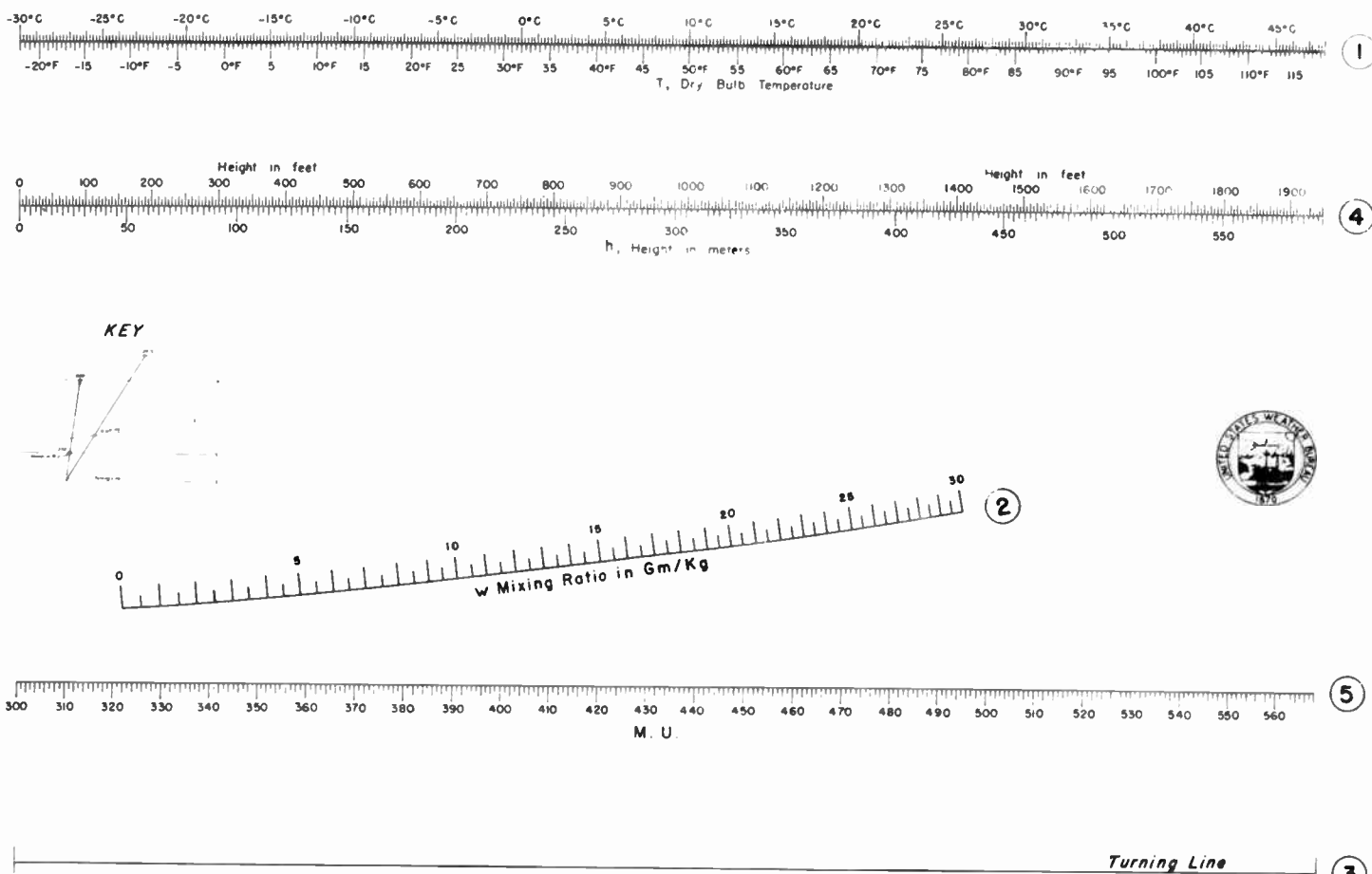


Fig. 156. M Nomographic Chart.

Adapted from Chart by Radiation Laboratory, M.I.T.

loss of range for surface targets may be serious.

The so-called *standard atmosphere*, frequently referred to in prior chapters as responsible for standard propagation, was defined by the NACA (National Advisory Committee for Aeronautics). It is an atmosphere whose sea-level temperature is 15° C (59° F) and whose temperature decrease is at the rate of 2° C (3.6° F) per 1000 feet. The heavy line in Fig. 154 indicates the temperature (but not the moisture) distribution in the standard atmosphere.

The NACA definition says nothing about water-vapor content. Yet we know that all atmospheres will contain more or less moisture. From observational data, we adopt a moist standard atmosphere in which the vapor pressure decreases uniformly from 10 millibars at sea level to 0 millibars at 10,000 feet. The temperature and moisture distributions are shown in Figs. 157 and 158. *M* curves for the dry and moist standard atmospheres appear in Fig. 159. The propagation features of the standard curve require no further discussion.

The superstandard *M* curve (section C of Fig. 150)

depicts a coverage situation slightly greater than standard in the lower level, with nearly normal coverage aloft. Such an *M* curve is transitional between the non-trapping and trapping conditions, the limit occurring when the lower segment of the *M* curve is vertical, indicating that the curvature of the rays is equal to the curvature of the earth. Instances have been recorded in which received signal strength beyond the line of sight was stronger when the lower segment of the *M* curve was approximately vertical for several hundred feet than when it sloped to the left for a 100 feet and became standard above. Superstandard cases embody all those curves whose angle of intersection at the base is greater than that of the standard.

A duct can exist only when the *M* curve bends back on itself at some point, so that *M* shows a decrease with height. Examples of the three principal trapping types of *M* curves and associated typical aerological soundings are shown in columns 1 and 2, Fig. 151. Again, these same *M* curves can result from many combinations of *T* and *w*. Even when a duct exists, *M*-curve information

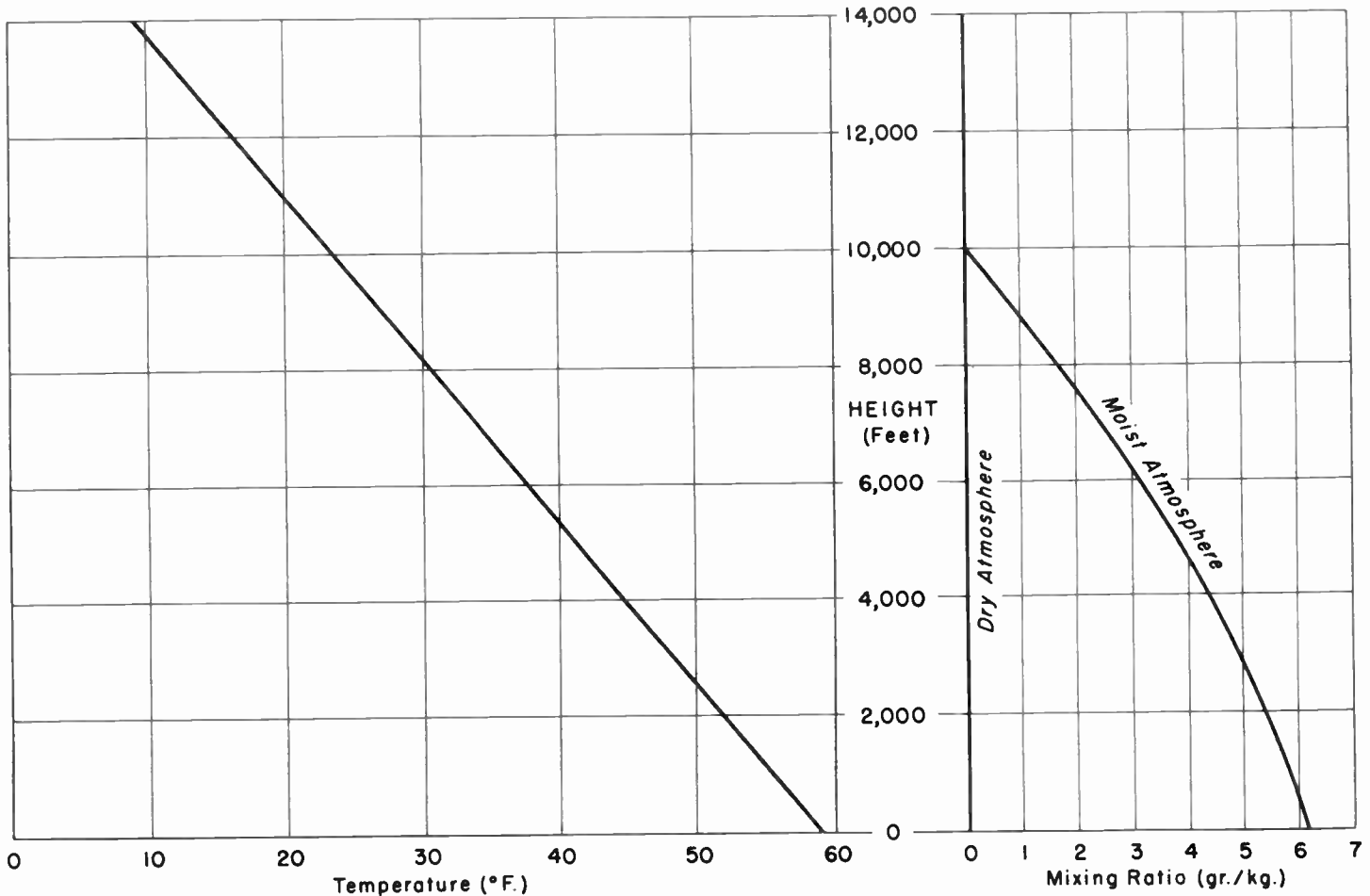


Fig. 157. Standard Atmosphere.

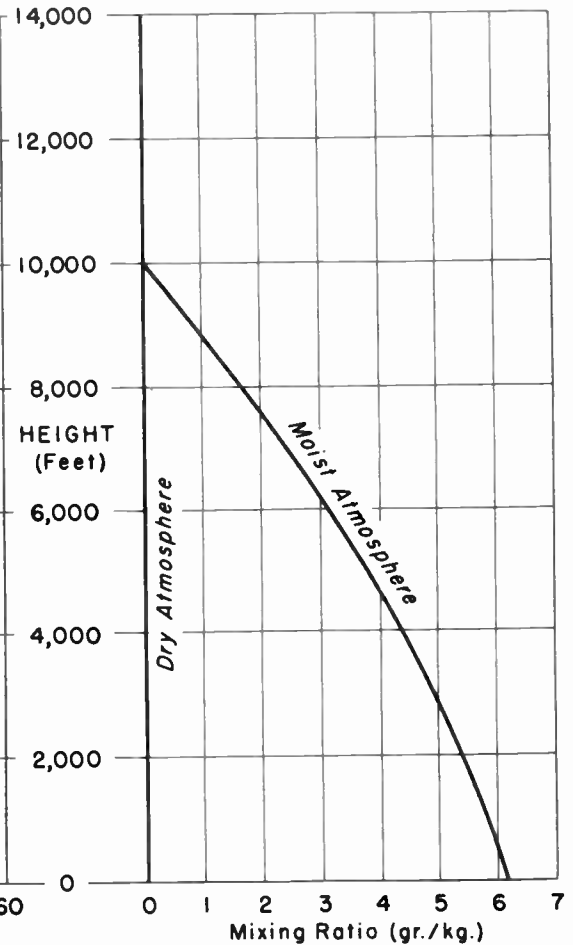


Fig. 158. Moisture Distribution in the Standard Atmosphere.

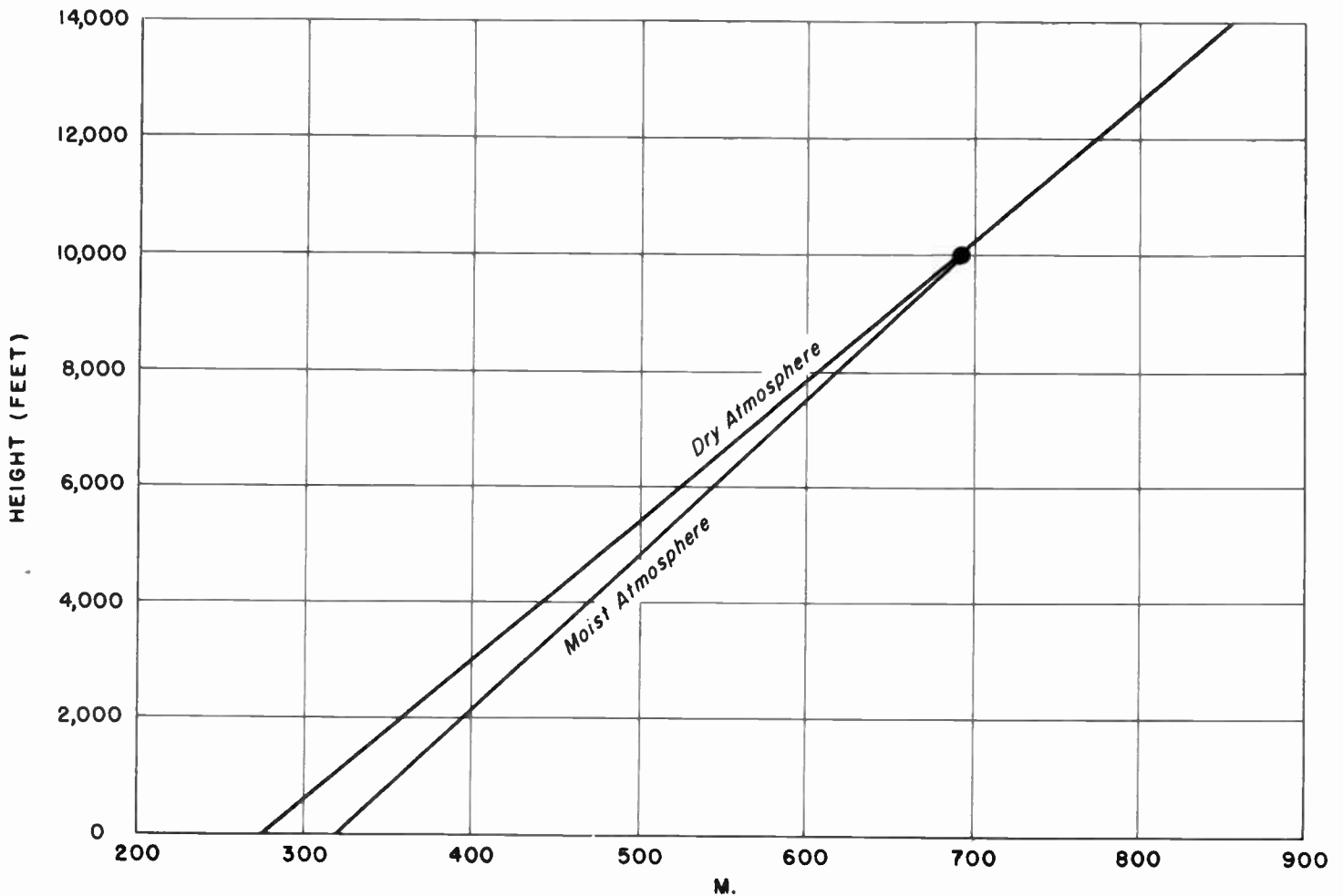


Fig. 159. *M* curves for Dry and Moist Atmospheres.

indicates that possible extensive trapping will occur only when the frequency is sufficiently high and, in the majority of cases, when the antenna is within the duct. Further discussion of these points will be given later.

All surface *M* inversions produce surface ducts. The *M* curve in section A-1, Fig. 151, shows that the top of the trapping layer is at 500 feet, that the duct is 500 feet thick, as illustrated by the shaded area, and that it is surface-based. An indication of the extent of the trapping to be expected from such a duct may be obtained from both the width of the duct and the difference between the value of *M* at the top and bottom of the duct. The greater these two values, the greater will be the expected trapping.

An *M*-curve inversion aloft may lead to a surface duct, as illustrated in section B, Fig. 151. Such an *M* curve is present if a vertical dropped from the minimum of *M* hits the earth before it crosses the *M* curve. It is again noted that in the associated typical aerological sounding for this example, the formation of the duct resulted principally from the reduction of moisture aloft. Radio waves

transmitted under these conditions may be trapped within the duct.

From the foregoing discussion, it follows that an elevated inversion—elevated duct is present when a vertical, dropped from the minimum *M*-value aloft, strikes the *M* curve at a point above the earth's surface. Such a situation is illustrated in section C, Fig. 151. The duct, as previously defined, lies between the minimum point of the *M* curve and the lower level where the *M* value is the same as at the top of the duct. Thus, if the radar of VHF or SHF radiator is placed within this duct and if the frequency is sufficiently high, abnormally great ranges again result.

Observed *M* curves are usually somewhat irregular, the breaks are not sharp, and the current representation in the form of straight lines is only a rough, but probably legitimate, approximation. The slope of the lowest segment may be classified as substandard, standard, or superstandard. The slope of the intermediate element is variable, and the upper slope of the *M* curve is always assumed to be standard.

When there is trapping, coverage directly above the duct, in what would be ordinarily the lowest lobe of standard coverage, may be somewhat modified. Lobes still exist, and their relative spacing with respect to one another is about the same as standard, but the intensity of the lowest lobe is often reduced. However, the reduction in coverage at higher levels is a good deal less striking than the increased coverage at low levels. The reason is that only a small fraction of the total power originally pertaining to the lowest lobe is ever trapped in the duct, but this small amount of power is prevented by the duct from spreading out vertically, and so gives a remarkably high field strength in the duct at long range.

Operationally, we can classify M curves into 10 different types as follows:

Nontrapping:

- Type 0, substandard
- Type 1, standard
- Type 2, superstandard

Trapping:

- Type 3, surface inversion—surface duct
- Type 4, elevated inversion—surface duct, substandard base
- Type 5, elevated inversion—surface duct, standard base
- Type 6, elevated inversion—surface duct, superstandard base
- Type 7, elevated inversion—elevated duct, substandard base
- Type 8, elevated inversion—elevated duct, standard base
- Type 9, elevated inversion—elevated duct, superstandard base

As previously stated, the higher frequencies tend to be trapped more readily than lower ones. Theoretical analysis shows that the atmospheric conditions leading to the trapping phenomenon are described by two parameters of the M curve. The first is the thickness of the duct D_t . If the duct is ground based, D_t will be the altitude (in feet) of the level where M reaches its minimum value. If the duct is elevated, the thickness is the distance from the minimum value of M in the inversion down to the point where M assumes this same minimum value. Duct thicknesses are shown shaded in column 1, Fig. 151.

The second parameter descriptive of the phenomenon is the so-called M deficit or *trapping index* M_t . This is the distance in M units between the value of M at the top of the duct and the maximum value of M to be found in the duct.

The greater M_t and D_t , the greater will be the trap-

ping. To get an approximate idea of the character of trapping, one may employ the following formula:

$$\log (n - \frac{1}{4}) = \frac{1}{2} \log M_t - \log D_t - \log f - 5.71. \quad (5)$$

All logarithms are to the base 10. M_t is the M deficit, in M units; D_t is the duct thickness, in feet, both read from the M curve; and f is the frequency, in megacycles. The quantity n , which is the real measure of expected trapping, determines the number of modes transmitted by the duct. If n , as determined from the diagram, is not an integer, adopt the next-lower integral value as the number of modes. For example, if $n = 2.75$ as calculated, take $n = 2$.

The nomograms of Figs. 160 to 165 present the solution of this equation for various selected frequencies. To construct similar nomograms for other frequencies, merely slide the central scale up or down to a position that may be determined from logarithmic interpolation between the given frequencies.

For the first mode of vibration, there is a single loop of electrical intensity confined within the duct. The second mode has two loops; the third mode, three; and so forth. These vibrational conditions are somewhat analogous to the higher harmonics of an oscillating wire, in which the first mode is the fundamental.

For trapping to be appreciable, n must exceed or at least be equal to 1. Otherwise, the duct will leak extremely rapidly. The higher modes leak more rapidly than the lowest.

For an absolutely uniform duct—that is, one whose M curve is constant over a long path, one can calculate the energy distribution with height and distance. In the actual atmosphere, however, such uniformity rarely exists. It is impracticable to attempt any special calculations of signal strength because of the wide variations of M in time and distance.

If a special circuit is to be set up on the frequencies greater than 30 megacycles, one should make a statistical analysis of meteorological data in order to determine the percentage of time that trapping conditions may obtain. Such studies should extend over an entire year, so that seasonal ducts will be detected.

The practical use of information concerning ducts will be given in a later chapter. For the moment we shall pause, reminding the reader that the transmitter within the duct is expected to give extended ranges, whereas a transmitter above or below the duct may experience a severe loss of coverage.

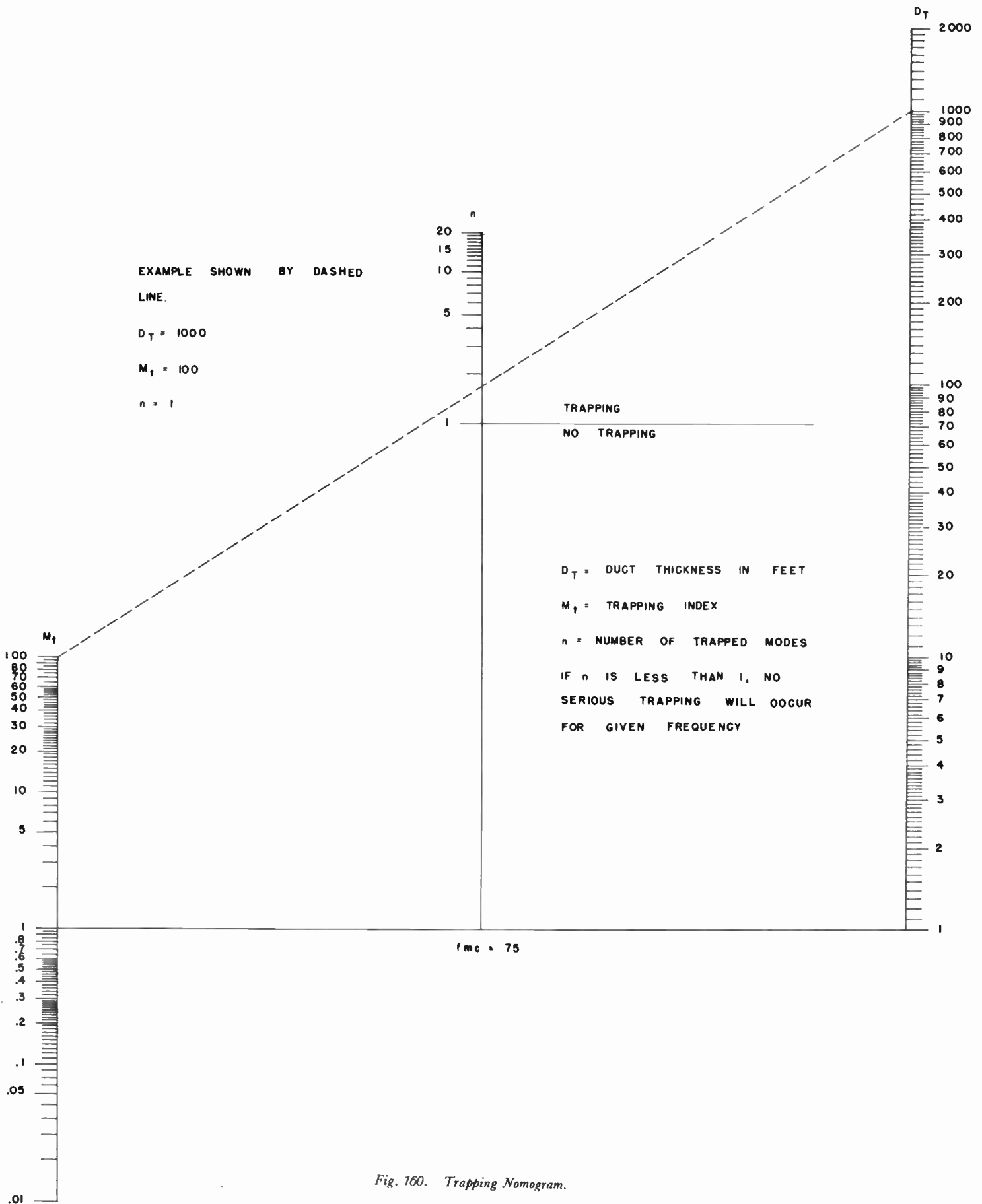


Fig. 160. Trapping Nomogram.

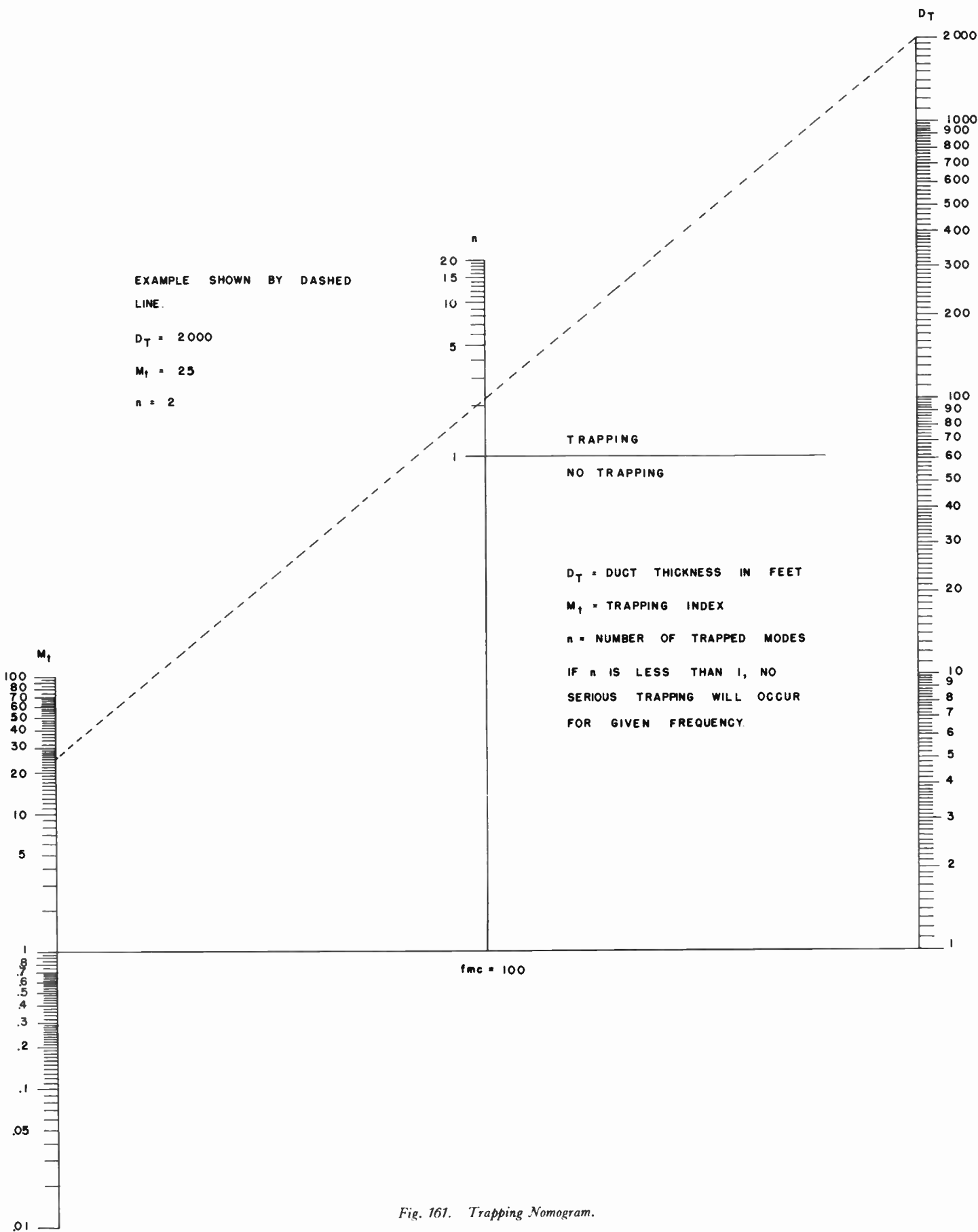


Fig. 161. Trapping Nomogram.

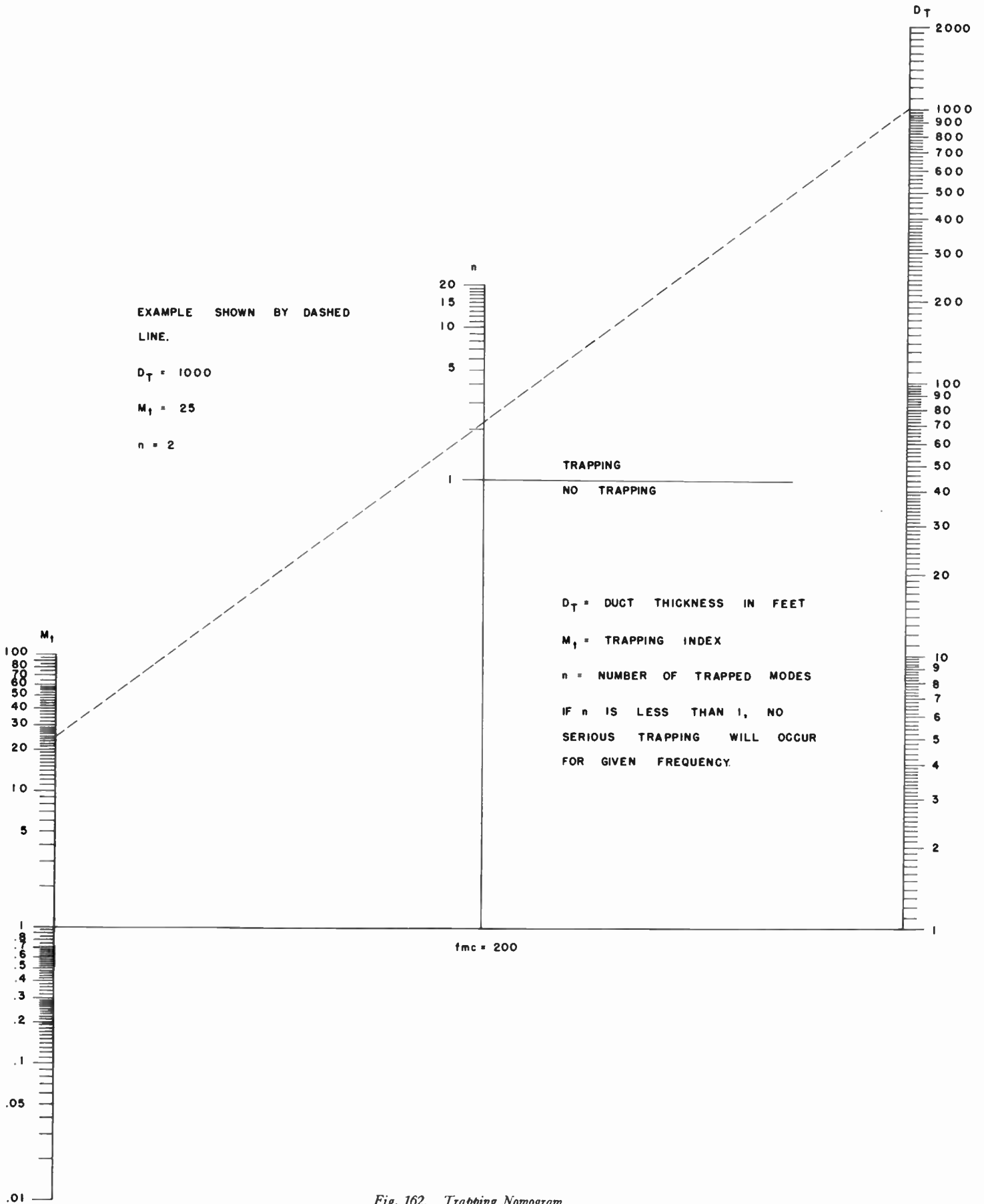


Fig. 162. Trapping Nomogram.

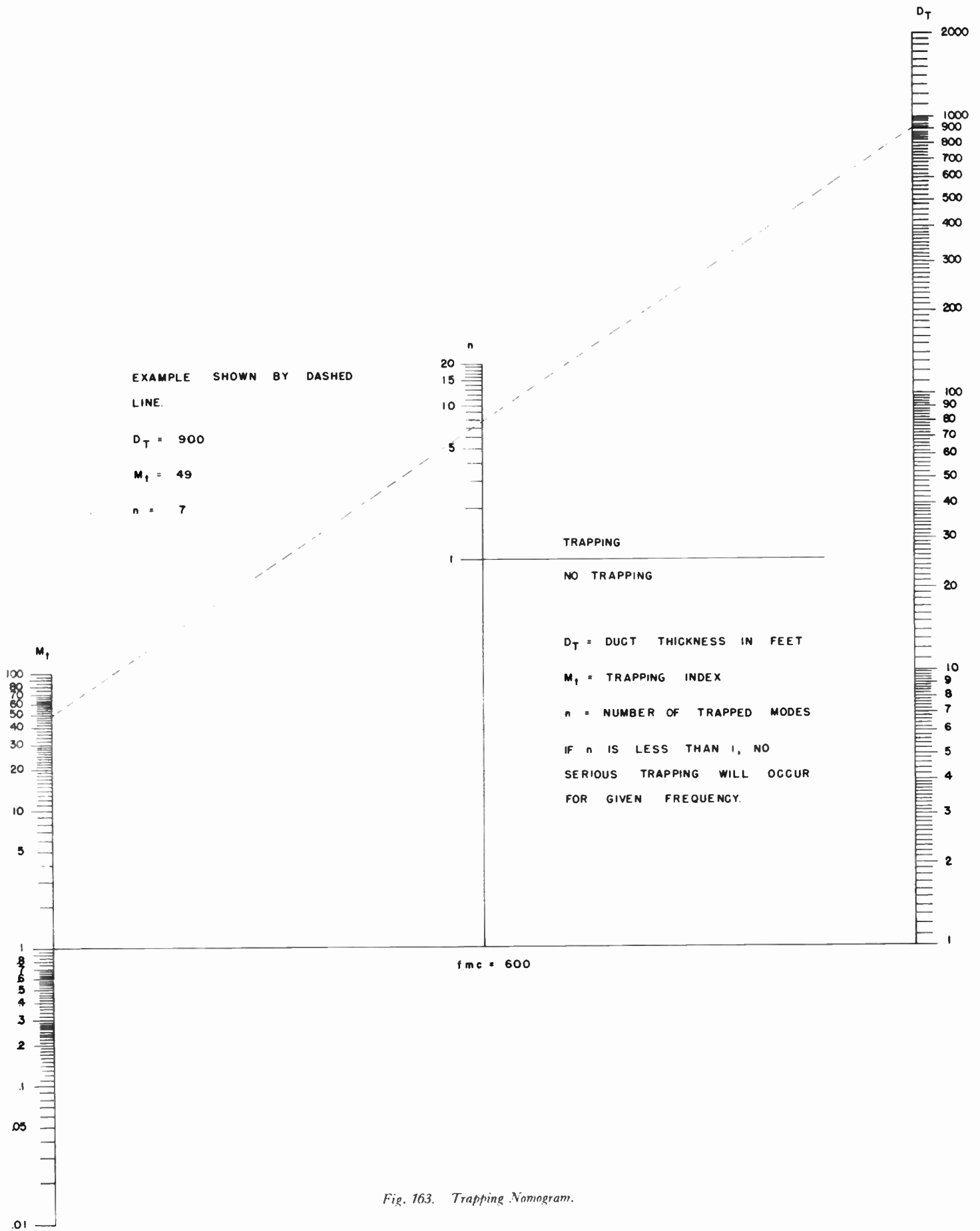


Fig. 163. Trapping Nomogram.

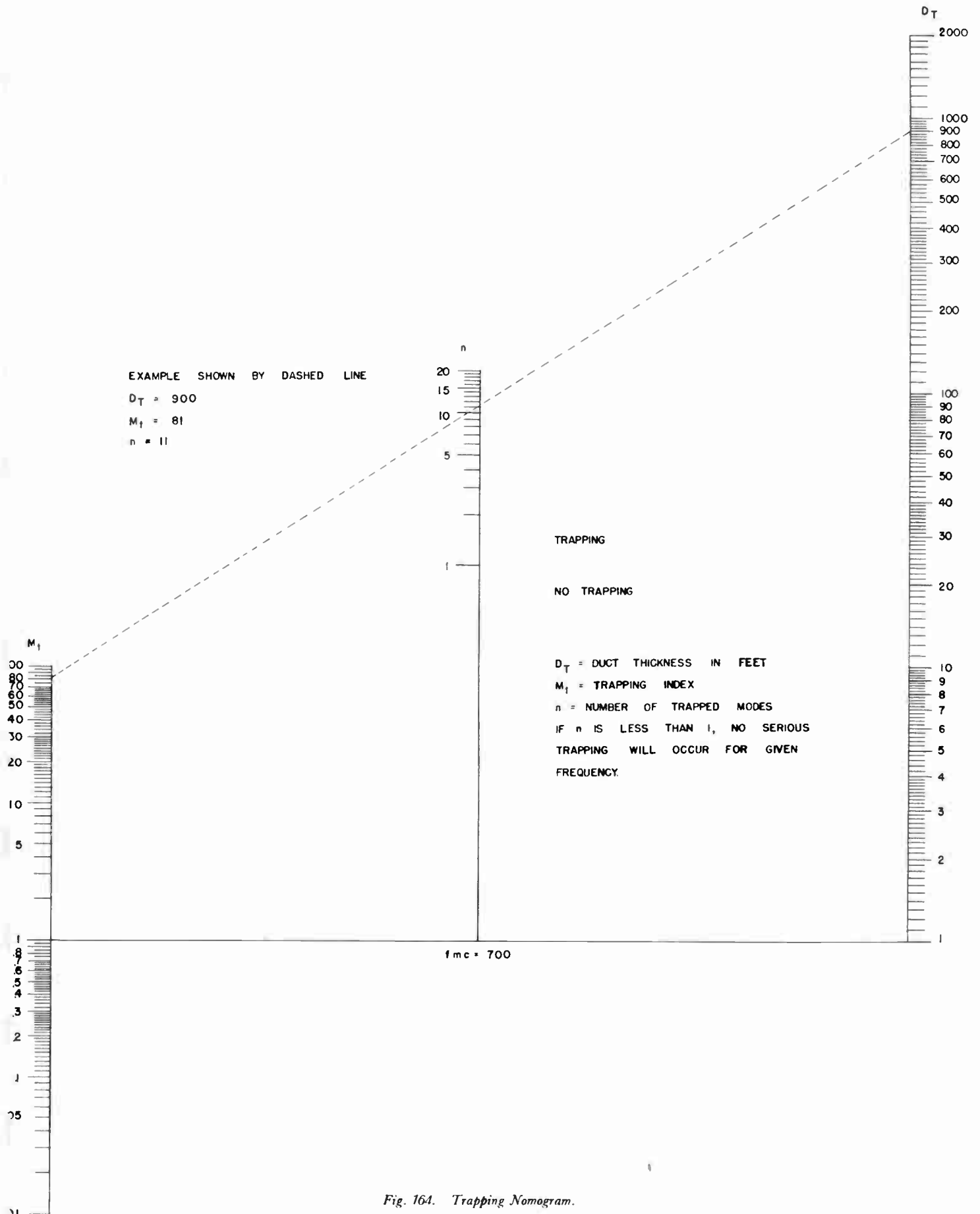


Fig. 164. Trapping Nomogram.

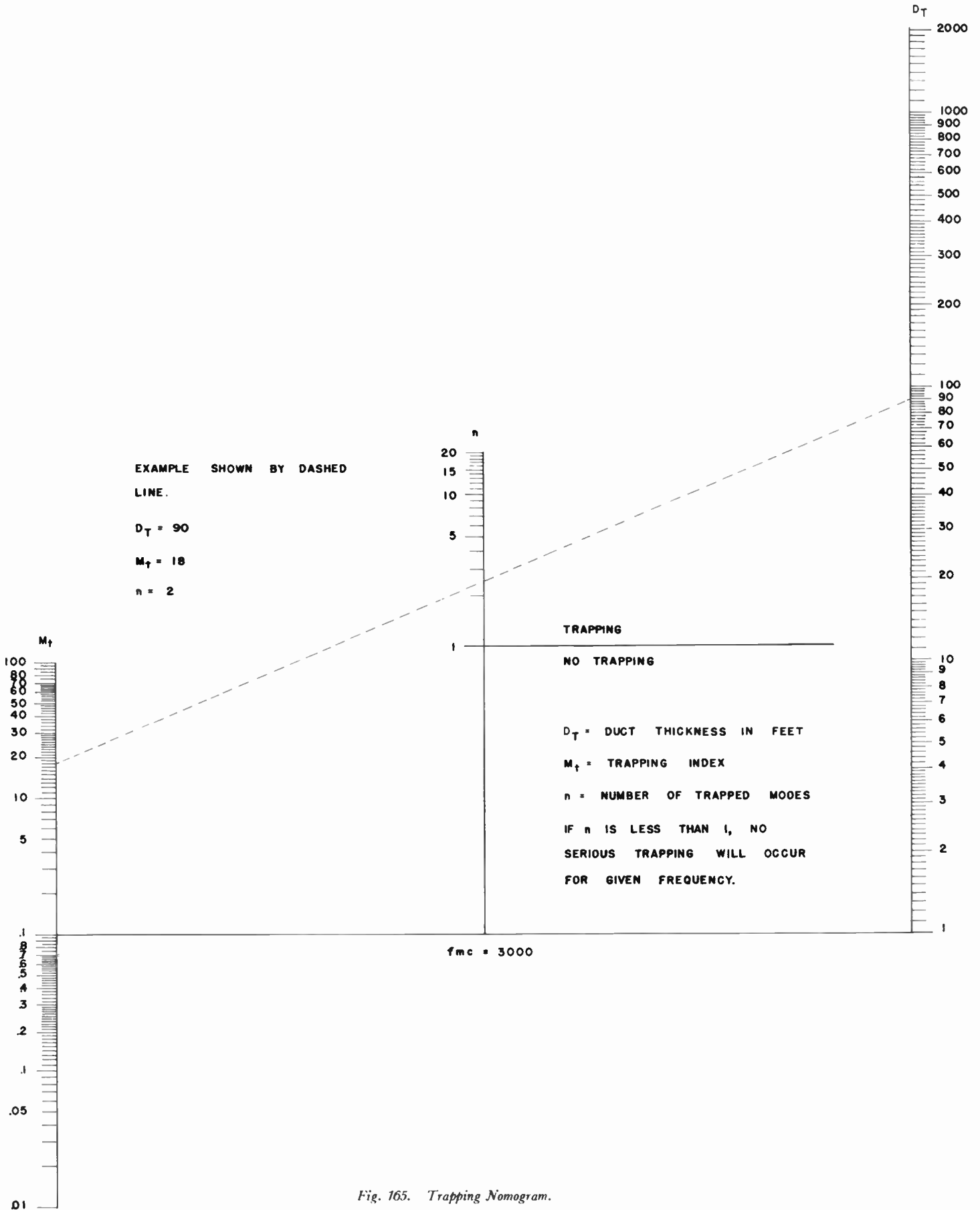


Fig. 165. Trapping Nomogram.

PROPAGATION EFFECTS DEDUCED FROM WEATHER CONDITIONS

IT IS NOT ALWAYS PRACTICABLE TO OBTAIN A SERIES OF moisture-temperature determinations with a sounding balloon or similar techniques. Are there any general rules that we can use to detect the presence of nonstandard atmospheric conditions?

Variations may lead not only to increased, but also to markedly reduced, ranges. This situation may be potentially more dangerous than that previously discussed. Again, such variation can be usually foretold only from knowledge concerning the state of the atmosphere. For example, substandard conditions often accompany low-level *advection fog*.

Advection fog results from warm, moist air flowing over colder water. The layers nearest the sea are cooled more than the elevated levels, so that a temperature inversion arises. The warmer upper levels can hold more water than the cooler low ones, so that moisture content also increases with height. This condition leads to substandard propagation. The colder the sea and the sharper the temperature increase, the more severe will be the substandard conditions.

The mere presence of fog, however, is not always an indication of the true meteorological condition. Fog, unaccompanied by a temperature inversion, will produce essentially standard propagation or may even give rise to the formation of a low-level duct. Also, over freezing water, the substandard conditions will not be marked, except where the temperature increase is very steep. It is also possible, and not uncommon, for fog to underlie an elevated duct that produces strong trapping. Generally, when the air at bridge level is warm and moist relative to the air at sea surface, conditions will be substandard whether fog is present or not.

The development of fog means that ordinary optical search fails and if, at the same time, there is a marked substandard coverage for radar operation, the situation may prove dangerous. Unfortunately, there is very little that the operator can do except to run his set at the greatest possible sensitivity, take extra precautions, and employ the higher antennas, which will tend to give the best available coverage for substandard conditions.

What types of atmospheric conditions give rise to the

trapping *M* curves and result in extraordinary ranges on VHF radio equipment? Important aerological factors that cause changes in the distribution of temperature and moisture throughout the atmosphere are the flow of warm, dry air from a land mass out over cooler sea; nocturnal cooling (principally over land); flow of cool air over warmer sea; and low-level subsidence. Subsidence is produced by descending or *subsiding* air, which tends to produce a warmer, dryer level. The phenomenon is pictured schematically in Figs. 166 and 167.

If the radar or communications operator were invariably equipped with aerological instruments and knowledge, he would be able to detect the presence of a dangerous situation. Unfortunately, under most operational conditions, he may find it inconvenient, if not impossible, to obtain accurate measurements of temperature and moisture from which to construct an *M* curve. He must, therefore, rely upon what evidence he can glean from visual observation and upon whatever rules of thumb the aerologist can give him. The aerologist is far from knowing all about the weather conditions that accompany trapping. His predictions, however, should be of considerable help to the operator.

Perhaps the best way to consider the whole question is to subdivide the significant aerological conditions into seven classifications, discussing their relative effects on radio propagation.

1. Surface (radiation) inversions.
2. Stratum of cool air blowing over warmer sea.
3. Inversions produced by warm continental air blowing over colder sea water.
4. Subsidence inversions in warm high-pressure areas.
5. Coastal stratus-type inversions.
6. Frontal inversions.
7. Post-frontal subsidence inversions in cold high-pressure areas.

Some general indications exist of surface trapping that should be emphasized before we discuss the characteristics of the various duct types.

Various rules have been stated concerning the temperature at bridge level as compared with the sea temperature. The temperature change for a standard

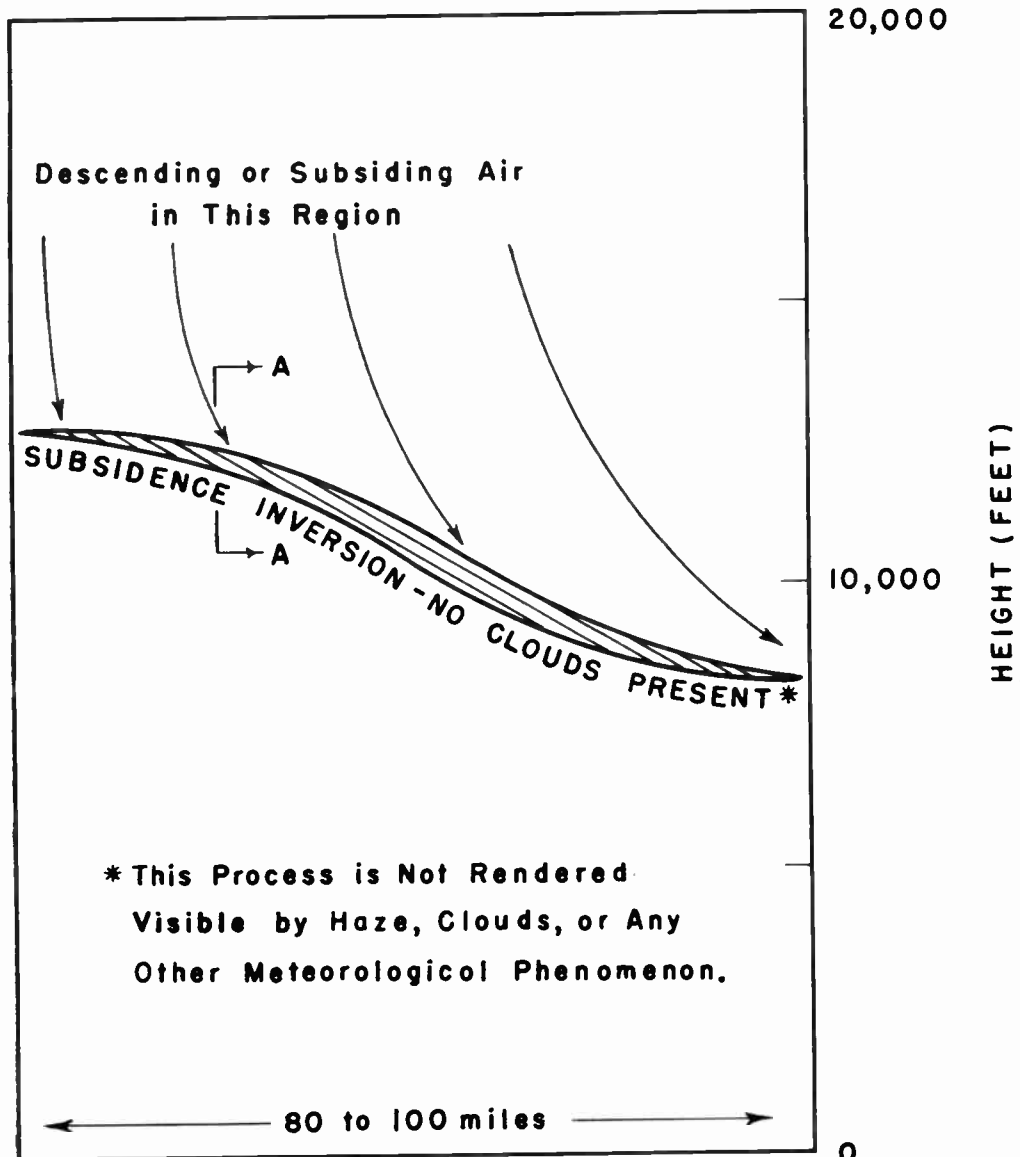


Fig. 166. Process of Subsidence.

atmosphere is a decrease of only 0.36 F per hundred feet. Thus, to expect standard propagation, one should find the temperatures at bridge and water level nearly identical.

At any rate, if the operator measures a significant difference of temperature of as much as 2°, irrespective of whether the sea is warmer or colder than the atmosphere, he may expect to find some propagation peculiarity. Trapping or partial trapping conditions may obtain in either case. The significant factor is the relative amount of water vapor in the air. If there is considerably less moisture in the atmosphere at bridge level compared with that in the air just above the sea surface, as evidenced by the wet- and dry-bulb temperatures, trapping is to be expected.

Essentially, the same condition applies over land as well as sea. If a pole or tower is available, one can check

the relative temperatures at different levels. During World War II, the British found it convenient to put recording thermometers at various elevations. The land observations have the distinct advantage over sea observations in that wet-bulb measures are simpler and more reliable at low levels.

Unfortunately, it is not always convenient to measure the moisture content, and the temperature difference between sea and bridge is not in itself a satisfactory guide of propagation conditions. If, however, the air at bridge level is 2° F or so warmer than the sea, and if this excess is clearly due to presence of a warm offshore wind, trapping may be expected. If, on the other hand, in open ocean, particularly in trade-wind areas, the bridge temperature is appreciably less than that of the water, some degree of trapping may be expected. Partial trapping of 3000-megacycle radar is a common occur-

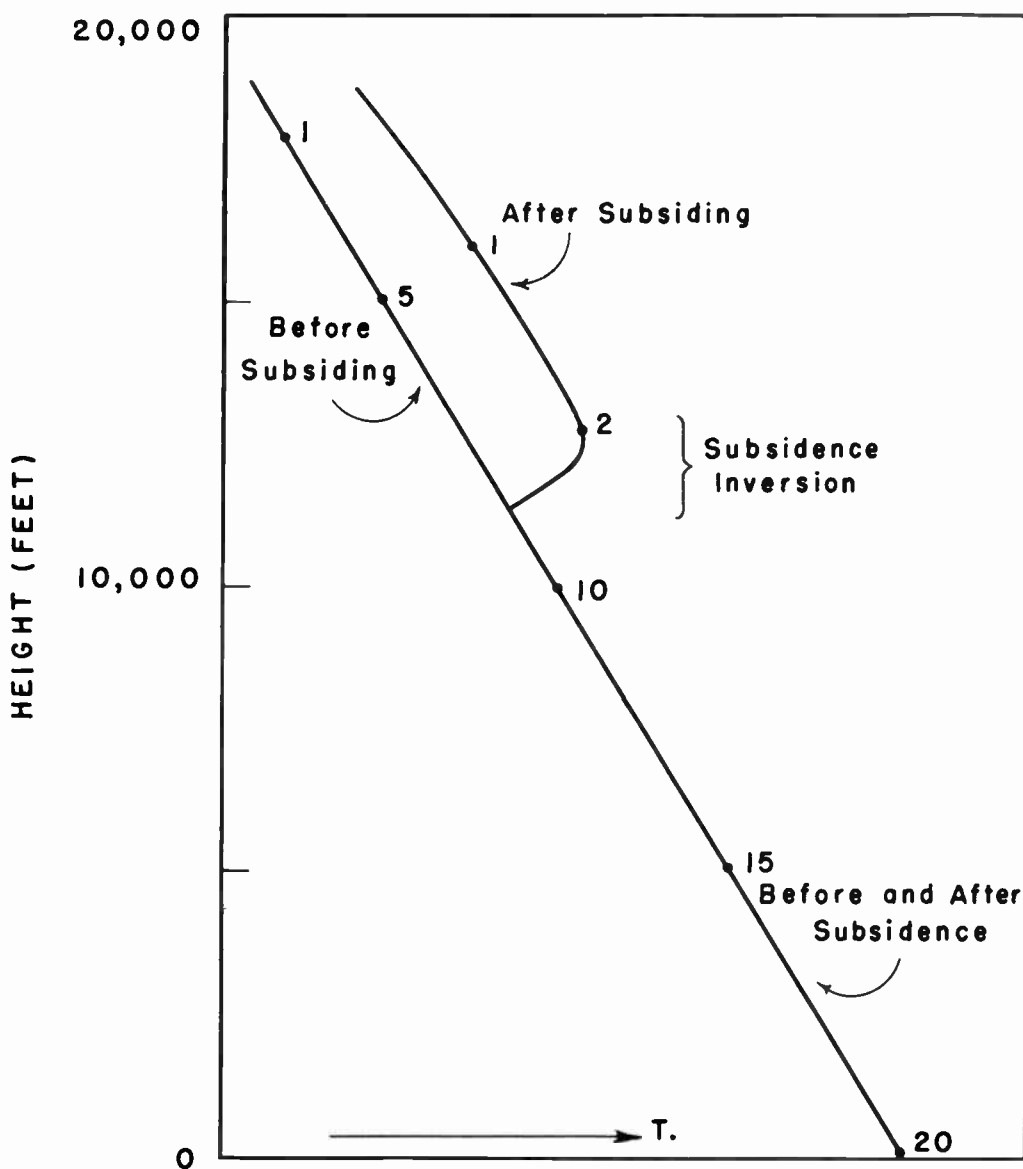


Fig. 16. Aerological Soundings before and after Subsidence. Cross-section AA of Figure 166.

rence in these areas, as extensive investigations made during World War II have proved.

Another aerological factor that materially affects propagation conditions is the presence of turbulence of the air. When the winds are gusty, the temperature and moisture variations characteristic of trapping tend to be smoothed out, and the atmosphere retains the homogeneous, well-mixed character favorable to standard propagation.

Surface (radiation) inversions result from nocturnal cooling—that is, loss of heat from the ground by radiation. Heat is radiated from the earth faster than it is dispersed by the lowest layer of the atmosphere, so that the temperature of the surface becomes appreciably lower than that of the air. A temperature inversion is established, and a low-level duct results. This nocturnal cooling is greatest when there is no overcast and, as a

result, trapping rarely occurs over land when the sky is cloudy.

Radiation ducts will be found chiefly over large, flat, land areas in the middle and higher latitudes. They will not ordinarily exist over atolls, small islands, ridges, hilltops, or large bodies of water in the tropics. They will be stronger in the higher latitudes and on the leeward shores of large islands and land masses. They are especially likely to occur over desert country. Over wooded terrain, the vegetation exerts an important effect on the cooling rate. Ground fog is often associated with surface inversions.

The operator should expect such inversions chiefly at night and in the early morning, when there are clear skies, little or no wind, and a low moisture content in the air. When the wind is strong, the skies clear, and there is little moisture in the atmosphere, the duct will generally

disappear early in the morning.

Radiation inversions rarely occur more than one or two miles offshore, and when one exists away from land the duct will be weakened and the base will gradually rise above the surface of the water.

There appear to be occasional, unexplained surface inversions over water. The reason we do not expect them is the fluid state of the water. When ground cools off, the surface remains cool. But when water cools, the layer becomes denser and sinks, a warmer layer taking its place. Since water holds so much heat energy, the cooling during the night is negligible. Consequently, the atmosphere immediately above is kept warm by its oceanic hot-water bottle.

Even so, duct formation sometimes occurs over water during the night. The phenomenon has all the characteristics of radiation inversions over land, except that the height is smaller. Despite the theoretical reasons against the existence of such inversions, it appears that the phenomenon can sometimes occur. Some of the operational aspects of such ducts will be detailed in the following chapter.

A stratum of cool air blowing over a warmer sea may also produce surface ducts. The exact aerological causes involved are not yet completely understood, but observations indicate that such ducts are extremely important for propagation over open ocean. With this particular phenomenon, there is no associated temperature inversion, and the entire effect is caused, apparently, by the evaporation of water into the lower levels of the atmosphere. Experiments conducted in the southwest and central Pacific oceanic areas show that ducts usually accompany winds that have blown for long distances over the open sea, that the height and size of the duct increase with the wind speed, and that at the higher wind speeds typical of the Pacific trade belt (10 to 20 knots), ducts of from 50 to 60 feet high occur quite generally.

These surface ducts seldom attain the height and intensity necessary to entrap the lower frequencies, but S-band and higher-frequency transmissions, from antennas situated within the duct, show marked increase in range on surface shipping and low-flying aircraft. These ducts are particularly important because they extend for such long distances and because they seem to occur so frequently. Later experiments show that the same phenomenon obtains in Atlantic waters.

Warm continental air blowing over colder sea water leads directly to duct formation by causing a temperature inversion as well as evaporation from the cooler sea into the lower levels of warm, dry air. The base of such inversions is usually at the sea surface, with the ducts themselves reaching several hundred feet upward. At

the higher latitudes (above 25° or 30°) they are most prevalent along the eastern shores of continents. If they are present in the lower latitudes, they are found instead chiefly on the western coasts. This distribution with latitude results from the normal direction of the prevailing wind, which must be offshore to produce the effect.

Ducts of this sort will form only when there is a distinct temperature difference between the sea and the air blowing from the land. Hence, conditions are most favorable to their occurrence during the summer. The height of the trapping area is usually from 200 to 600 feet, and it tends to remain level from 100 or 200 miles out to sea. At considerable distances offshore, the duct may become elevated, in which case it may funnel energy to great distances at considerable heights. Near the coast, the trapping will be strongest just after noon and weakest just after dawn.

Fog is usually not associated with inversions of this sort, but at times surface fog, observed from 5 to 10 miles out to sea, indicates the presence of such a duct. Associated with this front of warm continental air over cooler sea may be a coastal effect. The warm air may be cooled and moistened in contact with the water and may return landward in the form of a sea breeze. High-frequency radio sets located in the sea-breeze layer and directed seaward may obtain unusually long ranges.

The four types of inversions, to be discussed below, are all elevated. Unfortunately, these ducts, unlike surface ones, cannot be detected by obvious temperature and moisture variations near the surface of land or sea.

Subsidence is the slow vertical sinking of air. As a result of compression, some upper level of air becomes heated and often becomes partially dried out. This effect occurs most often in high-pressure areas, and hence is associated with clear weather rather than with storms. Subsidence produces a temperature inversion, as well as a layer of very dry air which spreads out horizontally and creates conditions favorable to the formation of a duct. Air-to-air or air-to-ground communications may be very materially affected. Such a duct is usually relatively high above the ground and may not materially affect surface propagation from a ground-based set. This statement is not always true, however, because the subsidence stratum may be intense and fall to a height of a few thousand feet. When this occurs, the purely trapping features may be sufficient to increase the ranges of all types of equipment appreciably, but the effects will generally be greater for the higher frequencies.

When the inversion boundary is sharply marked and the layer relatively thin, the radio waves may be directly reflected, and thus bounce on to greater distances. This effect, which resembles in some respects the behavior of

the ionosphere, is more pronounced for the lower frequencies and the ranges of 200-megacycle equipment may be markedly increased. The phenomenon of skip—that is, various zones of silence between the transmitter and the target—is usually associated with the reflections. Indeed, skip effects are commonly observed for most types of elevated ducts.

A phenomenon associated with subsidence ducts may be found over high, rugged country. The mountains may extend into the heated levels of the atmosphere which, having previously lost moisture by precipitation, will be hot and dry. The phenomenon is well known to those living in the Rocky Mountains, where it is referred to as a “Chinook Wind.” The more general term is “Fohn” or “Foehn” wind. If an antenna is used on a high mountain peak, around which a high-level duct is situated, a trapping condition of unusual interest may be expected. In some cases, however, the Foehn winds are forced to fairly low levels and flow out to sea where they may cause trapping.

Strong subsidence inversions in warm high-pressure areas, based from a few thousand to 20,000 feet above the ground, yield an elevated duct with associated trapping. Weak inversions of this type cause only slightly less than normal increase of M with height and have little effect on propagation. The height of such an inversion may be estimated from observation of the clouds, since stratified or thin alto-cumulus clouds usually form at the bottom of the inversions during the night or early morning. These formations persist until mid-morning.

Ducts of this type are often found in the tropics. In the trade-wind areas, they can be expected off the western coasts of continents. They are often present, but in high, weak form, in the doldrums and in moist, onshore summer monsoons. The radio operator should expect them to be more effective in summer than in winter, and he should find that a rising barometer is usually associated with lowering and intensification of the duct. The time of day is also known to have an effect upon trapping by ducts of this sort. Observations have revealed that there is a distinct tendency for the duct to rise and weaken after mid-morning and to lower and strengthen after sunset.

Coastal, stratus-type inversions—that is, underrunning of warm continental air by cool sea air—usually produce strong elevated inversions with surface ducts. When the inversions are weak and at a high level, the M curve will be of the elevated, inversion-elevated-duct variety. Ducts of this sort are produced by subsidence, but the flow of cool sea air under warm air tends to increase the inversions and produce ducts whose characteristics differ from those caused by simple subsidence. These ducts may be expected most often on the western shores of

continents in the lower middle latitudes, where the higher atmosphere is blowing offshore, with the lower, cooler portions stationary or perhaps even blowing onshore. The ducts seldom exist in the tropics, at high latitudes, or on the eastern shores of continents. They vary with the seasons, being present almost entirely in late spring, summer, and early fall. The trapping effects are found to be most pronounced during the night and early morning, and to be directly associated with the presence of abnormally cold sea water close to shore.

A front consists of a narrow zone of transition between two air masses of quite different moisture content. Through a frontal inversion, the temperature tends to decrease normally with height. The moisture content of the air, however, increases sharply through the transition region. As a result, the M curve for this region is substandard, whereas above and below the inversion conditions are standard.

The base of a frontal inversion usually starts at the ground and slowly rises with distance from the point of origin until it attains a height of from 10,000 to 12,000 feet. The mixing of the two varieties of air at the surface where they meet often leads to cloud formations. Clouds that form in layers often come with a warm front, whereas windy-looking, puffy clouds accompany a cold front. Below the boundary, rain areas, associated with masses of low-lying clouds, are frequently observed.

The propagation effects of a frontal inversion are usually small, unless the antenna or target lies close to the point where the front reaches the ground. The increase of moisture within the inversion layer leads to subnormal rather than trapping conditions.

Unusual propagation conditions caused by frontal inversions are almost entirely limited to the middle and high latitudes; they rarely extend into the trade-wind belt. The region in which they are prevalent varies with the season and with the hemisphere: in the northern hemisphere, in winter, the southern boundary is approximately 20° N, and the summer limit is 30° N; in the southern hemisphere, the winter boundary is approximately 10° S, and the summer boundary is 20° S.

Post-frontal subsidence inversions in cold, high-pressure areas are usually not strong enough to produce more than a slightly less than normal decrease in M with height. When they are intense, however, an elevated duct may form. The base of the inversion is always above the ground, with an average height of from 4000 to 8000 feet.

Except that they are found at lower elevations, these ducts are very difficult to distinguish from the warm, high-pressure-type subsidence inversions, and fleecy fair-weather clouds are often an indication of their presence.

These clouds tend to form below the base of the duct in the afternoon, to disappear in the evening, and they tend to flatten out on top. This flattened appearance can give the operator some idea as to the height of the base of the duct.

Post-frontal inversions are most frequently observed in the middle and high latitudes, never in the latitudes of

the doldrums; are stronger in winter than in summer; increase in intensity and decrease in height at night. They tend to slope upward toward, and disappear inside, the center of high-pressure areas. Their effects on propagation are similar to those produced by inversion in warm, high-pressure areas.

OPERATIONAL APPLICATIONS IN TROPOSPHERIC PROPAGATION

THE OPERATOR SHOULD EXERCISE GREAT CAUTION IN attributing failure or unexpected variations in the behavior of his equipment to trapping. It must be reemphasized that trapping rarely affects high-frequency waves unless they are transmitted at angles of less than 1° relative to the horizontal. Actually, trapping rarely occurs at angles greater than 0.5° , but since a duct may be inclined, this angle of inclination must be added to the 0.5° . It is safer, therefore, to consider the possibility of trapping at any angle up to 1° . When unusually short ranges occur, the operator should first check his equipment carefully before blaming atmospheric conditions.

Some operators have been mystified by the apparent fluctuations of reliable ranges for aircraft, where the ranges for surface craft show much smaller variations. Such variations are entirely to be expected. Fast-moving planes change aspect continually, and the signal may scintillate in consequence, whereas the slower-moving ship exhibits a much steadier signal. The roll and pitch of the ship, however, produce as much as five db change in signal strength.

Quite apart from this effect, it should be noted that a set operating, say, 6 db below normal, would find aircraft ranges diminished by approximately 40 per cent, whereas the limiting ranges for surface craft would be decreased only 20 per cent, or possibly even less. Even this 20 per cent loss might be masked by the presence of a small surface duct which could more than make up for the reduced power. In consequence, the operator might believe, from his observations of surface craft, that his set was functioning better than normal, whereas in reality, his aircraft coverage might be dangerously low. Thus, it becomes obvious that the use of standard targets, corner reflectors, mountains, or large surface craft to test the efficiency of radar equipment is extremely hazardous. Use the echo box, if one is available, to check your equipment.

Knowledge of atmospheric conditions and their effect on high-frequency propagation can be put to important operational use. All types of equipment are affected: search radar, beacons, and communication units—surface, air-to-ground, and air-to-air.

During World War II, when the danger of premature detection by the enemy was ever present, the operator always had to consider the possibility of trapping. When a duct is present, the enemy can intercept signals at far greater ranges than might ordinarily be expected.

When trapping was known to be present and a choice of frequencies was available, the lowest frequencies were safer, since the higher ones were far more susceptible to trapping.

An exception to this rule occurs, however, for a sharp, elevated inversion, which may reflect the lower frequencies more effectively than the high ones. Altering the height of the antenna may also diminish the trapping effect. Only if the antenna lies well within the duct will unusually great ranges be ordinarily expected to occur. When the antenna is above the top or below the bottom of the duct, the signal intensity within the duct will usually be fairly low and the effects of superrefraction reduced.

Remember that the *line of sight* theory for VHF, UHF, and SHF equipment is only a myth. On occasion, radio silence was as necessary on these frequencies as in the lower communication band. Operators were continually warned to guard against the unnecessary or unauthorized use of the equipment.

If the operator were aware of the atmospheric conditions and their effect upon transmission, he could improve his countermeasures and increase the likelihood of the success of specific operations. For example, if he knew that a duct was present, he would expect the enemy radar also to be operating with greater ranges and he could advise that jamming be turned on earlier than usual. The operator could also make helpful suggestions as to the best direction for attack. For example, winds, in passage over land, frequently become altered, and a duct forms on the leeward shore of the island. If the primary consideration is to avoid detection, one should attack with the wind rather than against it. In this respect the best procedure runs contrary to the old custom of the woodsman who stalks against the wind in order that the sensitive nostrils of his game will not be able to detect him.

A possible exception to this rule lies in the open ocean

when a duct is formed by a cool wind blowing over warmer water. Here, the duct extends in all directions, and there is little choice in direction of approach.

All of the effects mentioned above, used for tactical purposes of war, have their counterpart in peacetime operations. There are dangers of interfering signals from great distances under duct formation. There are losses of range that may prove equally troublesome. But an understanding of the atmospheric problems will greatly assist the operator in locating propagation troubles.

In the previous chapter, we mentioned that surface inversions occasionally were found over sea as well as over land, although the reason for their occurrence is not fully understood. In certain areas, radars, operating with very low antennas, displayed the long ranges that accompany trapping conditions.

Submarines were frequently troubled with ghost signals from multiple reflections. The radar impulse from the submarine *A* would strike target *B*, and return to *A*, where it would be reflected again to *B* and back to *A*. Or multiple reflections might involve several targets, as for example, over a path such as *ABCABA*. The total distance might well exceed the time delay for the first sweep, and the image would appear on a higher sweep. The effect is not dissimilar to that of the radar mirage discussed in Chapter 16.

The ghost images would often streak across the PPI scope at phenomenal speeds for surface craft. This peculiarity arose from the fact that the distance *ABABA* is changing twice as rapidly as the distance *ABA*.

This rapid motion called special attention to these images. As the time delay of *ABABA* decreased to just slightly more than the first-sweep delay, the image showed up on the screen very near the center. The operator seemed to be steering a collision course. Veering ship had little effect. Only reversal of course would have kept the image from moving in to the center. Just at the moment when the path delay corresponded to that of the pulsing frequency and collision seemed imminent, the image vanished.

These "galloping ghosts," as they came to be known, caused no end of worry until the phenomenon was identified with radio-propagation peculiarities, not with some mysterious countermeasure designed by the enemy. The point is that the low-level duct and low antenna conspired to concentrate the radar pulses in a thin layer just above the water. The beam, even after a number of scattered reflections, was still intense enough to record on the PPI screen.

Similar propagation effects are expected to give occasional trouble with racons and responder beacons. A

signal may trip, not only the nearest set, but a number of more distant ones, with resultant confusion. Or echoes from buildings or mountains may trigger a responder mechanism and produce records which, if improperly interpreted, can lead to calamitous results.

During World War II, the inverse effect was often encountered and, until it was recognized, led to the loss of many planes. When trapping exists, we expect extended ranges within the duct. But the increased ranges from below are usually counterbalanced by decreased ranges from above. A plane, flying within sight of its base, but with an altitude less than 1° above the horizontal, may not be able to get its VHF or SHF signal through the barrier formed by the top of the duct.

The ordinary procedure for increasing one's range is to increase altitude. Normally, this works well when standard atmospheric conditions prevail. But, if a duct exists, the gain in altitude may not be enough to overcome the reflective action of the duct. So frequently did planes come near enough to the base that was trying frantically to signal them and then move on out to sea and be lost, that the operational problem became very severe. When the source of the difficulty was finally recognized, the answer appeared to be quite simple. To establish contact, fly at a low level, within the duct if possible. The long ranges of reception enabled many planes, otherwise lost, to return safely.

Trapping may be the cause of apparently inexplicable failures in communication. Subsidence ducts, unless at a very low level (as on the western coast of continental areas), do not have much effect on ground-to-ground or ground-to-air communication. If a plane flying within the duct attempts to contact another above or below the trapping area, the duct may act as a barrier. The waves will be unable to penetrate this area, and communication will be impossible.

A pilot can combat the effect of a duct by selecting the proper altitude for flight. Since the top of a duct is often indicated by a stratum of very quiet air, the pilot may be tempted to select this level. The best procedure, however, is to avoid this area of uncertain communication and fly, instead, considerably higher or lower.

During World War II, pilots, by utilizing knowledge of aerological conditions, were often able to pick out paths where enemy signal strength was low. Especially was this true for low frequencies for which the lobes are spaced farther apart and are more clearly defined. The concentration of energy within the duct made it extremely dangerous to fly within the trapping area. The pilot was directed to select a height just above or, if possible, just below the top of the duct.

Planes employing radar to home on a target would

often be able to pick up the enemy signals in advance of the time when they themselves would be detected by the enemy. This is true because the enemy signal, being a two-way transmission, had to travel both to the plane and back to the transmitter. Thus, it had less intensity at the enemy listening post than at the plane's receiver. In this way, the pilot was able to select the *null* lines, or regions of lowest signal intensity, and fly along those paths, and thus delay detection.

Under conditions approaching those of standard propagation, the lobes of high intensity are separated by regions where the signal level is low. An approaching plane, flying at a constant (but unknown) altitude will alternately give strong and weak reflections as it moves through the different lobes. If the plane did not alter its altitude, the operator could often estimate the height from knowledge of the distance (obtained directly from the radar record) and of the lobe pattern, particularly the null lines. It is altogether probable that this principle may find some useful application to peacetime pursuits. If no direct way appears for employing the information, there is at least the inverse study of lobe positions to indicate the character of the radio-propagation conditions.

Since small differences in the antenna height may make an appreciable difference in the intensity of the received signal, the operator of land-based equipment should be aware that the rise and fall of the tide may affect the performance of his set. The lowering of the antenna when there is a surface duct may increase the range, whereas the customary high antenna may actually be less efficient.

Experiments in the Atlantic trade-wind area indicate the presence of persistent low-level ducts over the ocean, which effect a substantial increase in range of S-band and higher-frequency signals. On S-band transmissions, increasing the antenna height up to at least 100 feet tended to improve the signal strength, whereas still higher frequencies operated more efficiently with somewhat lower antennas.

Aerologists are at present studying carefully the various ways in which weather affects high-frequency radio propagation. It is hoped that some day they will have developed a program of forecasting duct conditions by means of which complete and accurate radio coverage may be predicted. Since this goal has not yet been attained, the operator must utilize the information at his disposal.

The rules here given are by no means infallible. Radio propagation for the frequencies under consideration is determined by atmospheric conditions and closely associated with the weather. No one expects the weather forecast to be 100 per cent accurate, but applications

even of imperfect rules will lead to useful results. Therefore, we would do well, before closing this discussion, to summarize several rules by which the operator may, without the aid of aerological equipment, detect the presence of a duct, and thus make use of the suggestions given above. The observer should expect trapping when:

1. A wind is blowing from land.
2. There is a stratum of quiet air.
3. There are clear skies, little wind, and high barometric conditions.
4. In open ocean when a cool breeze is blowing over warm ocean, especially in the tropic areas and in the trade-wind belt.
5. Smoke, haze, or dust fails to rise, but spreads out horizontally.
6. There are skips in the ground clutter on his scope; for example, when near-by islands are not received on the scope.
7. There is strong fading of the pip. A rapidly fading pip may indicate a duct with ranges on a higher sweep. This rule, however, is not universally true. The duct may be well formed and steady; or when there are standard conditions, changes in the aspect of the target may cause rapid scintillations of the signal.
8. The moisture content of the atmosphere at bridge level is considerably less than that just above the sea surface.
9. There is an offshore wind and the temperature at bridge level is 1 or 2° F greater than that of the sea.
10. In open ocean, the temperature at bridge level is definitely less than that of the sea.
11. In trade-wind areas, generally, for frequencies of 3000 megacycles and higher, with low-level antennas.
12. The potential temperature of the upper air (around 2000 feet) is 10 F or more greater than the surface value,* while at the same time the mixing ratio of the upper air is 5 grams per kilogram or more below the surface value.

Rain, snow, and hail have definite effects on the propagation of radio waves in the VHF to SHF range. Storm clouds and abrupt discontinuities in the air influence radio transmissions.

The magnitude of the disturbances increases with frequency. Frequencies of 3000 megacycles suffer a loss of only 3 to 4 db per 100 km through a rain storm where the precipitation is 10 cm per hour. But 30,000-megacycle signals are attenuated by as much as 2 db per km

* The surface temperature must be compared, not with the actual temperature of the upper atmosphere, but with this temperature corrected to the surface on the assumption that temperature increases by 5 F for every 1000 feet we descend. This corrected temperature of the upper atmosphere is known as its *potential temperature*. Thus, at a height of 2000 feet, an actual temperature of 60 F represents a potential temperature of 70 F.

through a precipitation of 1 cm per hr. Thick fog, with visibility of the order of 100 feet, produces attenuations of the same order as those given above for the rains.

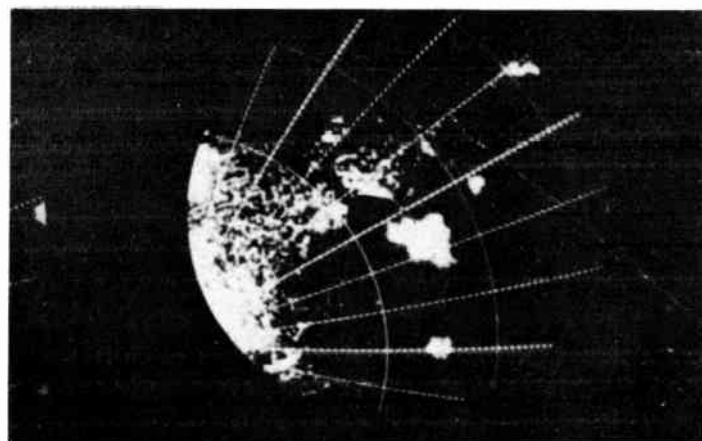
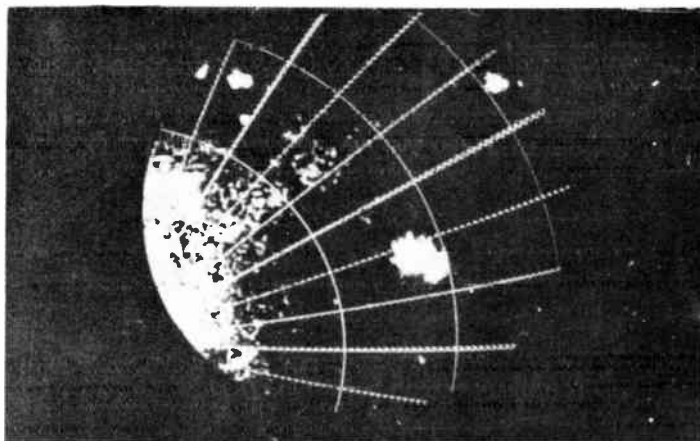
These effects indicate that the extremes of radio frequencies are subject to limitations. Within certain frequency intervals (at about 10,000 megacycles) absorption by water vapor and other gases of the atmosphere begins to be appreciable.

Scattering of radio waves from clouds or precipitation has certain uses, however. Radar of 3000 megacycles and higher gives one a picture of storms in the vicinity. A line of hazy patches may indicate a cold front. A series of spiral curves may denote the proximity of a hurricane.

Weather observers are thus finding radar a useful adjunct in the complex problem of forecasting. A pilot

ers are set at 10-mile intervals. The radials are 10° apart. The white return on the left side of each picture is ground clutter. However, the white spot in (a) at a range of about 18 miles is a return from a cloud. The top of this cloud, wherein there were sufficient water particles to give a visible return on the scope, was determined to be 35,000 feet. It was raining on the ground. Pictures (a) and (b) show both the direction and the velocity of the movement of the cloud during a 5-minute interval.

Fig. 169 shows a series taken on the USS Wasp. Fig. 169a was taken on December 18, 1944, 400 nautical miles due East of Manila, Philippine Islands, and shows a typhoon. This radar picture does not show the "eye," or center, of the typhoon as would be observed visibly on the surface of the sea because of the curvature of the earth. Furthermore, although visibly the eye of



Figs. 168(a) and (b). PPI Scopes.

of a plane may discern a heavy storm in his path and veer his course to avoid the most hazardous portions.

The various types of storms that imprint characteristic features on a radar scope of 3000 megacycles and above, are showers, squall lines, thunderstorms, cold fronts, warm fronts, occluded fronts, typhoons, hurricanes, and tornadoes. The range of detection depends upon the vertical extent of the storm. Approximate vertical extent and ranges are

Extent	Range of Detection
5,000 feet.....	85 miles
10,000 feet.....	120 miles
20,000 feet.....	175 miles

Typical echoes from various types of meteorological conditions are shown in Figs. 168 to 170. Figures 168a and 168b are PPI pictures taken in the vicinity of Orlando, Florida, at 5:25 p.m. and 5:35 p.m. on July 30, 1946. They were taken by the Weather Bureau Thunderstorm Research Project, which is a joint undertaking of the Weather Bureau, Army, Navy, and National Advisory Committee for Aeronautics. The range mark-

the typhoon might be completely filled in, it is not filled in from a radar-propagation viewpoint because of insufficient precipitation.

Figs. 169b to 169e show another typhoon about 200 miles SSW of the southern tip of Japan in the North Pacific on the edge of the East China Sea. This storm was moving along a trough oriented NNW-SSE. There were widely scattered rain showers throughout the area in the early period of the storm. There was light, continuous rain associated directly with the typhoon. At no time was there a great intensity of rain and blowing spray in this storm, as compared to other storms experienced in this general area. In other words, this disturbance might be classed as a *moderate typhoon*. Additional explanation of these four scope pictures is given in conjunction with the photographs. It is of considerable interest to note that this typhoon developed meteorological conditions that produced trapping wherein VHF and higher-frequency signals were picked up over approximately a 600-mile distance. No upper air soundings

were made to verify the exact M curve produced by the variations of temperature and mixing ratio aloft.

Fig. 170 is a photograph by the U.S. Army Signal Corps of a synoptic chart showing the Spring Lake area and giving the position of a cold front 15 minutes before the scope picture was taken, which shows the appearance of the radar PPI scope with the passage of a cold front.

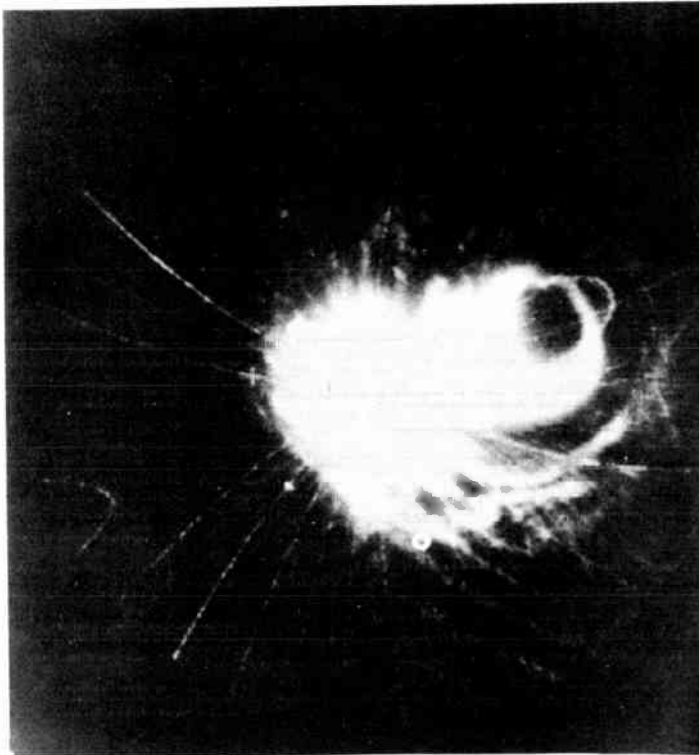


Fig. 169(a). Photo No. 1. Item Time: 1100. Approx. Ship's Position: $14^{\circ}29.4'N$. $127^{\circ}39'E$. True Bearing and Distance Storm Center: 077° , 39 miles. Wind Direction and Force: 336° , 57 knots, gusts to 66 knots. Pressure: 994.5 mbs. (29.37"). Precipitation ceiling of less 500'. Visibility: 800-1200 yds. State of sea: Very High. (20'-40'.)

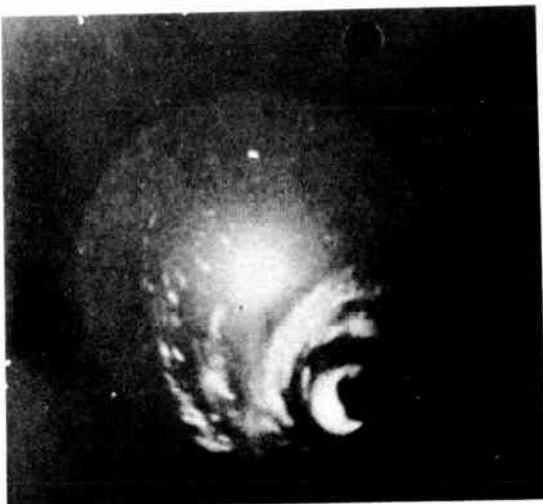


Fig. 169(b). Photo No. 1. Aug. 26, 1945. Item Time: 1115.



Fig. 169(c). Photo No. 2. Aug. 26, 1945. Item Time: 1130. True Bearing and Distance Storm Center: 149° , 68 miles. Wind Direction and Force: 035° , 32 knots. Pressure: 998.4 mbs. (29.48"). Stratus overcast at 1000 Feet. Visibility: 4 miles in haze. State of sea: Very rough. (18'-24'.)

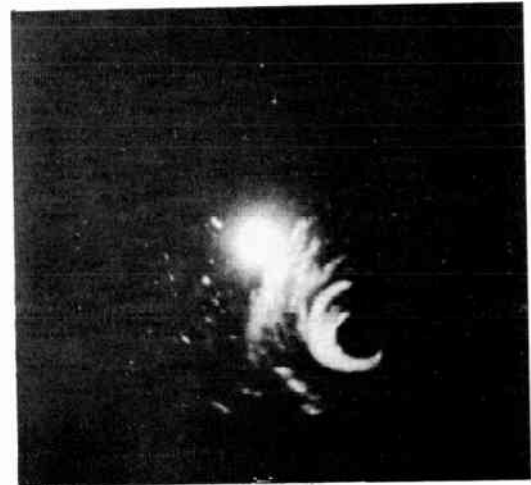


Fig. 169(d). Photo No. 3. Aug. 26, 1945. Item Time: 1145.



Fig. 169(e). Photo No. 4. Aug. 26, 1945. Item Time: 1200. Ship's Position: $29^{\circ}31.0'N$. $132^{\circ}40.2'E$. True Bearing and Distance Storm Center: 138° , 54 miles. Wind Direction and Force: 030° , 34 knots. Pressure: 997.0 mbs. (29.44"). Stratus overcast at 1000 feet. Visibility: 2 miles in blowing spray and haze. State of sea: High (20'-30').

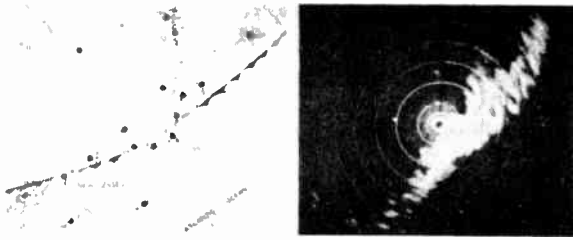


Fig. 170.

Fig. 171 depicts the development of trapping conditions. At 2200, the ranges, shown by the extent of ground clutter, were nearly normal. Beginning at 2400 and increasing from 0100 to 0300, the PPI scope shows extended ranges in the upper left-hand sector. By 0400, the duct had nearly disappeared.

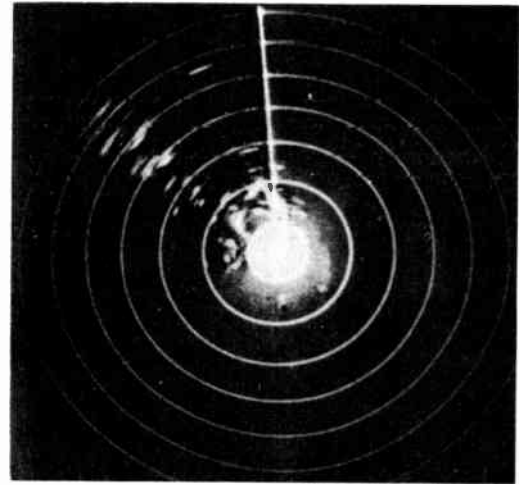


Fig. 171(c). 0100 EWT.

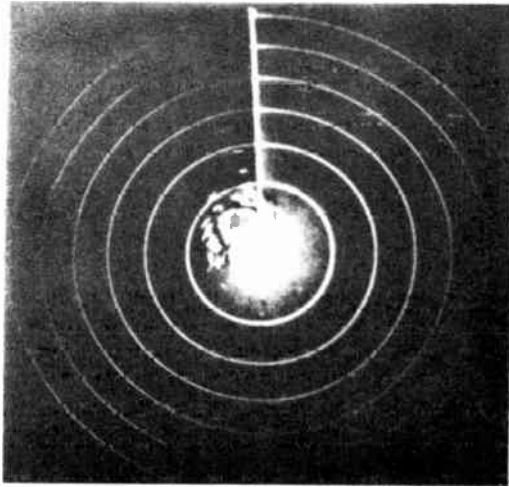


Fig. 171(a). 2200 EWT.

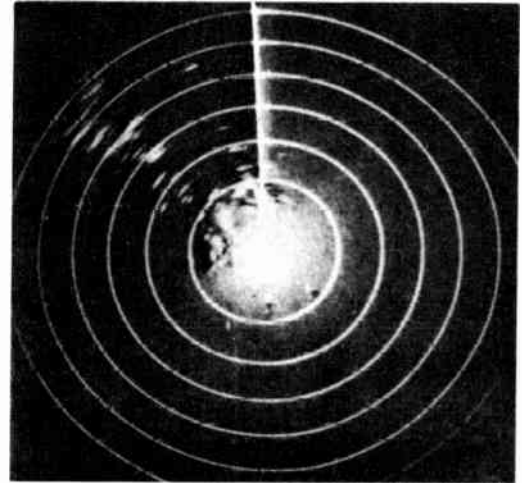


Fig. 171(d). 0300 EWT.

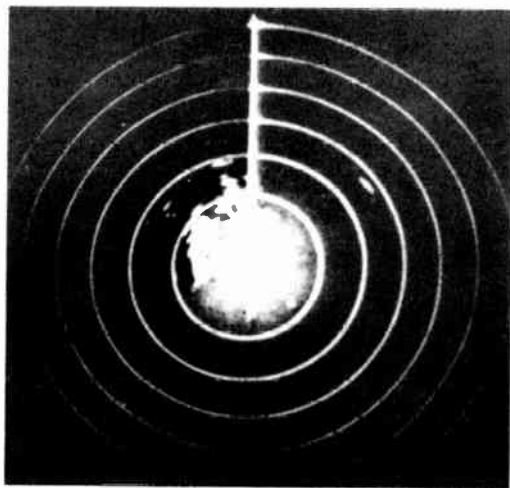


Fig. 171(b). 2400 EWT.

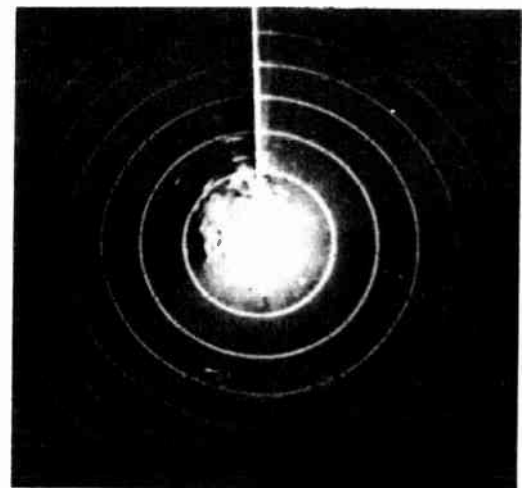


Fig. 171(e). 0400 EWT.

THEORY OF IONOSPHERIC PROPAGATION

FOR THE BENEFIT OF THOSE WHO ARE INTERESTED IN THE basic theory of radio propagation, the following technical summary provides an introduction to the subject. The starting point of the analysis, as for most studies involving electricity, magnetism, and radiation, lies in the fundamental equations of Maxwell. These are, in vector notation,

$$\text{Curl } \mathbf{H} = \nabla \times \mathbf{H} = \frac{\kappa}{c} \frac{\partial \mathbf{E}}{\partial t} + \frac{4\pi}{c} \mathbf{J}. \quad (1)$$

$$\text{Curl } \mathbf{E} = \nabla \times \mathbf{E} = -\frac{\mu}{c} \frac{\partial \mathbf{H}}{\partial t}. \quad (2)$$

$$\text{div } \mathbf{H} = \nabla \cdot \mathbf{H} = 0 \quad (3)$$

$$\text{div } \mathbf{E} = \nabla \cdot \mathbf{E} = 4\pi\rho/\kappa \quad (4)$$

$$\mathbf{F} = m \frac{d\mathbf{v}}{dt} = -\epsilon[\mathbf{E} + (\mu/c) \mathbf{v} \times \mathbf{H}] \quad (5)$$

∇ is the vector operator: $\nabla = \mathbf{i} \frac{\partial}{\partial x} + \mathbf{j} \frac{\partial}{\partial y} + \mathbf{k} \frac{\partial}{\partial z}$.

\mathbf{H} and \mathbf{E} are the intensities of the magnetic and electric fields.

\mathbf{J} is the current.

μ and κ are the magnetic permeability and dielectric constant, herein supposed to be independent of time.

ρ is the density of electric charge.

c is the velocity of light.

ϵ and m are the electronic charge and mass.

\mathbf{v} is the electronic velocity.

\mathbf{F} is the force acting on a moving electron.

First of all, let us develop the solution of these equations for free space, where $\mathbf{J} = 0$, $\rho = 0$.

Differentiating (1) and (2) partially with respect to t , we get

$$\nabla \times \frac{\partial \mathbf{H}}{\partial t} = -\frac{c}{\mu} \nabla \times \nabla \times \mathbf{E} = \frac{\kappa}{c} \frac{\partial^2 \mathbf{E}}{\partial t^2}, \quad (6)$$

and

$$\nabla \times \frac{\partial \mathbf{E}}{\partial t} = \frac{\kappa}{c} \nabla \times \nabla \times \mathbf{H} = -\frac{\mu}{c} \frac{\partial^2 \mathbf{H}}{\partial t^2}. \quad (7)$$

But

$$\text{curl curl} = \nabla \times \nabla \times = \nabla \nabla \cdot - \nabla^2 \quad (8)$$

by a familiar vector transformation. Thus

$$\nabla^2 \mathbf{E} = \frac{\mu\kappa}{c^2} \frac{\partial^2 \mathbf{E}}{\partial t^2} + \nabla \nabla \cdot \mathbf{E} \quad (9)$$

and

$$\nabla^2 \mathbf{H} = \frac{\mu\kappa}{c^2} \frac{\partial^2 \mathbf{H}}{\partial t^2} + \nabla \nabla \cdot \mathbf{H}, \quad (10)$$

where

$$\nabla^2 = \frac{\partial^2}{\partial x^2} + \frac{\partial^2}{\partial y^2} + \frac{\partial^2}{\partial z^2}.$$

But

$$\nabla \cdot \mathbf{E} = \nabla \cdot \mathbf{H} = 0 \quad (11)$$

so that \mathbf{E} and \mathbf{H} generally satisfy the wave equation:

$$\nabla^2 \psi = \frac{n^2}{c^2} \frac{\partial^2 \psi}{\partial t^2}. \quad (12)$$

In this equation, the wave velocity is c/n , so that n is the index of refraction. Since the velocity must be c in free space, we have

$$n = \mu\kappa = 1.$$

We have chosen our electrostatic system of units so that

$$\mu = \kappa = 1$$

for a vacuum. The wave equation has many possible solutions, whose forms are dictated by boundary conditions. For radio transmission, the boundary is simply the antenna itself. Our concern, however, is with the wave in the ionosphere. In this region we can, to a first approximation, consider the wave as plane.

Take the z axis as the direction of propagation, and assume the solution

$$\left. \begin{aligned} \mathbf{H} &= iH_0 e^{i\omega \left(t - \frac{nz}{c}\right)} \\ \mathbf{E} &= jE_0 e^{i\omega \left(t - \frac{nz}{c}\right)} \end{aligned} \right\} \quad (13)$$

The \mathbf{H} and \mathbf{E} vectors are perpendicular to each other and also to the axis of propagation. Setting $\psi = \mathbf{E}$ and \mathbf{H} in turn, we find that equations (13) satisfy the condition (12).

Now suppose that the wave passes through an ionized medium containing N electrons per unit volume. The electronic motions conform to equation 5,

$$\frac{d\mathbf{v}}{dt} = -\frac{\epsilon}{m} \mathbf{E} = -j \frac{\epsilon}{m} E_0 e^{i\omega \left(t - \frac{nz}{c}\right)}, \quad (14)$$

so that

$$\mathbf{v} = \mathbf{v}_0 - j \frac{\epsilon E_0}{im\omega} e^{i\omega \left(t - \frac{nz}{c}\right)} = \mathbf{v}_0 + \frac{\epsilon}{m\omega^2} \frac{\partial \mathbf{E}}{\partial t}, \quad (15)$$

where \mathbf{v}_0 is the initial velocity of the free electron. The total current density produced by N electrons is

$$\mathbf{J} = -\Sigma \epsilon \mathbf{v} \quad (16)$$

In the summation, the initial \mathbf{v}_0 's of the electrons are randomly

oriented. Hence the effect cancels out and we are left with the value:

$$\mathbf{J} = -\frac{N\epsilon^2}{m\omega^2} \frac{\partial \mathbf{E}}{\partial t}. \quad (17)$$

Introducing this value for \mathbf{J} in equation (1), wherein we take $\kappa = 1$ for the free-space portion, we get

$$\nabla \times \mathbf{H} = \frac{1}{c} \left(1 - \frac{4\pi N\epsilon^2}{m\omega^2} \right) \frac{\partial \mathbf{E}}{\partial t}. \quad (18)$$

The equation is of the original form if we set

$$\kappa = 1 - \frac{4\pi N\epsilon^2}{m\omega^2} = n^2. \quad (19)$$

The phase velocity, V_p ,

$$V_p = c/n = c / \left(1 - \frac{4\pi N\epsilon^2}{m\omega^2} \right)^{1/2}, \quad (20)$$

is therefore greater than c . The signal or group velocity, V_g , becomes

$$V_g = V_p / \left(1 - \frac{\omega}{V_p} \frac{\partial V_p}{\partial \omega} \right) = c \left(1 - \frac{4\pi N\epsilon^2}{m\omega^2} \right)^{1/2}. \quad (21)$$

Thus the presence of a charge retards the signal.

Since

$$\omega = 2\pi \cdot 10^6 f_{mc}, \quad (22)$$

where f_{mc} is the frequency in megacycles, we have

$$n^2 = 1 - \frac{N\epsilon^2 \times 10^{-12}}{\pi m f_{mc}^2}. \quad (23)$$

When we reduce the frequency to satisfy the equation

$$f_{mc}^2 = \frac{N\epsilon^2 \times 10^{-12}}{\pi m} = 8.1 \times 10^{-5} N, \quad (24)$$

where

$$\begin{aligned} \epsilon &= 4.77 \times 10^{-10} \text{ e.s.u.}, \\ m &= 9.01 \times 10^{-28} \text{ g.}, \end{aligned} \quad (25)$$

n becomes zero, and the phase velocity infinite. This critical frequency and all lower frequencies are simply reflected at the layer. Higher frequencies penetrate the layer. This relationship is, therefore, fundamental in ionospheric studies.

The presence of the earth's field somewhat complicates the picture. Let \mathbf{H}^0 represent the magnetic field of the earth. Choose the axis of the coordinates so that the z axis lies in the direction of propagation. Let \mathbf{H}^0 have a component \mathbf{H}_L in this direction. The transverse component, except for a minor effect caused by radiation pressure, can be neglected. We also can omit the small terms in v/c arising from the electromagnetic field. Thus our equations of motion become

$$\left. \begin{aligned} \frac{d^2x}{dt^2} &= -\frac{\epsilon}{m} E_x - \frac{\epsilon\mu}{mc} H_L \frac{dy}{dt}, \\ \frac{d^2y}{dt^2} &= -\frac{\epsilon}{m} E_y + \frac{\epsilon\mu}{mc} H_L \frac{dx}{dt}, \\ \frac{d^2z}{dt^2} &= 0. \end{aligned} \right\} \quad (26)$$

Multiply the second of these equations through by i and add to the first. Then

$$\frac{d}{dt} (v_x + iv_y) = -\frac{\epsilon}{m} (E_x + iE_y) + i \frac{\epsilon\mu}{mc} H_L (v_x + iv_y), \quad (27)$$

where v_x and v_y are the velocities. The field equations become

$$\left. \begin{aligned} \frac{\partial E_y}{\partial z} &= \frac{\mu}{c} \frac{\partial H_x}{\partial t}, & \frac{\partial E_x}{\partial z} &= -\frac{\mu}{c} \frac{\partial H_y}{\partial t}, \\ -\frac{\partial H_y}{\partial z} &= \frac{\kappa}{c} \frac{\partial E_x}{\partial t} - \frac{4\pi N\epsilon v_x}{c}, & \frac{\partial H_x}{\partial z} &= \frac{\kappa}{c} \frac{\partial E_y}{\partial t} - \frac{4\pi N\epsilon v_y}{c}. \end{aligned} \right\} \quad (28)$$

Combine them in a similar fashion to give

$$\frac{\partial}{\partial z} (E_x + iE_y) = \frac{\mu i}{c} \frac{\partial}{\partial t} (H_x + iH_y), \quad (29)$$

$$\frac{\partial}{\partial z} (H_x + iH_y) = -\frac{\kappa i}{c} \frac{\partial}{\partial t} (E_x + iE_y) + \frac{4\pi i N\epsilon}{c} (v_x + iv_y). \quad (30)$$

Now introduce the complex quantities

$$\left. \begin{aligned} v_x + iv_y &= V e^{\pm i\omega \left(t - \frac{nz}{c} \right)}, \\ E_x + iE_y &= E e^{\pm i\omega \left(t - \frac{nz}{c} \right)}, \\ H_x + iH_y &= H e^{\pm i\omega \left(t - \frac{nz}{c} \right)}, \end{aligned} \right\} \quad (31)$$

wherein V , E , and H are complex constants.

Setting these expressions into equations (27), (29), and (30), we get

$$\left. \begin{aligned} \pm i\omega V &= -\frac{\epsilon E}{m} + i \frac{\epsilon\mu}{mc} H_L V, \\ i n E &= \mu H, \\ i\omega n H &= -\kappa \omega E \pm 4\pi i N\epsilon V, \end{aligned} \right\} \quad (32)$$

three independent equations for the four complex constants, V , E , H , and n . By the form of the equations, we see that n is the only one uniquely determined. The remaining are given in terms of the here unspecified electric intensity of the incoming wave. Simultaneous solution gives for n the value

$$n^2 = 1 - \frac{4\pi N\epsilon^2}{m} \frac{1}{\omega^2 \pm \frac{\epsilon}{mc} H_L \omega}, \quad (33)$$

wherein we have set $\mu = \kappa = 1$, as appropriate for free space. Note that this equation reduces to (19) when $H_L = 0$.

There are thus two indices of refraction. The ionosphere, under the action of the earth's magnetic field, behaves like a birefringent crystal. For a given frequency, ω , the wave splits into two parts, which progress at different rates through the medium. The waves are circularly polarized and rotate in opposite senses. Also, there are two values of the critical frequency, for which $n = 0$, according to the sign adopted. The higher value is the extraordinary ray, the lower is the ordinary. Interference between the two beams is one of the causes of fading.

The quantity

$$\epsilon H_L / mc = \omega_L \quad (34)$$

is the Larmor precession frequency of an electron in the mag-

netic field of the earth. The radio frequency corresponding to the Larmor frequency is of the order of 1.5–1.6 megacycles near the magnetic poles and falls to 0.7–0.8 megacycles near the equator.

For denser layers and low frequencies still another phenomenon comes into account: the collisions of electrons with neighboring ions and atoms. We suppose that this resistance opposes the motion of the electron. On the right-hand sides of (26) we must add the resistance terms $-gv_x$ to the first, and $-gv_y$ to the second. We thus obtain, in place of (27), the equation

$$\frac{d}{dt}(v_x + iv_y) = -\frac{e}{m}(E_x + iE_y) + \left(i\frac{e\mu}{mc}H_L - g\right)(v_x + iv_y). \quad (35)$$

Equations (29) and (30) are unchanged.

The index of refraction turns out to be complex, and of the form

$$n^2 = 1 - \frac{4\pi N e^2}{m\omega} \frac{1}{\omega \pm \omega_L \pm ig}. \quad (36)$$

If we set

$$n = n_r \mp ik, \quad (37)$$

where n_r and k are real, we have the equations

$$n_r^2 - k^2 = 1 - \frac{4\pi N e^2}{m\omega} \frac{\omega \pm \omega_L}{(\omega \pm \omega_L)^2 + g^2}, \quad (38)$$

$$2n_r k = \frac{4\pi N e^2}{m\omega} \frac{g}{(\omega \pm \omega_L)^2 + g^2}, \quad (39)$$

from which to determine the parameters.

Introducing (37) into (31), we see that the general propagation factor becomes

$$e^{\pm i\omega\left(t - \frac{nz}{c}\right)} = e^{\pm i\omega\left(t - \frac{n_r z}{c}\right) - \frac{\omega k z}{c}} \quad (40)$$

The last term in the exponent causes the wave amplitude to diminish with z . The collision term thus introduces absorption of the wave. The amplitude diminishes by a factor e in the distance $c/\omega k$.

The lower sign in these formulas corresponds to the extraordinary ray, and the upper sign to the ordinary. Thus we see that the extraordinary critical is higher than the ordinary. Also, for a given frequency, absorption of the extraordinary is greater than for the ordinary.

The quantity, g , roughly corresponds to the collision frequency of the electrons. More accurately, $1/g$ is the time for the square root of the kinetic energy to fall to a value $1/e$. Maximum absorption tends to occur for those layers where ω and g are approximately equal to the Larmor frequency, ω_L .

SUGGESTED REFERENCES:

- Stratton, J. A., *Electromagnetic Theory*. New York: McGraw-Hill Book Company, 1941, pages 327ff.
 Mimno, Harry Rowe, "The Physics of the Ionosphere," *Reviews of Modern Physics*, Vol. 9, No. 1, January, 1937.
 The latter publication contains detailed references to propagation literature.

• APPENDIX TWO •

THEORY OF TROPOSPHERIC PROPAGATION

THIS SECTION WILL BE DEVOTED TO THE PROBLEM OF determining the field intensity for radio frequencies greater than 30 megacycles. The primary question is the preparation of coverage diagrams. Chapter 14 gave the essential features of the process. We must now investigate the basic theory underlying the formulas and nomograms previously presented without proof.

For the geometry of the problem turn to Fig. 108. Note that the angle of incidence must be equal to the angle of reflection. In other words, the elevations at *C* of *AC* and *BC* above the horizon must be equal to θ . Let *r* be the radius of the earth. Set *AC* = *d*, and *CB* = *d*₂. We suppose the transmitter to be located at *A*. The electric field, *E*_{*d*} at *B*, resulting from the direct beam, is

$$E_d = E_0 \frac{e^{-2\pi i d_2/\lambda + 2\pi i c t/\lambda}}{d_3},$$

where λ is the wave-length, *c* the velocity, *t* the time, and *E*₀ the maximum amplitude of the electric vector at unit distance from the transmitter, as measured in free space. A similar expression holds for the field intensity of the ground-reflected wave, with three complications, however. The beam may not be totally reflected at *C*; the phase will be rotated; the beam will be reduced in intensity because reflection from the convex earth tends to disperse the radiation.

Let ρ be the absolute value of the reflection coefficient and δ the magnitude of the phase shift. Then the electric field from the reflected beam is

$$E_r = \frac{E_0' e^{-2\pi i (d_1 + d_2)/\lambda + 2\pi i c t/\lambda + i\delta}}{\sqrt{(d_1 + d_2)(d_1' + d_2)}} \rho.$$

The factor $\sqrt{(d_1 + d_2)(d_1' + d_2)}$ allows for the spherical aberration of the beam produced by reflection from the spherical earth. In the vertical plane through the transmitter the beam diverges and appears to radiate from the image source at *A'*. In the horizontal plane the divergence is normal.

If we assume horizontal polarization (the electric vector lying perpendicular to the plane of the figure) and a perfectly conducting sphere, the component parallel to the ground must vanish when *d*₂ = 0. Thus $\delta = \pi$, $\rho = 1$, and *d*₃ = *d*₁.

$$E_r = E_d, \quad \text{or} \quad E_0' = E_0 \sqrt{d_1'/d_1},$$

and

$$E_r = \frac{-E_0}{d_1 + d_2} \left[\frac{d_1'(d_1 + d_2)}{d_1(d_1' + d_2)} \right]^{1/2} e^{-2\pi i (d_1 + d_2)/\lambda + 2\pi i c t/\lambda}.$$

Set

$$D^2 = \frac{d_1'(d_1 + d_2)}{d_1(d_1' + d_2)}. \quad (1)$$

Also, note that for the grazing angles under consideration we may take

$$d_1 + d_2 \sim d_3,$$

except where differences of the direct and reflected paths are considered. Then

$$|E|^2 = \frac{E_0^2}{d_3^2} \left\{ 1 - 2D \cos \left[\frac{2\pi}{\lambda} (d_1 + d_2 - d_3) \right] + D^2 \right\}. \quad (2)$$

E is the peak electric intensity at any point in space, resulting from the interference of the direct and reflected beams.

The important factors to determine, therefore, are *D* and

$$\Delta S = d_1 + d_2 - d_3, \quad (3)$$

the path difference. We start with the calculation of the latter. From triangles *AOC*, *BOC*, and *ABC*, we get the following equations from the law of cosines:

$$(r + h_1)^2 = d_1^2 + r^2 - 2d_1 r \cos(90^\circ + \theta),$$

$$(r + h_2)^2 = d_2^2 + r^2 - 2d_2 r \cos(90^\circ + \theta),$$

$$d_3^2 = d_1^2 + d_2^2 - 2d_1 d_2 \cos(180^\circ - 2\theta),$$

which reduce to

$$2h_1 r + h_1^2 = d_1^2 + 2d_1 r \sin \theta \quad (4)$$

$$2h_2 r + h_2^2 = d_2^2 + 2d_2 r \sin \theta \quad (5)$$

$$d_3^2 = d_1^2 + d_2^2 + 2d_1 d_2 \cos 2\theta. \quad (6)$$

From (4) and (5) we get

$$\sin \theta = \frac{2h_1 r + h_1^2 - d_1^2}{2d_1 r} = \frac{2h_2 r + h_2^2 - d_2^2}{2d_2 r}. \quad (7)$$

Let us now introduce the parameters α and β , defined as follows:

$$d_1^2 = 2h_1 r(1 - \alpha), \quad d_2^2 = 2h_2 r(1 - \beta). \quad (8)$$

Then equation (7) becomes:

$$\sin \theta = \left(\alpha + \frac{h_1}{2r} \right) \sqrt{\frac{h_1}{2r(1 - \alpha)}} = \left(\beta + \frac{h_2}{2r} \right) \sqrt{\frac{h_2}{2r(1 - \beta)}}. \quad (9)$$

$$\cos 2\theta = 1 - 2 \sin^2 \theta = 1 - 2 \left(\alpha + \frac{h_1}{2r} \right)^2 \left[\frac{h_1}{2r(1 - \alpha)} \right]. \quad (10)$$

$$\cos 2\theta = 1 - 2 \left(\beta + \frac{h_2}{2r} \right)^2 \left[\frac{h_2}{2r(1 - \beta)} \right]. \quad (11)$$

Substituting (10) into (6), and making use of (8), we get

$$(d_1 + d_2)^2 - d_3^2 = 4 \sqrt{h_1 h_2 (1 - \beta)} (1 - \alpha) h_1 \left(\alpha + \frac{h_1}{2r} \right)^2. \quad (12)$$

Factoring the left-hand side, taking

$$2S = d_1 + d_2 + d_3, \quad (13)$$

and employing (3), we have

$$\Delta S = \frac{2 \sqrt{h_1 h_2 (1 - \beta) / (1 - \alpha)}}{S} h_1 (\alpha + h_1 / 2r). \quad (14)$$

Similarly employing (11), instead of (10), we get

$$\Delta S = \frac{2 \sqrt{h_1 h_2 (1 - \alpha) / (1 - \beta)}}{S} h_2 (\beta + h_2 / 2r). \quad (15)$$

Multiplying the respective sides of (14) and (15), and taking the square root, we finally obtain

$$\Delta S = \frac{2h_1 h_2}{S} (\alpha + h_1 / 2r)(\beta + h_2 / 2r). \quad (16)$$

Also, dividing (15) by (14), we get

$$\frac{(1 - \alpha)}{h_1 (\alpha + h_1 / 2r)^2} = \frac{(1 - \beta)}{h_2 (\beta + h_2 / 2r)}. \quad (17)$$

To within accuracy sufficient for our purposes we may take

$$d_3 \sim d_1 + d_2 \sim S, \quad (18)$$

and interpret S as the distance between the two antennas, measured, if we prefer, along the surface of the earth. Then, from (8), we have

$$S = \sqrt{2r} [\sqrt{h_1(1 - \alpha)} + \sqrt{h_2(1 - \beta)}]. \quad (19)$$

In any actual problem we are given r , h_1 , h_2 , and S . ΔS , α , and β are to be determined. The three independent equations (16), (17), and (19) are sufficient for the problem. We should, of course, prefer to eliminate both of the intermediate parameters, α and β , but we shall find it possible to eliminate only one of them.

For all practical purposes we may take (16) and (17) in the form

$$\Delta S = \frac{2h_1 h_2}{S} \alpha \beta, \quad (20)$$

$$\frac{(1 - \alpha)}{h_1 \alpha^2} = \frac{(1 - \beta)}{h_2 \beta^2}, \quad (21)$$

and neglect terms of the order $h_1 / 2r$. The condition to be satisfied is that

$$\left(\frac{h}{2r}\right)^{5/2} \frac{h}{\lambda} \ll 1, \quad (22)$$

which is fulfilled even for 1 cm. wave lengths at heights of five miles. In (22) h is the greater of the two antenna heights. For derivation of (22) we have taken both antennae to lie at the same height, which is the worst possible case. Note that h , λ , and r are to be expressed in the same units.

With these simplifications, we take (19), (20), and (21) as the fundamental equations for the determination of path difference, ΔS .

Substitute the value of $1 - \beta$ from (21) into (19) and solve the resultant equation for β .

$$\beta = \alpha \frac{h_1}{h_2} \left[\frac{S}{\sqrt{2rh_1(1 - \alpha)}} - 1 \right]. \quad (23)$$

Set this expression for β back into (21) and reduce. The

result is

$$S^2 + \frac{(-2 + 3\alpha)}{(1 - \alpha)^{3/2}} S \sqrt{2rh_1} + 2rh_1(1 - \alpha) - 2rh_2 = 0. \quad (24)$$

An analogous symmetrical equation holds for β .

$$S^2 + \frac{(-2 + 3\beta)}{(1 - \beta)^{3/2}} S \sqrt{2rh_2} + 2rh_2(1 - \beta) - 2rh_1 = 0. \quad (25)$$

If we could solve these equations explicitly for α and β in terms of the given parameters h_1 and h_2 and of S , we should have our solution complete. Unfortunately, equations (24) and (25) are irreducible cubics. A fairly simple solution can be obtained in terms of nomograms, but we prefer to continue with the analysis.

To obtain a more general relationship, set

$$\phi = \frac{2\pi\Delta S}{\lambda} = \frac{4\pi h_1^2 \alpha^2}{\lambda} \left[\frac{1}{\sqrt{2rh_1(1 - \alpha)}} - \frac{1}{S} \right], \quad (26)$$

by (20) and (23). From (2) and (3), we get

$$|E|^2 = \frac{E_0^2}{S^2} [(1 - D)^2 + 4D \sin^2 \phi / 2]. \quad (27)$$

Let p = the power density per unit area from a transmitter of unit power. Express p in microwatts per square meter and assume a power of one watt for the transmitter. Then

$$p = \frac{10^6}{4\pi S^2} [(1 - D)^2 + 4D \sin^2 \phi / 2]. \quad (28)$$

With a unit of power density p_0 as standard, so that

$$p_0 = 1/S_0^2 \quad (29)$$

where S_0 is unity if measured in meters, we take the ratio

$$\frac{p}{p_0} = 10^{-db/10} = \frac{10^6}{\pi} \left(\frac{S_0}{S}\right)^2 \left[\frac{(1 - D)^2}{4} + D \sin^2 \phi / 2 \right], \quad (30)$$

where db is the number of decibels that the power density is below standard. We may regard S_0 as the conversion factor between meters and whatever units are used for S , so that the ratio is independent of the system employed.

We still must evaluate the divergence factor, D . Refer to Fig. 172 and consider two adjacent rays leaving A and striking the earth at angles θ_1 , and $\theta_2 = \theta_1 - \Delta\theta$. If γ is the angle at the center of the earth subtended by the points of reflection, we have

$$A = \theta_1 - \theta_2 - \gamma, \quad (31)$$

and

$$A' = \theta_1 - \theta_2 + \gamma.$$

$$\frac{d_1'}{d_1} = \lim_{\gamma \rightarrow 0} \left[\frac{\sin(\theta_2 - \gamma/2) \sin A}{\sin(\theta_2 + \gamma/2) \sin A'} \right] = \lim_{\gamma \rightarrow 0} \frac{A}{A'}$$

By definition,

$$\left. \begin{aligned} d_1 &= \sqrt{2rh_1(1 - \alpha)}, & \Delta d_1 &= -\frac{\sqrt{2rh_1} \Delta \alpha}{2(1 - \alpha)^{3/2}} \\ \gamma &= \frac{\Delta d_1}{r} = -\sqrt{\frac{h_1}{2r}} \frac{\Delta \alpha}{(1 - \alpha)^{3/2}} \end{aligned} \right\} \quad (32)$$

$$\theta_1 - \theta_2 = \Delta\theta = \sqrt{\frac{h_1}{2r}} \frac{2 - \alpha}{2(1 - \alpha)^{3/2}} \Delta\alpha, \quad (33)$$

from differentiation of (9). Thus,

$$\frac{d'_1}{d_1} = \frac{\alpha}{4 - 3\alpha}.$$

Finally, we have, from (1),

$$D^2 = \frac{\alpha}{4 - 3\alpha - \frac{4\sqrt{2rh_1}}{S}(1 - \alpha)^{3/2}}. \quad (34)$$

As α covers its range $0 \leq \alpha \leq 1$, D covers the same range. Note that if we set

$$S = \sqrt{2rh_1}(1 - \alpha), \quad (35)$$

which corresponds to a point on the surface of the earth, we get

$$D = 1,$$

as required.

Except for points near the ground and a small region near the point where the tangent ray from the transmitter touches the earth, we shall introduce no appreciable error by taking

$$D^2 \sim \frac{\alpha}{4 - 3\alpha}, \quad (36)$$

and we shall ordinarily make this approximation.

The following four equations, derived to this point, contain the solution of our problem.

$$10^{-db/10} = \frac{10^6}{\pi} \left(\frac{S_0}{S}\right)^2 \left[\frac{(1 - D)^2}{4} + D \sin^2 \phi/2 \right]. \quad (37)$$

$$D^2 = \frac{\alpha}{4 - 3\alpha - \frac{4\sqrt{2rh_1}}{S}(1 - \alpha)^{3/2}} \sim \frac{\alpha}{4 - 3\alpha}. \quad (38)$$

$$\phi = \frac{4\pi h_1^2 \alpha^2}{\lambda} \left[\frac{1}{\sqrt{2rh_1}(1 - \alpha)} - \frac{1}{S} \right]. \quad (39)$$

$$S^2 + \frac{(-2 + 3\alpha)}{(1 - \alpha)^{1/2}} S \sqrt{2rh_1} + 2rh_1(1 - 2\alpha) - 2rh_2 = 0. \quad (40)$$

An alternative exact expression for D , which may be useful, is

$$D^2 = \frac{1}{1 + \frac{\sqrt{2rh_1} \phi \lambda (1 - \alpha)^{3/2}}{\pi h_1^2 \alpha^3}} = \frac{1}{1 + \frac{4B(1 - \alpha)^{3/2}}{\alpha^3}}, \quad (41)$$

where B is defined in equation (49).

If we accept the approximate expression for D , we have the three equations, (39), and (40), to be solved simultaneously.

$$10^{-db/10} =$$

$$\frac{10^6}{\pi} \left(\frac{S_0}{S}\right)^2 \left\{ \frac{\left[1 - \left(\frac{\alpha}{4 - 3\alpha}\right)^{1/2}\right]^2}{4} + \left(\frac{\alpha}{4 - 3\alpha}\right)^{1/2} \sin^2 \phi/2 \right\}. \quad (42)$$

We are ordinarily given the quantities h_1 , λ , r , and S_0 .

The parameters α and β are to be eliminated so that the relationship between db , S , and h_2 will appear.

Eliminating the factor, $\sqrt{1 - \alpha}$, between (39) and (40),

$$\frac{S^2}{2r} + \frac{(-2 + 3\alpha) 150 (n - b)}{h_1 \alpha^2 f} S = h_2 + (1 - \alpha)h_1, \quad (43)$$

wherein we have set

$$\phi = 2(n - b)\pi \quad \text{and} \quad \lambda = 300/f; \quad (44)$$

f is the frequency in megacycles, n is an integer (1, 2, 3, . . .) specifying the number of the lobe, and b a "phase" factor specifying the position on the lobe.

$$0 \leq b \leq 1; \quad (45)$$

$b = 1/2$ corresponds to a lobe maximum, $b = 0$ to a minimum, and other values to intermediate positions. Thus (39) becomes

$$2(n - b)\pi = \frac{4\pi h_1^2 \alpha^2}{300/f} \left[\frac{1}{\sqrt{2rh_1}(1 - \alpha)} - \frac{1}{S} \right]. \quad (46)$$

$$\frac{150 (n - b) \sqrt{2r}}{h_1^{3/2} \alpha^2 f} = \frac{1}{\sqrt{1 - \alpha}} - \frac{\sqrt{2rh_1}}{S}. \quad (47)$$

We also get the result from (42) that

$$10^{-db/20} = \frac{10^3}{\sqrt{\pi}} \left(\frac{S_0}{S}\right)^2 \left\{ \frac{\left[1 - \left(\frac{\alpha}{4 - 3\alpha}\right)^{1/2}\right]^2}{4} + \left(\frac{\alpha}{4 - 3\alpha}\right)^{1/2} \sin^2 \pi b \right\}^{1/2}. \quad (48)$$

At this point we find it convenient to discuss two limiting cases, *viz.*, when $1 - \alpha \ll 1$ and when $\alpha \ll 1$. Let

$$B = \frac{150 (n - b) \sqrt{2r}}{h_1^{3/2} f}. \quad (49)$$

Then,

$$\alpha = 1 - \left[B + \frac{\sqrt{2rh_1}}{S} \right]^{-2}, \quad B^2 \gg 1. \quad (50)$$

$$\alpha \sim B^{1/2} \left[1 - \frac{\sqrt{2rh_1}}{S} \right]^{-1/2}, \quad B^{1/2} \ll 1. \quad (51)$$

Of these two approximations, the former is by far the more important. It holds well over a large region of space, whereas the latter is applicable only over a small region close to the ray from the transmitter after it passes the point of tangency to the earth's surface. Moreover, we frequently find the condition fulfilled that

$$B \gg \sqrt{2rh_1}/S, \quad (52)$$

whence

$$\alpha \sim 1 - B^{-2}. \quad (53)$$

Thus we should have

$$10^{-db/10} \sim \frac{10^6}{\pi} \left(\frac{S_0}{S}\right)^2 \left\{ \frac{1}{B^4} + \left(1 - \frac{1}{B^2}\right) \sin^2 \pi b \right\}. \quad (54)$$

B is known from (49). Hence, for assumed values of db and b , we may calculate the distance, S , for the selected point on

the given lobe. Then, from (43), we get the height h_2 as follows:

$$\frac{S^2}{2r} + \left(1 - \frac{1}{B^2}\right) B \frac{\sqrt{h_1}}{\sqrt{2r}} S = h_2 + h_1/B^2. \quad (55)$$

Equations (49), (54), and (55) thus contain a direct solution of the problem when the conditions of (50) and (52) are fulfilled. This holds for the higher lobes. For frequencies less than about 300 mc., it holds well above the maximum of the first lobe.

We require a more exact treatment for values of α less than about 0.95, say, which will include at least the lower part of the first lobe. Eliminate S between (47) and (48). The result is

$$10^{-Y/20} = \sqrt{2\pi r h_1} 10^{-(3+db/20)} \\ = \left(\frac{1}{\sqrt{1-\alpha}} - \frac{B}{\alpha^2}\right) \left\{ \frac{\left[1 - \left(\frac{\alpha}{4-3\alpha}\right)^{1/2}\right]^2}{4} + \left(\frac{\alpha}{4-3\alpha}\right)^{1/2} \sin^2 \pi b \right\}^{1/2}. \quad (56)$$

For given values of b , B , and db , we are to determine α . The solution can be effected by means of nomograms. Then, with b , db , and α given, we return to (48) to calculate S . Finally, from (43), written as follows, we determine h_2 :

$$\frac{S^2}{2r} + \frac{(-2+3\alpha)}{\alpha^2} B \frac{\sqrt{h_1}}{\sqrt{2r}} S = h_2 + (1-\alpha)h_1. \quad (57)$$

The set of equations (48), (49), (56), and (57) provides the complete answer to the problem.

We turn now to the development of nomograms for the practical solution of the general problem. Expressing h_1 in feet, we have

$$B = \frac{150(n-b)\sqrt{2r}(3.281)^{3/2}}{h_1^{3/2}f} = 3.676 \times 10^6 \frac{(n-b)}{h_1^{3/2}f}, \quad (58)$$

where we have taken $r = 8.50 \times 10^6$ meters as the approximate $\frac{4}{3}$ earth value. We have to decide on the interval for b . By taking $b = 0, \frac{1}{6}, \frac{2}{6}, \frac{3}{6}, \frac{4}{6}, \frac{5}{6}$, we actually obtain seven points on each lobe, which should be sufficient for the purpose of drawing a coverage diagram. Hence,

$$n-b = 0, \frac{1}{6}, \frac{1}{3}, \frac{1}{2}, \frac{2}{3}, \frac{5}{6}, 1, \frac{7}{6}, \dots \quad (59)$$

and so on. Define a quantity k by the equation

$$n-b = k/6, \quad (60)$$

so that $k = 3$ corresponds to the maximum of the first lobe, $k = 6$ to the minimum, $k = 9$ to the next maximum, $k = 12$ to the minimum, and so forth. $k = 15, 21,$ and 27 correspond to the 3rd, 4th, and 5th maxima, respectively. Other values of k determine intermediate points on the lobe.

It should be noted that the equation (58) is easy to solve, and the operator familiar with mathematical procedures may prefer to use direct calculation, by slide rule or logarithm tables, as more accurate. In general, however, the nomogram values are sufficiently accurate for the work.

As a preliminary step in the solution of (56) we must calculate Y , which is defined as

$$Y = db + 60 - 10 \log (2\pi r h_1). \quad (61)$$

One now proceeds to the determination of B and α . Having calculated α for a given point on the coverage chart, we now evaluate S from (48). The numerical form, for the selected units is:

$$10^{-db/20} = \frac{10^3}{\sqrt{\pi}} \left(\frac{1}{914S}\right) \left\{ \frac{\left[1 - \left(\frac{\alpha}{4-3\alpha}\right)^{1/2}\right]^2}{4} + \left(\frac{\alpha}{4-3\alpha}\right)^{1/2} \sin^2 \pi b \right\}^{1/2}. \quad (62)$$

Finally, we must calculate h_2 , from either equation (40) or equation (57). The latter is, perhaps, preferable. For heights expressed in feet, and ranges in thousands of yards, (57) becomes

$$H = h_2 + (1-\alpha)h_1 = \frac{(3.281)(914)^2}{2r} S^2 + \frac{(3.281)^2(914)(150)(n-b)}{h_1 f} - \frac{(-2+3\alpha)}{\alpha^2} S. \quad (63)$$

This equation, unfortunately, has too many variables for nomographic solution in a single step. We first define a quantity C , such that

$$C = \frac{(3.281)^2(914)(150)(n-b)(-2+3\alpha)}{h_1 f \alpha^2}. \quad (64)$$

Thus we determine H for each value of S and C . Finally, we get h_2 from the relation

$$h_2 = H - (1-\alpha)h_1. \quad (65)$$

Actually, for much of the range, $\alpha \sim 1$ and

$$h_2 \sim H. \quad (66)$$

For the upper lobes considerable simplification is possible. We may omit all the steps involving calculation of α . We determine the various B 's as before. Then, as long as

$$B \gg 1, \quad (67)$$

we employ (54), which becomes

$$10^{-db/10} = \frac{10^6}{\pi} \left(\frac{1}{914S}\right)^2 \left\{ \frac{1}{B^4} + \left(1 - \frac{1}{B^2}\right) \sin^2 \pi b \right\}. \quad (68)$$

This equation gives S directly for each db and assumed value of b . The nomogram for this problem appears in Fig. 141. We then obtain H from (63), with α set equal to unity.

$$H = \frac{(3.281)(914)^2}{2r} S^2 + \frac{(3.281)^2(914)(150)}{C'} S. \quad (69)$$

In equation (69) we have written C' instead of C . For much of the range, wherever B is very large, we may take

$$C' \sim C. \quad (70)$$

If greater accuracy is desired, we may compute C' directly by the equation

$$C' = \frac{(3.281)^2(914)(150)k}{6fh_1} \left(1 - \frac{1}{B^2}\right). \quad (71)$$

It is interesting to note that equation (69), apart from the correction factor $(1 - 1/B^2)$, which merely serves to improve the accuracy of the result, is familiar to many in the construction of so-called "fade charts." These diagrams depict merely the lobe minima (and sometimes also the maxima). If we set $b = 0$, we get the former, and if we take $b = \frac{1}{2}$, we determine the latter.

The total number of lobes, N , is approximately

$$N = 2h_1/\lambda = \frac{h_1 f}{(150)(3.281)} = 2.03 \times 10^{-3} h_1 f,$$

for h_1 in feet. These will be distributed over an angle of 90 degrees. Hence \bar{A} , the average angle per lobe, is

$$\bar{A} = 90^\circ/N = 4.^\circ43 \times 10^4/fh_1.$$

Near the horizon, however, the angle per lobe, A_0 , is somewhat larger, to wit:

$$A_0 = 360^\circ/\pi N = 5.^\circ64 \times 10^4/fh_1.$$

When

$$A_0 < 0.^\circ1,$$

the lower lobes are so closely packed that the drawing of a coverage diagram becomes almost impossible. For such cases one should determine, for a given db , the lower edge of the lowest lobe. Then, with the aid of the nomograms for $b = \frac{1}{2}$, calculate merely the positions of maxima of the other lobes.

During the calculations and tests of the foregoing method, one difficulty became apparent. Equation (56) proved to be inadequate for the determination of α when $b = 0$. The nomograms gave erroneous results. Two roots or no roots were invariably obtained when a single root was desired. Study has shown that the difficulty arose from the approximation for D , as given in (38). The error is still negligibly small as far as D is concerned, but the reverse calculation cannot be allowed.

To determine α we may have recourse to the exact equation derived from (37), (41), and (49):

$$10^{-r/20} = \left(\frac{1}{\sqrt{1-\alpha}} - \frac{B}{\alpha^2} \right) \left\{ \frac{1 - \frac{1}{\sqrt{1+4B(1-\alpha)^{3/2}\alpha^{-3}}}}{4} + \frac{\sin^2 \pi b}{\sqrt{1+4B(1-\alpha)^{3/2}\alpha^{-3}}} \right\}^{1/2}, \quad (72)$$

which is not too complicated when $b = 0$. Tables or curves could be provided for ready solution of the equation. Nevertheless, one will ordinarily obtain a sufficiently accurate value of α for $b = 0$ by averaging the values previously derived for $b = \frac{5}{6}$ and $\frac{1}{6}$, which have been entered into the work sheet in parentheses. Once α is given by this method, proceed as before to obtain S and continue to derive C , H , and h_2 , in turn.

The results are amply accurate—indeed, far more accurate than they will be fulfilled in nature, where minor variations will cause appreciable differences from the theoretical curve, especially at the minima.

When $B > 4.0$, we may omit the intermediate step of calculating α and proceed to derive S directly from equation 54.

Within the line of sight, the ray method is a quick and satisfactory means of calculating the field of a radio transmitter. When the receiver lies in the shadow zone below the horizon, however, the simple ray theory breaks down, and one must employ diffraction theory based on the wave equation. One then obtains an expression for the field as a series of normal modes, converging so rapidly within the shadow zone that only the first mode generally need be retained. One can calculate the field at points near the horizon ray by adding the higher normal modes, but the simplest procedure is to compute the field at points well within the line of sight (ray theory) and well within the shadow zone (first normal mode) and then to interpolate graphically.

Upon introducing the normalized modified index of refraction (N) to take account of both the earth's curvature and standard atmospheric refraction, one can simplify the mathematical problem to the following, referred now to a plane earth:

Find the solution of the wave equation

$$\nabla^2 \psi + k^2 N^2 \psi = 0 \quad (k = 2\pi/\lambda = \omega/c) \quad (73)$$

subject to the conditions that

- (a) ψ reduce to $\frac{e^{-ikR}}{R}$ at small distances R from the source,
- (b) ψ vanish at the surface ($h = 0$),
- (c) $\psi e^{i\omega t}$ represent an outgoing wave at large distances from the source.

N^2 is a function of height alone and has the form

$$N^2 = 1 + qh, \quad (q = 2/r), \quad (74)$$

where r is the effective ($\frac{4}{3}$) radius of the earth (8500 kilometers).

The solution of (73) can be expressed as the following series of normal modes:

$$\psi = -i\pi \sum_{m=1}^{\infty} H_0^{(2)}(kS \cos \alpha_m) U_m(h_1) U_m(h_2), \quad (75)$$

where $H_0^{(2)}$ denotes the second Hankel function of order zero, and the (complex) characteristic functions U_m and characteristic values $\sin^2 \alpha_m$ are determined by the conditions:

- (a) $U_m''(h) + k^2(\sin^2 \alpha_m + qh)U_m(h) = 0$,
- (b) $U(0) = 0$,
- (c) $\lim_{I(k) \rightarrow 0^-} \int_0^{\infty} U_m^2 dh = 1$
- (d) $U e^{i\omega t}$ is an outgoing wave for $h \gg 1$.

In order to put the solution in a non-dimensional form, one introduces the quantities:

$$\begin{aligned} L &= 2(kq^2)^{-1/4} && \text{(natural unit of distance)} \\ H &= (k^2q)^{-1/4} && \text{(natural unit of height)} \\ X &= S/L = \frac{1}{2}(kq^2)^{1/4} S, \\ Z &= h/H = (kq^2)^{1/4} h \\ D_m &= \left(\frac{k}{q}\right)^{3/4} \sin^2 \alpha_m = B_m + iA_m \end{aligned} \quad (76)$$

(characteristic value in natural units).

Upon replacing the Hankel functions $H_0^{(2)}$ by their asymptotic approximations and setting $\cos \alpha_m \sim 1 - \frac{1}{2} \sin^2 \alpha_m$ in the

exponent, $\cos \alpha_m \sim 1$ elsewhere—allowable since $|\sin^2 \alpha_m| \ll 1$ —one can transform the solution to the following standard form:

$$\psi = e^{-i(kS + \frac{\pi}{4})} \frac{2\pi^{1/2}}{L} x^{1/2} \sum_{m=1}^{\infty} e^{iD_m z} U_m^0(z_1) U_m^0(z_2), \quad (77)$$

where the standard height-gain functions, U_m^0 , are defined by

$$\begin{aligned} U_m^0(z) &= ih_2(D_m + z)/h_2'(D_m), \\ h_2''(\xi) + \xi h_2(\xi) &= 0, \\ h_2(\xi) &= (2/3 \xi^{3/2})^{1/2} H_{1/2}^{(2)}(2/3 \xi)^{3/2}, \\ h_2(D_m) &= 0, \\ D_m &= (3/2 S_m)^{2/3} e^{2\pi i/3}, \\ \mathcal{J}_{1/3}(S_m) + \mathcal{J}_{-1/3}(S_m) &= 0. \end{aligned} \quad (78)$$

($S_1 = 2.3834466$, $S_2 = 5.5101956$, . . . Cf. Watson's *Bessel Functions*, p. 751.

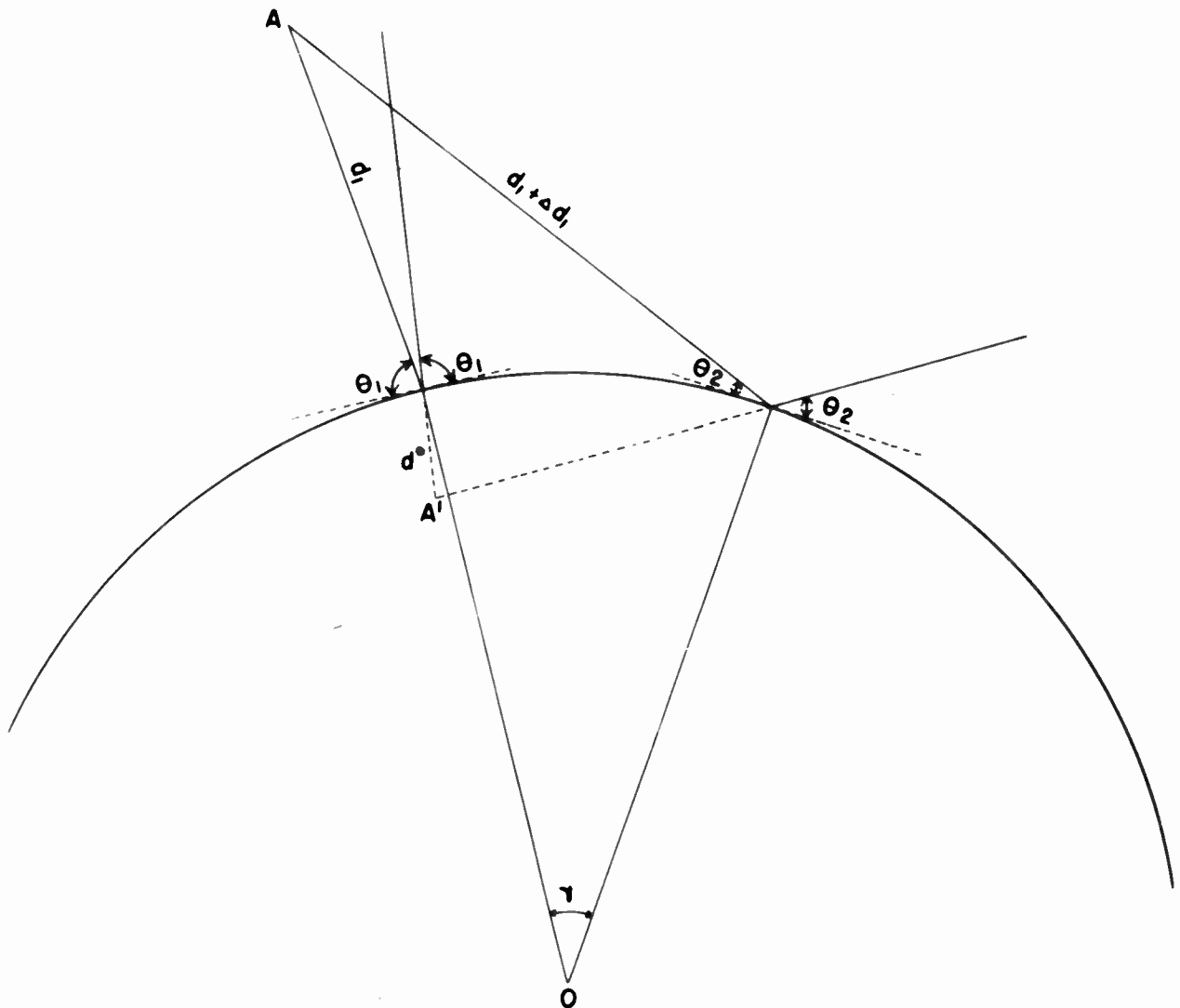
Although the series derived above is formally valid everywhere (including the optical region), convergence is slow outside the diffraction zone. Well within the diffraction zone, however, it is sufficient to retain only the first mode ($m = 1$) under standard conditions. If one assumes a one-watt isotropic source, the power density at the receiver in decibels below one micro-watt/sq. meter is then given by

$$-db = (-22.41 + 10/3 \log_{10} f) - 10 \log S - 8.448 \times 10^{-2} f^{3/8} S + 20 \log_{10} |U_1^0(z_1)| + 20 \log_{10} |U_1^0(z_2)|, \quad (79)$$

where f is the frequency (megacycles), S the horizontal distance between the transmitter and receiver (thousands of yards), and z_1, z_2 the height of the transmitter and receiver in natural units:

$$z = 1.433 \times 10^{-4} f^{2/3} h, \quad (h \text{ in feet}). \quad (80)$$

With a slight change of notation, these equations agree with those given in Chapter 15.



$$d_i^l = \lim_{\gamma \rightarrow 0} d^o$$

Fig. 172.

• APPENDIX THREE •

DEFINITIONS

CHARACTERISTICS OF RADIO WAVES

Atmospheric Wave. It is comprised of the direct wave and ground-reflected wave, which, together with the surface wave, form the ground wave.

***Direct Wave.** A wave that is propagated directly through space.

***Electromagnetic Wave.** A wave in which there are both electric and magnetic displacements. Electromagnetic waves are known as *radio waves, heat rays, light, X rays,* and so forth, depending on the frequency.

***Fading.** The variation of radio field intensity caused by changes in the transmission medium.

***Ground Wave.** A radio wave that is propagated over the earth and is ordinarily affected by the presence of the ground. The ground wave includes all components of a radio wave over the earth except ionospheric and tropospheric waves.

***Ground-reflected Wave.** The component of the ground wave that is reflected from the ground.

***Guided Wave.** A wave whose propagation is concentrated in certain directions within or near boundaries between materials of different properties located in a path between two places.

***Ionospheric Wave.** A radio wave that is propagated by reflection from the ionosphere.

***Radio Field Intensity.** The electric or magnetic field intensity at a given location resulting from the passage of radio waves. It is commonly expressed in terms of the electric field intensity. Unless otherwise stated, it is taken in the direction of maximum field intensity.

***Radio Frequency.** A frequency at which electromagnetic radiation of energy is useful for communication purposes. *Note:* The present useful limits of radio frequencies are roughly 10 kilocycles to 10,000 megacycles.

***Radio-Wave Propagation.** The transfer of energy by electromagnetic radiation at radio frequencies.

***Selective Fading.** Fading which is different at different frequencies in a frequency band occupied by a modulated wave.

Sky Wave. The ionospheric wave is sometimes known as the *sky wave.*

***Troposphere.** That region of the earth's atmosphere in which temperature generally decreases with altitude; and

* *Standards on radio-wave propagation, Definitions of Terms.* 1942. The Institute of Radio Engineers.

where clouds form and convection is active.

***Tropospheric Wave.** A radio wave that is propagated by reflection from a place of abrupt change, with position in the troposphere.

***Wave.** A disturbance propagated through a medium. Also, the graphical representation of a wave or of any periodic variation.

***Wave Duct.** A wave guide with tubular boundaries capable of concentrating the propagation of waves within its boundaries.

***Wave Interference.** The variation of wave amplitude with distance or time, caused by variations of relative phase in the combination of two or more waves.

***Wave Length.** In a periodic wave, the distance between corresponding phases of two consecutive cycles. It is equal to the quotient of phase velocity by frequency.

NOISE

***Atmospheric Noise.** Noise caused by natural electrical discharges in the atmosphere. *Note:* It is also called *static.*

***Electrical Interference.** Interference caused by the operation of electrical apparatus other than radio stations. It may be either selective interference or noise, usually the latter.

***Noise.** Interference whose energy is distributed over a wide band of frequencies.

***Radio Interference.** An undesired disturbance in reception, or that which causes the undesired disturbance. Radio interference may thus be a disturbance in the radio transmitter, the transmission medium, or the radio receiver. Some examples of radio interference are background interference in the transmitter, undesired electromagnetic disturbance in the transmission medium as by lightning or undesired radio waves, and hum or thermal agitation in the receiver.

***Selective Interference.** Radio interference whose energy is concentrated in a narrow band of frequencies. Some examples are other radio stations on the same or adjacent frequencies, harmonics of other radio stations, and unshielded diathermy equipment.

IONOSPHERE

Critical Frequency. The penetration frequency is sometimes called the *critical frequency.*

Diffraction. Diffraction is the bending of waves about an obstacle.

- *E Layer.** An ionized layer in the *E* region.
- *E Region.** The region of the ionosphere between about 90 and 140 km above the earth's surface.
- *F Layer.** An ionized layer in the *F* region, existing in the night hemisphere and in the weakly illuminated portion of the day hemisphere. Over the intensely illuminated portion of the day hemisphere, two layers exist (see F_1 layer and F_2 layer, below).
- * F_1 Layer.** The lower of the two ionized layers normally existing in the *F* region in the day hemisphere.
- * F_2 Layer.** The higher of the two ionized layers normally existing in the *F* region in the day hemisphere.
- *F Region.** The region of the ionosphere between about 140 and 400 km above the earth's surface.
- *Hop.** An excursion of a radio wave from the earth to the ionosphere and back to earth, in traveling from one point to another. It is usually used in expressions such as single-hop, double-hop, and multihop. The number of hops is called the *order of reflection*.
- *Ionosphere.** That part of the earth's atmosphere above the lowest level at which the ionization is large compared with that at the ground, so that it affects the transmission of radio waves. *Note:* Experiments indicate that this lowest level is about 50 km above the earth's surface.
- *Ionospheric Storm.** A period of disturbance in the ionosphere, during which there are anomalous variations of penetration frequencies, virtual heights, and absorption. The disturbance usually includes: turbulence of the ionosphere and poorly defined penetration frequencies, especially at night; great virtual heights and low penetration frequencies, especially of the *F* and F_2 layers; great absorption, especially at night at frequencies of the order of one megacycle. An ionospheric storm usually lasts a substantial part of a day or more than one day.
- *Line of Propagation.** Of a wave from one point to another, the line between these two points which is in the direction of the wave normal at all points in space. This is also called the *path* or *line of travel*.
- Lowest Useful High Frequency, (LUHF).** That frequency which will just penetrate the absorption layers and exceed the noise level. Any lower frequency would fail to be received, unless it could be sent on the long path around the earth.
- *Maximum Usable Frequency, (MUF).** The highest frequency that can be used for radio transmission at a specified time between two points on the earth by reflection from the regular ionized layers of the ionosphere. Higher frequencies are transmitted only by sporadic and scattered reflections.
- *Oblique-incidence Transmission.** The transmission of a radio wave obliquely up to the ionosphere and down again.
- Optimum Working Frequency, (OWF).** Ninety-seven per cent of the correct MUF for the *E*, F_1 layer or 85 per cent of the F_2 MUF values, whichever is higher. This is a safety valve for abnormal fluctuations or times when the frequencies may be abnormally low.
- *Penetration Frequency.** The frequency of an ionized layer of the ionosphere, at which the virtual height for a wave component at vertical incidence has a maximum value caused by penetration of the wave through the layer. Except for the occurrence of sporadic and scattered reflections, it is the highest frequency of waves reflected from the layer at vertical incidence.
- *Primary Skip Zone.** The area around a radio transmitter beyond the ground-wave range but within the skip distance. Radio reception is possible in the primary skip zone only by sporadic, scattered, and zigzag reflections.
- *Radio Fade-out.** A cessation or near cessation of propagation of radio waves through the parts of the ionosphere affected by a sudden ionospheric disturbance.
- Refraction.** Refraction is the bending a wave undergoes in passing from one medium into another, as from air into water or from a denser to rarer layer of the atmosphere.
- *Skip Distance.** The minimum distance at which radio waves of a specified frequency can be transmitted at a specified time between two points on the earth by reflection from the regular ionized layers of the ionosphere.
- *Sporadic Reflections.** From an ionized layer of the ionosphere, sharply defined reflections of substantial intensity from the layer at frequencies greater than the critical frequency of the layer. The intensity of the sporadic reflections generally decreases with increasing frequency. They are variable in respect to time of occurrence, geographic distribution, and frequency range. *Note:* Sporadic reflections are sometimes called *abnormal reflections*.
- *Sudden Ionospheric Disturbance.** A sudden increase of ionization density in low parts of the ionosphere, caused by a bright solar chromospheric eruption. It gives rise to a sudden increase of absorption in radio waves propagated through the low parts of the ionosphere, and sometimes to simultaneous disturbances of terrestrial magnetism and earth currents. The change takes place within one or a few minutes, and conditions usually return to normal within one or a few hours.
- *Vertical-incidence Transmission.** The transmission of a radio wave vertically to the ionosphere and back. The transmission is practically the same for slight departures from the vertical, as when the radio transmitter and receiver are separated by a few kilometers.
- *Virtual Height.** The height, of an ionized layer of the ionosphere, at which reflection from a definite boundary surface would cause the same time of travel as the actual reflection, for a wave transmitted from the ground to the ionosphere and reflected back. Virtual height depends on the wave components and the frequency. *Note:* This is sometimes called *equivalent height* or *effective height*.

GENERAL

- *Absorption.** The loss of energy from a wave by dissipation in propagation through or adjacent to a dissipative medium.
- *Attenuation.** Of a wave, the decrease in displacement with distance in the direction of propagation. If the attenua-

tion varies with frequency, it is defined for a sinusoidal wave of a certain frequency and of constant amplitude at any point. The attenuation of a wave may be defined relative to the attenuation in some ideal conditions such as in free space or over a perfectly conducting plane.

Coverage Diagram. A graphical representation of radio field intensity.

Db. See footnote Chapter 11; loudness is defined in decibels below standard; standard is considered as 1 microwatt per square meter.

Great Circle. An arc on the surface of a sphere whose center is also the center of the sphere.

***Horizon.** In radio-wave propagation over the earth, the line which bounds that part of the earth's surface reached by the direct wave. On a spherical surface, the horizon is a circle. The distance to the horizon is affected by atmospheric refraction.

Line of Sight. A straight line from the transmitting antenna striking the earth tangentially.

Lobe. A conic enclosing the field penetrable by radio waves.

Meridian. A great circle on a sphere passing through the poles and the zenith of a given place. On the earth, these are numbered according to degrees of longitude.

Nomogram. A nomogram consists of a series of curved or straight lines on a chart, with suitable indices. They are normally arranged for the solution of equations involving three variables. If a straightedge is set to read two of these variables, the value of the third can then be determined from the intersection of the straightedge with the other curve or line on the chart.

Prime Meridian. That of Greenwich, England. Longitude is counted both east and west along the equator from the point of intersection of this meridian with the equator.

***Refractive Index.** Of a wave-transmission medium, the ratio of the phase velocity in free space to that in the medium.

TABLE 8

kilometer (km)	1000 meters	1.6 km = 1 mile
		1.85 km = 1 nautical mile
meter		39.37 inches
centimeter (cm)	$\frac{1}{100}$ meter	2.54 cm = 1 inch
		30.5 cm = 1 foot
millimeter (mm)	$\frac{1}{1000}$ meter	

TABLE 9

	Wave Lengths (meters)	Frequency (megacycles)
Long wave telegraphy, marine and aviation beacons, etc.	10,000 to 500	0.03 to 0.55
Intermediate broadcasting	550 to 200	0.55 to 1.5
Short wave telephony, broadcasting, amateurs, etc.	200 to 20	1.5 to 15
Ultra-short wave television, local broadcasting	20 to 1	15 to 30
Radar	0.4 to 0.1	30 up

TABLE 10

Frequency Range	Nature of Range	Abbreviation
Below 30 kc	Very low frequencies	VLF
30 to 300 kc	Low frequencies	LF
300 to 3000 kc	Medium frequencies	MF
3000 to 30,000 kc	High frequencies	HF
30 to 300 mc	Very high frequencies	VHF
300 to 3000 mc	Ultra high frequencies	UHF
3000 to 30,000 mc	Super high frequencies	SHF

INDEX

A

Absorption, 3, 47ff
 auroral zone, 55
 deviative, 58
 non-deviative, 58
 variation with frequency, 58
 Adiabatic:
 dry, 186
 moist, 186
 Advection fog, 197
 Aerological factors, 197
 Angle of fire, 130
 Anomalous propagation, 178
 Antenna height, effect on trapping, 203
 Apparent Solar Time (A.S.T.), 11
 Atmosphere, 4
 Atmospheric temperature, 181
 Atmospheric variations, 196ff
 Atmospheric wave, 120
 Atmospherics, 131
 variations of, 47
 Aurora, 3
 Auroral zone, 118
 absorption, 58
 Austin-Cohen formula, 132
 Aviation, 119
 Azimuthal equal-area projection, 7
 Azimuthal equal-distance projection, 7

B

Beacons, 203
 Bearing, 5
 Birefringence, 16, 210

C

Chinook winds, 201
 Communication security, 203
 Conductivity, 1
 Conversion factors, 220
 Corner reflectors, 203
 Corona, 115
 Coronagraph, 118
 Countermeasure, 203
 Coverage diagrams, 136ff
 Coverage, radar, 181ff
 Critical frequency, 15, 18, 210
 Curved-earth charts, 144
 Cylindrical equal-area projection, 7
 Cylindrical equal-distance projection, 7

D

Dead spots, 128
 Definitions, 218ff
 Dellinger effect, 117
 Deviative absorption, 58
 Diffraction, 120, 172, 216
 D-layer, 14, 55
 Diversity antennas, 130
 Doldrums, 202
 Duct, 180, 189, 197, 203
 elevated, 190
 surface, 189
 Duct formation, 178

Ducts over water, 200
 Ducts, radiation, 199

E

Echo box, 180, 203
 E-layer, 14
 E, sporadic, 44, 117
 Equation of Time (E.T.), 11, 13
 Extended ranges, 134
 Extraordinary wave, 16, 27, 210

F

Faculae, 113
 Fade-outs, 117, 138
 Fading, 128, 179
 flutter, 128
 selective, 130
 Field intensity, 58
 unabsorbed, 58
 F₁-layer, 14
 F₂-layer, 14
 Fog, advection, 197
 Fohn wind, 201
 Free-space intensity, 121, 139
 Frequencies, broadcast, 131ff
 Frequency, critical, 15, 18
 Frontal inversions, 197

G

Galaxy, 139
 Galloping Ghosts, 204
 Ghost images, 178
 Ghost signals, 204
 Gnomonic projection, 6
 Great circles, 5, 7
 Great-circle distance, 42ff
 Great-circle maps, 36ff
 Greenwich Civil Time (G.C.T.), 7
 Ground return, 177
 Ground wave, 1, 120ff
 distance range, 126
 Group velocity, 210
 Gyro-frequency, 17, 59

H

Height-gain, 121
 Homing with radar, 204
 Humidity, relative, 184
 Hurricane, radar detection of, 206

I

Index of refraction, modified, 182
 Ionosphere, 14
 variation with solar zenith distance, 21
 Ionospheric propagation, theory of, 209ff
 Ionospheric splitting, 20
 Ionospheric storm, 118
 forecasting of, 118
 recurrence of, 118
 Ionospheric variations, 117ff

K

Kd, 57
 Kilometer, 13
 Kiska, 179

L

Latitude, 5
 Limiting angle of refraction, 180
 Line of sight, 203
 Lobes, 136, 144, 190, 204, 215
 Local Civil Time (L.C.T.), 9
 Longitude, 5
 Longitude effect, 23
 Longitude zones, 44
 Long path, 38
 transmission, 59
 Loran, 119, 128
 Lowest useful high frequency (*see* LUHF)
 LUHF, 3, 25, 53, 56ff, 118, 131
 (short path), 59

M

Magnetic effects, 3
 Magnetic storm, 118
 Map projections, 5ff
 Maximum usable frequency (*see* MUF)
 Maxwell's equations, 209
 M-curve, 181ff, 189
 M-curves, formula for, 183
 M-deficit, 190
 Mercator projections, 7
 Mile, 13
 Mirage, 176
 Mixing ratio, 183
 Modes, 190
 Moisture content, 198
 Moisture variations, 182
 M-type transmissions, 61
 MUF, 3, 17, 19, 25, 44ff, 117, 118
 MUF distance factors:
 (E, F₁), 22
 (F₂), 24
 (F₂-zero), 26
 Multi-hop transmissions, 18, 46
 Multiple reflections, 155, 204
 Multiple sweeps, 178

N

Nautical mile, 13
 Nocturnal cooling, 199
 Noise, 47ff, 131 (*see also* Atmospherics)
 Noise grades, 47
 Noise receiver, 4
 Nomograms, 13
 Non-deviative absorption, 58
 Null lines, 205

O

Operational problems in tropospheric propagation, 203ff
 Optimum working frequency (*see* OWF)
 Ordinary wave, 16, 210

Orthographic projection, 6
OWF, 20, 25

P

Phase shift, 212
Plane-to-ground communication, 180, 200, 204
Polarization, 16, 210
Polar regions, 182
Power density, 136
Power requirements, 61
PPI scope, 177
Precipitation static, 139
Projection:
 azimuthal equal-area, 7
 azimuthal equidistant, 7
 cylindrical equal-area, 7
 cylindrical equal-distance, 7
 gnomonic, 6
 mercator, 7
 orthographic, 6
 stereographic, 6
Prominence, 113
Pseudo-adiabatic diagram, 184
Pulse measurements, 15
Pulsing rate, 177

R

Racons, 204
Radar, 134
Radar coverage, 181ff
 variations of, 177
Radar echoes, 177
Radar observations:
 and meteorology, 206
 of the moon, 134
Radiation inversions, 200
Radio mirages, 177
Radiosonde, 186
Range fluctuations, 203
Range formula, 178
Range variation (Radar), 176
Ranges, 155
 diminished, 204
Receiver noise, 137
Reception at antipodes, 59
Reflected wave, 120

Refractive index, 177
Relative humidity, 184
Responder beacons, 204

S

Saturated air, 186
Search radar, 203
Sea return, 177
Service areas, 13
Shadow-loss, 127
Shadow-zone, 172ff
SHF, 134ff, 153
Short path, 38
Skip distance, 2
Skip zones in VHF, 201
Sky wave, 1
Small circles, 5
Solar activity, 132
Solar flares, 117, 138
Solar noise, 138
Solar radiation, 2
Solar variability, 113ff
Sounding techniques, 186
Sporadic E, 44, 60, 117, 132
Standard atmosphere, 188
Standard atmospheric conditions, 136
Standard propagation, 181, 187
Standard targets, 203
Standard time, 8
Static, 47
Static, precipitation, 139
Stereographic projection, 6
Storm:
 ionospheric, 118
 magnetic, 118
Stratus-type inversions, 197
Submarine, 204
Subsidence, 197
Substandard propagation, 187
Sun, 113ff
Sunspots, 114
Sunspot cycle, 115
Sunspot period, 115
Super-high frequencies (*see* SAF)
Superrefraction, 178
Superstandard propagation, 187
Surface inversions, 197
Surface wave, 120

T

Television, 138
Temperature:
 atmospheric, 181
 dry-bulb, 184
 inversion, 182
 wet-bulb, 184
Thunderstorms, radar detection of, 206
Time, 7
 apparent solar, 11
 equation of, 11
 Greenwich Civil, 7
 local civil, 7
 standard, 8
Tornado, radar detection of, 206
Trapping, 178, 182, 203
 index, 190
Tropical regions, 182
Troposphere, 134
Tropospheric propagation, theory of, 212
Turbulence, 199
Typhoons, radar detection of, 206
Twilight zone, 59

U

UHF, 134ff
Ultra-high frequencies (*see* UHF)

V

Vertical antenna, 120
Very high frequencies (*see* VHF)
Very low frequencies, 132
Virtual height, 15
VHF, 134ff
 communication, 203

W

Water vapor, 181, 198
Wave equation, 209
Weather:
 effect on VHF propagation, 197ff
 effect on VHF, summer, 205
Weather effects, 181
Weather forecasting from radar observations,
 206

